ISSN 1948-0210 (online)

World Journal of *Stem Cells*

World J Stem Cells 2023 June 26; 15(6): 502-653

Published by Baishideng Publishing Group Inc

WJSC

World Journal of Stem Cells

Contents

Monthly Volume 15 Number 6 June 26, 2023

REVIEW

MINIREVIEWS

ORIGINAL ARTICLE

Basic Study

SYSTEMATIC REVIEWS

World Journal of Stem Cells

Monthly Volume 15 Number 6 June 26, 2023

Contents

ABOUT COVER

Editorial Board Member of *World Journal of Stem Cells*, Luminita Labusca, MD, PhD, Senior Researcher, National Institute of Research and Development in Technical Physics Iasi, 47 D Mangeron Boulevard, Iasi 70050, Romania. drlluminita@yahoo.com

AIMS AND SCOPE

The primary aim of *World Journal of Stem Cells* (*WJSC*, *World J Stem Cells*) is to provide scholars and readers from various fields of stem cells with a platform to publish high-quality basic and clinical research articles and communicate their research findings online. *WJSC* publishes articles reporting research results obtained in the field of stem cell biology and regenerative medicine, related to the wide range of stem cells including embryonic stem cells, germline stem cells, tissue-specific stem cells, adult stem cells, mesenchymal stromal cells, induced pluripotent stem cells, embryonal carcinoma stem cells, hemangioblasts, lymphoid progenitor cells, *etc*.

INDEXING/ABSTRACTING

The *WJSC* is now abstracted and indexed in Science Citation Index Expanded (SCIE, also known as SciSearch®), Journal Citation Reports/Science Edition, PubMed, PubMed Central, Scopus, Biological Abstracts, BIOSIS Previews, Reference Citation Analysis, China National Knowledge Infrastructure, China Science and Technology Journal Database, and Superstar Journals Database. The 2023 Edition of Journal Citation Reports® cites the 2022 impact factor (IF) for *WJSC* as 4.1; IF without journal self cites: 3.9; 5-year IF: 4.5; Journal Citation Indicator: 0.53; Ranking: 15 among 29 journals in cell and tissue engineering; Quartile category: Q3; Ranking: 99 among 191 journals in cell biology; and Quartile category: Q3. The *WJSC*'s CiteScore for 2022 is 8.0 and Scopus CiteScore rank 2022: Histology is 9/57; Genetics is 68/325; Genetics (clinical) is 19/90; Molecular Biology is 119/380; Cell Biology is 95/274.

RESPONSIBLE EDITORS FOR THIS ISSUE

Production Editor: *Xiang-Di Zhang*; **Production Department Director:** *Xu Guo*; **Editorial Office Director:** *Jia-Ru Fan*.

NAME OF JOURNAL
World Journal of Stem Cells

ISSN
ISSN 1948-0210 (online)

LAUNCH DATE
December 31, 2009

FREQUENCY
Monthly

EDITORS-IN-CHIEF
Carlo Ventura, Shengwen Calvin Li

EDITORIAL BOARD MEMBERS
https://www.wjgnet.com/1948-0210/editorialboard.htm

PUBLICATION DATE
June 26, 2023

INSTRUCTIONS TO AUTHORS
https://www.wjgnet.com/bpg/gerinfo/204

GUIDELINES FOR ETHICS DOCUMENTS
https://www.wjgnet.com/bpg/GerInfo/287

GUIDELINES FOR NON-NATIVE SPEAKERS OF ENGLISH
https://www.wjgnet.com/bpg/gerinfo/240

PUBLICATION ETHICS
https://www.wjgnet.com/bpg/GerInfo/288

PUBLICATION MISCONDUCT
https://www.wjgnet.com/bpg/gerinfo/208

ARTICLE PROCESSING CHARGE
https://www.wjgnet.com/bpg/gerinfo/242

STEPS FOR SUBMITTING MANUSCRIPTS
https://www.wjgnet.com/bpg/GerInfo/239

ONLINE SUBMISSION
https://www.f6publishing.com

World Journal of Stem Cells

Submit a Manuscript: https://www.f6publishing.com

World J Stem Cells 2023 June 26; 15(6): 502-513

DOI: 10.4252/wjsc.v15.i6.502

ISSN 1948-0210 (online)

REVIEW

Adipokines regulate mesenchymal stem cell osteogenic differentiation

Zhong-Hua Xu, Chen-Wei Xiong, Kai-Song Miao, Zhen-Tang Yu, Jun-Jie Zhang, Chang-Lin Yu, Yong Huang, Xin-Die Zhou

Specialty type: Cell biology

Provenance and peer review: Invited article; Externally peer reviewed.

Peer-review model: Single blind

Peer-review report's scientific quality classification

Grade A (Excellent): 0
Grade B (Very good): B, B
Grade C (Good): 0
Grade D (Fair): 0
Grade E (Poor): 0

P-Reviewer: Scarfi S, Italy; Stogov MV, Russia

Received: November 14, 2022
Peer-review started: November 14, 2022
First decision: February 21, 2023
Revised: February 26, 2023
Accepted: April 24, 2023
Article in press: April 24, 2023
Published online: June 26, 2023

Zhong-Hua Xu, Department of Orthopedics, Jintan Hospital Affiliated to Jiangsu University, Changzhou 213200, Jiangsu Province, China

Chen-Wei Xiong, Kai-Song Miao, Zhen-Tang Yu, Jun-Jie Zhang, Chang-Lin Yu, Yong Huang, Xin-Die Zhou, Department of Orthopedics, The Affiliated Changzhou Second People's Hospital of Nanjing Medical University, Changzhou 213000, Jiangsu Province, China

Chen-Wei Xiong, Kai-Song Miao, Zhen-Tang Yu, Jun-Jie Zhang, Chang-Lin Yu, Yong Huang, Xin-Die Zhou, Changzhou Medical Center, Nanjing Medical University, Changzhou 213000, Jiangsu Province, China

Xin-Die Zhou, Department of Orthopedics, Gonghe County Hospital of Traditional Chinese Medicine, Hainan Tibetan Autonomous Prefecture 811800, Qinghai Province, China

Corresponding author: Xin-Die Zhou, MD, Department of Orthopedics, The Affiliated Changzhou Second People's Hospital of Nanjing Medical University, No. 29 Xinglong Lane, Tianning District, Changzhou 213000, Jiangsu Province, China. zhouxindie@njmu.edu.cn

Abstract

Mesenchymal stem cells (MSCs) can differentiate into various tissue cell types including bone, adipose, cartilage, and muscle. Among those, osteogenic differentiation of MSCs has been widely explored in many bone tissue engineering studies. Moreover, the conditions and methods of inducing osteogenic differentiation of MSCs are continuously advancing. Recently, with the gra-dual recognition of adipokines, the research on their involvement in different pathophysiological processes of the body is also deepening including lipid metabolism, inflammation, immune regulation, energy disorders, and bone homeostasis. At the same time, the role of adipokines in the osteogenic differentiation of MSCs has been gradually described more completely. Therefore, this paper reviewed the evidence of the role of adipokines in the osteogenic differentiation of MSCs, emphasizing bone formation and bone regeneration.

Key Words: Mesenchymal stem cells; Adipokines; Adipose tissue; Osteogenic differentiation; Osteogenesis; Bone regeneration

Core Tip: Bone tissue supports and protects the organs of the human body. There is a close relationship between the immune system and bone homeostasis. Adipose tissue is an essential accessory tissue around bone tissue, which regulates bone homeostasis through the secretion of adipocytokines. There are many types of adipokines, but only some have been studied in detail. Different adipokines affect the behavior and differentiation of mesenchymal stem cells under different local microenvironments and surrounding inflammation, thus coordinating and participating in the regulation of bone homeostasis.

Citation: Xu ZH, Xiong CW, Miao KS, Yu ZT, Zhang JJ, Yu CL, Huang Y, Zhou XD. Adipokines regulate mesenchymal stem cell osteogenic differentiation. *World J Stem Cells* 2023; 15(6): 502-513
URL: https://www.wjgnet.com/1948-0210/full/v15/i6/502.htm
DOI: https://dx.doi.org/10.4252/wjsc.v15.i6.502

INTRODUCTION

Adipose tissue is currently considered an endocrine organ[1] and comprises adipose cells, endothelial cells, fibroblasts, and immune cells[2]. Adipokines are factors secreted by adipose tissue and have multiple functions[3] involving various biological processes including immune responses, inflammation, glucose metabolism, insulin secretion, sensitivity regulation, regulation of blood pressure and myocardial contractility, blood vessel growth, and lipid metabolism[3,4]. Therefore, adipokines regulate different biological processes in different organs including the brain, liver, muscles, blood vessels, heart, and pancreas[5]. The function, characterization, molecular targets, and potential clinical disease correlation of adipokines are still unclear and the main focus of future adipokine research.

Mesenchymal stem cells (MSCs), pluripotent stem cells derived from the mesoderm, were identified by surface markers such as CD29, CD37, CD44, CD90, CD105, and CD166[6]. MSCs can be readily extracted from many tissues including bone marrow, umbilical cord, placenta, fat, liver, and skin[7]. However, the most well-studied source is bone marrow. MSCs have been shown to differentiate into mature cells of various tissues including cartilage, bone, tendon, ligament, and adipose tissue[8]. Due to its multipotential nature, MSCs have been used to treat many diseases including tumors, central nervous system disease, liver disease, graft-versus-host disease, inflammation, immune system disease, and bone regeneration[9-12]. In this review, we focus on the osteogenic differentiation of MSCs.

Bone is a rigid organ that supports and protects the other vital organs in the body. In adults, bones are renewed approximately every 7 years[13], and bone formation by osteoblasts and bone resorption by osteoclasts play a significant role. Osteoclasts originate from hematopoietic stem cell precursors, and osteoblasts originate from MSCs[14]. The dynamic balance of the two processes maintains the stability of bone metabolism, whereas the destruction of balance leads to various diseases including osteoporosis[15], osteopenia[16], and bone nonunion[17]. Osteoblasts promote the deposition of calcium salts in the bone matrix and stimulate bone remodeling and osteoblast differentiation of MSCs. It can be verified by the detection of runt-related transcription factor 2 (RUNX2), alkaline phosphatase (ALP), and osteopontin (OPN). Therefore, the biological characteristics of MSC osteogenic differentiation have been widely used in bone tissue engineering to treat bone defects caused by trauma, infection, and tumor surgery[18-20]. As a common progenitor of both adipocytes and osteoblasts, MSCs are in a delicate equilibrium state during differentiation, whereas adipose-inducing factors inhibit the osteogenic differentiation of MSCs. In contrast, bone-inducing factors inhibit the adipogenic differentiation of MSCs[6]. As an important active secretion of fat, the position and role of adipokine in the osteogenic differentiation of MSCs are worth further consideration. Therefore, we reviewed the role of adipokines in the osteogenic differentiation of MSCs.

CYTOKINE AND CYTOKINE-LIKE PROTEINS

Interleukin (IL) is an essential inflammatory adipokine that plays a vital role in the differentiation of MSCs in the early stage of bone reconstruction[21]. Lacey *et al*[22] found that low-dose IL-1β (0.001-1 ng/mL) inhibited ALP activity, reduced RUNX2 and procollagen expression, and inhibited the degree of mineralization of MSCs in mice. IL-6 is a multifunctional lymphoid factor with pro-inflammatory and anti-inflammatory effects[23]. At the same time, it can be secreted by osteoblasts to stimulate the secretion of osteoclasts and participate in bone homeostasis. IL-6 induces osteogenic differentiation in human bone marrow-derived MSCs (BMSCs) *via* mitogen-activated protein kinase signaling [24]. IL-10 can reduce the synthesis of pro-inflammatory cytokines and chemokines and inhibit the expression of IL-1 and tumor necrosis factor alpha (TNF-α)[25]. In mice, IL-10 inhibits the osteogenic differentiation of MSCs prior to ALP expression[26]. IL-17 cytokines act by binding to the IL-17 receptor family[27]. In the early stage of bone injury, IL-17 secretion increases, promoting the transformation of MSCs into bone progenitor cells or osteoblasts. In some cases, IL-17 can also act as an anti-osteoblast factor, leading to bone loss[28,29].

TNF-α is a pro-inflammatory cytokine that can bind to the TNF receptor superfamily and participate in the regulation of a variety of biological processes. Different doses of TNF-α showed different osteogenic differentiation activity of MSCs. Wang *et al*[30] showed that a high dose of TNF (50 ng/mL) could stimulate the upregulation of some osteogenic factors in MSCs, including vascular endothelial growth factor and insulin growth factor. Lacey *et al*[22] cultured BMSCs with different doses of TNF-α and found that low-dose TNF-α (0.1-10 ng/mL) inhibited the mineralization and activation of

ALP and OPN in cultured MSCs.

Monocyte chemotactic protein 1 (MCP-1), also known as C-C motif chemotactic factor ligand 2, can influence monocyte migration and subsequent macrophage polarization[31]. Xie *et al*[32] showed that in the process of osteogenic differentiation, MSCs from patients with ankylosing spondylitis secreted more MCP-1 than MSCs from healthy people. Enhanced MCP-1 secretion promoted monocyte migration, increased classical macrophage polarization, and enhanced TNF-α secretion[32]. Other adipokine-related cytokines, such as progranulin and resistin, have not been reported to correlate with MSC osteogenic differentiation.

Transforming growth factor β (TGF-β) has a unique correlation with the differentiation of adult MSCs[33]. Through the precise matching of ligands, receptors, and cell signaling molecules, TGF-β is involved in the lineage transformation process of the differentiation of various stem cells such as lipids, osteoblasts, chondrogenic and myogenic cells[34]. Tang *et al*[35] confirmed that TGF-β1 induced the migration of MSCs to the bone resorption site of mice by activating the activin receptor-like kinase 5-Smad2/3-Smad4 pathway and restricted the further recruitment of osteoclasts but did not induce osteogenic differentiation. However, other studies have reported that TGF-β inhibits osteogenic differentiation through Wnt signaling interactions and inhibits RUNX2 through the activation of Smad3[36,37]. However, TGF-β has also been reported to promote the osteogenic differentiation of MSCs[38,39]. However, further research needs to be carried out in the future.

Chemerin is a secreted protein derived from adipocytes and liver cells involved in physiological processes including inflammation, angiogenesis, and calcium mobilization[40,41]. Epidemiological studies have reported that patients with osteoporosis have higher circulating chemerin[42], and the knockout of chemerin or its receptor CMKLR1 inhibits lipogenesis and promotes the osteogenic differentiation of MSCs[43]. Li *et al*[41] showed that chemerin promoted the osteogenic differentiation of C3H10T1/2 cells and MSCs through Akt/Gsk3β/β-catenin signaling. However, Akt inhibitors (MK2206) inhibited chemerin's promotion of osteogenic differentiation and active β-catenin.

PROTEINS OF THE FIBRINOLYTIC SYSTEM

Plasminogen activator inhibitor-1 (PAI-1) is a serine protease inhibitor of the fibrinolytic system[44]. Adipose-derived PAI-1 is associated with various pathologic conditions including inflammation, diabetes, cancer, and obesity[44]. Takafuji *et al*[45] studied the role of PAI-1 in the osteogenic differentiation of MSCs using wild-type and PAI-1-deficient mice and found that the loss of PAI-1 significantly weakened the expression of BMSC osteogenic genes, such as bone morphogenetic protein 2 (BMP-2) and ALP.

Tissue factor, another adipokine that plays a crucial role in the clotting process[46], whose overexpression in the body can lead to multiple forms of thrombosis[47]. In a study aimed at improving coagulation activity, Rangasami *et al*[48] found that pluronic micelle-mediated tissue factor silencing could effectively induce the higher differentiation of MSCs in osteogenic and lipid-forming media.

COMPLEMENT AND COMPLEMENT-RELATED PROTEINS

Adipsin was the first adipocyte-secreted protein to be identified[49] and is currently named complement factor D[50]. Fat cells produce it through the activation of peroxisome proliferator-activated receptor gamma[51]. More recently, adipsin was shown to promote insulin secretion by pancreatic β cells and prevent β-cell death[52]. By activating Wnt signaling, adipsin initiates adipogenesis from BMSCs[53]. Experiments on BMSCs of adipsin knockout mice showed the increased expression of mineralized nodules and osteoblast markers including RUNX2, COL1A1, and osteocalcin compared with MSCs of normal origin[53].

Complement and complement-related proteins from adipose tissue include complement component 1q and TNF-related protein family, complement factor B, and acylating simulation protein[3,54]. However, it has not been reported whether they induce or inhibit the osteogenic differentiation of MSCs.

ADIPOKINES

Leptin, a hormone derived from adipose tissue, is involved in pathophysiological processes such as food absorption, energy metabolism, inflammation, immunity, and bone homeostasis[55-58]. Leptin binds to its leptin receptor, a marker specific to BMSCs[59]. Leptin has been shown to cross-regulate BMP-9 signaling through the JAK/STAT signaling pathway in MSCs, thereby enhancing BMP-9-induced osteogenesis[60].

Adiponectin plays a vital role in anti-inflammation, glucolipid metabolism, and insulin resistance regulation[61,62]. Wang *et al*[63] reported that adiponectin regulates BMSC osteogenic differentiation and osteogenesis through the Wnt/β-catenin pathway. Similar results have also been reported in other studies[64-66].

Visfatin is commonly produced by visceral adipose tissue and is also known as nicotinamide phosphoribosyltransferase (Nampt) or pre-B cell cluster enhancer. It is strongly expressed in osteogenic differentiation[67] and promotes the proliferation and mineralization activity of osteoblasts[68]. Visfatin induces the secretion of IL-6, IL-8, and MCP-1 during the osteogenic differentiation of MSCs and significantly increases matrix mineralization during osteogenic differentiation, while the expression of type I collagen is decreased[69].

Nicotinamide adenine dinucleotide (NAD) is involved in energy metabolism and protein modification[70]. Nampt has recently been identified as a novel adipokine[71]. Nampt is a rate-limiting enzyme and participates in all-around MC3T3 E1-osteogenesis prior to the cell differentiation process of NAD salvage pathways. Knocking out Nampt, or adding its specific inhibitor, Fk866, resulted in decreased intracellular NAD concentration and decreased osteogenic ability[67]. Thus, Nampt can be used as a specific marker for the osteogenic differentiation of MSCs[72].

Visceral adipose tissue-derived serine protease inhibitor (vaspin), an adipose-derived hormone, attenuates osteogenic differentiation of the preosteoblast cell line MC3T3-E1[73] and antagonizes the osteogenic differentiation of rat osteoblasts. However, the role of vaspin in the osteogenic differentiation of MSCs has not been reported[74].

BMPs, the largest component of the TGF-β ligand family, regulate multiple organogenetic pathways, fat formation, and energy metabolism[75,76]. BMP-2, BMP-3, BMP-4, BMP-5, BMP-6, and BMP-7 all strongly promote osteogenesis. Short-term addition of BMP-2 increases osteocalcin expression[77], and BMP-7 induces the increased expression of ALP, a marker of osteoblast differentiation, and accelerates calcification[78]. The absence of BMP-2 and BMP-4 results in severely impaired osteogenic function, but the limb skeleton still develops normally without BMP-4[79]. BMP-3 regulates adult bone mass by limiting the differentiation of bone progenitor cells into mature osteoblasts[80]. It is important to note that BMP-7 has been marketed and used in surgery to aid fracture healing, with no reported local or systemic adverse events [81]. The effects of BMP-5[82,83] and BMP-6[84,85] on the osteogenic differentiation of MSCs have also been reported.

Nesfatin-1 is a novel anorexia polypeptide that has a wide range of biological effects including energy metabolism, gastrointestinal function, anxiety and depression, and the regulation of cardiovascular and reproductive function[86-88]. The role of nesfatin-1 in the osteogenic differentiation of MSCs has not been reported, but it can promote the expression of osteogenic genes such as ALP and RUNX2 in newly derived rat stem cells[89]. Therefore, we speculate that Nesfatin-1 has a similar role in the osteogenic differentiation of MSCs, but this conclusion still needs to be confirmed by further studies.

Cathepsins are an important category of enzymes located within the lysosomes[90]. Cathepsins are produced by various tissues, which also include adipose tissue[91]. Cathepsin K is a crucial enzyme in the degradation of the organic bone matrix, and its expression in bone formation-related cells, including fibroblasts, osteoblasts, and MSCs, has also been confirmed[92,93]. Zhang *et al*[94] showed that knockout or inhibition of cathepsin K can promote the regeneration of BMSCs of jaw bone through glycolysis, thus promoting alveolar bone regeneration. Similarly, cathepsin S deficiency alters the balance between adipocyte and osteoblast differentiation, increases bone turnover, and alters bone microstructure[95].

Apelin is an endogenous ligand of the G protein-coupled apelin receptor[96]. Besides being an adipokine, apelin is also expressed in skeletal muscle, the central nervous system, the heart, and other tissues, and is involved in lipolysis, glucose metabolism, cell proliferation, and angiogenesis[97]. Exogenous addition of apelin protein or overexpression of apelin promotes postpositional MSC osteoblast differentiation by activating the Wnt/β-catenin signaling pathway[98].

Omentin-1 is the adipokine most commonly expressed in omental adipose tissue and is also abundant in plasma[99]. Omentin-1 is involved in the physiological processes of inflammation, insulin, and cardiovascular functions[99,100]. For bone effects, a study of postmenopausal women found a negative correlation between omentin-1 levels and lumbar bone density[101]. Tang *et al*[102] found that omentin-1 has a dose-dependent effect on the viability of MC3T3-E1 cells, which can significantly increase the expression of members of the TGF-β/Smad signaling pathway, and also significantly increase the expression levels of BMP-2, RUNX2, OPN, osteocalcin, and other proteins, thus promoting osteogenesis.

Lipocalin 2 (LCN2) is a protein involved in host defense, autoimmunity, insulin resistance, skin healing, tumor, and infection[103,104]. LCN2 disrupts osteoclast formation in bone tissue by negatively regulating the proliferation and differentiation of osteoclast precursors[105]. As a secretory bone factor, LCN2 positively affects the osteogenic differentiation and *in vivo* osteogenesis of MC3T3-E1[106].

Melatonin is an indoleamine that is synthesized and secreted primarily by the pineal gland in mammals but is also secreted by adipose tissue[107]. Melatonin mainly affects the circadian rhythm and sleep-wake cycle and is also involved in immune regulation and inhibition of tumor growth[108,109]. Melatonin is also involved in MSC differentiation, which is involved in developing and regenerating bone, muscle, and fat tissues. In BMSCs, melatonin enhances osteogenesis and inhibits lipogenesis. Melatonin also differentiates bone marrow progenitors from adipocytes to osteoblasts[110,111].

Gremlin-1 is a highly conserved glycoprotein, mainly distributed in the extracellular matrix, with a small amount in the endoplasmic reticulum[112]. As an adipokine, gremlin-1 plays an important role in adipose tissue homeostasis[113]. At the same time, studies have shown that gremlin-1 is a BMP protein inhibitor, which can inhibit their binding to BMP receptors on the cell membrane by binding to BMP-2, BMP-4, and BMP-7[112]. Specific overexpression of gremlin-1 in mouse bone tissue results in severe osteoporosis; however, conditional knockout of gremlin-1 increases trabecular volume and bone formation[114]. Gremlin-1 has also been shown to inhibit the viability and osteogenic differentiation of human BMSCs[115].

LIPID TRANSPORT

Apolipoprotein E (ApoE), one of the main components of plasma very low-density lipoprotein[116], regulates lipid homeostasis by regulating lipid transport between tissues and cells. ApoE4 is associated with hyperlipidemia and hypercholesterolemia, leading to coronary heart disease, stroke, and atherosclerosis[117-119]. BMP-2 can upregulate the ApoE level of the mouse mesenchymal progenitor cell line (C3H10T1/2), leading to enhanced osteogenic differentiation. At the same time, ApoE is also expressed *in vitro* in mouse cranial primary osteoblasts with advanced osteoblast sequences[120].

ENZYMES

Dipeptidyl peptidase 4 (DPP-4) is a protein secreted in the salivary glands, prostate, seminal vesicles, endometrium, small intestine, and decidual membrane, and has recently been identified in adipose tissue as well[121]. DPP-4 is an important drug target in type 2 diabetes and directly induces insulin resistance in adipocytes and skeletal muscle[121]. DPP-4 not only reflects but also promotes adipose tissue dysfunction. Choi *et al*[122] found that DPP-4, when overexpressed, could restrict the induction of osteogenic differentiation of heart artery flap-derived mesenchymal cells by the autocrine insulin-like growth factor-1 signaling pathway, but this result has not been verified on MSCs.

Tissue inhibitors of metalloproteinases (TIMPs) have four main members, TIMP-1, TIMP-2, TIMP-3, and TIMP-4, and are primarily responsible for degrading most proteins in the extracellular matrix[123,124]. TIMPs are generally considered to be inhibitors of matrix metalloproteinases (MMPs) through the action of their terminal N-domain[125]. Meanwhile, TIMPs exist in the extracellular matrix in a soluble form and preemptively bind to the extracellular matrix, thus inhibiting the effect of MMPs[126]. TIMPs can selectively inhibit different MMPs, metalloproteinase and a disintegrin and metalloproteinase with thrombospondin motifs[125,126]. Inhibition of endogenous TIMP-1 can inhibit the proliferation, metabolic activity, and osteogenic differentiation ability of MSCs by activating Wnt/β-catenin signaling [127]. However, Liang *et al*[128] found in the process of MSC osteogenic differentiation that TIMP-1 knockdown increased the deposition of calcium nodules, ALP activity, and the expression of osteocalcin protein by activating Wnt/β-catenin signaling. The conclusions here are contradictory and need further confirmation by other studies. Studies targeting TIMP-3 have shown that increased expression of TIMP-3 can significantly promote osteogenic differentiation of MSCs in the fracture model of diabetic rats[129].

CONCLUSION

The formation and regeneration of bone tissue usually require regulation of the local microenvironment. The balance between bone resorption and bone regeneration is essential for bone tissue regeneration. Adipokines are exogenous immune regulatory substances secreted by adipose tissue, and are widely involved in pathophysiological processes of surrounding tissues, including bone homeostasis and bone regeneration. Not all human adipokines have been identified, but the current literature has revealed that the surface adipose tissue secretes more than 600 factors or proteins involving many processes of human pathophysiology[130]. There are many types of adipokines, including cytokines[22], fibrinolysin[44], complement and related proteins[49], enzymes[121], lipid transport systems[116], endocannabinoids [131], and angiotensinogen[132] (Table 1).

In summary, this paper reviewed the current research on the regulation and influence of adipokine in the osteoblast differentiation of MSCs. However, this review did not include all currently discovered adipokines but only included published studies involving osteogenic differentiation of MSCs. Most of the included studies were conducted in BMSCs, with a small number involving osteoblast precursor cells, progenitor cells, and a small number of other tissue-derived stem cells. Our review suggests that different adipokines have different effects on the outcome of osteogenic differentiation, bone regeneration, and bone remodeling of MSCs. The progress of related research provides a good reference for subsequent preclinical and clinical studies and a new reference for treating osteogenic disorders and diseases of osteoblastic homeostasis.

Table 1 Key activities of factors released by adipose tissue

Classification	Appellation	Mechanism	Ref.
Cytokine and cytokine-like proteins	Interleukin	IL-6 induces osteogenic differentiation in human bone marrow-derived MSCs *via* MAPK signaling. IL-10 inhibits osteogenic differentiation of MSCs prior to ALP expression. IL-17 promoting the transformation of MSC into bone progenitor cells or osteoblasts	[24,26,28]
	TNF-α	High dose of TNF could stimulate the upregulation of some osteogenic factors in MSCs, including VEGF and insulin-like growth factor. Low-dose TNF-α inhibited the mineralization and activation of ALP and OPN in cultured MSCs	[22,30]
	MCP-1	Influencing monocyte migration and subsequent macrophage polarization	[31]
	TGF-β	Through the precise matching of ligands, receptors, and cell signaling molecules, TGF-β is involved in the lineage transformation process of the differentiation of various stem cells, such as lipid, osteoblast, chondrogenic, and myogenic	[34]
	Chemerin	Chemerin promotes lipogenesis and inhibits osteogenic differentiation of MSCs	[42]
Proteins of the fibrinolytic system	PAI-1	Loss of PAI-1 significantly weakened the expression of bone marrow-derived MSC osteogenic genes, such as BMP-2 and ALP	[45]
	Tissue factor	Tissue factor silencing could effectively induce higher differentiation of MSCs in osteogenic and lipid-forming media	[48]
Complement and complement-related proteins	Adipsin	Adipsin initiates adipogenesis from bone marrow MSCs by activating Wnt signaling	[53]
Adipokines	Leptin	Leptin has been shown to cross-regulate BMP-9 signaling through the JAK/STAT signaling pathway in MSCs, thereby enhancing BMP-9-induced osteogenesis	[60]
	Adiponectin	adiponectin regulates BMSC osteogenic differentiation and osteogenesis through the Wnt/β-catenin pathway	[63]
	Visfatin	Promoting the proliferation and mineralization activity of osteoblasts	[68]
	Nicotinamide	Nampt is a speed-limit enzyme and participates in the all-around MC3T3-E1. Osteogenesis prior to the cell differentiation process of NAD salvage pathways	[67]
	Visceral	Attenuating the osteogenic differentiation of preosteoblast cell line MC3T3-E1	[73]
	Bone morphogenetic proteins	BMP-7 induced increased expression of ALP, a marker of osteoblast differentiation, and accelerated calcification. The absence of BMP-2 and BMP-4 resulted in severely impaired osteogenic function. BMP-3 regulates adult bone mass by limiting the differentiation of bone progenitor cells into mature osteoblasts	[78-80]
	Nesfatin-1	Promoting the expression of osteogenic genes such as ALP and RUNX2 in rats' newly derived stem cells	[89]
	Cathepsins	Knockout or inhibition of cathepsin K could promote the regeneration of bone marrow MSCs of jaw bone through glycolysis. Cathepsin S deficiency alters the balance between adipocyte and osteoblast differentiation, increases bone turnover, and alters bone microstructure	[94,95]
	Apelin	Promoting postpositional MSC osteoblast differentiation by activating the Wnt/β-catenin signaling pathway	[98]
	Omentin-1	Increasing the expression of BMP2, RUNX2, OPN, and osteocalcin	[102]
	Lipocalin 2	Disrupting osteoclast formation in bone tissue by negatively regulating the proliferation and differentiation of osteoclast precursors	[105]
	Melatonin	Differentiating bone marrow progenitors from adipocytes to osteoblasts	[111]
	Gremlin-1	BMP protein inhibitor	[112]
Lipid transport	ApoE	Enhancing osteogenic differentiation of the mouse mesenchymal progenitor cell line	[120]
Enzymes	DPP-4	Restricting the induction of osteogenic differentiation of heart artery flap-derived mesenchymal cells by the autocrine insulin-like growth factor-1 signaling pathway	[122]
	Tissue inhibitors of metallo-	Inhibition of endogenous TIMP-1 can inhibit the proliferation, metabolic	[127]

proteinases	activity, and osteogenic differentiation ability of MSCs by activating the Wnt/β-catenin signal

ALP: Alkaline phosphatase; ApoE: Apolipoprotein E; BMP-2: Bone morphogenetic protein 2; DPP-4: Dipeptidyl peptidase 4; IL: Interleukin; JAK: Janus kinase; MAPK: Mitogen-activated protein kinase; MCP-1: Monocyte chemotactic protein 1; MSC: Mesenchymal stem cell; Nampt: Nicotinamide phosphoribosyltransferase; OPN: Osteopontin; PAI-1: Plasminogen activator inhibitor-1; RUNX2: Runt-related transcription factor 2; TIMP-1: Tissue inhibitors of metalloproteinase; TGF-β: Transforming growth factor beta; TNF: Tumor necrosis factor; VEGF: Vascular endothelial growth factor.

FOOTNOTES

Author contributions: Xu ZH and Xiong CW contributed equally to this work; Xu ZH contributed to the conceptualization, methodology, and software; Xiong CW contributed to the data curation, and writing-original draft preparation; Miao KS and Yu ZT contributed to the visualization and investigation; Zhang JJ and Yu CL contributed to the supervision, software, and validation; Huang Y contributed to the writing-reviewing and editing; Zhou XD contributed to the data collection.

Supported by the Changzhou Science & Technology Program, No. CJ20210104, CJ20220120, and CJ20210005; Qinghai Province Health System Guidance Plan Project, No. 2022-wjzdx-106; Young Talent Development Plan of Changzhou Health commission, No. CZQM2020059; and Top Talent of Changzhou "The 14th Five-Year Plan" High-Level Health Talents Training Project, No. 2022CZBJ059 and 2022CZBJ061.

Conflict-of-interest statement: The authors have no conflicts of interest to declare.

Country/Territory of origin: China

ORCID number: Jun-Jie Zhang 0000-0003-1062-3407; Xin-Die Zhou 0000-0003-4948-0191.

S-Editor: Zhang H
L-Editor: Filipodia
P-Editor: Liu JH

REFERENCES

1 **Klöting N**, Blüher M. Adipocyte dysfunction, inflammation and metabolic syndrome. *Rev Endocr Metab Disord* 2014; **15**: 277-287 [PMID: 25344447 DOI: 10.1007/s11154-014-9301-0]
2 **Blüher M**. Adipose tissue dysfunction contributes to obesity related metabolic diseases. *Best Pract Res Clin Endocrinol Metab* 2013; **27**: 163-177 [PMID: 23731879 DOI: 10.1016/j.beem.2013.02.005]
3 **Fasshauer M**, Blüher M. Adipokines in health and disease. *Trends Pharmacol Sci* 2015; **36**: 461-470 [PMID: 26022934 DOI: 10.1016/j.tips.2015.04.014]
4 **Blüher M**. Adipokines – removing road blocks to obesity and diabetes therapy. *Mol Metab* 2014; **3**: 230-240 [PMID: 24749053 DOI: 10.1016/j.molmet.2014.01.005]
5 **Blüher M**, Mantzoros CS. From leptin to other adipokines in health and disease: facts and expectations at the beginning of the 21st century. *Metabolism* 2015; **64**: 131-145 [PMID: 25497344 DOI: 10.1016/j.metabol.2014.10.016]
6 **Chen Q**, Shou P, Zheng C, Jiang M, Cao G, Yang Q, Cao J, Xie N, Velletri T, Zhang X, Xu C, Zhang L, Yang H, Hou J, Wang Y, Shi Y. Fate decision of mesenchymal stem cells: adipocytes or osteoblasts? *Cell Death Differ* 2016; **23**: 1128-1139 [PMID: 26868907 DOI: 10.1038/cdd.2015.168]
7 **Zuk PA**, Zhu M, Ashjian P, De Ugarte DA, Huang JI, Mizuno H, Alfonso ZC, Fraser JK, Benhaim P, Hedrick MH. Human adipose tissue is a source of multipotent stem cells. *Mol Biol Cell* 2002; **13**: 4279-4295 [PMID: 12475952 DOI: 10.1091/mbc.e02-02-0105]
8 **Pittenger MF**, Mackay AM, Beck SC, Jaiswal RK, Douglas R, Mosca JD, Moorman MA, Simonetti DW, Craig S, Marshak DR. Multilineage potential of adult human mesenchymal stem cells. *Science* 1999; **284**: 143-147 [PMID: 10102814 DOI: 10.1126/science.284.5411.143]
9 **Li T**, Xia M, Gao Y, Chen Y, Xu Y. Human umbilical cord mesenchymal stem cells: an overview of their potential in cell-based therapy. *Expert Opin Biol Ther* 2015; **15**: 1293-1306 [PMID: 26067213 DOI: 10.1517/14712598.2015.1051528]
10 **Das M**, Mayilsamy K, Mohapatra SS, Mohapatra S. Mesenchymal stem cell therapy for the treatment of traumatic brain injury: progress and prospects. *Rev Neurosci* 2019; **30**: 839-855 [PMID: 31203262 DOI: 10.1515/revneuro-2019-0002]
11 **Li A**, Guo F, Pan Q, Chen S, Chen J, Liu HF. Mesenchymal Stem Cell Therapy: Hope for Patients With Systemic Lupus Erythematosus. *Front Immunol* 2021; **12**: 728190 [PMID: 34659214 DOI: 10.3389/fimmu.2021.728190]
12 **Ding DC**, Chang YH, Shyu WC, Lin SZ. Human umbilical cord mesenchymal stem cells: a new era for stem cell therapy. *Cell Transplant* 2015; **24**: 339-347 [PMID: 25622293 DOI: 10.3727/096368915X686841]
13 **Teitelbaum SL**. Bone resorption by osteoclasts. *Science* 2000; **289**: 1504-1508 [PMID: 10968780 DOI: 10.1126/science.289.5484.1504]
14 **Caplan AI**. Mesenchymal stem cells. *J Orthop Res* 1991; **9**: 641-650 [PMID: 1870029 DOI: 10.1002/jor.1100090504]

15 **Jiang Y**, Zhang P, Zhang X, Lv L, Zhou Y. Advances in mesenchymal stem cell transplantation for the treatment of osteoporosis. *Cell Prolif* 2021; **54**: e12956 [PMID: 33210341 DOI: 10.1111/cpr.12956]

16 **Akbar MA**, Lu Y, Elshikha AS, Chen MJ, Yuan Y, Whitley EM, Holliday LS, Chang LJ, Song S. Transplantation of Adipose Tissue-Derived Mesenchymal Stem Cell (ATMSC) Expressing Alpha-1 Antitrypsin Reduces Bone Loss in Ovariectomized Osteoporosis Mice. *Hum Gene Ther* 2017; **28**: 179-189 [PMID: 27802778 DOI: 10.1089/hum.2016.069]

17 **Loi F**, Córdova LA, Pajarinen J, Lin TH, Yao Z, Goodman SB. Inflammation, fracture and bone repair. *Bone* 2016; **86**: 119-130 [PMID: 26946132 DOI: 10.1016/j.bone.2016.02.020]

18 **Fu X**, Liu G, Halim A, Ju Y, Luo Q, Song AG. Mesenchymal Stem Cell Migration and Tissue Repair. *Cells* 2019; **8** [PMID: 31357692 DOI: 10.3390/cells8080784]

19 **Brown C**, McKee C, Bakshi S, Walker K, Hakman E, Halassy S, Svinarich D, Dodds R, Govind CK, Chaudhry GR. Mesenchymal stem cells: Cell therapy and regeneration potential. *J Tissue Eng Regen Med* 2019; **13**: 1738-1755 [PMID: 31216380 DOI: 10.1002/term.2914]

20 **Grayson WL**, Bunnell BA, Martin E, Frazier T, Hung BP, Gimble JM. Stromal cells and stem cells in clinical bone regeneration. *Nat Rev Endocrinol* 2015; **11**: 140-150 [PMID: 25560703 DOI: 10.1038/nrendo.2014.234]

21 **Liu L**, Shi Z, Ji X, Zhang W, Luan J, Zahr T, Qiang L. Adipokines, adiposity, and atherosclerosis. *Cell Mol Life Sci* 2022; **79**: 272 [PMID: 35503385 DOI: 10.1007/s00018-022-04286-2]

22 **Lacey DC**, Simmons PJ, Graves SE, Hamilton JA. Proinflammatory cytokines inhibit osteogenic differentiation from stem cells: implications for bone repair during inflammation. *Osteoarthritis Cartilage* 2009; **17**: 735-742 [PMID: 19136283 DOI: 10.1016/j.joca.2008.11.011]

23 **Majumdar MK**, Thiede MA, Haynesworth SE, Bruder SP, Gerson SL. Human marrow-derived mesenchymal stem cells (MSCs) express hematopoietic cytokines and support long-term hematopoiesis when differentiated toward stromal and osteogenic lineages. *J Hematother Stem Cell Res* 2000; **9**: 841-848 [PMID: 11177595 DOI: 10.1089/152581600750062264]

24 **Rezaee F**, Rellick SL, Piedimonte G, Akers SM, O'Leary HA, Martin K, Craig MD, Gibson LF. Neurotrophins regulate bone marrow stromal cell IL-6 expression through the MAPK pathway. *PloS One* 2010; **5**: e9690 [PMID: 20300619 DOI: 10.1371/journal.pone.0009690]

25 **Carmody EE**, Schwarz EM, Puzas JE, Rosier RN, O'Keefe RJ. Viral interleukin-10 gene inhibition of inflammation, osteoclastogenesis, and bone resorption in response to titanium particles. *Arthritis Rheum* 2002; **46**: 1298-1308 [PMID: 12115237 DOI: 10.1002/art.10227]

26 **Van Vlasselaer P**, Borremans B, Van Den Heuvel R, Van Gorp U, de Waal Malefyt R. Interleukin-10 inhibits the osteogenic activity of mouse bone marrow. *Blood* 1993; **82**: 2361-2370 [PMID: 8400287 DOI: 10.1182/blood.V82.8.2361.bloodjournal8282361]

27 **Krstić J**, Mojsilović S, Mojsilović SS, Santibanez JF. Regulation of the mesenchymal stem cell fate by interleukin-17: Implications in osteogenic differentiation. *World J Stem Cells* 2021; **13**: 1696-1713 [PMID: 34909118 DOI: 10.4252/wjsc.v13.i11.1696]

28 **Ling L**, Nurcombe V, Cool SM. Wnt signaling controls the fate of mesenchymal stem cells. *Gene* 2009; **433**: 1-7 [PMID: 19135507 DOI: 10.1016/j.gene.2008.12.008]

29 **Chang J**, Wang Z, Tang E, Fan Z, McCauley L, Franceschi R, Guan K, Krebsbach PH, Wang CY. Inhibition of osteoblastic bone formation by nuclear factor-kappaB. *Nat Med* 2009; **15**: 682-689 [PMID: 19448637 DOI: 10.1038/nm.1954]

30 **Wang M**, Crisostomo PR, Herring C, Meldrum KK, Meldrum DR. Human progenitor cells from bone marrow or adipose tissue produce VEGF, HGF, and IGF-I in response to TNF by a p38 MAPK-dependent mechanism. *Am J Physiol Regul Integr Comp Physiol* 2006; **291**: R880-R884 [PMID: 16728464 DOI: 10.1152/ajpregu.00280.2006]

31 **Deshmane SL**, Kremlev S, Amini S, Sawaya BE. Monocyte chemoattractant protein-1 (MCP-1): an overview. *J Interferon Cytokine Res* 2009; **29**: 313-326 [PMID: 19441883 DOI: 10.1089/jir.2008.0027]

32 **Xie Z**, Wang P, Li J, Li Y, Wang S, Wu X, Sun S, Cen S, Su H, Deng W, Liu Z, Ouyang Y, Wu Y, Shen H. MCP1 triggers monocyte dysfunctions during abnormal osteogenic differentiation of mesenchymal stem cells in ankylosing spondylitis. *J Mol Med (Berl)* 2017; **95**: 143-154 [PMID: 27921117 DOI: 10.1007/s00109-016-1489-x]

33 **Crane JL**, Cao X. Bone marrow mesenchymal stem cells and TGF-β signaling in bone remodeling. *J Clin Invest* 2014; **124**: 466-472 [PMID: 24487640 DOI: 10.1172/JCI70050]

34 **Li SN**, Wu JF. TGF-β/SMAD signaling regulation of mesenchymal stem cells in adipocyte commitment. *Stem Cell Res Ther* 2020; **11**: 41 [PMID: 31996252 DOI: 10.1186/s13287-020-1552-y]

35 **Tang Y**, Wu X, Lei W, Pang L, Wan C, Shi Z, Zhao L, Nagy TR, Peng X, Hu J, Feng X, Van Hul W, Wan M, Cao X. TGF-beta1-induced migration of bone mesenchymal stem cells couples bone resorption with formation. *Nat Med* 2009; **15**: 757-765 [PMID: 19584867 DOI: 10.1038/nm.1979]

36 **Zhou S**. TGF-β regulates β-catenin signaling and osteoblast differentiation in human mesenchymal stem cells. *J Cell Biochem* 2011; **112**: 1651-1660 [PMID: 21344492 DOI: 10.1002/jcb.23079]

37 **Jian H**, Shen X, Liu I, Semenov M, He X, Wang XF. Smad3-dependent nuclear translocation of beta-catenin is required for TGF-beta1-induced proliferation of bone marrow-derived adult human mesenchymal stem cells. *Genes Dev* 2006; **20**: 666-674 [PMID: 16543220 DOI: 10.1101/gad.1388806]

38 **Du G**, Cheng X, Zhang Z, Han L, Wu K, Li Y, Lin X. TGF-Beta Induced Key Genes of Osteogenic and Adipogenic Differentiation in Human Mesenchymal Stem Cells and MiRNA-mRNA Regulatory Networks. *Front Genet* 2021; **12**: 759596 [PMID: 34899844 DOI: 10.3389/fgene.2021.759596]

39 **Igarashi Y**, Chosa N, Sawada S, Kondo H, Yaegashi T, Ishisaki A. VEGF-C and TGF-β reciprocally regulate mesenchymal stem cell commitment to differentiation into lymphatic endothelial or osteoblastic phenotypes. *Int J Mol Med* 2016; **37**: 1005-1013 [PMID: 26934950 DOI: 10.3892/ijmm.2016.2502]

40 **Bozaoglu K**, Bolton K, McMillan J, Zimmet P, Jowett J, Collier G, Walder K, Segal D. Chemerin is a novel adipokine associated with obesity and metabolic syndrome. *Endocrinology* 2007; **148**: 4687-4694 [PMID: 17640997 DOI: 10.1210/en.2007-0175]

41 **Li J**, Zhang T, Huang C, Xu M, Xie W, Pei Q, Xie X, Wang B, Li X. Chemerin located in bone marrow promotes osteogenic differentiation and bone formation *via* Akt/Gsk3β/β-catenin axis in mice. *J Cell Physiol* 2021; **236**: 6042-6054 [PMID: 33492671 DOI: 10.1002/jcp.30290]

42 **Kadric L**, Zylla S, Nauck M, Völzke H, Friedrich N, Hannemann A. Associations Between Plasma Chemerin Concentrations and Bone Quality in Adults From the General Population. *Endocrinology* 2018; **159**: 2378-2385 [PMID: 29701774 DOI: 10.1210/en.2018-00157]

43 **Muruganandan S**, Roman AA, Sinal CJ. Role of chemerin/CMKLR1 signaling in adipogenesis and osteoblastogenesis of bone marrow stem cells. *J Bone Miner Res* 2010; **25**: 222-234 [PMID: 19929432 DOI: 10.1359/jbmr.091106]

44 **Kaji H**. Adipose Tissue-Derived Plasminogen Activator Inhibitor-1 Function and Regulation. *Compr Physiol* 2016; **6**: 1873-1896 [PMID: 27783862 DOI: 10.1002/cphy.c160004]

45 **Takafuji Y**, Tatsumi K, Ishida M, Kawao N, Okada K, Matsuo O, Kaji H. Plasminogen activator inhibitor-1 deficiency suppresses osteoblastic differentiation of mesenchymal stem cells in mice. *J Cell Physiol* 2019; **234**: 9687-9697 [PMID: 30387130 DOI: 10.1002/jcp.27655]

46 **Drake TA**, Morrissey JH, Edgington TS. Selective cellular expression of tissue factor in human tissues. Implications for disorders of hemostasis and thrombosis. *Am J Pathol* 1989; **134**: 1087-1097 [PMID: 2719077]

47 **Nitori N**, Ino Y, Nakanishi Y, Yamada T, Honda K, Yanagihara K, Kosuge T, Kanai Y, Kitajima M, Hirohashi S. Prognostic significance of tissue factor in pancreatic ductal adenocarcinoma. *Clin Cancer Res* 2005; **11**: 2531-2539 [PMID: 15814630 DOI: 10.1158/1078-0432.CCR-04-0866]

48 **Rangasami VK**, Nawale G, Asawa K, Kadekar S, Samanta S, Nilsson B, Ekdahl KN, Miettinen S, Hilborn J, Teramura Y, Varghese OP, Oommen OP. Pluronic Micelle-Mediated Tissue Factor Silencing Enhances Hemocompatibility, Stemness, Differentiation Potential, and Paracrine Signaling of Mesenchymal Stem Cells. *Biomacromolecules* 2021; **22**: 1980-1989 [PMID: 33813822 DOI: 10.1021/acs.biomac.1c00070]

49 **Cook KS**, Min HY, Johnson D, Chaplinsky RJ, Flier JS, Hunt CR, Spiegelman BM. Adipsin: a circulating serine protease homolog secreted by adipose tissue and sciatic nerve. *Science* 1987; **237**: 402-405 [PMID: 3299705 DOI: 10.1126/science.3299705]

50 **Rosen BS**, Cook KS, Yaglom J, Groves DL, Volanakis JE, Damm D, White T, Spiegelman BM. Adipsin and complement factor D activity: an immune-related defect in obesity. *Science* 1989; **244**: 1483-1487 [PMID: 2734615 DOI: 10.1126/science.2734615]

51 **Choy LN**, Rosen BS, Spiegelman BM. Adipsin and an endogenous pathway of complement from adipose cells. *J Biol Chem* 1992; **267**: 12736-12741 [PMID: 1618777 DOI: 10.1016/S0021-9258(18)42338-1]

52 **Gómez-Banoy N**, Guseh JS, Li G, Rubio-Navarro A, Chen T, Poirier B, Putzel G, Rosselot C, Pabón MA, Camporez JP, Bhambhani V, Hwang SJ, Yao C, Perry RJ, Mukherjee S, Larson MG, Levy D, Dow LE, Shulman GI, Dephoure N, Garcia-Ocana A, Hao M, Spiegelman BM, Ho JE, Lo JC. Adipsin preserves beta cells in diabetic mice and associates with protection from type 2 diabetes in humans. *Nat Med* 2019; **25**: 1739-1747 [PMID: 31700183 DOI: 10.1038/s41591-019-0610-4]

53 **Aaron N**, Kraakman MJ, Zhou Q, Liu Q, Costa S, Yang J, Liu L, Yu L, Wang L, He Y, Fan L, Hirakawa H, Ding L, Lo J, Wang W, Zhao B, Guo E, Sun L, Rosen CJ, Qiang L. Adipsin promotes bone marrow adiposity by priming mesenchymal stem cells. *Elife* 2021; **10** [PMID: 34155972 DOI: 10.7554/eLife.69209]

54 **Bienertova-Vasku J**, Vinciguerra M, Buzga M, Villaroya F. Adipokines as Biomarkers in Health and Disease. *Dis Markers* 2018; **2018**: 5696815 [PMID: 30402169 DOI: 10.1155/2018/5696815]

55 **Reid IR**, Baldock PA, Cornish J. Effects of Leptin on the Skeleton. *Endocr Rev* 2018; **39**: 938-959 [PMID: 30184053 DOI: 10.1210/er.2017-00226]

56 **Park HK**, Ahima RS. Leptin signaling. *F1000Prime Rep* 2014; **6**: 73 [PMID: 25343030 DOI: 10.12703/P6-73]

57 **Yue R**, Zhou BO, Shimada IS, Zhao Z, Morrison SJ. Leptin Receptor Promotes Adipogenesis and Reduces Osteogenesis by Regulating Mesenchymal Stromal Cells in Adult Bone Marrow. *Cell Stem Cell* 2016; **18**: 782-796 [PMID: 27053299 DOI: 10.1016/j.stem.2016.02.015]

58 **Kelesidis T**, Kelesidis I, Chou S, Mantzoros CS. Narrative review: the role of leptin in human physiology: emerging clinical applications. *Ann Intern Med* 2010; **152**: 93-100 [PMID: 20083828 DOI: 10.7326/0003-4819-152-2-201001190-00008]

59 **Zhou BO**, Yue R, Murphy MM, Peyer JG, Morrison SJ. Leptin-receptor-expressing mesenchymal stromal cells represent the main source of bone formed by adult bone marrow. *Cell Stem Cell* 2014; **15**: 154-168 [PMID: 24953181 DOI: 10.1016/j.stem.2014.06.008]

60 **Zhang B**, Yang L, Zeng Z, Feng Y, Wang X, Wu X, Luo H, Zhang J, Zhang M, Pakvasa M, Wagstaff W, He F, Mao Y, Qin K, Ding H, Zhang Y, Niu C, Wu M, Zhao X, Wang H, Huang L, Shi D, Liu Q, Ni N, Fu K, Athiviraham A, Moriatis Wolf J, Lee MJ, Hynes K, Strelzow J, El Dafrawy M, Xia Y, He TC. Leptin Potentiates BMP9-Induced Osteogenic Differentiation of Mesenchymal Stem Cells Through the Activation of JAK/STAT Signaling. *Stem Cells Dev* 2020; **29**: 498-510 [PMID: 32041483 DOI: 10.1089/scd.2019.0292]

61 **Berg AH**, Combs TP, Du X, Brownlee M, Scherer PE. The adipocyte-secreted protein Acrp30 enhances hepatic insulin action. *Nat Med* 2001; **7**: 947-953 [PMID: 11479628 DOI: 10.1038/90992]

62 **Padmalayam I**, Suto M. Role of adiponectin in the metabolic syndrome: current perspectives on its modulation as a treatment strategy. *Curr Pharm Des* 2013; **19**: 5755-5763 [PMID: 23448486 DOI: 10.2174/13816128113199990360]

63 **Wang Y**, Zhang X, Shao J, Liu H, Liu X, Luo E. Adiponectin regulates BMSC osteogenic differentiation and osteogenesis through the Wnt/β-catenin pathway. *Sci Rep* 2017; **7**: 3652 [PMID: 28623357 DOI: 10.1038/s41598-017-03899-z]

64 **Chen T**, Wu YW, Lu H, Guo Y, Tang ZH. Adiponectin enhances osteogenic differentiation in human adipose-derived stem cells by activating the APPL1-AMPK signaling pathway. *Biochem Biophys Res Commun* 2015; **461**: 237-242 [PMID: 25892517 DOI: 10.1016/j.bbrc.2015.03.168]

65 **Pu Y**, Wu H, Lu S, Hu H, Li D, Wu Y, Tang Z. Adiponectin Promotes Human Jaw Bone Marrow Stem Cell Osteogenesis. *J Dent Res* 2016; **95**: 769-775 [PMID: 26961489 DOI: 10.1177/0022034516636853]

66 **Wang Y**, Du Y, Yuan H, Pan Y, Wu J, Du X, Hao S, Yan Z, Li X, Liu K, Xu F. Human amnion-derived mesenchymal stem cells enhance the osteogenic differentiation of human adipose-derived stem cells by promoting adiponectin excretion *via* the APPL1-ERK1/2 signaling pathway. *IUBMB Life* 2020; **72**: 296-304 [PMID: 31509344 DOI: 10.1002/iub.2165]

67 **Li Y**, He J, He X, Li Y, Lindgren U. Nampt expression increases during osteogenic differentiation of multi- and omnipotent progenitors. *Biochem Biophys Res Commun* 2013; **434**: 117-123 [PMID: 23537654 DOI: 10.1016/j.bbrc.2013.02.132]

68 **Otero M**, Lago R, Gomez R, Lago F, Dieguez C, Gómez-Reino JJ, Gualillo O. Changes in plasma levels of fat-derived hormones adiponectin, leptin, resistin and visfatin in patients with rheumatoid arthritis. *Ann Rheum Dis* 2006; **65**: 1198-1201 [PMID: 16414972 DOI: 10.1136/ard.2005.046540]

69 **Tsiklauri L**, Werner J, Kampschulte M, Frommer KW, Berninger L, Irrgang M, Glenske K, Hose D, El Khassawna T, Pons-Kühnemann J, Rehart S, Wenisch S, Müller-Ladner U, Neumann E. Visfatin alters the cytokine and matrix-degrading enzyme profile during osteogenic and adipogenic MSC differentiation. *Osteoarthritis Cartilage* 2018; **26**: 1225-1235 [PMID: 29908226 DOI: 10.1016/j.joca.2018.06.001]

70 **Braidy N**, Berg J, Clement J, Khorshidi F, Poljak A, Jayasena T, Grant R, Sachdev P. Role of Nicotinamide Adenine Dinucleotide and Related Precursors as Therapeutic Targets for Age-Related Degenerative Diseases: Rationale, Biochemistry, Pharmacokinetics, and Outcomes. *Antioxid Redox Signal* 2019; **30**: 251-294 [PMID: 29634344 DOI: 10.1089/ars.2017.7269]

71 **Sommer G**, Garten A, Petzold S, Beck-Sickinger AG, Blüher M, Stumvoll M, Fasshauer M. Visfatin/PBEF/Nampt: structure, regulation and potential function of a novel adipokine. *Clin Sci (Lond)* 2008; **115**: 13-23 [PMID: 19016657 DOI: 10.1042/CS20070226]

72 **He X**, He J, Shi Y, Pi C, Yang Y, Sun Y, Ma C, Lin L, Zhang L, Li Y. Nicotinamide phosphoribosyltransferase (Nampt) may serve as the marker for osteoblast differentiation of bone marrow-derived mesenchymal stem cells. *Exp Cell Res* 2017; **352**: 45-52 [PMID: 28159473 DOI: 10.1016/j.yexcr.2017.01.021]

73 **Liu Y**, Xu F, Pei HX, Zhu X, Lin X, Song CY, Liang QH, Liao EY, Yuan LQ. Vaspin regulates the osteogenic differentiation of MC3T3-E1 through the PI3K-Akt/miR-34c loop. *Sci Rep* 2016; **6**: 25578 [PMID: 27156573 DOI: 10.1038/srep25578]

74 **Wang H**, Chen F, Li J, Wang Y, Jiang C, Zhang M, Xu J. Vaspin antagonizes high fat-induced bone loss in rats and promotes osteoblastic differentiation in primary rat osteoblasts through Smad-Runx2 signaling pathway. *Nutr Metab (Lond)* 2020; **17**: 9 [PMID: 31993071 DOI: 10.1186/s12986-020-0429-5]

75 **Schulz TJ**, Huang P, Huang TL, Xue R, McDougall LE, Townsend KL, Cypess AM, Mishina Y, Gussoni E, Tseng YH. Brown-fat paucity due to impaired BMP signalling induces compensatory browning of white fat. *Nature* 2013; **495**: 379-383 [PMID: 23485971 DOI: 10.1038/nature11943]

76 **Schulz TJ**, Tseng YH. Emerging role of bone morphogenetic proteins in adipogenesis and energy metabolism. *Cytokine Growth Factor Rev* 2009; **20**: 523-531 [PMID: 19896888 DOI: 10.1016/j.cytogfr.2009.10.019]

77 **Huang Z**, Ren PG, Ma T, Smith RL, Goodman SB. Modulating osteogenesis of mesenchymal stem cells by modifying growth factor availability. *Cytokine* 2010; **51**: 305-310 [PMID: 20580248 DOI: 10.1016/j.cyto.2010.06.002]

78 **Gu K**, Zhang L, Jin T, Rutherford RB. Identification of potential modifiers of Runx2/Cbfa1 activity in C2C12 cells in response to bone morphogenetic protein-7. *Cells Tissues Organs* 2004; **176**: 28-40 [PMID: 14745233 DOI: 10.1159/000075025]

79 **Tsuji K**, Cox K, Bandyopadhyay A, Harfe BD, Tabin CJ, Rosen V. BMP4 is dispensable for skeletogenesis and fracture-healing in the limb. *J Bone Joint Surg Am* 2008; **90** Suppl 1: 14-18 [PMID: 18292351 DOI: 10.2106/JBJS.G.01109]

80 **Kokabu S**, Gamer L, Cox K, Lowery J, Tsuji K, Raz R, Economides A, Katagiri T, Rosen V. BMP3 suppresses osteoblast differentiation of bone marrow stromal cells *via* interaction with Acvr2b. *Mol Endocrinol* 2012; **26**: 87-94 [PMID: 22074949 DOI: 10.1210/me.2011-1168]

81 **Vaccaro AR**, Whang PG, Patel T, Phillips FM, Anderson DG, Albert TJ, Hilibrand AS, Brower RS, Kurd MF, Appannagari A, Patel M, Fischgrund JS. The safety and efficacy of OP-1 (rhBMP-7) as a replacement for iliac crest autograft for posterolateral lumbar arthrodesis: minimum 4-year follow-up of a pilot study. *Spine J* 2008; **8**: 457-465 [PMID: 17588821 DOI: 10.1016/j.spinee.2007.03.012]

82 **Rivera JC**, Strohbach CA, Wenke JC, Rathbone CR. Beyond osteogenesis: an in vitro comparison of the potentials of six bone morphogenetic proteins. *Front Pharmacol* 2013; **4**: 125 [PMID: 24101902 DOI: 10.3389/fphar.2013.00125]

83 **Tiaden AN**, Breiden M, Mirsaidi A, Weber FA, Bahrenberg G, Glanz S, Cinelli P, Ehrmann M, Richards PJ. Human serine protease HTRA1 positively regulates osteogenesis of human bone marrow-derived mesenchymal stem cells and mineralization of differentiating bone-forming cells through the modulation of extracellular matrix protein. *Stem Cells* 2012; **30**: 2271-2282 [PMID: 22865667 DOI: 10.1002/stem.1190]

84 **Zachos TA**, Shields KM, Bertone AL. Gene-mediated osteogenic differentiation of stem cells by bone morphogenetic proteins-2 or -6. *J Orthop Res* 2006; **24**: 1279-1291 [PMID: 16649180 DOI: 10.1002/jor.20068]

85 **Friedman MS**, Long MW, Hankenson KD. Osteogenic differentiation of human mesenchymal stem cells is regulated by bone morphogenetic protein-6. *J Cell Biochem* 2006; **98**: 538-554 [PMID: 16317727 DOI: 10.1002/jcb.20719]

86 **Goebel-Stengel M**, Stengel A. Role of Brain NUCB2/nesfatin-1 in the Stress-induced Modulation of Gastrointestinal Functions. *Curr Neuropharmacol* 2016; **14**: 882-891 [PMID: 27281021 DOI: 10.2174/1570159X14666160601153202]

87 **Levata L**, Dore R, Jöhren O, Schwaninger M, Schulz C, Lehnert H. Nesfatin-1 Acts Centrally to Induce Sympathetic Activation of Brown Adipose Tissue and Non-Shivering Thermogenesis. *Horm Metab Res* 2019; **51**: 678-685 [PMID: 31487748 DOI: 10.1055/a-0985-4272]

88 **Ranjan A**, Choubey M, Yada T, Krishna A. Nesfatin-1 ameliorates type-2 diabetes-associated reproductive dysfunction in male mice. *J Endocrinol Invest* 2020; **43**: 515-528 [PMID: 31691259 DOI: 10.1007/s40618-019-01136-0]

89 **Xu K**, Zhang Z, Chen M, Moqbel SAA, He Y, Ma C, Jiang L, Xiong Y, Wu L. Nesfatin-1 Promotes the Osteogenic Differentiation of Tendon-Derived Stem Cells and the Pathogenesis of Heterotopic Ossification in Rat Tendons *via* the mTOR Pathway. *Front Cell Dev Biol* 2020; **8**: 547342 [PMID: 33344440 DOI: 10.3389/fcell.2020.547342]

90 **Lecaille F**, Chazeirat T, Saidi A, Lalmanach G. Cathepsin V: Molecular characteristics and significance in health and disease. *Mol Aspects Med* 2022; **88**: 101086 [PMID: 35305807 DOI: 10.1016/j.mam.2022.101086]

91 **Fain JN**. Release of interleukins and other inflammatory cytokines by human adipose tissue is enhanced in obesity and primarily due to the nonfat cells. *Vitam Horm* 2006; **74**: 443-477 [PMID: 17027526 DOI: 10.1016/S0083-6729(06)74018-3]

92 **Liu F**, Zhou ZF, An Y, Yu Y, Wu RX, Yin Y, Xue Y, Chen FM. Effects of cathepsin K on Emdogain-induced hard tissue formation by human periodontal ligament stem cells. *J Tissue Eng Regen Med* 2017; **11**: 2922-2934 [PMID: 27401615 DOI: 10.1002/term.2195]

93 **Whitty C**, Wardale RJ, Henson FMD. The regulation of sclerostin by cathepsin K in periodontal ligament cells. *Biochem Biophys Res Commun* 2018; **503**: 550-555 [PMID: 29859187 DOI: 10.1016/j.bbrc.2018.05.160]

94 **Zhang W**, Dong Z, Li D, Li B, Liu Y, Zheng X, Liu H, Zhou H, Hu K, Xue Y. Cathepsin K deficiency promotes alveolar bone regeneration by promoting jaw bone marrow mesenchymal stem cells proliferation and differentiation *via* glycolysis pathway. *Cell Prolif* 2021; **54**: e13058 [PMID: 34053135 DOI: 10.1111/cpr.13058]

95 **Rauner M**, Föger-Samwald U, Kurz MF, Brünner-Kubath C, Schamall D, Kapfenberger A, Varga P, Kudlacek S, Wutzl A, Höger H, Zysset PK, Shi GP, Hofbauer LC, Sipos W, Pietschmann P. Cathepsin S controls adipocytic and osteoblastic differentiation, bone turnover, and bone microarchitecture. *Bone* 2014; **64**: 281-287 [PMID: 24780878 DOI: 10.1016/j.bone.2014.04.022]

96 **Fasshauer M**, Blüher M, Stumvoll M. Adipokines in gestational diabetes. *Lancet Diabetes Endocrinol* 2014; **2**: 488-499 [PMID: 24731659 DOI: 10.1016/S2213-8587(13)70176-1]

97 **Castan-Laurell I**, Dray C, Attané C, Duparc T, Knauf C, Valet P. Apelin, diabetes, and obesity. *Endocrine* 2011; **40**: 1-9 [PMID: 21725702 DOI: 10.1007/s12020-011-9507-9]

98 **Hang K**, Ye C, Xu J, Chen E, Wang C, Zhang W, Ni L, Kuang Z, Ying L, Xue D, Pan Z. Apelin enhances the osteogenic differentiation of human bone marrow mesenchymal stem cells partly through Wnt/β-catenin signaling pathway. *Stem Cell Res Ther* 2019; **10**: 189 [PMID: 31238979 DOI: 10.1186/s13287-019-1286-x]

99 **Yang RZ**, Lee MJ, Hu H, Pray J, Wu HB, Hansen BC, Shuldiner AR, Fried SK, McLenithan JC, Gong DW. Identification of omentin as a novel depot-specific adipokine in human adipose tissue: possible role in modulating insulin action. *Am J Physiol Endocrinol Metab* 2006; **290**: E1253-E1261 [PMID: 16531507 DOI: 10.1152/ajpendo.00572.2004]

100 **Yamawaki H**, Tsubaki N, Mukohda M, Okada M, Hara Y. Omentin, a novel adipokine, induces vasodilation in rat isolated blood vessels. *Biochem Biophys Res Commun* 2010; **393**: 668-672 [PMID: 20170632 DOI: 10.1016/j.bbrc.2010.02.053]

101 **Tohidi M**, Akbarzadeh S, Larijani B, Kalantarhormozi M, Ostovar A, Assadi M, Vahdat K, Farrokhnia M, Sanjdideh Z, Amirinejad R, Nabipour I. Omentin-1, visfatin and adiponectin levels in relation to bone mineral density in Iranian postmenopausal women. *Bone* 2012; **51**: 876-881 [PMID: 22971441 DOI: 10.1016/j.bone.2012.08.117]

102 **Tang C**, Liang D, Qiu Y, Zhu J, Tang G. Omentin1 induces osteoblast viability and differentiation *via* the TGFβ/Smad signaling pathway in osteoporosis. *Mol Med Rep* 2022; **25** [PMID: 35179221 DOI: 10.3892/mmr.2022.12648]

103 **Yan QW**, Yang Q, Mody N, Graham TE, Hsu CH, Xu Z, Houstis NE, Kahn BB, Rosen ED. The adipokine lipocalin 2 is regulated by obesity and promotes insulin resistance. *Diabetes* 2007; **56**: 2533-2540 [PMID: 17639021 DOI: 10.2337/db07-0007]

104 **Jung M**, Weigert A, Mertens C, Rehwald C, Brüne B. Iron Handling in Tumor-Associated Macrophages-Is There a New Role for Lipocalin-2? *Front Immunol* 2017; **8**: 1171 [PMID: 28979267 DOI: 10.3389/fimmu.2017.01171]

105 **Kim HJ**, Yoon HJ, Yoon KA, Gwon MR, Jin Seong S, Suk K, Kim SY, Yoon YR. Lipocalin-2 inhibits osteoclast formation by suppressing the proliferation and differentiation of osteoclast lineage cells. *Exp Cell Res* 2015; **334**: 301-309 [PMID: 25814363 DOI: 10.1016/j.yexcr.2015.03.008]

106 **Yin C**, Jia X, Zhao Q, Zhao Z, Wang J, Zhang Y, Li Z, Sun H. Transcription factor 7-like 2 promotes osteogenic differentiation and boron-induced bone repair *via* lipocalin 2. *Mater Sci Eng C Mater Biol Appl* 2020; **110**: 110671 [PMID: 32204099 DOI: 10.1016/j.msec.2020.110671]

107 **Luchetti F**, Canonico B, Bartolini D, Arcangeletti M, Ciffolilli S, Murdolo G, Piroddi M, Papa S, Reiter RJ, Galli F. Melatonin regulates mesenchymal stem cell differentiation: a review. *J Pineal Res* 2014; **56**: 382-397 [PMID: 24650016 DOI: 10.1111/jpi.12133]

108 **Cardinali DP**, Srinivasan V, Brzezinski A, Brown GM. Melatonin and its analogs in insomnia and depression. *J Pineal Res* 2012; **52**: 365-375 [PMID: 21951153 DOI: 10.1111/j.1600-079X.2011.00962.x]

109 **Rodriguez-Garcia A**, Mayo JC, Hevia D, Quiros-Gonzalez I, Navarro M, Sainz RM. Phenotypic changes caused by melatonin increased sensitivity of prostate cancer cells to cytokine-induced apoptosis. *J Pineal Res* 2013; **54**: 33-45 [PMID: 22738066 DOI: 10.1111/j.1600-079X.2012.01017.x]

110 **Murdolo G**, Piroddi M, Luchetti F, Tortoioli C, Canonico B, Zerbinati C, Galli F, Iuliano L. Oxidative stress and lipid peroxidation by-products at the crossroad between adipose organ dysregulation and obesity-linked insulin resistance. *Biochimie* 2013; **95**: 585-594 [PMID: 23274128 DOI: 10.1016/j.biochi.2012.12.014]

111 **Zhang L**, Zhang J, Ling Y, Chen C, Liang A, Peng Y, Chang H, Su P, Huang D. Sustained release of melatonin from poly (lactic-co-glycolic acid) (PLGA) microspheres to induce osteogenesis of human mesenchymal stem cells in vitro. *J Pineal Res* 2013; **54**: 24-32 [PMID: 22712496 DOI: 10.1111/j.1600-079X.2012.01016.x]

112 **Topol LZ**, Bardot B, Zhang Q, Resau J, Huillard E, Marx M, Calothy G, Blair DG. Biosynthesis, post-translation modification, and functional characterization of Drm/Gremlin. *J Biol Chem* 2000; **275**: 8785-8793 [PMID: 10722723 DOI: 10.1074/jbc.275.12.8785]

113 **Grillo E**, Ravelli C, Colleluori G, D'Agostino F, Domenichini M, Giordano A, Mitola S. Role of gremlin-1 in the pathophysiology of the adipose tissues. *Cytokine Growth Factor Rev* 2023; **69**: 51-60 [PMID: 36155165 DOI: 10.1016/j.cytogfr.2022.09.004]

114 **Gazzerro E**, Smerdel-Ramoya A, Zanotti S, Stadmeyer L, Durant D, Economides AN, Canalis E. Conditional deletion of gremlin causes a transient increase in bone formation and bone mass. *J Biol Chem* 2007; **282**: 31549-31557 [PMID: 17785465 DOI: 10.1074/jbc.M701317200]

115 **Hu K**, Sun H, Gui B, Sui C. Gremlin-1 suppression increases BMP-2-induced osteogenesis of human mesenchymal stem cells. *Mol Med Rep* 2017; **15**: 2186-2194 [PMID: 28260028 DOI: 10.3892/mmr.2017.6253]

116 **Shore VG**, Shore B. Heterogeneity of human plasma very low density lipoproteins. Separation of species differing in protein components. *Biochemistry* 1973; **12**: 502-507 [PMID: 4345806 DOI: 10.1021/bi00727a022]

117 **Marais AD**. Apolipoprotein E and Atherosclerosis. *Curr Atheroscler Rep* 2021; **23**: 34 [PMID: 33970359 DOI: 10.1007/s11883-021-00933-4]

118 **Marais AD**. Apolipoprotein E in lipoprotein metabolism, health and cardiovascular disease. *Pathology* 2019; **51**: 165-176 [PMID: 30598326 DOI: 10.1016/j.pathol.2018.11.002]

119 **Huang Y**, Mahley RW. Apolipoprotein E: structure and function in lipid metabolism, neurobiology, and Alzheimer's diseases. *Neurobiol Dis* 2014; **72** Pt A: 3-12 [PMID: 25173806 DOI: 10.1016/j.nbd.2014.08.025]

120 **Bächner D**, Schröder D, Betat N, Ahrens M, Gross G. Apolipoprotein E (ApoE), a Bmp-2 (bone morphogenetic protein) upregulated gene in mesenchymal progenitors (C3H10T1/2), is highly expressed in murine embryonic development. *Biofactors* 1999; **9**: 11-17 [PMID: 10221153 DOI: 10.1002/biof.5520090103]

121 **Lamers D**, Famulla S, Wronkowitz N, Hartwig S, Lehr S, Ouwens DM, Eckardt K, Kaufman JM, Ryden M, Müller S, Hanisch FG, Ruige J, Arner P, Sell H, Eckel J. Dipeptidyl peptidase 4 is a novel adipokine potentially linking obesity to the metabolic syndrome. *Diabetes* 2011; **60**: 1917-1925 [PMID: 21593202 DOI: 10.2337/db10-1707]

122 **Choi B**, Lee S, Kim SM, Lee EJ, Lee SR, Kim DH, Jang JY, Kang SW, Lee KU, Chang EJ, Song JK. Dipeptidyl Peptidase-4 Induces Aortic Valve Calcification by Inhibiting Insulin-Like Growth Factor-1 Signaling in Valvular Interstitial Cells. *Circulation* 2017; **135**: 1935-1950 [PMID: 28179397 DOI: 10.1161/CIRCULATIONAHA.116.024270]

123 **Lambert E**, Dassé E, Haye B, Petitfrère E. TIMPs as multifacial proteins. *Crit Rev Oncol Hematol* 2004; **49**: 187-198 [PMID: 15036259 DOI: 10.1016/j.critrevonc.2003.09.008]

124 **Lu P**, Takai K, Weaver VM, Werb Z. Extracellular matrix degradation and remodeling in development and disease. *Cold Spring Harb Perspect Biol* 2011; **3** [PMID: 21917992 DOI: 10.1101/cshperspect.a005058]

125 **Arpino V**, Brock M, Gill SE. The role of TIMPs in regulation of extracellular matrix proteolysis. *Matrix Biol* 2015; **44-46**: 247-254 [PMID: 25805621 DOI: 10.1016/j.matbio.2015.03.005]

126 **Jackson HW**, Defamie V, Waterhouse P, Khokha R. TIMPs: versatile extracellular regulators in cancer. *Nat Rev Cancer* 2017; **17**: 38-53 [PMID: 27932800 DOI: 10.1038/nrc.2016.115]

127 **Egea V**, Zahler S, Rieth N, Neth P, Popp T, Kehe K, Jochum M, Ries C. Tissue inhibitor of metalloproteinase-1 (TIMP-1) regulates mesenchymal stem cells through let-7f microRNA and Wnt/β-catenin signaling. *Proc Natl Acad Sci U S A* 2012; **109**: E309-E316 [PMID: 22223664 DOI: 10.1073/pnas.1115083109]

128 **Liang T**, Gao W, Zhu L, Ren J, Yao H, Wang K, Shi D. TIMP-1 inhibits proliferation and osteogenic differentiation of hBMSCs through Wnt/β-catenin signaling. *Biosci Rep* 2019; **39** [PMID: 30473539 DOI: 10.1042/BSR20181290]

129 **Jiang C**, Xia W, Wu T, Pan C, Shan H, Wang F, Zhou Z, Yu X. Inhibition of microRNA-222 up-regulates TIMP3 to promotes osteogenic differentiation of MSCs from fracture rats with type 2 diabetes mellitus. *J Cell Mol Med* 2020; **24**: 686-694 [PMID: 31691506 DOI: 10.1111/jcmm.14777]

130 **Lehr S**, Hartwig S, Sell H. Adipokines: a treasure trove for the discovery of biomarkers for metabolic disorders. *Proteomics Clin Appl* 2012; **6**: 91-101 [PMID: 22213627 DOI: 10.1002/prca.201100052]

131 **Kra G**, Daddam JR, Moallem U, Kamer H, Kočvarová R, Nemirovski A, Contreras GA, Tam J, Zachut M. Effects of omega-3

supplementation on components of the endocannabinoid system and metabolic and inflammatory responses in adipose and liver of peripartum dairy cows. *J Anim Sci Biotechnol* 2022; **13**: 114 [PMID: 36183098 DOI: 10.1186/s40104-022-00761-9]

132 **Cruz-López EO**, Uijl E, Danser AHJ. Perivascular Adipose Tissue in Vascular Function: Does Locally Synthesized Angiotensinogen Play a Role? *J Cardiovasc Pharmacol* 2021; **78**: S53-S62 [PMID: 34840262 DOI: 10.1097/FJC.0000000000001027]

World Journal of Stem Cells

Submit a Manuscript: https://www.f6publishing.com

World J Stem Cells 2023 June 26; 15(6): 514-529

DOI: 10.4252/wjsc.v15.i6.514

ISSN 1948-0210 (online)

REVIEW

Advances of nanotechnology applied to cancer stem cells

Miao Yue, Ting Guo, Deng-Yun Nie, Yin-Xing Zhu, Mei Lin

Specialty type: Cell biology

Provenance and peer review: Unsolicited article; Externally peer reviewed.

Peer-review model: Single blind

Peer-review report's scientific quality classification

Grade A (Excellent): 0
Grade B (Very good): 0
Grade C (Good): C, C, C
Grade D (Fair): 0
Grade E (Poor): 0

P-Reviewer: Kanaoujiya R, India; Nath L, India

Received: December 28, 2022
Peer-review started: December 28, 2022
First decision: February 14, 2023
Revised: March 1, 2023
Accepted: April 18, 2023
Article in press: April 18, 2023
Published online: June 26, 2023

Miao Yue, Deng-Yun Nie, Clinical Laboratory, Nanjing University of Chinese Medicine, Taizhou 225300, Jiangsu Province, China

Ting Guo, Yin-Xing Zhu, Mei Lin, Taizhou School of Clinical Medicine, The Affiliated Taizhou People's Hospital of Nanjing Medical University, Taizhou 225300, Jiangsu Province, China

Corresponding author: Mei Lin, MD, PhD, Senior Scientist, Taizhou School of Clinical Medicine, The Affiliated Taizhou People's Hospital of Nanjing Medical University, No. 366 Taihu Road, Taizhou 225300, Jiangsu Province, China. l_mei@163.com

Abstract

Cancer stem cells (CSCs) are a small proportion of the cells that exist in cancer tissues. They are considered to be the culprit of tumor genesis, development, drug resistance, metastasis and recurrence because of their self-renewal, proliferation, and differentiation potential. The elimination of CSCs is thus the key to cure cancer, and targeting CSCs provides a new method for tumor treatment. Due to the advantages of controlled sustained release, targeting and high biocompatibility, a variety of nanomaterials are used in the diagnosis and treatments targeting CSCs and promote the recognition and removal of tumor cells and CSCs. This article mainly reviews the research progress of nanotechnology in sorting CSCs and nanodrug delivery systems targeting CSCs. Furthermore, we identify the problems and future research directions of nanotechnology in CSC therapy. We hope that this review will provide guidance for the design of nanotechnology as a drug carrier so that it can be used in clinic for cancer therapy as soon as possible.

Key Words: Cancer stem cells; Nanotechnology; Nanoparticles; Nanodrug delivery systems; Drug resistance; Therapy

Core Tip: Cancer stem cells (CSCs) have the potential to self-renew, proliferate, and differentiate. CSCs play a key role in the occurrence, development, recurrence, and metastasis of tumors. Due to the good compatibility and biodegradability of nanomaterials, they are applied to target CSCs for drug delivery, photothermal therapy, and magnetic hyperthermia to treat cancer.

Citation: Yue M, Guo T, Nie DY, Zhu YX, Lin M. Advances of nanotechnology applied to cancer stem cells. *World J Stem Cells* 2023; 15(6): 514-529
URL: https://www.wjgnet.com/1948-0210/full/v15/i6/514.htm
DOI: https://dx.doi.org/10.4252/wjsc.v15.i6.514

INTRODUCTION

Cancer is a major threat to people's health and life worldwide[1]. One of every eight deaths is caused by cancer[2,3]. Current cancer treatments mainly include surgical intervention, radiation therapy, and chemotherapy, which often kill healthy cells and are harmful to patients. Therefore, researchers are seeking better ways to eliminate cancer cells, with less side effects. Some researchers are working on the use of various macrocyclic ligands for cancer therapy, making ruthenium an ideal choice over other transition metals due to its special chemical properties[4]. However, what plagues most cancer treatments is the presence of a small number of cancer stem cells (CSCs) in tumor tissues[5,6], which have the potential for self-renewal, unlimited proliferative capacity, and multidirectional differentiation[5,7]. These cells are in the G0 phase and hypoxic microenvironment and play a key role in tumorigenesis, progression, recurrence, and metastasis. The presence of CSCs in solid tumors such as breast cancer (BC)[8,9], human leukemia[10,11], colorectal cancer[12,13], glioblastoma multiforme (GBM)[14], and ovarian cancer[15] has been reported, and it has been confirmed that CSCs play an important role in the development of tumors.

CSCs have inherent properties such as phenotypic plasticity, drug efflux transporters, overexpression of antiapoptotic proteins, an efficient DNA repair system and a persistent stemness profile that make them resistant to conventional therapies such as chemotherapy and radiation[16-18]. In general, CSC resistance mainly occur through stem cell pathways including the hedgehog[19,20], Notch[21,22], Wnt/β-linked protein[23,24], Nanog[25,26], nuclear factor kappa B (NF-*k*B)[27], and epidermal growth factor receptor pathways[28]. They express ATP-binding cassette (ABC) transporter proteins that can abrogate potential drug damage. CSCs also activate DNA repair capacity within tumor cells and are resistant to cell death[29], which helps to prevent the recruitment of apoptotic factors[5,30]. Therefore, the development of effective anticancer strategies to specifically kill tumor cells and tumor stem cells will be central to cancer therapy.

In recent years, the popularity of nanotechnology has promoted the development of nanodrug delivery systems (NDDS), and various nanodrug carriers have been applied to the treatment of tumors. Due to their small size, biocompatibility, and biodegradability, nanoparticles (NPs) help to fully exploit the function of NDDSs as drug delivery systems/drug carriers, including as imaging agents and for photothermal therapy (PTT), recognition, and drug and gene delivery [31]. As the carrier of active drugs in the drug delivery model, NDDSs can ensure the specific release of active drugs in the patient's body, improve drug solubility and bioavailability and prolong maintenance to improve drug efficacy[32]. Nanocarriers offer remarkable specificity in targeted delivery through active and passive targeting mechanisms (Figure 1) [33,34]. In active targeting, NPs are conjugated to antibodies, peptides, aptamers, and other small molecules[34]. Drug delivery using NP targeting reduces toxicity in healthy cells, prevents drug degradation, and has the advantages of better specificity, biocompatibility, less cytotoxicity, extended half-lives, controlled drug release, and high drug loading capacity for NP-based cancer treatments compared to traditional chemo-cancer treatments[35]. In passive targeting, enhanced permeability and retention (EPR) effects result in NPs circulating slowly in the tumor microenvironment and being more concentrated there than in healthy tissue[36]. Some commonly used nanocarriers (Figure 2) include lipid and micelle-based NPs, polymer/non-polymer NPs, nanobinding, carbon nanotubes (CNTs), graphene oxide (GO), nanocapsules, dendritic macromolecules, polymer micelles, and quantum dots (QDs), which are used to enhance the effectiveness of therapeutic interventions by delivering nontoxic large payloads[37-39]. Recent advances in nanotherapeutics have led to the development and exploration of various nanomaterial carriers for efficient drug/therapeutic delivery.

CSCs have been identified as playing a central role in the setbacks currently faced in clinical trials and research. Therefore, designing a system that can target them at the cellular and system levels is the most promising avenue in the evolution of therapeutic design. By reviewing the application of nanotechnology in CSCs, we hope to provide guidance for the design and in-depth study of nanotechnology drug carriers so that they can be applied in clinic to treat cancer.

NANOTECHNOLOGY FOR CSC SORTING

To better understand the molecular basis of the contribution of CSCs to tumor progression, metastasis, and treatment resistance, many studies have identified biomarkers on the surface of CSC populations to distinguish them from the majority of tumor cells. Magnetic-activated cell sorting (MACS) is a CSC sorting technique. Magnetic NPs have unique magnetic activity and are one of the most actively studied NPs, usually ranging in diameter from 1 to 100 nanometers. Basically, magnetic NPs are classified as magnetically manipulated substances, consisting mainly of iron oxides or other metals (iron, nickel, or cobalt). MACS microbeads are superparamagnetic particles coupled to highly specific monoclonal antibodies. The cell surface-specific antigens are combined with stem cell markers such as CD44, CD133, and epithelial cell adhesion molecule (EpCAM), connected to the magnetic bead, and the cells labeled with the conjugated magnetic bead is separated by providing a uniform magnetic field to sort out the corresponding CSC population (Figure 3).

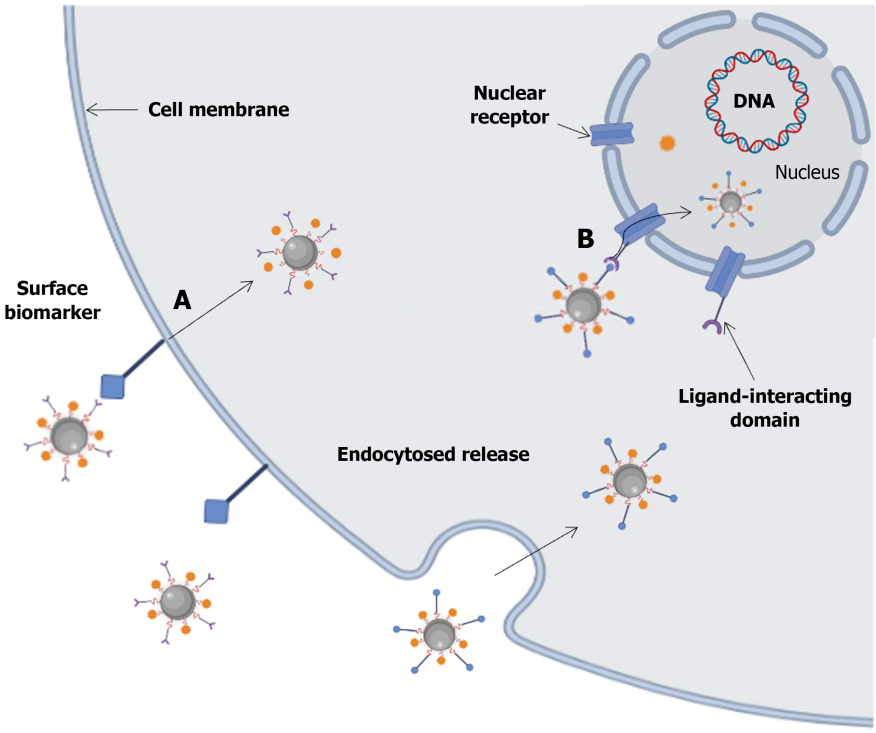

DOI: 10.4252/wjsc.v15.i6.514 **Copyright** ©The Author(s) 2023.

Figure 1 Different mechanisms of nanocarriers. A: Targeting through surface biomarkers; B: Targeting through the ligand-interacting domain on the nuclear receptor (created with BioRender).

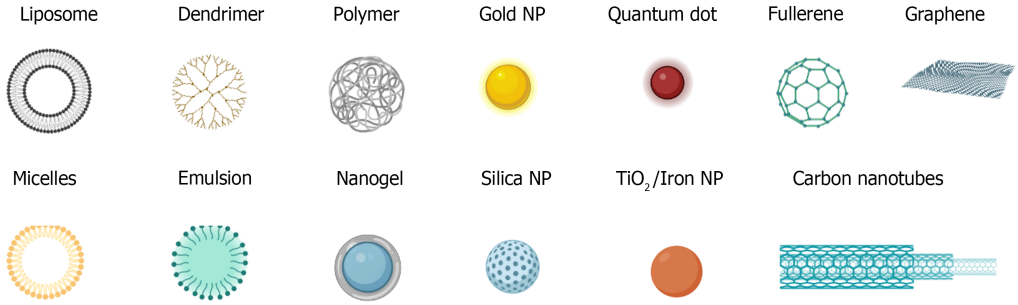

DOI: 10.4252/wjsc.v15.i6.514 **Copyright** ©The Author(s) 2023.

Figure 2 Different types of nanoparticles (created with BioRender). NPs: Nanoparticles.

KINDS OF NANODRUG DELIVERY SYSTEMS

To date, nanomedicine has been focused on identifying alternatives to tumor therapy, with researchers focusing on the design of various nanocarriers, which have been used to load various anticancer drugs and herbal medicines to target tumor cells. In fact, according to the National Institutes of Health, there have been clinical trials involving the use of nanotechnology in CSC therapy (Table 1). Because the mechanisms of multidrug resistance are very complex and varied, targeting one mechanism alone does not address clinical needs. Nanocarriers have good stability, a high encapsulation rate and a high drug loading rate and have been proven to be effective carriers for genes and drugs delivered to tumor cells. This delivery induces apoptotic pathways and inactivates resistance genes for targeting tumor tissue to eliminate CSCs. According to the classification of nanotechnology used to target CSCs, they can be divided into Polymeric NPs(PNPs), liposomes, gold (Au) nanorods (GNRs), QDs, CNTs, GO, PTT, and magnetic fluid hyperthermia (Table 2).

PNPs

PNPs can enhance the therapeutic effects of drugs, reduce the drug resistance of CSCs, and improve the therapeutic effects of chemotherapy drugs. The following is a summary of the classification of PNPs through different antibody-ligand recognition (Figure 4), mesoporous silica ($mSiO_2$) NPs (MSNs), and other nanodrug delivery systems.

Table 1 Clinical trials of advances in nanotechnology applied in cancer stem cells

Identifier	Trial name	Enrollment
NCT04907422	Cluster of differentiation 24-gold nanocomposite expression using quantitative polymerase chain reaction	60
NCT04907422	Nonconjugated cluster of differentiation 24 expression using quantitative polymerase chain reaction	60

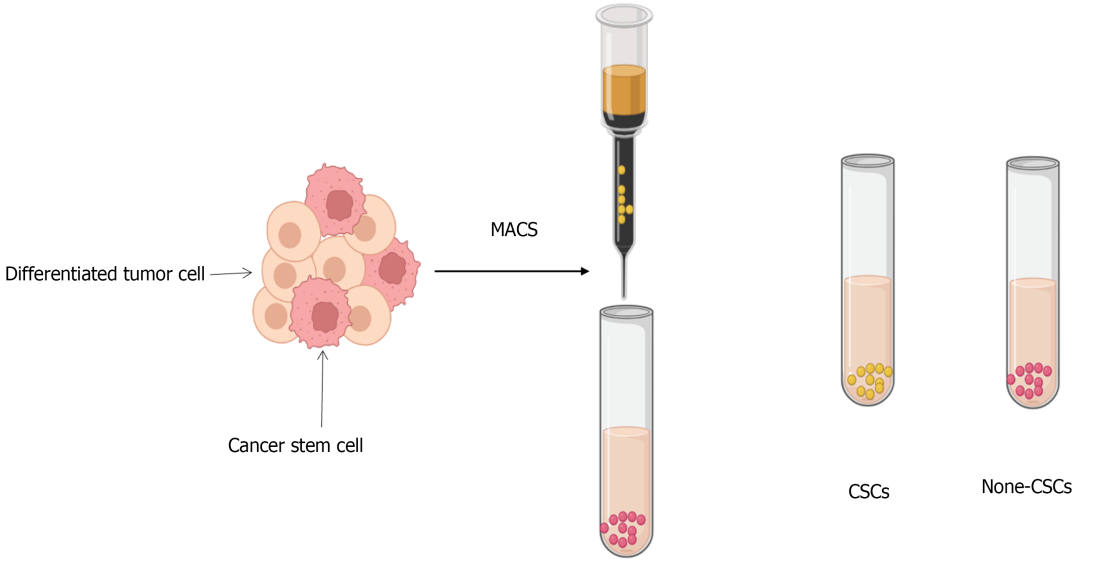

DOI: 10.4252/wjsc.v15.i6.514 **Copyright** ©The Author(s) 2023.

Figure 3 Magnetic-activated cell sorting (created with BioRender). CSCs: Cancer stem cells; MACS: Magnetic-activated cell sorting.

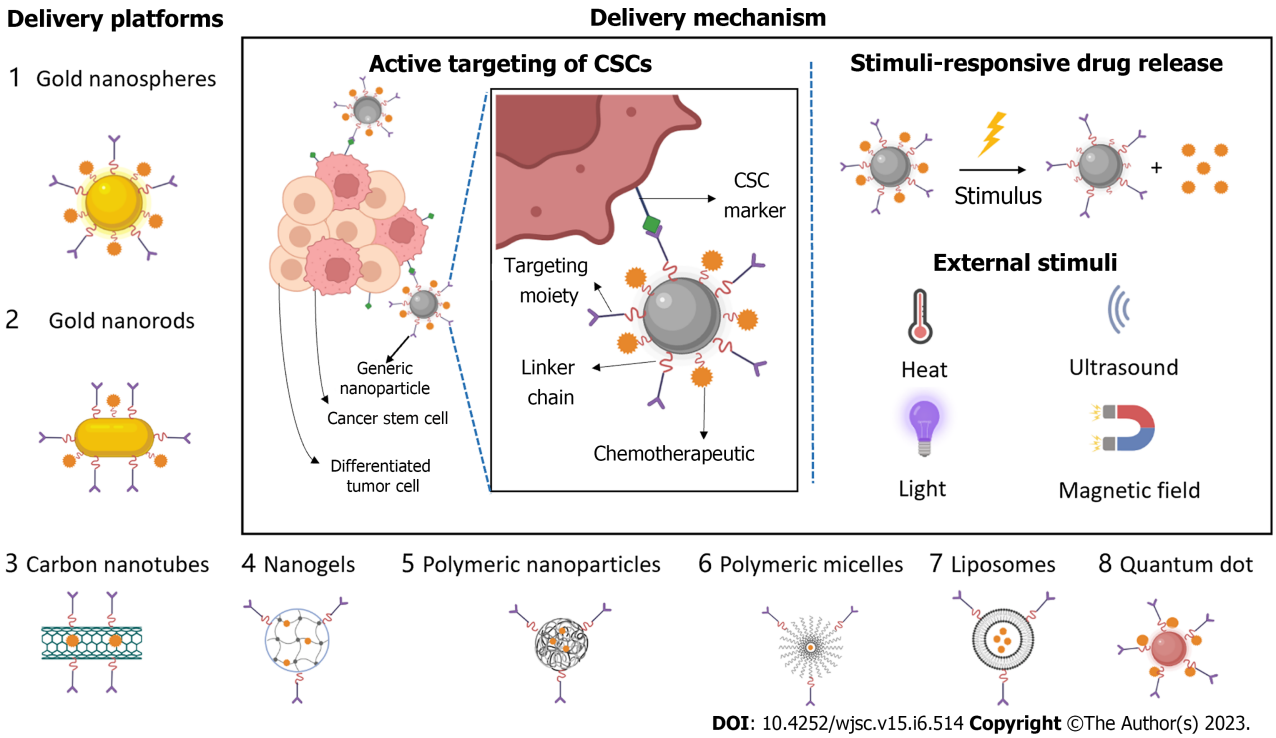

DOI: 10.4252/wjsc.v15.i6.514 **Copyright** ©The Author(s) 2023.

Figure 4 Nanoparticle-mediated targeted drug delivery to cancer stem cells (created with BioRender). CSCs: Cancer stem cells.

CD44

CD44[40,41] is a non-kinase transmembrane glycoprotein that is overexpressed in several cell types, including CSCs. Hyaluronic acid (HA) has become a research hotspot in drug release due to its simple chemical structure and inherent properties of targeting CD44. Kesharwani *et al*[42] designed a novel HA copolymerized styrene maleic acid and the

Table 2 Nanocarrier systems for cancer stem cells

Nanocarrier	Therapeutic agent	Cancer type	Delivery model	Cell line	CSC marker	Ref.
PNPs	CDF	Pancreas	HA-SMA could be engineered to form nanomicelles with a potent anticancer agent, CDF	MiaPaCa-2, AsPC-1	CD44	[42]
	DOX	Colon	HA-SS-MP	HCT116	CD44	[43]
	SFN	Breast	SFN/M-HA-SS-TA	MDA-MB-231, Hs578t, MCF7, MCF10A	CD44	[44]
	SN-38	Colon	CD133Ab-NP-SN-38	HCT116	CD133	[47]
	ITGA5	Breast	ITGA5-targeting NPs	MDA-MB-231	-	[48]
	DOX, tariquidar	Breast	mSiO2-dPG	MCF-7	-	[55]
	DOX, tariquidar	Cancer cell	TTNV	Hela, A547	CD44	[56]
	DS	GMB	PLGA	U87MG, U251MG, U373MG	ALDH	[57,58]
	miR-148a, miR-296-5p	GMB	nano-miRs	GBM1A	Oct4/Sox2	[60]
	TPZ	Breast	MSN	MCF-7	CD133	[54]
	Cyclopamine	Prostate	HPMA	RC-92a/hTERT	CD133	[57]
	HPI-1	Liver, pancreas	HPI-1 was loaded with PLGA-PEG NPs	Huh7, Pa03C	CD133	[58]
	RNA drugs	Liver	ET-tMNV	hep3B	EpCAM	[52]
	DOX, Cyc	Breast	HA-SS-PLGA	MCF-7 MDA-MB-231	CD44	[64]
	LDN193189	Liver	Fe_3O_4-OA-DHCA-PEI-HA	-	CD44	[61]
	DOX	Breast	Gold NPs coupled to adriamycin by nitrogen condensation bond	sk-3	-	[62]
	ZnS	Breast	ZnS	MCF-7	CD44	[63]
	DOX, all-trans retinoic acid	Liver	PLGA-b-PEG	Hepa1-6	EpCAM	[51]
	Epiampicin, arsenic trioxide	Liver	Nanomicelles	hepG2	CD44	[97]
	Resveratrol	Oral	NP	H-357	-	[69]
	Cisplatin	Liver	PEI-modified MSN	Huh7	CD133	[53]
Liposomes	SAL, DOX	Liver	Nanoliposomes	HepG2	CD133	[73]
	TRAIL, SAL	Cancer cell	Liposomes	CSCs	-	[72]
	DOX	Liver	HLs	HepG2	EpCAM, CD133	[74]
	DOX, SAL	Liver	Redox-triggered dual-targeted liposomes	Huh7	CD133EpCAM	[48]
	DTXPL, TEL	Lung	DOX loaded with polyethylene glycolized liposomes	NCI-H460	CD133	[76]
Gold nanorods	-	Head, neck	SPIONPs	Cal-27	CD44	[45]
	PKF, SAHA	Breast	PKF and SAHA loaded on the corona of GNPs	MCF-7	-	[81]
	-	Liver	CD133-targeting aptamers modified on the surface of quantum dots and gold NPs with partially complementary paired	Huh7	CD133	[82]

			RNA (ssRNA)			
	DOX	Liver	EpCAM antibody conjugated onto lipophilic Au-NR	Hepa 1-6	EpCAM	[51]
	siRNA	Breast	Glu-NP	MDA-MB-231	GLUT1	[84]
	SAL	Breast	SAL-conjugated gold NPs, SAL-AuNPs	MCF-7	CD44	[86]
	HA	Breast	HA-capped AuNPs	MDA-MB-231	CD44	[86]
	Teleglenastat	Brain	Au-PEG-CD133-CB-839	GBM-1, NCH-644	CD133	[83]
GO	SAL	Ovarian	rGO-Ag	A2780	ALDH, CD133	[93]
CNTs	Paclitaxel	Breast	Multiwalled carbon nanotubes	HMLER	CD44	[45]
	-	brain	CD133 monoclonal antibody onto chitosan-modified CNTs	GBM tissues	CD133	[89]
	Paclitaxel, SAL	Breast	CD44 antibody hydrazone-linked onto SWCNT with pH-activated release system	MDA-MB-231	CD44+	[91]
	SAL	Glioblastoma	SAL-SWCNT-CHI-HA	AGS	CD44+	[90]

CD: Cluster of differentiation; CDF: 3,4-Difluorobenzylidene curcumin; anti-CD133 antibody-conjugated SN-38-loaded nanoparticles CNTs: Carbon nanotubes; CSCs: Cancer stem cells; Cyc: Cyclophosphamide;CB-839:telaglenastat; dPG: Dendritic polyglycerol; DOX: Doxorubicin; DTXPL: Docetaxel liposome; EpCAM: Epithelial cell adhesion molecule; ET: EpCAM-targeted; Fe_3O_4-OA-DHCA-PEI- HA: Mgnetic nanocubes were synthesized and modified with PEI and HA; GBM: Glioblastoma multiforme; GO: Graphene oxide; GLS1: Glutaminase 1; Glu-NP: Glucose-installed sub-50-nm unimer polyion complex-assembled gold nanoparticle; HA: Hyaluronic acid; HA-SMA: Hyaluronic acid conjugate of copoly (styrene maleic acid); HA-SS-MP: Hyaluronic acid-SS-mercaptopurine; HPMA: N-(2-hydroxypropyl) methylacrylamide; HLs: Hybrid lipo plastids;ITGA5: Integrin subunit alpha 5; MNVs: Milk-derived nanovesicles: M-HA-SS-TA: Mineralized HA-SS-tetracylecyl nanocarrier; miR: MicroRNA; $miSO_2$: Mesoporous silica; MSNs: Mesoporous silica nanoparticles; MWCNTs: Multiwalled carbon nanotubes; NPs: Nanoparticles; PEG: Polyethylene glycol; PKF: PKF118-310; PLGA: Poly(L-lactide-co-glycolide); PNPs: Polymeric nanoparticles; PDT: Photodynamic therapy; ROS: Reactive oxygen species; rGO-Ag: Reduced graphene oxide–silver nanocomposite; SAHA: Vorinostat; SAL: Salomycin; SFN: Sulforaphane; siRNA: Small interfering RNA; SWCNT: Single-walled carbon nanotubes; SPIONPs: Superparamagnetic iron oxide NPs; SAL-SWCNT-CHI-HA:CHI-coated SWCNTs loaded with SAL and functionalized with HA;TEL: Telmisartan; TPZ: Tirapazamine; TRAIL: Tumor necrosis factor-associated apoptosis-inducing ligand; TTNV: Targeted theranostic nano vehicle; ZnS: Zinc sulfide.

effective anticancer agent 3,4-difluoromethylcurcumin to form nanomicelles. CD44+/CD133+/EpCAM+ pancreatic CSCs showed better uptake of HA-engineered nanomicelles and a better anticancer effect on CD44+ pancreatic CSCs. Furthermore, these nanomicelles significantly inhibited the expression of NF-κB, thereby reducing its proliferation and invasion. Debele *et al*[43] conjugated HA with hydrophobic 6-mercaptopurine (MP) and introduced doxorubicin (DOX) into colon cancer cells and colon CSCs through ligands. The inhibitory effect of the synthesized bisensitive polymer drug conjugate (HA-SS-MP) micelles on tumor growth was significantly higher than that of free drugs. In *vitro* cytotoxicity of HA-SS-MP and DOX-loaded HA-SS-MP micelles was great for CSCs (HCT116-CSCs). Gu *et al*[44] prepared mineralized HA-SS-tetracylecyl nanocarriers (M-HA-SS-TA) from oily, hydrophobic, and unstable sulforaphane (SFN), which showed a good response to highly reduced and weakly acidic tumor niches. The SFN nanomaterials (SFN/M-HA-SS-TA) can release SFN rapidly. Compared to free SFN, SFN/M-HA-SS-TA rapidly releases SFN in response to tumor niches, showing stronger inhibition of breast CSC (BCSC)-like properties (invasions, self-renewal, and tumor growth) *in vitro* and *in vivo*. However, magnetic fluid hyperthermia (MFH) mediated by anti-CD44 antibody-modified superparamagnetic iron oxide NPs (SPIONPs) can kill CSCs, and significantly inhibit the growth of transplanted Cal-27 tumors in mice[45].

CD133

The CD133 antigen is a five-fold transmembrane single-chain glycoprotein that exists on the surface of tumor stem cells. It is a key molecule that regulates the fate of stem cells and a functional marker of stem cells. It can be used to detect and isolate CSCs in various solid tumors[46]. NPs with SN-38 (anti-CD133 antibody-conjugated SN-38-loaded nanoparticles (CD133Ab-NPs-SN-38)), a topoisomerase inhibitor conjured by anti-CD133 antibody, targets CD133+HCT116 cells and inhibits colony formation. The CD133-targeted NP delivery system can eliminate CD133-positive cells[47]. The Wnt/β-catenin pathway plays critical roles in CSC generation and maintenance as well as in normal stem cells. Integrin subunit alpha 5-targeting NPs attenuate β-catenin and significantly reduce triple-negative BC (TNBC) metastasis and may provide a facile and unique strategy of specially attenuating β-catenin *in vivo* for treating metastatic TNBC[48]. Codelivery of DOX and salomycin (SAL) REDOX-triggered double-targeted liposomes CEP-LP@S/D can be used for the synergistic treatment of liver cancer. The system is based on the binding of CD133- and EpCAM-targeting peptides to form Y-shaped CEP ligands that anchor to the liposome surface and allow selective targeting of CD133EpCAMlCSC[49].

EpCAM

EpCAM, considered to be a homogenous cell-cell adhesion glycoprotein, is expressed in epithelial and circulating tumor cells (CTCs), as well as CSCs[50], and is involved in the regulation of cell adhesion, proliferation, migration, dryness, and the epithelial-to-mesenchymal transition (EMT) of cancer cells. Locatelli *et al*[51] coloaded GNRs and adriamycin (Adr) to label EpCAM by targeting the surface of CSCs and killed CSCs under laser ablation. Ishiguro *et al*[52] used RNA nanotechnology to pair milk source nanocapsules (MNVs) with synthetic oligonucleotide aptamers that could bind to EPCAM with high affinity and specificity and loaded small interfering RNA (siRNA) onto β-catenin. The EpCAM-targeted (ET) therapeutic MNV has been prepared. These ET-TMNVs can target EPCAM-positive stem cell populations and effectively release siRNAs within cells that inhibit β-catenin expression and tumor growth. For polymer nanomicelles (GNRS-1/curc@Pms) made from biocompatible poly(L-lactide-co-glycolide)-block-poly(ethylene glycol) (PLGA-b-PEG) copolymer as drug carriers for Adr and GNRs, when Adr/GNRs@Pms-antiEpCAM with EpCAM antibodies are modified, they are delivered to specific tumor stem cells and increase the drug concentration at the tumor site, thereby killing the entire tumor stem cell population[51].

MSN

MSN drug loading[53] can significantly enhance the cytotoxicity of anticancer drugs with low potency. Therefore, the positive polymer polyethylenimine (PEI) is usually coated and chemically modified to introduce a positive charge on the surface of MSNs, which can effectively bind the DNA structure, siRNAs, and other nucleic acids, thus enhancing their uptake by cells. The PEI-modified MSN was used for double delivery of the chemotherapy drug cisplatin, and the DNA encoding the hepatocyte nuclear factor 4 alpha transcription factor was used for gene therapy of liver cancer. This therapy inhibited the proliferation of CD133+ HUH7 cells, reduced the proportion of CSCs, and reduced the expression of dry-related genes. The nuclear targeting system of MSNs by Li *et al*[54] can directly target CSCs and enter the nucleus through anti-CD133 surface modification and heat-triggered exposure of the TAT polypeptide under an alternating magnetic field (AMF). Combined with hyperthermia and hypoxia-activated chemotherapy, the release of nuclear-targeted drugs eventually leads to complete apoptosis of CSCs. CSC-specific targeting of $mSiO_2$-dendritic polyglycerol (dPG) nanocarriers delivered the chemotherapy drug DOX and the P-glycoprotein (P-gp) inhibitor tariquidar (Tar) to reverse multidrug resistance (MDR) and enhance chemotherapy efficacy in bCSCs[55]. A targeted theranostic nano vehicle (TTNV) was designed using manganese-doped MSNs with an ideal surface area and pore volume for loading optimized ratios of antitumor DOX and the drug efflux inhibitor Tar. This strategically framed TTNV, which is chemically coupled with folic acid and HA, as a dual-targeted entity to promote folate receptor (FR)-mediated cancer cells and CD44-mediated CSC uptake, respectively[56].

Other nanodrug delivery systems

The N-(2-hydroxypropyl) methylacrylamide (HPMA) cyclopamine delivery system, as a selective macromolecular therapy for CSCs, has improved drug solubility and reduced systemic toxicity, allowing it to effectively remove CD133+ tumor stem cells in prostate tumors. HPI-1 was loaded with PLGA-PEG NPs to solve the problem of poor water solubility and effectively eliminate CD133+ CSCs in pancreatic and liver cancer[57,58].

GBM stem cells (GSCs) are the leading cause of chemotherapy failure in GBM. PLGA NP-encapsulated disulfiram effectively inhibited *in situ* and subcutaneous GSC xenografting in mouse models[59]. Although we are increasingly understanding GBM at the molecular level, treatment options are still limited. We have developed bioreducible poly(β-aminoester) NPs that exhibit high intracellular delivery efficacy and low cytotoxicity that have the ability to escape from endosomes and facilitate the release of cytoplasmic environment-triggered cargo for the delivery of microRNAs to tumor-reproducing human CSCs[60]. In the study by Wang *et al*[61], a high temperature thermal breakdown approach was used to create composite magnetic nanocubes modified by PEI and HA. The ferric oxide nanocubes recognized hepatocellular carcinoma (HCC) stem cells *via* receptor-ligand binding of HA and CD44 (HA receptor), while loading small molecule LDN193189 inhibited the expression of stemness-related genes octamer-binding transcription factor 4 and Nanog. Double pH-sensitive polymeric drug-conjugated NPs showed enhanced inhibition of the progression of drug-resistant SK-3 CSCs, whereas AuNPs conjugated to Adr *via* nitrogen reduction bonds overcame resistance by avoiding P-gp efflux, thereby delivering more DOX to tumor stem cells. This mechanism resulted in the elimination of all tumor cell subpopulations and prevented the potential reaggregation of CSCs[62]. Tran *et al*[63] inhibited the transfer of MCF-7-SCs by inhibiting the EMT process, revealing the potential role of nanozinc sulfide in inhibiting the migration and invasion of bCSCs, which opened up a new way of thinking and provided a potential approach for the treatment of BC.

It has also been shown that the constructed amphiphilic polymer, HA-cystine-PLGA, can be used to deliver DOX and cyclopamine to CD44-high-expressing bCSC subpopulations and a large number of BC cells, and allow on-demand release. The dual delivery particles effectively reduce the number and size of tumor spheroids, and HA shows targeting effects on bCSCs[64].

Gao *et al*[65] proposed a novel intravenous photodynamic therapy (PDT) platform based on stem cell simulation of SUCNPs@mSiO2 for tumor targeting and enhanced PDT efficacy. Due to the coating of the stem cell membrane, the prepared nano SUCNPs@mSiO2 has good stability and biocompatibility. Moreover, it has the ability to be intravenously injected and escape immunity, extend the blood circulation time, and improve the tumor targeting function of stem cells, paving the way for the development of photosensitizers with bioactive cell components, such as SUCNPs@mSiO2, as a platform for targeting PDT. Sorafenib and glucose oxidase were integrated into the N-acety-lgalactosamine-modified zeolite imidazolate framework (ZIF-8), designated SG@GR-ZIF-8, and this nano preparation exhibited significant antimetastatic HCC activity against C5 WN1 cells, a liver CSC-like cell line with tumorigenic and lung metastatic activity [66]. PT chemotherapy synergy was achieved by loading crocodile-based PT agents with natural cytotoxic heat shock

protein (HSP) inhibitors that had high potency biradical characteristics into a redox-sensitive chitosan (CHI) matrix. Within solid tumors, PEG shells that prevent nano-assembled mono nuclei from phagocytosing were cleared quickly to expose the positively charged CHI, and the isolated peptide iRGD was further activated. This step drives tumor penetration of CHI NPs and allows CSC targeting by selective identification of CD44 proteins. Due to the inhibition and chemosensitization of HSPs, the designed nano assembly can completely eliminate CSCs and non-CSCs, thereby inhibiting tumor growth and metastasis[67]. Chen *et al*[68] used PLGA/d-alpha-tocopherol PEG 1000 succinate (TPGS) NPs for the first time with the combination of chemotherapy drugs and ATP-binding cassette (ABC) transporter inhibitors (ATIs) and used TPGS and PLGA to prepare NPs. Due to the overexpression of ABC transporters in CSCs, the combination of ATIs and chemotherapy drugs can overcome the multidrug resistance of CSCs. PLGA/TPGS NPs were prepared for the codelivery of DOX and extracellular lipopeptide composite to reach the tumor site with an optimized synergistic ratio, and resveratrol NP reduces cancer activity and decreases inflammation in CSC-rich oral cancer[69]. In addition to active targeting strategies, relying on intelligent changes in nanodrug size to penetrate deep into tumor tissues and improve the clearance rate of CSCs is also an important strategy for efficient reversal of MDR. On this basis, a special morphologically tunable nanodrug was developed, which integrated chemotherapy and immune checkpoint blocking therapy for large tumor cells and CSCs into drug delivery systems. As NPs are transferred from circulation to tumor tissue, particle size shrinks, favoring pharmacokinetics and cellular uptake while enabling sequential drug release when needed. The nanomedicine reduced the proportion of CSCs and enhanced the therapeutic effect on tumors, thereby prolonging the survival time of mice[70].

Liposomes

Liposomes are spherical vesicles consisting of one or more concentric phospholipid bilayer layers that enclose a water core. Liposomes are both nontoxic and biodegradable, making them powerful drug delivery systems. They improve the therapeutic effect of drugs by stabilizing compounds, overcoming barriers to cell and tissue uptake, and increasing the biological distribution of drugs at target sites in the body while minimizing systemic toxicity[71].

Tumor necrosis factor-associated apoptosis-inducing ligands (TRAILs) have received much attention for their favorable ability to activate apoptosis in cancer cells by interacting with death receptors (DRs). However, CSC-like cells lack or express low levels of the death receptor DR and are highly resistant to apoptosis mediated by TRAIL, limiting therapeutic efficacy. The liposomal component of the plasmid DNA encoding TRAIL and SAL enables cancer cells to express TRAIL as protein generators, and more importantly, to upregulate DR expression through SAL-induced CSCs, making drug-resistant CSCs sensitive to TRAIL-triggered apoptosis. This liposome-based programmable drug codelivery system shows the potential to effectively eliminate CSCs and inhibit CSC-rich tumor growth in mouse models of colon tumors *in situ*[72].

Gong *et al*[73] prepared and characterized SAL-loaded nanoliposomes (SLNs), DOX-LNs (DLNs) and SAL and DOX simultaneously delivered nanoliposomes (SAL/DOX). Novel SDLNs and SLN-DLNs are used to deliver SAL and DOX to HCC cells and CSCs. Hybrid lipo plastids (HLs) are nanosized liposome particles that can be prepared by the ultrasonic mixing of capsule and micelle molecules in buffer solution. The inhibitory effect of HLs on the growth of the CSC subpopulation of HCC cells (HepG2) has proven that HLs are a new type of nanomaterial that can be used to target CSCs in the treatment of HCC[74]. Dual-targeted liposomes CEP-LP@S/D selectively target CD133EpCAMlCSCs. Upon arrival at CSCs, CEP-LP@S/D liposomes undergo cytoplasmic endocytosis, in which high concentrations of glutathione break the disulfide bonds, thereby degrading the liposomes[75]. The combination of docetaxel liposome (DTXPL) and telmisartan (TEL) increased the cytotoxicity of H460 WT 3D cells two-fold. In H460 WT and DTX-resistant CD133+ xenograft tumor models, tumors treated with the combination of DTXPL and TEL showed reduced tumor volume, increased apoptosis, and downregulated CSC marker expression[76].

Lipid nanocapsule (LNC) encapsulated with paclitaxel and SAL can induce apoptosis in bCSCs, which is enhanced by the codelivery of paclitaxel and SAL. Synergistic cytotoxic effects on cells, non-bCSCs, and bCSCs, as well as effective reduction in tumor mammary globular growth by encapsulating both paclitaxel and SAL, suggest that LNCs have potential for the treatment of BC[77].These studies demonstrate the great potential of nanoliposome-targeted drug delivery to tumor stem cells.

GNRs and QDs

GNRs are pseudo-one-dimensional rod-like NPs, which have become one of the emerging materials of interest in recent years due to their anisotropic shape and adjustable plasma properties[78]. QDs, also known as nanocrystals, are NPs composed of II-VI or III-V elements that are rich in energy electrons and quantum-confined holes[79]. QDs are widely studied as biomedical imaging probes due to their unique optical and electronic properties. They are usually nanoscale semiconductor microcrystals and are widely used to improve the efficacy of fluorescent markers in bioimaging[80].

PKF118-310 (PKF) and vorinostat (SAHA) loaded on GNP corona Protein corona (PC), a AuNP system with protein corona coating for simultaneous delivery of PKF and SAHA resulted in a reduction of stem cell populations and Snail marker in MCF7 bCSCs[81]. Coloaded with GNRs and Adr, EpCAM was labeled by targeting the surface of CSCs to kill CSCs under laser ablation[54]. A novel fluorescent on nano aptamer sensor for the quantitative detection of CD133 has also been designed. By hybridization of CD133-targeting aptamers modified on the surface of QDs and AuNPs with partially complementary paired RNA (single-stranded RNA), the distance between the QDs and AuNPs is shortened, resulting in fluorescence resonance energy transfer between them so that the fluorescence of the QDs is quenched by AuNPs. The QD fluorescence recovery aptamer sensor is a sensitive and reliable sensor for the detection of CD133, providing a simple and promising detection tool for CSC markers[82]. Inhibition of glutamine decomposition may be an effective anti-CSC strategy. The glutaminase 1 (GLS1) inhibitor telaglenastat (CB-839) was loaded into Au pegylated NPs (Au-PEG-CD133-CB-839) equipped with covalently coupled CD133 aptamer. In an *in vitro* exposure to a CD133-positive

brain tumor model, Au-PEG-CD133-CB-839 reduced the activity of CD133-positive cancer cells in a dose-dependent manner[83]. Glucose-installed-targeted NPs (Glu-NPs) demonstrated higher cellular uptake of siRNA payload in globular BC (MBA-MB-231) cell cultures compared to glucose-uncoupled control NPs (MeO-NPs). Glu-NPs, a promising nanocarrier design for CSC-targeted cancer therapy, caused significantly enhanced gene silencing in CSC-rich MDA-MB-231 tumor tissue in situ after systemic administration to tumor-bearing mice[84]. Liu *et al*[85] reported that SAL was conjugated with biocompatible AuNPs coated with PEG showed specific targeting ability and high antitumor efficacy against CD24 Low/CD44high subsets in BC cells. The biodegradable naturally negatively charged polysaccharide HA is used to synthesize AuNPs, while HA can act as a capping agent based on its hydroxyl group, thereby stabilizing newly produced AuNPs. HA-functionalized AuNPs exhibit excellent physical properties and high cell uptake and have a strong inhibitory effect on MDA-MB-231 cells and CSCs. In particular, synergistic chemothermal therapy with HA-capped AuNPs combined with NIR irradiation has shown more effective therapeutic results in terms of cytotoxicity, apoptosis, and necrosis compared with chemotherapy alone[86].

The disadvantage of metallic nanomaterials lies in their toxicity. Reactive oxygen species(ROS) generation, influence on cell structures and other characteristics of metallic NPs toxicity are similar to other NPs, and the toxicity is related to size, shape, dimensionality, surface charge. Therefore, metallic NPs should be carefully examined before used in clinic.

CNTs

The high surface-to-volume ratio, enhanced electrical conductivity, strength, biocompatibility, ease of functionalization, and optical properties of CNTs have led to their consideration as novel drug and gene delivery vehicles. CNTs are cylindrical tubes formed from sp2 hybrid carbon atoms, which can range in size from 1 nanometer to several microns. CNTs can be divided into single-walled CNTs (SWCNTs) and multiwalled CNTs (MWCNTs) according to the number of layers formed in them[87].

BCSCs have strong resistance to traditional hyperthermia, while PTT mediated by amino-modified multiwalled CNTs on the surface can effectively kill bCSCs[88]. CD133 is a currently recognized CSC marker for GBM. CNTs can be targeted to CD133-positive cells of GBM (GBM-CD133+) through a CD133 antibody. Wang *et al*[89] grafted a CD133 monoclonal antibody onto CHI-modified CNTs. Then, CSCs were effectively killed by PTT. The gastric CSC-specific targeted drug delivery system (SAL-SWNT-CHI-HA complex) is also based on CHI-coated SWCNTs loaded with SAL and functionalized with HA to selectively eliminate gastric CSCs[90]. SWCNTs facilitate active targeting due to their needle shape, significant transmembrane penetration, EPR effects, high drug loading capacity, and ease of functionalization of biological agents (*i.e.* antibodies). Surface functionalization with polymers such as PEG helps overcome the limitations of the original NTs, providing good water solubility, prolonging blood circulation, and reducing the toxic effects of SWCNT-based nanocarriers. The potential therapeutic effect of the combination of paclitaxel and SAL in BC and CSCs is mediated by a pH-responsive release mechanism near the acidic tumor microenvironment *via* a hydrazone junction[91].

GO

Driven by the achievements of CNTs, graphene, and GO are new types of drug nano carriers used to support a variety of therapeutic drugs, anticancer drugs, insoluble drugs, antibiotics, antibodies, *etc.*

GO is alleged to specifically target CSCs rather than normal cells and to induce CSC differentiation and inhibit tumor sphere formation in multiple cell lines, including breast, ovarian, prostate, lung, pancreas, and GBM cell lines, by inhibiting several key signaling pathways, including the Wnt, Notch, and signal tranducer and activator of transcription signaling pathways[92].

Choi *et al*[93] synthesized reduced graphene-silver nanocomposites (rGO-Ag) using the R-phycoglobin biomolecular mediated method. These composites have a toxic effect on ovarian CSCs (OvCSCs) and can reduce the survival rate of OvCSCs by decreasing the mitochondrial membrane potential and expression of apoptotic genes, leading to mitochondrial dysfunction and possibly apoptosis. RGO-Ag may be a novel nanotherapeutic molecule for specifically targeting highly tumorigenic ALDH+CD133+ cells and clearing CSCs.

PTT

PTT uses metal NPs to eradicate CSCs and stimulate a hyperthermal physiological response by converting light into heat [94]. MSNs under an alternating magnetic field eliminate CSCs by blocking the hypoxia signaling pathway and heating, thus effectively inhibiting tumor growth[56,95]. Burke *et al*[86] found that bCSCs have strong resistance to traditional hyperthermia, and PTT mediated by amino-modified multiwalled CNTs on the surface can effectively kill bCSCs. Wang *et al*[87] grafted CD133 monoclonal antibody onto CHI-modified CNTs. CD133 is currently recognized as a CSC marker for GBM, and CNTs can be targeted to GBM-CD133+ through the CD133 antibody. Then the CSCs were effectively killed by PTT. NPs loaded with bimodal metal cages and photodynamic therapys (PDT) PDTs target CSCs by reducing cell mobility under laser irradiation[96]. Researchers developed a CSC-specific-targeted, retinoic acid (RA)-loaded Au nanostar-dPG nanoplatform for the efficient eradication of CSCs. The nanocomposites possess good biocompatibility and exhibit effective CSC-specific multivalent-targeted capability due to HA decorated on the multiple attachment sites of the bioinert dPG. With the help of CSC differentiation induced by RA, the self-renewal of bCSCs and tumor growth were suppressed by the high therapeutic efficacy of PTT in a synergistic inhibitory manner[97]. Based on PTT properties of CNTs and metallic materials, nanoplatform functions with chemotherapy and PTT can be designed to produce synergistic effects.

Researchers have utilized MnO_2@Ce6 NPs and a PDT-based approach that improved tumor microenvironment-related therapeutic resistance by modulating the tumor microenvironment with excess hydrogen protons and water, resulting in subsequent radiation of CSCs[98]. Haldavnekar R *et al*. introduced nickel-based functionalized nanoprobe-facilitated

surface-enhanced Raman scattering for the prediction of cancer dissemination by CSC-based surveillance[99]. MoS_2 nanosheets and a moderate PTT treatment were applied to target a CSC surface receptor (*i.e.* CD44) and modulate its downstream signaling pathway. The treatment showed attenuated self-renewal capacity, more response to anticancer drugs, and less invasiveness[100].

Although PTT can inhibit tumor growth by eliminating tumor stem cells, it is usually difficult to completely eradicate tumors due to the limited penetration depth of near-infrared (NIR) light. Therefore, combining PTT with other therapies is expected to overcome these challenges.

Magnetic fluid hyperthermia

MFH uses the good magnetic thermal conversion ability of magnetic NPs under the influence of an external alternating magnetic field to rapidly heat the internal tumor, forming a high-temperature zone, to kill tumor cells or induce their apoptosis[101].

When anti-CD44 antibody-modified SPIONPs are prepared, SPIONP-mediated hyperthermia can kill CSCs, and MFH significantly inhibits the growth of transplanted Cal-27 tumors in mice[59]. Nuclear targeting systems coated with MSNs of superparamagnetic iron oxide-based NPs can directly target CSCs and can be used to combine thermotherapy and hypoxia-activated chemotherapy with nuclear-targeted drug release under an alternating magnetic field, ultimately leading to complete apoptosis of CSCs[73]. Biomimetic magnetic NPs induce apoptosis of stress-escape CSCs and inhibit their proliferation and metastasis *in vitro* and *in vivo* by the combined therapeutic effects of DOX chemotherapy and magnetic MSNs MFH under the action of an alternating magnetic field[102]. Antibody-modified NPs targeting lung CSCs enhance cellular uptake *in vitro* and prolong tumor accumulation *in vivo*. Due to the combined effects of hyperthermia and chemotherapy treatment, up to 98% of lung CSCs are killed by AMF within 30 min of application outside the body. In *in vivo* models, this combination therapy significantly inhibited tumor growth and metastasis in mice carrying lung CSC xenografts with minimal side effects and adverse reactions[103]. In summary, MFH shows great potential in targeting tumor stem cells.

FUTURE PERSPECTIVES AND CHALLENGES

The discovery of CSCs has made us gradually realize the complexity of tumors. CSCs are the roots of tumor occurrence, drug resistance, and postoperative recurrence. Therefore, the eradication of CSCs is of great significance for the treatment of cancer. At present, theoretical research on tumor stem cells is still in the initial stage, and many problems have not been solved. For example, CSCs and normal stem cells have very similar self-renewal, multidirectional differentiation, signaling pathways, and cell surface markers. How to effectively kill CSCs without damaging normal stem cells needs further research. Some regulatory mechanisms and biological behaviors of tumor stem cells have not been fully clarified. It is believed that with the continuous deepening of CSC research, more targets and a theoretical basis will be provided for clinical treatment.

In addition to effective drugs targeting CSCs, it is also necessary to consider the heterogeneity of CSCs to eliminate tumor cells and CSCs more effectively, inhibit recurrence and improve the survival rate of patients. Although great progress has been made in research on the molecular mechanism of cancer, cancer detection and treatment, and the treatment methods have been continuously improved, there is still a lack of effective treatments for cancer. The targeting, slow release, good biocompatibility, and stability of nanomaterials will play a huge role. In addition, nanotargeting technology is used to track the biological characteristics of CTCs[104]. The physical and chemical properties of each component of the tumor microenvironment are different from those of normal tissues, and the tumor microenvironment plays a huge role in the process of tumor occurrence and development, which makes the tumor microenvironment an important target for nanomaterial-targeted therapy[105]. Although there are still several difficulties in the wide application of nanomaterials in clinical practice, the most important of which is biosafety, there is still no convincing evidence that nanomaterials can be effectively metabolized in the body without accumulation and causing toxic side effects. In addition, how to improve the linking efficiency of targeted molecules and nanomaterials, the activity of targeted molecules after linking, the stability of the binding of targeted substances and drug carriers, and the metabolic pathways and toxicity of nanomaterials *in vivo* have not yet been solved. However, the strong ability shown in the early stages makes us hypothesize that nanomaterials for CSC-targeted therapy have broad prospects as a new generation of tumor treatment. With the continuous deepening of CSC research and the rapid development of nanotechnology, these fields will potentially overlap and provide a strong guarantee for cancer treatment.

CONCLUSION

Cancer is a huge barrier for researchers due to its high mortality rate and resistance to treatments. For example, multidrug resistance, recurrence, and the spreading nature of cancer cells make cancer extremely difficult to treat. CSCs are the main reason for inducing the characteristics of drug resistance and the regenerative ability of tumor cells. Therefore, the targeted system of cancer treatment began to turn to stem cell research. As an emerging field, nanotechnology is mainly applied to materials and carrier structures with diameters between 1 and 100 nanometers. Because nanomaterials have similar dimensions, they differ in composition, structure, hydrophobicity, magnetism, immunogenicity, and other properties. CSC therapies based on these unique properties have been extensively studied, but only a

few have entered clinical trials. To better improve clinical translation, further research on targeted drug delivery of nanocarriers is needed to reduce toxicity, enhance permeability and retention, and minimize the shielding effect of the protein corona. By rationally designing and constructing new NDDS to accurately target CSCs that have developed drug resistance, the efficiency of reversing multidrug resistance and inhibiting tumor growth can be effectively improved, providing a tremendous opportunity to improve cancer treatment or prognosis, which will ultimately improve the survival rate of cancer patients.

FOOTNOTES

Author contributions: Yue M wrote the original draft of the manuscript; Guo T and Nie DY drew the charts; Zhu YX wrote and edited the final paper; Lin M was responsible for the overall direction of the paper and for editing of the manuscript.

Supported by Natural Science Foundation of Nanjing University of Chinese Medicine China, No. XZR2020093.

Conflict-of-interest statement: The authors have no conflicts of interest to declare.

Country/Territory of origin: China

ORCID number: Miao Yue 0000-0002-4925-2191; Ting Guo 0000-0002-3794-9346; Deng-Yun Nie 0000-0001-6622-7513; Yin-Xing Zhu 0000-0002-7417-9109; Mei Lin 0000-0001-9815-2966.

S-Editor: Yan JP
L-Editor: Filipodia
P-Editor: Cai YX

REFERENCES

1 **Siegel RL**, Miller KD, Fuchs HE, Jemal A. Cancer Statistics, 2021. *CA Cancer J Clin* 2021; **71**: 7-33 [PMID: 33433946 DOI: 10.3322/caac.21654]
2 **Li F**, Tiede B, Massagué J, Kang Y. Beyond tumorigenesis: cancer stem cells in metastasis. *Cell Res* 2007; **17**: 3-14 [PMID: 17179981 DOI: 10.1038/sj.cr.7310118]
3 **Abdullah LN**, Chow EK. Mechanisms of chemoresistance in cancer stem cells. *Clin Transl Med* 2013; **2**: 3 [PMID: 23369605 DOI: 10.1186/2001-1326-2-3]
4 **Kanaoujiya R**, Singh D, Minocha T, Yadav SK, Srivastava S. Synthesis, characterization of ruthenium (III) macrocyclic complexes of 1, 4, 8, 11-tetraazacyclotetradecane (cyclam) and in vitro assessment of anti-cancer activity. *Mater Today Proceed* 2022; **65**: 3143-3149 [DOI: 10.1016/j.matpr.2022.05.354]
5 **Batlle E**, Clevers H. Cancer stem cells revisited. *Nat Med* 2017; **23**: 1124-1134 [PMID: 28985214 DOI: 10.1038/nm.4409]
6 **Reya T**, Morrison SJ, Clarke MF, Weissman IL. Stem cells, cancer, and cancer stem cells. *Nature* 2001; **414**: 105-111 [PMID: 11689955 DOI: 10.1038/35102167]
7 **Shibue T**, Weinberg RA. EMT, CSCs, and drug resistance: the mechanistic link and clinical implications. *Nat Rev Clin Oncol* 2017; **14**: 611-629 [PMID: 28397828 DOI: 10.1038/nrclinonc.2017.44]
8 **Bai X**, Ni J, Beretov J, Graham P, Li Y. Cancer stem cell in breast cancer therapeutic resistance. *Cancer Treat Rev* 2018; **69**: 152-163 [PMID: 30029203 DOI: 10.1016/j.ctrv.2018.07.004]
9 **Haiaty S**, Rashidi MR, Akbarzadeh M, Bazmani A, Mostafazadeh M, Nikanfar S, Zibaei Z, Rahbarghazi R, Nouri M. Thymoquinone inhibited vasculogenic capacity and promoted mesenchymal-epithelial transition of human breast cancer stem cells. *BMC Complement Med Ther* 2021; **21**: 83 [PMID: 33663486 DOI: 10.1186/s12906-021-03246-w]
10 **Uckun FM**, Sather H, Reaman G, Shuster J, Land V, Trigg M, Gunther R, Chelstrom L, Bleyer A, Gaynon P. Leukemic cell growth in SCID mice as a predictor of relapse in high-risk B-lineage acute lymphoblastic leukemia. *Blood* 1995; **85**: 873-878 [PMID: 7849309 DOI: 10.1182/blood.V85.4.873.bloodjournal854873]
11 **Wang X**, Huang S, Chen JL. Understanding of leukemic stem cells and their clinical implications. *Mol Cancer* 2017; **16**: 2 [PMID: 28137304 DOI: 10.1186/s12943-016-0574-7]
12 **Zeuner A**, Todaro M, Stassi G, De Maria R. Colorectal cancer stem cells: from the crypt to the clinic. *Cell Stem Cell* 2014; **15**: 692-705 [PMID: 25479747 DOI: 10.1016/j.stem.2014.11.012]
13 **Das PK**, Islam F, Lam AK. The Roles of Cancer Stem Cells and Therapy Resistance in Colorectal Carcinoma. *Cells* 2020; **9** [PMID: 32503256 DOI: 10.3390/cells9061392]
14 **Singh SK**, Hawkins C, Clarke ID, Squire JA, Bayani J, Hide T, Henkelman RM, Cusimano MD, Dirks PB. Identification of human brain tumour initiating cells. *Nature* 2004; **432**: 396-401 [PMID: 15549107 DOI: 10.1038/nature03128]
15 **Muinao T**, Deka Boruah HP, Pal M. Diagnostic and Prognostic Biomarkers in ovarian cancer and the potential roles of cancer stem cells - An updated review. *Exp Cell Res* 2018; **362**: 1-10 [PMID: 29079264 DOI: 10.1016/j.yexcr.2017.10.018]
16 **Najafi M**, Farhood B, Mortezaee K. Cancer stem cells (CSCs) in cancer progression and therapy. *J Cell Physiol* 2019; **234**: 8381-8395 [PMID:

30417375 DOI: 10.1002/jcp.27740]
17 **Najafi M**, Mortezaee K, Majidpoor J. Cancer stem cell (CSC) resistance drivers. *Life Sci* 2019; **234**: 116781 [PMID: 31430455 DOI: 10.1016/j.lfs.2019.116781]
18 **Tang L**, Mei Y, Shen Y, He S, Xiao Q, Yin Y, Xu Y, Shao J, Wang W, Cai Z. Nanoparticle-Mediated Targeted Drug Delivery to Remodel Tumor Microenvironment for Cancer Therapy. *Int J Nanomedicine* 2021; **16**: 5811-5829 [PMID: 34471353 DOI: 10.2147/IJN.S321416]
19 **Jia Y**, Wang Y, Xie J. The Hedgehog pathway: role in cell differentiation, polarity and proliferation. *Arch Toxicol* 2015; **89**: 179-191 [PMID: 25559776 DOI: 10.1007/s00204-014-1433-1]
20 **Wu C**, Zhu X, Liu W, Ruan T, Tao K. Hedgehog signaling pathway in colorectal cancer: function, mechanism, and therapy. *Onco Targets Ther* 2017; **10**: 3249-3259 [PMID: 28721076 DOI: 10.2147/OTT.S139639]
21 **BeLow M**, Osipo C. Notch Signaling in Breast Cancer: A Role in Drug Resistance. *Cells* 2020; **9** [PMID: 33003540 DOI: 10.3390/cells9102204]
22 **Meisel CT**, Porcheri C, Mitsiadis TA. Cancer Stem Cells, Quo Vadis? The Notch Signaling Pathway in Tumor Initiation and Progression. *Cells* 2020; **9** [PMID: 32796631 DOI: 10.3390/cells9081879]
23 **Nami B**, Wang Z. HER2 in Breast Cancer Stemness: A Negative Feedback Loop towards Trastuzumab Resistance. *Cancers (Basel)* 2017; **9** [PMID: 28445439 DOI: 10.3390/cancers9050040]
24 **Duchartre Y**, Kim YM, Kahn M. The Wnt signaling pathway in cancer. *Crit Rev Oncol Hematol* 2016; **99**: 141-149 [PMID: 26775730 DOI: 10.1016/j.critrevonc.2015.12.005]
25 **Yan Y**, Liu F, Han L, Zhao L, Chen J, Olopade OI, He M, Wei M. HIF-2α promotes conversion to a stem cell phenotype and induces chemoresistance in breast cancer cells by activating Wnt and Notch pathways. *J Exp Clin Cancer Res* 2018; **37**: 256 [PMID: 30340507 DOI: 10.1186/s13046-018-0925-x]
26 **Najafzadeh B**, Asadzadeh Z, Motafakker Azad R, Mokhtarzadeh A, Baghbanzadeh A, Alemohammad H, Abdoli Shadbad M, Vasefifar P, Najafi S, Baradaran B. The oncogenic potential of NANOG: An important cancer induction mediator. *J Cell Physiol* 2021; **236**: 2443-2458 [PMID: 32960465 DOI: 10.1002/jcp.30063]
27 **Volmar MNM**, Cheng J, Alenezi H, Richter S, Haug A, Hassan Z, Goldberg M, Li Y, Hou M, Herold-Mende C, Maire CL, Lamszus K, Flüh C, Held-Feindt J, Gargiulo G, Topping GJ, Schilling F, Saur D, Schneider G, Synowitz M, Schick JA, Kälin RE, Glass R. Cannabidiol converts NF-κB into a tumor suppressor in glioblastoma with defined antioxidative properties. *Neuro Oncol* 2021; **23**: 1898-1910 [PMID: 33864076 DOI: 10.1093/neuonc/noab095]
28 **Xu Y**, Afify SM, Du J, Liu B, Hassan G, Wang Q, Li H, Liu Y, Fu X, Zhu Z, Chen L, Seno M. The efficacy of PI3Kγ and EGFR inhibitors on the suppression of the characteristics of cancer stem cells. *Sci Rep* 2022; **12**: 347 [PMID: 35013447 DOI: 10.1038/s41598-021-04265-w]
29 **Codd AS**, Kanaseki T, Torigo T, Tabi Z. Cancer stem cells as targets for immunotherapy. *Immunology* 2018; **153**: 304-314 [PMID: 29150846 DOI: 10.1111/imm.12866]
30 **Yang L**, Shi P, Zhao G, Xu J, Peng W, Zhang J, Zhang G, Wang X, Dong Z, Chen F, Cui H. Targeting cancer stem cell pathways for cancer therapy. *Signal Transduct Target Ther* 2020; **5**: 8 [PMID: 32296030 DOI: 10.1038/s41392-020-0110-5]
31 **Kanaoujiya R**, Porwal D, Srivastava S. Applications of nanomaterials for gastrointestinal tumors: A review. *Front Med Technol* 2022; **4**: 997123 [PMID: 36119898 DOI: 10.3389/fmedt.2022.997123]
32 **Kumari A**, Yadav SK, Yadav SC. Biodegradable polymeric nanoparticles based drug delivery systems. *Colloids Surf B Biointerfaces* 2010; **75**: 1-18 [PMID: 19782542 DOI: 10.1016/j.colsurfb.2009.09.001]
33 **Harun NA**, Benning MJ, Horrocks BR, Fulton DA. Gold nanoparticle-enhanced luminescence of silicon quantum dots co-encapsulated in polymer nanoparticles. *Nanoscale* 2013; **5**: 3817-3827 [PMID: 23519376 DOI: 10.1039/c3nr00421j]
34 **Zhang H**, Lv J, Jia Z. Efficient Fluorescence Resonance Energy Transfer between Quantum Dots and Gold Nanoparticles Based on Porous Silicon Photonic Crystal for DNA Detection. *Sensors (Basel)* 2017; **17** [PMID: 28489033 DOI: 10.3390/s17051078]
35 **Zhang L**, Zhai BZ, Wu YJ, Wang Y. Recent progress in the development of nanomaterials targeting multiple cancer metabolic pathways: a review of mechanistic approaches for cancer treatment. *Drug Deliv* 2023; **30**: 1-18 [PMID: 36597205 DOI: 10.1080/10717544.2022.2144541]
36 **Bharti S**, Anant PS, Kumar A. Nanotechnology in stem cell research and therapy. *J Nanopart Res* 2023; **25**: 6 [DOI: 10.1007/s11051-022-05654-6]
37 **Su Z**, Dong S, Zhao SC, Liu K, Tan Y, Jiang X, Assaraf YG, Qin B, Chen ZS, Zou C. Novel nanomedicines to overcome cancer multidrug resistance. *Drug Resist Updat* 2021; **58**: 100777 [PMID: 34481195 DOI: 10.1016/j.drup.2021.100777]
38 **Chaturvedi VK**, Singh A, Singh VK, Singh MP. Cancer Nanotechnology: A New Revolution for Cancer Diagnosis and Therapy. *Curr Drug Metab* 2019; **20**: 416-429 [PMID: 30227814 DOI: 10.2174/1389200219666180918111528]
39 **Ali ES**, Sharker SM, Islam MT, Khan IN, Shaw S, Rahman MA, Uddin SJ, Shill MC, Rehman S, Das N, Ahmad S, Shilpi JA, Tripathi S, Mishra SK, Mubarak MS. Targeting cancer cells with nanotherapeutics and nanodiagnostics: Current status and future perspectives. *Semin Cancer Biol* 2021; **69**: 52-68 [PMID: 32014609 DOI: 10.1016/j.semcancer.2020.01.011]
40 **Ponta H**, Sherman L, Herrlich PA. CD44: from adhesion molecules to signalling regulators. *Nat Rev Mol Cell Biol* 2003; **4**: 33-45 [PMID: 12511867 DOI: 10.1038/nrm1004]
41 **Zöller M**. CD44: can a cancer-initiating cell profit from an abundantly expressed molecule? *Nat Rev Cancer* 2011; **11**: 254-267 [PMID: 21390059 DOI: 10.1038/nrc3023]
42 **Kesharwani P**, Banerjee S, Padhye S, Sarkar FH, Iyer AK. Hyaluronic Acid Engineered Nanomicelles Loaded with 3,4-Difluorobenzylidene Curcumin for Targeted Killing of CD44+ Stem-Like Pancreatic Cancer Cells. *Biomacromolecules* 2015; **16**: 3042-3053 [PMID: 26302089 DOI: 10.1021/acs.biomac.5b00941]
43 **Debele TA**, Yu LY, Yang CS, Shen YA, Lo CL. pH- and GSH-Sensitive Hyaluronic Acid-MP Conjugate Micelles for Intracellular Delivery of Doxorubicin to Colon Cancer Cells and Cancer Stem Cells. *Biomacromolecules* 2018; **19**: 3725-3737 [PMID: 30044910 DOI: 10.1021/acs.biomac.8b00856]
44 **Gu HF**, Ren F, Mao XY, Du M. Mineralized and GSH-responsive hyaluronic acid based nano-carriers for potentiating repressive effects of sulforaphane on breast cancer stem cells-like properties. *Carbohydr Polym* 2021; **269**: 118294 [PMID: 34294320 DOI: 10.1016/j.carbpol.2021.118294]
45 **Su Z**, Liu D, Chen L, Zhang J, Ru L, Chen Z, Gao Z, Wang X. CD44-Targeted Magnetic Nanoparticles Kill Head And Neck Squamous Cell Carcinoma Stem Cells In An Alternating Magnetic Field. *Int J Nanomedicine* 2019; **14**: 7549-7560 [PMID: 31571863 DOI: 10.2147/IJN.S215087]
46 **Kim WT**, Ryu CJ. Cancer stem cell surface markers on normal stem cells. *BMB Rep* 2017; **50**: 285-298 [PMID: 28270302 DOI:

10.5483/bmbrep.2017.50.6.039]
47 **Ning ST**, Lee SY, Wei MF, Peng CL, Lin SY, Tsai MH, Lee PC, Shih YH, Lin CY, Luo TY, Shieh MJ. Targeting Colorectal Cancer Stem-Like Cells with Anti-CD133 Antibody-Conjugated SN-38 Nanoparticles. *ACS Appl Mater Interfaces* 2016; **8**: 17793-17804 [PMID: 27348241 DOI: 10.1021/acsami.6b04403]
48 **Li Y**, Xiao Y, Lin HP, Reichel D, Bae Y, Lee EY, Jiang Y, Huang X, Yang C, Wang Z. In vivo β-catenin attenuation by the integrin α5-targeting nano-delivery strategy suppresses triple negative breast cancer stemness and metastasis. *Biomaterials* 2019; **188**: 160-172 [PMID: 30352320 DOI: 10.1016/j.biomaterials.2018.10.019]
49 **Wang Z**, Sun M, Li W, Fan L, Zhou Y, Hu Z. A Novel CD133- and EpCAM-Targeted Liposome With Redox-Responsive Properties Capable of Synergistically Eliminating Liver Cancer Stem Cells. *Front Chem* 2020; **8**: 649 [PMID: 32850663 DOI: 10.3389/fchem.2020.00649]
50 **Chenna V**, Hu C, Pramanik D, Aftab BT, Karikari C, Campbell NR, Hong SM, Zhao M, Rudek MA, Khan SR, Rudin CM, Maitra A. A polymeric nanoparticle encapsulated small-molecule inhibitor of Hedgehog signaling (NanoHHI) bypasses secondary mutational resistance to Smoothened antagonists. *Mol Cancer Ther* 2012; **11**: 165-173 [PMID: 22027695 DOI: 10.1158/1535-7163.MCT-11-0341]
51 **Locatelli E**, Li Y, Monaco I, Guo W, Maturi M, Menichetti L, Armanetti P, Martin RC, Comes Franchini M. A novel theranostic gold nanorods- and Adriamycin-loaded micelle for EpCAM targeting, laser ablation, and photoacoustic imaging of cancer stem cells in hepatocellular carcinoma. *Int J Nanomedicine* 2019; **14**: 1877-1892 [PMID: 30936691 DOI: 10.2147/IJN.S197265]
52 **Ishiguro K**, Yan IK, Lewis-Tuffin L, Patel T. Targeting Liver Cancer Stem Cells Using Engineered Biological Nanoparticles for the Treatment of Hepatocellular Cancer. *Hepatol Commun* 2020; **4**: 298-313 [PMID: 32025612 DOI: 10.1002/hep4.1462]
53 **Tsai PH**, Wang ML, Chang JH, Yarmishyn AA, Nhi Nguyen PN, Chen W, Chien Y, Huo TI, Mou CY, Chiou SH. Dual Delivery of HNF4α and Cisplatin by Mesoporous Silica Nanoparticles Inhibits Cancer Pluripotency and Tumorigenicity in Hepatoma-Derived CD133-Expressing Stem Cells. *ACS Appl Mater Interfaces* 2019; **11**: 19808-19818 [PMID: 31066542 DOI: 10.1021/acsami.9b04474]
54 **Li H**, Yan W, Suo X, Peng H, Yang X, Li Z, Zhang J, Liu D. Nucleus-targeted nano delivery system eradicates cancer stem cells by combined thermotherapy and hypoxia-activated chemotherapy. *Biomaterials* 2019; **200**: 1-14 [PMID: 30743049 DOI: 10.1016/j.biomaterials.2019.01.048]
55 **Pan Q**, Nie C, Hu Y, Yi J, Liu C, Zhang J, He M, Chen T, Chu X. Aptamer-Functionalized DNA Origami for Targeted Codelivery of Antisense Oligonucleotides and Doxorubicin to Enhance Therapy in Drug-Resistant Cancer Cells. *ACS Appl Mater Interfaces* 2020; **12**: 400-409 [PMID: 31815420 DOI: 10.1021/acsami.9b20707]
56 **Joseph MM**, Ramya AN, Vijayan VM, Nair JB, Bastian BT, Pillai RK, Therakathinal ST, Maiti KK. Targeted Theranostic Nano Vehicle Endorsed with Self-Destruction and Immunostimulatory Features to Circumvent Drug Resistance and Wipe-Out Tumor Reinitiating Cancer Stem Cells. *Small* 2020; **16**: e2003309 [PMID: 32797715 DOI: 10.1002/smll.202003309]
57 **Zhou Y**, Yang J, Kopeček J. Selective inhibitory effect of HPMA copolymer-cyclopamine conjugate on prostate cancer stem cells. *Biomaterials* 2012; **33**: 1863-1872 [PMID: 22138033 DOI: 10.1016/j.biomaterials.2011.11.029]
58 **Xu Y**, Chenna V, Hu C, Sun HX, Khan M, Bai H, Yang XR, Zhu QF, Sun YF, Maitra A, Fan J, Anders RA. Polymeric nanoparticle-encapsulated hedgehog pathway inhibitor HPI-1 (NanoHHI) inhibits systemic metastases in an orthotopic model of human hepatocellular carcinoma. *Clin Cancer Res* 2012; **18**: 1291-1302 [PMID: 21868763 DOI: 10.1158/1078-0432.CCR-11-0950]
59 **Kannappan V**, Liu Y, Wang Z, Azar K, Kurusamy S, Kilari RS, Armesilla AL, Morris MR, Najlah M, Liu P, Bian XW, Wang W. PLGA-Nano-Encapsulated Disulfiram Inhibits Hypoxia-Induced NF-κB, Cancer Stem Cells, and Targets Glioblastoma In Vitro and In Vivo. *Mol Cancer Ther* 2022; **21**: 1273-1284 [PMID: 35579893 DOI: 10.1158/1535-7163.MCT-22-0066]
60 **Lopez-Bertoni H**, Kozielski KL, Rui Y, Lal B, Vaughan H, Wilson DR, Mihelson N, Eberhart CG, Laterra J, Green JJ. Bioreducible Polymeric Nanoparticles Containing Multiplexed Cancer Stem Cell Regulating miRNAs Inhibit Glioblastoma Growth and Prolong Survival. *Nano Lett* 2018; **18**: 4086-4094 [PMID: 29927251 DOI: 10.1021/acs.nanolett.8b00390]
61 **Wang Y**, Ma S, Liu X, Wei Y, Xu H, Liang Z, Hu Y, Lian X, Huang D. Hyaluronic acid mediated Fe(3)O(4) nanocubes reversing the EMT through targeted cancer stem cell. *Colloids Surf B Biointerfaces* 2023; **222**: 113071 [PMID: 36473370 DOI: 10.1016/j.colsurfb.2022.113071]
62 **Sun R**, Liu Y, Li SY, Shen S, Du XJ, Xu CF, Cao ZT, Bao Y, Zhu YH, Li YP, Yang XZ, Wang J. Co-delivery of all-trans-retinoic acid and doxorubicin for cancer therapy with synergistic inhibition of cancer stem cells. *Biomaterials* 2015; **37**: 405-414 [PMID: 25453968 DOI: 10.1016/j.biomaterials.2014.10.018]
63 **Tran TA**, Krishnamoorthy K, Cho SK, Kim SJ. Inhibitory Effect of Zinc Sulfide Nanoparticles Towards Breast Cancer Stem Cell Migration and Invasion. *J Biomed Nanotechnol* 2016; **12**: 329-336 [PMID: 27305766 DOI: 10.1166/jbn.2016.2187]
64 **Hu K**, Zhou H, Liu Y, Liu Z, Liu J, Tang J, Li J, Zhang J, Sheng W, Zhao Y, Wu Y, Chen C. Hyaluronic acid functional amphipathic and redox-responsive polymer particles for the co-delivery of doxorubicin and cyclopamine to eradicate breast cancer cells and cancer stem cells. *Nanoscale* 2015; **7**: 8607-8618 [PMID: 25898852 DOI: 10.1039/c5nr01084e]
65 **Gao C**, Lin Z, Wu Z, Lin X, He Q. Stem-Cell-Membrane Camouflaging on Near-Infrared Photoactivated Upconversion Nanoarchitectures for in Vivo Remote-Controlled Photodynamic Therapy. *ACS Appl Mater Interfaces* 2016; **8**: 34252-34260 [PMID: 27936561 DOI: 10.1021/acsami.6b12865]
66 **Hu J**, Hu J, Wu W, Qin Y, Fu J, Zhou J, Liu C, Yin J. N-acetyl-galactosamine modified metal-organic frameworks to inhibit the growth and pulmonary metastasis of liver cancer stem cells through targeted chemotherapy and starvation therapy. *Acta Biomater* 2022; **151**: 588-599 [PMID: 36002126 DOI: 10.1016/j.actbio.2022.08.027]
67 **Zhu X**, Li L, Tang J, Yang C, Yu H, Liu K, Zheng Z, Gu X, Yu Q, Xu FJ, Gan Z. Cascade-responsive nano-assembly for efficient photothermal-chemo synergistic inhibition of tumor metastasis by targeting cancer stem cells. *Biomaterials* 2022; **280**: 121305 [PMID: 34890970 DOI: 10.1016/j.biomaterials.2021.121305]
68 **Chen D**, Pan X, Xie F, Lu Y, Zou H, Yin C, Zhang Y, Gao J. Codelivery of doxorubicin and elacridar to target both liver cancer cells and stem cells by polylactide-co-glycolide/d-alpha-tocopherol polyethylene glycol 1000 succinate nanoparticles. *Int J Nanomedicine* 2018; **13**: 6855-6870 [PMID: 30498347 DOI: 10.2147/IJN.S181928]
69 **Pradhan R**, Chatterjee S, Hembram KC, Sethy C, Mandal M, Kundu CN. Nano formulated Resveratrol inhibits metastasis and angiogenesis by reducing inflammatory cytokines in oral cancer cells by targeting tumor associated macrophages. *J Nutr Biochem* 2021; **92**: 108624 [PMID: 33705943 DOI: 10.1016/j.jnutbio.2021.108624]
70 **Lang T**, Liu Y, Zheng Z, Ran W, Zhai Y, Yin Q, Zhang P, Li Y. Cocktail Strategy Based on Spatio-Temporally Controlled Nano Device Improves Therapy of Breast Cancer. *Adv Mater* 2019; **31**: e1806202 [PMID: 30516854 DOI: 10.1002/adma.201806202]
71 **Guimarães D**, Cavaco-Paulo A, Nogueira E. Design of liposomes as drug delivery system for therapeutic applications. *Int J Pharm* 2021; **601**: 120571 [PMID: 33812967 DOI: 10.1016/j.ijpharm.2021.120571]

72 **Shen S**, Lin S, Chen Y, Zhang Y, He Y, Xu X, Feng Y, Lu Y, Mo R. Combating Cancer Stem-Like Cell-Derived Resistance to Anticancer Protein by Liposome-Mediated Acclimatization Strategy. *Nano Lett* 2022; **22**: 2419-2428 [PMID: 35254834 DOI: 10.1021/acs.nanolett.2c00004]

73 **Gong Z**, Chen D, Xie F, Liu J, Zhang H, Zou H, Yu Y, Chen Y, Sun Z, Wang X, Zhang G, Yin C, Gao J, Zhong Y, Lu Y. Codelivery of salinomycin and doxorubicin using nanoliposomes for targeting both liver cancer cells and cancer stem cells. *Nanomedicine (Lond)* 2016; **11**: 2565-2579 [PMID: 27647449 DOI: 10.2217/nnm-2016-0137]

74 **Inamura K**, Komizu Y, Yamakuchi M, Ishida S, Matsumoto Y, Matsushita T. Inhibitory effect of hybrid liposomes on the growth of liver cancer stem cells. *Biochem Biophys Res Commun* 2019; **509**: 268-274 [PMID: 30583860 DOI: 10.1016/j.bbrc.2018.12.118]

75 **Huang CW**, Jiang XX, Yin XB, Huang YY, Lei K, Xiong H. Research of FTC-CD133 Nanoparticles Inhibiting the Drug Resistance of Liver Cancer Stem Cell. *Zhongguo Quanke Yixue* 2016; **19**: 184-189

76 **Arthur P**, Patel N, Surapaneni SK, Mondal A, Gebeyehu A, Bagde A, Kutlehria S, Nottingham E, Singh M. Targeting lung cancer stem cells using combination of Tel and Docetaxel liposomes in 3D cultures and tumor xenografts. *Toxicol Appl Pharmacol* 2020; **401**: 115112 [PMID: 32540278 DOI: 10.1016/j.taap.2020.115112]

77 **Basu SM**, Yadava SK, Singh R, Giri J. Lipid nanocapsules co-encapsulating paclitaxel and salinomycin for eradicating breast cancer and cancer stem cells. *Colloids Surf B Biointerfaces* 2021; **204**: 111775 [PMID: 33940518 DOI: 10.1016/j.colsurfb.2021.111775]

78 **Oh E**, Hong MY, Lee D, Nam SH, Yoon HC, Kim HS. Inhibition assay of biomolecules based on fluorescence resonance energy transfer (FRET) between quantum dots and gold nanoparticles. *J Am Chem Soc* 2005; **127**: 3270-3271 [PMID: 15755131 DOI: 10.1021/ja0433323]

79 **Zheng J**, Cheng X, Zhang H, Bai X, Ai R, Shao L, Wang J. Gold Nanorods: The Most Versatile Plasmonic Nanoparticles. *Chem Rev* 2021; **121**: 13342-13453 [PMID: 34569789 DOI: 10.1021/acs.chemrev.1c00422]

80 **Dubertret B**, Skourides P, Norris DJ, Noireaux V, Brivanlou AH, Libchaber A. In vivo imaging of quantum dots encapsulated in phospholipid micelles. *Science* 2002; **298**: 1759-1762 [PMID: 12459582 DOI: 10.1126/science.1077194]

81 **Shamsian A**, Sepand MR, Javaheri Kachousangi M, Dara T, Ostad SN, Atyabi F, Ghahremani MH. Targeting Tumorigenicity of Breast Cancer Stem Cells Using SAHA/Wnt-b Catenin Antagonist Loaded Onto Protein Corona of Gold Nanoparticles. *Int J Nanomedicine* 2020; **15**: 4063-4078 [PMID: 32606664 DOI: 10.2147/IJN.S234636]

82 **Ding J**, Xu W, Tan J, Liu Z, Huang G, Wang S, He Z. Fluorescence Detection of Cancer Stem Cell Markers Using a Sensitive Nano-Aptamer Sensor. *Front Chem* 2022; **10**: 920123 [PMID: 35815217 DOI: 10.3389/fchem.2022.920123]

83 **Poonaki E**, Nickel AC, Shafiee Ardestani M, Rademacher L, Kaul M, Apartsin E, Meuth SG, Gorji A, Janiak C, Kahlert UD. CD133-Functionalized Gold Nanoparticles as a Carrier Platform for Telaglenastat (CB-839) against Tumor Stem Cells. *Int J Mol Sci* 2022; **23** [PMID: 35628289 DOI: 10.3390/ijms23105479]

84 **Yi Y**, Kim HJ, Zheng M, Mi P, Naito M, Kim BS, Min HS, Hayashi K, Perche F, Toh K, Liu X, Mochida Y, Kinoh H, Cabral H, Miyata K, Kataoka K. Glucose-linked sub-50-nm unimer polyion complex-assembled gold nanoparticles for targeted siRNA delivery to glucose transporter 1-overexpressing breast cancer stem-like cells. *J Control Release* 2019; **295**: 268-277 [PMID: 30639386 DOI: 10.1016/j.jconrel.2019.01.006]

85 **Zhao Y**, Zhao W, Lim YC, Liu T. Salinomycin-Loaded Gold Nanoparticles for Treating Cancer Stem Cells by Ferroptosis-Induced Cell Death. *Mol Pharm* 2019; **16**: 2532-2539 [PMID: 31009228 DOI: 10.1021/acs.molpharmaceut.9b00132]

86 **Burke AR**, Singh RN, Carroll DL, Wood JC, D'Agostino RB Jr, Ajayan PM, Torti FM, Torti SV. The resistance of breast cancer stem cells to conventional hyperthermia and their sensitivity to nanoparticle-mediated photothermal therapy. *Biomaterials* 2012; **33**: 2961-2970 [PMID: 22245557 DOI: 10.1016/j.biomaterials.2011.12.052]

87 **Wang J**, Liu N, Su Q, Lv Y, Yang C, Zhan H. Green Synthesis of Gold Nanoparticles and Study of Their Inhibitory Effect on Bulk Cancer Cells and Cancer Stem Cells in Breast Carcinoma. *Nanomaterials (Basel)* 2022; **12** [PMID: 36234451 DOI: 10.3390/nano12193324]

88 **Cheng Z**, Li M, Dey R, Chen Y. Nanomaterials for cancer therapy: current progress and perspectives. *J Hematol Oncol* 2021; **14**: 85 [PMID: 34059100 DOI: 10.1186/s13045-021-01096-0]

89 **Wang CH**, Chiou SH, Chou CP, Chen YC, Huang YJ, Peng CA. Photothermolysis of glioblastoma stem-like cells targeted by carbon nanotubes conjugated with CD133 monoclonal antibody. *Nanomedicine* 2011; **7**: 69-79 [PMID: 20620237 DOI: 10.1016/j.nano.2010.06.010]

90 **Yao HJ**, Zhang YG, Sun L, Liu Y. The effect of hyaluronic acid functionalized carbon nanotubes loaded with salinomycin on gastric cancer stem cells. *Biomaterials* 2014; **35**: 9208-9223 [PMID: 25115788 DOI: 10.1016/j.biomaterials.2014.07.033]

91 **Al Faraj A**, Shaik AS, Ratemi E, Halwani R. Combination of drug-conjugated SWCNT nanocarriers for efficient therapy of cancer stem cells in a breast cancer animal model. *J Control Release* 2016; **225**: 240-251 [PMID: 26827662 DOI: 10.1016/j.jconrel.2016.01.053]

92 **Fiorillo M**, Verre AF, Iliut M, Peiris-Pagés M, Ozsvari B, Gandara R, Cappello AR, Sotgia F, Vijayaraghavan A, Lisanti MP. Graphene oxide selectively targets cancer stem cells, across multiple tumor types: implications for non-toxic cancer treatment, *via* "differentiation-based nano-therapy". *Oncotarget* 2015; **6**: 3553-3562 [PMID: 25708684 DOI: 10.18632/oncotarget.3348]

93 **Choi YJ**, Gurunathan S, Kim JH. Graphene Oxide-Silver Nanocomposite Enhances Cytotoxic and Apoptotic Potential of Salinomycin in Human Ovarian Cancer Stem Cells (OvCSCs): A Novel Approach for Cancer Therapy. *Int J Mol Sci* 2018; **19** [PMID: 29494563 DOI: 10.3390/ijms19030710]

94 **Nunes T**, Hamdan D, Leboeuf C, El Bouchtaoui M, Gapihan G, Nguyen TT, Meles S, Angeli E, Ratajczak P, Lu H, Di Benedetto M, Bousquet G, Janin A. Targeting Cancer Stem Cells to Overcome Chemoresistance. *Int J Mol Sci* 2018; **19** [PMID: 30551640 DOI: 10.3390/ijms19124036]

95 **Li J**, Chen L, Su H, Yan L, Gu Z, Chen Z, Zhang A, Zhao F, Zhao Y. The pharmaceutical multi-activity of metallofullerenol invigorates cancer therapy. *Nanoscale* 2019; **11**: 14528-14539 [PMID: 31364651 DOI: 10.1039/c9nr04129j]

96 **Yang B**, Liu H, Yang H, Chen W, Wu J, Feng X, Tong R, Yu H, Chen Y, Lv Z, Sun W, He B, Yu G, Mao Z, Zheng S. Combinatorial photochemotherapy on liver cancer stem cells with organoplatinum(ii) metallacage-based nanoparticles. *J Mater Chem B* 2019; **7**: 6476-6487 [PMID: 31465082 DOI: 10.1039/c9tb01299k]

97 **Pan Y**, Ma X, Liu C, Xing J, Zhou S, Parshad B, Schwerdtle T, Li W, Wu A, Haag R. Retinoic Acid-Loaded Dendritic Polyglycerol-Conjugated Gold Nanostars for Targeted Photothermal Therapy in Breast Cancer Stem Cells. *ACS Nano* 2021; **15**: 15069-15084 [PMID: 34420298 DOI: 10.1021/acsnano.1c05452]

98 **Cao W**, Liu B, Xia F, Duan M, Hong Y, Niu J, Wang L, Liu Y, Li C, Cui D. MnO(2)@Ce6-loaded mesenchymal stem cells as an "oxygen-laden guided-missile" for the enhanced photodynamic therapy on lung cancer. *Nanoscale* 2020; **12**: 3090-3102 [PMID: 31965129 DOI: 10.1039/c9nr07947e]

99 **Haldavnekar R**, Vijayakumar SC, Venkatakrishnan K, Tan B. Prediction of Cancer Stem Cell Fate by Surface-Enhanced Raman Scattering

Functionalized Nanoprobes. *ACS Nano* 2020; **14**: 15468-15491 [PMID: 33175514 DOI: 10.1021/acsnano.0c06104]

100 **Liu J**, Smith S, Wang C. Photothermal Attenuation of Cancer Cell Stemness, Chemoresistance, and Migration Using CD44-Targeted MoS(2) Nanosheets. *Nano Lett* 2023; **23**: 1989-1999 [PMID: 36827209 DOI: 10.1021/acs.nanolett.3c00089]

101 **Laurent S**, Dutz S, Häfeli UO, Mahmoudi M. Magnetic fluid hyperthermia: focus on superparamagnetic iron oxide nanoparticles. *Adv Colloid Interface Sci* 2011; **166**: 8-23 [PMID: 21601820 DOI: 10.1016/j.cis.2011.04.003]

102 **Ni Z**, Nie X, Zhang H, Wang L, Geng Z, Du X, Qian H, Liu W, Liu T. Atranorin driven by nano materials SPION lead to ferroptosis of gastric cancer stem cells by weakening the mRNA 5-hydroxymethylcytidine modification of the Xc-/GPX4 axis and its expression. *Int J Med Sci* 2022; **19**: 1680-1694 [PMID: 36237989 DOI: 10.7150/ijms.73701]

103 **Yoon HJ**, Kim TH, Zhang Z, Azizi E, Pham TM, Paoletti C, Lin J, Ramnath N, Wicha MS, Hayes DF, Simeone DM, Nagrath S. Sensitive capture of circulating tumour cells by functionalized graphene oxide nanosheets. *Nat Nanotechnol* 2013; **8**: 735-741 [PMID: 24077027 DOI: 10.1038/nnano.2013.194]

104 **Liu D**, Hong Y, Li Y, Hu C, Yip TC, Yu WK, Zhu Y, Fong CC, Wang W, Au SK, Wang S, Yang M. Targeted destruction of cancer stem cells using multifunctional magnetic nanoparticles that enable combined hyperthermia and chemotherapy. *Theranostics* 2020; **10**: 1181-1196 [PMID: 31938059 DOI: 10.7150/thno.38989]

105 **Ji T**, Zhao Y, Ding Y, Nie G. Using functional nanomaterials to target and regulate the tumor microenvironment: diagnostic and therapeutic applications. *Adv Mater* 2013; **25**: 3508-3525 [PMID: 23703805 DOI: 10.1002/adma.201300299]

World Journal of Stem Cells

Submit a Manuscript: https://www.f6publishing.com

World J Stem Cells 2023 June 26; 15(6): 530-547

DOI: 10.4252/wjsc.v15.i6.530

ISSN 1948-0210 (online)

REVIEW

Neural lineage differentiation of human pluripotent stem cells: Advances in disease modeling

Yuan-Wei Yan, Eddie S Qian, Lauren E Woodard, Julie Bejoy

Specialty type: Neurosciences

Provenance and peer review: Invited article; Externally peer reviewed.

Peer-review model: Single blind

Peer-review report's scientific quality classification

Grade A (Excellent): 0
Grade B (Very good): B
Grade C (Good): C
Grade D (Fair): 0
Grade E (Poor): 0

P-Reviewer: Bagheri-Mohammadi S, Iran; Liu QS, China

Received: February 16, 2023
Peer-review started: February 16, 2023
First decision: February 28, 2023
Revised: March 14, 2023
Accepted: April 27, 2023
Article in press: April 24, 2023
Published online: June 26, 2023

Yuan-Wei Yan, Waisman Center, University of Wisconsin-Madison, Madison, WI 53705, United States

Eddie S Qian, Nephrology and Hypertension, Vanderbilt University Medical Center, Nashville, TN 37232, United States

Lauren E Woodard, Julie Bejoy, Department of Medicine, Vanderbilt University Medical Center, Nashville, TN 37232, United States

Lauren E Woodard, Department of Veterans Affairs, Tennessee Valley Healthcare System, Nashville, TN 37232, United States

Lauren E Woodard, Biomedical Engineering, Vanderbilt University, Nashville, TN 37232, United States

Corresponding author: Julie Bejoy, PhD, Research Fellow, Department of Medicine, Vanderbilt University Medical Center, 1161, No. 21 Avenue, Nashville, TN 37232, United States. julie.bejoy@vumc.org

Abstract

Brain diseases affect 1 in 6 people worldwide. These diseases range from acute neurological conditions such as stroke to chronic neurodegenerative disorders such as Alzheimer's disease. Recent advancements in tissue-engineered brain disease models have overcome many of the different shortcomings associated with the various animal models, tissue culture models, and epidemiologic patient data that are commonly used to study brain disease. One innovative method by which to model human neurological disease is *via* the directed differentiation of human pluripotent stem cells (hPSCs) to neural lineages including neurons, astrocytes, and oligodendrocytes. Three-dimensional models such as brain organoids have also been derived from hPSCs, offering more physiological relevance due to their incorporation of various cell types. As such, brain organoids can better model the pathophysiology of neural diseases observed in patients. In this review, we will emphasize recent developments in hPSC-based tissue culture models of neurological disorders and how they are being used to create neural disease models.

Key Words: Induced pluripotent stem cells; Astrocytes; Oligodendrocytes; Microglia; Brain organoids; Assembloids

Core Tip: This review discusses recent advances in the field of disease modeling using human-induced pluripotent stem cell-derived neural cell types as well as organoids. It also discusses challenges that exist with current approaches, in addition to considerations for possible improvements that will further advance the field of disease modeling.

Citation: Yan YW, Qian ES, Woodard LE, Bejoy J. Neural lineage differentiation of human pluripotent stem cells: Advances in disease modeling. *World J Stem Cells* 2023; 15(6): 530-547
URL: https://www.wjgnet.com/1948-0210/full/v15/i6/530.htm
DOI: https://dx.doi.org/10.4252/wjsc.v15.i6.530

INTRODUCTION

Human pluripotent stem cells (hPSCs) include both human embryonic stem cells (hESCs) and human-induced PSCs (hiPSCs). Current *in vitro* disease models that use hiPSCs begin with skin or blood cells that have been reprogramed with the four transcriptional elements octamer-binding transcription factor 4, SRY-box 2, Krüppel-like factor 4, and MYC[1]. Through differentiation, these hPSCs are the starting material to create models for different organs including the brain [2], kidney[3], liver[4,5], lung[6], and pancreas[7]. These models are able to simulate a "disease-in-a-dish", mimicking different disease phenotypes *in vitro*[8,9]. Both genetically modified hiPSCs and patient-derived hiPSCs can generate disease models[10-12]. These models are advantageous because of their accessibility, quick processing, and species-specific human attributes. Patient-derived hiPSCs can also be used to test personalized medicine approaches to effectively model gene mutations and chromosomal abnormalities. To study neurological diseases, scientists have generated multiple neural cell types from hPSCs including neurons[13], astrocytes[14], and oligodendrocytes (OLs)[15]. In the past decade, advancements in disease modeling and tissue engineering have also led to the "brain organoid" model[16]. Brain organoids are self-assembled structures that resemble the fetal human brain and are composed of progenitor, neuronal, and glial cells. A related system is the spheroid, a circular aggregate of cells that may reflect biological properties of an organ system but ultimately lacks structural complexity. Perhaps the most cutting-edge form of modeling technology in stem-cell research is the assembloid, which are three-dimensional (3D) structures made by fusing and integrating two or more cell types or organoids from different organ culture protocols[17]. These assembloids can model the organ crosstalk interactions that occur across physiological systems in the human body.

In this review, we discuss recent advancements in the field of disease modeling using hiPSC-derived neural cell types as well as organoids. We also discuss challenges that exist with current approaches, in addition to considerations for possible improvements that will further advance the field of disease modeling.

NEURAL CELL TYPE DIFFERENTIATION FROM HPSCS

Neural progenitors

The development of the mammalian brain initially occurs at the gastrula stage when the ectoderm differentiates to form the neural tube. This process is called neural induction, wherein neural tube cells become neural progenitors[18,19]. These progenitors subsequently give rise to specific neuronal subtypes along the rostral-caudal axis and dorsal-ventral axis[20]. Protocols for neural progenitor differentiation from hPSCs have been developed that reflect this neural induction principle (Table 1). In 2001, the first protocol of neural progenitor differentiation from hPSCs was developed using the embryoid body (EB) method, which was a combined two-dimensional (2D) monolayer and 3D suspension culture[21]. Without extrinsic factors, the EB method mainly derived dorsal forebrain cortical neurons. In 2008, advances in the EB method eventually gave rise to a complete 3D culture system called the serum-free floating culture of EB-like aggregates with quick aggregation (SFEBq)[22]. The SFEBq method generated neural tissues with self-organized structure using hPSCs, paving the way for the development of more complex systems such as brain spheroids and organoids. Following this advance, in 2009 the dual SMAD inhibition method was developed, which successfully directed over 80% of hESCs to induce neural differentiation[23]. The dual SMAD inhibition method was initially intended for 2D monolayer culture by inhibiting the bone morphogenetic protein (BMP) and transforming growth factor beta (TGF-β) signaling pathways, but it has been widely applied to 3D culture for neural progenitor differentiation from hPSCs. It is worth noting that both the SFEBq and dual SMAD inhibition methods can enable the generation of cortical spheroids and organoids[24-26]. In 2017, Studer's group modified the dual SMAD inhibition protocol to also block mitogen-activated protein kinase (MAPK), fibroblast growth factor (FGF), and Notch signaling, thereby accelerating forebrain cortical neuron derivation[27]. Although these protocols yield primarily deep-layer cortical neurons, deriving upper layer cortical neurons such as L2/3 and L4 cells is still a challenge.

Table 1 Comparison of methods for neural induction from human pluripotent stem cells

Method	Neural induction outcomes	Significance	Ref.
Embryoid bodies; selected neural rosettes; 2D and 3D culture	Neural tube-like rosettes stained with Nestin, Musashi-1 and NCAM; positive neuronal markers MAP2 and TUJ1 expression	First study of neural progenitor differentiation from hPSCs	Zhang *et al*[22], 2001
SFEBq aggregate; sorting cells; 3D culture	Self-organized structure with four distinct zones: ventricular, early and late cortical-plate, and Cajal-Retzius cell zones	Pure 3D culture, provides the basis for the brain organoid method	Eiraku *et al*[23], 2008
Dual SMAD inhibition; 2D monolayer culture	Complete neural conversion of > 80% of hESCs	Mostly wild used method; also enables neural induction in 3D culture	Chambers *et al*[24], 2009
Dual SMAD inhibition combined with retinoid signaling; 2D monolayer culture	More than 95% of hPSCs were PAX6 and OTX1/2 cortical progenitor cells in 15 d	Improved the dual SMAD inhibition protocol and higher neural induction efficiency	Shi *et al*[62], 2012
Cortical organoid/spheroid; 3D culture	Form layered structure tissues partially mimicking human cerebral cortex	Mostly brain-like tissue with some functions	Lancaster *et al*[17], 2013; Paşca *et al*[26], 2015; Qian *et al*[27], 2016
Dual SMAD inhibition combined with Wnt, FGF and Notch inhibition	Generate functional cortical neuron in 16 d	Improved the dual SMAD inhibition protocol and accelerated neural induction	Qi *et al*[28]

EB: Embryoid body; FGF: Fibroblast growth factor; hPSCs: Human pluripotent stem cells; MAP2: Microtubule-associated protein 2; NCAM: Neural cell adhesion molecule; OTX: Orthodenticle homeobox; PAX6: Paired box 6; SFEBq: Serum-free floating culture of EB-like aggregates with quick aggregation.

Astrocytes

Astrocytes are star-shaped populations of glial cells that help maintain homeostatic balance and support neuron growth within the central nervous system. There are two distinct groups of astrocytes: The highly branching protoplasmic astrocytes of the grey matter and the fibrous astrocytes found in the white matter that interact with OLs and axons[28]. Activated astrocytes can release neuroinflammatory cytokines and chemokines that mediate intercellular communication with microglia and invoke various neuroinflammatory responses. Similar to neurons, there are many subtypes of astrocytes depending on their location, morphology, molecular signature, and physiological function. The differentiation of glia cells from hPSCs usually takes more time and is more complicated than differentiating a neuron (Figure 1).

During brain development, astrocytes differentiate from radial glia or neural progenitors at the subventricular zone. It is currently unknown what signaling regulates the regional identity of astrocytes. The differentiation of astrocytes is usually initiated by inhibition of dual SMAD signaling using small molecules or by the EB method to generate neuroepithelial cells. Glial progenitors expressing nuclear factor IA (NFIA), S100β, and cluster of differentiation 44 (CD44) are derived from these neuroepithelial cells[29]. Ultimately, mature astrocytes are generated from radial glia by activating the signal transducer and activator of transcription 2 signaling pathway using ciliary neurotrophic factor. The most common marker for astrocytes is glial fibrillary acidic protein (GFAP)[30]. Mature astrocytes express aldehyde dehydrogenase family 1 member L1, aldolase C, glutamate transporter-1, and aquaporin 4[31]. In 2011, the first reported protocol for hPSC-derived astrocytes in a chemically defined system required long-term culture of up to 6 mo[29,32]. This protocol used the EB method and supported differentiation through the addition of the factors FGF2 and epidermal growth factor (EGF). To attenuate the culture time, shorter 4-6 wk long accelerated protocols for generating functional astrocytes through overexpression of the transcription factors SOX9 and NFIB were developed[33,34]. In 2017, the Pasca lab found a method to derive functional astrocytes using 3D cortical organoids. However, this protocol required up to 590 d, limiting its application[30]. The majority of recent studies use commercially available astrocyte differentiation medium to differentiate astrocytes from neural progenitor cells[35,36].

Astrocytopathies including Alexander disease[37,38], Aicardi-Goutières syndrome (AGS)[39], and vanishing white matter disease[40] can be effectively modeled with hiPSC-derived astrocytes[41]. Neurodegenerative diseases including Alzheimer's disease (AD)[36], Parkinson's disease (PD)[42], and Huntington's disease have also been modeled using similar methods. The familial presenilin-1 (*PS1*) mutation along with PD familial leucine-rich repeat kinase 2 (*LRRK2*) G2019S mutations were both modeled using hiPSC-derived astrocytes. The results showed the crucial role of astrocytes in the disease pathogenesis of AD and PD, respectively[36,42]. When co-cultured with neurons, astrocytes generated from Huntington's disease patient-derived hiPSCs displayed decreased electrophysiological activity and diminished neuroprotection consistent with Huntington's disease[43]. Regarding *in vitro* stroke modeling, ischemia-like conditions can be simulated by replacing normal oxygen (O_2)/carbon dioxide ($CO_{2)}$ conditions with nitrogen (N_2)/CO_2 and subjecting cells to glucose deprivation[44,45]. However, cultures in 2D cannot effectively model stroke due logistical difficulties in restricting oxygenation as well as maintaining nutrition deprivation. However, Wevers *et al*[46] used neurovascular unit on-a-chip, which included a triculture of brain vascular cells, hiPSC-astrocytes, and hiPSC-neurons to model ischemic stroke. The study used antimycin-A, an inhibitor of complex III of the electron transport chain, to induce hypoxic conditions[45]. Modeling the motor neuron pathology linked to amyotrophic lateral sclerosis (ALS) was achieved using hiPSC-derived astrocytes from a patient who had the C9ORF72 mutation[46,47]. Recent studies also reported generation of ventral spinal cord-like astrocytes, which better reflect ALS pathophysiology[48]. Zika virus targeting of astrocytes has

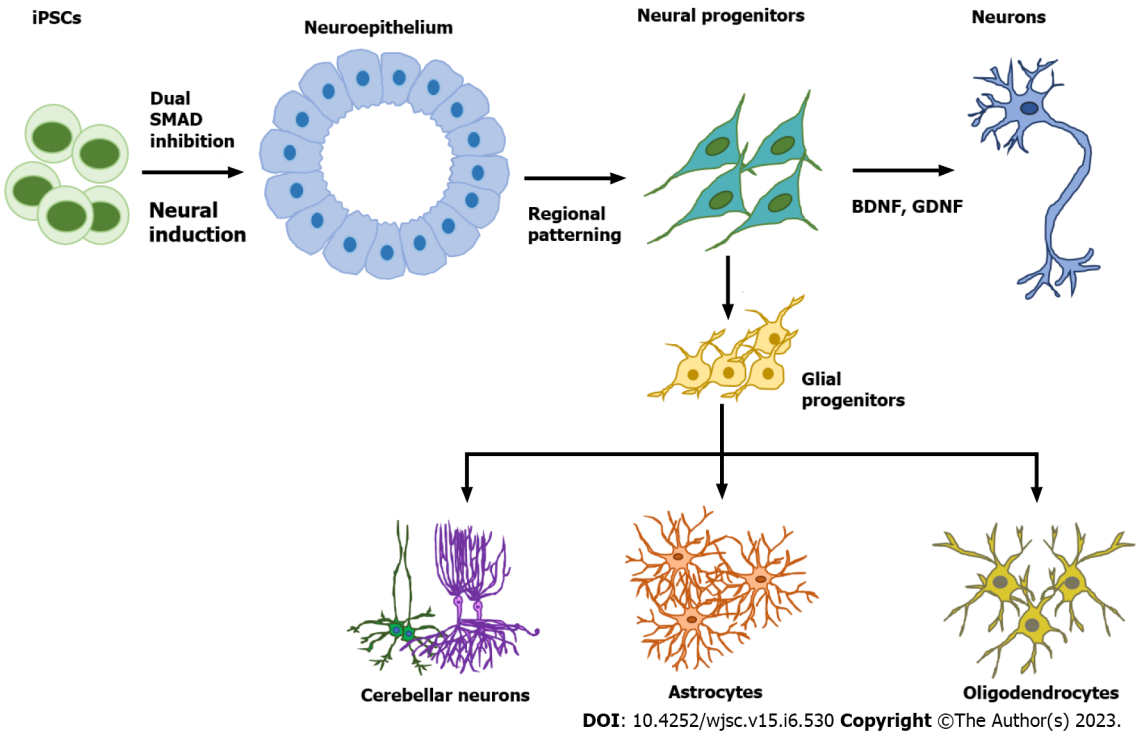

DOI: 10.4252/wjsc.v15.i6.530

Figure 1 Neural cell subtype differentiation from human pluripotent stem cells. The first step of neural cell differentiation is neural induction to generate neuroepithelial cells, usually by the dual SMAD inhibition method. Specific neural progenitors can be generated by tuning different signaling pathways such as Sonic Hedgehog, Wingless/integrated, retinoic acid, and bone morphogenetic protein. Neural progenitors can then be directed to become mature neurons through induction with neurotrophic factors such as brain-derived neurotrophic factor and glial cell line-derived neurotrophic factor or derived into glial progenitors through treatment with the growth factors fibroblast growth factor 2 and epidermal growth factor. Glial progenitors can give rise to either astrocytes or oligodendrocytes. BDNF: Brain-derived neurotrophic factor; GDNF: Glial cell line-derived neurotrophic factor.

also been studied using hiPSC-derived astrocytes, which corroborated the reactive oxygen species imbalance, mitochondrial abnormalities, and DNA damage observed after Zika virus infection[49]. Astrocytes derived from hiPSCs are also beneficial in modeling neurodevelopment disorders including Down's syndrome[50-53], Rett syndrome[54-57], and schizophrenia[58,59]. Rare genetic diseases such as the lysosomal storage disorder Gaucher disease can be modeled using patient hiPSC-derived astrocytes[60,61] (Figure 1, Table 1).

Oligodendrocytes

Protocols to differentiate hiPSCs into pre-OL progenitors were first established in 2012[62]. Retinoic acid (RA) and purmorphamine, a small-molecule agonist of Sonic Hedgehog (Shh) signaling, were used to make pre-OL progenitors that express the markers oligodendrocyte transcription factor 2 (OLIG2) and NK2 homeobox 2. Pre-OL progenitors were then further differentiated into bipotential OL progenitor cells (OPCs) that expressed markers SOX10 and platelet-derived growth factor receptor alpha (PDGFRA) using PDGF-AA, triiodothyronine, and neurotrophin-3. The OPCs at this stage were further developed into either $O4^+$ and myelin basic protein-positive (MBP^+) human-induced OLs or $GFAP^+$ astrocytes. OPCs ameliorate neurological deterioration and support survival of *shiverer* mice after engraftment[62]. However, this protocol requires a lengthy 120-d culture period. Efficient and robust generation of hiPSC-derived OPCs in 95 d has been achieved more recently[63,64]. Improved differentiation of myelinating OLs was obtained using brain extracellular matrix from decellularized human brain tissue[65]. Fast and efficient OL generation has additionally been achieved with SOX10 overexpression, either by introducing lentiviral vectors at the neuroepithelial stage or by direct transfection of hiPSCs prior to differentiation[66,67].

Shaker *et al*[68] published a 42-d protocol to derive organoids containing myelinating human OLs and astrocytes. Differentiated OLs that were produced using hiPSCs from primary progressive multiple sclerosis patients were found to be functional and supported *in vivo* myelination in *shiverer* mice[63]. Death of OLs is a hallmark of Pelizaeus-Merzbacher disease, an X-linked leukodystrophy caused by mutations in proteolipid protein 1 (PLP1)[63]. Human-induced OLs from individuals with PLP1 mutations have helped to identify important subgroups based on cell-intrinsic phenotypes and to elucidate the pathogenesis of various PLP1 mutations[15,68]. Involvement of OLs in neurodegenerative diseases, including AD and PD as well as multiple system atrophy[69], have also been studied using human-induced OLs.

OTHER CELL TYPES OF THE CENTRAL NERVOUS SYSTEM

Microglia

Although murine models have been the main tool for studying the genetics and function of microglia, there are important distinctions between murine microglia and human microglia when it comes to aging and associated diseases[70,71]. Historically, viable microglia cells have been obtained by extracting them from brain tumors or epileptic foci removed from surgery, but this procedure is logistically very challenging. These hurdles were reduced when multiple methods to differentiate microglia from hPSCs were developed[70-75]. Muffat *et al*[73] published the first protocol by producing microglia-like cells from regular and patient hESCs and hiPSCs. This method used serum-free neuroglial differentiation media, which contained various components with concentrations adjusted to biologically match human cerebrospinal fluid. Abud *et al*[76] described a two-step method to successfully derive microglia-like cells (iMGLs) from 10 different hiPSC lines in 5 wk. The transcriptome profile of the derived iMGLs was strikingly similar to that of both adult human and fetal microglia[75]. Most microglial directed differentiation protocols involve hematopoiesis[73,75,76]. Some reported studies use chemically-defined protocols to generate human microglia through the formation of myeloid progenitors in 30 d[77]. Ionized calcium binding adapter molecule 1, a protein that belongs to the calcium-binding protein family, is one of the main markers of microglia[78]. It is primarily involved in rearranging cytoskeleton and has been used as a marker for the 3D reconstruction of microglial cells[79,80]. Other general markers used for microglial identification are CD45 and CX3C motif chemokine receptor 1. In a recent study, Dräger *et al*[81] described an effective 8-d protocol for generating induced transcription factor microglia-like cells (iTF-Microglia) based on the inducible expression of six transcription factors (human MAF BZIP transcription factor B, CCAAT enhancer-binding protein, interferon regulatory factor (IRF8) PU.1, and IRF5).

The risk of developing late-onset AD is linked to several genes, including triggering receptor expressed on myeloid cells 2 (*TREM2*) and *CD33* expressed by microglia. Microglia accumulate around amyloid plaques during AD and exacerbate pathophysiology by secreting cytokines and chemokines that induce inflammation. Microglia that have been generated using hiPSCs can be effectively used to model neurological diseases *in vitro*[80,81]. Alternatively, microglia derived from patient hiPSCs have also been used for modeling neurodegenerative diseases. Recently, patient hiPSCs expressing the AD-linked R47Hhet *TREM2* variant was used to elucidate the signal transduction deficit observed during AD progression[82]. Another study using microglia derived from AD patient hiPSCs reported that dysregulated peroxisome proliferator-activated receptor gamma (PPARγ)/p38 MAPK signaling causes the phenotypic deficits observed in *TREM2* variants. The results of this study concluded that the activation of PPARγ/p38MAPK signaling can ameliorate metabolic deficits within these cells and consequently rescue critical microglial cellular functions such as β-amyloid phagocytosis[83].

BRAIN ORGANOID DEVELOPMENT FROM HPSCS

Protocols for producing brain organoids were derived from the EB and SFEBq methods for neural induction. The formation of brain organoids is based on the self-organization and self-renewal of stem cells to generate a mixed cell population in 3D suspension culture (Figure 2). In 2013, the first study on brain organoids was reported to generate whole brain tissues with regional specific structures using an EB-based culture involving Matrigel support in a spinning bioreactor[24]. The organoids were used to model microcephaly, a neurodevelopmental disease whose pathologic features are difficult to recapitulate using animal models. This was the first work done to generate brain-like tissue *in vitro* and apply them to study human pathological disorders. In the following years, a simpler method was developed to generate cortical spheroids in 3D static culture without Matrigel and agitation[25]. This method first derived neural progenitors using dual SMAD inhibition and then induced regional specific patterning by supplementing culture with the growth factors FGF2 and EGF. The last step of this protocol extended cultivation of brain aggregates and replaced the growth factors with the neurotrophic factors brain-derived neurotrophic factor (BDNF) and glial cell line-derived neurotrophic factor (GDNF) for up to 3 mo. The generated cortical spheroids exhibited a cortical layer-like structure and were developmentally comparable with the human fetal cortex. Brain spheroids and organoids have been widely used to model human brain development and neurological diseases *in vitro* and have provided a promising platform for drug screening[84] (Table 2, Figure 2).

Forebrain organoids

The areas of the brain originating from the telencephalon and diencephalon are referred to as the forebrain. The telencephalic region consists of the cerebral cortex and cerebellum, whereas the diencephalon includes the thalamus, hypothalamus, and pituitary glands. Self-organized cortical organoids or dorsal forebrain organoids were first reported using the SFEBq method. Multiple cortical layer tissues were generated through inhibition of TGF-β and Wnt signaling, resulting in dorsal-ventral patterning[22,85]. Lancaster *et al*[17] reported the first 3D culture system for deriving cortical organoids from hPSCs. Later, the Pasca lab generated more complex cortical spheroids and organoids from hPSCs, containing both neurons and astrocytes[25] (Figure 3). In following years, several groups attempted to develop protocols to derive cortical organoids from hPSCs. However, a common problem faced by many of these approaches was the presence of multiple ventricular subtypes within each organoid[26,86-91]. Cortical organoids derived from familial AD patient hiPSCs show increased levels of phosphorylated Tau and cytoplasmic neurofibrillary tangle-like deposits[92,93] (Table 1). Recent studies have shown that culture variations have an impact on the AD phenotypes seen in cerebral organoids and should be considered when using these models[94]. Cortical organoids were also used in stroke modeling

Table 2 Comparison of methods for brain organoids generation from human pluripotent stem cells

Organoid type or brain region modeled	Method brief description	Model application	Ref.
EB-like aggregates; cerebral cortex	SFEBq, static suspension culture with cell sorting	Form self-organized structure mimicking the early cortiogenesis	Eiraku *et al*[23], 2008
Cerebral organoid; whole brain	Spinning bioreactor with Matrigel supporting	Form pyramidal identities with spatial separation mimicking the developing human brain at early stage; modeling microcephaly	Lancaster *et al*[17], 2013
Cortical neuroepithelium; cerebral cortex	Improved SFEBq, in 40% oxygen in Lumox plates	Inside-out layer pattern for human cortex	Kadoshima *et al*[86], 2013
Cortical spheroid; cerebral cortex	Static suspension culture with FGF-2 and EGF	Generated laminated cerebral cortex-like structure with some functions	Paşca *et al*[26], 2015
Cerebellar-plate-like neuroepithelium; cerebellum	Static suspension culture with FGF-19 and SDF-1	Mimicking the early development of human cerebellum	Muguruma *et al*[129], 2015
Telencephalic organoids; forebrain	Static suspension culture after neural rosettes isolation manually	Modeling autism spectrum disorder	Mariani *et al*[130], 2015
Dorsomedial telencephalic-like tissue; hippocampus	Improved SFEBq, in 40% oxygen	Modeling the development of human hippocampus	Sakaguchi *et al*[107], 2015
Forebrain organoids; cerebral cortex	Miniaturized spinning bioreactor	Zika virus exposure	Qian *et al*[27], 2016
Midbrain organoids; midbrain	Miniaturized spinning bioreactor	Midbrain organoids contained TH^+ cells	Qian *et al*[27], 2016
Hypothalamic organoids; hypothalamus	Miniaturized spinning bioreactor	Modeling early hypothalamus development	Qian *et al*[27], 2016
Midbrain organoids; midbrain	Static suspension culture on orbital shaker	Midbrain produced neuromelanin and dopamine	Jo *et al*[131], 2016
Pituitary organoid; anterior pituitary	Improved SFEBq	Formed pituitary placode with pituitary hormone-producing cells	Ozone *et al*[132], 2016
Cerebral organoid; cerebral cortex	Microfilament-engineered organoids under agitation	Formed polarized cortical plate and radial units	Lancaster *et al*[133], 2017
Cerebral organoid; whole brain	Spinning bioreactor with Matrigel supporting	Brain organoids formed spontaneously active neuronal networks	Quadrato *et al*[134], 2017
Brain assembloids; assembly dorsal and ventral forebrain organoids	Static suspension culture	Modelling migration of human interneurons and their functional integration into microcircuits using healthy and timothy syndrome cell line	Birey *et al*[99], 2017
Fused cerebral organoids; assembly dorsal and ventral forebrain organoids	Static suspension culture with Matrigel supporting on orbital shaker	Modelling migration of human interneurons in cerebral cortex	Birey *et al*[99], 2017
Fused cortical organoids and MGE organoids	Static suspension culture on orbital shaker	Modelling migration of human interneurons	Xiang *et al*[101], 2017
Neoplastic cerebral organoid	Static suspension culture with Matrigel supporting on orbital shaker	Modelling brain tumorigenesis	Bian *et al*[135], 2018
Granted brain organoids in mouse	Spinning bioreactor	Formed functional networks and blood vessels in the grafts	Mansour *et al*[136], 2018
Cortical spheroid	Static suspension culture	Modelling Alzheimer's disease	Yan *et al*[87], 2018
Cerebral organoids	Static suspension culture with Geltrex supporting on orbital shaker	Modelling Alzheimer's disease	Gonzalez *et al*[93], 2018
Neuromuscular organoid	Static suspension culture supporting on orbital shaker	Formed functional neuromuscular junctions and modelling myasthenia gravis	Faustion Martins *et al*[137], 2020
Section spherical organoid	Manually slicing forebrain organoids	Sliced organoids exhibited separated upper and deep cortical layer	Qian *et al*[90], 2020
Cortico-motor assembloids; assembly cortical spheroids, spinal spheroids, and skeletal muscle spheroids	Static suspension culture	Modeling cortical-motor circuits	Andersen *et al*[18], 2020
Cortico-striatal assembloids; assembly cortical spheroids and striatal spheroids	Static suspension culture	Modeling cortical-striatal circuits and 22q13.3 deletion syndrome	Miura *et al*[102], 2020
Air-liquid interface cerebral organoids	Slicing mature organoids and cultured in air-liquid interface not completely submerged in liquid	Formed network with functional output	Giandomenico *et al*[138], 2019

ASD: Autism spectrum disorder; EGF: Epidermal growth factor; FGF2: Fibroblast growth factor 2; hPSCs: Human pluripotent stem cells; SDF: Stromal cell-derived factor; SFEBq: Serum-free floating culture of EB-like aggregates with quick aggregation.

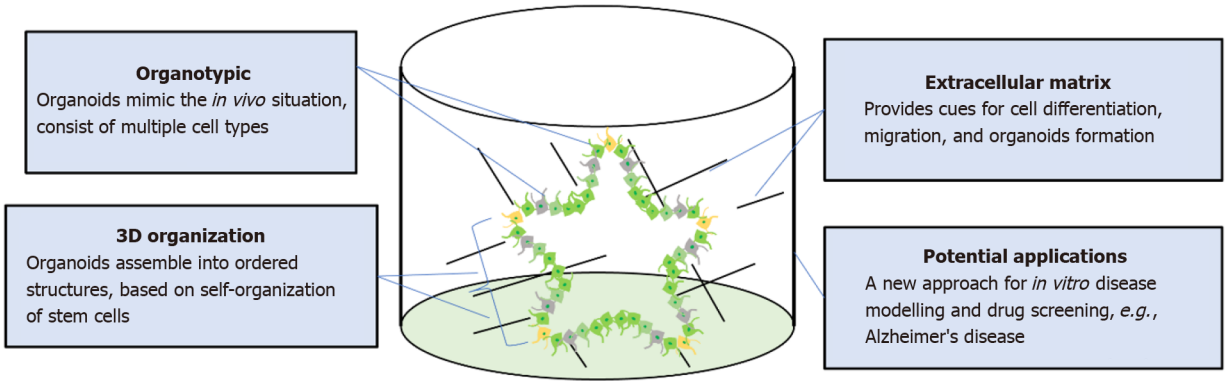

DOI: 10.4252/wjsc.v15.i6.530

Figure 2 Self-organization of brain organoids. Human brain organoids are generated based on the self-organizing properties of stem cells. Organoids usually contain multiple cell types including mature neurons and immature neural progenitors. The key to organoid regeneration is the extracellular matrix that is used to support stem cell growth and differentiation. Brain organoids have been widely utilized to model neurological pathology in disease such as Alzheimer's disease and microcephaly.

to study the effects of oxygen-glucose deprivation (OGD), neuronal death that followed, and damaged neural networks [95]. These models use 2-8 h of OGD with O_2 (0.1%), CO_2 (5.0%), and N_2 (95.0%) gas levels and deoxygenated glucose-free medium to induce ischemia[95]. It has also been discovered that hypoxic conditions can reduce the number of progenitors and impair the differentiation of immature neurons during the development stage of brain organoids[96,97]. Ventral forebrain tissue-like medial ganglionic eminence (MGE) organoids are usually patterned by high Shh and low Wnt signals[85,98]. These MGE organoids contain diverse GABAergic interneurons subtypes including somatostatin, parvalbumin, calretinin, and calbindin. These MGE organoids were assembled to model the migration of human interneurons towards the cerebral cortex[98-100]. In 2020, the Pasca lab reported a method to generate striatal organoids expressing medium spiny neuron markers such as DARPP32 using activin A, IWP-2, and SR11237[101]. Brain organoid technology has also been utilized to generate organoids that can model other regions of forebrain tissue including thalamic organoids[102], hypothalamic organoids[103-105], and hippocampal organoids[106,107].

The hippocampus plays a significant role in learning, memory, and emotion. Hippocampal atrophy or hyperexcitability can cause neurological disorders such as schizophrenia and neurodegenerative diseases like AD. Hippocampal spheroids can be derived from hiPSCs using dual SMAD inhibition, Shh, and Wnt pathway inhibition followed with Wnt activation[107,108]. Commonly reported hippocampal markers include zinc finger and BTB domain-containing 20 and prospero homeobox 1. Hippocampal spheroids can be used to model AD pathology either by the exogenous addition of amyloid beta 42 oligomer[107,108] or by using amyloid precursor protein/PS1 variant hiPSCs. Current hippocampal organoids reflect the early stages of embryonic hippocampus development and successfully can create dentate gyrus granule and carbonic anhydrase 3 (CA3) pyramidal-like neurons, but are unable to produce CA1 pyramidal-like neurons.

Midbrain organoids

The protocol to differentiate human midbrain-like organoids (hMLOs) employs several molecules to mediate the differentiation of neuroepithelial cells. These factors include hBDNF, hGDNF, dibutyryl cyclic adenosine monophosphate, ascorbic acid, TGF-β3, and 1 purmorphamine[109,110]. The presence of dopamine transporter tyrosine hydroxylase as well as the expression of G-protein-regulated inward-rectifier potassium channel 2 are both characteristics of midbrain dopaminergic (mDA) neurons in hMLOs. Common midbrain genes including engrailed, nuclear receptor 4A2, LIM homeobox transcription factor 1 beta (*LMX1B*), *LMX1A*, monoamine oxidase B, calbindin 1, tyrosine hydroxylase, catechol-O-methyltransferase, and dopa-decarboxylase have also been detected in these organoids. Additionally, neurons in hMLOs have been found to exhibit action potentials with large sag currents, indicating the existence of mDA neurons [111] (Figure 3).

According to single cell sequencing studies, hMLOs replicate early embryonic neurodevelopment and recapitulate disease characteristics[112,113]. However, the methods to generate midbrain organoids can take a significant amount of time, and can vary from batch to batch. To scale up the generation of midbrain organoids, Mohamed *et al*[114] recently published microfabricated disk technology using eNUVIO EB-Disks. Another study found that the use of recombinant spider-silk microfibers functionalized with full-length human laminin produced similar ventral midbrain organoids with lower inter-organoid variability[114,115]. Alternatively, an automated approach, termed automated midbrain organoids, was published by Renner *et al*[116] that produced high-throughput 3D midbrain organoids. The high-throughput production of hMLOs from hPSCs in spinner flasks was also reported using TH-TdTomato reporter hPSC lines as well [116].

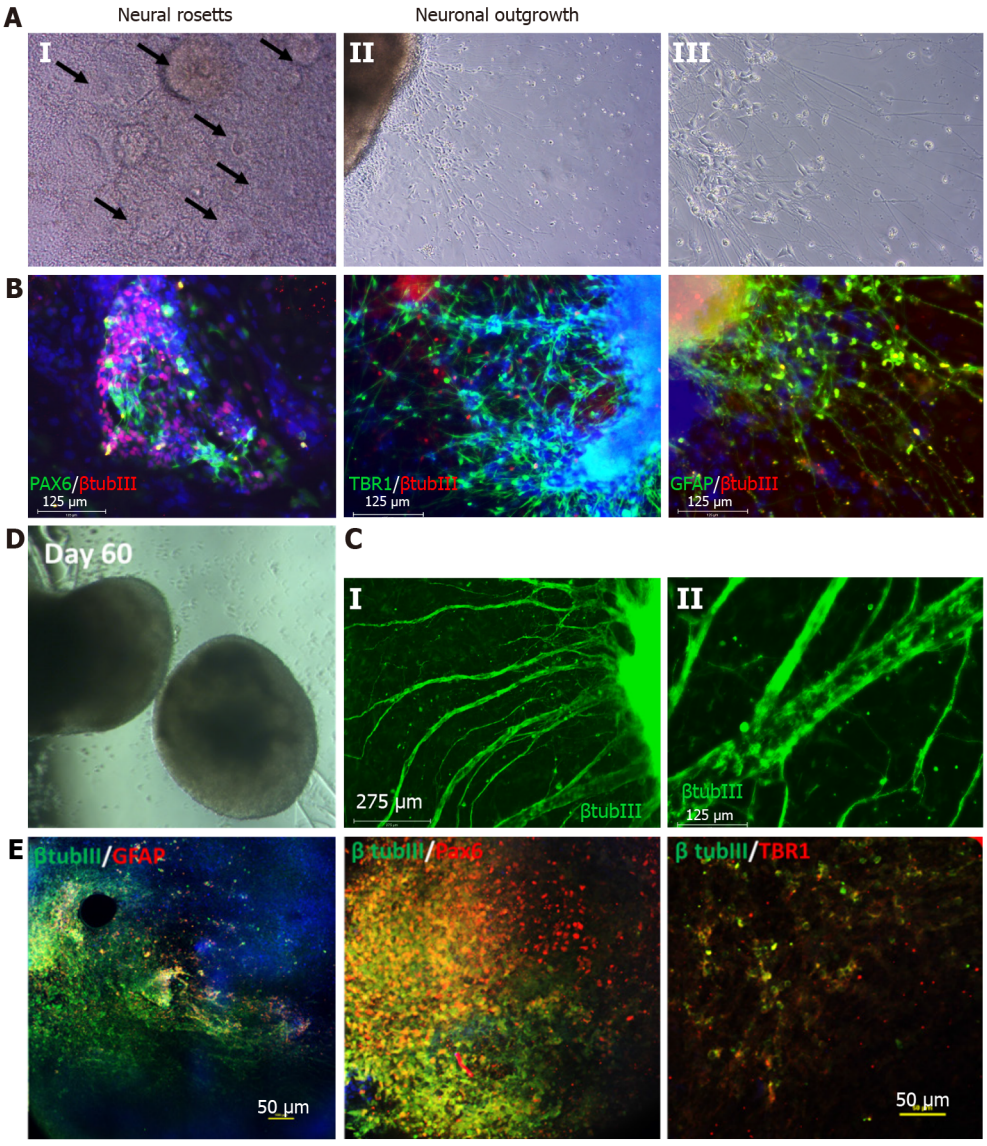

DOI: 10.4252/wjsc.v15.i6.530

Figure 3 Characterization of cortical organoids for neural and astrocyte marker expression. A: Brightfield images showing the neural rosettes and neuronal outgrowth from the organoids replated to an attachment plate at day 35 of differentiation; B: Resulting immunocytochemistry analysis of neural marker paired box 6 (PAX6), cortical deep layer VI marker T-box brain transcription factor 1 (TBR1), astrocyte marker glial fibrillary acidic protein (GFAP) co-stained with common neural marker β tubulin III, scale bar 125 μm; C: Immunostaining at later stage of the replating showing thick axon like extensions from the organoids, scale bar: 275 μm; D: Brightfield images of the day 60 cortical organoids; E: Confocal images of the day 60 organoids showing astrocyte marker GFAP, neural marker PAX6, cortical deep layer VI marker TBR1 co-stained with common neural marker β tubulin III, scale bar: 50 μm.

As the second most prevalent neurodegenerative disease worldwide[117], PD is frequently studied using hPSC-derived hMLOs[87,111,112,115,118-120]. The disease is characterized by the loss of dopaminergic neurons in the substantia nigra and is mainly caused by mutations in glucocerebrosidase and LRRK2 genes in addition to α-synuclein (α-syn; *SNCA*) gene triplications[111,121,122]. The hMLOs generated from patients with these mutations display PD traits such as oligomeric and fibrillar α-syn aggregates, loss of mDA neurons, and Lewy body-like inclusions[111,118,119]. Since hPSCs can be edited using clustered regularly interspaced short palindromic repeats (CRISPR)/CRISPR-associated protein 9 technology, *SNCA* gene genome correction has been demonstrated to revert PD patient hPSCs back to wild-type phenotypes[119,123]. These hMLOs have also been successfully generated from hiPSCs carrying the *LRRK2*-G2019S mutation[124]. Biallelic pathogenic variations in the phosphatase and tensin homolog-induced kinase 1 gene that controls mitochondrial function is also connected to the etiology of PD[125]. Human Parkinsonism can also have a more direct cause such as the toxicity of some drugs including 1-methyl-4-phenyl-1,2,3,6-tetrahydropyridine, which has also been modeled using hMLOs[126-128] (Table 2)[129-138].

Hindbrain organoids

The medulla, pons, and cerebellum make up the hindbrain region, which is developed from the metencephalon and myelencephalon. Methods to generate hindbrain organoids commonly involve purmorphamine-mediated Shh signaling activation to convert neuroepithelial cells into ventral identity neurons. RA is used as a potent caudalizing agent to

promote the fate of hindbrain cells instead of Wnt signaling activation, which is required for midbrain patterning[138]. Markers of hindbrain neurons include serotonergic neuron marker serotonin, human fifth Ewing variant, gastrulation brain homeobox 2, choline acetyltransferase (ChAT), and HB9. Due to their location, cerebellar neurons cannot be easily studied at the cellular or molecular level. Thus, using hiPSC-derived technologies is advantageous in this situation. The cerebellum can be divided into inhibitory GABAergic neurons known as Purkinje cells, which are derived from pancreas-specific transcription factor 1α progenitors, and excitatory glutamatergic neurons known as granule cells, which are descended from atonal homolog 1 (also known as MATH1) progenitors[139].

The first published granule cell differentiation protocol using hiPSCs involved several factors including FGF8B, Wnt proteins, BMPs, and RA. This method recapitulates anteroposterior and dorsoventral patterning and thereby induces *MATH1*-expressing mitotic neural progenitors, which can later be differentiated into cerebellar granule cells. Purkinje cells derived from hiPSCs initially had an immature phenotype, and thus needed to be co-cultured with mouse cerebellar granule cell precursors to allow for maturation[129,140]. However, cells made using this approach had substantial functional variability. Silva *et al*[141] recently published a protocol that generates mature cerebellar neurons without the need of such a co-culture system. This method involves stimulating the development of cerebellar precursors with FGF19, followed by self-organization and differentiation using stromal cell-derived factor 1 and BDNF/GDNF. Cerebellar neurons derived from hiPSCs are also helpful for modeling diseases, particularly cerebellar ataxia, a neurodegenerative disease that affects cerebellar neurons and eventually leads to motor incoordination. Cerebellar neurons derived from hiPSCs of either healthy human participants or ataxia patients were used in several recent studies to create an *in vitro* disease model. Spinocerebellar ataxia type 6 patient hiPSC-derived Purkinje cells have been used to model both thyroid hormone depletion-dependent degeneration and downregulation of the transcriptional targets TATA-Box Binding Protein Associated Factor 1 and BTG anti-proliferation factor 1, indicating their potential as a pathogenesis tool[141].

Recently, protocols for generating brain stem organoids have also been published, offering a new tool for evaluating the pathophysiology of disorders that impact the brainstem. Human brain stem organoids express the medullary marker ChAT, the pons marker hydroxylase, and the mature and functioning excitatory and inhibitory neuron markers vesicular glutamate transporter 1 and glutamic acid decarboxylase 67 in addition to various other relevant markers[142]. Both $OLIG2^+$ and MBP^+ OLs, as well as $S100^+$ astrocytes, are expressed in brain stem organoids[142].

Assembloids

Assembloids are systems that combine one type of spheroid or organoid with another type of spheroid or organoid. For example, assembloids can be produced by combining the dorsal and ventral forebrain, the cerebral cortex with the thalamus, or the cerebral cortex with any other non-neural cell type such as microglia, immunological cells, pericytes, and endothelial cells. The Pasca lab published the first assembloid study in 2017, in which human cortical spheroids were mixed with human subpallium spheroids[98]. The assembloids were created using human subpallium spheroids and cortical spheroids differentiated from hiPSCs from timothy syndrome (TS) patients with mutations in the α1c subunit of the L-type calcium channel (*CACNA1C*) gene. The two types of spheroids were combined in simple conical tubes and left undisturbed for 3 d to produce assembloids. The interneurons within the assembloids migrated, suggesting high potential for the study of certain aspects of migratory disorders such as TS. These patient-derived assembloids showed less effective interneuron movement, which was reversed by the administration of L-type calcium channel blockers.

Since then, many labs have sought to use assembloids to elucidate the interactions that occur between different physiological systems. The Knoblich lab reported the use of fused cerebral organoids that combined dorsal and ventral forebrain tissue cultures. They showed migration of C-X-C chemokine receptor type 4-dependent GABAergic interneurons from the ventral forebrain to the dorsal forebrain, which had a more MGE identity[143]. Assembloids of cortical organoids with integrated pericyte-like cells which express angiotensin-converting enzyme 2 have also been shown to enhance severe acute respiratory syndrome coronavirus 2 infection, suggesting the involvement of multiple cell types[100]. Another study employed cortico-striatal assembloids to recapitulate neurodevelopmental disorders that impair the cortico-striatal pathway, including schizophrenia, obsessive-compulsive disorder, and autism spectrum disorder[144-146]. These cortico-striatal assembloids were developed from patients with Phelan-McDermid Syndrome, a severe developmental disorder also known as 22q13.3DS. It is important to note that these patient-derived assembloids had a higher number of calcium spike events than striatal organoids, offering a better representation of altered neural activity. Interneuron migration has also been reported in a separate assembloids study that fused human MGE organoids with human cortical organoids[147].

CURRENT LIMITATIONS AND POTENTIAL ADVANCEMENTS

The extended culture times required by current methods to produce neural cell types as well as organoids restrict their application. Another consideration is the cell-line-to-cell-line and batch-to-batch variabilities of hiPSC differentiation. Therefore, accelerated protocols with less variable outcomes should be developed. For hiPSC-derived astrocytes, the major drawback is their lack of regional identity. Most protocols derive astrocytes with cortical identity, which may not be useful for modeling disease pathophysiology affecting the ventral part of the brain. Therefore, it is essential to employ experimental approaches that can produce astrocyte subtypes with the appropriate rostro-caudal and dorso-ventral identities. In the case of hiPSC-derived OLs, the lack of advanced OL disease models created using genetically-modified hiPSCs also limits their application. Finally, the lack of vascularization in current organoid and assembloid systems prevents the important study of cell-type crosstalk. Therefore, incorporating vasculature as well as reducing culture time would benefit multiple methods of neural lineage disease modeling.

CONCLUSION

Research in hPSCs has proven to be extremely helpful in creating disease models that can corroborate results gleaned from animal models and overcome their associated limitations. Distinct brain cell types can be produced using hPSCs including neurons, astrocytes, OLs, microglia, in addition to more advanced heterogeneous systems such as brain organoids. These systems have contributed to the development of models for neurological diseases such as AD, PD, and many others. Current models that employ hPSCs have certain shortcomings related to the absence of vasculature as well as microglia. However, developing research in the field of tissue engineering that use cocultures, organ-on-chip and assembloids may be able to get around these limitations in the years to come.

ACKNOWLEDGEMENTS

The VA Tennessee Valley Healthcare System provided resources and facilities for the research that was reported in this article. Images were obtained with the resources of the Vanderbilt Cell Imaging Shared Resource.

FOOTNOTES

Author contributions: Yuan Y and Bejoy J wrote the manuscript; Qian ES and Woodard LE edited the manuscript; all authors have read and approved the final manuscript.

Supported by the CTSA Award from the National Center for Advancing Translational Sciences to the Vanderbilt Institute for Clinical and Translational Research, No. UL1 TR002243; A Pilot and Feasibility Award from the NIDDK to the Vanderbilt Diabetes Research and Training Center, No. DK020593; and a VA MERIT Award, No. BX004845.

Conflict-of-interest statement: Lauren E Woodard and Julie Bejoy have two patent applications submitted on "Accelerated protocol for deriving podocytes from hiPSCs" and "nephron progenitor exosomes" listed below; Inventors: Bejoy J and Woodard LE accelerated the protocol for the differentiation of podocytes from human pluripotent stem cells. Patent Application filed August 26, 2022. PCT/US2022/075447; Inventors: Bejoy J and Woodard LE Nephron progenitor exosomes, patent Application filed October 6, 2022. PCT/US2022/077692.

Country/Territory of origin: United States

ORCID number: Julie Bejoy 0000-0002-6406-077X.

S-Editor: Chen YL
L-Editor: Filipodia
P-Editor: Liu JH

REFERENCES

1 **Takahashi K**, Tanabe K, Ohnuki M, Narita M, Ichisaka T, Tomoda K, Yamanaka S. Induction of pluripotent stem cells from adult human fibroblasts by defined factors. *Cell* 2007; **131**: 861-872 [PMID: 18035408 DOI: 10.1016/j.cell.2007.11.019]

2 **Takahashi K**, Yamanaka S. Induction of pluripotent stem cells from mouse embryonic and adult fibroblast cultures by defined factors. *Cell* 2006; **126**: 663-676 [PMID: 16904174 DOI: 10.1016/j.cell.2006.07.024]

3 **Lancaster MA**, Knoblich JA. Generation of cerebral organoids from human pluripotent stem cells. *Nat Protoc* 2014; **9**: 2329-2340 [PMID: 25188634 DOI: 10.1038/nprot.2014.158]

4 **Takasato M**, Er PX, Chiu HS, Maier B, Baillie GJ, Ferguson C, Parton RG, Wolvetang EJ, Roost MS, Chuva de Sousa Lopes SM, Little MH. Kidney organoids from human iPS cells contain multiple lineages and model human nephrogenesis. *Nature* 2015; **526**: 564-568 [PMID: 26444236 DOI: 10.1038/nature15695]

5 **Wang Y**, Wang H, Deng P, Chen W, Guo Y, Tao T, Qin J. In situ differentiation and generation of functional liver organoids from human iPSCs in a 3D perfusable chip system. *Lab Chip* 2018; **18**: 3606-3616 [PMID: 30357207 DOI: 10.1039/c8lc00869h]

6 **Takebe T**, Sekine K, Enomura M, Koike H, Kimura M, Ogaeri T, Zhang RR, Ueno Y, Zheng YW, Koike N, Aoyama S, Adachi Y, Taniguchi H. Vascularized and functional human liver from an iPSC-derived organ bud transplant. *Nature* 2013; **499**: 481-484 [PMID: 23823721 DOI: 10.1038/nature12271]

7 **Dye BR**, Hill DR, Ferguson MA, Tsai YH, Nagy MS, Dyal R, Wells JM, Mayhew CN, Nattiv R, Klein OD, White ES, Deutsch GH, Spence JR. In vitro generation of human pluripotent stem cell derived lung organoids. *Elife* 2015; **4** [PMID: 25803487 DOI: 10.7554/eLife.05098]

8 **Hohwieler M**, Illing A, Hermann PC, Mayer T, Stockmann M, Perkhofer L, Eiseler T, Antony JS, Müller M, Renz S, Kuo CC, Lin Q, Sendler

M, Breunig M, Kleiderman SM, Lechel A, Zenker M, Leichsenring M, Rosendahl J, Zenke M, Sainz B Jr, Mayerle J, Costa IG, Seufferlein T, Kormann M, Wagner M, Liebau S, Kleger A. Human pluripotent stem cell-derived acinar/ductal organoids generate human pancreas upon orthotopic transplantation and allow disease modelling. *Gut* 2017; **66**: 473-486 [PMID: 27633923 DOI: 10.1136/gutjnl-2016-312423]

9 **Gerakis Y**, Hetz C. Brain organoids: a next step for humanized Alzheimer's disease models? *Mol Psychiatry* 2019; **24**: 474-478 [PMID: 30617271 DOI: 10.1038/s41380-018-0343-7]

10 **Lancaster MA**, Knoblich JA. Organogenesis in a dish: modeling development and disease using organoid technologies. *Science* 2014; **345**: 1247125 [PMID: 25035496 DOI: 10.1126/science.1247125]

11 **Shimizu T**, Mae SI, Araoka T, Okita K, Hotta A, Yamagata K, Osafune K. A novel ADPKD model using kidney organoids derived from disease-specific human iPSCs. *Biochem Biophys Res Commun* 2020; **529**: 1186-1194 [PMID: 32819584 DOI: 10.1016/j.bbrc.2020.06.141]

12 **Raja WK**, Mungenast AE, Lin YT, Ko T, Abdurrob F, Seo J, Tsai LH. Self-Organizing 3D Human Neural Tissue Derived from Induced Pluripotent Stem Cells Recapitulate Alzheimer's Disease Phenotypes. *PLoS One* 2016; **11**: e0161969 [PMID: 27622770 DOI: 10.1371/journal.pone.0161969]

13 **Li R**, Sun L, Fang A, Li P, Wu Q, Wang X. Recapitulating cortical development with organoid culture *in vitro* and modeling abnormal spindle-like (ASPM related primary) microcephaly disease. *Protein Cell* 2017; **8**: 823-833 [PMID: 29058117 DOI: 10.1007/s13238-017-0479-2]

14 **Dolmetsch R**, Geschwind DH. The human brain in a dish: the promise of iPSC-derived neurons. *Cell* 2011; **145**: 831-834 [PMID: 21663789 DOI: 10.1016/j.cell.2011.05.034]

15 **Juopperi TA**, Kim WR, Chiang CH, Yu H, Margolis RL, Ross CA, Ming GL, Song H. Astrocytes generated from patient induced pluripotent stem cells recapitulate features of Huntington's disease patient cells. *Mol Brain* 2012; **5**: 17 [PMID: 22613578 DOI: 10.1186/1756-6606-5-17]

16 **Douvaras P**, Wang J, Zimmer M, Hanchuk S, O'Bara MA, Sadiq S, Sim FJ, Goldman J, Fossati V. Efficient generation of myelinating oligodendrocytes from primary progressive multiple sclerosis patients by induced pluripotent stem cells. *Stem Cell Reports* 2014; **3**: 250-259 [PMID: 25254339 DOI: 10.1016/j.stemcr.2014.06.012]

17 **Lancaster MA**, Renner M, Martin CA, Wenzel D, Bicknell LS, Hurles ME, Homfray T, Penninger JM, Jackson AP, Knoblich JA. Cerebral organoids model human brain development and microcephaly. *Nature* 2013; **501**: 373-379 [PMID: 23995685 DOI: 10.1038/nature12517]

18 **Andersen J**, Revah O, Miura Y, Thom N, Amin ND, Kelley KW, Singh M, Chen X, Thete MV, Walczak EM, Vogel H, Fan HC, Paşca SP. Generation of Functional Human 3D Cortico-Motor Assembloids. *Cell* 2020; **183**: 1913-1929.e26 [PMID: 33333020 DOI: 10.1016/j.cell.2020.11.017]

19 **Muñoz-Sanjuán I**, Brivanlou AH. Neural induction, the default model and embryonic stem cells. *Nat Rev Neurosci* 2002; **3**: 271-280 [PMID: 11967557 DOI: 10.1038/nrn786]

20 **Stern CD**. Neural induction: old problem, new findings, yet more questions. *Development* 2005; **132**: 2007-2021 [PMID: 15829523 DOI: 10.1242/dev.01794]

21 **Suzuki IK**, Vanderhaeghen P. Is this a brain which I see before me? *Development* 2015; **142**: 3138-3150 [PMID: 26395142 DOI: 10.1242/dev.120568]

22 **Zhang SC**, Wernig M, Duncan ID, Brüstle O, Thomson JA. In vitro differentiation of transplantable neural precursors from human embryonic stem cells. *Nat Biotechnol* 2001; **19**: 1129-1133 [PMID: 11731781 DOI: 10.1038/nbt1201-1129]

23 **Eiraku M**, Watanabe K, Matsuo-Takasaki M, Kawada M, Yonemura S, Matsumura M, Wataya T, Nishiyama A, Muguruma K, Sasai Y. Self-organized formation of polarized cortical tissues from ESCs and its active manipulation by extrinsic signals. *Cell Stem Cell* 2008; **3**: 519-532 [PMID: 18983967 DOI: 10.1016/j.stem.2008.09.002]

24 **Chambers SM**, Fasano CA, Papapetrou EP, Tomishima M, Sadelain M, Studer L. Highly efficient neural conversion of human ES and iPS cells by dual inhibition of SMAD signaling. *Nat Biotechnol* 2009; **27**: 275-280 [PMID: 19252484 DOI: 10.1038/nbt.1529]

25 **Hattori N**. Cerebral organoids model human brain development and microcephaly. *Mov Disord* 2014; **29**: 185 [PMID: 24375826 DOI: 10.1002/mds.25740]

26 **Paşca AM**, Sloan SA, Clarke LE, Tian Y, Makinson CD, Huber N, Kim CH, Park JY, O'Rourke NA, Nguyen KD, Smith SJ, Huguenard JR, Geschwind DH, Barres BA, Paşca SP. Functional cortical neurons and astrocytes from human pluripotent stem cells in 3D culture. *Nat Methods* 2015; **12**: 671-678 [PMID: 26005811 DOI: 10.1038/nmeth.3415]

27 **Qian X**, Nguyen HN, Song MM, Hadiono C, Ogden SC, Hammack C, Yao B, Hamersky GR, Jacob F, Zhong C, Yoon KJ, Jeang W, Lin L, Li Y, Thakor J, Berg DA, Zhang C, Kang E, Chickering M, Nauen D, Ho CY, Wen Z, Christian KM, Shi PY, Maher BJ, Wu H, Jin P, Tang H, Song H, Ming GL. Brain-Region-Specific Organoids Using Mini-bioreactors for Modeling ZIKV Exposure. *Cell* 2016; **165**: 1238-1254 [PMID: 27118425 DOI: 10.1016/j.cell.2016.04.032]

28 **Qi Y**, Zhang XJ, Renier N, Wu Z, Atkin T, Sun Z, Ozair MZ, Tchieu J, Zimmer B, Fattahi F, Ganat Y, Azevedo R, Zeltner N, Brivanlou AH, Karayiorgou M, Gogos J, Tomishima M, Tessier-Lavigne M, Shi SH, Studer L. Combined small-molecule inhibition accelerates the derivation of functional cortical neurons from human pluripotent stem cells. *Nat Biotechnol* 2017; **35**: 154-163 [PMID: 28112759 DOI: 10.1038/nbt.3777]

29 **Tabata H**. Diverse subtypes of astrocytes and their development during corticogenesis. *Front Neurosci* 2015; **9**: 114 [PMID: 25904839 DOI: 10.3389/fnins.2015.00114]

30 **Krencik R**, Weick JP, Liu Y, Zhang ZJ, Zhang SC. Specification of transplantable astroglial subtypes from human pluripotent stem cells. *Nat Biotechnol* 2011; **29**: 528-534 [PMID: 21602806 DOI: 10.1038/nbt.1877]

31 **Sloan SA**, Darmanis S, Huber N, Khan TA, Birey F, Caneda C, Reimer R, Quake SR, Barres BA, Paşca SP. Human Astrocyte Maturation Captured in 3D Cerebral Cortical Spheroids Derived from Pluripotent Stem Cells. *Neuron* 2017; **95**: 779-790.e6 [PMID: 28817799 DOI: 10.1016/j.neuron.2017.07.035]

32 **Jurga AM**, Paleczna M, Kadluczka J, Kuter KZ. Beyond the GFAP-Astrocyte Protein Markers in the Brain. *Biomolecules* 2021; **11** [PMID: 34572572 DOI: 10.3390/biom11091361]

33 **Krencik R**, Zhang SC. Directed differentiation of functional astroglial subtypes from human pluripotent stem cells. *Nat Protoc* 2011; **6**: 1710-1717 [PMID: 22011653 DOI: 10.1038/nprot.2011.405]

34 **Li X**, Tao Y, Bradley R, Du Z, Kong L, Dong Y, Jones J, Yan Y, Harder CRK, Friedman LM, Bilal M, Hoffmann B, Zhang SC. Fast Generation of Functional Subtype Astrocytes from Human Pluripotent Stem Cells. *Stem Cell Reports* 2018; **11**: 998-1008 [PMID: 30269954 DOI: 10.1016/j.stemcr.2018.08.019]

35 **Canals I**, Ginisty A, Quist E, Timmerman R, Fritze J, Miskinyte G, Monni E, Hansen MG, Hidalgo I, Bryder D, Bengzon J, Ahlenius H. Rapid and efficient induction of functional astrocytes from human pluripotent stem cells. *Nat Methods* 2018; **15**: 693-696 [PMID: 30127505 DOI: 10.1038/s41592-018-0103-2]

36 **Soubannier V**, Maussion G, Chaineau M, Sigutova V, Rouleau G, Durcan TM, Stifani S. Characterization of human iPSC-derived astrocytes with potential for disease modeling and drug discovery. *Neurosci Lett* 2020; **731**: 135028 [PMID: 32380146 DOI: 10.1016/j.neulet.2020.135028]

37 **Brezovakova V**, Sykova E, Jadhav S. Astrocytes Derived from Familial and Sporadic Alzheimer's Disease iPSCs Show Altered Calcium Signaling and Respond Differently to Misfolded Protein Tau. *Cells* 2022; **11** [PMID: 35563735 DOI: 10.3390/cells11091429]

38 **Kondo T**, Funayama M, Miyake M, Tsukita K, Era T, Osaka H, Ayaki T, Takahashi R, Inoue H. Modeling Alexander disease with patient iPSCs reveals cellular and molecular pathology of astrocytes. *Acta Neuropathol Commun* 2016; **4**: 69 [PMID: 27402089 DOI: 10.1186/s40478-016-0337-0]

39 **Li L**, Tian E, Chen X, Chao J, Klein J, Qu Q, Sun G, Huang Y, Warden CD, Ye P, Feng L, Li X, Cui Q, Sultan A, Douvaras P, Fossati V, Sanjana NE, Riggs AD, Shi Y. GFAP Mutations in Astrocytes Impair Oligodendrocyte Progenitor Proliferation and Myelination in an hiPSC Model of Alexander Disease. *Cell Stem Cell* 2018; **23**: 239-251.e6 [PMID: 30075130 DOI: 10.1016/j.stem.2018.07.009]

40 **Thomas CA**, Tejwani L, Trujillo CA, Negraes PD, Herai RH, Mesci P, Macia A, Crow YJ, Muotri AR. Modeling of TREX1-Dependent Autoimmune Disease using Human Stem Cells Highlights L1 Accumulation as a Source of Neuroinflammation. *Cell Stem Cell* 2017; **21**: 319-331.e8 [PMID: 28803918 DOI: 10.1016/j.stem.2017.07.009]

41 **Zhou L**, Li P, Chen N, Dai LF, Gao K, Liu YN, Shen L, Wang JM, Jiang YW, Wu Y. Modeling vanishing white matter disease with patient-derived induced pluripotent stem cells reveals astrocytic dysfunction. *CNS Neurosci Ther* 2019; **25**: 759-771 [PMID: 30720246 DOI: 10.1111/cns.13107]

42 **Lanciotti A**, Brignone MS, Macioce P, Visentin S, Ambrosini E. Human iPSC-Derived Astrocytes: A Powerful Tool to Study Primary Astrocyte Dysfunction in the Pathogenesis of Rare Leukodystrophies. *Int J Mol Sci* 2021; **23** [PMID: 35008700 DOI: 10.3390/ijms23010274]

43 **di Domenico A**, Carola G, Calatayud C, Pons-Espinal M, Muñoz JP, Richaud-Patin Y, Fernandez-Carasa I, Gut M, Faella A, Parameswaran J, Soriano J, Ferrer I, Tolosa E, Zorzano A, Cuervo AM, Raya A, Consiglio A. Patient-Specific iPSC-Derived Astrocytes Contribute to Non-Cell-Autonomous Neurodegeneration in Parkinson's Disease. *Stem Cell Reports* 2019; **12**: 213-229 [PMID: 30639209 DOI: 10.1016/j.stemcr.2018.12.011]

44 **Garcia VJ**, Rushton DJ, Tom CM, Allen ND, Kemp PJ, Svendsen CN, Mattis VB. Huntington's Disease Patient-Derived Astrocytes Display Electrophysiological Impairments and Reduced Neuronal Support. *Front Neurosci* 2019; **13**: 669 [PMID: 31316341 DOI: 10.3389/fnins.2019.00669]

45 **Holloway PM**, Gavins FN. Modeling Ischemic Stroke In Vitro: Status Quo and Future Perspectives. *Stroke* 2016; **47**: 561-569 [PMID: 26742797 DOI: 10.1161/STROKEAHA.115.011932]

46 **Wevers NR**, Nair AL, Fowke TM, Pontier M, Kasi DG, Spijkers XM, Hallard C, Rabussier G, van Vught R, Vulto P, de Vries HE, Lanz HL. Modeling ischemic stroke in a triculture neurovascular unit on-a-chip. *Fluids Barriers CNS* 2021; **18**: 59 [PMID: 34906183 DOI: 10.1186/s12987-021-00294-9]

47 **Zhao C**, Devlin AC, Chouhan AK, Selvaraj BT, Stavrou M, Burr K, Brivio V, He X, Mehta AR, Story D, Shaw CE, Dando O, Hardingham GE, Miles GB, Chandran S. Mutant C9orf72 human iPSC-derived astrocytes cause non-cell autonomous motor neuron pathophysiology. *Glia* 2020; **68**: 1046-1064 [PMID: 31841614 DOI: 10.1002/glia.23761]

48 **Birger A**, Ben-Dor I, Ottolenghi M, Turetsky T, Gil Y, Sweetat S, Perez L, Belzer V, Casden N, Steiner D, Izrael M, Galun E, Feldman E, Behar O, Reubinoff B. Human iPSC-derived astrocytes from ALS patients with mutated C9ORF72 show increased oxidative stress and neurotoxicity. *EBioMedicine* 2019; **50**: 274-289 [PMID: 31787569 DOI: 10.1016/j.ebiom.2019.11.026]

49 **Soubannier V**, Chaineau M, Gursu L, Haghi G, Franco Flores AK, Rouleau G, Durcan TM, Stifani S. Rapid Generation of Ventral Spinal Cord-like Astrocytes from Human iPSCs for Modeling Non-Cell Autonomous Mechanisms of Lower Motor Neuron Disease. *Cells* 2022; **11** [PMID: 35159209 DOI: 10.3390/cells11030399]

50 **Ledur PF**, Karmirian K, Pedrosa CDSG, Souza LRQ, Assis-de-Lemos G, Martins TM, Ferreira JCCG, de Azevedo Reis GF, Silva ES, Silva D, Salerno JA, Ornelas IM, Devalle S, Madeiro da Costa RF, Goto-Silva L, Higa LM, Melo A, Tanuri A, Chimelli L, Murata MM, Garcez PP, Filippi-Chiela EC, Galina A, Borges HL, Rehen SK. Zika virus infection leads to mitochondrial failure, oxidative stress and DNA damage in human iPSC-derived astrocytes. *Sci Rep* 2020; **10**: 1218 [PMID: 31988337 DOI: 10.1038/s41598-020-57914-x]

51 **Araujo BHS**, Kaid C, De Souza JS, Gomes da Silva S, Goulart E, Caires LCJ, Musso CM, Torres LB, Ferrasa A, Herai R, Zatz M, Okamoto OK, Cavalheiro EA. Down Syndrome iPSC-Derived Astrocytes Impair Neuronal Synaptogenesis and the mTOR Pathway In Vitro. *Mol Neurobiol* 2018; **55**: 5962-5975 [PMID: 29128905 DOI: 10.1007/s12035-017-0818-6]

52 **Chen C**, Jiang P, Xue H, Peterson SE, Tran HT, McCann AE, Parast MM, Li S, Pleasure DE, Laurent LC, Loring JF, Liu Y, Deng W. Role of astroglia in Down's syndrome revealed by patient-derived human-induced pluripotent stem cells. *Nat Commun* 2014; **5**: 4430 [PMID: 25034944 DOI: 10.1038/ncomms5430]

53 **Mizuno GO**, Wang Y, Shi G, Sun J, Papadopoulos S, Broussard GJ, Unger EK, Deng W, Weick J, Bhattacharyya A, Chen CY, Yu G, Looger LL, Tian L. Aberrant Calcium Signaling in Astrocytes Inhibits Neuronal Excitability in a Human Down Syndrome Stem Cell Model. *Cell Rep* 2018; **24**: 355-365 [PMID: 29996097 DOI: 10.1016/j.celrep.2018.06.033]

54 **Ponroy Bally B**, Farmer WT, Jones EV, Jessa S, Kacerovsky JB, Mayran A, Peng H, Lefebvre JL, Drouin J, Hayer A, Ernst C, Murai KK. Human iPSC-derived Down syndrome astrocytes display genome-wide perturbations in gene expression, an altered adhesion profile, and increased cellular dynamics. *Hum Mol Genet* 2020; **29**: 785-802 [PMID: 31943018 DOI: 10.1093/hmg/ddaa003]

55 **Williams EC**, Zhong X, Mohamed A, Li R, Liu Y, Dong Q, Ananiev GE, Mok JC, Lin BR, Lu J, Chiao C, Cherney R, Li H, Zhang SC, Chang Q. Mutant astrocytes differentiated from Rett syndrome patients-specific iPSCs have adverse effects on wild-type neurons. *Hum Mol Genet* 2014; **23**: 2968-2980 [PMID: 24419315 DOI: 10.1093/hmg/ddu008]

56 **Yasui T**, Uezono N, Nakashima H, Noguchi H, Matsuda T, Noda-Andoh T, Okano H, Nakashima K. Hypoxia Epigenetically Confers Astrocytic Differentiation Potential on Human Pluripotent Cell-Derived Neural Precursor Cells. *Stem Cell Reports* 2017; **8**: 1743-1756 [PMID: 28591654 DOI: 10.1016/j.stemcr.2017.05.001]

57 **Andoh-Noda T**, Akamatsu W, Miyake K, Matsumoto T, Yamaguchi R, Sanosaka T, Okada Y, Kobayashi T, Ohyama M, Nakashima K, Kurosawa H, Kubota T, Okano H. Differentiation of multipotent neural stem cells derived from Rett syndrome patients is biased toward the astrocytic lineage. *Mol Brain* 2015; **8**: 31 [PMID: 26012557 DOI: 10.1186/s13041-015-0121-2]

58 **Kim JJ**, Savas JN, Miller MT, Hu X, Carromeu C, Lavallée-Adam M, Freitas BCG, Muotri AR, Yates JR 3rd, Ghosh A. Proteomic analyses reveal misregulation of LIN28 expression and delayed timing of glial differentiation in human iPS cells with MECP2 Loss-of-function. *PLoS One* 2019; **14**: e0212553 [PMID: 30789962 DOI: 10.1371/journal.pone.0212553]

59 **Liu Z**, Osipovitch M, Benraiss A, Huynh NPT, Foti R, Bates J, Chandler-Militello D, Findling RL, Tesar PJ, Nedergaard M, Windrem MS,

Goldman SA. Dysregulated Glial Differentiation in Schizophrenia May Be Relieved by Suppression of SMAD4- and REST-Dependent Signaling. *Cell Rep* 2019; **27**: 3832-3843.e6 [PMID: 31242417 DOI: 10.1016/j.celrep.2019.05.088]

60 **Akkouh IA**, Ueland T, Hansson L, Inderhaug E, Hughes T, Steen NE, Aukrust P, Andreassen OA, Szabo A, Djurovic S. Decreased IL-1β-induced CCL20 response in human iPSC-astrocytes in schizophrenia: Potential attenuating effects on recruitment of regulatory T cells. *Brain Behav Immun* 2020; **87**: 634-644 [PMID: 32109548 DOI: 10.1016/j.bbi.2020.02.008]

61 **Aflaki E**, Stubblefield BK, McGlinchey RP, McMahon B, Ory DS, Sidransky E. A characterization of Gaucher iPS-derived astrocytes: Potential implications for Parkinson's disease. *Neurobiol Dis* 2020; **134**: 104647 [PMID: 31669751 DOI: 10.1016/j.nbd.2019.104647]

62 **Shi Y**, Kirwan P, Smith J, Robinson HP, Livesey FJ. Human cerebral cortex development from pluripotent stem cells to functional excitatory synapses. *Nat Neurosci* 2012; **15**: 477-486, S1 [PMID: 22306606 DOI: 10.1038/nn.3041]

63 **Wang S**, Bates J, Li X, Schanz S, Chandler-Militello D, Levine C, Maherali N, Studer L, Hochedlinger K, Windrem M, Goldman SA. Human iPSC-derived oligodendrocyte progenitor cells can myelinate and rescue a mouse model of congenital hypomyelination. *Cell Stem Cell* 2013; **12**: 252-264 [PMID: 23395447 DOI: 10.1016/j.stem.2012.12.002]

64 **Nobuta H**, Yang N, Ng YH, Marro SG, Sabeur K, Chavali M, Stockley JH, Killilea DW, Walter PB, Zhao C, Huie P Jr, Goldman SA, Kriegstein AR, Franklin RJM, Rowitch DH, Wernig M. Oligodendrocyte Death in Pelizaeus-Merzbacher Disease Is Rescued by Iron Chelation. *Cell Stem Cell* 2019; **25**: 531-541.e6 [PMID: 31585094 DOI: 10.1016/j.stem.2019.09.003]

65 **Douvaras P**, Fossati V. Generation and isolation of oligodendrocyte progenitor cells from human pluripotent stem cells. *Nat Protoc* 2015; **10**: 1143-1154 [PMID: 26134954 DOI: 10.1038/nprot.2015.075]

66 **Cho AN**, Jin Y, Kim S, Kumar S, Shin H, Kang HC, Cho SW. Aligned Brain Extracellular Matrix Promotes Differentiation and Myelination of Human-Induced Pluripotent Stem Cell-Derived Oligodendrocytes. *ACS Appl Mater Interfaces* 2019; **11**: 15344-15353 [PMID: 30974942 DOI: 10.1021/acsami.9b03242]

67 **Neyrinck K**, García-León JA. Single Transcription Factor-Based Differentiation Allowing Fast and Efficient Oligodendrocyte Generation *via* SOX10 Overexpression. *Methods Mol Biol* 2021; **2352**: 149-170 [PMID: 34324186 DOI: 10.1007/978-1-0716-1601-7_11]

68 **Shaker MR**, Pietrogrande G, Martin S, Lee JH, Sun W, Wolvetang EJ. Rapid and Efficient Generation of Myelinating Human Oligodendrocytes in Organoids. *Front Cell Neurosci* 2021; **15**: 631548 [PMID: 33815061 DOI: 10.3389/fncel.2021.631548]

69 **Numasawa-Kuroiwa Y**, Okada Y, Shibata S, Kishi N, Akamatsu W, Shoji M, Nakanishi A, Oyama M, Osaka H, Inoue K, Takahashi K, Yamanaka S, Kosaki K, Takahashi T, Okano H. Involvement of ER stress in dysmyelination of Pelizaeus-Merzbacher Disease with PLP1 missense mutations shown by iPSC-derived oligodendrocytes. *Stem Cell Reports* 2014; **2**: 648-661 [PMID: 24936452 DOI: 10.1016/j.stemcr.2014.03.007]

70 **Azevedo C**, Teku G, Pomeshchik Y, Reyes JF, Chumarina M, Russ K, Savchenko E, Hammarberg A, Lamas NJ, Collin A, Gouras GK, Klementieva O, Hallbeck M, Taipa R, Vihinen M, Roybon L. Parkinson's disease and multiple system atrophy patient iPSC-derived oligodendrocytes exhibit alpha-synuclein-induced changes in maturation and immune reactive properties. *Proc Natl Acad Sci U S A* 2022; **119**: e2111405119 [PMID: 35294277 DOI: 10.1073/pnas.2111405119]

71 **Friedman BA**, Srinivasan K, Ayalon G, Meilandt WJ, Lin H, Huntley MA, Cao Y, Lee SH, Haddick PCG, Ngu H, Modrusan Z, Larson JL, Kaminker JS, van der Brug MP, Hansen DV. Diverse Brain Myeloid Expression Profiles Reveal Distinct Microglial Activation States and Aspects of Alzheimer's Disease Not Evident in Mouse Models. *Cell Rep* 2018; **22**: 832-847 [PMID: 29346778 DOI: 10.1016/j.celrep.2017.12.066]

72 **Ueda Y**, Gullipalli D, Song WC. Modeling complement-driven diseases in transgenic mice: Values and limitations. *Immunobiology* 2016; **221**: 1080-1090 [PMID: 27371974 DOI: 10.1016/j.imbio.2016.06.007]

73 **Muffat J**, Li Y, Yuan B, Mitalipova M, Omer A, Corcoran S, Bakiasi G, Tsai LH, Aubourg P, Ransohoff RM, Jaenisch R. Efficient derivation of microglia-like cells from human pluripotent stem cells. *Nat Med* 2016; **22**: 1358-1367 [PMID: 27668937 DOI: 10.1038/nm.4189]

74 **Haenseler W**, Sansom SN, Buchrieser J, Newey SE, Moore CS, Nicholls FJ, Chintawar S, Schnell C, Antel JP, Allen ND, Cader MZ, Wade-Martins R, James WS, Cowley SA. A Highly Efficient Human Pluripotent Stem Cell Microglia Model Displays a Neuronal-Co-culture-Specific Expression Profile and Inflammatory Response. *Stem Cell Reports* 2017; **8**: 1727-1742 [PMID: 28591653 DOI: 10.1016/j.stemcr.2017.05.017]

75 **Takata K**, Kozaki T, Lee CZW, Thion MS, Otsuka M, Lim S, Utami KH, Fidan K, Park DS, Malleret B, Chakarov S, See P, Low D, Low G, Garcia-Miralles M, Zeng R, Zhang J, Goh CC, Gul A, Hubert S, Lee B, Chen J, Low I, Shadan NB, Lum J, Wei TS, Mok E, Kawanishi S, Kitamura Y, Larbi A, Poidinger M, Renia L, Ng LG, Wolf Y, Jung S, Önder T, Newell E, Huber T, Ashihara E, Garel S, Pouladi MA, Ginhoux F. Induced-Pluripotent-Stem-Cell-Derived Primitive Macrophages Provide a Platform for Modeling Tissue-Resident Macrophage Differentiation and Function. *Immunity* 2017; **47**: 183-198.e6 [PMID: 28723550 DOI: 10.1016/j.immuni.2017.06.017]

76 **Abud EM**, Ramirez RN, Martinez ES, Healy LM, Nguyen CHH, Newman SA, Yeromin AV, Scarfone VM, Marsh SE, Fimbres C, Caraway CA, Fote GM, Madany AM, Agrawal A, Kayed R, Gylys KH, Cahalan MD, Cummings BJ, Antel JP, Mortazavi A, Carson MJ, Poon WW, Blurton-Jones M. iPSC-Derived Human Microglia-like Cells to Study Neurological Diseases. *Neuron* 2017; **94**: 278-293.e9 [PMID: 28426964 DOI: 10.1016/j.neuron.2017.03.042]

77 **Pandya H**, Shen MJ, Ichikawa DM, Sedlock AB, Choi Y, Johnson KR, Kim G, Brown MA, Elkahloun AG, Maric D, Sweeney CL, Gossa S, Malech HL, McGavern DB, Park JK. Differentiation of human and murine induced pluripotent stem cells to microglia-like cells. *Nat Neurosci* 2017; **20**: 753-759 [PMID: 28253233 DOI: 10.1038/nn.4534]

78 **Douvaras P**, Sun B, Wang M, Kruglikov I, Lallos G, Zimmer M, Terrenoire C, Zhang B, Gandy S, Schadt E, Freytes DO, Noggle S, Fossati V. Directed Differentiation of Human Pluripotent Stem Cells to Microglia. *Stem Cell Reports* 2017; **8**: 1516-1524 [PMID: 28528700 DOI: 10.1016/j.stemcr.2017.04.023]

79 **McQuade A**, Blurton-Jones M. Human Induced Pluripotent Stem Cell-Derived Microglia (hiPSC-Microglia). *Methods Mol Biol* 2022; **2454**: 473-482 [PMID: 34773245 DOI: 10.1007/7651_2021_429]

80 **Bejoy J**, Yuan X, Song L, Hua T, Jeske R, Sart S, Sang QA, Li Y. Genomics Analysis of Metabolic Pathways of Human Stem Cell-Derived Microglia-Like Cells and the Integrated Cortical Spheroids. *Stem Cells Int* 2019; **2019**: 2382534 [PMID: 31827525 DOI: 10.1155/2019/2382534]

81 **Dräger NM**, Sattler SM, Huang CT, Teter OM, Leng K, Hashemi SH, Hong J, Aviles G, Clelland CD, Zhan L, Udeochu JC, Kodama L, Singleton AB, Nalls MA, Ichida J, Ward ME, Faghri F, Gan L, Kampmann M. A CRISPRi/a platform in human iPSC-derived microglia uncovers regulators of disease states. *Nat Neurosci* 2022; **25**: 1149-1162 [PMID: 35953545 DOI: 10.1038/s41593-022-01131-4]

82 **Ito D**, Imai Y, Ohsawa K, Nakajima K, Fukuuchi Y, Kohsaka S. Microglia-specific localisation of a novel calcium binding protein, Iba1. *Brain Res Mol Brain Res* 1998; **57**: 1-9 [PMID: 9630473 DOI: 10.1016/S0169-328X(98)00040-0]

83 **Andreone BJ**, Przybyla L, Llapashtica C, Rana A, Davis SS, van Lengerich B, Lin K, Shi J, Mei Y, Astarita G, Di Paolo G, Sandmann T, Monroe KM, Lewcock JW. Alzheimer's-associated PLCγ2 is a signaling node required for both TREM2 function and the inflammatory response in human microglia. *Nat Neurosci* 2020; **23**: 927-938 [PMID: 32514138 DOI: 10.1038/s41593-020-0650-6]

84 **McQuade A**, Blurton-Jones M. Microglia in Alzheimer's Disease: Exploring How Genetics and Phenotype Influence Risk. *J Mol Biol* 2019; **431**: 1805-1817 [PMID: 30738892 DOI: 10.1016/j.jmb.2019.01.045]

85 **Tan HY**, Cho H, Lee LP. Human mini-brain models. *Nat Biomed Eng* 2021; **5**: 11-25 [PMID: 33318650 DOI: 10.1038/s41551-020-00643-3]

86 **Kadoshima T**, Sakaguchi H, Nakano T, Soen M, Ando S, Eiraku M, Sasai Y. Self-organization of axial polarity, inside-out layer pattern, and species-specific progenitor dynamics in human ES cell-derived neocortex. *Proc Natl Acad Sci USA* 2013; **110**: 20284-20289 [PMID: 24277810 DOI: 10.1073/pnas.1315710110]

87 **Yan Y**, Song L, Bejoy J, Zhao J, Kanekiyo T, Bu G, Zhou Y, Li Y. Modeling Neurodegenerative Microenvironment Using Cortical Organoids Derived from Human Stem Cells. *Tissue Eng Part A* 2018; **24**: 1125-1137 [PMID: 29361890 DOI: 10.1089/ten.TEA.2017.0423]

88 **Boreström C**, Jonebring A, Guo J, Palmgren H, Cederblad L, Forslöw A, Svensson A, Söderberg M, Reznichenko A, Nyström J, Patrakka J, Hicks R, Maresca M, Valastro B, Collén A. A CRISP(e)R view on kidney organoids allows generation of an induced pluripotent stem cell-derived kidney model for drug discovery. *Kidney Int* 2018; **94**: 1099-1110 [PMID: 30072040 DOI: 10.1016/j.kint.2018.05.003]

89 **Yan Y**, Song L, Tsai AC, Ma T, Li Y. Generation of Neural Progenitor Spheres from Human Pluripotent Stem Cells in a Suspension Bioreactor. *Methods Mol Biol* 2016; **1502**: 119-128 [PMID: 26837215 DOI: 10.1007/7651_2015_310]

90 **Qian X**, Su Y, Adam CD, Deutschmann AU, Pather SR, Goldberg EM, Su K, Li S, Lu L, Jacob F, Nguyen PTT, Huh S, Hoke A, Swinford-Jackson SE, Wen Z, Gu X, Pierce RC, Wu H, Briand LA, Chen HI, Wolf JA, Song H, Ming GL. Sliced Human Cortical Organoids for Modeling Distinct Cortical Layer Formation. *Cell Stem Cell* 2020; **26**: 766-781.e9 [PMID: 32142682 DOI: 10.1016/j.stem.2020.02.002]

91 **Trujillo CA**, Gao R, Negraes PD, Gu J, Buchanan J, Preissl S, Wang A, Wu W, Haddad GG, Chaim IA, Domissy A, Vandenberghe M, Devor A, Yeo GW, Voytek B, Muotri AR. Complex Oscillatory Waves Emerging from Cortical Organoids Model Early Human Brain Network Development. *Cell Stem Cell* 2019; **25**: 558-569.e7 [PMID: 31474560 DOI: 10.1016/j.stem.2019.08.002]

92 **Gordon A**, Yoon SJ, Tran SS, Makinson CD, Park JY, Andersen J, Valencia AM, Horvath S, Xiao X, Huguenard JR, Pașca SP, Geschwind DH. Long-term maturation of human cortical organoids matches key early postnatal transitions. *Nat Neurosci* 2021; **24**: 331-342 [PMID: 33619405 DOI: 10.1038/s41593-021-00802-y]

93 **Gonzalez C**, Armijo E, Bravo-Alegria J, Becerra-Calixto A, Mays CE, Soto C. Modeling amyloid beta and tau pathology in human cerebral organoids. *Mol Psychiatry* 2018; **23**: 2363-2374 [PMID: 30171212 DOI: 10.1038/s41380-018-0229-8]

94 **Alić I**, Goh PA, Murray A, Portelius E, Gkanatsiou E, Gough G, Mok KY, Koschut D, Brunmeir R, Yeap YJ, O'Brien NL, Groet J, Shao X, Havlicek S, Dunn NR, Kvartsberg H, Brinkmalm G, Hithersay R, Startin C, Hamburg S, Phillips M, Pervushin K, Turmaine M, Wallon D, Rovelet-Lecrux A, Soininen H, Volpi E, Martin JE, Foo JN, Becker DL, Rostagno A, Ghiso J, Krsnik Ž, Šimić G, Kostović I, Mitrečić D; LonDownS Consortium, Francis PT, Blennow K, Strydom A, Hardy J, Zetterberg H, Nižetić D. Patient-specific Alzheimer-like pathology in trisomy 21 cerebral organoids reveals BACE2 as a gene dose-sensitive AD suppressor in human brain. *Mol Psychiatry* 2021; **26**: 5766-5788 [PMID: 32647257 DOI: 10.1038/s41380-020-0806-5]

95 **Hernández D**, Rooney LA, Daniszewski M, Gulluyan L, Liang HH, Cook AL, Hewitt AW, Pébay A. Culture Variabilities of Human iPSC-Derived Cerebral Organoids Are a Major Issue for the Modelling of Phenotypes Observed in Alzheimer's Disease. *Stem Cell Rev Rep* 2022; **18**: 718-731 [PMID: 33725267 DOI: 10.1007/s12015-021-10147-5]

96 **De Paola M**, Pischiutta F, Comolli D, Mariani A, Kelk J, Lisi I, Cerovic M, Fumagalli S, Forloni G, Zanier ER. Neural cortical organoids from self-assembling human iPSC as a model to investigate neurotoxicity in brain ischemia. *J Cereb Blood Flow Metab* 2023; **43**: 680-693 [PMID: 36655331 DOI: 10.1177/0271678X231152023]

97 **Boisvert EM**, Means RE, Michaud M, Madri JA, Katz SG. Minocycline mitigates the effect of neonatal hypoxic insult on human brain organoids. *Cell Death Dis* 2019; **10**: 325 [PMID: 30975982 DOI: 10.1038/s41419-019-1553-x]

98 **Pașca AM**, Park JY, Shin HW, Qi Q, Revah O, Krasnoff R, O'Hara R, Willsey AJ, Palmer TD, Pașca SP. Human 3D cellular model of hypoxic brain injury of prematurity. *Nat Med* 2019; **25**: 784-791 [PMID: 31061540 DOI: 10.1038/s41591-019-0436-0]

99 **Birey F**, Andersen J, Makinson CD, Islam S, Wei W, Huber N, Fan HC, Metzler KRC, Panagiotakos G, Thom N, O'Rourke NA, Steinmetz LM, Bernstein JA, Hallmayer J, Huguenard JR, Pașca SP. Assembly of functionally integrated human forebrain spheroids. *Nature* 2017; **545**: 54-59 [PMID: 28445465 DOI: 10.1038/nature22330]

100 **Bagley JA**, Reumann D, Bian S, Lévi-Strauss J, Knoblich JA. Fused cerebral organoids model interactions between brain regions. *Nat Methods* 2017; **14**: 743-751 [PMID: 28504681 DOI: 10.1038/nmeth.4304]

101 **Xiang Y**, Tanaka Y, Patterson B, Kang YJ, Govindaiah G, Roselaar N, Cakir B, Kim KY, Lombroso AP, Hwang SM, Zhong M, Stanley EG, Elefanty AG, Naegele JR, Lee SH, Weissman SM, Park IH. Fusion of Regionally Specified hPSC-Derived Organoids Models Human Brain Development and Interneuron Migration. *Cell Stem Cell* 2017; **21**: 383-398.e7 [PMID: 28757360 DOI: 10.1016/j.stem.2017.07.007]

102 **Miura Y**, Li MY, Birey F, Ikeda K, Revah O, Thete MV, Park JY, Puno A, Lee SH, Porteus MH, Pașca SP. Generation of human striatal organoids and cortico-striatal assembloids from human pluripotent stem cells. *Nat Biotechnol* 2020; **38**: 1421-1430 [PMID: 33273741 DOI: 10.1038/s41587-020-00763-w]

103 **Xiang Y**, Tanaka Y, Cakir B, Patterson B, Kim KY, Sun P, Kang YJ, Zhong M, Liu X, Patra P, Lee SH, Weissman SM, Park IH. hESC-Derived Thalamic Organoids Form Reciprocal Projections When Fused with Cortical Organoids. *Cell Stem Cell* 2019; **24**: 487-497.e7 [PMID: 30799279 DOI: 10.1016/j.stem.2018.12.015]

104 **Wataya T**, Ando S, Muguruma K, Ikeda H, Watanabe K, Eiraku M, Kawada M, Takahashi J, Hashimoto N, Sasai Y. Minimization of exogenous signals in ES cell culture induces rostral hypothalamic differentiation. *Proc Natl Acad Sci U S A* 2008; **105**: 11796-11801 [PMID: 18697938 DOI: 10.1073/pnas.0803078105]

105 **Merkle FT**, Maroof A, Wataya T, Sasai Y, Studer L, Eggan K, Schier AF. Generation of neuropeptidergic hypothalamic neurons from human pluripotent stem cells. *Development* 2015; **142**: 633-643 [PMID: 25670790 DOI: 10.1242/dev.117978]

106 **Huang WK**, Wong SZH, Pather SR, Nguyen PTT, Zhang F, Zhang DY, Zhang Z, Lu L, Fang W, Chen L, Fernandes A, Su Y, Song H, Ming GL. Generation of hypothalamic arcuate organoids from human induced pluripotent stem cells. *Cell Stem Cell* 2021; **28**: 1657-1670.e10 [PMID: 33961804 DOI: 10.1016/j.stem.2021.04.006]

107 **Sakaguchi H**, Kadoshima T, Soen M, Narii N, Ishida Y, Ohgushi M, Takahashi J, Eiraku M, Sasai Y. Generation of functional hippocampal neurons from self-organizing human embryonic stem cell-derived dorsomedial telencephalic tissue. *Nat Commun* 2015; **6**: 8896 [PMID: 26573335 DOI: 10.1038/ncomms9896]

108 **Pomeshchik Y**, Klementieva O, Gil J, Martinsson I, Hansen MG, de Vries T, Sancho-Balsells A, Russ K, Savchenko E, Collin A, Vaz AR, Bagnoli S, Nacmias B, Rampon C, Sorbi S, Brites D, Marko-Varga G, Kokaia Z, Rezeli M, Gouras GK, Roybon L. Human iPSC-Derived Hippocampal Spheroids: An Innovative Tool for Stratifying Alzheimer Disease Patient-Specific Cellular Phenotypes and Developing Therapies. *Stem Cell Reports* 2020; **15**: 256-273 [PMID: 32589876 DOI: 10.1016/j.stemcr.2020.06.001]

109 **Bejoy J**, Song L, Wang Z, Sang QX, Zhou Y, Li Y. Neuroprotective Activities of Heparin, Heparinase III, and Hyaluronic Acid on the Aβ42-Treated Forebrain Spheroids Derived from Human Stem Cells. *ACS Biomater Sci Eng* 2018; **4**: 2922-2933 [PMID: 30533518 DOI: 10.1021/acsbiomaterials.8b00021]

110 **Sozzi E**, Nilsson F, Kajtez J, Parmar M, Fiorenzano A. Generation of Human Ventral Midbrain Organoids Derived from Pluripotent Stem Cells. *Curr Protoc* 2022; **2**: e555 [PMID: 36121202 DOI: 10.1002/cpz1.555]

111 **Monzel AS**, Smits LM, Hemmer K, Hachi S, Moreno EL, van Wuellen T, Jarazo J, Walter J, Brüggemann I, Boussaad I, Berger E, Fleming RMT, Bolognin S, Schwamborn JC. Derivation of Human Midbrain-Specific Organoids from Neuroepithelial Stem Cells. *Stem Cell Reports* 2017; **8**: 1144-1154 [PMID: 28416282 DOI: 10.1016/j.stemcr.2017.03.010]

112 **Jo J**, Yang L, Tran HD, Yu W, Sun AX, Chang YY, Jung BC, Lee SJ, Saw TY, Xiao B, Khoo ATT, Yaw LP, Xie JJ, Lokman H, Ong WY, Lim GGY, Lim KL, Tan EK, Ng HH, Je HS. Lewy Body-like Inclusions in Human Midbrain Organoids Carrying Glucocerebrosidase and α-Synuclein Mutations. *Ann Neurol* 2021; **90**: 490-505 [PMID: 34288055 DOI: 10.1002/ana.26166]

113 **Zagare A**, Barmpa K, Smajic S, Smits LM, Grzyb K, Grünewald A, Skupin A, Nickels SL, Schwamborn JC. Midbrain organoids mimic early embryonic neurodevelopment and recapitulate LRRK2-p.Gly2019Ser-associated gene expression. *Am J Hum Genet* 2022; **109**: 311-327 [PMID: 35077669 DOI: 10.1016/j.ajhg.2021.12.009]

114 **Mohamed NV**, Lépine P, Lacalle-Aurioles M, Sirois J, Mathur M, Reintsch W, Beitel LK, Fon EA, Durcan TM. Microfabricated disk technology: Rapid scale up in midbrain organoid generation. *Methods* 2022; **203**: 465-477 [PMID: 34314827 DOI: 10.1016/j.ymeth.2021.07.008]

115 **Fiorenzano A**, Sozzi E, Birtele M, Kajtez J, Giacomoni J, Nilsson F, Bruzelius A, Sharma Y, Zhang Y, Mattsson B, Emnéus J, Ottosson DR, Storm P, Parmar M. Single-cell transcriptomics captures features of human midbrain development and dopamine neuron diversity in brain organoids. *Nat Commun* 2021; **12**: 7302 [PMID: 34911939 DOI: 10.1038/s41467-021-27464-5]

116 **Renner H**, Grabos M, Becker KJ, Kagermeier TE, Wu J, Otto M, Peischard S, Zeuschner D, TsyTsyura Y, Disse P, Klingauf J, Leidel SA, Seebohm G, Schöler HR, Bruder JM. A fully automated high-throughput workflow for 3D-based chemical screening in human midbrain organoids. *Elife* 2020; **9** [PMID: 33138918 DOI: 10.7554/eLife.52904]

117 **Sarrafha L**, Parfitt GM, Reyes R, Goldman C, Coccia E, Kareva T, Ahfeldt T. High-throughput generation of midbrain dopaminergic neuron organoids from reporter human pluripotent stem cells. *STAR Protoc* 2021; **2**: 100463 [PMID: 33997803 DOI: 10.1016/j.xpro.2021.100463]

118 **Maserejian N**, Vinikoor-Imler L, Dilley A. Estimation of the 2020 Global Population of Parkinson's Disease (PD) [abstract]. Mov Disord 2020. [cited 16 March 2023]. Available from: https://www.mdsabstracts.org/abstract/estimation-of-the-2020-global-population-of-parkinsons-disease-pd/

119 **Modamio Chamarro**, Saraiva C, Gomez Giro G, Louise Nickels S, Jarazo J, M A Antony P, Barbuti P, Halder R, Jäger C, Krüger R, Glaab E. Synaptic decline precedes dopaminergic neuronal loss in human midbrain organoids harboring a triplication of the SNCA gene. July 15, 2021. [cited 16 March 2023]. Available from: https://www.researchgate.net/publication/353290998_Synaptic_decline_precedes_dopaminergic_neuronal_loss_in_human_midbrain_organoids_harboring_a_triplication_of_the_SNCA_gene

120 **Mohamed NV**, Sirois J, Ramamurthy J, Mathur M, Lépine P, Deneault E, Maussion G, Nicouleau M, Chen CX, Abdian N, Soubannier V, Cai E, Nami H, Thomas RA, Wen D, Tabatabaei M, Beitel LK, Singh Dolt K, Karamchandani J, Stratton JA, Kunath T, Fon EA, Durcan TM. Midbrain organoids with an SNCA gene triplication model key features of synucleinopathy. *Brain Commun* 2021; **3**: fcab223 [PMID: 34632384 DOI: 10.1093/braincomms/fcab223]

121 **Smits LM**, Reinhardt L, Reinhardt P, Glatza M, Monzel AS, Stanslowsky N, Rosato-Siri MD, Zanon A, Antony PM, Bellmann J, Nicklas SM, Hemmer K, Qing X, Berger E, Kalmbach N, Ehrlich M, Bolognin S, Hicks AA, Wegner F, Sterneckert JL, Schwamborn JC. Modeling Parkinson's disease in midbrain-like organoids. *NPJ Parkinsons Dis* 2019; **5**: 5 [PMID: 30963107 DOI: 10.1038/s41531-019-0078-4]

122 **Alexander GE**. Biology of Parkinson's disease: pathogenesis and pathophysiology of a multisystem neurodegenerative disorder. *Dialogues Clin Neurosci* 2004; **6**: 259-280 [PMID: 22033559 DOI: 10.31887/DCNS.2004.6.3/galexander]

123 **Poewe W**, Seppi K, Tanner CM, Halliday GM, Brundin P, Volkmann J, Schrag AE, Lang AE. Parkinson disease. *Nat Rev Dis Primers* 2017; **3**: 17013 [PMID: 28332488 DOI: 10.1038/nrdp.2017.13]

124 **Jarazo J**, Barmpa K, Modamio J, Saraiva C, Sabaté-Soler S, Rosety I, Griesbeck A, Skwirblies F, Zaffaroni G, Smits LM, Su J, Arias-Fuenzalida J, Walter J, Gomez-Giro G, Monzel AS, Qing X, Vitali A, Cruciani G, Boussaad I, Brunelli F, Jäger C, Rakovic A, Li W, Yuan L, Berger E, Arena G, Bolognin S, Schmidt R, Schröder C, Antony PMA, Klein C, Krüger R, Seibler P, Schwamborn JC. Parkinson's Disease Phenotypes in Patient Neuronal Cultures and Brain Organoids Improved by 2-Hydroxypropyl-β-Cyclodextrin Treatment. *Mov Disord* 2022; **37**: 80-94 [PMID: 34637165 DOI: 10.1002/mds.28810]

125 **Zanetti C**, Spitz S, Berger E, Bolognin S, Smits LM, Crepaz P, Rothbauer M, Rosser JM, Marchetti-Deschmann M, Schwamborn JC, Ertl P. Monitoring the neurotransmitter release of human midbrain organoids using a redox cycling microsensor as a novel tool for personalized Parkinson's disease modelling and drug screening. *Analyst* 2021; **146**: 2358-2367 [PMID: 33625407 DOI: 10.1039/d0an02206c]

126 **Larsen SB**, Hanss Z, Krüger R. The genetic architecture of mitochondrial dysfunction in Parkinson's disease. *Cell Tissue Res* 2018; **373**: 21-37 [PMID: 29372317 DOI: 10.1007/s00441-017-2768-8]

127 **Goldman SM**. Environmental toxins and Parkinson's disease. *Annu Rev Pharmacol Toxicol* 2014; **54**: 141-164 [PMID: 24050700 DOI: 10.1146/annurev-pharmtox-011613-135937]

128 **Langston JW**, Ballard P, Tetrud JW, Irwin I. Chronic Parkinsonism in humans due to a product of meperidine-analog synthesis. *Science* 1983; **219**: 979-980 [PMID: 6823561 DOI: 10.1126/science.6823561]

129 **Muguruma K**, Nishiyama A, Kawakami H, Hashimoto K, Sasai Y. Self-organization of polarized cerebellar tissue in 3D culture of human pluripotent stem cells. *Cell Rep* 2015; **10**: 537-550 [PMID: 25640179 DOI: 10.1016/j.celrep.2014.12.051]

130 **Mariani J**, Coppola G, Zhang P, Abyzov A, Provini L, Tomasini L, Amenduni M, Szekely A, Palejev D, Wilson M, Gerstein M, Grigorenko EL, Chawarska K, Pelphrey KA, Howe JR, Vaccarino FM. FOXG1-Dependent Dysregulation of GABA/Glutamate Neuron Differentiation in Autism Spectrum Disorders. *Cell* 2015; **162**: 375-390 [PMID: 26186191 DOI: 10.1016/j.cell.2015.06.034]

131 **Jo J**, Xiao Y, Sun AX, Cukuroglu E, Tran HD, Göke J, Tan ZY, Saw TY, Tan CP, Lokman H, Lee Y, Kim D, Ko HS, Kim SO, Park JH, Cho NJ, Hyde TM, Kleinman JE, Shin JH, Weinberger DR, Tan EK, Je HS, Ng HH. Midbrain-like Organoids from Human Pluripotent Stem Cells

Contain Functional Dopaminergic and Neuromelanin-Producing Neurons. *Cell Stem Cell* 2016; **19**: 248-257 [PMID: 27476966 DOI: 10.1016/j.stem.2016.07.005]

132 **Ozone C**, Suga H, Eiraku M, Kadoshima T, Yonemura S, Takata N, Oiso Y, Tsuji T, Sasai Y. Functional anterior pituitary generated in self-organizing culture of human embryonic stem cells. *Nat Commun* 2016; **7**: 10351 [PMID: 26762480 DOI: 10.1038/ncomms10351]

133 **Lancaster MA**, Corsini NS, Wolfinger S, Gustafson EH, Phillips AW, Burkard TR, Otani T, Livesey FJ, Knoblich JA. Guided self-organization and cortical plate formation in human brain organoids. *Nat Biotechnol* 2017; **35**: 659-666 [PMID: 28562594 DOI: 10.1038/nbt.3906]

134 **Quadrato G**, Nguyen T, Macosko EZ, Sherwood JL, Min Yang S, Berger DR, Maria N, Scholvin J, Goldman M, Kinney JP, Boyden ES, Lichtman JW, Williams ZM, McCarroll SA, Arlotta P. Cell diversity and network dynamics in photosensitive human brain organoids. *Nature* 2017; **545**: 48-53 [PMID: 28445462 DOI: 10.1038/nature22047]

135 **Bian S**, Repic M, Guo Z, Kavirayani A, Burkard T, Bagley JA, Krauditsch C, Knoblich JA. Genetically engineered cerebral organoids model brain tumor formation. *Nat Methods* 2018; **15**: 631-639 [PMID: 30038414 DOI: 10.1038/s41592-018-0070-7]

136 **Mansour AA**, Gonçalves JT, Bloyd CW, Li H, Fernandes S, Quang D, Johnston S, Parylak SL, Jin X, Gage FH. An *in vivo* model of functional and vascularized human brain organoids. *Nat Biotechnol* 2018; **36**: 432-441 [PMID: 29658944 DOI: 10.1038/nbt.4127]

137 **Faustino Martins JM**, Fischer C, Urzi A, Vidal R, Kunz S, Ruffault PL, Kabuss L, Hube I, Gazzerro E, Birchmeier C, Spuler S, Sauer S, Gouti M. Self-Organizing 3D Human Trunk Neuromuscular Organoids. *Cell Stem Cell* 2020; **26**: 172-186.e6 [PMID: 31956040 DOI: 10.1016/j.stem.2019.12.007]

138 **Giandomenico SL**, Mierau SB, Gibbons GM, Wenger LMD, Masullo L, Sit T, Sutcliffe M, Boulanger J, Tripodi M, Derivery E, Paulsen O, Lakatos A, Lancaster MA. Cerebral organoids at the air-liquid interface generate diverse nerve tracts with functional output. *Nat Neurosci* 2019; **22**: 669-679 [PMID: 30886407 DOI: 10.1038/s41593-019-0350-2]

139 **Valiulahi P**, Vidyawan V, Puspita L, Oh Y, Juwono VB, Sittipo P, Friedlander G, Yahalomi D, Sohn JW, Lee YK, Yoon JK, Shim JW. Generation of caudal-type serotonin neurons and hindbrain-fate organoids from hPSCs. *Stem Cell Reports* 2021; **16**: 1938-1952 [PMID: 34242615 DOI: 10.1016/j.stemcr.2021.06.006]

140 **Bekman E**, Silva TP, Cotovio JP, de Almeida RM. Concepts and Applications of Stem Cell Biology: A Guide for Students. Rodrigues G, Roelen BAG, editors. Cham: Springer International Publishing, 2020: 213-228 [DOI: 10.1007/978-3-030-43939-2_11]

141 **Silva TP**, Bekman EP, Fernandes TG, Vaz SH, Rodrigues CAV, Diogo MM, Cabral JMS, Carmo-Fonseca M. Maturation of Human Pluripotent Stem Cell-Derived Cerebellar Neurons in the Absence of Co-culture. *Front Bioeng Biotechnol* 2020; **8**: 70 [PMID: 32117945 DOI: 10.3389/fbioe.2020.00070]

142 **Ishida Y**, Kawakami H, Kitajima H, Nishiyama A, Sasai Y, Inoue H, Muguruma K. Vulnerability of Purkinje Cells Generated from Spinocerebellar Ataxia Type 6 Patient-Derived iPSCs. *Cell Rep* 2016; **17**: 1482-1490 [PMID: 27806289 DOI: 10.1016/j.celrep.2016.10.026]

143 **Eura N**, Matsui TK, Luginbühl J, Matsubayashi M, Nanaura H, Shiota T, Kinugawa K, Iguchi N, Kiriyama T, Zheng C, Kouno T, Lan YJ, Kongpracha P, Wiriyasermkul P, Sakaguchi YM, Nagata R, Komeda T, Morikawa N, Kitayoshi F, Jong M, Kobashigawa S, Nakanishi M, Hasegawa M, Saito Y, Shiromizu T, Nishimura Y, Kasai T, Takeda M, Kobayashi H, Inagaki Y, Tanaka Y, Makinodan M, Kishimoto T, Kuniyasu H, Nagamori S, Muotri AR, Shin JW, Sugie K, Mori E. Brainstem Organoids From Human Pluripotent Stem Cells. *Front Neurosci* 2020; **14**: 538 [PMID: 32670003 DOI: 10.3389/fnins.2020.00538]

144 **Wang L**, Sievert D, Clark AE, Lee S, Federman H, Gastfriend BD, Shusta EV, Palecek SP, Carlin AF, Gleeson JG. A human three-dimensional neural-perivascular 'assembloid' promotes astrocytic development and enables modeling of SARS-CoV-2 neuropathology. *Nat Med* 2021; **27**: 1600-1606 [PMID: 34244682 DOI: 10.1038/s41591-021-01443-1]

145 **Shepherd GM**. Corticostriatal connectivity and its role in disease. *Nat Rev Neurosci* 2013; **14**: 278-291 [PMID: 23511908 DOI: 10.1038/nrn3469]

146 **Milad MR**, Rauch SL. Obsessive-compulsive disorder: beyond segregated cortico-striatal pathways. *Trends Cogn Sci* 2012; **16**: 43-51 [PMID: 22138231 DOI: 10.1016/j.tics.2011.11.003]

147 **Peça J**, Feliciano C, Ting JT, Wang W, Wells MF, Venkatraman TN, Lascola CD, Fu Z, Feng G. Shank3 mutant mice display autistic-like behaviours and striatal dysfunction. *Nature* 2011; **472**: 437-442 [PMID: 21423165 DOI: 10.1038/nature09965]

World Journal of Stem Cells

Submit a Manuscript: https://www.f6publishing.com

World J Stem Cells 2023 June 26; 15(6): 548-560

DOI: 10.4252/wjsc.v15.i6.548

ISSN 1948-0210 (online)

REVIEW

Factors affecting osteogenesis and chondrogenic differentiation of mesenchymal stem cells in osteoarthritis

Yi Peng, Hai Jiang, Hou-Dong Zuo

Specialty type: Cell biology

Provenance and peer review: Unsolicited article; Externally peer reviewed.

Peer-review model: Single blind

Peer-review report's scientific quality classification

Grade A (Excellent): 0
Grade B (Very good): 0
Grade C (Good): C, C
Grade D (Fair): 0
Grade E (Poor): 0

P-Reviewer: Wong CY, Malaysia; Liu AF, China

Received: March 17, 2023
Peer-review started: March 17, 2023
First decision: April 10, 2023
Revised: April 21, 2023
Accepted: May 5, 2023
Article in press: May 5, 2023
Published online: June 26, 2023

Yi Peng, Hai Jiang, Hou-Dong Zuo, Medical Imaging Key Laboratory of Sichuan Province, Department of Radiology, Affiliated Hospital of North Sichuan Medical College, Nanchong 637000, Sichuan Province, China

Hou-Dong Zuo, Department of Radiology, Chengdu Xinhua Hospital, Chengdu 610067, Sichuan Province, China

Corresponding author: Hou-Dong Zuo, MD, Doctor, Teacher, Medical Imaging Key Laboratory of Sichuan Province, Department of Radiology, Affiliated Hospital of North Sichuan Medical College, No. 1 Maoyuan South Road, Shunqing District, Nanchong 637000, Sichuan Province, China. zuohoud@163.com

Abstract

Osteoarthritis (OA) is a common degenerative joint disease that often involves progressive cartilage degeneration and bone destruction of subchondral bone. At present, clinical treatment is mainly for pain relief, and there are no effective methods to delay the progression of the disease. When this disease progresses to the advanced stage, the only treatment option for most patients is total knee replacement surgery, which causes patients great pain and anxiety. As a type of stem cell, mesenchymal stem cells (MSCs) have multidirectional differentiation potential. The osteogenic differentiation and chondrogenic differentiation of MSCs can play vital roles in the treatment of OA, as they can relieve pain in patients and improve joint function. The differentiation direction of MSCs is accurately controlled by a variety of signaling pathways, so there are many factors that can affect the differentiation direction of MSCs by acting on these signaling pathways. When MSCs are applied to OA treatment, the microenvironment of the joints, injected drugs, scaffold materials, source of MSCs and other factors exert specific impacts on the differentiation direction of MSCs. This review aims to summarize the mechanisms by which these factors influence MSC differentiation to produce better curative effects when MSCs are applied clinically in the future.

Key Words: Osteoarthritis; Mesenchymal stem cells; Differentiation; Hypoxia; Dexamethasone; Cell therapy

Core Tip: Several reviews have summarized the current status of mesenchymal stem cells (MSCs) in the treatment of osteoarthritis (OA). These studies usually focus on the paracrine function of MSCs. However, the differentiation function of MSCs also plays an important role in the treatment of diseases. This is the first review to report the factors that may affect the differentiation direction of MSCs in the treatment of OA and aims to provide guidance for more accurate regulation when MSC therapy is applied in the future.

Citation: Peng Y, Jiang H, Zuo HD. Factors affecting osteogenesis and chondrogenic differentiation of mesenchymal stem cells in osteoarthritis. *World J Stem Cells* 2023; 15(6): 548-560
URL: https://www.wjgnet.com/1948-0210/full/v15/i6/548.htm
DOI: https://dx.doi.org/10.4252/wjsc.v15.i6.548

INTRODUCTION

Osteoarthritis (OA) is one of the most common degenerative joint diseases, and its incidence increases with age[1]. With the rapid growth of the aging population, the prevalence of OA is increasing[2]. At present, there are more than 300 million OA patients worldwide[3]. The major symptoms of OA are pain and joint dysfunction, which seriously affect the quality of life of patients. Intra-articular microenvironment changes occur as OA develops. Due to tissue injury, severe hypoxia occurs in the joint cavity, and the expression level of hypoxia inducible factor 1 alpha increases significantly[4]. Many inflammatory cytokines infiltrate joints with OA, including interleukin-1 and tumour necrosis factor alpha (TNF-α). The expression of transforming growth factor-beta (TGF-β) in cartilage is significantly lower than that in healthy joints, which can lead to metabolic disorders of chondrocytes[5].

OA is an incurable disease at present, and cartilage degeneration and subchondral bone remodeling are considered the main pathogenic mechanisms of OA. There are no drugs that can delay the progres-sion of OA[6]. The goal of clinical treatment is to relieve symptoms such as pain and loss of function[7]. The common treatments for OA include physiotherapy, pain relievers and nonsteroidal anti-inflammatory drug administration, intra-articular glucocorticoid injection and surgery. When OA progresses to the advanced stage, the only treatment option for most patients is total knee replacement surgery, which causes patients great pain and anxiety[8]. Some innovative new treatment options have been proposed, including mesenchymal stem cell (MSC) therapy.

Mesenchymal stem cells are a branch of stem cells, with the stem cell characteristics of self-renewal and differentiation potential[9]. MSCs can repair tissue damage after injury by differentiating into different tissue cells, so they can play an important role in disease treatment. In 1968, Professor Friedenstein[10] first discovered the existence of MSCs in bone marrow and established an adherent method to isolate and culture MSCs *in vitro*. Pittenger *et al*[11] proved for the first time that MSCs have multidirectional differentiation ability. Since then, MSCs have been widely studied and applied to the treatment of clinical diseases. In 2006, the International Society for Cell Therapy (ISCT)[12] established three minimal criteria for defining MSCs unequivocally: (1) The cells must have the ability to adhere to plastic surfaces when cultivated in standard conditions; (2) they must express CD105, CD73, and CD90, but not CD45, CD34, CD14/CD11b, CD79a/CD19, or HLA-D; and (3) they must have the ability to differentiate into at least the following cell types *in vitro*: Osteoblasts, adipocytes, and chondroblasts.

MSCs can be isolated from various tissues, such as bone marrow, adipose tissue, cord blood and placenta. MSCs from different sources have different characteristics[13]. At present, bone marrow MSCs (BMSCs) and adipose MSCs (ADSCs) are the most commonly used. Heo *et al*[14] found that only BMSCs and ADSCs have the ability to differentiate into three lineages, including osteoblasts, adipocytes and chondrocytes, to meet the minimum MSC standard proposed by the ISCT [15]. However, Beeravolu *et al*[16] believe that MSCs from the human umbilical cord and fetal placenta can also differentiate into three lineages.

At present, there are approximately 1519 studies on "mesenchymal stem cells" registered, according to clinicaltrials.gov (April 2023). MSCs have been used as cellular therapy for various degenerative, inflammatory and autoimmune diseases in a large number of clinical trials. These clinical trials include diseases of the musculoskeletal system, respiratory system, blood system and cardiovascular system and have already shown the effectiveness and safety of MSCs. These cells are most commonly used for the treatment of OA in the musculoskeletal system. At present, the pathogenesis of OA is not completely clear. A large number of studies have shown that subchondral bone destruction[17, 18] and cartilage degeneration[19-21] participate in pathogenesis. Osteogenesis and chondrogenesis of MSCs play a key role in the treatment of OA.

Lamo-Espinosa *et al*[22] recruited 30 patients with OA and injected MSCs into the experimental group and hyaluronic acid (HA) into the control group. After 12 mo, magnetic resonance imaging (MRI) showed that the experimental group receiving the high dose of MSCs had a greater cartilage thickness, which is an indicator of the regeneration of cartilage in OA patients, than the control group. Tang *et al*[23] injected MSCs into rabbit models of OA. Nine weeks later, the knee joints of the rabbits were collected and analyzed. They found that when MSCs were injected, the articular cartilage of the rabbit showed characteristics of good reconstruction, such as a regular surface, restored cartilage thickness, nearly normal chondrocyte morphology, and uniformly distributed red Safranin O staining in the articular cartilage. At present, no experiment has been performed on the differentiation of MSCs in isolated subchondral bone tissue. However, many similar studies that applied MSCs to bone defects have been performed and proved the feasibility of osteogenic differen-

tiation of MSCs *in vivo*. For example, in the treatment of femoral head necrosis in the same hypoxic environment, after MSCs are implanted, the expression of bone-related genes is improved, and alkaline phosphatase and type I collagen are increased, which are indicators of bone formation[24]. MSCs are considered promising candidates for bone and cartilage repair and regeneration in OA. But the differentiation of transplanted MSCs is influenced by the microenvironment. Therefore, this article reviews the factors affecting the osteogenesis and chondrogenesis of MSCs (Figure 1).

MECHANISM OF OSTEOGENIC AND CHONDROGENIC DIFFERENTIATION OF MSCS

The differentiation of MSCs depends on a number of factors, including chemical, physical and biological factors. These factors activate different signaling pathways and transcription factors that regulate MSC differentiation into different cells [25]. The differentiation of MSCs is precisely controlled by various signaling pathways[26]. These signaling pathways activate lineage-specific transcription factors[27].

Chondrogenesis and osteogenesis of MSCs are interrelated processes. There are two ways for MSCs to form bone: Endochondral or intramembranous ossification. In endochondral ossification, MSCs first differentiate into chondrocytes and secrete cartilage matrix, and then they are stimulated by osteoblasts to form bone. In contrast, in intramembranous ossification, MSCs differentiate into osteoblasts directly[28]. Therefore, there are some common signaling pathways and transcription factors involved in the osteogenic differentiation and chondrogenic differentiation of MSCs.

TGF-β signaling, Wnt/β-catenin signaling and Notch signaling are the key pathways involved in chondrogenic differentiation of MSCs. The key cytokines include Sox9, Runx2, TGF-β, FGF and others[29]. Sox9 plays an essential role during chondrogenic differentiation and is considered an early sign of chondrocyte formation. Complete deletion of Sox9 can prevent the formation of cartilage. When it is overexpressed, it significantly inhibits the proliferation of chondrocytes[30]. Sox9 is a regulator of the type II collagen (*ColII*) gene, which is a specific marker of cartilage formation. The expression of *ColII* in chondrocytes has been found to be in direct proportion to the concentration of Sox9[31]. TGF-β can promote the differentiation of MSCs into chondrocytes and inhibit the terminal differentiation of chondrocytes into mast cells[32]. The differentiation of chondrocytes induced by TGF-β is mainly mediated by the Smad signaling pathway[33], which can upregulate the expression of Sox9 trans-cription factors and promote the synthesis of collagen and proteoglycan.

The main paracrine signaling pathways involved in the osteogenic differentiation of MSCs include bone morphogenetic protein (BMP) signaling, Wnt signaling, and Notch signaling[28,34-36]. The key transcriptional regulatory factors include Runx2, β-catenin, and osterix[27]. Runx2 is indispensable for the osteogenic differentiation of MSCs because it is a common convergence point for many signaling pathways[25,37]. It leads to the differentiation of MSCs into osteoblasts and inhibits the differentiation of adipogenesis and chondrogenesis. Runx2 promotes the differentiation of MSCs into osteoblasts in the early stage and promotes the maturation and mineralization of osteoblasts in the later stage by regulating extracellular matrix proteins, such as ColI and alkaline phosphatase (ALP). When Runx2 is absent, neither periosteal nor endochondral ossification occurs[38]. BMP2 is also an effective osteogenic induction factor that promotes the expression of Runx2, thus promoting the differentiation and maturation of osteoblasts[28]. Osterix is an osteoblast-specific transcription factor that is only expressed in osseous tissue and plays a decisive role in the differentiation of MSCs into osteoblasts[39]. Activation of the Wnt signaling pathway induces osterix expression. Overexpression of osterix in MSCs leads to osteogenic differentiation and an enhanced bone regeneration ability of MSCs[40]. The activity of β-catenin is also regulated by Wnt signaling. β-catenin can facilitate the shift of MSC fate to osteoblasts and enhance endochondral ossification. Its deficiency hinders the osteogenesis of MSCs and promotes the formation of cartilage and fat[41,42] (Figure 2).

FACTORS AFFECTING THE OSTEOGENIC AND CHONDROGENIC DIFFERENTIATION OF MSCS IN THE MICROENVIRONMENT OF OA

Oxygen concentration

The effect of oxygen concentration on MSCs has been studied for over twenty years (hypoxia promotes murine bone marrow-derived stromal cell migration and tube formation). Although there are still some controversies, a large number of studies have proven that low oxygen tension (hereinafter "hypoxia") exerts a significant impact on the differentiation of MSCs. Hypoxia often occurs in the stem cell microenvironment, which induces beneficial signals, such as upregulation of pluripotency markers, for MSCs to maintain their functions[43]. In the general microenvironment *in vivo*, the oxygen concentration is usually low. For example, the oxygen concentration in healthy bone marrow is only 1.3% to 7.0%[44], and that in articular cartilage is only 2% to 5%[45]. In particular, OA often occurs in a hypoxic environment. Nitric oxide synthase and hypoxia-inducible factor-1 are often upregulated in OA and aggravate the hypoxic environment[46]. Although the oxygen concentration in the microenvironment of MSCs is low, a 21% O_2 concentration (hereinafter "normoxia") is routinely used in cell culture.

Ciapetti *et al*[22] isolated and cultured BM-MSCs under 2% O_2. They observed a higher tendency of osteogenic differentiation of these cells compared with the cells cultured in standard normoxia. Significant changes in the MSC immunophenotype, such as increased CD73 and CD90 expression, were observed, but CD105 expression was reduced. MSCs cultured under hypoxia have better mineralization, higher mineral density and higher calcium matrix deposition than those cultured under normoxia. Alizarin red S staining is a convenient method for detecting calcium salt deposition. The positive area observed in hypoxic cultured MSCs was greater than that in cells cultured in normoxia, which means

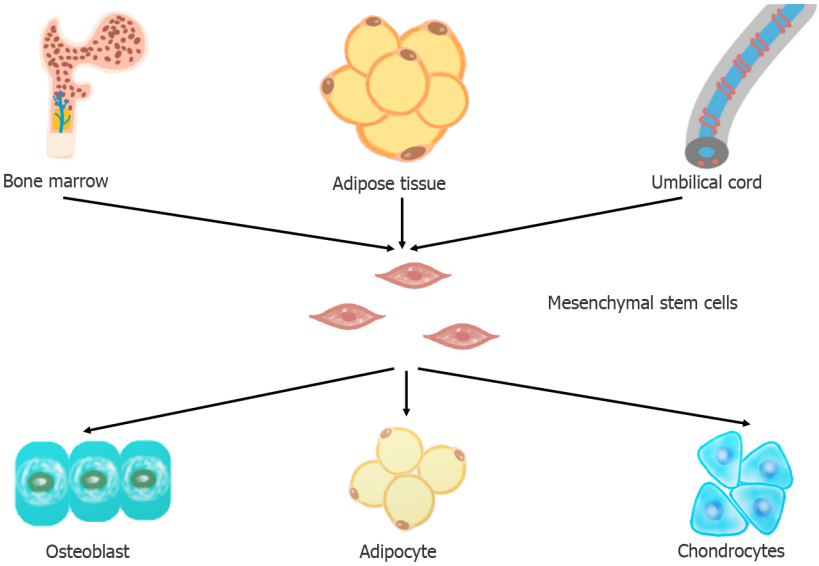

DOI: 10.4252/wjsc.v15.i6.548 **Copyright** ©The Author(s) 2023.

Figure 1 Common sources and differentiation potential of mesenchymal stem cells.

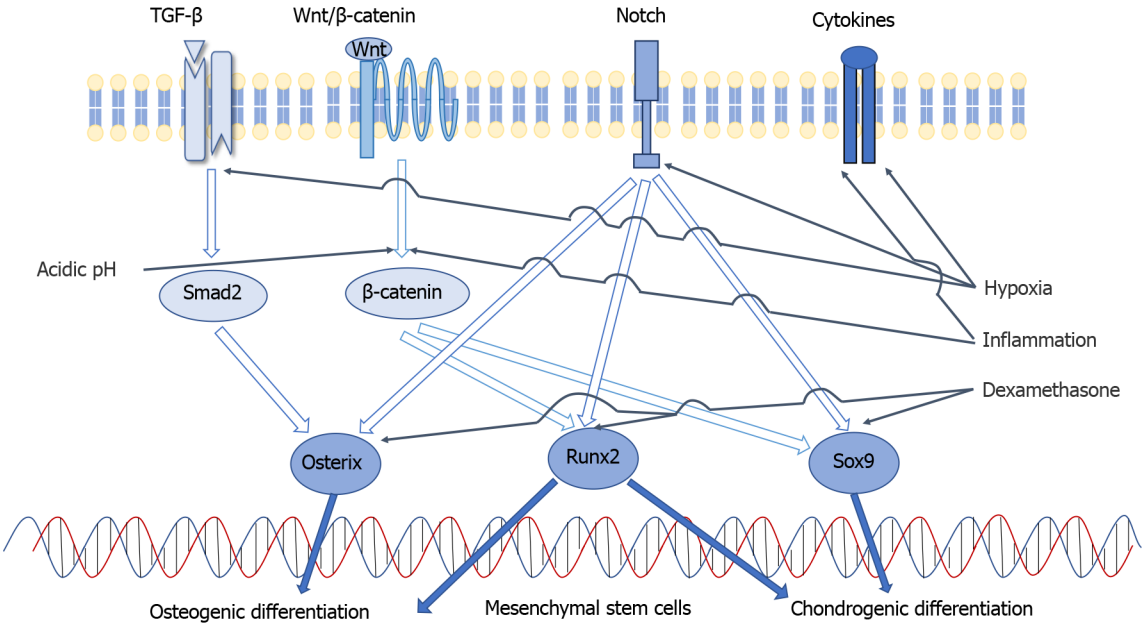

DOI: 10.4252/wjsc.v15.i6.548 **Copyright** ©The Author(s) 2023.

Figure 2 Signaling pathways involved in osteogenic and chondrogenic differentiation of mesenchymal stem cells and the mechanism of certain factors. TGF-β: Transforming growth factor-beta.

that osteoblast differentiation was enhanced[47,48]. Fennema *et al*[49] found that hypoxic culture increased the levels of osteogenic genes, such as osteopontin, osteocalcin, ALP and ColI[50]. Hypoxia activates the Notch signaling pathway, increases the expression of CBF-1α, and promotes the osteogenic differentiation of MSCs[51,52].

Similarly, hypoxic conditions increased the chondrogenic differentiation efficiency compared to normoxic conditions. Chondrogenic differentiation of MSCs can be quantitatively assessed by Safranin O staining[53,54], and the positive area increases after hypoxic culture. Immunohistochemistry demonstrated that the expression of *ColII* increased[50]. Hypoxia may enhance the chondrogenic differentiation capacity of MSCs by enhancing the expression of chondrogenic genes[55]. This may be manifested as increased mRNA expression of glycosaminoglycans, aggrecan, transcription factor and Sox9 [56,57]. The level of cartilage oligomeric matrix protein is higher under hypoxic conditions[53]. These factors play crucial roles in chondrocyte differentiation. Hypoxia affects the overall cellular response through TGF-β, leading to upregulation of cartilage molecular markers, such as *ColII* and Sox9[58]. However, some studies have shown that hypoxia can enhance chondrogenesis and inhibit osteogenesis of MSCs[59,60]. These differences between studies may be due to differences in culture conditions and sources of MSCs and therefore larger sample sizes and more precise experiments are required to

fully elucidate the effect of hypoxia on MSC differentiation.

Inflammation

OA was once referred to as noninflammatory arthritis, but it is now considered a persistent low-grade inflammatory disease, and many inflammatory cells are involved[61]. Chronic inflammation activates the Wnt/β-catenin pathway, which leads to mitochondrial damage and further impairs the differentiation of MSCs[62]. Interferon-gamma (IFN-γ) and TNF-α are two important inflammatory cytokines involved in OA inflammation[63]. Li *et al*[64] pretreated MSCs with IFN-γ and TNF-α to simulate the inflammatory microenvironment. They found that the inflammatory microenvironment promoted chondrogenic differentiation of MSCs and inhibited their osteogenic differentiation.

Acidic pH

Inflammation decreases the extracellular pH and makes the OA joint cavity a weakly acidic microenvironment[65]. The pH of joints with OA (6.40 ± 0.08) was obviously lower than that of normal joints (7.01 ± 0.26)[66]. Decreasing pH was shown to inhibit the proliferation and metabolism of MSCs in culture. Furthermore, the activity of alkaline phosphatase was reduced, which means that the osteogenic differentiation of MSCs was decreased[67]. At physiologic pH (8.0), MSCs exhibit the strongest osteogenic differentiation potential[68]. A pH of 8.0 is recommended for a greater therapeutic effect of MSCs in OA.

Osmolar pressure

The osmolar pressure in the joint cavity of healthy adults is 404 mOsm/L ± 57 mOsm/L, while that in OA patients is 297.0 mOsm/L ± 16.9 mOsm/L. The joint cavity of OA patients is exposed to a hypoosmotic environment[69,70]. At present, there is little research on the effect of osmotic pressure on the osteogenic and chondrogenic differentiation of MSCs. Some studies have demonstrated that hyperosmolarity promotes the chondrogenic differentiation of MSCs and cartilage repair[71-73]. No study on the effect of hypo-osmotic stress has been conducted.

Cytokines

In contrast to normal bone, subchondral bone in advanced OA is characterized by osteosclerosis, including a higher bone volume fraction, a greater number of trabecular bones in the load-bearing area, and an increase in the thickness of the original trabeculae. This may be due to the overexpression of growth factors in the joints of patients with OA, such as insulin-like growth factor 1 and TGF-β[74]. Both of these cytokines have been shown to promote osteogenic and chondrogenic differentiation of MSCs[75,76]. The local expression of basic fibroblast growth factor (bFGF) in the joints of patients with OA is significantly higher than that in healthy people[77]. bFGF has been proven to be an important growth factor for maintaining the stemness of MSCs[78].

OTHER COMMON INFLUENCING FACTORS IN THE TREATMENT OF OA

Glucocorticoids

Dexamethasone is a member of the glucocorticoid class, and it is considered to be the mildest corticosteroid drug used for OA treatment[79]. Intra-articular injection of glucocorticoids is one of the treatment methods for OA[80], and dexamethasone can also be used as an immunosuppressive agent for MSC transplantation. Moreover, dexamethasone is generally considered one of the main components that induces MSCs to differentiate toward osteogenic, adipogenic and chondrogenic lineages[81]. The osteogenic differentiation of MSCs mainly relies on osteogenic induction medium, which is usually composed of dexamethasone, ascorbic acid and β-sodium glycerophosphate. Dexamethasone induces increased expression of Runx2, osterix, and bone matrix proteins. Furthermore, it can induce osteogenic differentiation by inhibiting Sox9 expression[82]. Ascorbic acid and β-sodium glycerophosphate increase the content of ColI and stimulate the formation of a mineralized matrix[11]. Human MSCs need dexamethasone to produce ALP, a marker used to distinguish osteoblasts in culture[83,84]. The chondrogenic differentiation medium often includes dexamethasone, ascorbic acid and TGF-β3. Dexamethasone enhances the expression of the cartilage-specific gene Sox9[85]. The adipogenic differentiation medium often contains dexamethasone, ascorbic acid, 3-isobutyl-1-methylxanthine, insulin and other components[86]. Although the detailed mechanism of differentiation induced by dexa-methasone is currently unknown, dexamethasone clearly affects the direction of MSC differentiation[87].

Doi *et al*[88] found that dexamethasone had certain effects on the osteogenic differentiation of MSCs. The effect of dexamethasone on inducing MSCs to differentiate into osteoblasts depends on the dosage and exposure time of the drugs [89]. It has been reported that short-term use of low-dose (10^{-8}, 10^{-7} mol/L) dexamethasone can stimulate the osteogenesis of MSCs and significantly increase the formation of mineralized nodules and the expression of osteogenic markers (BSPII and Runx-2) in cells[90,91]. It has also been reported that high concentrations of dexamethasone (10^{-6} mol/L) can inhibit the osteogenic differentiation of MSCs and induce them to differentiate into adipocytes. A high dose can reduce the osteogenic differentiation-related surface phenotype, as indicated, for example, by decreased surface expression of CD73. The higher concentration of dexamethasone resulted in enhanced lipid droplet formation and higher expression of lipid-forming markers (PPAR-γ and CEBP-α) in cells. In addition, a high concentration of dexamethasone exacerbates apoptosis of MSCs, inhibits MSC proliferation, and promotes senescence of MSCs[83]. A concentration of dexamethasone up to 10^{-6} mol/L imposes toxic effects on MSCs[89,92]. When the concentration of dexamethasone was lower than 10^{-8} mol/L, no differentiation of osteoblasts was detected[93,94]. Therefore, 10^{-7} mol/L is considered the most appropriate concentration

for inducing MSCs to differentiate into bone[91].

Similarly, dexamethasone can also promote chondrogenic differentiation of MSCs[93]. Tangtrongsup *et al*[95] found that chondrogenic differentiation was suppressed in dexamethasone-free cultures. It can increase the proteoglycan content and collagen type II intracellular content. Dexamethasone may not function as a specific chondrogenic factor to directly promote cartilage differentiation, rather, it may promote it by inducing cells to upregulate cartilage factors, such as Runx2 and Noggin[96]. Its influence is mainly dependent on the context[97].

In addition to the dosage, the duration of dexamethasone treatment also affected the differentiation of MSCs. Dexamethasone is commonly used in bone trauma to relieve edema and pain, but long-term use may lead to osteoporosis through bone loss and bone marrow lipogenesis. Some studies suggest that long-term exposure of MSCs to dexamethasone may negatively impact their differentiation[91]. Others found that a lack of dexamethasone inhibits the differentiation of MSCs, so continuous delivery *in vivo* should be given priority[95]. Moreover, Song *et al*[98] found that within 4 wk, as exposure time increased, stimulation of osteogenic differentiation by dexamethasone strengthened, and calcium deposition increased. According to some authors, the sensitivity of MSCs to dexamethasone depends on the stage of cell maturation. Dexamethasone mainly acts on early stem cells, so it should be applied in the early stage[84]. It has also been suggested that early exposure to dexamethasone has little effect on MSC differentiation, and thus, continuous exposure for at least one week is required[89]. At present, there is little research on the effect of the duration of dexamethasone exposure on MSC differentiation, and more accurate experiments are needed to verify this hypothesis. As a glucocorticoid, dexa-methasone is not suitable for systematic use to regenerate local tissue defects due to possible negative effects on healthy tissues and organs. Therefore, the application of local controlled release devices of dexamethasone in MSC therapy is reasonable.

Scaffolds

MSCs can be injected directly into the damaged site or differentiate into target cells together with the tissue engineering scaffold. Many tissue engineering experiments have proven that biological scaffolds can enhance the osteogenic and chondrogenic differentiation of MSCs. HA is often used to form a stable 3D environment for MSC chondrogenesis *in vitro*, which allows for better provision of oxygen and nutrients to MSCs. HA can promote the osteogenic process of endochondral ossification of MSCs[99]. Three-dimensional nanofibrous scaffolds, such as poly-((D,L)-lactide-ε-caprolactone)dimethacrylate scaffolds and poly(-caprolactone) nanofibrous scaffolds, have been shown to enhance chondrogenic differentiation of MSCs[100,101]. The combination of MSCs with biomaterials can improve the differentiation ability of MSCs. These studies have demonstrated that better efficacy can be achieved by injection of scaffolds loaded with MSCs.

Sources of MSCs

The source of MSCs also significantly impact their differentiation. By reviewing clinical trials, we found that bone marrow-derived MSCs (BM-MSCs), adipose tissue-derived MSCs (AD-MSCs) and umbilical cord-derived MSCs (UC-MSCs) are mainly used in OA research. MSCs from different sources have different characteristics and differentiation potentials[102].

BM-MSCs offer the advantages of strong differentiation ability, mild implantation reaction and strong expansion ability *in vitro*. However, BM-MSCs need to be obtained from the patient's bone marrow, and bone marrow collection is a painful and invasive process. The number of BM-MSCs derived *in vivo* is quite low and requires *in vitro* amplification. Moreover, the differentiation potential and proliferative capacity of BM-MSCs decrease with the age of the donor[103]. Adipose tissue was first identified as an alternative source of MSCs in 2001[104,105]. AD-MSCs offer the advantage that they can be obtained in large quantities in a simple, minimally invasive manner. They can be extracted from excess adipose tissue that is discarded as waste during liposuction, avoiding immunogenicity and ethical concerns. The quantity and quality of MSCs from adipose tissues were significantly higher than those of other tissues[106]. Some studies have suggested that the differentiation potential of AD-MSCs depends on the source of adipose tissue[107]. MSCs from visceral adipose tissues have greater osteogenic differentiation capacity[108,109]. UC-MSCs exhibit superior clonogenic, proliferation and migration capacities[43,110]. They can secrete relevant chondrogenic factors[111,112]. Furthermore, UC-MSCs are less mature, which makes them a better choice for allogeneic therapy[113]. Wharton's jelly (WJ) is the most frequently used source of umbilical cord tissue[114]. WJ-MSCs are relatively novel for cell and tissue engineering therapy and are considered promising candidates for the development of cell-based therapies[113,115].

Many studies have shown that BM-MSCs have higher osteogenic and chondrogenic differentiation potential[116,117]. They exhibit a relatively high incidence of bone and cartilage formation[50], and they can generate more mature bone tissue and more compact cartilage pellets[118]. BM-MSCs express high levels of CD90, which means that they are more suitable for bone repair and regeneration[119].

AD-MSCs are more inclined to differentiate into adipocytes, and their potential for osteogenic differentiation and chondrogenic differentiation is relatively low[107]. Some studies hypothesize that the chondrogenic potential of MSCs derived from adipose tissue is higher than that of MSCs derived from UC sources[120]. However, other studies have suggested that AD-MSCs and UC-MSCs show similar chondrogenic potential[110].

Although BM-MSCs have stronger differentiation ability, AD-MSCs and UB-MSCs perform better for pain relief and functional improvement in OA[121]. AD-MSCs are considered the most effective MSCs in relieving pain, while UC-MSCs are considered the most effective MSCs in improving function in OA patients[122]. Therefore, AD-MSCs and UC-MSCs showed better anti-arthritis efficacy than BM-MSCs[123].

CONCLUSION

In this review, we summarize the common factors that affect the differentiation of MSCs in the OA microenvironment. MSCs can differentiate into different lineages, and these processes are precisely regulated by signaling pathways. Many factors can affect the differentiation direction of MSCs by acting on these signaling pathways. The multidirectional differentiation potential and tunability of MSCs make them a promising treatment for OA and other diseases. A large number of studies have confirmed their safety and effectiveness.

At present, a large number of studies focus on the paracrine effect of MSCs. However, the differentiation function of MSCs can also play an important role in disease treatment. Chemical, physical and biological factors can affect the differentiation of MSCs. Therefore, there are many conditions that can affect the efficacy of MSCs. To control the differentiation of MSCs more precisely to improve their efficacy in the treatment of diseases, it is necessary to understand how various influencing factors work. However, there are few studies on the factors that affect the differentiation direction of MSCs, and we are still at a preliminary stage in understanding how these factors determine the fate of MSCs. More research is needed on the differentiation of MSCs, which is of great value for developing novel therapies for diseases and applying MSCs to clinical practice.

FOOTNOTES

Author contributions: Yi P wrote the paper; Hai J reviewed the literature; Zuo HD designed the outline and coordinated the writing of the paper; and all authors have read and approved the final manuscript.

Supported by the Nature Science Foundation of China, No. 81701756; Sichuan Provincial Department of Education, No. 18ZB0215; City-School Cooperation Project, No. 18SXHZ0389 and No. 22SXZRKX0005; and Chengdu Medical Project, No. 2022573.

Conflict-of-interest statement: There is no conflict of interest associated with any of the senior author or other coauthors contributed their efforts in this manuscript.

Country/Territory of origin: China

ORCID number: Yi Peng 0009-0000-6460-1700; Hai Jiang 0000-0002-5799-016X; Hou-Dong Zuo 0000-0002-1530-3018.

S-Editor: Chen YL
L-Editor: A
P-Editor: Ma YJ

REFERENCES

1 **Sacitharan PK**. Ageing and Osteoarthritis. *Subcell Biochem* 2019; **91**: 123-159 [PMID: 30888652 DOI: 10.1007/978-981-13-3681-2_6]
2 **Allen KD**, Thoma LM, Golightly YM. Epidemiology of osteoarthritis. *Osteoarthritis Cartilage* 2022; **30**: 184-195 [PMID: 34534661 DOI: 10.1016/j.joca.2021.04.020]
3 **Safiri S**, Kolahi AA, Smith E, Hill C, Bettampadi D, Mansournia MA, Hoy D, Ashrafi-Asgarabad A, Sepidarkish M, Almasi-Hashiani A, Collins G, Kaufman J, Qorbani M, Moradi-Lakeh M, Woolf AD, Guillemin F, March L, Cross M. Global, regional and national burden of osteoarthritis 1990-2017: a systematic analysis of the Global Burden of Disease Study 2017. *Ann Rheum Dis* 2020; **79**: 819-828 [PMID: 32398285 DOI: 10.1136/annrheumdis-2019-216515]
4 **Sha Y**, Cai W, Mohanad Khalid A, Chi Q, Wang J, Sun T, Wang C. Pretreatment with mechano growth factor E peptide attenuates osteoarthritis through improving cell proliferation and extracellular matrix synthesis in chondrocytes under severe hypoxia. *Int Immunopharmacol* 2021; **97**: 107628 [PMID: 34015701 DOI: 10.1016/j.intimp.2021.107628]
5 **Zhang RK**, Li GW, Zeng C, Lin CX, Huang LS, Huang GX, Zhao C, Feng SY, Fang H. Mechanical stress contributes to osteoarthritis development through the activation of transforming growth factor beta 1 (TGF-β1). *Bone Joint Res* 2018; **7**: 587-594 [PMID: 30581556 DOI: 10.1302/2046-3758.711.BJR-2018-0057.R1]
6 **Xuan A**, Chen H, Chen T, Li J, Lu S, Fan T, Zeng D, Wen Z, Ma J, Hunter D, Ding C, Zhu Z. The application of machine learning in early diagnosis of osteoarthritis: a narrative review. *Ther Adv Musculoskelet Dis* 2023; **15**: 1759720X231158198 [PMID: 36937823 DOI: 10.1177/1759720X231158198]
7 **Michael JW**, Schlüter-Brust KU, Eysel P. The epidemiology, etiology, diagnosis, and treatment of osteoarthritis of the knee. *Dtsch Arztebl Int* 2010; **107**: 152-162 [PMID: 20305774 DOI: 10.3238/arztebl.2010.0152]
8 **Jang S**, Lee K, Ju JH. Recent Updates of Diagnosis, Pathophysiology, and Treatment on Osteoarthritis of the Knee. *Int J Mol Sci* 2021; **22** [PMID: 33807695 DOI: 10.3390/ijms22052619]
9 **Potten CS**, Loeffler M. Stem cells: attributes, cycles, spirals, pitfalls and uncertainties. Lessons for and from the crypt. *Development* 1990; **110**: 1001-1020 [PMID: 2100251 DOI: 10.1242/dev.110.4.1001]

10 **Friedenstein AJ**, Piatetzky-Shapiro II, Petrakova KV. Osteogenesis in transplants of bone marrow cells. *J Embryol Exp Morphol* 1966; **16**: 381-390 [PMID: 5336210 DOI: 10.1242/dev.16.3.381]

11 **Pittenger MF**, Mackay AM, Beck SC, Jaiswal RK, Douglas R, Mosca JD, Moorman MA, Simonetti DW, Craig S, Marshak DR. Multilineage potential of adult human mesenchymal stem cells. *Science* 1999; **284**: 143-147 [PMID: 10102814 DOI: 10.1126/science.284.5411.143]

12 **Dominici M**, Le Blanc K, Mueller I, Slaper-Cortenbach I, Marini F, Krause D, Deans R, Keating A, Prockop Dj, Horwitz E. Minimal criteria for defining multipotent mesenchymal stromal cells. The International Society for Cellular Therapy position statement. *Cytotherapy* 2006; **8**: 315-317 [PMID: 16923606 DOI: 10.1080/14653240600855905]

13 **Markov A**, Thangavelu L, Aravindhan S, Zekiy AO, Jarahian M, Chartrand MS, Pathak Y, Marofi F, Shamlou S, Hassanzadeh A. Mesenchymal stem/stromal cells as a valuable source for the treatment of immune-mediated disorders. *Stem Cell Res Ther* 2021; **12**: 192 [PMID: 33736695 DOI: 10.1186/s13287-021-02265-1]

14 **Heo JS**, Choi Y, Kim HS, Kim HO. Comparison of molecular profiles of human mesenchymal stem cells derived from bone marrow, umbilical cord blood, placenta and adipose tissue. *Int J Mol Med* 2016; **37**: 115-125 [PMID: 26719857 DOI: 10.3892/ijmm.2015.2413]

15 **Kern S**, Eichler H, Stoeve J, Klüter H, Bieback K. Comparative analysis of mesenchymal stem cells from bone marrow, umbilical cord blood, or adipose tissue. *Stem Cells* 2006; **24**: 1294-1301 [PMID: 16410387 DOI: 10.1634/stemcells.2005-0342]

16 **Beeravolu N**, McKee C, Alamri A, Mikhael S, Brown C, Perez-Cruet M, Chaudhry GR. Isolation and Characterization of Mesenchymal Stromal Cells from Human Umbilical Cord and Fetal Placenta. *J Vis Exp* 2017 [PMID: 28447991 DOI: 10.3791/55224]

17 **Aspden RM**. Subchondral bone - a welcome distraction in OA treatment. *Osteoarthritis Cartilage* 2022; **30**: 911-912 [PMID: 35247544 DOI: 10.1016/j.joca.2022.02.617]

18 **Chien SY**, Tsai CH, Liu SC, Huang CC, Lin TH, Yang YZ, Tang CH. Noggin Inhibits IL-1β and BMP-2 Expression, and Attenuates Cartilage Degeneration and Subchondral Bone Destruction in Experimental Osteoarthritis. *Cells* 2020; **9** [PMID: 32290085 DOI: 10.3390/cells9040927]

19 **Vina ER**, Kwoh CK. Epidemiology of osteoarthritis: literature update. *Curr Opin Rheumatol* 2018; **30**: 160-167 [PMID: 29227353 DOI: 10.1097/BOR.0000000000000479]

20 **Peng Z**, Sun H, Bunpetch V, Koh Y, Wen Y, Wu D, Ouyang H. The regulation of cartilage extracellular matrix homeostasis in joint cartilage degeneration and regeneration. *Biomaterials* 2021; **268**: 120555 [PMID: 33285440 DOI: 10.1016/j.biomaterials.2020.120555]

21 **Ajami S**, Javaheri B, Chang YM, Maruthainar N, Khan T, Donaldson J, Pitsillides AA, Liu C. Spatial links between subchondral bone architectural features and cartilage degeneration in osteoarthritic joints. *Sci Rep* 2022; **12**: 6694 [PMID: 35461315 DOI: 10.1038/s41598-022-10600-6]

22 **Lamo-Espinosa JM**, Mora G, Blanco JF, Granero-Moltó F, Nuñez-Córdoba JM, Sánchez-Echenique C, Bondía JM, Aquerreta JD, Andreu EJ, Ornilla E, Villarón EM, Valentí-Azcárate A, Sánchez-Guijo F, Del Cañizo MC, Valentí-Nin JR, Prósper F. Intra-articular injection of two different doses of autologous bone marrow mesenchymal stem cells *versus* hyaluronic acid in the treatment of knee osteoarthritis: multicenter randomized controlled clinical trial (phase I/II). *J Transl Med* 2016; **14**: 246 [PMID: 27565858 DOI: 10.1186/s12967-016-0998-2]

23 **Tang S**, Chen P, Zhang H, Weng H, Fang Z, Chen C, Peng G, Gao H, Hu K, Chen J, Chen L, Chen X. Comparison of Curative Effect of Human Umbilical Cord-Derived Mesenchymal Stem Cells and Their Small Extracellular Vesicles in Treating Osteoarthritis. *Int J Nanomedicine* 2021; **16**: 8185-8202 [PMID: 34938076 DOI: 10.2147/IJN.S336062]

24 **Ciapetti G**, Granchi D, Fotia C, Savarino L, Dallari D, Del Piccolo N, Donati DM, Baldini N. Effects of hypoxia on osteogenic differentiation of mesenchymal stromal cells used as a cell therapy for avascular necrosis of the femoral head. *Cytotherapy* 2016; **18**: 1087-1099 [PMID: 27421741 DOI: 10.1016/j.jcyt.2016.06.005]

25 **Kim P**, Park J, Lee DJ, Mizuno S, Shinohara M, Hong CP, Jeong Y, Yun R, Park H, Park S, Yang KM, Lee MJ, Jang SP, Kim HY, Lee SJ, Song SU, Park KS, Tanaka M, Ohshima H, Cho JW, Sugiyama F, Takahashi S, Jung HS, Kim SJ. Mast4 determines the cell fate of MSCs for bone and cartilage development. *Nat Commun* 2022; **13**: 3960 [PMID: 35803931 DOI: 10.1038/s41467-022-31697-3]

26 **Chen Q**, Shou P, Zheng C, Jiang M, Cao G, Yang Q, Cao J, Xie N, Velletri T, Zhang X, Xu C, Zhang L, Yang H, Hou J, Wang Y, Shi Y. Fate decision of mesenchymal stem cells: adipocytes or osteoblasts? *Cell Death Differ* 2016; **23**: 1128-1139 [PMID: 26868907 DOI: 10.1038/cdd.2015.168]

27 **Almalki SG**, Agrawal DK. Key transcription factors in the differentiation of mesenchymal stem cells. *Differentiation* 2016; **92**: 41-51 [PMID: 27012163 DOI: 10.1016/j.diff.2016.02.005]

28 **Beederman M**, Lamplot JD, Nan G, Wang J, Liu X, Yin L, Li R, Shui W, Zhang H, Kim SH, Zhang W, Zhang J, Kong Y, Denduluri S, Rogers MR, Pratt A, Haydon RC, Luu HH, Angeles J, Shi LL, He TC. BMP signaling in mesenchymal stem cell differentiation and bone formation. *J Biomed Sci Eng* 2013; **6**: 32-52 [PMID: 26819651 DOI: 10.4236/jbise.2013.68A1004]

29 **Robert AW**, Marcon BH, Dallagiovanna B, Shigunov P. Adipogenesis, Osteogenesis, and Chondrogenesis of Human Mesenchymal Stem/Stromal Cells: A Comparative Transcriptome Approach. *Front Cell Dev Biol* 2020; **8**: 561 [PMID: 32733882 DOI: 10.3389/fcell.2020.00561]

30 **Lefebvre V**, Dvir-Ginzberg M. SOX9 and the many facets of its regulation in the chondrocyte lineage. *Connect Tissue Res* 2017; **58**: 2-14 [PMID: 27128146 DOI: 10.1080/03008207.2016.1183667]

31 **Feng L**, Yang ZM, Li YC, Wang HX, Lo JHT, Zhang XT, Li G. Linc-ROR promotes mesenchymal stem cells chondrogenesis and cartilage formation *via* regulating SOX9 expression. *Osteoarthritis Cartilage* 2021; **29**: 568-578 [PMID: 33485931 DOI: 10.1016/j.joca.2020.12.020]

32 **Wang C**, Shen J, Ying J, Xiao D, O'Keefe RJ. FoxO1 is a crucial mediator of TGF-β/TAK1 signaling and protects against osteoarthritis by maintaining articular cartilage homeostasis. *Proc Natl Acad Sci U S A* 2020; **117**: 30488-30497 [PMID: 33199631 DOI: 10.1073/pnas.2017056117]

33 **Ma N**, Teng X, Zheng Q, Chen P. The regulatory mechanism of p38/MAPK in the chondrogenic differentiation from bone marrow mesenchymal stem cells. *J Orthop Surg Res* 2019; **14**: 434 [PMID: 31831024 DOI: 10.1186/s13018-019-1505-2]

34 **Ahmadi A**, Mazloomnejad R, Kasravi M, Gholamine B, Bahrami S, Sarzaeem MM, Niknejad H. Recent advances on small molecules in osteogenic differentiation of stem cells and the underlying signaling pathways. *Stem Cell Res Ther* 2022; **13**: 518 [PMID: 36371202 DOI: 10.1186/s13287-022-03204-4]

35 **Cai H**, Zou J, Wang W, Yang A. BMP2 induces hMSC osteogenesis and matrix remodeling. *Mol Med Rep* 2021; **23** [PMID: 33300084 DOI: 10.3892/mmr.2020.11764]

36 **Wagley Y**, Chesi A, Acevedo PK, Lu S, Wells AD, Johnson ME, Grant SFA, Hankenson KD. Canonical Notch signaling is required for bone morphogenetic protein-mediated human osteoblast differentiation. *Stem Cells* 2020; **38**: 1332-1347 [PMID: 32535942 DOI: 10.1002/stem.3245]

37 **Gao X**, Xue Y, Yang K. LINC00899 promotes osteogenic differentiation by targeting miR-374a and RUNX2 expression. *Exp Ther Med* 2021; **22**: 1071 [PMID: 34447464 DOI: 10.3892/etm.2021.10505]

38 **Komori T**. Roles of Runx2 in Skeletal Development. *Adv Exp Med Biol* 2017; **962**: 83-93 [PMID: 28299652 DOI: 10.1007/978-981-10-3233-2_6]

39 **Zhang C**. Transcriptional regulation of bone formation by the osteoblast-specific transcription factor Osx. *J Orthop Surg Res* 2010; **5**: 37 [PMID: 20550694 DOI: 10.1186/1749-799X-5-37]

40 **Wang B**, Huang S, Pan L, Jia S. Enhancement of bone formation by genetically engineered human umbilical cord-derived mesenchymal stem cells expressing osterix. *Oral Surg Oral Med Oral Pathol Oral Radiol* 2013; **116**: e221-e229 [PMID: 22819334 DOI: 10.1016/j.oooo.2011.12.024]

41 **Chen XJ**, Shen YS, He MC, Yang F, Yang P, Pang FX, He W, Cao YM, Wei QS. Polydatin promotes the osteogenic differentiation of human bone mesenchymal stem cells by activating the BMP2-Wnt/β-catenin signaling pathway. *Biomed Pharmacother* 2019; **112**: 108746 [PMID: 30970530 DOI: 10.1016/j.biopha.2019.108746]

42 **Zhou X**, Beilter A, Xu Z, Gao R, Xiong S, Paulucci-Holthauzen A, Lozano G, de Crombrugghe B, Gorlick R. Wnt/ß-catenin-mediated p53 suppression is indispensable for osteogenesis of mesenchymal progenitor cells. *Cell Death Dis* 2021; **12**: 521 [PMID: 34021120 DOI: 10.1038/s41419-021-03758-w]

43 **Musiał-Wysocka A**, Kot M, Sułkowski M, Badyra B, Majka M. Molecular and Functional Verification of Wharton's Jelly Mesenchymal Stem Cells (WJ-MSCs) Pluripotency. *Int J Mol Sci* 2019; **20** [PMID: 31013696 DOI: 10.3390/ijms20081807]

44 **Spencer JA**, Ferraro F, Roussakis E, Klein A, Wu J, Runnels JM, Zaher W, Mortensen LJ, Alt C, Turcotte R, Yusuf R, Côté D, Vinogradov SA, Scadden DT, Lin CP. Direct measurement of local oxygen concentration in the bone marrow of live animals. *Nature* 2014; **508**: 269-273 [PMID: 24590072 DOI: 10.1038/nature13034]

45 **Pattappa G**, Markway BD, Docheva D, Johnstone B. Physioxic Culture of Chondrogenic Cells. *Methods Mol Biol* 2023; **2598**: 45-63 [PMID: 36355284 DOI: 10.1007/978-1-0716-2839-3_5]

46 **McCulloch K**, Litherland GJ, Rai TS. Cellular senescence in osteoarthritis pathology. *Aging Cell* 2017; **16**: 210-218 [PMID: 28124466 DOI: 10.1111/acel.12562]

47 **Kwon SY**, Chun SY, Ha YS, Kim DH, Kim J, Song PH, Kim HT, Yoo ES, Kim BS, Kwon TG. Hypoxia Enhances Cell Properties of Human Mesenchymal Stem Cells. *Tissue Eng Regen Med* 2017; **14**: 595-604 [PMID: 30603513 DOI: 10.1007/s13770-017-0068-8]

48 **Valorani MG**, Montelatici E, Germani A, Biddle A, D'Alessandro D, Strollo R, Patrizi MP, Lazzari L, Nye E, Otto WR, Pozzilli P, Alison MR. Pre-culturing human adipose tissue mesenchymal stem cells under hypoxia increases their adipogenic and osteogenic differentiation potentials. *Cell Prolif* 2012; **45**: 225-238 [PMID: 22507457 DOI: 10.1111/j.1365-2184.2012.00817.x]

49 **Gu Q**, Gu Y, Shi Q, Yang H. Hypoxia Promotes Osteogenesis of Human Placental-Derived Mesenchymal Stem Cells. *Tohoku J Exp Med* 2016; **239**: 287-296 [PMID: 27477937 DOI: 10.1620/tjem.239.287]

50 **Fennema EM**, Tchang LAH, Yuan H, van Blitterswijk CA, Martin I, Scherberich A, de Boer J. Ectopic bone formation by aggregated mesenchymal stem cells from bone marrow and adipose tissue: A comparative study. *J Tissue Eng Regen Med* 2018; **12**: e150-e158 [PMID: 28485099 DOI: 10.1002/term.2453]

51 **Landor SK**, Lendahl U. The interplay between the cellular hypoxic response and Notch signaling. *Exp Cell Res* 2017; **356**: 146-151 [PMID: 28456549 DOI: 10.1016/j.yexcr.2017.04.030]

52 **Huang J**, Deng F, Wang L, Xiang XR, Zhou WW, Hu N, Xu L. Hypoxia induces osteogenesis-related activities and expression of core binding factor α1 in mesenchymal stem cells. *Tohoku J Exp Med* 2011; **224**: 7-12 [PMID: 21498965 DOI: 10.1620/tjem.224.7]

53 **Bornes TD**, Jomha NM, Mulet-Sierra A, Adesida AB. Hypoxic culture of bone marrow-derived mesenchymal stromal stem cells differentially enhances *in vitro* chondrogenesis within cell-seeded collagen and hyaluronic acid porous scaffolds. *Stem Cell Res Ther* 2015; **6**: 84 [PMID: 25900045 DOI: 10.1186/s13287-015-0075-4]

54 **Solchaga LA**, Penick KJ, Welter JF. Chondrogenic differentiation of bone marrow-derived mesenchymal stem cells: tips and tricks. *Methods Mol Biol* 2011; **698**: 253-278 [PMID: 21431525 DOI: 10.1007/978-1-60761-999-4_20]

55 **Adesida AB**, Mulet-Sierra A, Jomha NM. Hypoxia mediated isolation and expansion enhances the chondrogenic capacity of bone marrow mesenchymal stromal cells. *Stem Cell Res Ther* 2012; **3**: 9 [PMID: 22385573 DOI: 10.1186/scrt100]

56 **Bae HC**, Park HJ, Wang SY, Yang HR, Lee MC, Han HS. Hypoxic condition enhances chondrogenesis in synovium-derived mesenchymal stem cells. *Biomater Res* 2018; **22**: 28 [PMID: 30275971 DOI: 10.1186/s40824-018-0134-x]

57 **Elabd C**, Ichim TE, Miller K, Anneling A, Grinstein V, Vargas V, Silva FJ. Comparing atmospheric and hypoxic cultured mesenchymal stem cell transcriptome: implication for stem cell therapies targeting intervertebral discs. *J Transl Med* 2018; **16**: 222 [PMID: 30097061 DOI: 10.1186/s12967-018-1601-9]

58 **Foyt DA**, Taheem DK, Ferreira SA, Norman MDA, Petzold J, Jell G, Grigoriadis AE, Gentleman E. Hypoxia impacts human MSC response to substrate stiffness during chondrogenic differentiation. *Acta Biomater* 2019; **89**: 73-83 [PMID: 30844569 DOI: 10.1016/j.actbio.2019.03.002]

59 **Hwang OK**, Noh YW, Hong JT, Lee JW. Hypoxia Pretreatment Promotes Chondrocyte Differentiation of Human Adipose-Derived Stem Cells *via* Vascular Endothelial Growth Factor. *Tissue Eng Regen Med* 2020; **17**: 335-350 [PMID: 32451775 DOI: 10.1007/s13770-020-00265-5]

60 **Peck SH**, Bendigo JR, Tobias JW, Dodge GR, Malhotra NR, Mauck RL, Smith LJ. Hypoxic Preconditioning Enhances Bone Marrow-Derived Mesenchymal Stem Cell Survival in a Low Oxygen and Nutrient-Limited 3D Microenvironment. *Cartilage* 2021; **12**: 512-525 [PMID: 30971109 DOI: 10.1177/1947603519841675]

61 **Robinson WH**, Lepus CM, Wang Q, Raghu H, Mao R, Lindstrom TM, Sokolove J. Low-grade inflammation as a key mediator of the pathogenesis of osteoarthritis. *Nat Rev Rheumatol* 2016; **12**: 580-592 [PMID: 27539668 DOI: 10.1038/nrrheum.2016.136]

62 **Zhai Q**, Chen X, Fei D, Guo X, He X, Zhao W, Shi S, Gooding JJ, Jin F, Jin Y, Li B. Nanorepairers Rescue Inflammation-Induced Mitochondrial Dysfunction in Mesenchymal Stem Cells. *Adv Sci (Weinh)* 2022; **9**: e2103839 [PMID: 34894103 DOI: 10.1002/advs.202103839]

63 **Schuerwegh AJ**, Dombrecht EJ, Stevens WJ, Van Offel JF, Bridts CH, De Clerck LS. Influence of pro-inflammatory (IL-1 alpha, IL-6, TNF-alpha, IFN-gamma) and anti-inflammatory (IL-4) cytokines on chondrocyte function. *Osteoarthritis Cartilage* 2003; **11**: 681-687 [PMID: 12954239 DOI: 10.1016/s1063-4584(03)00156-0]

64 **Lu S**, Qiao X. Single-cell profiles of human bone marrow-derived mesenchymal stromal cells after IFN-γ and TNF-α licensing. *Gene* 2021; **771**: 145347 [PMID: 33333228 DOI: 10.1016/j.gene.2020.145347]

65 **Li R**, Guan Z, Bi S, Wang F, He L, Niu X, You Y, Liu Y, Ding Y, Siwko S, Wang N, Zhang Z, Jin Y, Luo J. The proton-activated G protein-coupled receptor GPR4 regulates the development of osteoarthritis *via* modulating CXCL12/CXCR7 signaling. *Cell Death Dis* 2022; **13**: 152 [PMID: 35165253 DOI: 10.1038/s41419-021-04455-4]

66 **Lombardi AF**, Ma Y, Jang H, Jerban S, Tang Q, Searleman AC, Meyer RS, Du J, Chang EY. AcidoCEST-UTE MRI Reveals an Acidic

Microenvironment in Knee Osteoarthritis. *Int J Mol Sci* 2022; **23** [PMID: 35457284 DOI: 10.3390/ijms23084466]

67 **Chen T**, Zhou Y, Tan WS. Influence of lactic acid on the proliferation, metabolism, and differentiation of rabbit mesenchymal stem cells. *Cell Biol Toxicol* 2009; **25**: 573-586 [PMID: 19130272 DOI: 10.1007/s10565-008-9113-7]

68 **Nuttelman CR**, Kloxin AM, Anseth KS. Temporal changes in peg hydrogel structure influence human mesenchymal stem cell proliferation and matrix mineralization. *Adv Exp Med Biol* 2006; **585**: 135-149 [PMID: 17120782 DOI: 10.1007/978-0-387-34133-0_10]

69 **Wang Z**, Irianto J, Kazun S, Wang W, Knight MM. The rate of hypo-osmotic challenge influences regulatory volume decrease (RVD) and mechanical properties of articular chondrocytes. *Osteoarthritis Cartilage* 2015; **23**: 289-299 [PMID: 25450844 DOI: 10.1016/j.joca.2014.11.003]

70 **Deng Z**, Lin Z, Zhong Q, Lu M, Fang H, Liu J, Duan L, Chen L, Wang L, Wang D, Li W. Interleukin 1 beta-induced chloride currents are important in osteoarthritis onset: an *in vitro* study. *Acta Biochim Biophys Sin (Shanghai)* 2021; **53**: 400-409 [PMID: 33677475 DOI: 10.1093/abbs/gmab010]

71 **Konar E**, Khatami SR, Pezeshki SP, Shafiei M, Hajjari MR. The effect of PRP and hyperosmolarity simultaneous use on expression profile alteration of miRNAs associated with cartilage differentiation in human adipose tissue-derived mesenchymal stem cells. *Gene* 2023; **859**: 147188 [PMID: 36632912 DOI: 10.1016/j.gene.2023.147188]

72 **Ahmadyan S**, Kabiri M, Hanaee-Ahvaz H, Farazmand A. Osmolyte Type and the Osmolarity Level Affect Chondrogenesis of Mesenchymal Stem Cells. *Appl Biochem Biotechnol* 2018; **185**: 507-523 [PMID: 29196933 DOI: 10.1007/s12010-017-2647-5]

73 **Alinezhad-Bermi S**, Kabiri M, Rad I, Irani S, Hanaee-Ahvaz H. Hyperosmolarity benefits cartilage regeneration by enhancing expression of chondrogenic markers and reducing inflammatory markers. *In Vitro Cell Dev Biol Anim* 2021; **57**: 290-299 [PMID: 33580417 DOI: 10.1007/s11626-020-00430-z]

74 **Zhang L**, Wen C. Osteocyte Dysfunction in Joint Homeostasis and Osteoarthritis. *Int J Mol Sci* 2021; **22** [PMID: 34204587 DOI: 10.3390/ijms22126522]

75 **Levi B**, James AW, Wan DC, Glotzbach JP, Commons GW, Longaker MT. Regulation of human adipose-derived stromal cell osteogenic differentiation by insulin-like growth factor-1 and platelet-derived growth factor-alpha. *Plast Reconstr Surg* 2010; **126**: 41-52 [PMID: 20220555 DOI: 10.1097/PRS.0b013e3181da8858]

76 **Blaney Davidson EN**, van der Kraan PM, van den Berg WB. TGF-beta and osteoarthritis. *Osteoarthritis Cartilage* 2007; **15**: 597-604 [PMID: 17391995 DOI: 10.1016/j.joca.2007.02.005]

77 **Honsawek S**, Yuktanandana P, Tanavalee A, Saetan N, Anomasiri W, Parkpian V. Correlation between plasma and synovial fluid basic fibroblast growth factor with radiographic severity in primary knee osteoarthritis. *Int Orthop* 2012; **36**: 981-985 [PMID: 22173563 DOI: 10.1007/s00264-011-1435-z]

78 **Youssef A**, Aboalola D, Han VK. The Roles of Insulin-Like Growth Factors in Mesenchymal Stem Cell Niche. *Stem Cells Int* 2017; **2017**: 9453108 [PMID: 28298931 DOI: 10.1155/2017/9453108]

79 **Wyles CC**, Houdek MT, Wyles SP, Wagner ER, Behfar A, Sierra RJ. Differential cytotoxicity of corticosteroids on human mesenchymal stem cells. *Clin Orthop Relat Res* 2015; **473**: 1155-1164 [PMID: 25187334 DOI: 10.1007/s11999-014-3925-y]

80 **Orchard JW**. Is there a place for intra-articular corticosteroid injections in the treatment of knee osteoarthritis? *BMJ* 2020; **368**: l6923 [PMID: 31941647 DOI: 10.1136/bmj.l6923]

81 **Rawat S**, Dadhwal V, Mohanty S. Dexamethasone priming enhances stemness and immunomodulatory property of tissue-specific human mesenchymal stem cells. *BMC Dev Biol* 2021; **21**: 16 [PMID: 34736395 DOI: 10.1186/s12861-021-00246-4]

82 **Della Bella E**, Buetti-Dinh A, Licandro G, Ahmad P, Basoli V, Alini M, Stoddart MJ. Dexamethasone Induces Changes in Osteogenic Differentiation of Human Mesenchymal Stromal Cells *via* SOX9 and PPARG, but Not RUNX2. *Int J Mol Sci* 2021; **22** [PMID: 33946412 DOI: 10.3390/ijms22094785]

83 **Wang H**, Pang B, Li Y, Zhu D, Pang T, Liu Y. Dexamethasone has variable effects on mesenchymal stromal cells. *Cytotherapy* 2012; **14**: 423-430 [PMID: 22364108 DOI: 10.3109/14653249.2011.652735]

84 **Fiorentini E**, Granchi D, Leonardi E, Baldini N, Ciapetti G. Effects of osteogenic differentiation inducers on *in vitro* expanded adult mesenchymal stromal cells. *Int J Artif Organs* 2011; **34**: 998-1011 [PMID: 22161283 DOI: 10.5301/ijao.5000001]

85 **Richardson SM**, Kalamegam G, Pushparaj PN, Matta C, Memic A, Khademhosseini A, Mobasheri R, Poletti FL, Hoyland JA, Mobasheri A. Mesenchymal stem cells in regenerative medicine: Focus on articular cartilage and intervertebral disc regeneration. *Methods* 2016; **99**: 69-80 [PMID: 26384579 DOI: 10.1016/j.ymeth.2015.09.015]

86 **Lu H**, Guo L, Wozniak MJ, Kawazoe N, Tateishi T, Zhang X, Chen G. Effect of cell density on adipogenic differentiation of mesenchymal stem cells. *Biochem Biophys Res Commun* 2009; **381**: 322-327 [PMID: 19309772 DOI: 10.1016/j.bbrc.2009.01.174]

87 **Lavrentieva A**, Hatlapatka T, Neumann A, Weyand B, Kasper C. Potential for osteogenic and chondrogenic differentiation of MSC. *Adv Biochem Eng Biotechnol* 2013; **129**: 73-88 [PMID: 22457052 DOI: 10.1007/10_2012_133]

88 **Doi M**, Nagano A, Nakamura Y. Genome-wide screening by cDNA microarray of genes associated with matrix mineralization by human mesenchymal stem cells in vitro. *Biochem Biophys Res Commun* 2002; **290**: 381-390 [PMID: 11779180 DOI: 10.1006/bbrc.2001.6196]

89 **Li X**, Xu L, Nie H, Lei L. Dexamethasone-loaded β-cyclodextrin for osteogenic induction of mesenchymal stem/progenitor cells and bone regeneration. *J Biomed Mater Res A* 2021; **109**: 1125-1135 [PMID: 32981208 DOI: 10.1002/jbm.a.37104]

90 **Song IH**, Caplan AI, Dennis JE. Dexamethasone inhibition of confluence-induced apoptosis in human mesenchymal stem cells. *J Orthop Res* 2009; **27**: 216-221 [PMID: 18683880 DOI: 10.1002/jor.20726]

91 **Li T**, Xu Y, Wang Y, Jiang Y. Differential expression profiles of long noncoding RNAs and mRNAs in human bone marrow mesenchymal stem cells after exposure to a high dosage of dexamethasone. *Stem Cell Res Ther* 2021; **12**: 9 [PMID: 33407832 DOI: 10.1186/s13287-020-02040-8]

92 **de Girolamo L**, Sartori MF, Albisetti W, Brini AT. Osteogenic differentiation of human adipose-derived stem cells: comparison of two different inductive media. *J Tissue Eng Regen Med* 2007; **1**: 154-157 [PMID: 18038404 DOI: 10.1002/term.12]

93 **Cárcamo-Orive I**, Gaztelumendi A, Delgado J, Tejados N, Dorronsoro A, Fernández-Rueda J, Pennington DJ, Trigueros C. Regulation of human bone marrow stromal cell proliferation and differentiation capacity by glucocorticoid receptor and AP-1 crosstalk. *J Bone Miner Res* 2010; **25**: 2115-2125 [PMID: 20499359 DOI: 10.1002/jbmr.120]

94 **Kim HJ**, Yi SW, Oh HJ, Lee JS, Park JS, Park KH. Transfection of gene regulation nanoparticles complexed with pDNA and shRNA controls multilineage differentiation of hMSCs. *Biomaterials* 2018; **177**: 1-13 [PMID: 29883913 DOI: 10.1016/j.biomaterials.2018.05.035]

95 **Tangtrongsup S**, Kisiday JD. Effects of Dexamethasone Concentration and Timing of Exposure on Chondrogenesis of Equine Bone Marrow-Derived Mesenchymal Stem Cells. *Cartilage* 2016; **7**: 92-103 [PMID: 26958321 DOI: 10.1177/1947603515595263]

96 **Stewart AA**, Byron CR, Pondenis HC, Stewart MC. Effect of dexamethasone supplementation on chondrogenesis of equine mesenchymal stem cells. *Am J Vet Res* 2008; **69**: 1013-1021 [PMID: 18672964 DOI: 10.2460/ajvr.69.8.1013]

97 **Shintani N**, Hunziker EB. Differential effects of dexamethasone on the chondrogenesis of mesenchymal stromal cells: influence of microenvironment, tissue origin and growth factor. *Eur Cell Mater* 2011; **22**: 302-19; discussion 319 [PMID: 22116649 DOI: 10.22203/ecm.v022a23]

98 **Song IH**, Caplan AI, Dennis JE. In vitro dexamethasone pretreatment enhances bone formation of human mesenchymal stem cells in vivo. *J Orthop Res* 2009; **27**: 916-921 [PMID: 19137580 DOI: 10.1002/jor.20838]

99 **Guo P**, Liu X, Zhang P, He Z, Li Z, Alini M, Richards RG, Grad S, Stoddart MJ, Zhou G, Zou X, Chan D, Tian W, Chen D, Gao M, Zhou Z, Liu S. A single-cell transcriptome of mesenchymal stromal cells to fabricate bioactive hydroxyapatite materials for bone regeneration. *Bioact Mater* 2022; **9**: 281-298 [PMID: 34820571 DOI: 10.1016/j.bioactmat.2021.08.009]

100 **Li WJ**, Tuli R, Okafor C, Derfoul A, Danielson KG, Hall DJ, Tuan RS. A three-dimensional nanofibrous scaffold for cartilage tissue engineering using human mesenchymal stem cells. *Biomaterials* 2005; **26**: 599-609 [PMID: 15282138 DOI: 10.1016/j.biomaterials.2004.03.005]

101 **Spreda M**, Hauptmann N, Lehner V, Biehl C, Liefeith K, Lips KS. Porous 3D Scaffolds Enhance MSC Vitality and Reduce Osteoclast Activity. *Molecules* 2021; **26** [PMID: 34684837 DOI: 10.3390/molecules26206258]

102 **Fan XL**, Zhang Y, Li X, Fu QL. Mechanisms underlying the protective effects of mesenchymal stem cell-based therapy. *Cell Mol Life Sci* 2020; **77**: 2771-2794 [PMID: 31965214 DOI: 10.1007/s00018-020-03454-6]

103 **Babenko VA**, Silachev DN, Danilina TI, Goryunov KV, Pevzner IB, Zorova LD, Popkov VA, Chernikov VP, Plotnikov EY, Sukhikh GT, Zorov DB. Age-Related Changes in Bone-Marrow Mesenchymal Stem Cells. *Cells* 2021; **10** [PMID: 34063923 DOI: 10.3390/cells10061273]

104 **Zuk PA**, Zhu M, Mizuno H, Huang J, Futrell JW, Katz AJ, Benhaim P, Lorenz HP, Hedrick MH. Multilineage cells from human adipose tissue: implications for cell-based therapies. *Tissue Eng* 2001; **7**: 211-228 [PMID: 11304456 DOI: 10.1089/107632701300062859]

105 **Zuk PA**, Zhu M, Ashjian P, De Ugarte DA, Huang JI, Mizuno H, Alfonso ZC, Fraser JK, Benhaim P, Hedrick MH. Human adipose tissue is a source of multipotent stem cells. *Mol Biol Cell* 2002; **13**: 4279-4295 [PMID: 12475952 DOI: 10.1091/mbc.e02-02-0105]

106 **Russell AL**, Lefavor R, Durand N, Glover L, Zubair AC. Modifiers of mesenchymal stem cell quantity and quality. *Transfusion* 2018; **58**: 1434-1440 [PMID: 29582436 DOI: 10.1111/trf.14597]

107 **Nepali S**, Park M, Lew H, Kim O. Comparative Analysis of Human Adipose-Derived Mesenchymal Stem Cells from Orbital and Abdominal Fat. *Stem Cells Int* 2018; **2018**: 3932615 [PMID: 30210548 DOI: 10.1155/2018/3932615]

108 **Ong WK**, Chakraborty S, Sugii S. Adipose Tissue: Understanding the Heterogeneity of Stem Cells for Regenerative Medicine. *Biomolecules* 2021; **11** [PMID: 34206204 DOI: 10.3390/biom11070918]

109 **Ritter A**, Friemel A, Roth S, Kreis NN, Hoock SC, Safdar BK, Fischer K, Möllmann C, Solbach C, Louwen F, Yuan J. Subcutaneous and Visceral Adipose-Derived Mesenchymal Stem Cells: Commonality and Diversity. *Cells* 2019; **8** [PMID: 31640218 DOI: 10.3390/cells8101288]

110 **Ju Y**, Yi L, Li C, Wang T, Zhang W, Chai W, Yin X, Weng T. Comparison of biological characteristics of human adipose- and umbilical cord-derived mesenchymal stem cells and their effects on delaying the progression of osteoarthritis in a rat model. *Acta Histochem* 2022; **124**: 151911 [PMID: 35764040 DOI: 10.1016/j.acthis.2022.151911]

111 **Matas J**, Orrego M, Amenabar D, Infante C, Tapia-Limonchi R, Cadiz MI, Alcayaga-Miranda F, González PL, Muse E, Khoury M, Figueroa FE, Espinoza F. Umbilical Cord-Derived Mesenchymal Stromal Cells (MSCs) for Knee Osteoarthritis: Repeated MSC Dosing Is Superior to a Single MSC Dose and to Hyaluronic Acid in a Controlled Randomized Phase I/II Trial. *Stem Cells Transl Med* 2019; **8**: 215-224 [PMID: 30592390 DOI: 10.1002/sctm.18-0053]

112 **Bartolucci J**, Verdugo FJ, González PL, Larrea RE, Abarzua E, Goset C, Rojo P, Palma I, Lamich R, Pedreros PA, Valdivia G, Lopez VM, Nazzal C, Alcayaga-Miranda F, Cuenca J, Brobeck MJ, Patel AN, Figueroa FE, Khoury M. Safety and Efficacy of the Intravenous Infusion of Umbilical Cord Mesenchymal Stem Cells in Patients With Heart Failure: A Phase 1/2 Randomized Controlled Trial (RIMECARD Trial [Randomized Clinical Trial of Intravenous Infusion Umbilical Cord Mesenchymal Stem Cells on Cardiopathy]). *Circ Res* 2017; **121**: 1192-1204 [PMID: 28974553 DOI: 10.1161/CIRCRESAHA.117.310712]

113 **Avercenc-Léger L**, Guerci P, Virion JM, Cauchois G, Hupont S, Rahouadj R, Magdalou J, Stoltz JF, Bensoussan D, Huselstein C, Reppel L. Umbilical cord-derived mesenchymal stromal cells: predictive obstetric factors for cell proliferation and chondrogenic differentiation. *Stem Cell Res Ther* 2017; **8**: 161 [PMID: 28676126 DOI: 10.1186/s13287-017-0609-z]

114 **Mushahary D**, Spittler A, Kasper C, Weber V, Charwat V. Isolation, cultivation, and characterization of human mesenchymal stem cells. *Cytometry A* 2018; **93**: 19-31 [PMID: 29072818 DOI: 10.1002/cyto.a.23242]

115 **Vieira Paladino F**, de Moraes Rodrigues J, da Silva A, Goldberg AC. The Immunomodulatory Potential of Wharton's Jelly Mesenchymal Stem/Stromal Cells. *Stem Cells Int* 2019; **2019**: 3548917 [PMID: 31281372 DOI: 10.1155/2019/3548917]

116 **Kim HJ**, Kim KW, Kwon YR, Kim BM, Kim YJ. Forced expression of CD200 improves the differentiation capability and immunoregulatory functions of mesenchymal stromal cells. *Biotechnol Lett* 2018; **40**: 1425-1433 [PMID: 29740779 DOI: 10.1007/s10529-018-2561-0]

117 **Jeyaraman M**, Muthu S, Ganie PA. Does the Source of Mesenchymal Stem Cell Have an Effect in the Management of Osteoarthritis of the Knee? Meta-Analysis of Randomized Controlled Trials. *Cartilage* 2021; **13**: 1532S-1547S [PMID: 32840122 DOI: 10.1177/1947603520951623]

118 **Wang JP**, Liao YT, Wu SH, Huang HK, Chou PH, Chiang ER. Adipose Derived Mesenchymal Stem Cells from a Hypoxic Culture Reduce Cartilage Damage. *Stem Cell Rev Rep* 2021; **17**: 1796-1809 [PMID: 33893621 DOI: 10.1007/s12015-021-10169-z]

119 **Sangeetha KN**, Vennila R, Secunda R, Sakthivel S, Pathak S, Jeswanth S, Surendran R. Functional variations between Mesenchymal Stem Cells of different tissue origins: A comparative gene expression profiling. *Biotechnol Lett* 2020; **42**: 1287-1304 [PMID: 32372268 DOI: 10.1007/s10529-020-02898-x]

120 **Tsvetkova AV**, Vakhrushev IV, Basok YB, Grigor'ev AM, Kirsanova LA, Lupatov AY, Sevastianov VI, Yarygin KN. Chondrogeneic Potential of MSC from Different Sources in Spheroid Culture. *Bull Exp Biol Med* 2021; **170**: 528-536 [PMID: 33725253 DOI: 10.1007/s10517-021-05101-x]

121 **Zhang Y**, Yang H, He F, Zhu X. Intra-articular injection choice for osteoarthritis: making sense of cell source-an updated systematic review and dual network meta-analysis. *Arthritis Res Ther* 2022; **24**: 260 [PMID: 36443838 DOI: 10.1186/s13075-022-02953-0]

122 **Wei ZJ**, Wang QQ, Cui ZG, Inadera H, Jiang X, Wu CA. Which is the most effective one in knee osteoarthritis treatment from mesenchymal stem cells obtained from different sources?-A systematic review with conventional and network meta-analyses of randomized controlled trials. *Ann Transl Med* 2021; **9**: 452 [PMID: 33850849 DOI: 10.21037/atm-20-5116]

123 **Chahal J**, Gómez-Aristizábal A, Shestopaloff K, Bhatt S, Chaboureau A, Fazio A, Chisholm J, Weston A, Chiovitti J, Keating A, Kapoor M, Ogilvie-Harris DJ, Syed KA, Gandhi R, Mahomed NN, Marshall KW, Sussman MS, Naraghi AM, Viswanathan S. Bone Marrow Mesenchymal Stromal Cell Treatment in Patients with Osteoarthritis Results in Overall Improvement in Pain and Symptoms and Reduces Synovial Inflammation. *Stem Cells Transl Med* 2019; **8**: 746-757 [PMID: 30964245 DOI: 10.1002/sctm.18-0183]

World Journal of Stem Cells

Submit a Manuscript: https://www.f6publishing.com

World J Stem Cells 2023 June 26; 15(6): 561-575

DOI: 10.4252/wjsc.v15.i6.561

ISSN 1948-0210 (online)

MINIREVIEWS

Potential regulatory effects of stem cell exosomes on inflammatory response in ischemic stroke treatment

Na Chen, Yan-Lin Wang, Hui-Fang Sun, Zhuo-Ya Wang, Qi Zhang, Fei-Yan Fan, Yu-Cheng Ma, Fei-Xiang Liu, Yun-Ke Zhang

Specialty type: Cell and tissue engineering

Provenance and peer review: Unsolicited article; Externally peer reviewed.

Peer-review model: Single blind

Peer-review report's scientific quality classification

Grade A (Excellent): 0
Grade B (Very good): B
Grade C (Good): C, C
Grade D (Fair): 0
Grade E (Poor): 0

P-Reviewer: Chen X, United States; Song BW, South Korea; Liu W, China

Received: January 7, 2023
Peer-review started: January 7, 2023
First decision: April 10, 2023
Revised: April 22, 2023
Accepted: May 16, 2023
Article in press: May 16, 2023
Published online: June 26, 2023

Na Chen, Fei-Yan Fan, Yu-Cheng Ma, First School of Clinical Medicine, Henan University of Chinese Medicine, Zhengzhou 450046, Henan Province, China

Yan-Lin Wang, Hui-Fang Sun, Zhuo-Ya Wang, Qi Zhang, Department of Neurology, The First Affiliated Hospital of Zhengzhou University, Zhengzhou 450052, Henan Province, China

Fei-Xiang Liu, Yun-Ke Zhang, Department of Neurology, The First Affiliated Hospital of Henan University of Chinese Medicine, Zhengzhou 450000, Henan Province, China

Yun-Ke Zhang, School of Rehabilitation Medicine, Henan University of Chinese Medicine, Zhengzhou 450008, Henan Province, China

Corresponding author: Yun-Ke Zhang, PhD, Doctor, School of Rehabilitation Medicine, Henan University of Chinese Medicine, No. 156 Jinshui East Road, Zhengdong New District, Zhengzhou 450008, Henan Province, China. henanzyk@126.com

Abstract

The high incidence and disability rates of stroke pose a heavy burden on society. Inflammation is a significant pathological reaction that occurs after an ischemic stroke. Currently, therapeutic methods, except for intravenous thrombolysis and vascular thrombectomy, have limited time windows. Mesenchymal stem cells (MSCs) can migrate, differentiate, and inhibit inflammatory immune responses. Exosomes (Exos), which are secretory vesicles, have the characteristics of the cells from which they are derived, making them attractive targets for research in recent years. MSC-derived exosomes can attenuate the inflammatory response caused by cerebral stroke by modulating damage-associated molecular patterns. In this review, research on the inflammatory response mechanisms associated with Exos therapy after an ischemic injury is discussed to provide a new approach to clinical treatment.

Key Words: Mesenchymal stem cell-derived exosome; MicroRNA; Inflammation; Ischemic stroke; Adipose-derived stem cell; Toll-like receptor

Core Tip: Mesenchymal stem cell-derived exosome (MSC-Exos) transplantation is a novel treatment method for ischemic stroke that exhibits certain achievements in trials. Here, we review the strategies developed for MSC-Exos in the neuroinflammatory response of patients with stroke and provide potential therapeutic targets. These methods provide new insights for the future clinical application of MSC-Exos in the treatment of ischemic stroke.

Citation: Chen N, Wang YL, Sun HF, Wang ZY, Zhang Q, Fan FY, Ma YC, Liu FX, Zhang YK. Potential regulatory effects of stem cell exosomes on inflammatory response in ischemic stroke treatment. *World J Stem Cells* 2023; 15(6): 561-575
URL: https://www.wjgnet.com/1948-0210/full/v15/i6/561.htm
DOI: https://dx.doi.org/10.4252/wjsc.v15.i6.561

INTRODUCTION

Stroke is a common clinical condition that frequently occurs in middle-aged and elderly people and is a global public health problem with high disability and mortality rates; it ranks third in the list of diseases affecting human lifespan[1]. The main goals of stroke treatment are vascular recanalization and reduction of cerebral ischemic injury. At present, the main recanalization methods are intravenous thrombolysis and endovascular mechanical thrombectomy; however, owing to the restricted time window and various comorbidities, few patients can benefit from these procedures[2,3]. Increasing evidence has suggested that inflammatory cytokines promote the migration of immune cells to damaged tissues through the blood-brain barrier (BBB) after stroke, aggravating the inflammatory response and leading to nerve cell injury[4,5]. However, the exact molecular mechanisms underlying the inflammatory response after stroke remain unclear, hindering the development of effective and specific treatments.

The effectiveness of stem cell transplantation, which can regulate the immune-inflammatory response and the permeability of the BBB, in the treatment of ischemic stroke (IS) has been verified[6,7]. However, pluripotent stem cells are obstructed by the BBB and cannot effectively enter the central nervous system, leading to risks, such as tumorigenicity, thrombosis, and pulmonary embolism, limiting their clinical application. It has been suggested that the therapeutic mechanism of mesenchymal stem cells (MSCs) may involve secreted exosomes (Exos) rather than the direct replacement of brain cells[8]. MSC-derived extracellular vesicles (MSC-EVs) possess the biological characteristics of cells and can penetrate the BBB, reduce the risk of tumors and pulmonary embolism, considerably improve therapeutic efficiency, and reduce complications, thereby having broad therapeutic prospects. MSC-derived Exos (MSC-Exos) reduce inflammatory responses after stroke[9-12]. However, the specific mechanism by which Exos alleviate the inflammatory response after stroke has not yet been explored.

Therefore, in this review, we present the current progress in research on the unique biological characteristics of MSC-Exos and the specific mechanism of action of MSC-Exos in the neuroinflammatory response after stroke. This review aims to explore the role of Exos in the neuroinflammatory response in stroke and provide potential therapeutic targets, with the expectation of offering a reference for future clinical treatments.

PATHOLOGICAL CHANGES AFTER CEREBRAL ISCHEMIA

Brain cell death after stroke can lead to a series of pathological processes including cell energy failure, neuronal apoptosis, leukocyte infiltration, inflammatory immune responses, tight junction (TJ) protein breakage and degradation, BBB destruction, and increased permeability[13,14]. The main goals of IS treatment are to restore blood flow and improve functional outcomes as soon as possible[15]. In addition, methods of regulating immune inflammation and oxidative stress responses, anti-apoptosis, and promotion of angiogenesis and neurogenesis are of great significance for the treatment of cerebral apoplexy in ischemic and hypoxic injured brain tissues[16]. The BBB controls the inflow and outflow of biological substances necessary for metabolic activity and neuronal function in the brain; therefore, its structural and functional integrity is essential for maintaining the brain microenvironment. The BBB is mainly comprised of vascular endothelial cells, pericytes, the basement membrane, astrocytes, neurons, and microglia, which exchange substances that connect the central and peripheral nervous systems. The mechanisms of BBB injury after stroke include modification of TJ proteins, regulation of transporter expression, and inflammatory damage[17]. The intravascular inflammatory response marks the beginning of BBB disruption and leukocyte infiltration in ischemic brain tissue[18]. The inflammatory response after stroke is an important factor in BBB disruption and nerve cell edema, leading to damage to mental function and even death (Figure 1).

Microglia are the resident immune cells of the brain that polarize into different phenotypes (M1 or M2)[19]. M1 inflamed microglia lead to BBB dysfunction and vascular 'leakage,' whereas M2 microglia have inflammation-inhibiting, immune-regulating, tissue-repair, and damage-eliminating functions; they also protect the BBB[20]. Activated M1 microglia release the pro-inflammatory factors tumor necrosis factor-α (TNF-α), interleukin (IL)-1, and IL-6, which activate the nuclear factor kappa-B (NF-κB)-mediated inflammatory response of reactive astrocytes (A1s) and further amplify this effect[21]. Owing to inflammatory response stimulation, the structure of the neurovascular unit (NVU) changes, which inhibits central nervous system restoration. This change in the microenvironment stimulates M2 microglia to initiate phagocytosis and secrete transforming growth factor-β (TGFβ), IL-4, and IL-10, and the engulfment of

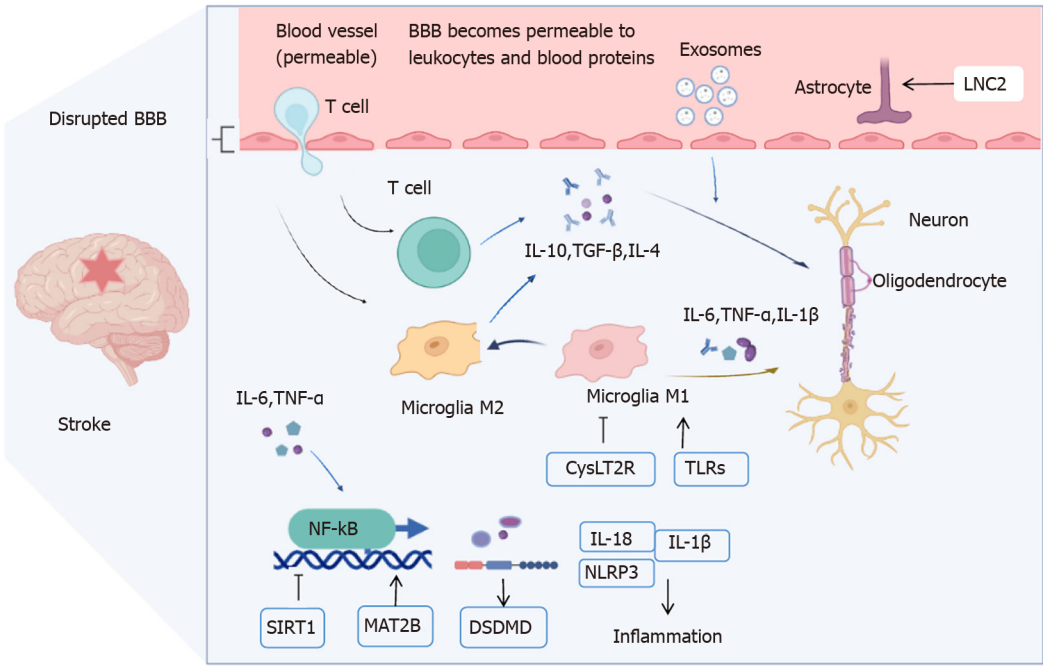

DOI: 10.4252/wjsc.v15.i6.561

Figure 1 Pathological changes after stroke. Blood-brain barrier (BBB) disruption after stroke is permeable to leukocytes and blood proteins. Microglia are stimulated, and these activated microglia (M1), in turn, release tumor necrosis factor-α, interleukin (IL)-6, and IL-1β, which activate the nuclear factor kappa-B inflammatory response of reactive astrocytes (A1) and further amplify this effect. Exosomes can penetrate BBB, promote microglial M1 polarization to M2 and T cell activation, mediate lipocalin-2, sirtuin 1, methionine adenosyl transferase 2B, pyrin domain-containing protein, cysteinyl leukotriene receptor 2, and other signaling pathways to promote the release of anti-inflammatory cytokines IL-10, transforming growth factor-β, and IL-4. By BioRender.com. BBB: Blood-brain barrier; CysLT2: Cysteinyl leukotriene receptor 2; IL: Interleukin; LNC2: Lipocalin-2; MAT2B: Methionine adenosyl transferase 2B; NF-κB: Nuclear factor kappa-B; SIRT1: Sirtuin 1; TLRs: Pyrin domain-containing protein; TNF-α: Tumor necrosis factor-α.

immune cells, indirectly protecting against inflammation-induced BBB disruption[22]. M2 polarization promotes the release of anti-inflammatory cytokines and tissue repair, including neurogenesis, axonal remodeling, angiogenesis, and oligodendrogenesis[21,23]. Activated matrix metalloproteinase (MMP)-2 and MMP-9 by microglia after stroke degrade the basement membrane and TJ proteins, resulting in BBB disruption, leukocyte infiltration, and angioedema, thus aggravating brain injury[17,24,25]. Pericytes also release cytokines that play vital roles in maintaining the structural integrity of the BBB. Under pathological conditions, dysfunctional pericytes can cause basement membrane degradation or alter NVU coordination, leading to BBB instability[17]. In addition, BBB injury along with the activation of TGFβ signaling in astrocytes may be a mechanism to disrupt NVU structure, as TGFβ overproduction affects the function of pericytes and vascular smooth muscle cells[26,27]. Microglial polarization is closely related to stroke progression; M1 microglia promote astrocyte differentiation to the A1 phenotype through a variety of signaling pathways, including the immune inflammatory response, angioedema, BBB disruption, neuronal apoptosis, and glutamate excitotoxicity, thereby exacerbating brain injury caused by IS[28,29]. The inflammatory reaction of the nervous system is closely related to the polarization of microglia, pericyte-secreted factors, astrocyte differentiation, and leukocyte species. However, the underlying mechanism of action of Exos in the treatment of neuroinflammation in stroke remains unclear.

BIOLOGICAL CHARACTERISTICS OF MESENCHYMAL STEM CELL EXOSOMES

MSCs are pluripotent stem cells with self-renewal, differentiation, secretion, and homing properties. They were first discovered in the bone marrow, where they are abundant and easily extractable, and are also found in the dental pulp, umbilical cord, hemocytes, and adipose tissue (such as bone marrow MSCs, dental MSCs, umbilical cord-derived MSCs, adipose-derived MSCs, and hematopoietic stem cells)[30,31]. To overcome the problems with primary MSCs, human pluripotent stem cells (hPSCs), including human embryonic stem cells (hESCs) and pluripotent stem cells (iPSCs), represent a promising solution[32]. MSCs can differentiate into lipogenic, chondrogenic, osteoblastic, endothelial, neural, and epithelial lineages, both *in vivo* and *in vitro*[33,34]. MSCs can reduce inflammatory responses, release trophic factors to promote therapeutic effects, induce angiogenesis, promote neurogenesis, reduce infarct volume, and replace damaged cells *via* immunomodulation[10,35,36]. Extracellular vesicles secreted by MSCs can be divided into three types based on their size and intracellular origin: Apoptotic bodies, microvesicles, and Exos. Apoptotic bodies are ≥ 1000 nm and microvesicles are 100–1000 nm in diameter. Exos (30–100 nm in diameter) originate from multivesicular bodies and are released by exocytosis, which is dependent on cytoskeletal reorganization, but independent of intracellular Ca^{2+} concentration[37,38]. When multivesicular bodies fuse with the cell membrane, Exos are released from the cells. Previously, these vesicles were considered waste products actively excreted by cells; however, studies have shown that Exos have key

functions, such as transmitting information between cells, tissue regeneration, and immune regulation[39] (Figure 2).

Exos are released upon fusion with the cell membrane and trigger the release of different cellular substances. Exos can carry the same bioactive substances as their source cells and are vital for information transmission between cells, such as immune regulation and promotion of cell migration, proliferation, differentiation, and matrix synthesis[40]. Moreover, the exogenous Exos of stem cells express specific surface markers (CD9, CD63, CD81, and CD92), express specific phenotypes of stem cells (CD29, CD44, CD73, and CD90)[41], and carry heat shock proteins (HSP) proteins (HSP8, HSP60, HSP70, and HSP9), signal transduction proteins, and multivesicular production-related proteins. More importantly, they can directly transfer bioactive molecules, including non-coding regulatory microRNAs (miRNAs), messenger RNAs (mRNAs), and proteins from donor cells to recipient cells. MiRNAs are short (approximately 22 nucleotides), single-stranded, non-coding RNAs transcribed in the nucleus by RNA polymerase II from one gene or between two different genes to regulate different cellular processes such as differentiation, proliferation, metabolism, inflammation, stress response, angiogenesis, and signaling transduction[42]. miRNAs mainly affect gene expression by degrading the corresponding miRNAs or suppressing translation[43]. Alexander *et al*[44] showed that exosomal miRNAs participate in regulating inflammatory responses; miR-146a-containing Exos can inhibit inflammation, whereas miR-155-containing Exos promote inflammation following exposure to the same inflammatory stimulus.

Exos contain a variety of active substances that form the basis for disease treatment. These bioactive substances carried by Exos can target specific cells for information transmission and enter the cytoplasm by fusion with receptor cell membranes or endocytosis, thereby changing the target cell function by transmitting proteins, lipids, and nucleic acids [45]. Exos can be effectively isolated from donor cells and protect their contents from the external environment, ensuring the complete transmission of effective information[46]. Exos act as mediators that facilitate intercellular communication and influence the recipient cell activity by delivering content. DiR-labeled MSC-Exos were injected into a rat model of stroke *via* the caudal vein, and the *in vivo* tracer showed that Exos could penetrate the BBB and reach the brain tissue. The fluorescence signal peaked on the third day and then gradually decreased[47]. Matsumoto *et al*[48] also demonstrated that Exos can increase long-term neuroprotective effects after stroke, modulate peripheral immune responses, and increase angiogenesis and axonal dendritic remodeling. Therefore, the use of Exos for the treatment of neurological diseases has great potential[49,50]. These results suggest that Exos is an important therapeutic target for the treatment of stroke (Figure 3).

MSC-EVS REGULATE INFLAMMATORY RESPONSE IN IS TREATMENT

The potential therapeutic mechanisms of stem cell Exos involve promoting dendritic and axonal growth, repairing nerves, and promoting angiogenesis through direct actions[51,52]. Through indirect action, it can promote the secretion of inflammatory factors by cells by exogenously producing Exos that appear to interact with recipient brain cells, thereby stimulating them to release their own Exos and playing a role in anti-inflammation and neurological repair. Transplantation of MSC-Exos improves inflammatory responses in IS, maintaining BBB function, decreasing brain edema, regulating energy metabolism, and promoting antioxidant, anti-inflammatory, and anti-apoptotic effects[53]. In IS, miRNAs are involved in a variety of cellular functions, such as injured tissue repair and remodeling, and different neuronal activities. Their target genes play a crucial regulatory role in the inflammatory process of post-ischemic reperfusion injury, which explains their potential use as therapeutic targets in IS and is the focus of Exos research[54,55]. According to current research, the main signaling pathways mediated by Exos after cerebral ischemia are as follows (Table 1)[12,41,56-63].

NF-kB signaling pathway

The transcription factor NF-κB regulates many aspects of innate and adaptive immunity and plays an important role in the inflammatory response. It is also involved in the migration of immune effector cells to the inflammatory system, thereby allowing the secretion of pro-inflammatory cytokines[64]. Han *et al*[65] showed that MSCs-Exos protect MCAO-injured rats, possibly by regulating the AMP-activated protein kinase (AMPK) and JAK2/STAT3/NF-κB signaling pathways. NF-κB is a central inflammatory mediator responding to many immune receptors. NF-κB mediates the induction of pro-inflammatory cytokines, such as TNF-α, IL-1, and IL-6, in monocytes/macrophages[66]. Fann *et al*[67] confirmed the involvement of NF-κB signaling in the activation of pyrin domain-containing inflammasomes following IS. Preconditioning MSCs with lithium modifies EV secretion patterns, enhancing the therapeutic potential of the derived EVs (Li-EVs) and significantly increasing the resistance of cultured astrocytes, microglia, and neurons to hypoxic injury compared with control and native EVs. Li-EVs reduce the abundance of post-hypoxic and post-ischemic TLR4 (leading to activation of the NF-κB signaling pathway) and decrease proteasomal activity, which together contribute to reduced levels of poststroke encephalitis[68]. The miRNAs carried by Exos play a significant physiological role. Cai *et al*[56] confirmed that MSC-derived exosomal microRNA-542-3p (miR-542-3p) prevented ischemia-induced glial cell inflammatory responses by inhibiting TLR4. Interleukin-1 receptor-associated kinase 1 (IRAK1) and tumor necrosis factor receptor-associated factor 6 (TRAF6) may be parts of an NF-κB-induced negative feedback loop[69]. Zhang *et al*[57] found that injected Exos produced by human umbilical cord MSCs (HUMSC-Exos) enter the site of ischemic injury and be internalized by cells, both *in vivo* and *in vitro*. *In vitro*, HUMSC-Exos treatment attenuates microglial inflammation induced by oxygen-glucose deprivation (OGD). *In vivo*, HUMSC-Exos treatment significantly reduced infarct volume, alleviated behavioral deficits, and improved microglial activation 3 d after transient cerebral ischemia. MiR-146a-5p from HUMSC-Exos can attenuate microglial-mediated neuroinflammation through the IRAK1/TRAF6 pathway and ensuing neurological deficits after IS. NF-κB signaling pathway activation is a 'master regulator' of inflammation and is associated

Table 1 Application of stem cell exogenous exosomal miRNA in treatment of ischemic stroke

MicroRNA	Source	Model(s)	Functional effects	Pathway(s)	Ref.
miR-21a-5p	MSCs	OGD microglia	Induces microglial M2 polarization by targeting STAT3	STAT3	Xin *et al*[12], 2022
miR-138-5p	BMSCs	MCAO mouse, OGD astrocytes	Promotes astrocyte proliferation and inhibits inflammatory response	LCN2	Deng *et al*[41], 2019
miR-542-3p	MSCs	MCAO mice, OGD human glial cells	Suppresses inflammation and prevents cerebral infarction	TLR4	Cai *et al*[56], 2021
miR-146a-5p	HUMSCs	MCAO mouse, OGD microglia	Anti-inflammation	IRAK1/TRAF6	Zhang *et al*[57], 2021
miR-223-3p	MSCs	MCAO Rats, OGD microglia	Anti-inflammation	CysLT2R	Zhao *et al*[58,59], 2020
miR-21-3p	MSCs	MCAO rats	BBB protection, anti-inflammation, anti-apoptosis	MAT2B	Li *et al*[60], 2019
miR-26a-5p	HUMSCs	I/R mice, OGD microglia	Inhibits microglial M1 polarization	TLRs	Li *et al*[61], 2020
miR-150-5p	BMSCs	MCAO rats	Decelerates neuronal apoptosis, reduces inflammation	TLR5	Li *et al*[62], 2022
miR-30d-5p	ADSCs	Patients, MCAO rats, OGD microglia	Promotes M2 microglial/macrophage polarization	Inflammatory mediators	Jiang *et al*[63], 2018

ADSCs: Adipose-derived stem cells; BMSCs: Bone marrow mesenchymal stem cell; CysLT2R: Cysteinyl leukotriene receptor 2; HUMSCs: Human umbilical cord blood mesenchymal stem cells; I/R: Ischemia/reperfusion; IRAK1: Interleukin-1receptor-associated kinase 1; MCAO: Middle cerebral artery occlusion; MAT2B: Methionine adenosyl transferase 2B; MSCs: Mesenchymal stem cells; OGD: Oxygen-glucose deprivation; STAT3: Signal transducer and activator of transcription 3; TLRs: Toll-like receptors; TRAF6: Tumor necrosis factor receptor-associated factor 6; TLR4: Toll-like receptor 4; TLR5: Toll-like receptor 5.

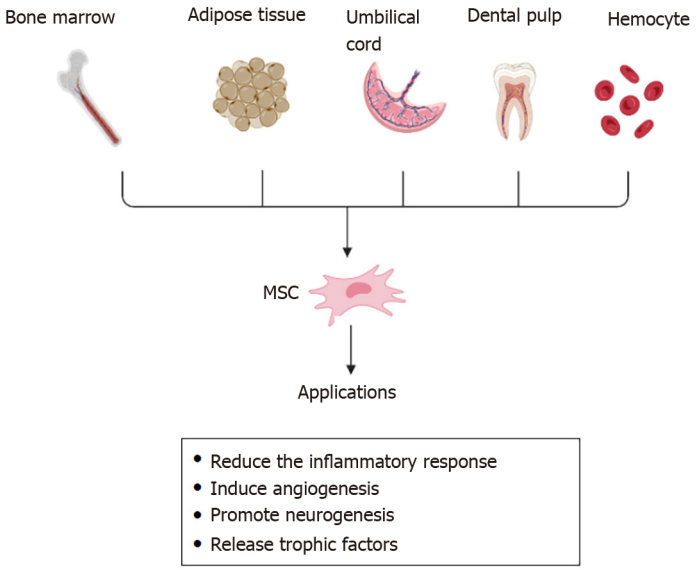

DOI: 10.4252/wjsc.v15.i6.561

Figure 2 Sources and potential function for stroke of mesenchymal stromal cells. These cells are found in bone marrow, dental pulp, umbilical cord, hemocyte, and adipose tissue. Mesenchymal stromal cells reduce the inflammatory response, release trophic factors, induce angiogenesis, and promote neurogenesis in stroke. By BioRender.com. MSC: Mesenchymal stem cell.

with the generation of free radicals and the activation of proteolytic enzymes and pro-inflammatory cytokines, playing an important role in regulating apoptosis after stroke[70,71]. Taken together, these results show that NF-κB signaling is essential for the regulation of brain tissue inflammasomes under ischemic conditions. In addition, MSC-Exos treatment decreased the activation of the NF-κB signaling pathway, thereby attenuating inflammasome expression and activation under ischemic conditions. These findings suggest that therapeutic interventions targeting neuroinflammasome activation may provide new opportunities for the treatment of IS.

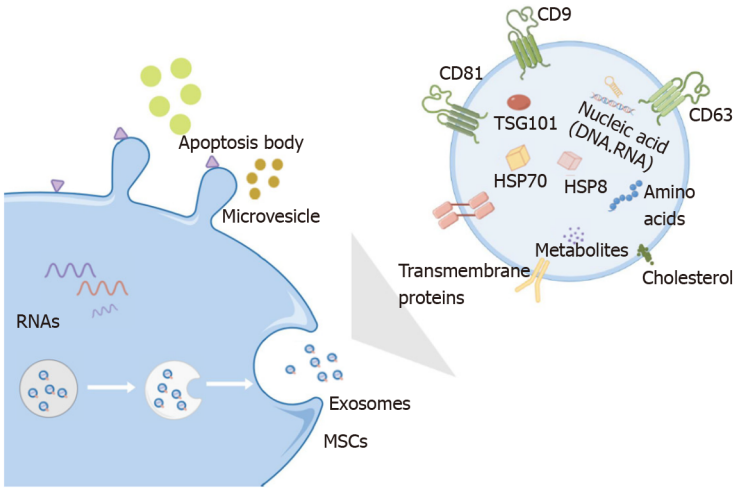

DOI: 10.4252/wjsc.v15.i6.561 **Copyright** ©The Author(s) 2023.

Figure 3 Exosomes. Extracellular vesicles are classified into three types: Apoptotic bodies, microvesicles, and exosomes (Exos). Apoptotic bodies are ≥ 1000 nm, microvesicles are 100–1000 nm, and Exos are 30–100 nm in diameter. The contents carried by the Exos are mainly DNA, mRNA, microRNA, functional proteins, and other active substances. The membrane structure can express a variety of antigens and antibody molecules. The surface markers of the Exos mainly include CD63, CD81, CD9, and heat shock protein 70. By Figdiaw. MSCs: Mesenchymal stem cells.

NOD-like receptor family pyrin domain-containing 3 signaling pathway

NOD-like receptor family pyrin domain-containing 3 (NLRP3) plays an important role in mediating the inflammatory responses during cerebral IS[72]. The NLRP3 inflammasome is a multiprotein complex comprising NLRP3 and pyroptosis-related factors (ASC and caspase 1)[73]. The NF-κB and mitogen-activated protein kinase (MAPK) pathways play a major role in the expression and activation of NLRP1 and NLRP3 inflammasomes in primary cortical neurons[67]. Bone marrow MSC-Exos (BMSC-Exos) can reduce brain infarct area and cerebral edema, thus improving neurological function. MSC-Exos can downregulate the expression of NLRP3 inflammasome and pyroptosis-related proteins on the surface of neurons[74]. Moreover, it improved the transition from M1 to M2 phenotype both *in vivo* and *in vitro*. BMSC-Exos relieve cerebral ischemia/reperfusion (I/R) injury by suppressing NLRP3 inflammasome-mediated inflammation and pyroptosis *via* modulation of microglial polarization[74]. Sarmah *et al*[75] came to similar conclusions by treating a rat MCAO model with intra-arterial injections of MSCs; the levels of NLRP-1 and NLRP-3 inflammasomes and their related components IL-1β, caspase-1, and ASC were significantly reduced. NLRP3 apoptotic bodies are involved in astrocyte and microglial polarization and are closely related to the development of the inflammatory cascade after stroke, and BMSC-Exos reduce the inflammatory response after stroke by inhibiting NLRP3 activation.

Sirtuin signaling pathway

Sirtuins (SIRTs) are NAD+-dependent deacylases with multiple roles in energy metabolism regulation, cell survival, transcriptional regulation, inflammation, circadian regulation, and DNA repair[76]. SIRT-1 and SIRT-3 are both associated with the inflammatory response in stroke patients. Xin *et al*[12] used an *in vivo* neonatal male mouse model of hypoxic-ischemic (HI) injury and induced *in vitro* hypoxia-glucose deficiency, thus simulating microglial BV-2 cells to deliver miR-21a-5p (miR-21a-5p) as a therapeutic intervention through MSC-Exos. Treatment of BV-2 cells with MSC-EVs increased cell viability and miR-21a-5p levels, which were decreased after glucose-oxygen deprivation. In both *in vitro* and *in vivo* models of HI injury, the effects on microglial polarization and STAT3 phosphorylation decreased when miR-21a-5p levels were reduced in MSC-Exos. These results suggest that MSC-Exos attenuate HI brain injury in neonatal mice by delivering miR-21a-5p, which induces microglial M2 polarization by targeting STAT3. Adipose-derived MSC-derived miR-22-3p reduces infarct volume and apoptosis in a stroke model[77]. Sarmah *et al*[75] demonstrated that intraarterial MSCs increase SIRT-1 to inhibit the NF-κB pathway, reducing inflammasome signaling and apoptosis, thereby exerting a neuroprotective effect. SIRT1 may be an independent risk factor for cerebral infarction, and a high concentration of SIRT1 in cerebral infarction may be associated with disruption of the BBB[78].

Cysteinyl leukotriene signaling pathway

Cysteinyl leukotrienes (CysLTs), including leukotriene C4 (LTC4), leukotriene D4 (LTD4), and leukotriene E4 (LTE4), are derived from 5-lipoxygenase metabolites of arachidonic acid after cell necrosis and are effective mediators of inflammation[79]. The effects of CysLTs are mainly mediated by the CysLT1 and CysLT2 receptors (CysLT1R and CysLT2R), which are active in various cell types during pathological brain injury. CysLT2 is expressed in the cerebral cortex, hippocampus, substantia nigra, and lateral ventricle[80]. Zhao *et al*[58,59] showed that the overexpression of miR-223-3p (miR-223-3p) in MSC-Exos can reduce MCAO-induced infarction, improve neurological deficits, and promote learning and memorization. MiR-223-3p inhibits the expression of pro-inflammatory factors and promotes the secretion of anti-inflammatory factors in the ischemic cortex and hippocampus. Western blot and quantitative real-time PCR analyses also showed that exosomal miR-223-3p reduced the mRNA and protein expression of CysLT2R *in vitro* and *in vivo*. Exosomal

miR-223-3p from MSCs alleviated cerebral I/R injury by inhibiting the pro-inflammatory response mediated by M1 polarization of microglia, which may be related to the inhibition of CysLT2R by exosomal miR-223-3p.

Lipocalin-2

Lipocalin-2 (LCN2), a 25 kDa protein, is a neutrophil gelatinase-associated protein that affects different cellular processes during stroke. The pro-inflammatory mediator LCN2 plays a key role in I/R injury[81]. Genetic or pharmacological inhibition of these pro-inflammatory mediators (iNOS, IL-6, CCL2, and CCL9) provides neuroprotection against stroke and reduces the expression of inflammatory factors by down-regulating LCN2[41]. Deng *et al*[41] used a mouse MCAO model to explore the effects of BMSC-derived exosomal miR-138-5p in IS *in vivo*. Overexpression of miR-138-5p promoted cell proliferation and inhibited apoptosis of OGD-damaged astrocytes, accompanied by decreased expression of inflammatory factors. This was achieved by downregulating LCN2, and the expression of LCN2 protein was subsequently detected by Western blot analysis. More importantly, BMSCs attenuated neuronal injury in IS mice by delivering miR-138-5p to astrocyte Exos. Therefore, the exogenous exosomal miR-138-5p from BMSCs promotes astrocyte proliferation and inhibits the inflammatory response after IS by targeting LCN2, thereby reducing neurological impairment, which may provide a new target for IS treatment.

Methionine adenosyl transferase 2B

Methionine adenosyl transferase (MAT) is an enzyme involved in cell cycle regulation. Mammals have three major MAT genes: MAT1A, MAT2A, and MAT2B[60]. TNF-induced activation of MAT2B promotes tumor growth through the NF-κB pathway in hepatoma cells[81]. MiR-21-3p antagomir can control the inflammatory response by inhibiting NF-κB signaling; these functions of miR-21-3p are exerted by directly targeting MAT2B[82]. This interaction forms the basis of the function of miR-21-3p/MAT2B in regulating inflammation. Li *et al*[60] found that miR-21-3p expression was elevated in the MCAO model, and the inhibition of exogenous adipose-derived stem cell Exos miR-21-3p could inhibit the expression of MAT2B in neural cells, thereby improving the BBB status and inhibiting apoptosis and inflammatory responses. MiR-21-3p antagomir could inhibit the expression of pro-inflammatory cytokines (TNF-α, IL-1β, and IL6) and promote the expression of anti-inflammatory cytokines (IL-10). Thus, miR-21-3p can protect neural cells by inhibiting the expression of MAT2B and thus inhibiting apoptosis and inflammatory responses.

Toll-like receptors (TLRS)

Evidence suggests that Toll-like receptors (TLRs) play important roles in the development of ischemic brain injury in adults[83]. TLRs, comprising 13 members (TLR-1 to TLR-13), are type 1 integral membrane proteins responsible for detecting invading pathogens and initiating immune responses[84,85]. The microglial TLR pathway is activated following cerebral ischemia and inhibition of TLR signaling by exosomal miR-26a-5p decreases cholesterol 25-hydroxylase protein expression, which in turn inhibits microglial M1 polarization and relieves nerve injury after brain injury[61]. The gene expression of many inflammatory mediators, such as TNF-α, IL-1, and IL-6, can reduce the development of nervous system inflammation by inhibiting TLR4 transduction pathway downregulation[86]. Upregulation of miR-326 attenuates IL-10, IL-1β, and TNF-α pro-inflammatory cytokine expression in response to lipopolysaccharide stimulation by targeting TLR4[87]. TLR5 activates NF-kB and MAPK pathways that regulate the transcription of genes encoding immune mediators[88]. Qiao *et al*[89] elucidated that TLR5 downregulation is accompanied by alleviated neurological deficits, reduced infarct volume, and reduced edema after IS[90]. Li *et al*[62] validated that BMSC-Exos can improve neurological function and pathological changes, decelerate neuronal apoptosis, and reduce inflammatory factors in MCAO rats. Exosomal miR-150-5p from BMSCs mitigates cerebral I/R injury by inhibiting TLR5 expression. These studies showed that TLRs and their related miRNAs are associated with inflammation after IS.

Inflammatory mediators

Dabrowska *et al*[91] transplanted human bone marrow stem cells and their secreted Exos into a rat model of local brain injury. The results showed that monocyte chemoattractant protein-1 (MCP-1) expression increased locally after brain injury, whereas MCP-1 expression decreased in the transplanted HUMSCs and Exos groups. In addition, they observed that the infusion of pro-inflammatory cytokines and chemokines with HUMSCs or EVs in rats with untreated focal brain injury was associated with reduced microglial/macrophage and astrocyte activation. MSC-Exos therapy can reduce the expression of the inflammatory cytokines TNF-α and IL-6, increase the expression of the cytokines IL-4 and IL-10, and reduce brain injury. Exos from stem cells can enhance the activation of CD4+ and CD8+ lymphocytes, decrease the number of dendritic cells, regulate peripheral immunosuppression caused by stroke[9], and pass antigens to the immune system through the BBB[92]. IL-4, CD206, and IL-10 are markers of M2 microglial secretion, whereas TNF-α, IL-6, and iNOS are markers of M1 microglial secretion[93]. Yang *et al*[94] found that the MCAO model also verified that Exos intervention reduced the infarct volume and promoted the polarization of microglia to M2 phenotype. These results demonstrate that adipose-derived stem cell Exos can prevent stroke by shifting microglia from an M1 to M2 phenotype in the hippocampus[94].

Microglial polarization

Microglia are macrophages of the central nervous system and are important components of innate and adaptive immune responses[95]. The microglial M1 type can secrete pro-inflammatory factors, whereas the M2 type can secrete anti-inflammatory factors; therefore, the fact that MSCs and Exos can promote the polarization of microglia to M2 is notable for the treatment of IS. The M2 type protects nerve cells mainly by engulfing debris and promoting the repair and regeneration of brain tissue. In contrast, inflammatory factors of the M1 phenotype aggravate post-stroke symptoms. Therefore, the

microglial response after stroke is an important prognostic factor[96]. Different miRNAs transported by Exos contribute to the differentiation of microglia into distinct phenotypes. Increased levels of miR-124-3p in microglial Exos promote M2 microglial polarization, reduce brain damage, and improve stroke outcomes[97]. Adipose-derived MSCs (ADMSCs) participate in the repair process of tissues through paracrine effects after relieving nerve injury; ADMSCs have similar biological characteristics to MSCs. Stimulation of AMSC-derived Exos with inflammatory factors was found to convert M1 microglia into M2 microglia, suggesting that AMSC-derived Exos promote microglial polarization by activating pro-inflammatory microenvironment signals[98]. miRNAs are critical regulators of genes involved in various biological processes; miR-146a-5p-enriched BMSC-Exos directly target IRAK1 and nuclear factor-activated T cell 5 (NFAT5), which contributes to inflammatory responses and polarize M1 microglia/macrophages[99]. Exos containing miR-216a-5p, miR-124, miR-155, miR-182, miR-17-5p, miR-30d-5p, and miR-223-3p were found to promote microglial M2 polarization[63, 100-103]. BMSC-Exos promote microglial polarization from M1 to M2, inhibit inflammation-related signaling pathways, and reduce endothelial cell injury and neurological impairment caused by IS[104-106]. Although astrocytes may play a role in brain inflammation, little is known about their role in stroke pathology[107].

Activated regulatory T cells

Changes in regulatory T cell (Treg) numbers and function after stroke are accompanied by a decrease in immunosuppressive function, which affects stroke prognosis[108]. The immunosuppressive function of Tregs is largely impaired during stroke and Treg-derived anti-inflammatory factors, including transforming growth factor-beta (TGF-b) and IL-10, are reduced[109,110]. MiRNAs delivered by stem cell Exos can induce anti-inflammatory polarization as important regulators of Treg homeostasis and function[111,112]. MSC-Exos induce anti-inflammatory IL-10 and TGF-β transcription, attenuate pro-inflammatory factors IL-1β, IL-6, and TNF-β, and inhibit the differentiation and activation of Tregs[113, 114]. Furthermore, MSC-Exos are absorbed by endothelial cells, impair T-cell function by inhibiting T-cell proliferation *in vitro*, and increase endothelial cell proliferation, migration, and capillary formation in a dose-dependent manner[115]. Wang *et al*[116] showed that the intravenous injection of MSC-EVs reduced neurological deficits, cerebral infarct volume, brain edema, and neuronal injury in both young and old mice. The neuroprotective and anti-inflammatory effects of MSC-EVs were demonstrated through a decrease in leukocyte infiltration and, specifically, polymorphonuclear neutrophil, monocyte, and macrophage infiltration, in the cerebral ischemic areas of aged mice. In addition, MSC-EVs significantly decreased the number of monocytes and activated Tregs. The expression and phos-phorylation of signal transducer and activator 1 (STAT1) are increased in mice with miR-146a deficient Tregs, and miR-125a is involved in the differentiation of Tregs[117]. Exosomal miR-16 and miR-21, derived from bone marrow stem cells, can increase the production of Tregs and exert anti-inflammatory effects[118]. Although breakthroughs have been made in elucidating the working mechanism of Tregs over the past decade, the mechanism by which this minor population of peripheral immune cells has a significant beneficial effect after stroke injury remains largely unknown[108].

CONCLUSION

Brain injury after stroke is a complex pathological process. This review summarizes the recent studies on the mechanism of action of MSC-Exos in regulating inflammatory responses during IS treatment. MSC-Exos regulate microglial polarization through various pathways such as NF-κB, NLRP3, and STATs, indicating that microglial M1 to M2 phenotype polarization is closely related to the inflammatory response after IS.

However, some essential questions remain unanswered. Stroke-induced brain injury involves multiple mechanisms that cannot be explained by a single one. Immune inflammation plays a crucial role in this process, especially the NF-κB, NLRP3, and other signaling pathways. After immune inflammation, microglia, leukocytes, and other inflammatory cells are activated and release many pro-inflammatory factors. Additionally, nerve cells are affected by varying degrees of damage caused by ischemia and hypoxia after stroke.

However, these studies have some limitations. MSC-Exos can mediate different signaling pathways to reduce inflammatory responses after stroke in animal models. However, these results have not been translated into clinical practice. Most studies have focused on exosomal miRNAs, indicating that they play an important role in regulating cellular functions. However, research on other bioactive molecules contained in Exos, such as miRNAs, mRNAs, and proteins, is limited. This does not mean that this mechanism of action of miRNAs can explain how Exos attenuate post-stroke inflammation. The dosage, mode of administration, and duration of action of the Exos should be elucidated. Exos are considered ideal biomarkers and drug delivery vehicles, with great potential for overcoming the limitations of stem cell therapy [119]. The use of Exos as drug-loaded systems will facilitate breakthroughs in the research and development of targeted drugs for clinical treatment. Moreover, new directions and methods will be provided for stroke treatment.

FOOTNOTES

Author contributions: Chen N drafted the manuscript; Wang YL, Sun HF, Wang ZY, and Zhang Q reviewed the literature, and designed and revised the manuscript; Fan FY, Liu FX, and Ma YC generated the graphs; Zhang YK guided the construction of the manuscript; all the authors have read and approved the manuscript.

Supported by the National Natural Science Foundation of China, No. 81974564 and No. 82104730; the Zhongyuan Science and Technology Innovation Leading Talent Project, No. 224200510027; the National Natural Science Foundation of China, No. 82001973; the

Youth Project Co-established by Henan Province and a Ministry grant, No. SBGJ2020003017; and the Health Science and Technology Innovation Excellent Youth Training Project in Henan Province, No. YXKC2020057.

Conflict-of-interest statement: The authors declare no conflict of interest. The funding body played no role in the design of the study; collection, analysis, and interpretation of data; or in writing the manuscript.

Country/Territory of origin: China

ORCID number: Na Chen 0000-0001-6862-4635; Yan-Lin Wang 0009-0005-6539-8456; Hui-Fang Sun 0000-0002-5450-0962; Zhuo-Ya Wang 0009-0007-5595-4089; Qi Zhang 0009-0003-5471-9301; Fei-Yan Fan 0009-0004-0075-2453; Yu-Cheng Ma 0009-0004-0783-8655; Fei-Xiang Liu 0000-0001-7713-8049; Yun-Ke Zhang 0000-0003-1500-1535.

Corresponding Author's Membership in Professional Societies: Henan Stroke Association.

S-Editor: Li L
L-Editor: Wang TQ
P-Editor: Li L

REFERENCES

1 **Yang L**, Qian J, Yang B, He Q, Wang J, Weng Q. Challenges and Improvements of Novel Therapies for Ischemic Stroke. *Front Pharmacol* 2021; **12**: 721156 [PMID: 34658860 DOI: 10.3389/fphar.2021.721156]
2 **Ungvari Z**, Tarantini S, Donato AJ, Galvan V, Csiszar A. Mechanisms of Vascular Aging. *Circ Res* 2018; **123**: 849-867 [PMID: 30355080 DOI: 10.1161/CIRCRESAHA.118.311378]
3 **Yang P**, Zhang Y, Zhang L, Treurniet KM, Chen W, Peng Y, Han H, Wang J, Wang S, Yin C, Liu S, Wang P, Fang Q, Shi H, Yang J, Wen C, Li C, Jiang C, Sun J, Yue X, Lou M, Zhang M, Shu H, Sun D, Liang H, Li T, Guo F, Ke K, Yuan H, Wang G, Yang W, Li Z, Xing P, Zhang P, Zhou Y, Wang H, Xu Y, Huang Q, Wu T, Zhao R, Li Q, Fang Y, Wang L, Lu J, Li Y, Fu J, Zhong X, Wang Y, Goyal M, Dippel DWJ, Hong B, Deng B, Roos YBWEM, Majoie CBLM, Liu J; DIRECT-MT Investigators. Endovascular Thrombectomy with or without Intravenous Alteplase in Acute Stroke. *N Engl J Med* 2020; **382**: 1981-1993 [PMID: 32374959 DOI: 10.1056/NEJMoa2001123]
4 **Tariq MB**, Lee J, McCullough LD. Sex differences in the inflammatory response to stroke. *Semin Immunopathol* 2022 [PMID: 36355204 DOI: 10.1007/s00281-022-00969-x]
5 **Zou L**, Han R. Inflammatory Response and Immune Regulation in Brain-Heart Interaction after Stroke. *Cardiovasc Ther* 2022; **2022**: 2406122 [PMID: 36474712 DOI: 10.1155/2022/2406122]
6 **Pittenger MF**, Discher DE, Péault BM, Phinney DG, Hare JM, Caplan AI. Mesenchymal stem cell perspective: cell biology to clinical progress. *NPJ Regen Med* 2019; **4**: 22 [PMID: 31815001 DOI: 10.1038/s41536-019-0083-6]
7 **Stonesifer C**, Corey S, Ghanekar S, Diamandis Z, Acosta SA, Borlongan CV. Stem cell therapy for abrogating stroke-induced neuroinflammation and relevant secondary cell death mechanisms. *Prog Neurobiol* 2017; **158**: 94-131 [PMID: 28743464 DOI: 10.1016/j.pneurobio.2017.07.004]
8 **Li Y**, Cheng Q, Hu G, Deng T, Wang Q, Zhou J, Su X. Extracellular vesicles in mesenchymal stromal cells: A novel therapeutic strategy for stroke. *Exp Ther Med* 2018; **15**: 4067-4079 [PMID: 29725359 DOI: 10.3892/etm.2018.5993]
9 **Doeppner TR**, Herz J, Görgens A, Schlechter J, Ludwig AK, Radtke S, de Miroschedji K, Horn PA, Giebel B, Hermann DM. Extracellular Vesicles Improve Post-Stroke Neuroregeneration and Prevent Postischemic Immunosuppression. *Stem Cells Transl Med* 2015; **4**: 1131-1143 [PMID: 26339036 DOI: 10.5966/sctm.2015-0078]
10 **Dabrowska S**, Andrzejewska A, Lukomska B, Janowski M. Neuroinflammation as a target for treatment of stroke using mesenchymal stem cells and extracellular vesicles. *J Neuroinflammation* 2019; **16**: 178 [PMID: 31514749 DOI: 10.1186/s12974-019-1571-8]
11 **Yu H**, Xu Z, Qu G, Wang H, Lin L, Li X, Xie X, Lei Y, He X, Chen Y, Li Y. Hypoxic Preconditioning Enhances the Efficacy of Mesenchymal Stem Cells-Derived Conditioned Medium in Switching Microglia toward Anti-inflammatory Polarization in Ischemia/Reperfusion. *Cell Mol Neurobiol* 2021; **41**: 505-524 [PMID: 32424775 DOI: 10.1007/s10571-020-00868-5]
12 **Xin DQ**, Zhao YJ, Li TT, Ke HF, Gai CC, Guo XF, Chen WQ, Liu DX, Wang Z. The delivery of miR-21a-5p by extracellular vesicles induces microglial polarization *via* the STAT3 pathway following hypoxia-ischemia in neonatal mice. *Neural Regen Res* 2022; **17**: 2238-2246 [PMID: 35259844 DOI: 10.4103/1673-5374.336871]
13 **An H**, Zhou B, Ji X. Mitochondrial quality control in acute ischemic stroke. *J Cereb Blood Flow Metab* 2021; **41**: 3157-3170 [PMID: 34551609 DOI: 10.1177/0271678X211046992]
14 **Datta A**, Sarmah D, Mounica L, Kaur H, Kesharwani R, Verma G, Veeresh P, Kotian V, Kalia K, Borah A, Wang X, Dave KR, Yavagal DR, Bhattacharya P. Cell Death Pathways in Ischemic Stroke and Targeted Pharmacotherapy. *Transl Stroke Res* 2020; **11**: 1185-1202 [PMID: 32219729 DOI: 10.1007/s12975-020-00806-z]
15 **Mendelson SJ**, Prabhakaran S. Diagnosis and Management of Transient Ischemic Attack and Acute Ischemic Stroke: A Review. *JAMA* 2021; **325**: 1088-1098 [PMID: 33724327 DOI: 10.1001/jama.2020.26867]
16 **Onose G**, Anghelescu A, Blendea D, Ciobanu V, Daia C, Firan FC, Oprea M, Spinu A, Popescu C, Ionescu A, Busnatu Ş, Munteanu C. Cellular and Molecular Targets for Non-Invasive, Non-Pharmacological Therapeutic/Rehabilitative Interventions in Acute Ischemic Stroke. *Int*

J Mol Sci 2022; **23** [PMID: 35055089 DOI: 10.3390/ijms23020907]
17 **Abdullahi W**, Tripathi D, Ronaldson PT. Blood-brain barrier dysfunction in ischemic stroke: targeting tight junctions and transporters for vascular protection. *Am J Physiol Cell Physiol* 2018; **315**: C343-C356 [PMID: 29949404 DOI: 10.1152/ajpcell.00095.2018]
18 **Jurcau A**, Simion A. Neuroinflammation in Cerebral Ischemia and Ischemia/Reperfusion Injuries: From Pathophysiology to Therapeutic Strategies. *Int J Mol Sci* 2021; **23** [PMID: 35008440 DOI: 10.3390/ijms23010014]
19 **Xiong XY**, Liu L, Yang QW. Functions and mechanisms of microglia/macrophages in neuroinflammation and neurogenesis after stroke. *Prog Neurobiol* 2016; **142**: 23-44 [PMID: 27166859 DOI: 10.1016/j.pneurobio.2016.05.001]
20 **Durafourt BA**, Moore CS, Zammit DA, Johnson TA, Zaguia F, Guiot MC, Bar-Or A, Antel JP. Comparison of polarization properties of human adult microglia and blood-derived macrophages. *Glia* 2012; **60**: 717-727 [PMID: 22290798 DOI: 10.1002/glia.22298]
21 **Hu X**, Leak RK, Shi Y, Suenaga J, Gao Y, Zheng P, Chen J. Microglial and macrophage polarization—new prospects for brain repair. *Nat Rev Neurol* 2015; **11**: 56-64 [PMID: 25385337 DOI: 10.1038/nrneurol.2014.207]
22 **Qiu YM**, Zhang CL, Chen AQ, Wang HL, Zhou YF, Li YN, Hu B. Immune Cells in the BBB Disruption After Acute Ischemic Stroke: Targets for Immune Therapy? *Front Immunol* 2021; **12**: 678744 [PMID: 34248961 DOI: 10.3389/fimmu.2021.678744]
23 **Wang N**, Liang H, Zen K. Molecular mechanisms that influence the macrophage m1-m2 polarization balance. *Front Immunol* 2014; **5**: 614 [PMID: 25506346 DOI: 10.3389/fimmu.2014.00614]
24 **Shu ZM**, Shu XD, Li HQ, Sun Y, Shan H, Sun XY, Du RH, Lu M, Xiao M, Ding JH, Hu G. Ginkgolide B Protects Against Ischemic Stroke Via Modulating Microglia Polarization in Mice. *CNS Neurosci Ther* 2016; **22**: 729-739 [PMID: 27306494 DOI: 10.1111/cns.12577]
25 **Zhu J**, Cao D, Guo C, Liu M, Tao Y, Zhou J, Wang F, Zhao Y, Wei J, Zhang Y, Fang W, Li Y. Berberine Facilitates Angiogenesis Against Ischemic Stroke Through Modulating Microglial Polarization *via* AMPK Signaling. *Cell Mol Neurobiol* 2019; **39**: 751-768 [PMID: 31020571 DOI: 10.1007/s10571-019-00675-7]
26 **Sweeney MD**, Ayyadurai S, Zlokovic BV. Pericytes of the neurovascular unit: key functions and signaling pathways. *Nat Neurosci* 2016; **19**: 771-783 [PMID: 27227366 DOI: 10.1038/nn.4288]
27 **Kato T**, Sekine Y, Nozaki H, Uemura M, Ando S, Hirokawa S, Onodera O. Excessive Production of Transforming Growth Factor β1 Causes Mural Cell Depletion From Cerebral Small Vessels. *Front Aging Neurosci* 2020; **12**: 151 [PMID: 32581764 DOI: 10.3389/fnagi.2020.00151]
28 **Wan T**, Huang Y, Gao X, Wu W, Guo W. Microglia Polarization: A Novel Target of Exosome for Stroke Treatment. *Front Cell Dev Biol* 2022; **10**: 842320 [PMID: 35356292 DOI: 10.3389/fcell.2022.842320]
29 **Jolivel V**, Bicker F, Binamé F, Ploen R, Keller S, Gollan R, Jurek B, Birkenstock J, Poisa-Beiro L, Bruttger J, Opitz V, Thal SC, Waisman A, Bäuerle T, Schäfer MK, Zipp F, Schmidt MHH. Perivascular microglia promote blood vessel disintegration in the ischemic penumbra. *Acta Neuropathol* 2015; **129**: 279-295 [PMID: 25500713 DOI: 10.1007/s00401-014-1372-1]
30 **Sherman LS**, Romagano MP, Williams SF, Rameshwar P. Mesenchymal stem cell therapies in brain disease. *Semin Cell Dev Biol* 2019; **95**: 111-119 [PMID: 30922957 DOI: 10.1016/j.semcdb.2019.03.003]
31 **Srithanyarat SS**, Choosiri M, Sa-Ard-Iam N, Petcharat P, Osathanon T. Characteristics of mesenchymal stem cells from supracrestal gingival connective tissue. *J Periodontol* 2023; **94**: 439-450 [PMID: 36218191 DOI: 10.1002/JPER.22-0306]
32 **Liu TM**. Application of mesenchymal stem cells derived from human pluripotent stem cells in regenerative medicine. *World J Stem Cells* 2021; **13**: 1826-1844 [PMID: 35069985 DOI: 10.4252/wjsc.v13.i12.1826]
33 **Chen YH**, Pruett-Miller SM. Improving single-cell cloning workflow for gene editing in human pluripotent stem cells. *Stem Cell Res* 2018; **31**: 186-192 [PMID: 30099335 DOI: 10.1016/j.scr.2018.08.003]
34 **Maqsood M**, Kang M, Wu X, Chen J, Teng L, Qiu L. Adult mesenchymal stem cells and their exosomes: Sources, characteristics, and application in regenerative medicine. *Life Sci* 2020; **256**: 118002 [PMID: 32585248 DOI: 10.1016/j.lfs.2020.118002]
35 **Zhang Y**, Dong N, Hong H, Qi J, Zhang S, Wang J. Mesenchymal Stem Cells: Therapeutic Mechanisms for Stroke. *Int J Mol Sci* 2022; **23** [PMID: 35269692 DOI: 10.3390/ijms23052550]
36 **Gu Y**, Zhang Y, Bi Y, Liu J, Tan B, Gong M, Li T, Chen J. Mesenchymal stem cells suppress neuronal apoptosis and decrease IL-10 release *via* the TLR2/NFκB pathway in rats with hypoxic-ischemic brain damage. *Mol Brain* 2015; **8**: 65 [PMID: 26475712 DOI: 10.1186/s13041-015-0157-3]
37 **Willms E**, Johansson HJ, Mäger I, Lee Y, Blomberg KE, Sadik M, Alaarg A, Smith CI, Lehtiö J, El Andaloussi S, Wood MJ, Vader P. Cells release subpopulations of exosomes with distinct molecular and biological properties. *Sci Rep* 2016; **6**: 22519 [PMID: 26931825 DOI: 10.1038/srep22519]
38 **Yang Y**, Ye Y, Su X, He J, Bai W, He X. MSCs-Derived Exosomes and Neuroinflammation, Neurogenesis and Therapy of Traumatic Brain Injury. *Front Cell Neurosci* 2017; **11**: 55 [PMID: 28293177 DOI: 10.3389/fncel.2017.00055]
39 **Jafari D**, Shajari S, Jafari R, Mardi N, Gomari H, Ganji F, Forouzandeh Moghadam M, Samadikuchaksaraei A. Designer Exosomes: A New Platform for Biotechnology Therapeutics. *BioDrugs* 2020; **34**: 567-586 [PMID: 32754790 DOI: 10.1007/s40259-020-00434-x]
40 **Kawabori M**, Shichinohe H, Kuroda S, Houkin K. Clinical Trials of Stem Cell Therapy for Cerebral Ischemic Stroke. *Int J Mol Sci* 2020; **21** [PMID: 33036265 DOI: 10.3390/ijms21197380]
41 **Deng Y**, Chen D, Gao F, Lv H, Zhang G, Sun X, Liu L, Mo D, Ma N, Song L, Huo X, Yan T, Zhang J, Miao Z. Exosomes derived from microRNA-138-5p-overexpressing bone marrow-derived mesenchymal stem cells confer neuroprotection to astrocytes following ischemic stroke *via* inhibition of LCN2. *J Biol Eng* 2019; **13**: 71 [PMID: 31485266 DOI: 10.1186/s13036-019-0193-0]
42 **Rahmani A**, Saleki K, Javanmehr N, Khodaparast J, Saadat P, Nouri HR. Mesenchymal stem cell-derived extracellular vesicle-based therapies protect against coupled degeneration of the central nervous and vascular systems in stroke. *Ageing Res Rev* 2020; **62**: 101106 [PMID: 32565329 DOI: 10.1016/j.arr.2020.101106]
43 **Chen TS**, Lai RC, Lee MM, Choo AB, Lee CN, Lim SK. Mesenchymal stem cell secretes microparticles enriched in pre-microRNAs. *Nucleic Acids Res* 2010; **38**: 215-224 [PMID: 19850715 DOI: 10.1093/nar/gkp857]
44 **Alexander M**, Hu R, Runtsch MC, Kagele DA, Mosbruger TL, Tolmachova T, Seabra MC, Round JL, Ward DM, O'Connell RM. Exosome-delivered microRNAs modulate the inflammatory response to endotoxin. *Nat Commun* 2015; **6**: 7321 [PMID: 26084661 DOI: 10.1038/ncomms8321]
45 **Chen J**, Chopp M. Exosome Therapy for Stroke. *Stroke* 2018; **49**: 1083-1090 [PMID: 29669873 DOI: 10.1161/STROKEAHA.117.018292]
46 **Choi DS**, Kim DK, Kim YK, Gho YS. Proteomics of extracellular vesicles: Exosomes and ectosomes. *Mass Spectrom Rev* 2015; **34**: 474-490 [PMID: 24421117 DOI: 10.1002/mas.21420]
47 **Xu R**, Bai Y, Min S, Xu X, Tang T, Ju S. In vivo Monitoring and Assessment of Exogenous Mesenchymal Stem Cell-Derived Exosomes in

Mice with Ischemic Stroke by Molecular Imaging. *Int J Nanomedicine* 2020; **15**: 9011-9023 [PMID: 33235449 DOI: 10.2147/IJN.S271519]
48 **Matsumoto J**, Stewart T, Sheng L, Li N, Bullock K, Song N, Shi M, Banks WA, Zhang J. Transmission of α-synuclein-containing erythrocyte-derived extracellular vesicles across the blood-brain barrier *via* adsorptive mediated transcytosis: another mechanism for initiation and progression of Parkinson's disease? *Acta Neuropathol Commun* 2017; **5**: 71 [PMID: 28903781 DOI: 10.1186/s40478-017-0470-4]
49 **Xiong Y**, Mahmood A, Chopp M. Emerging potential of exosomes for treatment of traumatic brain injury. *Neural Regen Res* 2017; **12**: 19-22 [PMID: 28250732 DOI: 10.4103/1673-5374.198966]
50 **Liu W**, Bai X, Zhang A, Huang J, Xu S, Zhang J. Role of Exosomes in Central Nervous System Diseases. *Front Mol Neurosci* 2019; **12**: 240 [PMID: 31636538 DOI: 10.3389/fnmol.2019.00240]
51 **Xu Y**, Hu Y, Xu S, Liu F, Gao Y. Exosomal microRNAs as Potential Biomarkers and Therapeutic Agents for Acute Ischemic Stroke: New Expectations. *Front Neurol* 2021; **12**: 747380 [PMID: 35173663 DOI: 10.3389/fneur.2021.747380]
52 **Otero-Ortega L**, Laso-García F, Gómez-de Frutos MD, Rodríguez-Frutos B, Pascual-Guerra J, Fuentes B, Díez-Tejedor E, Gutiérrez-Fernández M. White Matter Repair After Extracellular Vesicles Administration in an Experimental Animal Model of Subcortical Stroke. *Sci Rep* 2017; **7**: 44433 [PMID: 28300134 DOI: 10.1038/srep44433]
53 **Wang J**, Chen S, Zhang W, Chen Y, Bihl JC. Exosomes from miRNA-126-modified endothelial progenitor cells alleviate brain injury and promote functional recovery after stroke. *CNS Neurosci Ther* 2020; **26**: 1255-1265 [PMID: 33009888 DOI: 10.1111/cns.13455]
54 **Vasudeva K**, Munshi A. miRNA dysregulation in ischaemic stroke: Focus on diagnosis, prognosis, therapeutic and protective biomarkers. *Eur J Neurosci* 2020; **52**: 3610-3627 [PMID: 32022336 DOI: 10.1111/ejn.14695]
55 **Ghoreishy A**, Khosravi A, Ghaemmaghami A. Exosomal microRNA and stroke: A review. *J Cell Biochem* 2019; **120**: 16352-16361 [PMID: 31219202 DOI: 10.1002/jcb.29130]
56 **Cai G**, Cai G, Zhou H, Zhuang Z, Liu K, Pei S, Wang Y, Wang H, Wang X, Xu S, Cui C, Sun M, Guo S, Jia K, Zhang D. Mesenchymal stem cell-derived exosome miR-542-3p suppresses inflammation and prevents cerebral infarction. *Stem Cell Res Ther* 2021; **12**: 2 [PMID: 33407827 DOI: 10.1186/s13287-020-02030-w]
57 **Zhang Z**, Zou X, Zhang R, Xie Y, Feng Z, Li F, Han J, Sun H, Ouyang Q, Hua S, Lv B, Hua T, Liu Z, Cai Y, Zou Y, Tang Y, Jiang X. Human umbilical cord mesenchymal stem cell-derived exosomal miR-146a-5p reduces microglial-mediated neuroinflammation *via* suppression of the IRAK1/TRAF6 signaling pathway after ischemic stroke. *Aging (Albany NY)* 2021; **13**: 3060-3079 [PMID: 33479185 DOI: 10.18632/aging.202466]
58 **Zhao Y**, Gan Y, Xu G, Hua K, Liu D. Exosomes from MSCs overexpressing microRNA-223-3p attenuate cerebral ischemia through inhibiting microglial M1 polarization mediated inflammation. *Life Sci* 2020; **260**: 118403 [PMID: 32926923 DOI: 10.1016/j.lfs.2020.118403]
59 **Zhao Y**, Gan Y, Xu G, Yin G, Liu D. MSCs-Derived Exosomes Attenuate Acute Brain Injury and Inhibit Microglial Inflammation by Reversing CysLT2R-ERK1/2 Mediated Microglia M1 Polarization. *Neurochem Res* 2020; **45**: 1180-1190 [PMID: 32112178 DOI: 10.1007/s11064-020-02998-0]
60 **Li C**, Fei K, Tian F, Gao C, Yang S. Adipose-derived mesenchymal stem cells attenuate ischemic brain injuries in rats by modulating miR-21-3p/MAT2B signaling transduction. *Croat Med J* 2019; **60**: 439-448 [PMID: 31686458 DOI: 10.3325/cmj.2019.60.439]
61 **Li G**, Xiao L, Qin H, Zhuang Q, Zhang W, Liu L, Di C, Zhang Y. Exosomes-carried microRNA-26b-5p regulates microglia M1 polarization after cerebral ischemia/reperfusion. *Cell Cycle* 2020; **19**: 1022-1035 [PMID: 32208888 DOI: 10.1080/15384101.2020.1743912]
62 **Li X**, Bi T, Yang S. Exosomal microRNA-150-5p from bone marrow mesenchymal stromal cells mitigates cerebral ischemia/reperfusion injury *via* targeting toll-like receptor 5. *Bioengineered* 2022; **13**: 3030-3043 [PMID: 34898357 DOI: 10.1080/21655979.2021.2012402]
63 **Jiang M**, Wang H, Jin M, Yang X, Ji H, Jiang Y, Zhang H, Wu F, Wu G, Lai X, Cai L, Hu R, Xu L, Li L. Exosomes from MiR-30d-5p-ADSCs Reverse Acute Ischemic Stroke-Induced, Autophagy-Mediated Brain Injury by Promoting M2 Microglial/Macrophage Polarization. *Cell Physiol Biochem* 2018; **47**: 864-878 [PMID: 29807362 DOI: 10.1159/000490078]
64 **Barnabei L**, Laplantine E, Mbongo W, Rieux-Laucat F, Weil R. NF-κB: At the Borders of Autoimmunity and Inflammation. *Front Immunol* 2021; **12**: 716469 [PMID: 34434197 DOI: 10.3389/fimmu.2021.716469]
65 **Han M**, Cao Y, Xue H, Chu X, Li T, Xin D, Yuan L, Ke H, Li G, Wang Z. Neuroprotective Effect of Mesenchymal Stromal Cell-Derived Extracellular Vesicles Against Cerebral Ischemia-Reperfusion-Induced Neural Functional Injury: A Pivotal Role for AMPK and JAK2/STAT3/NF-κB Signaling Pathway Modulation. *Drug Des Devel Ther* 2020; **14**: 2865-2876 [PMID: 32764885 DOI: 10.2147/DDDT.S248892]
66 **Liu T**, Zhang L, Joo D, Sun SC. NF-κB signaling in inflammation. *Signal Transduct Target Ther* 2017; **2**: 17023-17023 [PMID: 29158945 DOI: 10.1038/sigtrans.2017.23]
67 **Fann DY**, Lim YA, Cheng YL, Lok KZ, Chunduri P, Baik SH, Drummond GR, Dheen ST, Sobey CG, Jo DG, Chen CL, Arumugam TV. Evidence that NF-κB and MAPK Signaling Promotes NLRP Inflammasome Activation in Neurons Following Ischemic Stroke. *Mol Neurobiol* 2018; **55**: 1082-1096 [PMID: 28092085 DOI: 10.1007/s12035-017-0394-9]
68 **Haupt M**, Zheng X, Kuang Y, Lieschke S, Janssen L, Bosche B, Jin F, Hein K, Kilic E, Venkataramani V, Hermann DM, Bähr M, Doeppner TR. Lithium modulates miR-1906 levels of mesenchymal stem cell-derived extracellular vesicles contributing to poststroke neuroprotection by toll-like receptor 4 regulation. *Stem Cells Transl Med* 2021; **10**: 357-373 [PMID: 33146943 DOI: 10.1002/sctm.20-0086]
69 **Zilahi E**, Tarr T, Papp G, Griger Z, Sipka S, Zeher M. Increased microRNA-146a/b, TRAF6 gene and decreased IRAK1 gene expressions in the peripheral mononuclear cells of patients with Sjögren's syndrome. *Immunol Lett* 2012; **141**: 165-168 [PMID: 22033216 DOI: 10.1016/j.imlet.2011.09.006]
70 **Harari OA**, Liao JK. NF-κB and innate immunity in ischemic stroke. *Ann N Y Acad Sci* 2010; **1207**: 32-40 [PMID: 20955423 DOI: 10.1111/j.1749-6632.2010.05735.x]
71 **Vidale S**, Consoli A, Arnaboldi M, Consoli D. Postischemic Inflammation in Acute Stroke. *J Clin Neurol* 2017; **13**: 1-9 [PMID: 28079313 DOI: 10.3988/jcn.2017.13.1.1]
72 **Gong Z**, Pan J, Shen Q, Li M, Peng Y. Mitochondrial dysfunction induces NLRP3 inflammasome activation during cerebral ischemia/reperfusion injury. *J Neuroinflammation* 2018; **15**: 242 [PMID: 30153825 DOI: 10.1186/s12974-018-1282-6]
73 **Alfonso-Loeches S**, Ureña-Peralta JR, Morillo-Bargues MJ, Oliver-De La Cruz J, Guerri C. Role of mitochondria ROS generation in ethanol-induced NLRP3 inflammasome activation and cell death in astroglial cells. *Front Cell Neurosci* 2014; **8**: 216 [PMID: 25136295 DOI: 10.3389/fncel.2014.00216]
74 **Liu X**, Zhang M, Liu H, Zhu R, He H, Zhou Y, Zhang Y, Li C, Liang D, Zeng Q, Huang G. Bone marrow mesenchymal stem cell-derived exosomes attenuate cerebral ischemia-reperfusion injury-induced neuroinflammation and pyroptosis by modulating microglia M1/M2 phenotypes. *Exp Neurol* 2021; **341**: 113700 [PMID: 33741350 DOI: 10.1016/j.expneurol.2021.113700]
75 **Sarmah D**, Datta A, Kaur H, Kalia K, Borah A, Rodriguez AM, Yavagal DR, Bhattacharya P. Sirtuin-1 - Mediated NF-κB Pathway

Modulation to Mitigate Inflammasome Signaling and Cellular Apoptosis is One of the Neuroprotective Effects of Intra-arterial Mesenchymal Stem Cell Therapy Following Ischemic Stroke. *Stem Cell Rev Rep* 2022; **18**: 821-838 [PMID: 35112234 DOI: 10.1007/s12015-021-10315-7]

76 **Kane AE**, Sinclair DA. Sirtuins and NAD(+) in the Development and Treatment of Metabolic and Cardiovascular Diseases. *Circ Res* 2018; **123**: 868-885 [PMID: 30355082 DOI: 10.1161/CIRCRESAHA.118.312498]

77 **Li B**, Wang Z, Yu M, Wang X, Chen C, Zhang Z, Zhang M, Sun C, Zhao C, Li Q, Wang W, Wang T, Zhang L, Ning G, Feng S. miR-22-3p enhances the intrinsic regenerative abilities of primary sensory neurons *via* the CBL/p-EGFR/p-STAT3/GAP43/p-GAP43 axis. *J Cell Physiol* 2020; **235**: 4605-4617 [PMID: 31663116 DOI: 10.1002/jcp.29338]

78 **Liang X**, Liu Y, Jia S, Xu X, Dong M, Wei Y. SIRT1: The Value of Functional Outcome, Stroke-Related Dementia, Anxiety, and Depression in Patients with Acute Ischemic Stroke. *J Stroke Cerebrovasc Dis* 2019; **28**: 205-212 [PMID: 30361109 DOI: 10.1016/j.jstrokecerebrovasdis.2018.09.037]

79 **Sasaki F**, Yokomizo T. The leukotriene receptors as therapeutic targets of inflammatory diseases. *Int Immunol* 2019; **31**: 607-615 [PMID: 31135881 DOI: 10.1093/intimm/dxz044]

80 **Wang Y**, Yang Y, Zhang S, Li C, Zhang L. Modulation of neuroinflammation by cysteinyl leukotriene 1 and 2 receptors: implications for cerebral ischemia and neurodegenerative diseases. *Neurobiol Aging* 2020; **87**: 1-10 [PMID: 31986345 DOI: 10.1016/j.neurobiolaging.2019.12.013]

81 **Iadecola C**, Anrather J. The immunology of stroke: from mechanisms to translation. *Nat Med* 2011; **17**: 796-808 [PMID: 21738161 DOI: 10.1038/nm.2399]

82 **Yang H**, Ara AI, Magilnick N, Xia M, Ramani K, Chen H, Lee TD, Mato JM, Lu SC. Expression pattern, regulation, and functions of methionine adenosyltransferase 2beta splicing variants in hepatoma cells. *Gastroenterology* 2008; **134**: 281-291 [PMID: 18045590 DOI: 10.1053/j.gastro.2007.10.027]

83 **Ge X**, Li W, Huang S, Yin Z, Yang M, Han Z, Chen F, Wang H, Lei P, Zhang J. Increased miR-21-3p in Injured Brain Microvascular Endothelial Cells after Traumatic Brain Injury Aggravates Blood-Brain Barrier Damage by Promoting Cellular Apoptosis and Inflammation through Targeting MAT2B. *J Neurotrauma* 2019; **36**: 1291-1305 [PMID: 29695199 DOI: 10.1089/neu.2018.5728]

84 **Paschon V**, Takada SH, Ikebara JM, Sousa E, Raeisossadati R, Ulrich H, Kihara AH. Interplay Between Exosomes, microRNAs and Toll-Like Receptors in Brain Disorders. *Mol Neurobiol* 2016; **53**: 2016-2028 [PMID: 25862375 DOI: 10.1007/s12035-015-9142-1]

85 **Vaure C**, Liu Y. A comparative review of toll-like receptor 4 expression and functionality in different animal species. *Front Immunol* 2014; **5**: 316 [PMID: 25071777 DOI: 10.3389/fimmu.2014.00316]

86 **Lester SN**, Li K. Toll-like receptors in antiviral innate immunity. *J Mol Biol* 2014; **426**: 1246-1264 [PMID: 24316048 DOI: 10.1016/j.jmb.2013.11.024]

87 **Zhang XS**, Li W, Wu Q, Wu LY, Ye ZN, Liu JP, Zhuang Z, Zhou ML, Zhang X, Hang CH. Resveratrol Attenuates Acute Inflammatory Injury in Experimental Subarachnoid Hemorrhage in Rats *via* Inhibition of TLR4 Pathway. *Int J Mol Sci* 2016; **17** [PMID: 27529233 DOI: 10.3390/ijms17081331]

88 **Chaurasiya V**, Kumari S, Onteru SK, Singh D. Up-regulation of miR-326 regulates pro-inflammatory cytokines targeting TLR-4 in buffalo granulosa cells. *Mol Immunol* 2020; **119**: 154-158 [PMID: 32035362 DOI: 10.1016/j.molimm.2020.01.019]

89 **Qiao H**, Zhang X, Zhu C, Dong L, Wang L, Xing Y, Wang C, Ji Y, Cao X. Luteolin downregulates TLR4, TLR5, NF-κB and p-p38MAPK expression, upregulates the p-ERK expression, and protects rat brains against focal ischemia. *Brain Res* 2012; **1448**: 71-81 [PMID: 22377454 DOI: 10.1016/j.brainres.2012.02.003]

90 **Gu L**, Huang J, Tan J, Wei Q, Jiang H, Shen T, Liang B, Tang N. Impact of TLR5 rs5744174 on stroke risk, gene expression and on inflammatory cytokines, and lipid levels in stroke patients. *Neurol Sci* 2016; **37**: 1537-1544 [PMID: 27262705 DOI: 10.1007/s10072-016-2607-9]

91 **Dabrowska S**, Andrzejewska A, Strzemecki D, Muraca M, Janowski M, Lukomska B. Human bone marrow mesenchymal stem cell-derived extracellular vesicles attenuate neuroinflammation evoked by focal brain injury in rats. *J Neuroinflammation* 2019; **16**: 216 [PMID: 31722731 DOI: 10.1186/s12974-019-1602-5]

92 **Zhang L**, Yu D. Exosomes in cancer development, metastasis, and immunity. *Biochim Biophys Acta Rev Cancer* 2019; **1871**: 455-468 [PMID: 31047959 DOI: 10.1016/j.bbcan.2019.04.004]

93 **Jiang CT**, Wu WF, Deng YH, Ge JW. Modulators of microglia activation and polarization in ischemic stroke (Review). *Mol Med Rep* 2020; **21**: 2006-2018 [PMID: 32323760 DOI: 10.3892/mmr.2020.11003]

94 **Yang H**, Tu Z, Yang D, Hu M, Zhou L, Li Q, Yu B, Hou S. Exosomes from hypoxic pre-treated ADSCs attenuate acute ischemic stroke-induced brain injury *via* delivery of circ-Rps5 and promote M2 microglia/macrophage polarization. *Neurosci Lett* 2022; **769**: 136389 [PMID: 34896256 DOI: 10.1016/j.neulet.2021.136389]

95 **Wang J**, Xing H, Wan L, Jiang X, Wang C, Wu Y. Treatment targets for M2 microglia polarization in ischemic stroke. *Biomed Pharmacother* 2018; **105**: 518-525 [PMID: 29883947 DOI: 10.1016/j.biopha.2018.05.143]

96 **Hu X**, Li P, Guo Y, Wang H, Leak RK, Chen S, Gao Y, Chen J. Microglia/macrophage polarization dynamics reveal novel mechanism of injury expansion after focal cerebral ischemia. *Stroke* 2012; **43**: 3063-3070 [PMID: 22933588 DOI: 10.1161/STROKEAHA.112.659656]

97 **Huang S**, Ge X, Yu J, Han Z, Yin Z, Li Y, Chen F, Wang H, Zhang J, Lei P. Increased miR-124-3p in microglial exosomes following traumatic brain injury inhibits neuronal inflammation and contributes to neurite outgrowth *via* their transfer into neurons. *FASEB J* 2018; **32**: 512-528 [PMID: 28935818 DOI: 10.1096/fj.201700673R]

98 **Domenis R**, Cifù A, Quaglia S, Pistis C, Moretti M, Vicario A, Parodi PC, Fabris M, Niazi KR, Soon-Shiong P, Curcio F. Pro inflammatory stimuli enhance the immunosuppressive functions of adipose mesenchymal stem cells-derived exosomes. *Sci Rep* 2018; **8**: 13325 [PMID: 30190615 DOI: 10.1038/s41598-018-31707-9]

99 **Duan S**, Wang F, Cao J, Wang C. Exosomes Derived from MicroRNA-146a-5p-Enriched Bone Marrow Mesenchymal Stem Cells Alleviate Intracerebral Hemorrhage by Inhibiting Neuronal Apoptosis and Microglial M1 Polarization. *Drug Des Devel Ther* 2020; **14**: 3143-3158 [PMID: 32821084 DOI: 10.2147/DDDT.S255828]

100 **Liu W**, Rong Y, Wang J, Zhou Z, Ge X, Ji C, Jiang D, Gong F, Li L, Chen J, Zhao S, Kong F, Gu C, Fan J, Cai W. Exosome-shuttled miR-216a-5p from hypoxic preconditioned mesenchymal stem cells repair traumatic spinal cord injury by shifting microglial M1/M2 polarization. *J Neuroinflammation* 2020; **17**: 47 [PMID: 32019561 DOI: 10.1186/s12974-020-1726-7]

101 **Zha Z**, Gao YF, Ji J, Sun YQ, Li JL, Qi F, Zhang N, Jin LY, Xue B, Yang T, Fan YP, Zhao H, Wang L. Bu Shen Yi Sui Capsule Alleviates Neuroinflammation and Demyelination by Promoting Microglia toward M2 Polarization, Which Correlates with Changes in miR-124 and miR-155 in Experimental Autoimmune Encephalomyelitis. *Oxid Med Cell Longev* 2021; **2021**: 5521503 [PMID: 33815654 DOI:

10.1155/2021/5521503]
102 **Yang J**, Chen Y, Jiang K, Zhao G, Guo S, Liu J, Yang Y, Deng G. MicroRNA-182 supplies negative feedback regulation to ameliorate lipopolysaccharide-induced ALI in mice by targeting TLR4. *J Cell Physiol* 2020; **235**: 5925-5937 [PMID: 32003008 DOI: 10.1002/jcp.29504]
103 **Li Y**, Guo W, Cai Y. NEAT1 Promotes LPS-induced Inflammatory Injury in Macrophages by Regulating MiR-17-5p/TLR4. *Open Med (Wars)* 2020; **15**: 38-49 [PMID: 32099901 DOI: 10.1515/med-2020-0007]
104 **Zhang Q**, Bian G, Chen P, Liu L, Yu C, Liu F, Xue Q, Chung SK, Song B, Ju G, Wang J. Aldose Reductase Regulates Microglia/Macrophages Polarization Through the cAMP Response Element-Binding Protein After Spinal Cord Injury in Mice. *Mol Neurobiol* 2016; **53**: 662-676 [PMID: 25520004 DOI: 10.1007/s12035-014-9035-8]
105 **Lin L**, Yihao T, Zhou F, Yin N, Qiang T, Haowen Z, Qianwei C, Jun T, Yuan Z, Gang Z, Hua F, Yunfeng Y, Zhi C. Inflammatory Regulation by Driving Microglial M2 Polarization: Neuroprotective Effects of Cannabinoid Receptor-2 Activation in Intracerebral Hemorrhage. *Front Immunol* 2017; **8**: 112 [PMID: 28261199 DOI: 10.3389/fimmu.2017.00112]
106 **Zhang Y**, Xu N, Ding Y, Zhang Y, Li Q, Flores J, Haghighiabyaneh M, Doycheva D, Tang J, Zhang JH. Chemerin suppresses neuroinflammation and improves neurological recovery *via* CaMKK2/AMPK/Nrf2 pathway after germinal matrix hemorrhage in neonatal rats. *Brain Behav Immun* 2018; **70**: 179-193 [PMID: 29499303 DOI: 10.1016/j.bbi.2018.02.015]
107 **Coulibaly AP**, Provencio JJ. Aneurysmal Subarachnoid Hemorrhage: an Overview of Inflammation-Induced Cellular Changes. *Neurotherapeutics* 2020; **17**: 436-445 [PMID: 31907877 DOI: 10.1007/s13311-019-00829-x]
108 **Wang M**, Thomson AW, Yu F, Hazra R, Junagade A, Hu X. Regulatory T lymphocytes as a therapy for ischemic stroke. *Semin Immunopathol* 2022 [PMID: 36469056 DOI: 10.1007/s00281-022-00975-z]
109 **Ruhnau J**, Schulze J, von Sarnowski B, Heinrich M, Langner S, Pötschke C, Wilden A, Kessler C, Bröker BM, Vogelgesang A, Dressel A. Reduced Numbers and Impaired Function of Regulatory T Cells in Peripheral Blood of Ischemic Stroke Patients. *Mediators Inflamm* 2016; **2016**: 2974605 [PMID: 27073295 DOI: 10.1155/2016/2974605]
110 **Hu Y**, Zheng Y, Wu Y, Ni B, Shi S. Imbalance between IL-17A-producing cells and regulatory T cells during ischemic stroke. *Mediators Inflamm* 2014; **2014**: 813045 [PMID: 24991091 DOI: 10.1155/2014/813045]
111 **Zhu D**, Johnson TK, Wang Y, Thomas M, Huynh K, Yang Q, Bond VC, Chen YE, Liu D. Macrophage M2 polarization induced by exosomes from adipose-derived stem cells contributes to the exosomal proangiogenic effect on mouse ischemic hindlimb. *Stem Cell Res Ther* 2020; **11**: 162 [PMID: 32321589 DOI: 10.1186/s13287-020-01669-9]
112 **Okoye IS**, Coomes SM, Pelly VS, Czieso S, Papayannopoulos V, Tolmachova T, Seabra MC, Wilson MS. MicroRNA-containing T-regulatory-cell-derived exosomes suppress pathogenic T helper 1 cells. *Immunity* 2014; **41**: 89-103 [PMID: 25035954 DOI: 10.1016/j.immuni.2014.05.019]
113 **Blazquez R**, Sanchez-Margallo FM, de la Rosa O, Dalemans W, Alvarez V, Tarazona R, Casado JG. Immunomodulatory Potential of Human Adipose Mesenchymal Stem Cells Derived Exosomes on in vitro Stimulated T Cells. *Front Immunol* 2014; **5**: 556 [PMID: 25414703 DOI: 10.3389/fimmu.2014.00556]
114 **Zhang B**, Yin Y, Lai RC, Tan SS, Choo AB, Lim SK. Mesenchymal stem cells secrete immunologically active exosomes. *Stem Cells Dev* 2014; **23**: 1233-1244 [PMID: 24367916 DOI: 10.1089/scd.2013.0479]
115 **Bian S**, Zhang L, Duan L, Wang X, Min Y, Yu H. Extracellular vesicles derived from human bone marrow mesenchymal stem cells promote angiogenesis in a rat myocardial infarction model. *J Mol Med (Berl)* 2014; **92**: 387-397 [PMID: 24337504 DOI: 10.1007/s00109-013-1110-5]
116 **Wang C**, Börger V, Mohamud Yusuf A, Tertel T, Stambouli O, Murke F, Freund N, Kleinschnitz C, Herz J, Gunzer M, Popa-Wagner A, Doeppner TR, Giebel B, Hermann DM. Postischemic Neuroprotection Associated With Anti-Inflammatory Effects by Mesenchymal Stromal Cell-Derived Small Extracellular Vesicles in Aged Mice. *Stroke* 2022; **53**: e14-e18 [PMID: 34847707 DOI: 10.1161/STROKEAHA.121.035821]
117 **Bellon M**, Lepelletier Y, Hermine O, Nicot C. Deregulation of microRNA involved in hematopoiesis and the immune response in HTLV-I adult T-cell leukemia. *Blood* 2009; **113**: 4914-4917 [PMID: 19246560 DOI: 10.1182/blood-2008-11-189845]
118 **Zhang M**, Johnson-Stephenson TK, Wang W, Wang Y, Li J, Li L, Zen K, Chen X, Zhu D. Mesenchymal stem cell-derived exosome-educated macrophages alleviate systemic lupus erythematosus by promoting efferocytosis and recruitment of IL-17(+) regulatory T cell. *Stem Cell Res Ther* 2022; **13**: 484 [PMID: 36153633 DOI: 10.1186/s13287-022-03174-7]
119 **Chen J**, Jin J, Li K, Shi L, Wen X, Fang F. Progresses and Prospects of Neuroprotective Agents-Loaded Nanoparticles and Biomimetic Material in Ischemic Stroke. *Front Cell Neurosci* 2022; **16**: 868323 [PMID: 35480961 DOI: 10.3389/fncel.2022.868323]

World Journal of Stem Cells

Submit a Manuscript: https://www.f6publishing.com

World J Stem Cells 2023 June 26; 15(6): 576-588

DOI: 10.4252/wjsc.v15.i6.576

ISSN 1948-0210 (online)

MINIREVIEWS

Clinical relevance of stem cells in lung cancer

Horacio Eduardo Romeo, María Laura Barreiro Arcos

Specialty type: Cell and tissue engineering

Provenance and peer review: Invited article; Externally peer reviewed.

Peer-review model: Single blind

Peer-review report's scientific quality classification

Grade A (Excellent): 0
Grade B (Very good): B
Grade C (Good): C
Grade D (Fair): 0
Grade E (Poor): 0

P-Reviewer: Lei X, China; Zhao W, China

Received: January 31, 2023
Peer-review started: January 31, 2023
First decision: February 10, 2023
Revised: March 18, 2023
Accepted: May 8, 2023
Article in press: May 8, 2023
Published online: June 26, 2023

Horacio Eduardo Romeo, María Laura Barreiro Arcos, School of Engineering and Agrarian Sciences, Pontifical Catholic University of Argentina, Institute of Biomedical Research (BIOMED-UCA-CONICET), CABA C1107AAZ, Buenos Aires, Argentina

Corresponding author: María Laura Barreiro Arcos, PhD, Research Scientist, School of Engineering and Agrarian Sciences, Pontifical Catholic University of Argentina, Institute of Biomedical Research (BIOMED-UCA-CONICET), Av. Alicia Moreau de Justo 1600, CABA C1107AZZ, Buenos Aires, Argentina. mlbarreiro@yahoo.com.ar

Abstract

Lung cancer is the major cause of cancer-related deaths worldwide, it has one of the lowest 5-year survival rate, mainly because it is diagnosed in the late stage of the disease. Lung cancer is classified into two groups, small cell lung cancer (SCLC) and non-SCLC (NSCLC). In turn, NSCLC is categorized into three distinct cell subtypes: Adenocarcinoma, squamous cell carcinoma, and large cell carcinoma. NSCLC is the most common lung cancer, accounting for 85% of all lung cancers. Treatment for lung cancer is linked to the cell type and stage of the disease, involving chemotherapy, radiation therapy, and surgery. Despite improvements in therapeutic treatments, lung cancer patients show high rates of recurrence, metastasis, and resistance to chemotherapy. Lung stem cells (SCs) are undifferentiated cells capable of self-renewal and proliferation, are resistant to chemotherapy and radiotherapy and, due to their properties, could be involved in the development and progression of lung cancer. The presence of SCs in the lung tissue could be the reason why lung cancer is difficult to treat. The identification of lung cancer stem cells biomarkers is of interest for precision medicine using new therapeutic agents directed against these cell populations. In this review, we present the current knowledge on lung SCs and discuss their functional role in the initiation and progression of lung cancer, as well as their role in tumor resistance to chemotherapy.

Key Words: Lung cancer; Cancer stem cells; Biomarkers; Chemoresistance

Core Tip: Lung cancer stem cells (CSCs) could have a functional role in primary tumor initiation, invasion and metastasis, resistance to chemotherapeutic drugs, and recurrence in lung cancer. To improve lung cancer treatments, it is necessary to identify and characterize CSCs populations in lung tissue and develop targeted therapies against these cell types. This review discusses the current knowledge on CSCs in lung tissue and future perspectives in lung cancer treatment.

Citation: Romeo HE, Barreiro Arcos ML. Clinical relevance of stem cells in lung cancer. *World J Stem Cells* 2023; 15(6): 576-588
URL: https://www.wjgnet.com/1948-0210/full/v15/i6/576.htm
DOI: https://dx.doi.org/10.4252/wjsc.v15.i6.576

INTRODUCTION

Lung cancer is the leading cause of cancer death worldwide, in both men and women. Lung cancer is classified into two histological types, small cell lung cancer (SCLC) derived from cells of the neuroendocrine lineage and non-SCLC (NSCLC) derived from epithelial cells. The latter is the most frequent type of lung cancer in the population, since represents approximately 85% of all lung tumors, while SCLC represents the remaining 15%[1].

Based on the morphology of the transformed cells, NSCLC is classified into three subtypes: Squamous cell carcinoma (SCC), adenocarcinoma (AD), and large cell carcinoma (LCC). AD arises in peripheral lung tissue from type II alveolar epithelial cells that line the small alveoli, while SCC arises in the central lung region from cells of the stratified squamous epithelium that line the airways from the trachea to the main bronchi. LCC is a heterogeneous group of tumors that lack the morphological characteristics of AD and SCC sub-types or SCLC and arise from epithelial cells that line the lungs[1,2].

SCLC arises from lung epithelial cells from the main bronchi to the terminal alveoli. Their histologic features correlate with the site of origin and reflect epithelial variations of the airways[2]. The classification and main characteristics of lung cancer are shown in Figure 1.

All forms of lung cancer have a poor prognosis, mainly SCLC and SCC, which are typically seen in smokers. SCLC is the most aggressive lung cancer because it grows quickly and spreads to other tissues, generating metastases in the liver, brain, bones, and adrenal glands[3]. LCC has a better prognosis, which depends on the cell subtype. The poor prognosis is generally associated with the ability of the cells to metastasize and the late diagnosis of the disease, since the symptoms and signs do not usually appear in the early stages[4]. People with lung cancer may have chest pain, frequent coughing, blood in the mucus, trouble breathing, swallowing or speaking, loss of appetite and weight, and tiredness[5].

The prevalence of lung cancer worldwide is 13%, with an incidence of 1.8 million new cases per year. Lung cancer is responsible for about 20% of all cancer-related deaths worldwide and has one of the lowest 5-year survival rates (7% in SCLC and 11-17% in NSCLC, depending on the subtype and stage of the cancer[6].

The main cause of lung cancer is long-term smoking, with a 25-fold increase in the risk of developing the disease. However, there are other risk factors such as genetic factors, long-term menopausal hormone replacement therapy, exposure to radon, asbestos, metals (arsenic, cadmium, and chromium), organic chemicals found in smoke coal, and a history of lung disease such as tuberculosis, emphysema, or chronic bronchitis[7]. Smoking can cause all types of lung cancer, but is most strongly linked to SCLC and SCC, while AD is the most common type of lung cancer in patients who have never smoked. In the first two, cancer development frequently occurs in people 60 to 70 years of age with a long-term history of tobacco smoking, while AD occurs in younger people[7].

In this review, we update knowledge about the properties of SCs and their participation in the initiation and progression of lung cancer, pointing out the biomarkers that may be useful in therapeutic strategies or as a prognosis of the disease. In addition, we discuss the role of SCs in the resistance to therapeutic treatments.

SOMATIC MUTATIONS IN LUNG CANCER

Lung carcinogenesis is a chronic process that involves multiple genetic, cellular, and tissue alterations as a consequence of mutations in genes that regulate growth, differentiation, and apoptosis. Cancers are caused by the accumulation of mutations in critical genes, specifically those that control cell growth and division or the repair of damaged DNA. These changes allow cells to grow and divide uncontrollably to form a tumor. In almost all cases of lung cancer, these genetic changes, which are present only in certain lung cells, are acquired during life as a result of exposure to carcinogens, long-term hormone therapy, or chronic lung disease[8].

The most frequently mutated genes in lung cancer are *epidermal growth factor receptor* (*EGFR*), *Kirsten rat sarcoma virus* (*KRAS*) and *tumor protein 53* (*TP53*)[9,10]. The proteins encoded by these genes participate in signaling pathways that contribute to lung tumorigenesis. Mutations in the *EGFR* gene cause the expression of receptors on the cell membrane that are constitutively activated, triggering signaling pathways within cells involved in lung tumorigenesis. Binding of epidermal growth factor (EGF) to EGFR induces receptor phosphorylation at tyrosine residues and activates multiple downstream signaling pathways, such as the Ras-Raf-MAPK, PI3K, and STAT pathways, which induce proliferation and cell invasion, angiogenesis, inhibition of apoptosis and metastasis. The constitutive activity of EGFR has been observed in more than 60% of patients with NSCLC and is due to different mutations present in the receptor[11]. *KRAS* was first identified as a viral oncogene in the Kirsten RAt Sarcoma virus. The *KRAS* gene encodes the Ras proteins, low molecular

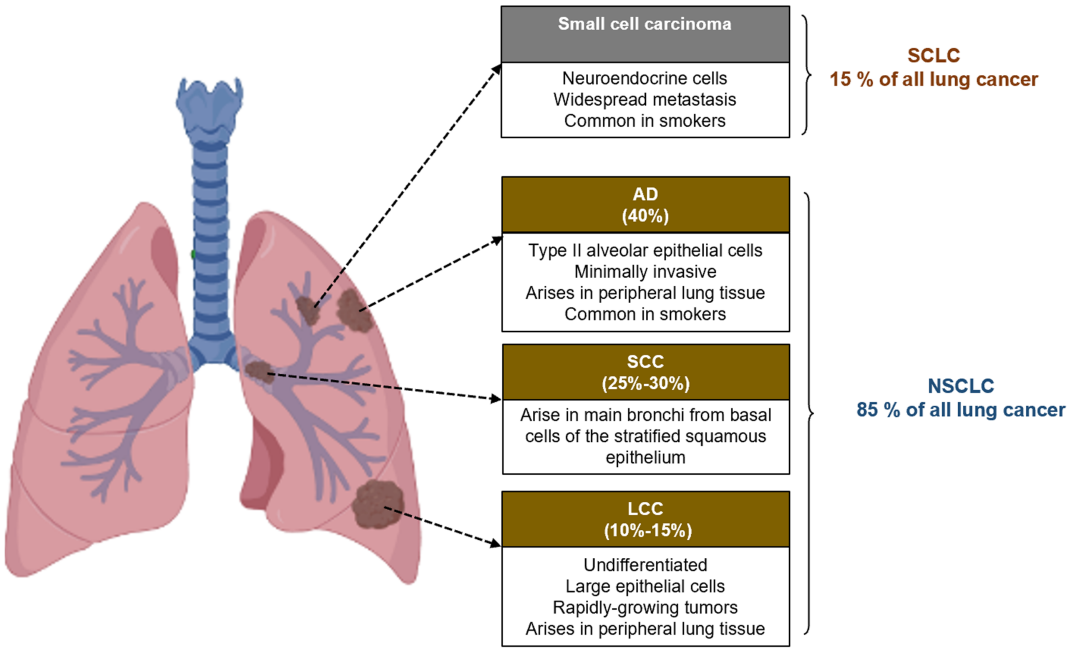

DOI: 10.4252/wjsc.v15.i6.576

Figure 1 Classification and main characteristics of lung cancer. Lung cancer is classified into two histological types, small cell lung cancer (SCLC) derived from cells of the neuroendocrine lineage and non-SCLC (NSCLC) derived from epithelial cells. NSCLC is classified into three subtypes: Adenocarcinoma, squamous cell carcinoma, and large cell carcinoma. SCLC: Small cell lung cancer; NSCLC: Non-SCLC; AD: Adenocarcinoma; SCC: Squamous cell carcinoma; LCC: Large cell carcinoma.

weight enzymes with guanosine triphosphate hydrolase (GTPase) activity located on the inside of the plasma membrane. Ras GTPases are activated in response to the binding of ligands to several receptors such as EGF, platelet-derived growth factor, integrin, and cytokine receptors. Mutations in the *KRAS* gene cause loss of the ability of Ras to hydrolyze GTP to guanosine diphosphate leading to constant activation of Ras[12]. Similar to constitutive activation of EGFR, mutated Ras stimulates multiple signaling pathways relevant to tumor development. Mutations in the *KRAS* gene are of high frequency in NSCLC but are also present in other types of cancer such as colorectal and pancreatic cancer[13]. Another protein associated with the onset of lung cancer is the p53 tumor suppressor protein encoded by the *TP53* gene. This tumor suppressor responds to several cellular stresses to regulate expression of target genes, thereby inducing DNA repair or cell cycle arrest and apoptosis[14]. Mutations in the *TP53* gene synthesize a non-functional p53 protein, causing accumulation of damaged DNA in cells and dysregulation of the cell cycle. Mutations in the *KRAS* and *TP53* genes have been found in up to 30% of patients with lung cancer and have been considered as predictors of poor prognosis[9]. Mutations in other genes such as *CDKN2A*, *STK11*, *BRAF*, *PIK3CA*, *RB1*, *PTEN* or *MET* have been associated with the onset of lung cancer, although they showed a lower mutation rate than the *EGFR*, *KRAS* or *TP53* genes. Most of them are involved in the regulation of cell proliferation, differentiation, or apoptosis[9].

Lung tumor tissue is characterized by a heterogeneity of cell types with different phenotypic characteristics and properties as a result of the accumulation of gene mutations and differential cell signaling in the tumor microenvironment. However, it has been shown that only a small fraction of cells in tumor tissue have the ability to form tumor spheroids *in vitro* and develop tumors when they are transplanted into immunodeficient animals. These observations raise the need to study which are the cell populations in the tumor with tumorigenic potential.

ROLE OF STEM CELLS IN TUMORIGENESIS

Cancer stem cells (CSCs) are defined as a subpopulation of tumor cells residing in the tumor with SCs characteristics. CSCs have the ability to self-renew, generate identical daughter cells with stem cell properties, differentiate into multiple cancer cell lineages, facilitate tumor growth and survival, and metastasize to distal sites. In addition, they could be the cause of evasion of the immune system, resistance to chemotherapy and radiation therapy, and cancer relapse[15]. CSCs differ from normal tissue-specific SCs only in their uncontrolled growth and altered genotypes[16].

The seminal proposition that CSCs could be responsible for tumor initiation was introduced by the end of XIX century [17], however the first conclusive evidence for CSCs in acute myeloid leukemia was demonstrated in 1997 by Bonnet and Dick[18]. These authors isolated a subpopulation of CD34+/CD38- leukemic cells capable of initiating tumors in non-obese diabetic/severe combined immunodeficiency disease (NOD/SCID) mice histologically similar to the donor. In recent years, CSCs have been identified in several tumors, including breast, brain, colon, and lung cancer[19].

CSCs are a small proportion of the cell population of a tumor (less than 1%) that exhibit high tumorigenic potential. This is supported by experiments where thousands of tumor cells need to be inoculated into syngeneic or immunodeficient animals for a solid tumor to develop. Some years ago, this requirement was thought to be due to the loss of viability of tumor cells during transfer or the absence of a suitable niche for tumor growth. The new paradigm indicates that only CSCs (a small fraction of the transplanted cells) has the potential to generate a tumor[20]. This hypothesis can be reinforced by the fact that metastases are histologically heterogeneous and similar to the primary tumor, which implies that the cell that gave rise to it has the potential to differentiate into multiple cell types, such as a SCs[19].

Several questions have been raised about the origin of CSCs in tumor tissue. The first hypothesis is that CSCs could originate from tissue-specific normal SCs that have dysregulated cell growth. In this sense, it has been shown that all tissues harbor SCs that play an essential role in tissue repair[16]. These normal SCs could be transformed into CSCs due to the accumulation of gene mutations or the action of chemical mediators released under conditions of tissue damage [21]. This hypothesis is accepted for tissues with a high degree of cell renewal, such as intestinal epithelium or skin, but it is controversial for tissues that are quiescent or that renew slowly, such as lung epithelium. In this sense, some authors have identified a fraction of cells in active division (less than 1.3%) located in specific niches of the tracheal and bronchiolar epithelium with characteristics of SCs that could become CSCs[22,23]. The second hypothesis is that CSCs could originate from more differentiated progenitor cells that have acquired the capacity for self-renewal or differentiated tumor cells (called CSCs-like cells) due to mutations in genes that regulate the cell cycle, hypoxia, or chemical mediators of the tumor microenvironment such as nitric oxide or certain interleukin[24].

STEM CELL MARKERS IN LUNG CANCER

Tumor tissue is heterogeneous, showing different cell populations that have their own signaling pathways, leading to more complex therapeutic strategies. Factors contributing to intratumoral heterogeneity include genetic mutations, epigenetic changes, interactions with the microenvironment and CSCs[25]. CSCs represent only a small group of cells within the heterogeneity of tumor tissue. SCs trigger specific signaling pathways, such as Notch, Hedgehog, and Wnt, that allow them to self-renew and proliferate in tissue repair processes. These pathways are tightly controlled, but their aberrant activation in CSCs can induce the expression of tumor molecular markers, leading to tumorigenicity and chemoresistance[26].

CSCs have been identified in several types of cancer through proteins that are differentially expressed in these cells. These proteins include cell membrane receptors, cell adhesion molecules, cell membrane transporters, enzymes involved in metabolism, and transcription factors. Its are used as biomarkers to predict the prognosis of the disease, evaluate the most appropriate chemotherapy treatments and the efficacy of the therapies in tumor remission[15].

Biomarkers that have been identified in lung cancer include cluster of differentiation-133 (CD133), cluster of differentiation-44 (CD44), epithelial cell adhesion molecule (EpCAM), aldehyde dehydrogenase 1A1 (ALDH1A1), ATP-binding cassette sub-family G member 2 (ABCG2) and the transcription factors octamer-binding transcription factor 4 (Oct-4), sex-determining region Y-box 2 (Sox2), and Nanog[15,26]. Although these biomarkers have different structures and functional roles, its are linked to the SCs properties and uncontrolled proliferation of tumor cells. The biomarkers identified in lung CSCs are shown in Figure 2.

Biomarkers are not specific for lung CSCs and may be expressed in other types of cancer, such as breast, brain, colon or liver cancer. Since a single marker is not sufficient to accurately identify CSCs, combinations of several markers are used to identify and isolate CSCs in tumor tissue[27].

Cluster of differentiation

CD133: CD133, also known as prominin-1, is a transmembrane glycoprotein involved in cell growth and differentiation through its involvement in multiple signaling pathways[27,28]. It has been identified as the main biomarker of SCs in normal tissue and of stemness in tumor tissue from patients with NSCLC or SCLC.CD133 expression is essential to maintain CSCs characteristics such as tumor cell proliferation, migration, and invasion, and the ability to resist chemotherapy[27].

In lung cancer, the high level of expression of CD133 has been correlated with epithelial to mesenchymal transitions and the formation of metastases in lymph nodes and other tissues, which reveals that CD133 is a biomarker of tumor aggressiveness and poor prognosis of the pathology[29-31]. The molecular mechanisms involved in CD133-mediated cell growth and resistance to chemotherapy are still under study, but appear to be associated with the Wnt/catenin, PI3K-AKT and SRC-FAK signaling pathways[32,33]. Furthermore, CD133 has been shown to directly interact with vascular endothelial growth factor (VEGF), stimulating angiogenesis and leading to tumor growth[34]. CD133 is also used as diagnostic, predictive, or therapeutic biomarkers in other types of cancer including breast, stomach, liver, prostate, colorectal, pancreatic, and renal[28].

CD44: CD44 is a transmembrane glycoprotein of high structural and functional diversity due to alternative splicing processes and post-translational modifications. It can bind to a wide variety of ligands on the cell surface, including hyaluronic acid (HA), and trigger multiple cellular processes such as cell-cell signaling, cell growth and differentiation, cell adhesion and migration, angiogenesis, or cell survival[26].

CD44 regulates several signaling pathways to promote cancer progression, including Notch, Hedgehog, and Wnt pathways[26]. In addition, it can act as a co-receptor and heterodimerizes with growth factor receptors [EGFR, fibroblast growth factor receptor (FGFR), hepatocyte growth factor receptor, VEGF receptor, transforming growth factorβ receptor]

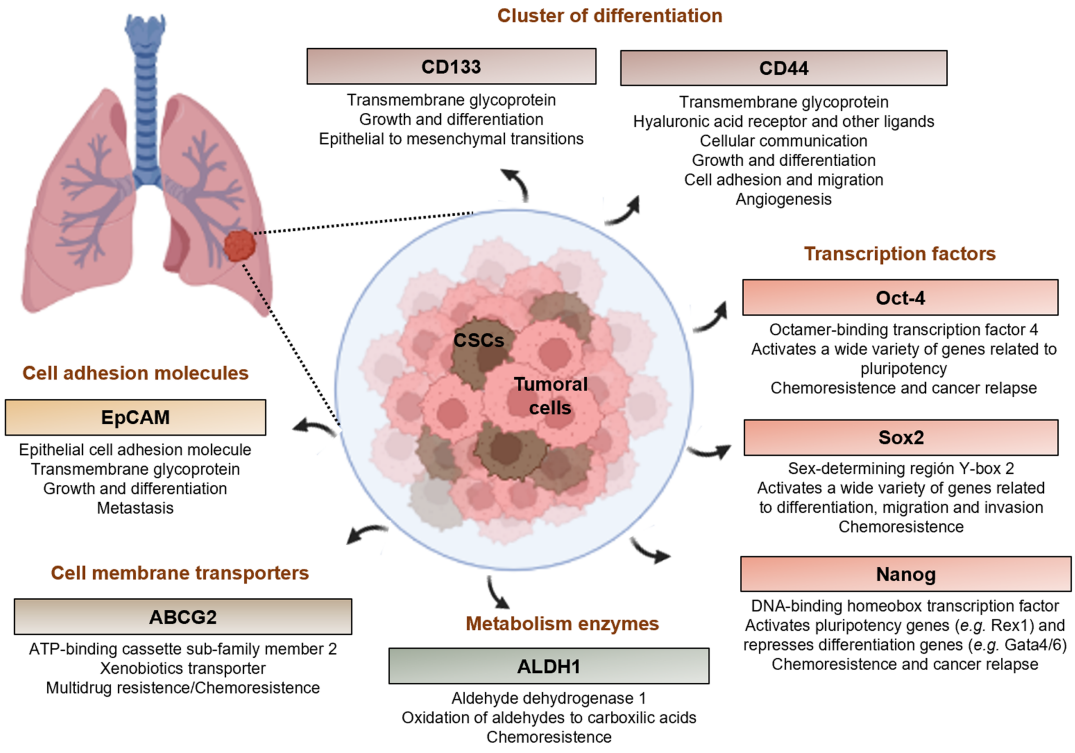

DOI: 10.4252/wjsc.v15.i6.576 **Copyright** ©The Author(s) 2023.

Figure 2 Stem cell biomarkers in lung cancer. Biomarkers identified in cancer stem cells in lung tissue include clusters of differentiation, cell adhesion molecules, cell membrane transporters, enzymes of cell metabolism, and transcription factors. CSCs: Cancer stem cells; ABCG2: ATP-binding cassette subfamily G member 2; ALDH: Aldehyde dehydrogenase.

and leads to activation of the PI3K-AKT and MAPK pathways[15]. It is hypothesized that CD44 could play an important role in tumorigenesis mediated by the constitutive activation of EGFR, whose expression is frequently mutated in patients with NSCLC. In this last sense, CD44 could be an important marker to predict the efficacy of chemotherapy using EGFR-specific tyrosine kinase inhibitors in patients with lung cancer[15].

CD44 is expressed in almost all tumor types, but it has been identified as the main CSCs biomarker in lung ADs and in SCC. Its expression is associated with a more aggressive tumor phenotype, with the ability to metastasize and resist chemotherapy[35].

Cell adhesion molecules

EpCAM: EpCAM is a transmembrane protein and acts as an adhesion molecule on the lung epithelium. It is a potential biomarker for lung tumors of epithelial origin[36]. EpCAM expression in lung tumor epithelium is upregulated by metastasis-associated protein 1 and leads to increased metastatic capacity of tumor cells[36]. The co-expression of EpCAM with CD44 and CD166 in NSCLC indicates a greater self-renewal capacity, clonal heterogeneity and stemness. These biomarkers in lung tumor tissue indicate a poor prognosis for the disease[37].

Cell membrane transporters

ABCG2: ABCG2 is a transporter of xenobiotic compounds into the extracellular space, which has been implicated in the development of multidrug resistance (MDR) in cancer. The wide variety of ABCG2 substrates includes several antitumoral drugs such as paclitaxel, doxorubicin, cisplatin, topotecan, mitoxantrone and irinotecan. ABCG2 also expels the fluorescent dye Hoechst 33342 out of the cell, a property that is unique to SCs and is used for identification of these cells[38]. The expression of ABCG2 in SCs has been conserved in many tissues, such as the pancreas, lung, heart, testis, liver, brain, prostate, and embryonic tissue, demonstrating the importance of this transporter for cell survival[39]. In lung cancer, increased expression of ABCG2 has been found in SCs, associated with the upregulation and activity of the transcription factors Sp1, Sp3, YAP1 and Nrf2[40-42]. Its expression in lung CSCs is associated with cancer relapse and poor prognosis[42].

Enzymes involved in metabolic pathways

ALDH1: ALDH1 is an enzyme that participates in cellular metabolism through the oxidation of aldehydes to carboxylic acids and is a marker of SCs of normal and tumor tissue[43]. It has three main isotypes, ALDH1A1, ALDH1A2 and ALDH1A3, but its activity is mainly attributed to the ALDH1A1 isotype[43].

Increased expression of ALDH has been found in NSCLC overexpressing a subpopulation of CD44+/EpCAM+ cells [44]. Overexpression of the ALDH1 and CD133 markers was found exclusively in SCC and AD[45]. ALDH1A1 overexpression is associated with an aggressive chemotherapy-resistant tumor phenotype. Despite this, ALDH1 could be a

useful therapeutic target for tumors growing in tissues that do not normally express high levels of ALDH1A1, such as the lung, breast, colon, and stomach[43].

Transcription factors

Otherwise, the transcription factors involved in the normal activity of SCs could be deregulated in cancer, and activate cellular pluripotency genes and suppress differentiation genes, triggering signaling pathways responsible for the characteristics of CSCs. Transcription factors that regulate the functions of lung CSCs, such as Oct-4, Sox2, and Nanog, have been identified.

Oct-4: Oct-4 also known as POU5F1, is a member of the POU transcription factor family that contains a binding domain to the ATGCAAAT sequence in target genes[15]. The *Oct-4* gene encodes four protein isoforms called Oct4A, Oct4B-190, Oct4B-265, and Oct4B-164. Of these, Oct4A is known to transcribe a wide variety of genes that regulate SCs stemming. Several Oct-4A target genes have been identified in CSCs of lung cancer, including Fgf4, Utf1, Opn, Rex1/Zfp42, and Fbx15[15].

Oct-4A transcriptional activity is upregulated by post-translational modifications, through phosphorylation at residues Ser229, Ser236 and tyr327 or sumoylation at residue Lys118. Its expression is high in SCs, however Oct-4 is ubiquitinated and degraded by the proteasome in the cell differentiation process[15].

In lung cancer, Oct4 activity is associated with chemotherapy resistance, cancer relapse, and worse outcomes[15].

Sox2: Sox2 is a member of the high mobility group (HMG) box gene family encoded by the sex-determining region Y-box gene. HMG is a sequence of 80 amino acids that acts as a DNA-binding domain in several target genes related to the maintenance of pluripotency in embryonic SCs and CSCs[46]. Sox2 is closely associated with early embryonic development, neuronal differentiation, bronchial morphogenesis, and airway epithelial maturation[46].

In lung cancer, Sox2 can regulate the transcription of the c-MYC, Wnt and Notch oncogenes and increase metastatic capacity through the FGFR-ERK1/2-SOX2 signaling pathway[47]. In SCC, Sox2 can induce expression of tumor-related factors p63 and keratin 6 and lead to cancer differentiation, migration, and invasion. In SCLC, Sox2 is crucial in the PI3K-Akt-Sox2 signaling pathway and may mediate chemoresistance[47]. In addition, Sox2 together with Oct-4 increase its expression under hypoxia in tumor tissue, which induces the expression of the CD133 marker and the self-renewal and maintenance of lung CSCs[48].

Sox2 transcriptional activity can be increased by phosphorylation at amino acid residue Thr118 or methylation at Arg113, which inhibits its proteasome degradation or promotes its homodimerization, respectively[49].

Sox2 and Oct4 have been located in the cell nucleus of SCLC and lung AD, but not in their paracancerous tissues or benign tumor tissues, pointing to the importance of Sox2 and Oct4 as potential markers for cancer therapies[50].

Nanog: Nanog, a DNA-binding homeobox transcription factor, may promote cell proliferation, renewal, and stem properties. Nanog can regulate cell pluripotency through two mechanisms of action. Thus, Nanog can repress the transcription of genes essential for cell differentiation, such as Gata4 and Gata6, or it can activate the transcription of genes necessary for self-renewal, such as Rex1[15].

Nanog expression is upregulated by Nr5a2 promoting CSCs properties and tumorigenesis in NSCLC[51]. Nanog is highly expressed in pluripotent cells and its expression is downregulated during differentiation. Its transcriptional activity is increased by phosphorylation at amino acid residues Ser52, 65 and 71 and Thr287, which abolishes its ubiquitination and degradation by the proteasome[52].

Nanog is increased in many types of carcinomas, including lung cancers, and is associated with chemoresistance, cancer relapse, and poor prognosis[15,52].

STEM CELL MARKERS AS THERAPEUTIC TARGETS FOR THE TREATMENT OF LUNG CANCER

Most clinical trials involve the use of drugs whose targets of action are protein tyrosine kinases, regulators of the cell cycle or cell signaling pathways. Several chemotherapy drugs are not effective in controlling tumor growth and metastases. Thus, novel therapeutic agents directed against CSCs are a hope for patients who do not respond to conventional therapies or who relapse after cancer treatment. These therapies include the use of synthetic or natural inhibitors, monoclonal or bispecific antibodies (BsAb), antibodies-drug conjugates, aptamer-drug conjugates, or chimeric antigen receptor T (CAR-T) therapies. Novel therapies using stem cell biomarkers as pharmacological targets are summarized in Table 1.

Inhibitory drugs

Salazosulfapyridine in combination with cisplatin and pemetrexed is under phase I study for advanced NSCLC (Trial registration-UMIN 000017854). This drug inhibits the intracellular uptake of cysteine by the cysteine-glutamate antiporter in CSCs that overexpress CD44 marker, preventing the synthesis of the antioxidant GSH, essential for cellular redox homeostasis, and leading to the inhibition of tumor growth[53].

Phase II trial using disulfiram in combination with cisplatin plus vinorelbine have shown to be effective for the treatment of metastatic NSCLC (Trial registration-NCT 00312819)[54]. *In vitro* studies in NSCLC cell lines treated with cisplatin have shown the growth of chemoresistant ALDH1+ cell subpopulations. These cells were sensitive to the cytotoxic effects of cisplatin after treatment with diethylaminobenzaldehyde and disulfiram, inhibitors of ALDH1 activity [55]. In xenograft models in NOD/SCID mice, it has been shown that disulfaran inhibits the activity of ALDH1A1 and the

Table 1 Potential therapeutic strategies targeting lung cancer stem cell markers

Stem cell marker-target	Therapeutic strategies in clinical trials and preclinical studies
Differentiation cluster	
CD133	Docetaxel-loaded liposomes conjugated to anti-CD133 aptamers
	Gefitinib-loaded nanomicelles conjugated to anti-CD133 aptamers
	Salinomycin sodium-loaded nanoparticles conjugated to anti-CD133 antibody
	CD133-specific CAR-T cells plus anti-PD-1 antibody and a CD73 inhibitor
CD44	Salazosulfapyridine plus cisplatin and pemetrexed (Phase I clinical trial for the treatment of advanced non-squamous NSCLC)
	mAb MEM-85 (monoclonal antibody)
	HA-Cisplatin conjugated
	HA-Irinotecan conjugated (Phase II study for treatment of SCLC)
	HA-Apoferritin conjugated
	HA-conjugated cisplatin-loaded nanoparticles
Cell adhesion molecules	
EpCAM	Doxorubicin-loaded nanoparticles conjugated to EpCAM aptamer
	Catumaxomab BsAb anti-human EpCAM/CD3 T-cell antigen (Phase I study for treatment of NSCLC)
	MT110 BsAb anti-EpCAM/CD3 T-cell antigen (Phase I clinical trial for treatment of lung adenocarcinoma)
	MuS110 BsAb anti-human EpCAM/CD3 T-cell antigen
	2C11x4-7 BsAb anti-murine EpCAM/CD3 T-cell antigen
Cell membrane transporters	
ABCG2	Secalonic acid D
	Axitinib in combination with topotecan or mitoxantrone
	FL118 (topoisomerase 1 inhibitor) in combination with irinotecan, topotecan or cisplatino
	A-803467 (tetrodotoxin-resistant sodium channel blocker) in combination with topotecan, doxorubicin or mitoxantrone
	Verteporfin (YAP1 inhibitor)
Metabolic enzymes	
ALDH	Disulfiram in combination with cisplatin plus vinorelbine (Phase II clinical trial for the treatment of NSCLC)
	Disulfiram alone or in combination with diethylaminobenzaldehyde and cisplatin
	FL118 in combination withirinotecan, topotecan or cisplatino
Transcription factors and signaling pathway	
Oct-4	FL118 in combination with irinotecan, topotecan or cisplatino
Notch-signaling pathway	BsAb-5 directed against c-MET and CTLA-4 in CD166+ NSCLC

mAb: Monoclonal antibody; HA: Hyaluronic acid; BsAb: Bispecific antibody; CAR-T: Chimeric antigen receptor T; c-MET: Cellular mesenchymal-to-epithelial transition factor; CTLA-4: Cytotoxic T-lymphocyte-associated protein 4; NSCLC: Non-small cell lung cancer; ABCG2: ATP-binding cassette subfamily G member 2; CD133: Cluster of differentiation-133; CD44: Cluster of differentiation-44; EpCAM: Epithelial cell adhesion molecule; ALDH: Aldehyde dehydrogenase; Oct-4: Octamer-binding transcription factor 4.

expression of Sox2, Oct-4 and Nanog, reducing the size of tumors derived from ALDH+ CSCs and cancer recurrence[56].

ABCG2 transporter is one of the main CSCs markers under study due to its role in MDR. It has been found that the secalonic acid D, a metabolite of marine-derived mangrove endophytic fungus, can down-regulate the expression of ABCG2 by activation of Calpaina 1, a protease that shortens the half-life of the transporter[57]. In addition, Verteporfin, an inhibitor of the YAP1 transcription factor, was found to down-regulate the expression of the ABCG2 transporter in lung CSCs[41].

A-803467, a tetrodotoxin-resistant sodium channel blocker, inhibits ABCG2 transporter activity, increasing the sensitivity to chemotherapeutic drugs such as topotecan, doxorubicin and mitoxantrone in multidrug resistant cells. A combination of A-803467 and ABCG2 substrates may potentially be a novel therapeutic treatment in tumors overexpressing the ABCG2 protein[58].

FL118, a topoisomerase 1 inhibitor similar to camptothecin analogues (such as irinotecan or topotecan) used in the clinic, selectively inhibits the expression of several members of the proapoptotic protein family such as Survivin, Xiap, CIAP2 and BCL-2. It has also been found that FL118 down-regulate the expression of ABCG2, ALDH1A1 and Oct-4. FL118 improves sensitivity to chemotherapy and inhibits the growth of CSCs and metastases. Moreover, FL118 is effective for human tumors that acquire irinotecan, topotecan and cisplatino resistance due to its ability to bypass the drug resistance induced by ABC transporters[59].

Monospecific and Biespecific antibodies

mAbMEM-85 is a monoclonal antibody of therapeutic interest since it inhibits the growth of lung cancer cells in murine models. It has been shown that mAbMEM-85 recognizes the hyaluronate binding site in the C-terminal region of CD44 in lung cancer SCs[60].

Axitinib is a monoclonal antibody that inhibits the activity of the ABCG2 transporter in CSCs, and reverses MDR. Studies in A549 human lung cancer cells and nude mice bearing S1-M1-80 xenografts that overexpress ABCG2 have shown that axitinib increases tumor cell apoptosis induced by chemotherapeutic drugs such as topotecan and mitoxantrone without causing additional toxicity[61].

BsAb target two different epitopes or antigens simultaneously. One of the Fab fragments recognizes epitopes on cytotoxic drugs or CD8+ T or NK immune cells, while the other Fab fragment can bind epitopes on CSCs. Then, BsAbs can selectively direct effector cells or chemotherapeutic drugs towards CSCs, promoting their destruction. BsAb have been extensively explored in translational and clinical studies in lung cancer.

Catumaxomab is a BsAb with binding sites directed to human EpCAM and CD3 T-cell antigen. A phase I study has shown that catumaxomab is safe and tolerable when administered intravenously in patients with NSCLC[62]. Other anti-CD3-EpCAM BsAbs have been studied in immunocompetent mice bearing lung tumors, showing potent inhibition of local and disseminated tumor growth[63]. MT110 BsAb targeting EpCAM/CD3 T-cell antigen has been tested in patients with colorectal, gastric, and lung cancer[64]. MuS110 BsAb was found to have similar *in vitro* characteristics and *in vivo* antitumor activity as MT110[65].

BsAb-5 target cellular mesenchymal-to-epithelial transition factor (c-MET) and cytotoxic T-lymphocyte-associated protein 4 in CD166+ lung CSCs with high affinity and specificity. BsAb-5 has been shown to reduce tumor size in mouse models by a mechanism that involves inhibition of the c-MET-Notch pathway in CSCs and the up-regulating effector T cells. BsAb could be a possible drug for the treatment of human NSCLC[66].

Drugs conjugated to specific ligands of CSCs

The extracellular domain of CD44 contains a HA binding site, a property that is used for the development of HA-conjugated antitumor drugs. Preclinical studies have shown that HA can be effectively used to deliver chemotherapy and selectively decrease CD44+ lung CSCs. Thus, a phase II clinical trial (ACTRN 12611000520932) using HA-irinotecan has shown to be effective in the treatment of SCLC[67]. Other studies show that cisplatin or apoferritin conjugated to HA are effective in eliminating lung CSCs[68,69].

Drugs-loaded nanoparticles

In recent years, nanoparticulate systems have been developed to encapsulate antitumor drugs. The efficacy of these systems in the treatment of cancer has been improved by the conjugation of the nanoparticles to specific ligands, antibodies or aptamers directed against SC markers. In this sense, it has been shown that the intratracheal administration of HA-conjugated cisplatin-loaded nanoparticles attenuated lung cancer growth in mice[70]. Other systems such as salinomycin sodium-loaded nanoparticles conjugated to anti-CD133 antibody, doxorubicin-loaded nanoparticles conjugated to EpCAM aptamer and gefitinib or docetaxel-loaded liposomes conjugated to anti-CD133 aptamers have been shown to be effective in inhibiting tumor growth[71-74].

CAR-T therapies

CAR-T cell is a new therapeutic approach that involves the development of a receptor expressed in T cells that recognizes certain specific antigens on the membrane of cancer cells, triggering an antitumor immune response. The efficacy of specific CAR-T therapy against the AC133 epitope of CD133 has been studied in a mouse model with orthotopic xenograft. AC133-specific CAR-T cells reduced tumor size and prolonged survival in the humanized orthotopic SCLC model but were unable to eliminate tumors completely. However, the combination of AC133-specific CAR-T cells with an anti-PD-1 antibody and a CD73 inhibitor was able to eliminate chemoresistant CSCs[75].

CONCLUSION

Current chemotherapies for lung cancer involve the use of drugs whose targets of action are protein tyrosine kinases, regulators of the cell cycle or cell signaling pathways. Despite improvements in treatments, some patients do not respond to therapies or have cancer relapses months or years after treatment. It is hypothesized that one of the main causes of cancer relapse is the ineffectiveness of anticancer drugs to eliminate CSCs in tumor tissue. Chemotherapy and

radiotherapy induce senescence of tumor cells. Factors released by senescent cells into the tumor microenvironment could activate signaling pathways that induce phenotypic and functional changes in SCs, increasing their plasticity and uncontrolled growth. In addition, CSCs could be chemoresistant due to the expression of transporters in cell membranes that expel xenobiotic compounds into the extracellular space.

In lung cancer, several biomarkers have been identified in CSCs associated with the maintenance of tumorigenicity, metastasis and chemoresistance. These biomarkers could be useful as targets for the effective treatment of lung cancer. Thus, new drugs directed against CSCs include the use of inhibitors, monoclonal and BsAb, antibody-drug conjugates or aptamer-drug conjugates, and CAR-T therapies. These therapies are a hope for patients who do not respond to conventional treatments or relapse in lung cancer.

FOOTNOTES

Author contributions: Romeo HE and Barreiro Arcos ML compiled the updated information, wrote the manuscript and prepared the figures.

Conflict-of-interest statement: All the authors report no relevant conflicts of interest for this article.

Country/Territory of origin: Argentina

ORCID number: Horacio Eduardo Romeo 0000-0002-3613-1884; María Laura Barreiro Arcos 0000-0002-7976-9183.

S-Editor: Fan JR
L-Editor: A
P-Editor: Cai YX

REFERENCES

1 **Blandin Knight S**, Crosbie PA, Balata H, Chudziak J, Hussell T, Dive C. Progress and prospects of early detection in lung cancer. *Open Biol* 2017; **7** [PMID: 28878044 DOI: 10.1098/rsob.170070]
2 **Thai AA**, Solomon BJ, Sequist LV, Gainor JF, Heist RS. Lung cancer. *Lancet* 2021; **398**: 535-554 [PMID: 34273294 DOI: 10.1016/S0140-6736(21)00312-3]
3 **Wang WZ**, Shulman A, Amann JM, Carbone DP, Tsichlis PN. Small cell lung cancer: Subtypes and therapeutic implications. *Semin Cancer Biol* 2022; **86**: 543-554 [PMID: 35398266 DOI: 10.1016/j.semcancer.2022.04.001]
4 **Nooreldeen R**, Bach H. Current and Future Development in Lung Cancer Diagnosis. *Int J Mol Sci* 2021; **22** [PMID: 34445366 DOI: 10.3390/ijms22168661]
5 **Beckles MA**, Spiro SG, Colice GL, Rudd RM. Initial evaluation of the patient with lung cancer: symptoms, signs, laboratory tests, and paraneoplastic syndromes. *Chest* 2003; **123**: 97S-104S [PMID: 12527569 DOI: 10.1378/chest.123.1_suppl.97s]
6 **Bray F**, Ferlay J, Soerjomataram I, Siegel RL, Torre LA, Jemal A. Global cancer statistics 2018: GLOBOCAN estimates of incidence and mortality worldwide for 36 cancers in 185 countries. *CA Cancer J Clin* 2018; **68**: 394-424 [PMID: 30207593 DOI: 10.3322/caac.21492]
7 **Malhotra J**, Malvezzi M, Negri E, La Vecchia C, Boffetta P. Risk factors for lung cancer worldwide. *Eur Respir J* 2016; **48**: 889-902 [PMID: 27174888 DOI: 10.1183/13993003.00359-2016]
8 **Schwartz AG**, Cote ML. Epidemiology of Lung Cancer. *Adv Exp Med Biol* 2016; **893**: 21-41 [PMID: 26667337 DOI: 10.1007/978-3-319-24223-1_2]
9 **Chen Y**, Shi JX, Pan XF, Feng J, Zhao H. Identification of candidate genes for lung cancer somatic mutation test kits. *Genet Mol Biol* 2013; **36**: 455-464 [PMID: 24130455 DOI: 10.1590/S1415-47572013000300022]
10 **Wadowska K**, Bil-Lula I, Trembecki Ł, Śliwińska-Mossoń M. Genetic Markers in Lung Cancer Diagnosis: A Review. *Int J Mol Sci* 2020; **21** [PMID: 32604993 DOI: 10.3390/ijms21134569]
11 **Harrison PT**, Vyse S, Huang PH. Rare epidermal growth factor receptor (EGFR) mutations in non-small cell lung cancer. *Semin Cancer Biol* 2020; **61**: 167-179 [PMID: 31562956 DOI: 10.1016/j.semcancer.2019.09.015]
12 **Ferrer I**, Zugazagoitia J, Herbertz S, John W, Paz-Ares L, Schmid-Bindert G. KRAS-Mutant non-small cell lung cancer: From biology to therapy. *Lung Cancer* 2018; **124**: 53-64 [PMID: 30268480 DOI: 10.1016/j.lungcan.2018.07.013]
13 **Timar J**, Kashofer K. Molecular epidemiology and diagnostics of KRAS mutations in human cancer. *Cancer Metastasis Rev* 2020; **39**: 1029-1038 [PMID: 32725342 DOI: 10.1007/s10555-020-09915-5]
14 **Yang L**, Zhou Y, Li Y, Zhou J, Wu Y, Cui Y, Yang G, Hong Y. Mutations of p53 and KRAS activate NF-κB to promote chemoresistance and tumorigenesis *via* dysregulation of cell cycle and suppression of apoptosis in lung cancer cells. *Cancer Lett* 2015; **357**: 520-526 [PMID: 25499080 DOI: 10.1016/j.canlet.2014.12.003]
15 **Maiuthed A**, Chantarawong W, Chanvorachote P. Lung Cancer Stem Cells and Cancer Stem Cell-targeting Natural Compounds. *Anticancer Res* 2018; **38**: 3797-3809 [PMID: 29970499 DOI: 10.21873/anticanres.12663]
16 **Pathak S**. Organ- and tissue-specific stem cells and carcinogenesis. *Anticancer Res* 2002; **22**: 1353-1356 [PMID: 12168810]

17 **Cohnheim J**. Congenitales, quergestreiftes Muskelsarkom der Nieren. *Archiv f pathol Anat* 1875; **65**: 64-69 [DOI: 10.1007/BF01978936]
18 **Bonnet D**, Dick JE. Human acute myeloid leukemia is organized as a hierarchy that originates from a primitive hematopoietic cell. *Nat Med* 1997; **3**: 730-737 [PMID: 9212098 DOI: 10.1038/nm0797-730]
19 **Rahman M**, Deleyrolle L, Vedam-Mai V, Azari H, Abd-El-Barr M, Reynolds BA. The cancer stem cell hypothesis: failures and pitfalls. *Neurosurgery* 2011; **68**: 531-45; discussion 545 [PMID: 21135745 DOI: 10.1227/NEU.0b013e3181ff9eb5]
20 **Naveen SV**, Kalaivani K. Cancer stem cells and evolving novel therapies: a paradigm shift. *Stem Cell Investig* 2018; **5**: 4 [PMID: 29430460 DOI: 10.21037/sci.2018.01.03]
21 **Chen Y**, Xue Y, Jin Y, Ji H. Lung stem cells in regeneration and tumorigenesis. *J Genet Genomics* 2021; **48**: 268-276 [PMID: 33896738 DOI: 10.1016/j.jgg.2020.12.004]
22 **Borthwick DW**, Shahbazian M, Krantz QT, Dorin JR, Randell SH. Evidence for stem-cell niches in the tracheal epithelium. *Am J Respir Cell Mol Biol* 2001; **24**: 662-670 [PMID: 11415930 DOI: 10.1165/ajrcmb.24.6.4217]
23 **Kim CF**, Jackson EL, Woolfenden AE, Lawrence S, Babar I, Vogel S, Crowley D, Bronson RT, Jacks T. Identification of bronchioalveolar stem cells in normal lung and lung cancer. *Cell* 2005; **121**: 823-835 [PMID: 15960971 DOI: 10.1016/j.cell.2005.03.032]
24 **Sasai K**, Takao-Rikitsu E, Sukezane T, Yanagita E, Nakagawa H, Itoh-Yagi M, Izumi Y, Itoh T, Akagi T. Engineering cancer stem-like cells from normal human lung epithelial cells. *PLoS One* 2017; **12**: e0175147 [PMID: 28380052 DOI: 10.1371/journal.pone.0175147]
25 **Dawood S**, Austin L, Cristofanilli M. Cancer stem cells: implications for cancer therapy. *Oncology (Williston Park)* 2014; **28**: 1101-1107, 1110 [PMID: 25510809]
26 **Zheng Y**, Wang L, Yin L, Yao Z, Tong R, Xue J, Lu Y. Lung Cancer Stem Cell Markers as Therapeutic Targets: An Update on Signaling Pathways and Therapies. *Front Oncol* 2022; **12**: 873994 [PMID: 35719973 DOI: 10.3389/fonc.2022.873994]
27 **Prabavathy D**, Swarnalatha Y, Ramadoss N. Lung cancer stem cells-origin, characteristics and therapy. *Stem Cell Investig* 2018; **5**: 6 [PMID: 29682513 DOI: 10.21037/sci.2018.02.01]
28 **Walcher L**, Kistenmacher AK, Suo H, Kitte R, Dluczek S, Strauß A, Blaudszun AR, Yevsa T, Fricke S, Kossatz-Boehlert U. Cancer Stem Cells-Origins and Biomarkers: Perspectives for Targeted Personalized Therapies. *Front Immunol* 2020; **11**: 1280 [PMID: 32849491 DOI: 10.3389/fimmu.2020.01280]
29 **Koren A**, Rijavec M, Kern I, Sodja E, Korosec P, Cufer T. BMI1, ALDH1A1, and CD133 Transcripts Connect Epithelial-Mesenchymal Transition to Cancer Stem Cells in Lung Carcinoma. *Stem Cells Int* 2016; **2016**: 9714315 [PMID: 26770215 DOI: 10.1155/2016/9714315]
30 **Wu H**, Qi XW, Yan GN, Zhang QB, Xu C, Bian XW. Is CD133 expression a prognostic biomarker of non-small-cell lung cancer? A systematic review and meta-analysis. *PLoS One* 2014; **9**: e100168 [PMID: 24940615 DOI: 10.1371/journal.pone.0100168]
31 **Yamashita N**, Oyama T, So T, Miyata T, Yoshimatsu T, Nakano R, Matsunaga W, Gotoh A. Association Between CD133 Expression and Prognosis in Human Lung Adenocarcinoma. *Anticancer Res* 2021; **41**: 905-910 [PMID: 33517296 DOI: 10.21873/anticanres.14843]
32 **Jang JW**, Song Y, Kim SH, Kim J, Seo HR. Potential mechanisms of CD133 in cancer stem cells. *Life Sci* 2017; **184**: 25-29 [PMID: 28697984 DOI: 10.1016/j.lfs.2017.07.008]
33 **Aghajani M**, Mansoori B, Mohammadi A, Asadzadeh Z, Baradaran B. New emerging roles of CD133 in cancer stem cell: Signaling pathway and miRNA regulation. *J Cell Physiol* 2019; **234**: 21642-21661 [PMID: 31102292 DOI: 10.1002/jcp.28824]
34 **Adini A**, Adini I, Ghosh K, Benny O, Pravda E, Hu R, Luyindula D, D'Amato RJ. The stem cell marker prominin-1/CD133 interacts with vascular endothelial growth factor and potentiates its action. *Angiogenesis* 2013; **16**: 405-416 [PMID: 23150059 DOI: 10.1007/s10456-012-9323-8]
35 **Leung EL**, Fiscus RR, Tung JW, Tin VP, Cheng LC, Sihoe AD, Fink LM, Ma Y, Wong MP. Non-small cell lung cancer cells expressing CD44 are enriched for stem cell-like properties. *PLoS One* 2010; **5**: e14062 [PMID: 21124918 DOI: 10.1371/journal.pone.0014062]
36 **Zhou N**, Wang H, Liu H, Xue H, Lin F, Meng X, Liang A, Zhao Z, Liu Y, Qian H. MTA1-upregulated EpCAM is associated with metastatic behaviors and poor prognosis in lung cancer. *J Exp Clin Cancer Res* 2015; **34**: 157 [PMID: 26698569 DOI: 10.1186/s13046-015-0263-1]
37 **Satar NA**, Fakiruddin KS, Lim MN, Mok PL, Zakaria N, Fakharuzi NA, Abd Rahman AZ, Zakaria Z, Yahaya BH, Baharuddin P. Novel triplepositive markers identified in human nonsmall cell lung cancer cell line with chemotherapy-resistant and putative cancer stem cell characteristics. *Oncol Rep* 2018; **40**: 669-681 [PMID: 29845263 DOI: 10.3892/or.2018.6461]
38 **Smith PJ**, Furon E, Wiltshire M, Campbell L, Feeney GP, Snyder RD, Errington RJ. ABCG2-associated resistance to Hoechst 33342 and topotecan in a murine cell model with constitutive expression of side population characteristics. *Cytometry A* 2009; **75**: 924-933 [PMID: 19802874 DOI: 10.1002/cyto.a.20800]
39 **Gorczyca L**, Aleksunes LM. Transcription factor-mediated regulation of the BCRP/ABCG2 efflux transporter: a review across tissues and species. *Expert Opin Drug Metab Toxicol* 2020; **16**: 239-253 [PMID: 32077332 DOI: 10.1080/17425255.2020.1732348]
40 **Yang WJ**, Song MJ, Park EY, Lee JJ, Park JH, Park K, Kim HP. Transcription factors Sp1 and Sp3 regulate expression of human ABCG2 gene and chemoresistance phenotype. *Mol Cells* 2013; **36**: 368-375 [PMID: 23996530 DOI: 10.1007/s10059-013-0191-x]
41 **Dai Y**, Liu S, Zhang WQ, Yang YL, Hang P, Wang H, Cheng L, Hsu PC, Wang YC, Xu Z, Jablons DM, You L. YAP1 regulates ABCG2 and cancer cell side population in human lung cancer cells. *Oncotarget* 2017; **8**: 4096-4109 [PMID: 27911857 DOI: 10.18632/oncotarget.13686]
42 **Yang B**, Ma YF, Liu Y. Elevated Expression of Nrf-2 and ABCG2 Involved in Multi-drug Resistance of Lung Cancer SP Cells. *Drug Res (Stuttg)* 2015; **65**: 526-531 [PMID: 25368906 DOI: 10.1055/s-0034-1390458]
43 **Tomita H**, Tanaka K, Tanaka T, Hara A. Aldehyde dehydrogenase 1A1 in stem cells and cancer. *Oncotarget* 2016; **7**: 11018-11032 [PMID: 26783961 DOI: 10.18632/oncotarget.6920]
44 **Masciale V**, Grisendi G, Banchelli F, D'Amico R, Maiorana A, Sighinolfi P, Stefani A, Morandi U, Dominici M, Aramini B. CD44+/EPCAM+ cells detect a subpopulation of ALDH(high) cells in human non-small cell lung cancer: A chance for targeting cancer stem cells? *Oncotarget* 2020; **11**: 1545-1555 [PMID: 32391123 DOI: 10.18632/oncotarget.27568]
45 **Roudi R**, Korourian A, Shariftabrizi A, Madjd Z. Differential Expression of Cancer Stem Cell Markers ALDH1 and CD133 in Various Lung Cancer Subtypes. *Cancer Invest* 2015; **33**: 294-302 [PMID: 26046383 DOI: 10.3109/07357907.2015.1034869]
46 **Wang J**, Zeng H, Li H, Zhang J, Wang S. Roles of sex-determining region Y-box 2 in cell pluripotency and tumor-related signaling pathways. *Mol Clin Oncol* 2015; **3**: 1203-1207 [PMID: 26807221 DOI: 10.3892/mco.2015.639]
47 **Grimm D**, Bauer J, Wise P, Krüger M, Simonsen U, Wehland M, Infanger M, Corydon TJ. The role of SOX family members in solid tumours and metastasis. *Semin Cancer Biol* 2020; **67**: 122-153 [PMID: 30914279 DOI: 10.1016/j.semcancer.2019.03.004]
48 **Wang P**, Wan WW, Xiong SL, Feng H, Wu N. Cancer stem-like cells can be induced through dedifferentiation under hypoxic conditions in glioma, hepatoma and lung cancer. *Cell Death Discov* 2017; **3**: 16105 [PMID: 28179999 DOI: 10.1038/cddiscovery.2016.105]

49 **Cai N**, Li M, Qu J, Liu GH, Izpisua Belmonte JC. Post-translational modulation of pluripotency. *J Mol Cell Biol* 2012; **4**: 262-265 [PMID: 22679102 DOI: 10.1093/jmcb/mjs031]

50 **Li X**, Wang J, Xu Z, Ahmad A, Li E, Wang Y, Qin S, Wang Q. Expression of Sox2 and Oct4 and their clinical significance in human non-small-cell lung cancer. *Int J Mol Sci* 2012; **13**: 7663-7675 [PMID: 22837720 DOI: 10.3390/ijms13067663]

51 **Ye T**, Li J, Sun Z, Liu Y, Kong L, Zhou S, Tang J, Wang J, Xing HR. Nr5a2 promotes cancer stem cell properties and tumorigenesis in nonsmall cell lung cancer by regulating Nanog. *Cancer Med* 2019; **8**: 1232-1245 [PMID: 30740909 DOI: 10.1002/cam4.1992]

52 **Gong S**, Li Q, Jeter CR, Fan Q, Tang DG, Liu B. Regulation of NANOG in cancer cells. *Mol Carcinog* 2015; **54**: 679-687 [PMID: 26013997 DOI: 10.1002/mc.22340]

53 **Otsubo K**, Nosaki K, Imamura CK, Ogata H, Fujita A, Sakata S, Hirai F, Toyokawa G, Iwama E, Harada T, Seto T, Takenoyama M, Ozeki T, Mushiroda T, Inada M, Kishimoto J, Tsuchihashi K, Suina K, Nagano O, Saya H, Nakanishi Y, Okamoto I. Phase I study of salazosulfapyridine in combination with cisplatin and pemetrexed for advanced non-small-cell lung cancer. *Cancer Sci* 2017; **108**: 1843-1849 [PMID: 28667792 DOI: 10.1111/cas.13309]

54 **Nechushtan H**, Hamamreh Y, Nidal S, Gotfried M, Baron A, Shalev YI, Nisman B, Peretz T, Peylan-Ramu N. A phase IIb trial assessing the addition of disulfiram to chemotherapy for the treatment of metastatic non-small cell lung cancer. *Oncologist* 2015; **20**: 366-367 [PMID: 25777347 DOI: 10.1634/theoncologist.2014-0424]

55 **MacDonagh L**, Gallagher MF, Ffrench B, Gasch C, Breen E, Gray SG, Nicholson S, Leonard N, Ryan R, Young V, O'Leary JJ, Cuffe S, Finn SP, O'Byrne KJ, Barr MP. Targeting the cancer stem cell marker, aldehyde dehydrogenase 1, to circumvent cisplatin resistance in NSCLC. *Oncotarget* 2017; **8**: 72544-72563 [PMID: 29069808 DOI: 10.18632/oncotarget.19881]

56 **Liu X**, Wang L, Cui W, Yuan X, Lin L, Cao Q, Wang N, Li Y, Guo W, Zhang X, Wu C, Yang J. Targeting ALDH1A1 by disulfiram/copper complex inhibits non-small cell lung cancer recurrence driven by ALDH-positive cancer stem cells. *Oncotarget* 2016; **7**: 58516-58530 [PMID: 27542268 DOI: 10.18632/oncotarget.11305]

57 **Hu YP**, Tao LY, Wang F, Zhang JY, Liang YJ, Fu LW. Secalonic acid D reduced the percentage of side populations by down-regulating the expression of ABCG2. *Biochem Pharmacol* 2013; **85**: 1619-1625 [PMID: 23583455 DOI: 10.1016/j.bcp.2013.04.003]

58 **Anreddy N**, Patel A, Zhang YK, Wang YJ, Shukla S, Kathawala RJ, Kumar P, Gupta P, Ambudkar SV, Wurpel JN, Chen ZS, Guo H. A-803467, a tetrodotoxin-resistant sodium channel blocker, modulates ABCG2-mediated MDR in vitro and in vivo. *Oncotarget* 2015; **6**: 39276-39291 [PMID: 26515463 DOI: 10.18632/oncotarget.5747]

59 **Wang J**, Liu Z, Zhang D, Liu R, Lin Q, Liu J, Yang Z, Ma Q, Sun D, Zhou X, Jiang G. FL118, a novel survivin inhibitor, wins the battle against drug-resistant and metastatic lung cancers through inhibition of cancer stem cell-like properties. *Am J Transl Res* 2017; **9**: 3676-3686 [PMID: 28861158]

60 **Škerlová J**, Král V, Kachala M, Fábry M, Bumba L, Svergun DI, Tošner Z, Veverka V, Řezáčová P. Molecular mechanism for the action of the anti-CD44 monoclonal antibody MEM-85. *J Struct Biol* 2015; **191**: 214-223 [PMID: 26066970 DOI: 10.1016/j.jsb.2015.06.005]

61 **Wang F**, Mi YJ, Chen XG, Wu XP, Liu Z, Chen SP, Liang YJ, Cheng C, To KK, Fu LW. Axitinib targeted cancer stemlike cells to enhance efficacy of chemotherapeutic drugs *via* inhibiting the drug transport function of ABCG2. *Mol Med* 2012; **18**: 887-898 [PMID: 22549112 DOI: 10.2119/molmed.2011.00444]

62 **Sebastian M**, Passlick B, Friccius-Quecke H, Jäger M, Lindhofer H, Kanniess F, Wiewrodt R, Thiel E, Buhl R, Schmittel A. Treatment of non-small cell lung cancer patients with the trifunctional monoclonal antibody catumaxomab (anti-EpCAM x anti-CD3): a phase I study. *Cancer Immunol Immunother* 2007; **56**: 1637-1644 [PMID: 17410361 DOI: 10.1007/s00262-007-0310-7]

63 **Schlereth B**, Kleindienst P, Fichtner I, Lorenczewski G, Brischwein K, Lippold S, da Silva A, Locher M, Kischel R, Lutterbüse R, Kufer P, Baeuerle PA. Potent inhibition of local and disseminated tumor growth in immunocompetent mouse models by a bispecific antibody construct specific for Murine CD3. *Cancer Immunol Immunother* 2006; **55**: 785-796 [PMID: 16187083 DOI: 10.1007/s00262-005-0082-x]

64 **Fiedler WM**, Ritter B, Seggewiss R, Bokemeyer C, Fettes P, Klinger M, Vieser E, Ruettinger D, Kaubitzsch S, Wolf M. Phase I safety and pharmacology study of the EpCAM/CD3-bispecific BiTE antibody MT110 in patients with metastatic colorectal, gastric, or lung cancer. *J Clin Oncol* 2010; **28**: 2573-2573

65 **Amann M**, Brischwein K, Lutterbuese P, Parr L, Petersen L, Lorenczewski G, Krinner E, Bruckmeier S, Lippold S, Kischel R, Lutterbuese R, Kufer P, Baeuerle PA, Schlereth B. Therapeutic window of MuS110, a single-chain antibody construct bispecific for murine EpCAM and murine CD3. *Cancer Res* 2008; **68**: 143-151 [PMID: 18172306 DOI: 10.1158/0008-5472.CAN-07-2182]

66 **Li JF**, Niu YY, Xing YL, Liu F. A novel bispecific c-MET/CTLA-4 antibody targetting lung cancer stem cell-like cells with therapeutic potential in human non-small-cell lung cancer. *Biosci Rep* 2019; **39** [PMID: 29187584 DOI: 10.1042/BSR20171278]

67 **Alamgeer M**, Neil Watkins D, Banakh I, Kumar B, Gough DJ, Markman B, Ganju V. A phase IIa study of HA-irinotecan, formulation of hyaluronic acid and irinotecan targeting CD44 in extensive-stage small cell lung cancer. *Invest New Drugs* 2018; **36**: 288-298 [PMID: 29277856 DOI: 10.1007/s10637-017-0555-8]

68 **Quan YH**, Kim B, Park JH, Choi Y, Choi YH, Kim HK. Highly sensitive and selective anticancer effect by conjugated HA-cisplatin in non-small cell lung cancer overexpressed with CD44. *Exp Lung Res* 2014; **40**: 475-484 [PMID: 25299431 DOI: 10.3109/01902148.2014.905656]

69 **Luo Y**, Wang X, Du D, Lin Y. Hyaluronic acid-conjugated apoferritin nanocages for lung cancer targeted drug delivery. *Biomater Sci* 2015; **3**: 1386-1394 [PMID: 26301700 DOI: 10.1039/c5bm00067j]

70 **Ishiguro S**, Cai S, Uppalapati D, Turner K, Zhang T, Forrest WC, Forrest ML, Tamura M. Intratracheal Administration of Hyaluronan-Cisplatin Conjugate Nanoparticles Significantly Attenuates Lung Cancer Growth in Mice. *Pharm Res* 2016; **33**: 2517-2529 [PMID: 27335023 DOI: 10.1007/s11095-016-1976-3]

71 **Zhou J**, Sun J, Chen H, Peng Q. Promoted delivery of salinomycin sodium to lung cancer cells by dual targeting PLGA hybrid nanoparticles. *Int J Oncol* 2018; **53**: 1289-1300 [PMID: 30015824 DOI: 10.3892/ijo.2018.4474]

72 **Alibolandi M**, Ramezani M, Abnous K, Sadeghi F, Atyabi F, Asouri M, Ahmadi AA, Hadizadeh F. In vitro and in vivo evaluation of therapy targeting epithelial-cell adhesion-molecule aptamers for non-small cell lung cancer. *J Control Release* 2015; **209**: 88-100 [PMID: 25912964 DOI: 10.1016/j.jconrel.2015.04.026]

73 **Huang X**, Huang J, Leng D, Yang S, Yao Q, Sun J, Hu J. Gefitinib-loaded DSPE-PEG2000 nanomicelles with CD133 aptamers target lung cancer stem cells. *World J Surg Oncol* 2017; **15**: 167 [PMID: 28854941 DOI: 10.1186/s12957-017-1230-4]

74 **Ma J**, Zhuang H, Zhuang Z, Lu Y, Xia R, Gan L, Wu Y. Development of docetaxel liposome surface modified with CD133 aptamers for lung cancer targeting. *Artif Cells Nanomed Biotechnol* 2018; **46**: 1864-1871 [PMID: 29082764 DOI: 10.1080/21691401.2017.1394874]

75 **Taromi S**, Firat E, Simonis A, Braun LM, Apostolova P, Elze M, Passlick B, Schumacher A, Lagies S, Frey A, Schmitt-Graeff A, Burger M,

Schmittlutz K, Follo M, von Elverfeldt D, Zhu X, Kammerer B, Diederichs S, Duyster J, Manz MG, Niedermann G, Zeiser R. Enhanced AC133-specific CAR T cell therapy induces durable remissions in mice with metastatic small cell lung cancer. *Cancer Lett* 2022; **538**: 215697 [PMID: 35487310 DOI: 10.1016/j.canlet.2022.215697]

World Journal of Stem Cells

Submit a Manuscript: https://www.f6publishing.com

World J Stem Cells 2023 June 26; 15(6): 589-606

DOI: 10.4252/wjsc.v15.i6.589

ISSN 1948-0210 (online)

ORIGINAL ARTICLE

Basic Study

Single cell RNA sequencing reveals mesenchymal heterogeneity and critical functions of *Cd271* in tooth development

Yan-Yan Zhang, Feng Li, Xiao-Ke Zeng, Yan-Hui Zou, Bing-Bing Zhu, Jia-Jia Ye, Yun-Xiao Zhang, Qiu Jin, Xin Nie

Specialty type: Cell and tissue engineering

Provenance and peer review: Unsolicited article; Externally peer reviewed.

Peer-review model: Single blind

Peer-review report's scientific quality classification

Grade A (Excellent): A
Grade B (Very good): B
Grade C (Good): 0
Grade D (Fair): 0
Grade E (Poor): 0

P-Reviewer: Elchaninov AV, Russia; Stogov MV, Russia

Received: February 9, 2023
Peer-review started: February 9, 2023
First decision: April 10, 2023
Revised: April 18, 2023
Accepted: May 5, 2023
Article in press: May 5, 2023
Published online: June 26, 2023

Yan-Yan Zhang, Feng Li, Xiao-Ke Zeng, Yan-Hui Zou, Bing-Bing Zhu, Jia-Jia Ye, Yun-Xiao Zhang, Qiu Jin, Xin Nie, School & Hospital of Stomatology, Wenzhou Medical University, Wenzhou 325027, Zhejiang Province, China

Corresponding author: Xin Nie, PhD, Professor, School & Hospital of Stomatology, Wenzhou Medical University, Xueyuan West Road, Lucheng District, Wenzhou 325027, Zhejiang Province, China. dr.xinnie@qq.com

Abstract

BACKGROUND

Accumulating evidence suggests that the maxillary process, to which cranial crest cells migrate, is essential to tooth development. Emerging studies indicate that *Cd271* plays an essential role in odontogenesis. However, the underlying mechanisms have yet to be elucidated.

AIM

To establish the functionally heterogeneous population in the maxillary process, elucidate the effects of *Cd271* deficiency on gene expression differences.

METHODS

p75NTR knockout (*Cd271*$^{-/-}$) mice (from American Jackson laboratory) were used to collect the maxillofacial process tissue of p75NTR knockout mice, and the wild-type maxillofacial process of the same pregnant mouse wild was used as control. After single cell suspension, the cDNA was prepared by loading the single cell suspension into the 10x Genomics Chromium system to be sequenced by NovaSeq6000 sequencing system. Finally, the sequencing data in Fastq format were obtained. The FastQC software is used to evaluate the quality of data and CellRanger analyzed the data. The gene expression matrix is read by R software, and Seurat is used to control and standardize the data, reduce the dimension and cluster. We search for marker genes for subgroup annotation by consulting literature and database; explore the effect of p75NTR knockout on mesenchymal stem cells (MSCs) gene expression and cell proportion by cell subgrouping, differential gene analysis, enrichment analysis and protein-protein interaction network analysis; understand the interaction between MSCs cells and the differentiation trajectory and gene change characteristics of p75NTR knockout MSCs by cell communication analysis and pseudo-time analysis. Last we verified the findings

single cell sequencing *in vitro*.

RESULTS

We identified 21 cell clusters, and we re-clustered these into three subclusters. Importantly, we revealed the cell–cell communication networks between clusters. We clarified that *Cd271* was significantly associated with the regulation of mineralization.

CONCLUSION

This study provides comprehensive mechanistic insights into the maxillary- process-derived MSCs and demonstrates that *Cd271* is significantly associated with the odontogenesis in mesenchymal populations.

Key Words: *Cd271*; Mesenchymal stem cells; Single cell RNA sequencing; Osteogenesis; Mineralization; Tooth development

Core Tip: Our study reveals the following findings: (1) High cellular heterogeneity and molecular details; (2) Significant functional and signaling differences between cell types; (3) Novel subclusters of mesenchymal stem cells; and (4) Crucial cell-cell interactions of mesenchymal subpopulations. We provided new insights into the biological features of mesenchymal stem cells at the single cell level. Our findings contribute to thorough exploration of the mechanism of *Cd271* in regulating odontogenesis and osteogenesis which add to the theory of tooth development.

Citation: Zhang YY, Li F, Zeng XK, Zou YH, Zhu BB, Ye JJ, Zhang YX, Jin Q, Nie X. Single cell RNA sequencing reveals mesenchymal heterogeneity and critical functions of *Cd271* in tooth development. *World J Stem Cells* 2023; 15(6): 589-606
URL: https://www.wjgnet.com/1948-0210/full/v15/i6/589.htm
DOI: https://dx.doi.org/10.4252/wjsc.v15.i6.589

INTRODUCTION

During the early stage of embryogenesis, cranial neural crest cells migrate throughout the maxillary and mandibular processes, which are defined as ecto-mesenchymal stem cells (MSCs)[1,2]. Ecto-MSCs were regarded as the primitive dental cells in the classical theory of tooth development. To date, in-depth studies of the odontogenesis and osteogenesis of MSCs are still lacking.

Cd271 (low-affinity nerve growth factor receptor, p75 neurotrophic receptor) is a member of the tumor necrosis factor receptor superfamily, and is implicated in various biological functions[3]. It is used as a specific cell surface marker for purifying and identifying MSCs[4]. Previous studies focused on cellular physiological functions in processes, such as migration, proliferation, differentiation, survival and apoptosis[5-8]. *Cd271* is involved in the regulation of morphogenesis and the development of various tissues, including nerves, fat, liver and teeth[9-13]. In addition to these features, emerging studies indicate that *Cd271* plays a critical role in initiating tooth development, differentiation and mineralization of odontogenic stem cells. Mitsiadis *et al*[14] indicated that *Cd271* surrounded the developing tooth germ within nerve fibers and was highly expressed in the epithelium and mesenchyme in the early stages of odontogenesis within the cells of origin[14]. The spatial–temporal expression of *Cd271* was similar to the mineralization factor *Runx2* during the early development of tooth germ[15], which was supported by other studies[16,17]. These studies indicate that *Cd271* is involved in the physiological processes of tooth development and biomineralization. However, the molecular mechanisms of *Cd271*, as a transmembrane signaling molecule, in the morphogenesis and development of teeth remains largely unknown.

Conventionally, MSCs were considered a unified group of fusiform cells. Nevertheless, accumulating evidence suggests that MSCs are functionally and morphologically heterogeneous in essence[18,19]. High-throughput single cell RNA sequencing (scRNA-Seq) is powerful for disclosing the complexity and diversity of cells and relationships among genes involved in tissues, and offers an opportunity to explore unbiased gene expression profiling of cells[20]. scRNA-Seq also provides insights into specific changes in cell lineages, trajectory inference, and the identification of biomarkers[21, 22]. scRNA-seq has been used to study MSCs derived from adipose tissue, bone marrow, endometrium, placenta and dental pulp[23-27]. However, application of scRNA-seq in maxillary-process-derived MSCs is still absent.

Herein, we used the maxillary process from mouse embryos as a model to understand the development of maxillary-process-derived MSCs. We applied scRNA-Seq analysis to elucidate the cellular heterogeneity and explore molecular details better compared with conventional methods. Our study provides novel insights into the biological features of MSCs at the single cell level and the mechanism of *Cd271* in regulating odontogenesis and osteogenesis.

MATERIALS AND METHODS

Animal preparation and tissues dissection

Cd271 knockout (*Cd271*$^{-/-}$) and wild-type (*Cd271* $^{+/+}$) mice were used in this study. The *Cd271*$^{-/-}$ mice were gifts from The Jackson Laboratory (Bar Harbor, ME, United States). These mutant mice that exhibit the targeted deletion of exon III of the *Cd271* locus do not express functional full-length *Cd271*. All animal experiments were performed according to the protocols approved by the Medical Ethics Committee of Wenzhou Medical University (No. wydw2019-0224). We completed experimental steps under ethical guidelines. The animal protocol was designed to minimize pain or discomfort to the animals. The animals were housed to laboratory conditions (23 °C, 12 h/12 h light/dark, 50% humidity, ad libitum access to food and water) prior to experimentation. The homozygotes of *Cd271* $^{+/+}$ and *Cd271*$^{-/-}$ mice were mated to produce heterozygous offspring. The heterozygous mice were mated to generate three types of genotype embryos, *Cd271* $^{+/+}$ and *Cd271*$^{-/-}$and *Cd271*$^{+/-}$. We obtained embryos through abdominal surgery, and chose homozygous embryos from embryonic day 16.5. The embryos were placed in a 6-cm Petri dish and washed with Phosphate buffer saline (PBS). We cut the amniotic membrane with ophthalmic scissors to separate the fetal mice and washed them with PBS again. After cutting the head of the fetus, we cut the maxillary process tissue under a stereomicroscope. After the removal of nonpurpose tissues like blood stains and fatty layers, we rinsed the tissue twice in PBS. The genotype of wild-type and *Cd271* knockout mice was confirmed with a one-step genotyping kit (Vazyme, Nanjing, China).

Single cell isolation and library preparation

Maxillary processes were dissociated into single cells in dissociation solution (0.35% collagenase IV5, 2 mg/mL papain, and 120 U/mL DNase I) in 37 °C water bath with shaking for 20 min at 100 rpm. Single cell suspensions were washed and resuspended to load to the 10X Chromium platform. More than 25000 single cells were captured and subjected to 10X Chromium Controller machine to generate gel beads-in-emulsion (GEMs). mRNA was prepared using the 10X Genomics Chromium Single Cell 3′ Reagent Kit V2 (10X Genomics, Pleasanton, CA, United States). Cells were divided by partitions into the GEMs along with GelBeads coated with oligos in this step. These oligos utilized poly-dT sequences to capture mRNAs and cell-specific and transcript-specific barcodes. The following cDNA amplification generated adequate quantities for library construction according to the standard protocol. Libraries were sequenced on an Illumina NovaSeq 6000 sequencing system (paired-end multiplexing run, 150 bp) by the LC-Bio Technology (Hangzhou, China) at a minimum depth of 20000 reads per cell.

scRNA-Seq data processing

We processed sequencing reads using CellRanger (version 6.0.1). Then we created objects by Seurat (version 4.0.5) R package, and merged data using the function of Merge[28]. The ratio of mitochondrial genes to all genetic material was used to judge whether a cell was in a steady state. Generally, it was thought that a cell might be in a state of stress when it had a higher proportion of mitochondrial genes. Therefore, we filtered cells with > 10% mitochondrial gene content. Considering potential cellular diploidy, we filtered cells with < 1000 or > 6000 genes. After the above steps, we finally obtained 17426 cells.

Data were normalized using the log-normalization method. After controlling for the relationship between mean expression and dispersion, we identified highly variable genes in individual cells. We input variable genes to perform principal component analysis (PCA) and identified significant principal components based on the function of JackStraw [29]. A total of 20 principal components were selected as statistically significant inputs to the Uniform Manifold Approximation and Projection (UMAP). We examined the distribution of UMAP and PCA between these samples. The data showed correlations. We compared the mean expression of genes between samples and found an excellent Pearson correlation between them. We divided the cells clustered by the FindCluster into 21 clusters.

Cell annotation

We identified cell types based on specific maker genes. The MSCs lineage was identified by *Col1a1* and *Col3a1*. *Lgals7* and *Krtdap* marked the epithelial cell lineage; muscle cell marker genes included *Actc1* and *Tnnt1*; macrophage marker genes included *Pf4* and *C1qb*; glial marker genes included *Dct* and *Ptgds*; T cell marker genes included *Cma1* and *Cpa3*; endothelial cell marker genes included *Egfl7* and *Cdh5*; and perivascular cell marker genes included *Rgs5* and *Ndufa4 L2*. The FindAllMarkers function was used to find differentially expressed genes between each cell type.

Gene set enrichment analysis

Gene set enrichment analysis (GSEA) can identify whether predefined gene sets show significant differences between biological processes by a computational method. Typically, GSEA is used to estimate expression in dataset samples. To study differences in the biological processes between the two groups, we downloaded the reference gene set c2.cp.kegg.v7.4.entrez.gmt from the MSigDB database on the basis of the gene expression profiling dataset[30]. We used GSEA included in the R package ClusterProfiler to perform enrichment analysis and visualization of the dataset. The cut-off standards were set as nominal $P < 0.05$, FDR q < 0.25 and normalized enrichment score (NES) > 0.6.

MSCs reclustering

On account of our main focus on MSCs, we extracted a subpopulation of MSCs. Based on hierarchical clustering and defined marker genes, we reclustered the MSCs using the FindClusters function and assigned the MSCs to 13 cell subpopulations. The progenitor subpopulation was identified by *Cdk1* and *Dkk1*, the osteoblasts subpopulation was identified by *Runx2* and *Sp7*, and the fibroblasts subpopulation was determined by maker genes *Dlk1* and *Shox2*. We next

counted the proportions and number of these cell subpopulations in wild-type or *Cd271* knockout mice.

Gene ontology functional enrichment analysis and protein–protein interaction network

Gene Ontology (GO) is an approach for functional enrichment analysis of genes in diverse levels and dimensions. GO analysis comprises three levels: Biological process, molecular function and cellular components. The Wilcoxon rank-sum test was used to identify genes differentially expressed in MSCs between wild-type and *Cd271* knockout samples (logFC > 0.25, $P < 0.05$). Differentially expressed genes that were identified between wild-type and *Cd271* knockout samples were subjected to GO functional annotation by the ClusterProfiler (version 4.2.0) R package to identify the significantly enriched biological processes[31].The enrichment results were visualized in the form of a lollipop plot, and the significance threshold for the enrichment analysis was set at a corrected $P < 0.05$.

The STRING online database (https://string-db.org/) analyzed the interaction between the marker genes. We constructed a protein–protein interaction (PPI) network for the results obtained by Cytoscape (3.9.0). The functional interactions between the proteins expressed by the genes were mapped, including direct physical interactions and indirect functional correlations.

Pseudotemporal analysis

Cell differentiation of MSCs (progenitors, osteoblasts and fibroblasts) was inferred by the Monocle (2.22.0) R package and default parameters recommended by the developers[32]. The integrated gene expression profiling of each cell type was exported from Seurat into Monocle to establish the cellular gene dataset. The variable genes were defined by the process of DispersionTable, and the cells were sorted with the function of setOrderingFilter. The DDRTree method was used to reduce the dimension, and the orderCells function was used to estimate the cell arrangement along the trajectory. Based on clustering characteristics and marker gene analysis, we obtained the trajectory map of the differentiation time of MSCs. The study of each trajectory used a standard protocol with default parameters.

Cell–cell communication analysis

We identified the underlying interactions between MSCs and other cell populations by CellChat (version 1.1.3) (http://www.cellchat.org/) R package, which is commonly used to analyze cell–cell communication networks from single cell transcriptome sequencing profiling[33]. Taking advantage of CellChat, we inferred the scRNA-Seq data quantitatively and researched cell–cell communication networks. We predicted the main ingoing and outgoing signal patterns by network analysis and pattern recognition methods, as well as the coordination function between cells and signals. We counted all the important receptor–ligand pairs in the intercellular signal transmission by bubble chart, and we selected the signaling with a higher contribution to the cell for network centrality analysis.

Cell culture and mineralization induction

MSCs were isolated from embryonic maxillary processes. After washing with high-glucose Dulbecco's modified Eagle's medium (DMEM; Gibco, United States) three times, the cells were digested with trypsin–EDTA (Gibco) at 37 °C for 10 min, and centrifuged at 1000 rpm for 5 min. The cells were resuspended in a growth medium with DMEM, 10% fetal bovine serum (FBS) (Gibco), and 1% antibiotics (100 mg/mL penicillin and 100 μg/mL streptomycin) to generate primary MSCs. We maintained the cells at 37 °C in a 5% CO_2 humidified incubator and replaced the medium every 3 d.

For mineralization induction, cells were seeded in DMEM supplemented with 10% FBS at 4×10^4 cells per well in 24-well plates. At 75%–80% confluence, we changed the medium to mineralization induction medium, which consisted of DMEM with 10% FBS, 100 IU/mL penicillin, 100 IU/mL streptomycin, 0.1 μM dexamethasone, 10 mmol/L β-glycerol phosphate (Sigma–Aldrich, St. Louis, MO, United States) and 50 μM ascorbic acid (Sigma–Aldrich). We cultured the cells for up to 7 d, and replaced the medium every 3 d.

Alkaline phosphatase activity and staining

The alkaline phosphatase (ALP) activity kit (Nanjing Jiancheng Biotech, China) was used to detect intracellular ALP activity. Cells were lysed in RIPA lysis buffer (Beyotime, China) without protease and phosphatase inhibitors to induce mineralization for 7 d. We centrifuged the lysate at 12000 rpm and 4 °C for 30 min, and incubated the supernatant with reaction buffer at 37 °C for 15 min. We stopped the color development and measured the absorbance at 520 nm. We measured the protein concentration of the lysate with a Bicinchoninic Acid Assay (BCA) protein assay kit (Beyotime). The ALP staining assay was performed with a Beyotime kit. On day 7 of induction, the cells were fixed for 30 min and stained with Alkaline Phosphatase Assay Kit (Beyotime, China) in the dark for 30 min. The cells were observed and imaged for histochemical detection of ALP with a Nikon microscope.

Alizarin Red staining and quantification

After osteogenic inducting for 14 d, the cells were fixed with 4% paraformaldehyde for 30 min. They were stained with 1% Alizarin Red (pH 4.3) (Beyotime) for 20 min at room temperature and washed three times with deionized water. We observed and imaged the calcium deposits under a Nikon microscope. To quantify calcium deposits, we destained the stained cells with 10% cetylpyridinium chloride monohydrate (Sigma–Aldrich) in 10 mmol/L sodium phosphate (pH 7.0) for 30 min. We transferred a 200-μL aliquot to a 96-well plate to measure the absorbance at 550 nm by a Varioskan Flash Spectral Scanning Multimode Reader (ThermoFisher Scientific, United States).

Quantitative real-time polymerase chain reaction

Total RNA was isolated from the cells by an RNA prep pure Cell Kit (TIANGEN, Beijing, China). cDNA was synthesized following the instructions for the HiScript® III RT Super Mix for quantitative real time polymerase chain reaction (qPCR) kit (Vazyme, Nanjing, China). Quantitative real-time polymerase chain reaction (PCR) was performed with ChamQ Universal SYBR qPCR Master Mix kit (Vazyme) and Real-Time PCR Detection System (Quantstudio5, United States). Gene-specific primer pairs are show in Supplementary Table 1.

Cell Counting Kit-8 proliferation

Cell Counting Kit-8 (CCK-8; Dojindo Kagaku, Japan) was used to investigate the proliferation rate of E16.5d *Cd271* knockout and wild-type MSCs. The cells were seeded at 2 × 10^3 cells/well in a 96-well plate. After mixing the CCK-8 solution, the cells were cultured at 37 °C for 2 h in the dark. Absorbance was detected for 7 d continuously by a microplate reader at 450 nm.

Statistical analysis

Except the scRNA Seq, all the experiments were repeated more than three times. A one-way analysis of variance (ANOVA) or t test (GraphPad Prism 9.0 software, La Jolla, CA, United States) was used to identify significant differences. $P < 0.05$ was considered statistically significant.

RESULTS

scRNA-Seq analysis showed high cellular heterogeneity of murine maxillary process

To reveal cellular heterogeneity, we performed scRNA-Seq with murine maxillary processes from wild-type and *Cd271* knockout embryo tissues (Figure 1A and Supplementary Figure 1). After quality controlling and normalizing scRNA-Seq data, we obtained transcriptomes of 17426 cells (Supple-ementary Figure 2). UMAP clustering divided the cells into 21 independent clusters. Based on established lineage-specific marker genes, these 21 clusters were assigned to eight cell lineages (Figure 1B). We identified differentially expressed genes by comparing the gene expression profiles of one cluster with the others (Figure 1C). The MSC lineage was identified by *Col1a1* and *Col3a1*, and epithelial cells were marked by *Lgals7*. Based on these established lineage-specific maker genes, we assigned these clusters to eight cell types and plotted them (Figure 1D). We identified nine mesenchymal clusters (0–6, 11 and 17), a total of 12712 cells, which constituted the majority of sequenced cells by > 72.94%. Clusters 7, 18 and 20 were annotated as epithelial cells with a relative proportion of 6.14%. Muscle cells consisted of clusters 8, 9 and 12 with a relative proportion of 11.43%, while cluster 10 accounted for 3.11% as macrophages. Clusters 13 and 19 were annotated as glial cells (341, 1.95%). Clusters 14–16 were annotated as T cells (276, 1.58%), endothelial cells (269, 1.54%), and perivascular cells (162, 0.92%), respectively (Figure 1E).

We also analyzed the single cell sequence profiling from wild-type and *Cd271* knockout mice to establish the distribution of different types of cells and the source of samples. We counted the number and proportion of each cell type using histograms (Figure 1F). MSCs occupied most of the cell transcriptomes from the maxillary process, and the proportion of these cells between *Cd271* knockout and wild-type was similar.

GSEA showed significant functional and signaling differences between cell types

To identify the relevant molecular mechanisms and possible pathways, we subjected all expressions to GSEA. The results showed a high correlation with MSCs and a close relationship with biomineralization. The results suggested that biomineralization (NES = 2.51, $P < 0.01$) and bone mineralization (NES = 2.49, $P < 0.001$) associated pathways enriched in MSCs (Figure 2A and B). GSEA also revealed that the differentially expressed genes enriched endothelial development, epithelial and glial cell differentiation, immune response, myofilament sliding and vascular smooth muscle contraction (Figure 2C–I).

Unsupervised clustering revealed novel subclusters of MSCs

As MSCs contribute much to embryogenesis and are essential in odontogenesis and osteogenesis, we performed unsupervised reclustering of MSCs. We performed the Subcluster analysis to investigate the heterogeneity within the mesenchymal populations. We observed further heterogeneity in subclusters 0–12 (Figure 3A). We used the published markers to identify the subclusters in MSCs. For instance, *Cdk1* and *Dkk1* marked progenitors, *Runx2* and *sp7* marked osteoblasts, and *Dlk1* and *Shox2* marked fibroblasts. We scored these marker genes in MSC clusters (Figure 3B). In this way, MSC clusters could also be identified into three subpopulations: Progenitors, fibroblasts and osteoblasts. We counted the cell proportions of the MSCs subclusters from wild-type and *Cd271* knockout maxillary processes. The results showed that the numbers of subclusters 1, 3 and 10 were lower, while the other subclusters were higher in *Cd271* knockout compared with wild-type mice (Figure 3C).

Cd271 knockout MSCs exhibited weaker proliferation and osteogenic differentiation potential

We compared MSCs between wild-type and *Cd271* knockout maxillary processes. GO functional enrichment analysis revealed that differentially expressed genes were enriched in ossification, myeloid cell differentiation and biomineralization cell proliferation-related signaling (Figure 4A). To compare the differences in proliferation and osteogenic differentiation between wild-type and *Cd271* knockout MSCs, we investigated the potential for MSC proliferation. As the CCK-8 assay showed, the *Cd271* knockout MSCs exhibited weaker cell proliferation (Figure 4B). We induced the cells with an

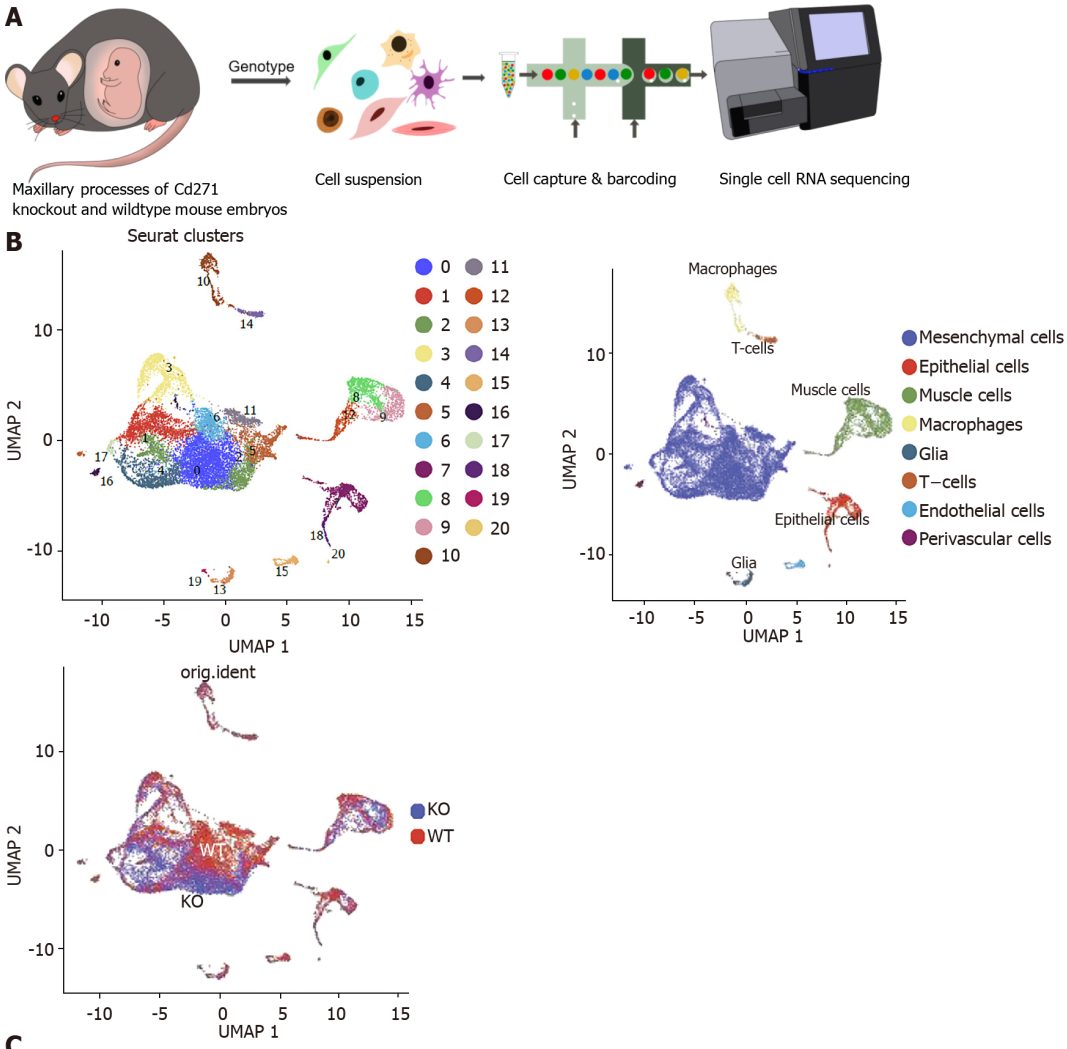
A
Genotype
Maxillary processes of Cd271 knockout and wildtype mouse embryos
Cell suspension
Cell capture & barcoding
Single cell RNA sequencing
B
Seurat clusters
UMAP 1
UMAP 2
Macrophages
T-cells
Muscle cells
Epithelial cells
Glia
Mesenchymal cells
Epithelial cells
Muscle cells
Macrophages
Glia
T−cells
Endothelial cells
Perivascular cells
orig.ident
KO
WT
C
Col1a1
Dcn
Agtr2
Col3a1
Col1a2
Smoc2
Ptn
Lum
Aldoa
Bsg
Ap2s1
Fis1
Timm13
Eif3l
Drg1
Itga1
Myh9
Nid1
Sntb1
Cald1
Tns1
Egfl7
Esam
Fabp4
Emcn
Ecscr
Plvap
Pf4
C1qc
Selenop
Fcrls
Ctsb
Fcer1g
Cluster 0
Cluster 6
Cluster 11
Cluster 1
Cluster 2
Cluster 3
Cluster 4
Cluster 5
Cluster 7
Cluster 18
Cluster 20
Cluster 8
Cluster 9
Cluster 12
Cluster 19
Cluster 13
Cluster 17
Cluster 16
Cluster 15
Cluster 10
Cluster 14

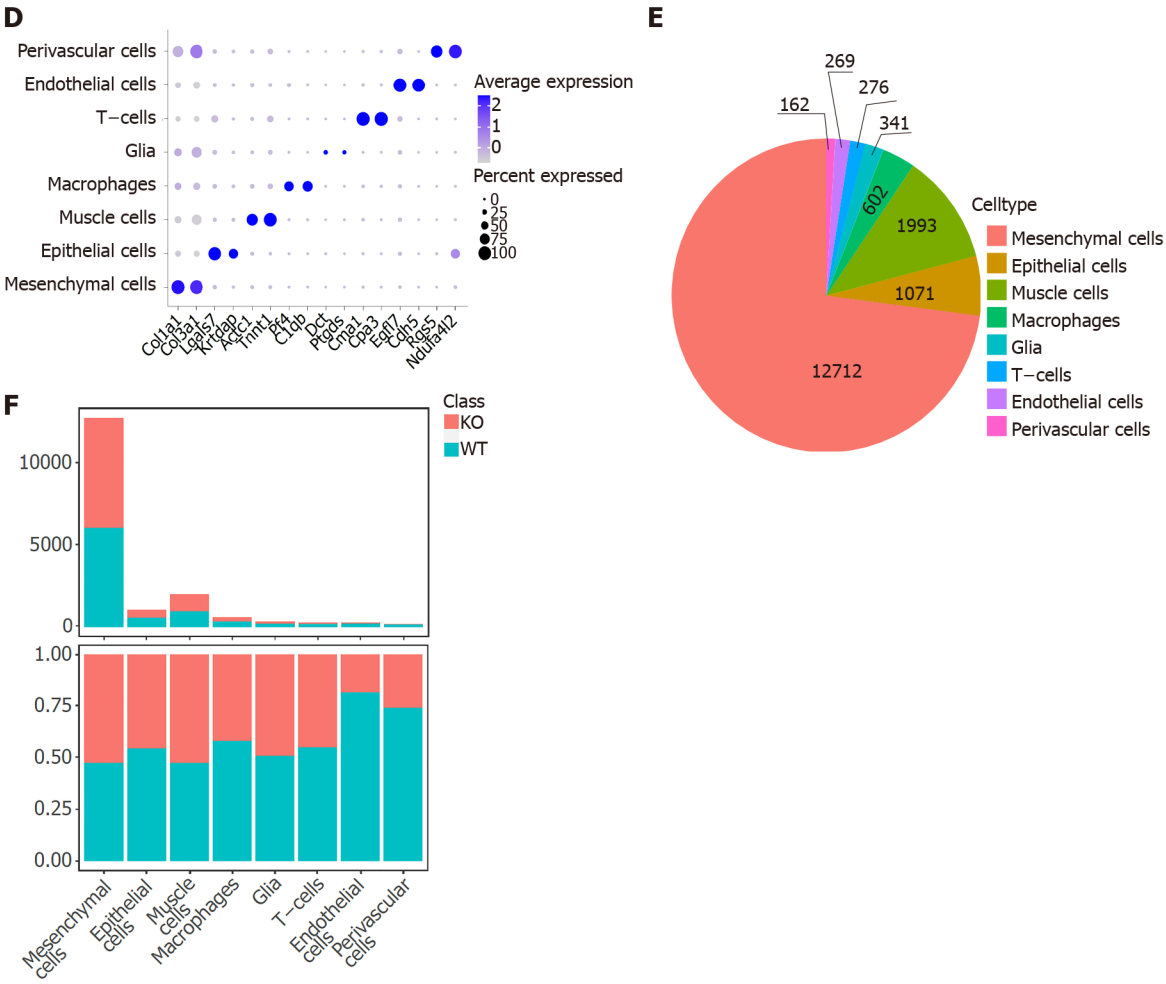

DOI: 10.4252/wjsc.v15.i6.589

Figure 1 Single cell RNA sequencing analysis of maxillary processes from wild-type and *Cd271* knockout mice. We identified 21 clusters of cells, and the single cell RNA sequencing data were characterized. A: Schematic representation of the experimental workflow. The *Cd271* knockout and wild-type maxillary processes were collected from mouse embryos at 16.5 d. After genotyping, cells were suspended as single cells, and the cDNA library was constructed and sequenced; B: Cells extracted from the samples were subjected to Uniform Manifold Approximation and Projection hierarchical clustering and color-coded by cluster grouping, predominant cell type, and sample origin; C: Heatmap showing expression levels of differentially expressed genes in each cluster; D: Dot plot showing prominent marker genes for each cell type (mesenchymal cells, epithelial, muscle cell, macrophage, glial, T cell, endothelial, and perivascular); E: Pie chart showing the number of each cell type; F: Histogram showing the number and proportion of cells from wild-type and *Cd271* knockout mice. UMAP: Uniform Manifold Approximation and Projection; KO: Knockout; WT: Wild-type.

osteogenic induction medium and performed the mineralization assay. ALP staining and a quantitative assay revealed a lower and lighter mineralization level of *Cd271* knockout than wild-type MSCs. Lighter and fewer mineralized nodules were observed by Alizarin Red staining in *Cd271* knock out MSCs (Figure 4C). These results indicated more inadequate osteogenic differentiation potential in *Cd271* knockout MSCs. We selected several differentially expressed genes with considerable interaction by Cytoscape, and measured the gene expression by real-time quantitative PCR (Figure 4D). Proliferation, ossification and osteoblast differentiation-related genes, such as *Col4a1*, *Col6a1*, *Sparc*, *Vim*, *Col1a1* and *Col3a1*, were significantly decreased in *Cd271* knockout MSCs (Figure 4E). *Cd271* was involved in regulating osteogenic differentiation in MSCs, and our results implied a weaker potential of proliferation and osteogenic differentiation in *Cd271* knockout MSCs.

Different sets of genes appeared to shift along the differentiation trajectory

We selected MSCs to institute a pseudotemporal trajectory map that contained terminals consistent with distinct cell fates. The progenitor cells aggregated at the root and branches, indicating a good cell cycle of the progenitor cells. Osteoblasts and fibroblasts were scattered in various branches, showing high invasive potential (Figure 5A–C). We extracted differentially expressed genes over pseudotemporal changes and plotted heatmaps. Different sets of genes were also found to be shifted during the progression of MSCs, stressing the actional change of the progenitor cells, which managed the cell fate transition in the mesenchyme. We clustered the differentially expressed genes into three and performed GO analysis. Clusters 1 and 2 were significantly enriched in biological processes of osteoblast differentiation, biomineralization and odontogenesis, while cluster 3 was mainly enriched in cell metabolism (Figure 5D).

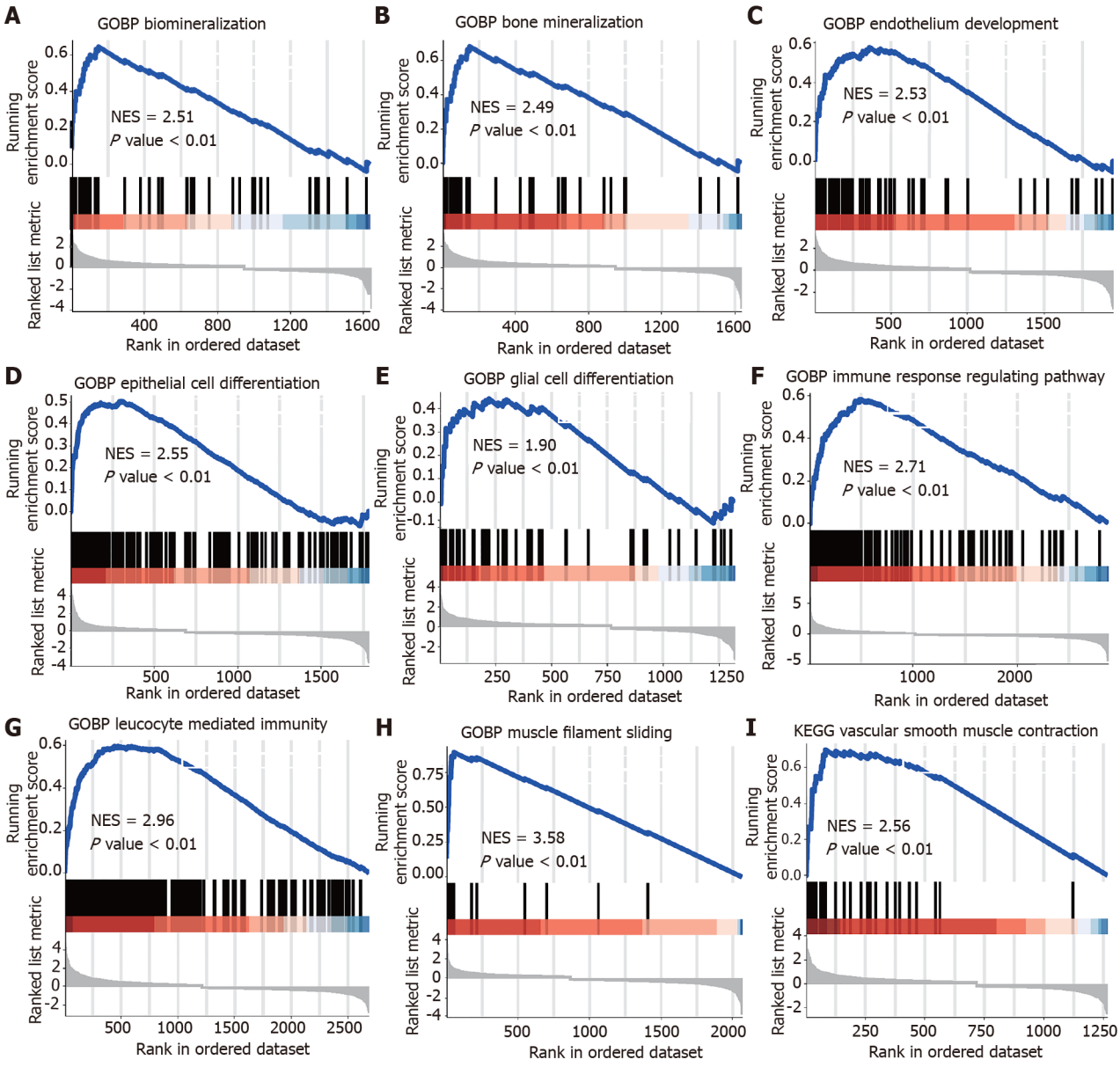

DOI: 10.4252/wjsc.v15.i6.589

Figure 2 Gene set enrichment analysis plots for representative signaling pathways upregulated in maxillary process. Gene set enrichment analysis enriched differentially expressed genes into multifunctional gene networks. A and B: Representative gene set enrichment analysis maps for mesenchymal stem cells; C: Endothelial cells; D: Epithelial cells; E: Glia; F: T cells; G: Macrophages; H: Muscle cells; I: Perivascular cells. Normalized enrichment score normalized enrichment score, corrected for multiple comparisons using false discovery rate method, *P* values shown in plots. NES: Normalized enrichment score.

Cell–cell interactions of mesenchymal subpopulations were crucial in the maxillary process

The dataset of scRNA-Seq provided an opportunity to analyze intercellular communication mediated by ligand–receptor interactions. To gain insights into potential signaling interactions between different cellular subpopulations, we interrogated our data with CellChat (version 1.1.3) (http://www.cellchat.org/) R package, which could predict the ligand and receptor interactions at single cell resolution[33]. We found dense communication between MSCs and other cells, and the most concentrated interactions occurred in the mesenchymal subpopulation (Figure 6A and B). It revealed the importance of mesenchymal interaction signaling. We detected 30 signaling pathways in eight cell groups, including MK, PTN, ncWNT, IGF, PDGF, WNT and VEGF signaling pathways. We compared the contribution of efferent (or afferent) signaling between cells, confirming that MSCs had higher interaction than other cell types while acting as outgoing signaling pathways (Figure 6C). We analyzed the potential signaling of MSCs, revealing a series of signaling pathways, such as odontogenesis-related signaling such as WNT, BMP and HH signaling (Figure 6D).

We explored ligand–receptor signals broadcast by MSCs, which revealed that MSCs might affect other cells in the ligand–receptor interaction of MK and PTN signaling (Figure 6E). We performed network centrality analysis on MK and PTN signaling, which confirmed that MSCs were important signal senders in intercellular communication (Figure 6F and G). The expression of *Mdk* and *Ptn* in wild-type and *Cd271*$^{-/-}$ MSCs exhibited significant differences by quantitative real-

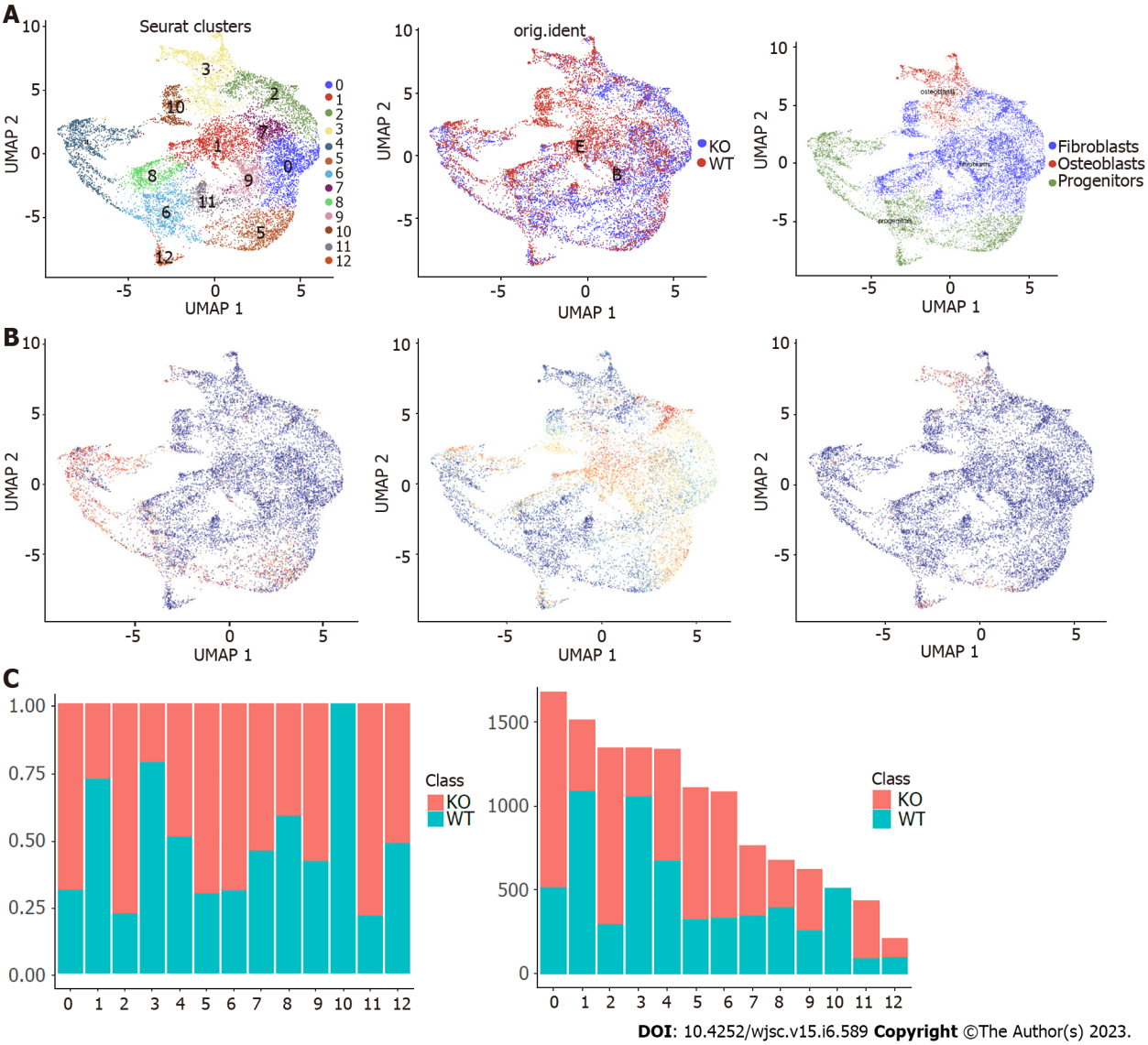

DOI: 10.4252/wjsc.v15.i6.589 **Copyright** ©The Author(s) 2023.

Figure 3 Further cluster analysis of mesenchymal stem cells. A: Mesenchymal stem cells were reclustered and color-coded according to cluster, sample origin and cell type; B: Feature scores of progenitors, fibroblasts and osteoblasts marker genes were displayed in the Uniform Manifold Approximation and Projection plot; C: Histogram showing the proportion and the number of cells in each cluster of wild-type and *Cd271* knockout mice. UMAP: Uniform Manifold Approximation and Projection; KO: Knockout; WT: Wild-type.

time PCR assay. The expression of *Mdk* and *Ptn* was higher in the *Cd271* knockout MSCs (Figure 6H). These results disclosed underlying ligand–receptor interactions and suggested that MK and PTN signaling may be influenced by *Cd271* in mesenchymal subpopulations.

DISCUSSION

Although MSCs have been extensively studied, there is still a lack of knowledge about the key mechanisms in tooth development. Researchers have found that the maxillary process included various cell subpopulations with diverse phenotypic and functional characteristics[34]. How this heterogeneity appears in osteogenesis and odontogenesis remains unclear. *Cd271* used to be a marker of the MSCs, and it had been reported that *Cd271* promotes differentiation in MSCs [35-37]. Hence, we used *Cd271* knockout mouse embryos to investigate what happens to MSCs in their initial developmental stage. We constructed a single cell profiling of representative mouse embryo maxillary processes and selected MSCs to explore their characteristics and critical regulatory mechanism *Cd271* related.

Maxillary-process-derived MSCs are recognized as primitive odontogenic stem cells. For instance, researchers obtained the MSCs from the first branchial arch of mice and the maxillary process tissue of rats in succession, and revealed the pluripotency of MSCs[38,39]. Wen *et al*[40] found that $p75^{+/+}$ MSCs have good multidirectional differentiation potential [40]. We identified nine MSC clusters among 21 clusters identified using scRNA-Seq in mouse embryo maxillary processes. MSC clusters accounted for the majority, suggesting that MSCs contribute much to embryogenesis. Emerging

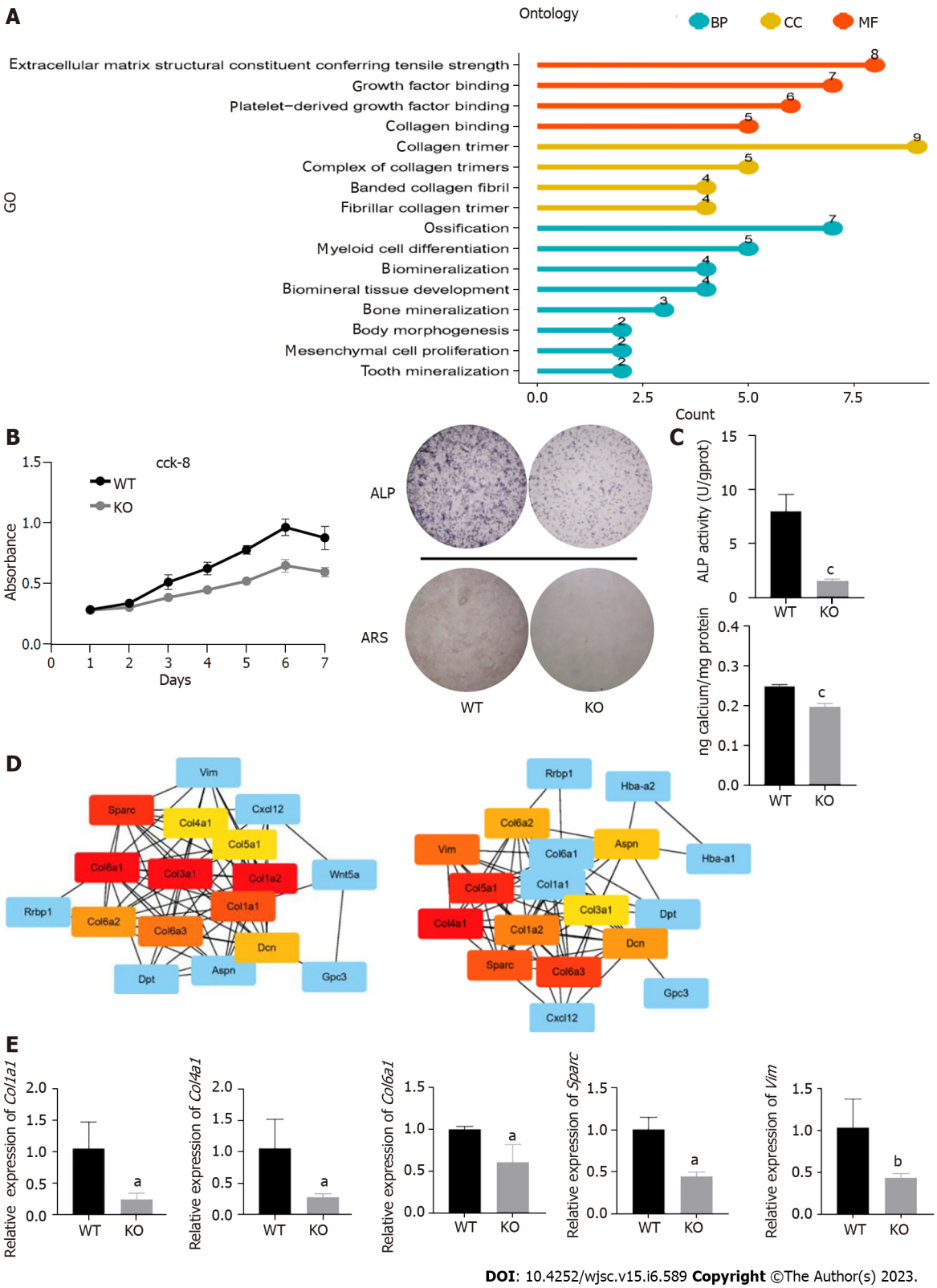

DOI: 10.4252/wjsc.v15.i6.589 **Copyright** ©The Author(s) 2023.

Figure 4 *Cd271* knockout mesenchymal stem cells showed weaker proliferation and osteogenic differentiation potential. A: Gene Ontology enrichment analysis of differentially expressed genes between *Cd271* knockout and wild-type mesenchymal stem cells (MSCs); B: Growth curves of *Cd271* knockout and wild-type MSCs; C: Mineralization assay of *Cd271* knockout and wild-type MSCs. Alkaline phosphatase (ALP) and Alizarin red staining of *Cd271* knockout MSCs was significantly lighter. ALP activity and calcium quantification were significantly lower in *Cd271* knockout compared with wild-type MSCs; D: Protein–protein interaction network interaction analysis of wildtype *vs* *Cd271* knockout differentially expressed genes; E: Quantitative real-time polymerase chain reaction assay of some differentially expressed genes in *Cd271* knockout and wild-type MSCs. Data are presented as mean values ± SD (n = 3 biologically independent experiments. Two-sided unpaired t-test, $^{a}P < 0.05$, $^{b}P < 0.01$, $^{c}P < 0.001$) BP: Biological Process; CC: Cell component; MF: Molecular function; ARS: Alizarin red S; ALP: Alkaline phosphatase; KO: Knockout; WT: Wild-type.

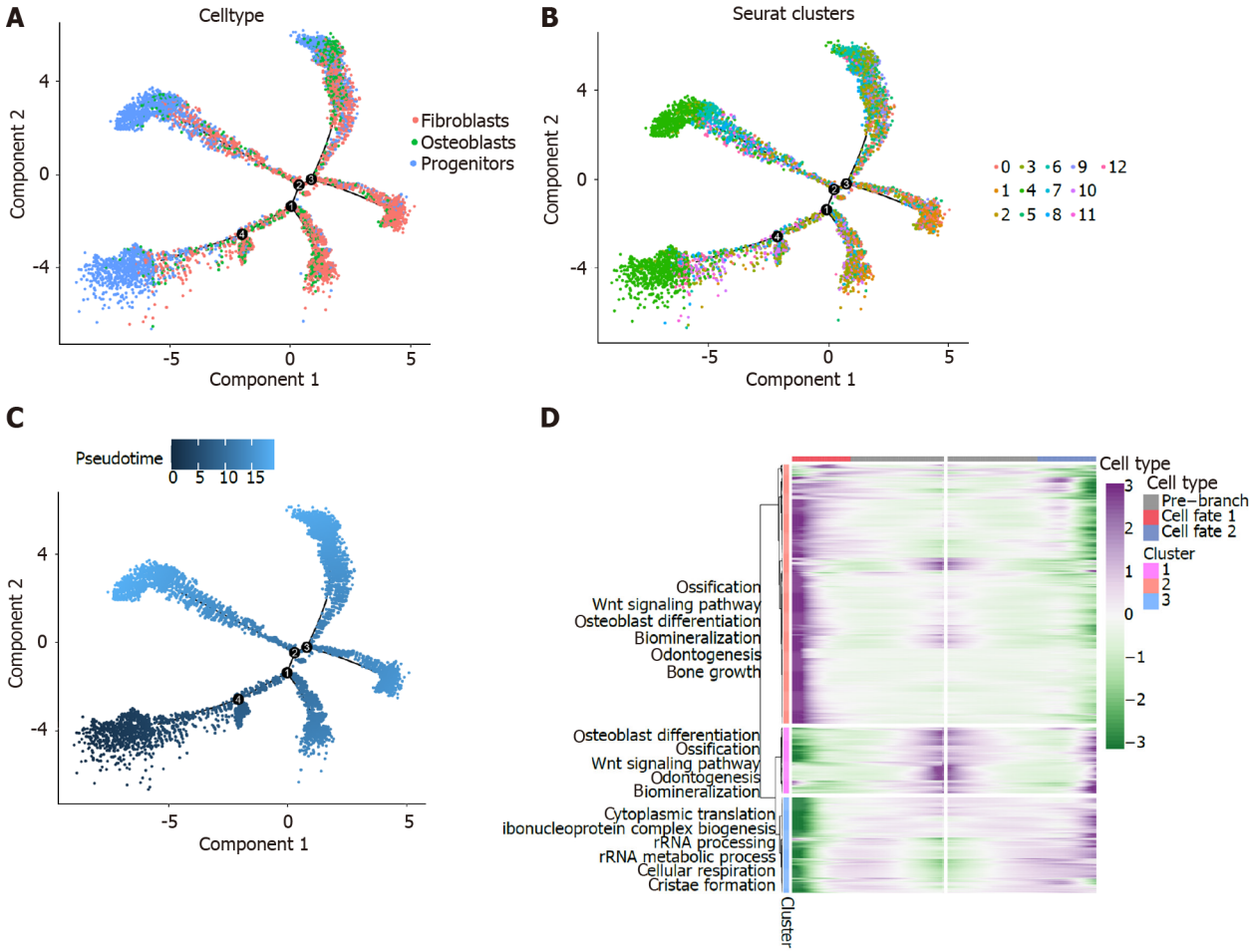

DOI: 10.4252/wjsc.v15.i6.589

Figure 5 The potential developmental trajectories of mesenchymal stem cells by Monocle. A: Pseudo-sequential diagram based on the differentiation process of mesenchymal stem cell (MSC) subpopulations; B: Pseudo-sequence plot of MSCs colored by cluster classification; C: Pseudo-sequential diagram of MSCs drawn with timeline coloring; D: Heatmap of differentially expressed genes in pseudotemporal analysis. The differentially expressed genes were divided into three gene clusters and gene ontology biological process enrichment analysis was performed.

studies have revealed that the marker genes of MSCs, *Col1a1* and *Col3a1*, promote collagen production and influence odontogenesis or osteogenesis[41-43]. The decreased expression of these two genes in *Cd271* knockout MSCs compared to wild-type, suggested that *Cd271* was related to MSC regulation of odontogenesis or osteogenesis.

In the past, several studies concentrated on the whole population of MSCs rather than the relationships among the subclusters. Our subcluster analysis disclosed that these MSC clusters could be separated into three subpopulations: Fibroblast, progenitors and osteoblast, which had not been separated before. One of the characteristics of MSC clusters is the expression of osteoblast differentiation-associated genes such as *Runx2*, *Sox9*, *Msx1* and *Omd*[44-47]. Previous studies showed that proteins such as Runx2 and Sox9 were positively regulated by *Cd271* in MSCs[48-50]. However, these studies did not show the heterogeneity of MSCs, or which subpopulations of MSCs these proteins derived from. Our results revealed that these proteins were mainly expressed in the osteoblast subpopulation. The number of osteoblast subpopulations decreased while progenitor subpopulations increased. This suggested that some progenitors were hindered from differentiating into osteoblasts in the *Cd271* knockout MSC clusters. Consistently, GO enrichment analysis and GSEA verified significant enrichment of the ossification, biomineralization and bone mineralization pathways in the *Cd271* knockout and wild-type cells. Based on our scRNA-Seq data, we gained differentially expressed genes between two groups for the first time. We picked out several differentially expressed genes with extensive interactions; for instance, *Sparc*, *Vim*, *Col4a1*, *Col6a1*, *Col1a1* and *Col3a1*. These genes are considered to relate to cell proliferation, bone mineralization and multipotent differentiation[41-43,51-54]. In *Cd271* knockout MSCs, we verified by quantitative real-time PCR that these differentially expressed gene clusters had lower expression. Functional experiments also demonstrated a weaker odontogenic and osteogenic differentiation and proliferation in the *Cd271* knockout MSCs. Consistent with previous studies, our results confirmed that the MSC clusters had an essential role in odontogenesis and osteogenesis and *Cd271* possibly regulated it.

Pseudotemporal analysis uncovered a developmental trajectory among these three subpopulations. Significantly, the progenitor subpopulation was found to develop into the osteoblast and fibroblast subpopulations. We concluded that the progenitors were the base subpopulation and increasingly transformed into the osteoblast and fibroblast subpopulations in MSCs. Consistent with our GO and GSEA findings, the differentially expressed genes that emerged in pseudotemporal

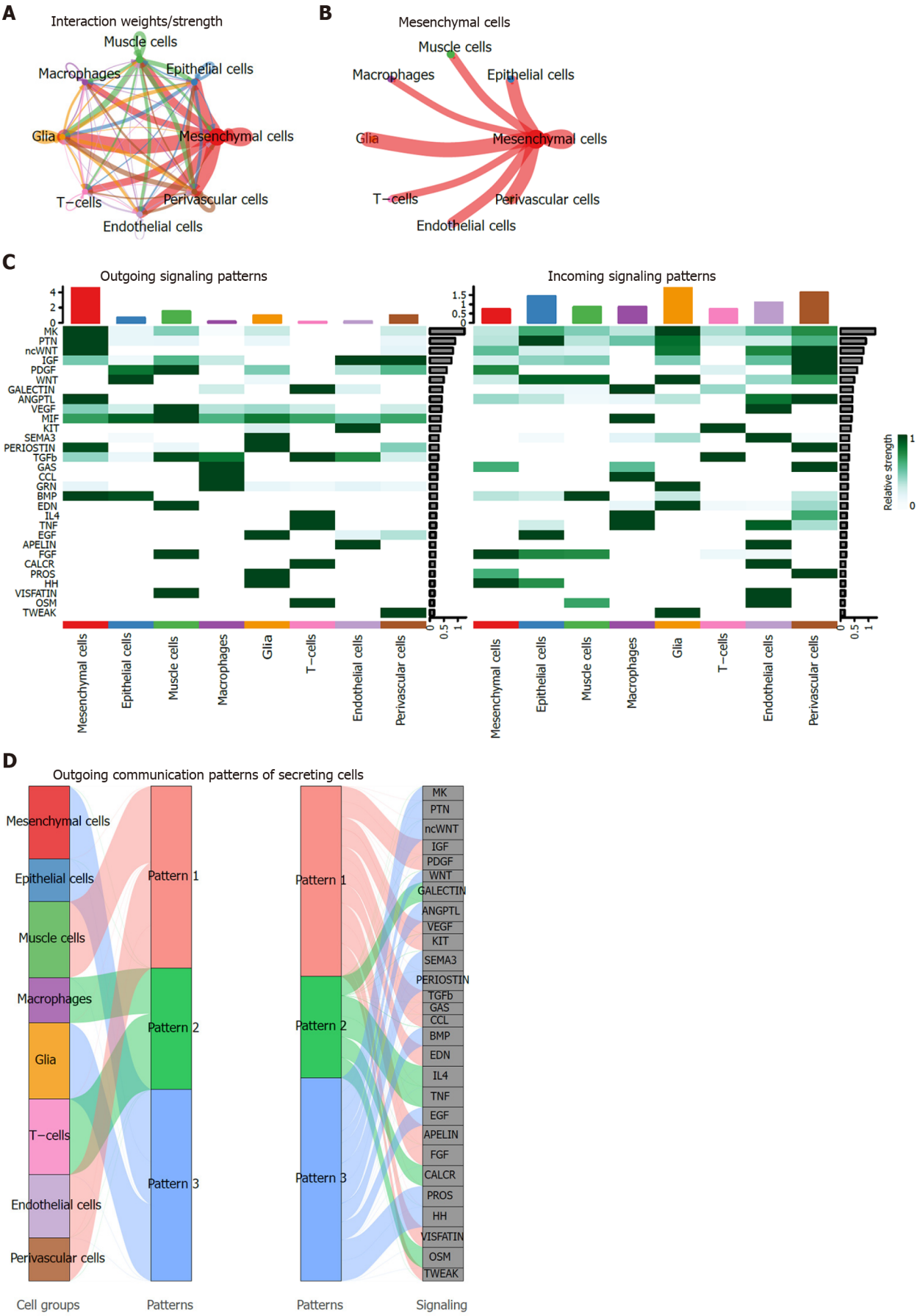
A
Interaction weights/strength
Muscle cells
Macrophages
Epithelial cells
Glia
Mesenchymal cells
T−cells
Perivascular cells
Endothelial cells
B
Mesenchymal cells
Muscle cells
Macrophages
Epithelial cells
Glia
Mesenchymal cells
T−cells
Perivascular cells
Endothelial cells
C
Outgoing signaling patterns
Incoming signaling patterns
MK
PTN
ncWNT
IGF
PDGF
WNT
GALECTIN
ANGPTL
VEGF
MIF
KIT
SEMA3
PERIOSTIN
TGFb
GAS
CCL
GRN
BMP
EDN
IL4
TNF
EGF
APELIN
FGF
CALCR
PROS
HH
VISFATIN
OSM
TWEAK
Relative strength
Mesenchymal cells
Epithelial cells
Muscle cells
Macrophages
Glia
T−cells
Endothelial cells
Perivascular cells
D
Outgoing communication patterns of secreting cells
Mesenchymal cells
Epithelial cells
Muscle cells
Macrophages
Glia
T−cells
Endothelial cells
Perivascular cells
Pattern 1
Pattern 2
Pattern 3
Cell groups
Patterns
Signaling

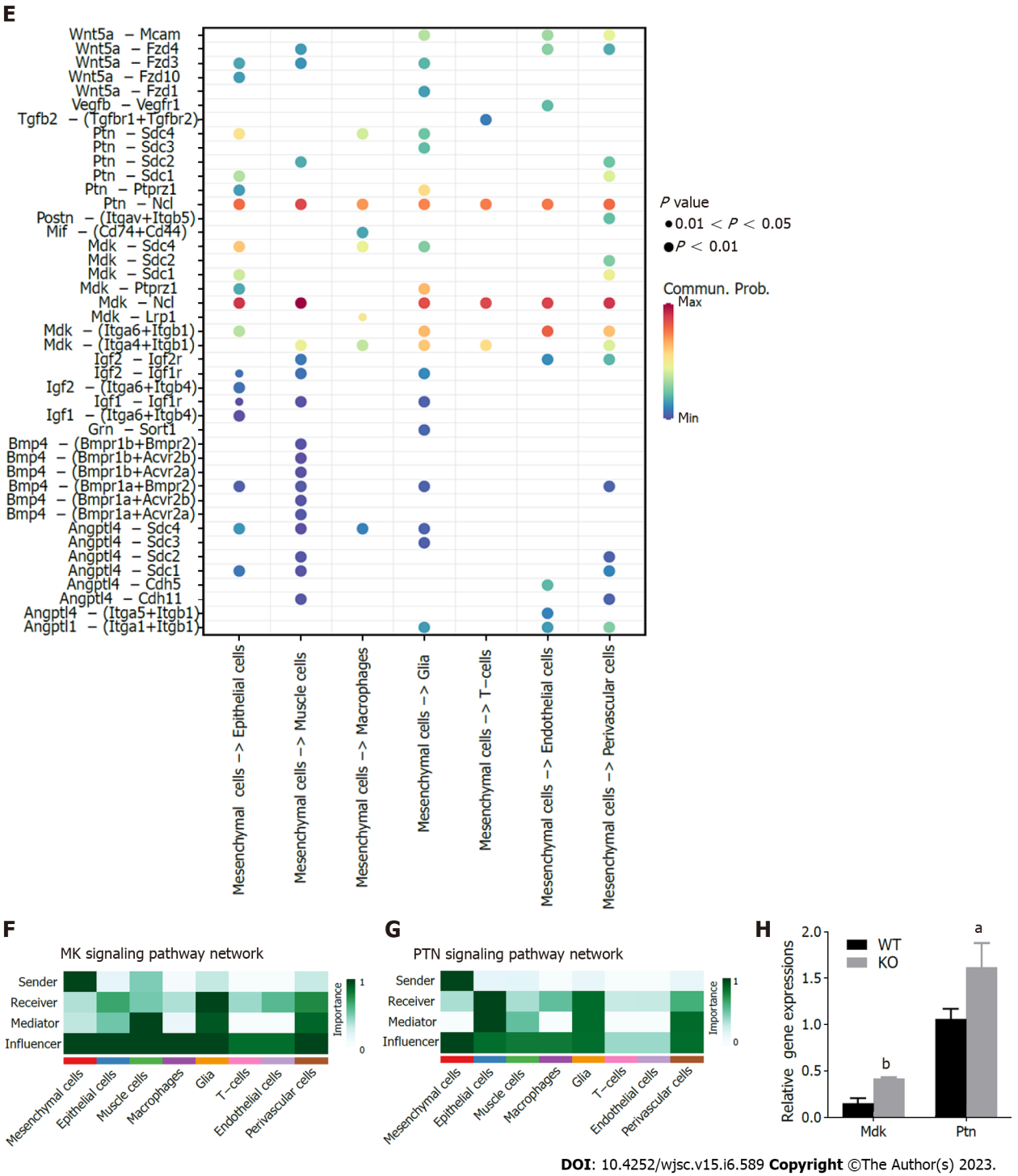

DOI: 10.4252/wjsc.v15.i6.589

Figure 6 Inference, analysis and visualization of cellular communication networks from a single dataset *via* CellChat. A: Interaction intensity plot between cells in single cell sequence profiling; B: Interaction intensity map between mesenchymal stem cells (MSCs) and other cell types; C: Contribution map of 30 signaling pathways detected by CellChat to intercellular efferent (or afferent) signaling; D: Alluvial plot of cell outgoing signaling patterns, showing the correspondence between cell populations and signaling pathways; E: Important ligand–receptor pairs for MSCs sending signals to other cell types. F and G: Contribution of efferent (or afferent) signals between cells, the MK signaling pathway (F) and PTN signaling pathway (G) were selected for visualization of network centrality scores; H: Expression of *Mdk* and *Ptn* in *Cd271* knockout and wild-type MSCs was analyzed by quantitative real-time polymerase chain reaction. Data are presented as mean values ± SD (n = 3 biologically independent experiments. Two-sided unpaired t-test, $^{a}P < 0.05$, $^{b}P < 0.01$). KO: Knockout; WT: Wild-type.

analysis showed a significant relation with ossification and osteoblast differentiation in MSCs. Collectively, our results revealed that MSCs were progressively diversified and determined to the odontogenic fate. Thus, the mesenchyme in the maxillary process provides a remarkable model to study the development of maxillary-process-derived MSCs.

It is known that the interactions between dental mesenchyme and epithelium play a crucial part in the integral tooth developmental process. Nevertheless, the cell–cell interactions within the maxillary process have not been extensively studied[55]. In our study, scRNA-Seq offered the opportunity to identify communicating pairs on the basis of the expression of their cell-surface receptors and ligands. CellChat showed that the most concentrated interactions occurred

between mesenchymal and other cells. It indicated that MSCs play a vital role in cell communication. It is worth noting that MSCs mainly participated in MK, PTN, ncWNT, WNT and BMP signaling. Previous studies reported that *Cd271* might regulate the odontogenic differentiation of MSCs through the BMP, WNT and PI3K pathways[17,49,56]. However, there are no reports that MDK signaling participates in regulating MSCs. In the CellChat, the receptor interactions of MDK and PTN appeared to be obvious. It reminded us that the *Mdk* and *Ptn* might play a primary role in the developmental process of MSCs. *Mdk* and *Ptn* expression notably increased in *Cd271* knockout cells during induction of mineralization for 7 d. Our subsequent study will explore the molecular mechanism of how *Cd271* regulates *Mdk* to influence osteogenesis.

Although our studies revealed several significant discoveries, there were some limitations. First, different clustering can generate different results; thus, further groupings are needed to perform future analysis. Second, the current study was based on scRNA-Seq. Therefore, we did some biological observation but did not illustrate the direct mechanisms of *Cd271* involved in tooth development. Therefore, further studies about direct mechanisms and *in vivo* studies are needed.

CONCLUSION

Our study reveals high cellular heterogeneity, molecular details and cell-cell interactions in MSCs. It provides a valuable resource for understanding the development of maxillary-process-derived MSCs. And it enables the maxillary process to serve as an excellent model to explore tooth development and cell fate determinations. Furthermore, we have found significant functional and signaling differences between *Cd271* knockout and wildtype MSCs. We have clarified that *Cd271* is significantly associated with the regulation of mineralization. We tentatively propose that *Mdk* signaling is involved in the regulatory mechanism of mineralization. These findings contribute to thorough exploration of the mechanism of *Cd271* in regulating odontogenesis and osteogenesis which add to the theory of tooth development.

ARTICLE HIGHLIGHTS

Research background

Tooth loss has become a common problem in human life. Compared with traditional denture restoration, dental tissue engineering has become the most ideal means to solve this problem, and it is also one of the most active research fields of stomatology in recent years. The tooth development involves complex signal pathways. Ecto-mesenchymal stem cells (MSCs) were regarded as the primitive dental cells in the classical theory of tooth development. To date, in-depth studies of the odontogenesis and osteogenesis of MSCs are still lacking.

Research motivation

We contribute to thorough exploration of the mechanism of odontogenesis and osteogenesis to add to the theory of tooth development.

Research objectives

Our study provides novel insights into the biological features of MSCs at the single cell level and the mechanism of *Cd271* in regulating odontogenesis and osteogenesis.

Research methods

We used the maxillary process from mouse embryos as a model to understand the development of maxillary-process-derived MSCs. We applied single cell RNA sequence analysis to elucidate the cellular heterogeneity and explore molecular details. And we verified the findings from single cell sequencing *in vitro* by lab experience such as cell staining, cell counting and quantitative real time polymerase chain reaction.

Research results

Our study reveals: (1) High cellular heterogeneity and molecular details; (2) Significant functional and signaling differences between cell types; (3) Novel subclusters of mesenchymal stem cells; and (4) Crucial cell-cell interactions of mesenchymal subpopulations. Besides, we contribute to thorough exploration of the mechanism of *Cd271* in regulating odontogenesis and osteogenesis.

Research conclusions

Our study reveals high cellular heterogeneity, molecular details and cell-cell interactions in MSCs. We found significant functional and signaling differences between *Cd271* knockout and wildtype MSCs. We clarified that *Cd271* is significantly associated with the regulation of mineralization.

Research perspectives

We need illustrate that *Mdk* signaling is involved in the regulatory mechanism of mineralization in future research. And direct mechanisms of *Cd271* involved in tooth development are needed in further studies.

FOOTNOTES

Author contributions: Zhang YY conceived experiments, interpreted data and wrote a manuscript; Li F, Zeng XK and Zou YH performed the experiment; Zhu BB, Ye JJ, Zhang YX, and Jin Q provided a critical insight into this study; Nie X supervised this study; All authors read and approved the final version for submission.

Supported by National Natural Science Foundation of China (General Program), No. 31870971; and Medical Health Science and Technology Project of Zhejiang Province, No. 2023KY155.

Institutional animal care and use committee statement: All animal experiments were performed according to the protocols approved by the Medical Ethics Committee of Wenzhou Medical University, No. wydw2019-0224.

Conflict-of-interest statement: All the authors report no relevant conflicts of interest for this article.

Data sharing statement: The datasets analyzed for this study can be found in the NCBI SRA: 506PRJNA891206. https://www.ncbi.nlm.nih.gov/sra/PRJNA891206.

ARRIVE guidelines statement: The authors have read the ARRIVE guidelines, and the manuscript was prepared and revised according to the ARRIVE guidelines.

Country/Territory of origin: China

ORCID number: Yan-Yan Zhang 0000-0001-6233-5752; Feng Li 0000-0002-0172-388X; Xiao-Ke Zeng 0000-0003-1643-1932; Yan-Hui Zou 0000-0002-6543-3796; Bing-Bing Zhu 0000-0001-8306-6109; Jia-Jia Ye 0000-0001-5901-3453; Yun-Xiao Zhang 0000-0002-0799-2642; Qiu Jin 0000-0003-3830-2613; Xin Nie 0000-0002-4645-226X.

S-Editor: Li L
L-Editor: A
P-Editor: Ma YJ

REFERENCES

1 **Egbuniwe O**, Idowu BD, Funes JM, Grant AD, Renton T, Di Silvio L. P16/p53 expression and telomerase activity in immortalized human dental pulp cells. *Cell Cycle* 2011; **10**: 3912-3919 [PMID: 22067611 DOI: 10.4161/cc.10.22.18093]
2 **Strobl-Mazzulla PH**, Bronner ME. Epithelial to mesenchymal transition: new and old insights from the classical neural crest model. *Semin Cancer Biol* 2012; **22**: 411-416 [PMID: 22575214 DOI: 10.1016/j.semcancer.2012.04.008]
3 **Abbasian M**, Langlois A, Gibon J. Sexual Dimorphism in Balance and Coordination in p75NTR(exonIII) Knock-Out Mice. *Front Behav Neurosci* 2022; **16**: 842552 [PMID: 35283743 DOI: 10.3389/fnbeh.2022.842552]
4 **Alvarez R**, Lee HL, Hong C, Wang CY. Single CD271 marker isolates mesenchymal stem cells from human dental pulp. *Int J Oral Sci* 2015; **7**: 205-212 [PMID: 26674422 DOI: 10.1038/ijos.2015.29]
5 **Akiyama Y**, Mikami Y, Watanabe E, Watanabe N, Toriumi T, Takahashi T, Komiyama K, Isokawa K, Shimizu N, Honda MJ. The P75 neurotrophin receptor regulates proliferation of the human MG63 osteoblast cell line. *Differentiation* 2014; **87**: 111-118 [PMID: 24582280 DOI: 10.1016/j.diff.2014.01.002]
6 **Castellini C**, Mattioli S, Cotozzolo E, Pistilli A, Rende M, Bartolini D, Di Sante G, Menchetti L, Dal Bosco A, Stabile AM. The Effect of Interaction NGF/p75(NTR) in Sperm Cells: A Rabbit Model. *Cells* 2022; **11** [PMID: 35326486 DOI: 10.3390/cells11061035]
7 **Zanin JP**, Friedman WJ. p75NTR prevents the onset of cerebellar granule cell migration *via* RhoA activation. *Elife* 2022; **11** [PMID: 36040414 DOI: 10.7554/eLife.79934]
8 **Zhao H**, Fan S, Sun J. Delayed wound healing in the elderly and a new therapeutic target: CD271. *Curr Stem Cell Res Ther* 2023 [PMID: 37016526 DOI: 10.2174/1574888X18666230403083603]
9 **Passino MA**, Adams RA, Sikorski SL, Akassoglou K. Regulation of hepatic stellate cell differentiation by the neurotrophin receptor p75NTR. *Science* 2007; **315**: 1853-1856 [PMID: 17395831 DOI: 10.1126/science.1137603]
10 **Wen X**, Liu L, Deng M, Liu R, Zhang L, Nie X. In vitro cementoblast-like differentiation of postmigratory neural crest-derived p75(+) stem cells with dental follicle cell conditioned medium. *Exp Cell Res* 2015; **337**: 76-86 [PMID: 26165934 DOI: 10.1016/j.yexcr.2015.07.001]
11 **Baeza-Raja B**, Sachs BD, Li P, Christian F, Vagena E, Davalos D, Le Moan N, Ryu JK, Sikorski SL, Chan JP, Scadeng M, Taylor SS, Houslay MD, Baillie GS, Saltiel AR, Olefsky JM, Akassoglou K. p75 Neurotrophin Receptor Regulates Energy Balance in Obesity. *Cell Rep* 2016; **14**: 255-268 [PMID: 26748707 DOI: 10.1016/j.celrep.2015.12.028]
12 **Gonçalves NP**, Mohseni S, El Soury M, Ulrichsen M, Richner M, Xiao J, Wood RJ, Andersen OM, Coulson EJ, Raimondo S, Murray SS, Vægter CB. Peripheral Nerve Regeneration Is Independent From Schwann Cell p75(NTR) Expression. *Front Cell Neurosci* 2019; **13**: 235 [PMID: 31191256 DOI: 10.3389/fncel.2019.00235]
13 **Smith RJP**, Faroni A, Barrow JR, Soul J, Reid AJ. The angiogenic potential of CD271+ human adipose tissue-derived mesenchymal stem cells. *Stem Cell Res Ther* 2021; **12**: 160 [PMID: 33653407 DOI: 10.1186/s13287-021-02177-0]

14 **Mitsiadis TA**, Pagella P. Expression of Nerve Growth Factor (NGF), TrkA, and p75(NTR) in Developing Human Fetal Teeth. *Front Physiol* 2016; **7**: 338 [PMID: 27536251 DOI: 10.3389/fphys.2016.00338]

15 **Zhao X**, Ning L, Xie Z, Jie Z, Li X, Wan X, Sun X, Huang B, Tang P, Shen S, Qin A, Ma Y, Song L, Fan S, Wan S. The Novel p38 Inhibitor, Pamapimod, Inhibits Osteoclastogenesis and Counteracts Estrogen-Dependent Bone Loss in Mice. *J Bone Miner Res* 2019; **34**: 911-922 [PMID: 30615802 DOI: 10.1002/jbmr.3655]

16 **Colosimo A**, Rofani C, Ciraci E, Salerno A, Oliviero M, Maio ED, Iannace S, Netti PA, Velardi F, Berardi AC. Osteogenic differentiation of CD271(+) cells from rabbit bone marrow cultured on three phase PCL/TZ-HA bioactive scaffolds: comparative study with mesenchymal stem cells (MSCs). *Int J Clin Exp Med* 2015; **8**: 13154-13162 [PMID: 26550238]

17 **Xing Y**, Nie X, Chen G, Wen X, Li G, Zhou X, Tian W, Liu L. Comparison of P75 NTR-positive and -negative etcomesenchymal stem cell odontogenic differentiation through epithelial-mesenchymal interaction. *Cell Prolif* 2016; **49**: 185-194 [PMID: 27038014 DOI: 10.1111/cpr.12248]

18 **Li Z**, Zhang C, Weiner LP, Zhang Y, Zhong JF. Molecular characterization of heterogeneous mesenchymal stem cells with single-cell transcriptomes. *Biotechnol Adv* 2013; **31**: 312-317 [PMID: 23266308 DOI: 10.1016/j.biotechadv.2012.12.003]

19 **Chen Y**, Zhang Z, Yang X, Liu A, Liu S, Feng J, Xuan K. Odontogenic MSC Heterogeneity: Challenges and Opportunities for Regenerative Medicine. *Front Physiol* 2022; **13**: 827470 [PMID: 35514352 DOI: 10.3389/fphys.2022.827470]

20 **Tanay A**, Regev A. Scaling single-cell genomics from phenomenology to mechanism. *Nature* 2017; **541**: 331-338 [PMID: 28102262 DOI: 10.1038/nature21350]

21 **Yan H**, Ye Y, Zhao H, Zuo H, Li Y. Single-Cell RNA Sequencing for Analyzing the Intestinal Tract in Healthy and Diseased Individuals. *Front Cell Dev Biol* 2022; **10**: 915654 [PMID: 35874838 DOI: 10.3389/fcell.2022.915654]

22 **Li Y**, Ju S, Li X, Li W, Zhou S, Wang G, Cai Y, Dong Z. Characterization of the microenvironment of diabetic foot ulcers and potential drug identification based on scRNA-seq. *Front Endocrinol (Lausanne)* 2022; **13**: 997880 [PMID: 36686438 DOI: 10.3389/fendo.2022.997880]

23 **Liu X**, Xiang Q, Xu F, Huang J, Yu N, Zhang Q, Long X, Zhou Z. Single-cell RNA-seq of cultured human adipose-derived mesenchymal stem cells. *Sci Data* 2019; **6**: 190031 [PMID: 30806636 DOI: 10.1038/sdata.2019.31]

24 **Kirkwood PM**, Gibson DA, Smith JR, Wilson-Kanamori JR, Kelepouri O, Esnal-Zufiaurre A, Dobie R, Henderson NC, Saunders PTK. Single-cell RNA sequencing redefines the mesenchymal cell landscape of mouse endometrium. *FASEB J* 2021; **35**: e21285 [PMID: 33710643 DOI: 10.1096/fj.202002123R]

25 **Wang Z**, Li X, Yang J, Gong Y, Zhang H, Qiu X, Liu Y, Zhou C, Chen Y, Greenbaum J, Cheng L, Hu Y, Xie J, Yang X, Li Y, Schiller MR, Tan L, Tang SY, Shen H, Xiao HM, Deng HW. Single-cell RNA sequencing deconvolutes the in vivo heterogeneity of human bone marrow-derived mesenchymal stem cells. *Int J Biol Sci* 2021; **17**: 4192-4206 [PMID: 34803492 DOI: 10.7150/ijbs.61950]

26 **Bayarsaihan D**, Enkhmandakh B, Vijaykumar A, Robson P, Mina M. Single-cell transcriptome analysis defines mesenchymal stromal cells in the mouse incisor dental pulp. *Gene Expr Patterns* 2022; **43**: 119228 [PMID: 34915194 DOI: 10.1016/j.gep.2021.119228]

27 **Li J**, Wang Q, An Y, Chen X, Xing Y, Deng Q, Li Z, Wang S, Dai X, Liang N, Hou Y, Yang H, Shang Z. Integrative Single-Cell RNA-Seq and ATAC-Seq Analysis of Mesenchymal Stem/Stromal Cells Derived from Human Placenta. *Front Cell Dev Biol* 2022; **10**: 836887 [PMID: 35450295 DOI: 10.3389/fcell.2022.836887]

28 **Satija R**, Farrell JA, Gennert D, Schier AF, Regev A. Spatial reconstruction of single-cell gene expression data. *Nat Biotechnol* 2015; **33**: 495-502 [PMID: 25867923 DOI: 10.1038/nbt.3192]

29 **Kim S**, Kang D, Huo Z, Park Y, Tseng GC. Meta-analytic principal component analysis in integrative omics application. *Bioinformatics* 2018; **34**: 1321-1328 [PMID: 29186328 DOI: 10.1093/bioinformatics/btx765]

30 **Liberzon A**, Birger C, Thorvaldsdóttir H, Ghandi M, Mesirov JP, Tamayo P. The Molecular Signatures Database (MSigDB) hallmark gene set collection. *Cell Syst* 2015; **1**: 417-425 [PMID: 26771021 DOI: 10.1016/j.cels.2015.12.004]

31 **Yu G**, Wang LG, Han Y, He QY. clusterProfiler: an R package for comparing biological themes among gene clusters. *OMICS* 2012; **16**: 284-287 [PMID: 22455463 DOI: 10.1089/omi.2011.0118]

32 **Qiu X**, Hill A, Packer J, Lin D, Ma YA, Trapnell C. Single-cell mRNA quantification and differential analysis with Census. *Nat Methods* 2017; **14**: 309-315 [PMID: 28114287 DOI: 10.1038/nmeth.4150]

33 **Jin S**, Guerrero-Juarez CF, Zhang L, Chang I, Ramos R, Kuan CH, Myung P, Plikus MV, Nie Q. Inference and analysis of cell-cell communication using CellChat. *Nat Commun* 2021; **12**: 1088 [PMID: 33597522 DOI: 10.1038/s41467-021-21246-9]

34 **Fabian P**, Crump JG. Reassessing the embryonic origin and potential of craniofacial ectomesenchyme. *Semin Cell Dev Biol* 2023; **138**: 45-53 [PMID: 35331627 DOI: 10.1016/j.semcdb.2022.03.018]

35 **Colombo E**, Romaggi S, Medico E, Menon R, Mora M, Falcone C, Lochmüller H, Confalonieri P, Mantegazza R, Morandi L, Farina C. Human neurotrophin receptor p75NTR defines differentiation-oriented skeletal muscle precursor cells: implications for muscle regeneration. *J Neuropathol Exp Neurol* 2011; **70**: 133-142 [PMID: 21343882 DOI: 10.1097/NEN.0b013e3182084391]

36 **Mikami Y**, Suzuki S, Ishii Y, Watanabe N, Takahashi T, Isokawa K, Honda MJ. The p75 neurotrophin receptor regulates MC3T3-E1 osteoblastic differentiation. *Differentiation* 2012; **84**: 392-399 [PMID: 22906707 DOI: 10.1016/j.diff.2012.07.001]

37 **Yang K**, Wang Y, Ju Y, Li G, Liu C, Liu J, Liu Q, Wen X, Liu LC. p75 neurotrophin receptor regulates differential mineralization of rat ectomesenchymal stem cells. *Cell Prolif* 2017; **50** [PMID: 27672006 DOI: 10.1111/cpr.12290]

38 **Deng MJ**, Jin Y, Shi JN, Lu HB, Liu Y, He DW, Nie X, Smith AJ. Multilineage differentiation of ectomesenchymal cells isolated from the first branchial arch. *Tissue Eng* 2004; **10**: 1597-1606 [PMID: 15588419 DOI: 10.1089/ten.2004.10.1597]

39 **Zhang J**, Duan X, Zhang H, Deng Z, Zhou Z, Wen N, Smith AJ, Zhao W, Jin Y. Isolation of neural crest-derived stem cells from rat embryonic mandibular processes. *Biol Cell* 2006; **98**: 567-575 [PMID: 16719840 DOI: 10.1042/BC20060012]

40 **Wen X**, Liu L, Deng M, Zhang L, Liu R, Xing Y, Zhou X, Nie X. Characterization of p75(+) ectomesenchymal stem cells from rat embryonic facial process tissue. *Biochem Biophys Res Commun* 2012; **427**: 5-10 [PMID: 22982680 DOI: 10.1016/j.bbrc.2012.08.109]

41 **Liu Y**, Wang Z, Ju M, Zhao Y, Jing Y, Li J, Shao C, Fu T, Lv Z, Li G. Modification of COL1A1 in Autologous Adipose Tissue-Derived Progenitor Cells Rescues the Bone Phenotype in a Mouse Model of Osteogenesis Imperfecta. *J Bone Miner Res* 2021; **36**: 1521-1534 [PMID: 33950576 DOI: 10.1002/jbmr.4326]

42 **Malmgren B**, Andersson K, Lindahl K, Kindmark A, Grigelioniene G, Zachariadis V, Dahllöf G, Åström E. Tooth agenesis in osteogenesis imperfecta related to mutations in the collagen type I genes. *Oral Dis* 2017; **23**: 42-49 [PMID: 27510842 DOI: 10.1111/odi.12568]

43 **Boban I**, Jacquin C, Prior K, Barisic-Dujmovic T, Maye P, Clark SH, Aguila HL. The 3.6 kb DNA fragment from the rat Col1a1 gene promoter drives the expression of genes in both osteoblast and osteoclast lineage cells. *Bone* 2006; **39**: 1302-1312 [PMID: 16938497 DOI:

10.1016/j.bone.2006.06.025]
44 **Long F**. Building strong bones: molecular regulation of the osteoblast lineage. *Nat Rev Mol Cell Biol* 2011; **13**: 27-38 [PMID: 22189423 DOI: 10.1038/nrm3254]
45 **Liao J**, Hu N, Zhou N, Lin L, Zhao C, Yi S, Fan T, Bao W, Liang X, Chen H, Xu W, Chen C, Cheng Q, Zeng Y, Si W, Yang Z, Huang W. Sox9 potentiates BMP2-induced chondrogenic differentiation and inhibits BMP2-induced osteogenic differentiation. *PLoS One* 2014; **9**: e89025 [PMID: 24551211 DOI: 10.1371/journal.pone.0089025]
46 **Goto N**, Fujimoto K, Fujii S, Ida-Yonemochi H, Ohshima H, Kawamoto T, Noshiro M, Shukunami C, Kozai K, Kato Y. Role of MSX1 in Osteogenic Differentiation of Human Dental Pulp Stem Cells. *Stem Cells Int* 2016; **2016**: 8035759 [PMID: 27648077 DOI: 10.1155/2016/8035759]
47 **Lin W**, Zhu X, Gao L, Mao M, Gao D, Huang Z. Osteomodulin positively regulates osteogenesis through interaction with BMP2. *Cell Death Dis* 2021; **12**: 147 [PMID: 33542209 DOI: 10.1038/s41419-021-03404-5]
48 **Chen J**, Wang N, Zhang H, Zhang X, Zhao L, Zhu L, Li Z, Bei C. [Lentivirus-mediated silencing of P75 neurotrophin receptor combined with nerve growth factor overexpression and transfection of bone marrow mesenchymal stem cells combined with demineralized bone matrix for heterotopic osteogenesis]. *Zhongguo Xiu Fu Chong Jian Wai Ke Za Zhi* 2020; **34**: 1438-1445 [PMID: 33191703 DOI: 10.7507/1002-1892.202003166]
49 **Wang Y**, Yang K, Li G, Liu R, Liu J, Li J, Tang M, Zhao M, Song J, Wen X. p75NTR(-/-) mice exhibit an alveolar bone loss phenotype and inhibited PI3K/Akt/β-catenin pathway. *Cell Prolif* 2020; **53**: e12800 [PMID: 32215984 DOI: 10.1111/cpr.12800]
50 **Shan P**, Wang X, Zhang Y, Teng Z, Jin Q, Liu J, Ma J, Nie X. P75 neurotrophin receptor positively regulates the odontogenic/osteogenic differentiation of ectomesenchymal stem cells *via* nuclear factor kappa-B signaling pathway. *Bioengineered* 2022; **13**: 11201-11213 [PMID: 35485233 DOI: 10.1080/21655979.2022.2063495]
51 **Rosset EM**, Bradshaw AD. SPARC/osteonectin in mineralized tissue. *Matrix Biol* 2016; **52-54**: 78-87 [PMID: 26851678 DOI: 10.1016/j.matbio.2016.02.001]
52 **Castro-Muñozledo F**, Meza-Aguilar DG, Domínguez-Castillo R, Hernández-Zequinely V, Sánchez-Guzmán E. Vimentin as a Marker of Early Differentiating, Highly Motile Corneal Epithelial Cells. *J Cell Physiol* 2017; **232**: 818-830 [PMID: 27404216 DOI: 10.1002/jcp.25487]
53 **Wang H**, Ning T, Song C, Luo X, Xu S, Zhang X, Deng Z, Ma D, Wu B. Priming integrin α5 promotes human dental pulp stem cells odontogenic differentiation due to extracellular matrix deposition and amplified extracellular matrix-receptor activity. *J Cell Physiol* 2019; **234**: 12897-12909 [PMID: 30556904 DOI: 10.1002/jcp.27954]
54 **Du C**, Li Y, Xia X, Du E, Lin Y, Lian J, Ren C, Li S, Wei W, Qin Y. Identification of a novel collagen-like peptide by high-throughput screening for effective wound-healing therapy. *Int J Biol Macromol* 2021; **173**: 541-553 [PMID: 33493562 DOI: 10.1016/j.ijbiomac.2021.01.104]
55 **Mantesso A**, Sharpe P. Dental stem cells for tooth regeneration and repair. *Expert Opin Biol Ther* 2009; **9**: 1143-1154 [PMID: 19653863 DOI: 10.1517/14712590903103795]
56 **Li G**, Liu J, Wang Y, Yang K, Zhao M, Xiao Y, Wen X, Liu L. LNGFR targets the Wnt/β-catenin pathway and promotes the osteogenic differentiation in rat ectomesenchymal stem cells. *Sci Rep* 2017; **7**: 11021 [PMID: 28887537 DOI: 10.1038/s41598-017-11555-9]

World Journal of Stem Cells

Submit a Manuscript: https://www.f6publishing.com

World J Stem Cells 2023 June 26; 15(6): 607-616

DOI: 10.4252/wjsc.v15.i6.607

ISSN 1948-0210 (online)

ORIGINAL ARTICLE

Basic Study

Culture and identification of neonatal rat brain-derived neural stem cells

Qing-Zhong Zhou, Xiao-Lan Feng, Xu-Feng Jia, Nurul Huda Binti Mohd Nor, Mohd Hezery Bin Harun, Da-Xiong Feng, Wan Aliaa Wan Sulaiman

Specialty type: Cell Biology

Provenance and peer review: Unsolicited article; Externally peer reviewed.

Peer-review model: Single blind

Peer-review report's scientific quality classification

Grade A (Excellent): A
Grade B (Very good): B
Grade C (Good): 0
Grade D (Fair): 0
Grade E (Poor): 0

P-Reviewer: Mekinian A, France; Steiger P, Switzerland

Received: March 21, 2023
Peer-review started: March 21, 2023
First decision: April 9, 2023
Revised: April 20, 2023
Accepted: April 27, 2023
Article in press: April 27, 2023
Published online: June 26, 2023

Qing-Zhong Zhou, Da-Xiong Feng, Department of Orthopedics, The Affiliated Hospital of Southwest Medical University, Luzhou 646000, Sichuan Province, China

Qing-Zhong Zhou, Wan Aliaa Wan Sulaiman, Department of Neurology, Faculty of Medicine and Health Sciences, Universiti Putra Malaysia, Serdang 43400, Selangor, Malaysia

Xiao-Lan Feng, Department of Radiology, The Affiliated Hospital of Southwest Medical University, Luzhou 646000, Sichuan Province, China

Xu-Feng Jia, Department of Orthopedics, The Peoples' Hospital of Jianyang City, Jianyang 641400, Sichuan Province, China

Nurul Huda Binti Mohd Nor, Department of Human Anatomi, Faculty of Medicine and Health Sciences, Universiti Putra Malaysia, Serdang Selangor, 43400, Malaysia

Mohd Hezery Bin Harun, Department of Orthopedics, Faculty of Medicine and Health Sciences, Universiti Putra Malaysia, Serdang 43400, Selangor, Malaysia

Corresponding author: Wan Aliaa Wan Sulaiman, BMedSci, MBChB BCh BAO, MRCP(UK), FRCP (Edin), Associate Professor, Department of Neurology, Faculty of Medicine and Health Sciences, Universiti Putra Malaysia, Serdang 43400, Selangor, Malaysia.
wanaliaa@upm.edu.my

Abstract

BACKGROUND

Timing of passaging, passage number, passaging approaches and methods for cell identification are critical factors influencing the quality of neural stem cells (NSCs) culture. How to effectively culture and identify NSCs is a continuous interest in NSCs study while these factors are comprehensively considered.

AIM

To establish a simplified and efficient method for culture and identification of neonatal rat brain-derived NSCs.

METHODS

First, curved tip operating scissors were used to dissect brain tissues from new born rats (2 to 3 d) and the brain tissues were cut into approximately 1 mm^3

sections. Filter the single cell suspension through a nylon mesh (200-mesh) and culture the sections in suspensions. Passaging was conducted with TrypL™ Express combined with mechanical tapping and pipetting techniques. Second, identify the 5th generation of passaged NSCs as well as the revived NSCs from cryopreservation. BrdU incorporation method was used to detect self-renew and proliferation capabilities of cells. Different NSCs specific antibodies (anti-nestin, NF200, NSE and GFAP antibodies) were used to identify NSCs specific surface markers and muti-differentiation capabilities by immunofluorescence staining.

RESULTS

Brain derived cells from newborn rats (2 to 3 d) proliferate and aggregate into spherical-shaped clusters with sustained continuous and stable passaging. When BrdU was incorporated into the 5th generation of passaged cells, positive BrdU cells and nestin cells were observed by immunofluorescence staining. After induction of dissociation using 5% fetal bovine serum, positive NF200, NSE and GFAP cells were observed by immunofluorescence staining.

CONCLUSION

This is a simplified and efficient method for neonatal rat brain-derived neural stem cell culture and identification.

Key Words: Neonatal rats; Brain-derived neural stem cells; Culture; Identification

Core Tip: How to harvest sufficient neural stem cells (NSCs) is a basic requirement for the study and clinical application of NSCs. This study describes a simplified and efficient method for neonatal rat brain-derived NSC culture and identification comprehensively considering the influencing factors including timing of passaging, passage number, passaging approaches and methods for cell identification. It demonstrates that combination of TrypL™ Express and mechanical tapping and pipetting techniques makes a more efficient way of passaging. The optimal timing for NSC passage is on the fourth to fifth day of primary or passage NSC culture.

Citation: Zhou QZ, Feng XL, Jia XF, Mohd Nor NHB, Harun MHB, Feng DX, Wan Sulaiman WA. Culture and identification of neonatal rat brain-derived neural stem cells. *World J Stem Cells* 2023; 15(6): 607-616
URL: https://www.wjgnet.com/1948-0210/full/v15/i6/607.htm
DOI: https://dx.doi.org/10.4252/wjsc.v15.i6.607

INTRODUCTION

Spinal cord injuries (SCIs) are associated with high morbidity, disability and medical costs around the world[1-3]. Prevention, treatment and rehabilitation of SCIs remains one of the global health issues. Pathophysiological basis for sensory, motor and sphincter dysfunction below the neurological level of injury is the substantial variations, necrosis and loss of neurons along with ruptured tracts of spinal cord as well as demyelination induced by primary and/or secondary SCIs[4,5]. Therefore, the research fucus on the key to promoting recovery of function following SCIs falls on how to replenish the lost neurons and boost the regeneration of axis cylinder and myelin sheath. It should be noted that neural stem cells (NSCs) have the capacity to self-renew and proliferate, and differentiate into nerve cells of central nervous system including neuron, astrocyte and oligodendrocyte[6]. Hence, by replenishing neurons, forming axis cylinder, increasing oligodendrocyte and reconstructing medullary sheath and then remolding the injured structure and function of spinal cord, NSCs replacement as a possible therapeutic approach could bring hope to SCI patients. In view that rapid and simplified accesses to a large number of pure NSCs for research are needed, it is necessary to develop a method for NSC amplification, culture, purification and identification *in vitro* to provide sufficient-necessary condition for further investigation of NSCs.

The present study cultured, passaged and harvested large amounts of high pure NSCs with growth factor containing serum-free medium using TrypLE™ Express digestion method combined with mechanical disassociation method[4,7,8], which provide the platform for the further study of NSCs.

MATERIALS AND METHODS

Rats

In this study, Brain-derived NSCs were abstracted from several two-to-three-day old newborn SD rats provided by Southwest Medical University Animal Resource Center.

Reagents

Hyclone DEME/F12 (1:1); Hyclone standard fetal bovine serum; Peprotech EGF (20 μg); Peprotech bFGF (10 μg); Gibco B27 Plus Supplement (50×); Gibco TrypL™ Express (1×); rabbit anti-nestin polyclonal antibody (Wuhan Boster Biological Technology, Ltd.); mouse anti-NSE monoclonal antibody and mouse anti-GFAP monoclonal antibody (Wuhan Boster Biological Technology, Ltd.); RBITC-labeled goat anti-mouse IgG (Beijing Biosynthesis Biotechnology Co., Ltd.); RBITC-labeled goat anti-rabbit IgG (Beijing Biosynthesis Biotechnology Co., Ltd.).

Preparation of serum free medium for NSC culture

Take 100 mL of DMEM/F12 (1:1) and add EGF (20 ng/mL), bFGF (20 ng/mL), B27 Plus Supplement (2%), glutamine (2 mmol/L) and 1 mL of penicillin-streptomycin solution (100 U/mL). NaOH filtered with 0.22 μm microporous membrane filter were used to adjust PH of the solution between 7.2 and 7.4. After preparation, the medium was stored at 4°C. Serum free medium (SFM) should be kept fresh. A weekly dosage of 100 mL for on preparation is generally recommended.

Primary culture, passage, cryopreservation, resuscitation and identification of NCSs

Preparation of extracts and primary NSC culture: Newborn SD rats (2–3 d old) were selected and immersed in 75% alcohol for 10 min for disinfection. In supine position, the rats were fixed to foam board and placed on the clean bench with cranial cavity exposed. Brain tissues were isolated and placed in sterilization incubators containing phosphate-buffered saline (PBS) (0.01 M, PH 7.2, pre-warmed to 37°C, 10 min, the same below) for washing to remove blood stains on the surface. Then pia mater as well as choroid plexus tissues were removed under a dissecting microscope. The dissected brain tissues were washed and transferred to a new sterilization incubator. Using curved tip operating scissors, dissected brain tissues were cut into approximately 1 mm^3 sections and were transferred to centrifuge tubes (10 mL, the same below) using sterile pipettes. Centrifuge the sections at 1000 rpm for 1 min and remove the supernatant. Save the cerebral cortex in three separate tubes, each containing 1 mL of mixed enzyme, shake them gently for 5 min in a 37°C water-bath and centrifuge them at 1000 rpm for 5 min, and then remove the supernatant. Add 5% fetal bovine serum, pipette and tap gently 10 times using pipettes, shake gently in a 37°C water-bath, centrifuge for 5 min at 1800 rpm, and remove the supernatant. Then add DMEM/F12 (1:1), pipette and tap gently 20 times using pipettes, filter using stainless-steel cell strainers (200-mesh), centrifuge for 5 min at 1000 rpm and remove the supernatant. Use 0.5 mL of SFM to resuspend cells. Pipette and tap the cells gently and form single-cell suspensions. Seed the cells at a rate of 1 × 10^6/mL (cell density determined by trypan blue method excluding dead cells) in 25 mL glass culture flasks and cultured in carbon dioxide constant temperature incubators (stable temperatures of 37°C, saturated humidity, a CO_2 level of 5%). Centrifuge the cells for 5 min at 1000 rpm every other day or every two days depending on how the cells developed and refresh half of the media with fresh growth media. Approximately, four or five days later, initiate passaging. Observe and record cell growth status under inverted phase contrast microscope every day including medium color, impurities in medium, cell refraction, density, size of neurosphere formation and neurosphere refraction.

Passaging of NSCs: After four to five days of primary culture, which is dependent on the growth process of cell and neurospheres, gather all neurospheres and culture solution and place in a 15 mL cone shaped tube, centrifuge for 5 min at 1000 rpm and remove the supernatant. Add 1 mL of TrypLE™, pipette cells gently using pipettes, shake them gently for 5 min in a 37°C water-bath and centrifuge them at 1800 rpm for 5 min, and then remove the supernatant. Add 0.5 mL of SFM to resuspend cells. Using 1000 μL pipettes, tap the cells gently 10 times (for 200 μL pipettes, approximately 20 times). Seed the cells at a rate of 1 × 10^6/mL (cell density determined by trypan blue method excluding dead cells) in a 25 mL glass culture flask and cultured in the above described constant temperature incubators (stable temperatures of 37°C, saturated humidity, a CO_2 level of 5%).

Cryopreservation and resuscitation of NSCs: Add 1 mL of freshly prepared cell freezing medium (DMEM/F12:fetal bovine serum:DMSO = 7:2:1) to the single-cell suspensions. Adjust the cell density to 5×10^6/mL, and preserve the suspension in a 4°C refrigerator for three hours. Place the cryovials in a small plastic storage box and keep the box immediately in a −80°C gas-phase liquid nitrogen freezer overnight and finally cryopreserve the cryovials in a liquid-phase liquid nitrogen freezer. For cell resuscitation, remove cryovials from the liquid-phase liquid nitrogen freezer and place the cryovials in a 37°C water-bath for rapid melting. Transfer the cells to centrifuge tubes and add 4 mL of basal media. Centrifuge the cells for 5 min at 1000 rpm and remove the supernatant. Add SFM and resuspend cells. Seed the cells at a rate of 1 × 10^6/mL (cell density determined by trypan blue method excluding dead cells) in 25 mL glass culture flasks and cultured in the above described constant temperature incubators.

Identification of NCSs: Identify the 5th generation of passaged NSCs and the revived NSCs from cryopreservation. Use bromodeoxyuridine (BrdU) incorporation method to detect the self-renew and proliferation abilities of cells. Use diverse neurocyte-specific antibodies such as anti-nestin, anti-NF200, anti-NSE and anti-GFAP antibodies to examine NSC specific surface markers and muti-differentiation capabilities by immunofluorescence staining.

BrdU incorporation method for the detection of the proliferation of NSCs: (1) At 24 h after the culture of 5th generation of passaged NSCs, add BrdU to SFM to make BrdU reach a concentration of 10 μmol/L. Continue to culture the cells for five days and seed the NSCs cultured in suspensions at a rate of 1 × 10^6/mL (500 μL) in a carbon dioxide constant temperature incubator containing 24-well culture plates with polylysine coated coverslips (stable temperatures of 37°C, moderate saturated humidity, a CO_2 level of 5%) for four hours; (2) Draw the solution and gently wash 3 × 5 min with PBS (0.01 mol/L, PH7.2); (3) Add 4% paraformaldehyde for a fixation for 15 min at room temperatures; (4) Draw the stationary fluids and wash 3 × 5 min with PBS (0.01 mol/L, PH7.2); (5) Use 37°C blocking buffer (10% sheep serum and 0.3% Triton) for 1 h closed incubation (150 μL per well, almost spread the coverslips) and then draw the stationary fluids.

Add 150 μL of mouse anti-BrdU primary monoclonal antibody (dilute the fluids with PBS to adjust the concentration to 1:200) and cover coverslips. Use PBS (0.01mol/L, PH7.2) as positive control to replace mouse anti-BrdU primary monoclonal antibody. Continue to culture the cells in a 37°C constant temperature incubator for two hours; (6) Blot fluids in the last step and wash 3 × 5 min with PBS (0.01 mol/L, PH7.2); (7) Add FITC labeled goat anti-mouse IgG second antibody (dilute the fluids with PBS to adjust the concentration to 1:40) (cells should be protected against exposure to light for each of the following steps). Continue to culture the cells in a 37°C constant temperature incubator for one hour; (8) Blot the second antibody and wash 3 × 5 min with PBS (0.01 mol/L, PH7.2); (9) Add 20 μL of anti-fluorescence quencher over the slide; and (10) Lift the coverslip using a self-made right-angled tip needle and then press it with the side containing the cells down avoiding creating air bubbles. View the cells under a fluorescence microscope, take photos and make records.

Nestin immunofluorescence staining: (1) Take a small amount of 5th generation of cultured neuro-sphere containing NSCs and seed them in a carbon dioxide constant temperature incubator containing 24-well culture plates with polylysine coated coverslips (stable temperatures of 37°C, moderate saturated humidity, a CO_2 level of 5%) for four hours; (2) Discard the solution and wash gently 3 × 5 min with PBS; (3) Add 4% paraformaldehyde for a stationary phase for 15 min at room temperatures; (4) Discard the stationary liquid and wash gently 3 × 5 min with PBS; (5) Use 37°C blocking buffer (10% sheep serum and 0.3% Triton) for 1 h closed incubation (150 μL per well, almost spread the coverslips) and then blot the stationary fluids. Add rabbit anti-nestin monoclonal primary antibody (dilute the fluids with PBS solution to adjust the concentration to 1:200). The primary antibody was substituted for PBS solution as a negative control. Continue to culture the cells in a 37°C constant temperature incubator for two hours; (6) Discard the liquid used in the last step and gently wash 3 × 5 min with PBS (0.01 M, PH7.2); (7) Add RBITC labeled goat anti-rabbit IgG second antibody (dilute the fluids with PBS solution to adjust the concentration to 1:40) (avoid light exposure for each of the following steps). Then culture the cells in a 37°C constant temperature incubator for one hour; (8) Blot the second antibody. Wash 3 × 5 min with PBS (0.01 mol/L, PH7.2); (9) Add DAPI staining solution (150 μL per well, almost spread the coverslips) for 3 min at room temperatures and then blot the DAPI staining solution. Wash 3 × 5 min with PBS (0.01mol/L, PH7.2). Add 20 μL of anti-fluorescence quencher over the slide; and (10) Lift the coverslip and then press it with the side containing the cells down on the slide containing 20 μL of anti-fluorescence quencher (Be careful to avoid creating air bubbles).

Observe the cells under a fluorescence microscope, take photos and make records. Differentiation of NSCs and immunofluorescence staining of GFAP, NF200 and NSE. (1) Using SFM containing 5% fetal bovine serum, seed the 5th generation of NSCs in 24-well culture plates with polylysine coated coverslips and culture the cells for 5 d; Repeat steps (2), (3) and (4) in the section of BrdU incorporation method for the detection of the proliferation of NSCs or in nestin immunofluorescence staining; (5) Use 37°C blocking buffer (0.3% Triton X-100 and 10% sheep serum) for 1 h closed incubation (150 μL per well, almost spread the coverslips, similarly hereinafter) and then discard the stationary fluids. Add mouse anti-GFAP monoclonal antibody, mouse anti-NSE monoclonal antibody and mouse anti- NF200 monoclonal antibody, respectively (all as primary antibody, dilute the fluids with PBS to adjust the concentration to 1:200), and the primary antibody was substituted for prepared PBS solution as a negative control and then cultured in the above described constant temperature incubators for two hours; (6) Discard the liquid in the last step, and wash 3 × 5 min with prepared PBS; (7) Add RBITC-labeled goat anti-mouse IgG secondary anti-body (dilute the fluids with PBS to adjust the concentration to 1:40), and incubate the cell in a above mentioned incubator for 1 h; Repeat steps (8), (9) and (10) in the section of BrdU incorporation method for the detection of the proliferation of NSCs or in nestin immunofluorescence staining.

RESULTS

Development and identification of NSCs

The first-generation cells derived from newborn SD rats appear small, equal sized, glossy spheres. At 24 h after the primary culture, larger amounts of cells aggregate in the middle of potion of the growth medium. These single floating cells can differentiate and renew (Figure 1A). There are also plenty of glossy, spherical-shaped, adherent single cells at the bottom of the culture bottle. Moreover, many structural looseness, highly refractile, spherical-shaped clusters and membraniform flocculation also exist in the culture medium, which are considered as clumps of dead cells and unelim-inated tissues such as blood vessels and pia mater, respectively. At 2 to 3 d after the primary culture, several and even dozens of translucent, highly refractile, spherical-shaped or thyrsiform cell clusters are discovered (Figure 1B). What's more, only a small amount dead cell clusters were left in the culture medium. At four to five days after the primary culture (Figure 1C), the cell mass bulks up to a spherical shape when large numbers of cell clusters aggregate and form translucent slippery spheres under an inverted phase-contrast microscope. However, refractivity at the center of the sphere decreases and few aggregated dead cells are observed. Compared with that of neurospheres at five days after the primary culture, the volume of neurospheres at eight days after the primary culture is obviously big and the refractivity is poor and it shows dark brown in most parts of the sphere center (Figure 1D). Passaging conducted at that time only dissociates neurospheres into smaller cell clumps and few single floating cells rather than single-cell suspensions. It is speculated that this is associated with tight cell-cell junction around the neurospheres. Moreover, many small sized adherent cells are observed at two days after the passaging with small quantity of low density single floating cells. Adherent differentiation occurs in plenty of large volume neurospheres during the continuous culture.

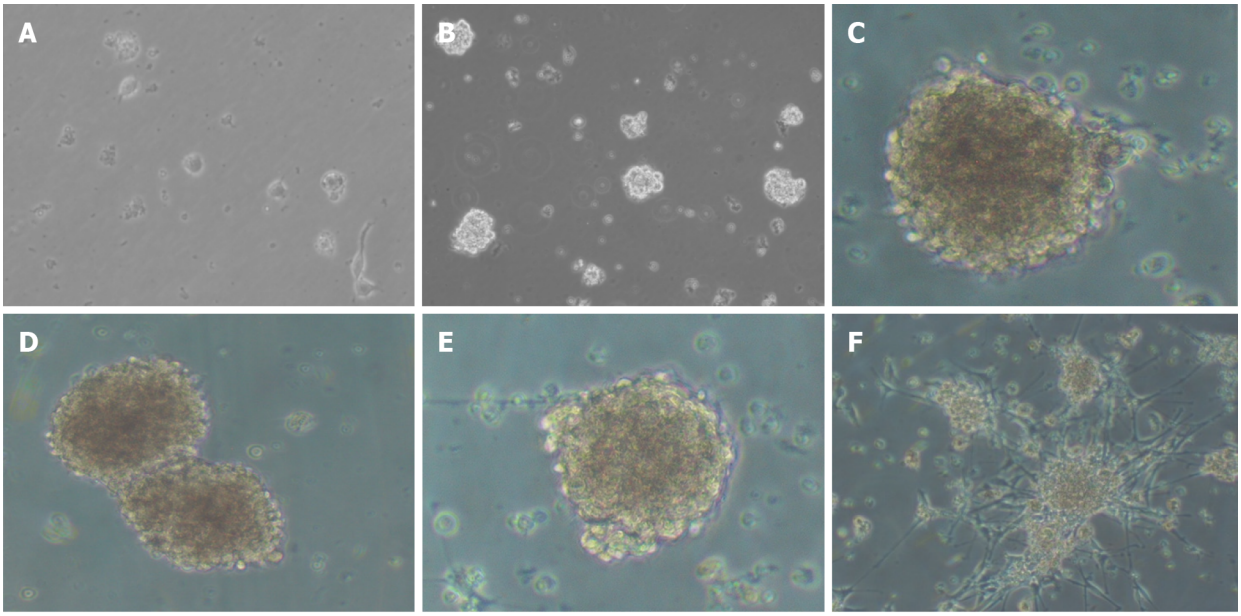

DOI: 10.4252/wjsc.v15.i6.607

Figure 1 Development of neural stem cells derived from newborn rats (inverted phase-contrast microscope). A: At 24 h after the primary culture (100×); B: 3 d after the primary culture (100×); C: 5 d after the primary culture (100×); D: 8 d after the primary culture (100×); E: 4 d after 5 passages (×200); F: 5 d after induction of dissociation (×200).

Generally, there are two methods of cell dissociation: mechanical and enzymatic. It is discovered that it is hard to control enzyme concentration and time, which easily lead to cell death. Comparatively, TrypLE™ Express digestion method combined with mechanical disassociation method can harvest sufficient normomorph, uniform size single floating cells with glossy cytoplasm and there are relatively few cell debris and impurities in the culture medium. In addition, medium-sized cloned neurospheres in good shape can be observed in the passaged NSC culturation (Figure 1E). At four hours after the induction of dissociation of 5th generation of passaged NSCs using 5% fetal bovine serum, adherent neurospheres and gradual migration of cells away from neurospheres are observed. At approximately five days after the induction of dissociation, spheres become flattened and form various shaped cells surrounding the neurospheres. At approximately five days after the induction of dissociation, the spheres flatten and make up lots of various shapes of cells. These cells connect to each other into a mesh-structure (Figure 1F).

Identification of NCSs

The incorporation of BrdU into the 5th generation of passaged cells showed positive after BrdU immunofluorescence staining (green fluorescence, Figure 2A) and nestin immunofluorescence staining (red fluorescence, Figure 2B). At five days after the induction of dissociation of 5th generation of passaged cells using 5% fetal bovine serum, NF200 (green fluorescence, DAPI nucleic acid stain revealed the blue fluorescent cell nucleus, Figure 2C), NSE (red fluorescence, blue fluorescent obtained with DAPI nucleic acid stain, Figure 2D) and GFAP (red fluorescence, DAPI nucleic acid stain revealed the blue fluorescent cell nucleus, Figure 2E) positive immunoreactivities were found.

DISCUSSION

Since 1990s, many researchers have demonstrated that NSCs are widely present in central nervous system (CNS) including spinal cord[6,9-17]. NSCs not only have the probabilities of division, regeneration proliferation and multidirectional differentiation (differentiate into nearly all types of CNS nerve cells such as neuron and glial cell), but also exhibit low immunogenicity and good histocompatibility[6,9-17]. This refutes the theory that the damaged cells are unable to be regenerated and repaired following the injuries to the nerve and the spinal cord, and provides new hope to the reconstruction of structure and function in CNS disorders such as SCIs and cerebral injuries[6,18]. NSCs, as the seed cells enhancing CNS regeneration, spontaneously become cores and foundation of neurological research. Efficient approaches for enhancing pure NSC yield in the research thus becomes crucial. The present study established a method for NSC amplification, culture, purification and identification *in vitro* to provide sufficient-necessary condition for further investigation of NSCs. Cell culture technology is the basic premise for the investigation of NSCs. Mature techniques for the isolation and culture of NSCs have been developed. In addition to proving the presence of NSCs and its potential of self-renewal and multidirectional differentiation, Reynolds and Weiss *et al*[9] also demonstrated that NSCs could proliferate massively *in vitro*, which establish crucial conditions for future investigation of NSCs. However, application of methods for *in vitro* amplification of stem cells is currently restricted to CNS. By contrast, cloning of monolayer cells[6,19] offers an alternative approach for NSC culture. This approach is widely used because using this approach we can not only derive

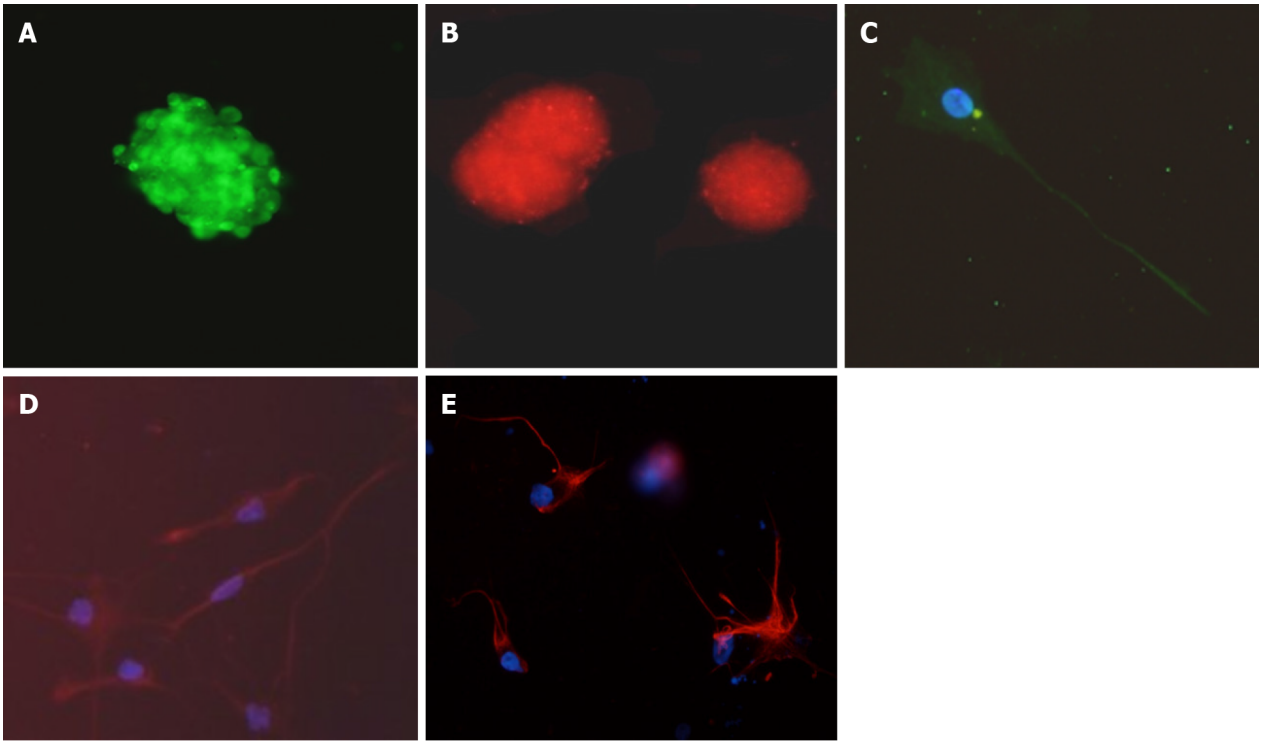

DOI: 10.4252/wjsc.v15.i6.607 **Copyright** ©The Author(s) 2023.

Figure 2 Immunofluorescence staining. A: BrdU immunofluorescence staining (green fluorescence, ×100); B: Nestin immunofluorescence staining (red fluorescence, ×100); C: NF200 + DAPI immunofluorescence staining (green fluorescence refers to NF200, blue fluorescence refers to DAPI, ×200); D: NSE + DAPI immunofluorescence staining (green fluorescence refers to NSE, blue fluorescence refers to DAPI, ×200); E: GFAP + DAPI immunofluorescence staining (green fluorescence refers to GFAP, blue fluorescence refers to DAPI, ×200).

an abundant amount of pure NSCs in a short time but also determine the differentiation capacity for a single NSC or its precursor cells.

For the timing of NSC passaging, the present study found that although passaging at two-to-three-day primary culture could facilitate the dissociation of neurospheres and formation of single-cell suspensions, the number of single cells derived was unsatisfactory at low densities which was not conductive to amplification and proliferation of NSCs after passage. Passaging performed when primary NSCs are cultured for seven to eight days could only dissociate neurospheres into small clusters of cells with a small amount of single floating cells instead of single-cell suspensions, which was presumably related to the tight junctions between peripheral neurosphere cells[20]. Moreover, small clusters of adherent cells with small portion of low density single floating cells were discovered after only two days of passage. Differentiation of adherent large neurospheres occurred after a continued cultivation. The observation of nine-to-ten-day primary NSC culture revealed that differentiation occurred in plenty of adherent large neurospheres with lots of dead cells, which also inhibits passaging. Comparatively, when passaging was performed after four to five days of primary culture, it not only promotes easy generation of single-cell suspensions dissociated from neurospheres but also harvests sufficient single floating cells with fewer dead cells and improved amplification and proliferation capabilities of NSCs. It follows that the optimal timing for NSC passage is after four-to-five-day primary or passage NSC culture. During the progress of *in vitro* culture, junctions can be formed between NSCs, which assemble to form neurospheres, through cytoskeletal protein and calnexin induced cell-cell adhesion mediation[20]. For neurospheres formed through primary culture or passage culture carried out for two to three days, the junction between NSCs is relatively loose making dissociation and formation for single floating cells easy. However, an analysis of the grow curve over this period displayed that passaging which is carried out when NSCs entered the logarithmic growth phase from the incubation phase might destroy the rapid amplification of NSCs resulting in passaged NSCs' repeated incubating and missing the optimal timing for amplification and at last failure to yielding sufficient NSCs in a short time. On the fourth to fifth day of primary culture or subculture, the number of NSCs increased significantly, the volume of neurospheres grew bigger and cell-cell junctions became tight when the junctions were still able to be dismantled by some means to obtain single cells comfortably. Notably, cell culture gradually reached a plateau period with anchoring cell-cell junctions over time. Oppositely, when the primary or passage culture last for seven to eight days, cell-cell junctions would become so tight that it was difficult to cleave or dissociate. Forced disconnection might end up with NSC damage, dissolution, death, adherence and differentiation. Furthermore, it was observed that the number of neurospheres decreased with their increasing volume suggesting the bulked volume of neurospheres might arise from neurosphere fusion instead of large amplification of NSCs. This can be interpreted as with the increasing volume of neurospheres, it is difficult for the cells within the spheres to contact the culture medium, which then prevents cells within the spheres from absorbing nutrition and affecting the process of metabolism, causing decline in the proliferation abilities of cells within the neurospheres,

death of a large number of cells and generation of necrotic cores[21]. From this view, balance should be reached between easy dissociation of neurospheres into single cells and rapid amplification of NSCs without damaging the proliferation abilities of cells within spheres by the excessive volume of neurospheres or causing death during the choice of timing for NSC passage. After summarizing the results of experiments, it is believed that the optimal timing for NSC passage is on the fourth to fifth day of primary or passage NSC culture.

Currently, the commonly used methods for passaging are enzymatic digestion method and mechanical method. After analyzing the investigations[4,7,8], the present study discovered that: (1) Although mechanical method alone is easy to operate and needs a very few of centrifugation, the force and times of tapping and pipetting is difficult to control and it increases the probability of mechanical damage to cells, which is not conducive to the experimental operation; (2) for enzymatic digestion method, trypsin is mainly used. However, the effect of trypsin in digestion is likely to cause chemical damage to NSCs. Moreover, usage of serum or enzyme inhibitor to counteract the digestive effect of trypsin may reduce the vitality and proliferation rate of NSCs and then influence the experimental results; (3) concerning the combination of enzymatic digestion method and mechanical tapping and pipetting method, in spite of a very few of blasting is needed and small scale of blasting can dissociate neurospheres into single-cell suspensions, it does not elevate the number of single cells while the amplification capability of NSCs and number of neurospheres decrease significantly; and (4) in terms of TrypL™ Express digestion method combined with mechanical tapping and pipetting method, TrypL™ Express, a high purity recombinant enzyme, has trypsin-like property, which cleaves peptide bonds on the C-terminal sides of lysine and arginine. TrypL™ Express has high thermostability compared with trypsin. There is no need to use serum or enzyme inhibitor to compromise its digestive effect. Instead, the effect of TrypL™ Express is mild with less toxicity. However, the action of TrypL™ Express should not last long. This study used TrypL™ Express combined with mechanical tapping and pipetting methods as the passaging method. Using this passaging method, sufficient regular shaped, even sized sheen floating single cells were harvested. What's more, cell culture medium is clear with few fragments and elemental impurities, and NSCs holds vigorous growth and proliferation abilities. After observing the process of NSC culture post passaging, it discovered proper sized and good shaped colony-like neurospheres. Based on this, this study recommend using TrypL™ Express combined with mechanical tapping and pipetting method as the method for NSCs passaging.

Additionally, immunofluorescence staining was used to identify whether the cultured cells derived from newborn rats' brains were NSCs. The 5th generation of passaged cells showed positive after both BrdU immunofluorescence staining and nestin immunofluorescence staining. BrdU, a thymidine analog, can incorporate into newly synthesized DNA during the S-phase of the cell cycle[22]. Its property of continuous self-replication and self-reproduction by stem cells makes it take in labeled Brdu during replication. Thus, when immunocytochemical detection is carried out, BrdU positive suggests the cells are in the division and proliferation phrase. Accordingly, NSCs' potential of division and proliferation can be identified by Brdu detention. Nestin, also called NES, is a major cytoskeletal protein in stem cells in the mammalian CNS and its expression is inversely associated with cell differentiation[23-25]. Nestin is a specific biomarker for NSCs and functions as one of factors to identify NSCs. However, nestin is also expressed in pancreatic progenitor cells and endodermal cells. Therefore, nestin positive cells are not necessarily NSCs. The identification of NSCs cannot only based on a certain feature. Apart from nestin immunofluorescence staining, specific biomarkers for NSC differentiation should be considered. The present study selected neuron-specific biomarkers NF200 and NSE and astrocyte-specific biomarker GFAP respectively for the identification of muti-differentiation of NSCs. This study used immunofluorescence staining for the detection of cultured cells derived from newborn rat brains in respect of the above described some characteristics of NSCs. It was observed that the 5th generation of passaged culture cells showed BrdU positive after BrdU immunofluorescence staining and nestin positive after nestin immunofluorescence staining. NF-200, NSE, GFAP positive cells were discovered following immunofluorescence staining at five days after induction of dissociation was performed in 5% fetal bovine serum. This implied that the cultured cells fulfil the criteria for NSC identification - expression of nestin, abilities of differentiation, renewal and proliferation and moreover the capabilities of dissociation. The composition of all these factors can demonstrate the cultured cells are NSCs.

There still are limitations on the development of methodologies to efficiently isolate, culture, and identify NSCs *in vitro*, and evaluating these obtained NSCs is the precondition for its clinical application. Further studies should try to find relevant influencing factors behind these issues.

CONCLUSION

Above all, the approaches used in this study yields sufficient purified NSCs, which then are employed for the further study of NSCs.

ARTICLE HIGHLIGHTS

Research background

The present study explores to establish a simplified and efficient method for culture and identification of neural stem cells (NSCs) derived from newborn rats in the aspects of timing of passaging, passage number, passaging approaches and methods for cell identification.

Research motivation

The study of NSCs is crucial for it will provide important insight into understanding and treating brain disorders. Efficient way to harvest sufficient neural stem cells will facilitate the use of NSCs in clinical scenarios.

Research objectives

This study aimed to explore a more effective protocol for culturing and identifying NSCs derived from newborn rats.

Research methods

Passaging of brain tissues sections dissected from new born rats (2 to 3 d) was conducted using TrypL™ Express combined with mechanical tapping and pipetting techniques. After five passages, NSCs as well as the revived NSCs from cryopreservation were identified. BrdU incorporation method was used to detect self-renew and proliferation capabilities of cells. Different NSCs specific antibodies (anti-nestin, NF200, NSE and GFAP antibodies) were used to identify NSCs specific surface markers and muti-differentiation capabilities with immunofluorescence staining.

Research results

With TrypL™ Express combined with mechanical tapping and pipetting techniques, spherical-shaped cell clusters were successfully obtained. When BrdU was incorporated into the 5th generation of passaged cells, positive BrdU cells and nestin cells were observed by immunofluorescence staining. After induction of dissociation using 5% fetal bovine serum, positive NF200, NSE and GFAP cells were observed by immunofluorescence staining.

Research conclusions

The present study developed a simplified and efficient method for neonatal rat brain-derived neural stem cell culture and identification.

Research perspectives

First, there still are limitations on the development of methodologies to efficiently isolate, culture, and identify NSCs *in vitro*. Second, evaluating these obtained NSCs is the precondition for its clinical application. Further studies should try to find relevant influencing factors behind these issues.

FOOTNOTES

Author contributions: Zhou QZ designed the study; all authors contributed to the data collect and manuscript writing; all authors have read and approve the final manuscript.

Supported by Project of Sichuan Department of Science and Technology, No. 2016PJ552; the Project of Luzhou Department of Science and Technology, No. 2016-R-70(18/24); the Project of Southwest Medical University of Science and Technology, No.15073 and 2015-YJ021; and Orthopaedic diseases (Shang Antong) special research Project of Sichuan Medical Association, No. 20220206070192.

Institutional animal care and use committee statement: This study was approved by the Institutional Animal Care and Use Committee of Southwest Medical University.

Conflict-of-interest statement: The authors declare no conflict of interest.

Data sharing statement: No additional data are available.

ARRIVE guidelines statement: The authors have read the ARRIVE Guidelines, and the manuscript was prepared and revised according to the ARRIVE Guidelines.

Country/Territory of origin: China

ORCID number: Wan Aliaa Wan Sulaiman 0000-0003-4969-0308.

S-Editor: Wang JL
L-Editor: A
P-Editor: Liu JH

REFERENCES

1 **Post MW**, van Leeuwen CM. Psychosocial issues in spinal cord injury: a review. *Spinal Cord* 2012; **50**: 382-389 [PMID: 22270190 DOI: 10.1038/sc.2011.182]

2 **Gomes-Osman J**, Cortes M, Guest J, Pascual-Leone A. A Systematic Review of Experimental Strategies Aimed at Improving Motor Function after Acute and Chronic Spinal Cord Injury. *J Neurotrauma* 2016; **33**: 425-438 [PMID: 26415105 DOI: 10.1089/neu.2014.3812]

3 **Ma VY**, Chan L, Carruthers KJ. Incidence, prevalence, costs, and impact on disability of common conditions requiring rehabilitation in the United States: stroke, spinal cord injury, traumatic brain injury, multiple sclerosis, osteoarthritis, rheumatoid arthritis, limb loss, and back pain. *Arch Phys Med Rehabil* 2014; **95**: 986-995.e1 [PMID: 24462839 DOI: 10.1016/j.apmr.2013.10.032]

4 **Zhou QZ**, Zhang G, Long HB, Lei F, Ye F, Jia XF, Zhou YL, Kang JP, Feng DX. Effect of spinal cord extracts after spinal cord injury on proliferation of rat embryonic neural stem cells and Notch signal pathway in vitro. *Asian Pac J Trop Med* 2014; **7**: 562-567 [PMID: 25063287 DOI: 10.1016/S1995-7645(14)60094-8]

5 **Oyinbo CA**. Secondary injury mechanisms in traumatic spinal cord injury: a nugget of this multiply cascade. *Acta Neurobiol Exp (Wars)* 2011; **71**: 281-299 [PMID: 21731081]

6 **Gage FH**. Mammalian neural stem cells. *Science* 2000; **287**: 1433-1438 [PMID: 10688783 DOI: 10.1126/science.287.5457.1433]

7 **Feng X**, Zhang G, Feng D, Jia X, Zhou Q. Spinal cord extracts from injured spinal cord impede differentiation of rat embryonic neural stem cells into neurons through regulating Notch signaling pathway. *Int J Clin Exp Pathol* 2019; **12**: 3855-3861 [PMID: 31933774]

8 **Zhou QZ**, Feng XL, He P, Zhang G, Zhao M, Bai YH, Feng DX. DAPT inhibits transforming growth factor-β1-induced differentiation of neural stem cells *via* blocking Notch signaling. *Zhonghua Linchuang Dianzi Zazhi* 2022; **16**: 579-587 [DOI: 10.3877/cma.j.issn.1674-0785.2022.06.020]

9 **Reynolds BA**, Weiss S. Generation of neurons and astrocytes from isolated cells of the adult mammalian central nervous system. *Science* 1992; **255**: 1707-1710 [PMID: 1553558 DOI: 10.1126/science.1553558]

10 **Lois C**, Alvarez-Buylla A. Proliferating subventricular zone cells in the adult mammalian forebrain can differentiate into neurons and glia. *Proc Natl Acad Sci U S A* 1993; **90**: 2074-2077 [PMID: 8446631 DOI: 10.1073/pnas.90.5.2074]

11 **Morshead CM**, Reynolds BA, Craig CG, McBurney MW, Staines WA, Morassutti D, Weiss S, van der Kooy D. Neural stem cells in the adult mammalian forebrain: a relatively quiescent subpopulation of subependymal cells. *Neuron* 1994; **13**: 1071-1082 [PMID: 7946346 DOI: 10.1016/0896-6273(94)90046-9]

12 **Johansson CB**, Momma S, Clarke DL, Risling M, Lendahl U, Frisén J. Identification of a neural stem cell in the adult mammalian central nervous system. *Cell* 1999; **96**: 25-34 [PMID: 9989494 DOI: 10.1016/s0092-8674(00)80956-3]

13 **Suh H**, Consiglio A, Ray J, Sawai T, D'Amour KA, Gage FH. In vivo fate analysis reveals the multipotent and self-renewal capacities of Sox2+ neural stem cells in the adult hippocampus. *Cell Stem Cell* 2007; **1**: 515-528 [PMID: 18371391 DOI: 10.1016/j.stem.2007.09.002]

14 **Weiss S**, Dunne C, Hewson J, Wohl C, Wheatley M, Peterson AC, Reynolds BA. Multipotent CNS stem cells are present in the adult mammalian spinal cord and ventricular neuroaxis. *J Neurosci* 1996; **16**: 7599-7609 [PMID: 8922416 DOI: 10.1523/JNEUROSCI.16-23-07599.1996]

15 **Ohori Y**, Yamamoto S, Nagao M, Sugimori M, Yamamoto N, Nakamura K, Nakafuku M. Growth factor treatment and genetic manipulation stimulate neurogenesis and oligodendrogenesis by endogenous neural progenitors in the injured adult spinal cord. *J Neurosci* 2006; **26**: 11948-11960 [PMID: 17108169 DOI: 10.1523/JNEUROSCI.3127-06.2006]

16 **Yamamoto S**, Yamamoto N, Kitamura T, Nakamura K, Nakafuku M. Proliferation of parenchymal neural progenitors in response to injury in the adult rat spinal cord. *Exp Neurol* 2001; **172**: 115-127 [PMID: 11681845 DOI: 10.1006/exnr.2001.7798]

17 **Martens DJ**, Seaberg RM, van der Kooy D. In vivo infusions of exogenous growth factors into the fourth ventricle of the adult mouse brain increase the proliferation of neural progenitors around the fourth ventricle and the central canal of the spinal cord. *Eur J Neurosci* 2002; **16**: 1045-1057 [PMID: 12383233 DOI: 10.1046/j.1460-9568.2002.02181.x]

18 **English D**, Sharma NK, Sharma K, Anand A. Neural stem cells-trends and advances. *J Cell Biochem* 2013; **114**: 764-772 [PMID: 23225161 DOI: 10.1002/jcb.24436]

19 **Shimojo H**, Ohtsuka T, Kageyama R. Oscillations in notch signaling regulate maintenance of neural progenitors. *Neuron* 2008; **58**: 52-64 [PMID: 18400163 DOI: 10.1016/j.neuron.2008.02.014]

20 **Lobo MV**, Alonso FJ, Redondo C, López-Toledano MA, Caso E, Herranz AS, Paíno CL, Reimers D, Bazán E. Cellular characterization of epidermal growth factor-expanded free-floating neurospheres. *J Histochem Cytochem* 2003; **51**: 89-103 [PMID: 12502758 DOI: 10.1177/002215540305100111]

21 **Mori H**, Ninomiya K, Kino-oka M, Shofuda T, Islam MO, Yamasaki M, Okano H, Taya M, Kanemura Y. Effect of neurosphere size on the growth rate of human neural stem/progenitor cells. *J Neurosci Res* 2006; **84**: 1682-1691 [PMID: 17044035 DOI: 10.1002/jnr.21082]

22 **Ngwenya LB**, Rosene DL, Peters A. An ultrastructural characterization of the newly generated cells in the adult monkey dentate gyrus. *Hippocampus* 2008; **18**: 210-220 [PMID: 18058825 DOI: 10.1002/hipo.20384]

23 **Gritti A**, Parati EA, Cova L, Frolichsthal P, Galli R, Wanke E, Faravelli L, Morassutti DJ, Roisen F, Nickel DD, Vescovi AL. Multipotential stem cells from the adult mouse brain proliferate and self-renew in response to basic fibroblast growth factor. *J Neurosci* 1996; **16**: 1091-1100 [PMID: 8558238 DOI: 10.1523/JNEUROSCI.16-03-01091.1996]

24 **Rietze RL**, Valcanis H, Brooker GF, Thomas T, Voss AK, Bartlett PF. Purification of a pluripotent neural stem cell from the adult mouse brain. *Nature* 2001; **412**: 736-739 [PMID: 11507641 DOI: 10.1038/35089085]

25 **Cattaneo E**, McKay R. Proliferation and differentiation of neuronal stem cells regulated by nerve growth factor. *Nature* 1990; **347**: 762-765 [PMID: 2172829 DOI: 10.1038/347762a0]

World Journal of Stem Cells

Submit a Manuscript: https://www.f6publishing.com

World J Stem Cells 2023 June 26; 15(6): 617-631

DOI: 10.4252/wjsc.v15.i6.617

ISSN 1948-0210 (online)

ORIGINAL ARTICLE

Basic Study

Synergism of calycosin and bone marrow-derived mesenchymal stem cells to combat podocyte apoptosis to alleviate adriamycin-induced focal segmental glomerulosclerosis

Qiong-Dan Hu, Rui-Zhi Tan, Yuan-Xia Zou, Jian-Chun Li, Jun-Ming Fan, Fahsai Kantawong, Li Wang

Specialty type: Urology and nephrology

Provenance and peer review: Unsolicited article; Externally peer reviewed.

Peer-review model: Single blind

Peer-review report's scientific quality classification

Grade A (Excellent): 0
Grade B (Very good): B, B
Grade C (Good): 0
Grade D (Fair): 0
Grade E (Poor): 0

P-Reviewer: Jena MK, India; Sheykhhasan M, Iran

Received: March 29, 2023
Peer-review started: March 29, 2023
First decision: April 25, 2023
Revised: April 28, 2023
Accepted: May 25, 2023
Article in press: May 25, 2023
Published online: June 26, 2023

Qiong-Dan Hu, Rui-Zhi Tan, Fahsai Kantawong, Department of Medical Technology, Faculty of Associated Medical Sciences, Chiang Mai University, Chiang Mai 50200, Thailand

Qiong-Dan Hu, Rui-Zhi Tan, Yuan-Xia Zou, Jian-Chun Li, Li Wang, Research Center of Integrated Traditional Chinese and Western Medicine, The Affiliated Traditional Chinese Medicine Hospital of Southwest Medical University, Luzhou 646000, Sichuan Province, China

Qiong-Dan Hu, Department of Nephrology, The Affiliated Traditional Chinese Medicine Hospital of Southwest Medical University, Luzhou 646000, Sichuan Province, China

Yuan-Xia Zou, Jian-Chun Li, Molecular Imaging and Therapy Research Unit, Department of Radiologic Technology, Faculty of Associated Medical Sciences, Chiang Mai University, Chiang Mai 50200, Thailand

Jun-Ming Fan, Department of Nephrology, The Affiliated Hospital of Chengdu Medical College, Chengdu 610500, Sichuan Province, China

Corresponding author: Li Wang, PhD, Professor, Research Center of Integrated Traditional Chinese and Western Medicine, The Affiliated Traditional Chinese Medicine Hospital of Southwest Medical University, No. 182 Chunhui Road, Longmatan District, Luzhou 646000, Sichuan Province, China. wangli120@swmu.edu.cn

Abstract

BACKGROUND

Bone marrow-derived mesenchymal stem cells (MSCs) show podocyte-protective effects in chronic kidney disease. Calycosin (CA), a phytoestrogen, is isolated from *Astragalus membranaceus* with a kidney-tonifying effect. CA preconditioning enhances the protective effect of MSCs against renal fibrosis in mice with unilateral ureteral occlusion. However, the protective effect and underlying mechanism of CA-pretreated MSCs ($MSCs^{CA}$) on podocytes in adriamycin (ADR)-induced focal segmental glomerulosclerosis (FSGS) mice remain unclear.

AIM

To investigate whether CA enhances the role of MSCs in protecting against podocyte injury induced by ADR and the possible mechanism involved.

METHODS
ADR was used to induce FSGS in mice, and MSCs, CA, or MSCs^{CA} were administered to mice. Their protective effect and possible mechanism of action on podocytes were observed by Western blot, immunohistochemistry, immunofluorescence, and real-time polymerase chain reaction. *In vitro*, ADR was used to stimulate mouse podocytes (MPC5) to induce injury, and the supernatants from MSC-, CA-, or MSCs^{CA}-treated cells were collected to observe their protective effects on podocytes. Subsequently, the apoptosis of podocytes was detected *in vivo* and *in vitro* by Western blot, TUNEL assay, and immunofluorescence. Overexpression of Smad3, which is involved in apoptosis, was then induced to evaluate whether the MSCs^{CA}-mediated podocyte protective effect is associated with Smad3 inhibition in MPC5 cells.

RESULTS
CA-pretreated MSCs enhanced the protective effect of MSCs against podocyte injury and the ability to inhibit podocyte apoptosis in ADR-induced FSGS mice and MPC5 cells. Expression of p-Smad3 was upregulated in mice with ADR-induced FSGS and MPC5 cells, which was reversed by MSC^{CA} treatment more significantly than by MSCs or CA alone. When Smad3 was overexpressed in MPC5 cells, MSCs^{CA} could not fulfill their potential to inhibit podocyte apoptosis.

CONCLUSION
MSCs^{CA} enhance the protection of MSCs against ADR-induced podocyte apoptosis. The underlying mechanism may be related to MSCs^{CA}-targeted inhibition of p-Smad3 in podocytes.

Key Words: Calycosin; Mesenchymal stem cells; Focal segmental glomerulosclerosis; Apoptosis; Smad3

Core Tip: Calycosin (CA)-pretreated mesenchymal stem cells (MSCs^{CA}) enhanced the protective effect of MSCs against adriamycin (ADR)-induced podocyte injury *in vitro* and *in vivo* by inhibiting apoptosis, accompanied by more reversal of the upregulated expression of p-Smad3 after ADR induction. Smad3 overexpression eliminated the inhibitory effect of MSCs^{CA} on podocyte apoptosis, suggesting that MSCs^{CA} inhibit podocyte apoptosis by targeting p-Smad3. These results broaden our understanding of the potential of MSCs pretreated with herbal extract and provide new theories for possible therapeutic mechanisms for ADR-induced focal segmental glomerulosclerosis.

Citation: Hu QD, Tan RZ, Zou YX, Li JC, Fan JM, Kantawong F, Wang L. Synergism of calycosin and bone marrow-derived mesenchymal stem cells to combat podocyte apoptosis to alleviate adriamycin-induced focal segmental glomerulosclerosis. *World J Stem Cells* 2023; 15(6): 617-631
URL: https://www.wjgnet.com/1948-0210/full/v15/i6/617.htm
DOI: https://dx.doi.org/10.4252/wjsc.v15.i6.617

INTRODUCTION

Focal segmental glomerulosclerosis (FSGS) is the most common primary glomerulopathy and the dominant pathological type of chronic kidney disease (CKD)[1,2], associated with high albuminuria and end-stage renal disease (ESRD) with a poor prognosis[3,4]. FSGS is linked with injury or even depletion of podocytes, manifested by the gradual disappearance of podocyte-specific markers such as podocin[5,6]. As podocyte injury plays a critical role in FSGS progression, protecting podocytes is promising to prevent ESRD in patients with FSGS[7].

Apoptosis of podocytes has been widely studied in previous studies[8-10], and inhibition of podocyte apoptosis has been reported to delay FSGS progression[11]. Podocyte apoptosis is characterized by the loss of Bcl-2 protein and the increase of Bax protein[12,13]. Recently, Smad3-related pathways have been reported to be involved in podocyte apoptosis[14]. However, the underlying mechanism remains unclear, and no specific effective treatment can prevent podocyte apoptosis.

Mesenchymal stem cells (MSCs) are multipotent stem cells that exhibit varying potential for multilineage cell differentiation as well as the capacity for self-renewal[15]. Therefore, using MSCs to treat various diseases is worth exploring[16-18]. MSCs treat diabetic nephropathy by protecting podocytes[19-21], and bone marrow-derived MSC (BMSC) transplantation can attenuate FSGS progression in a rat model of FSGS[22,23]. In addition, the protective effects of MSC derivatives or exosomes on podocytes have also been reported[24,25]. However, the application of MSCs is also limited. For instance, MSCs may be losing their biological function after being isolated and cultured for a long time. After infusion, MSCs must face harsh environments with various stressors such as inflammation, hypoxia, high acidity, or reduced energy reserve. On this account, preconditioning, genetic modification, and delivering MSCs with biomaterials have been developed[26]. Thus, it is important to explore how MSCs can overcome adverse microenvironments to

enhance their therapeutic benefits.

Calycosin (CA), a phytoestrogen with a kidney-tonifying effect, is isolated from *Astragalus membranaceus*. It has been reported that CA is the top component of potentially active compounds for the treatment of nephrotic syndrome[27]. Moreover, CA has also been found to be an active ingredient in the treatment of adriamycin (ADR) nephropathy using network pharmacology combined with transcriptomics[28]. Our research group used Ca-pretreated MSCs to treat mice with unilateral ureteral occlusion (UUO) and found that they improved renal fibrosis and inhibited necrosis of renal tubular epithelial cells more than normal MSCs did[29]. However, the protective effect on podocytes and their mechanism of action remain unknown.

In rodents, ADR can induce rapid podocyte injury characterized by massive foot process effacement and glomerulosclerosis, which serves as a model of FSGS[30,31]. In the present study, we compared the antiapoptotic efficacy of CA-pretreated MSCs ($MSCs^{CA}$) to that of MSCs or CA in a mouse model of FSGS induced with ADR and *in vitro*, as well as the possible mechanisms of action involved.

MATERIALS AND METHODS

Animal experiments

The C57BL/6 mice utilized in this investigation were bought from Chengdu Dashuo Biotechnology Co., LTD. in China. They were male, 8 wk old, and weighed 22-25 g. All the mice were kept in a specific disease-free space with 12 h of light and dark cycles and had free access to water and food. The mice were randomly divided into the following six groups: Normal control group; ADR injection group; ADR with Dulbecco's modified Eagle's medium (DMEM; 200 μL) injection (ADR + DMEM); ADR with 200 μL MSCs (10^6 cells/mL) (ADR + MSCs); ADR with 200 μg/mL CA (10^6 cells/mL) (ADR + CA); and ADR with MSCs preconditioned with 200 μg/mL CA (10^6 cells/mL) (ADR + $MSCs^{CA}$). For ADR-induced FSGS, the mice were injected with 10 mg/kg ADR (Shenzhen Main Luck Pharmaceuticals Inc.) *via* the tail vein. The normal control mice were injected with vehicle (saline). MSCs, CA dissolved in DMEM, and $MSCs^{CA}$ were injected *via* the tail vein 4 wk after ADR injection once weekly. Since both MSCs and CA are soluble in DMEM, mice in the ADR + DMEM group were given an equal volume of normal DMEM as the solvent control. All mice were killed at 8 wk after ADR injection. All animal experiments were carried out in accordance with the recommendations of the Institute of Nutrition and Health's Animal Care and Utilization Committee, and were approved by the Southwest Medical University's Animal Ethics Committee (No. 20210223-024).

Isolation of MSCs

As previously described, MSCs were isolated from the leg bone marrow of male C57BL/6 mice aged 6-8 wk[32]. Briefly, cells were grown at 37 °C and 5% CO_2 in DMEM Petri plates with 10% fetal bovine serum (FBS, Gibco, Carlsbad, CA, United States), 1 g/L glucose, and 1% penicillin-streptomycin (Beyotime, Shanghai, China). At 24 h, the medium was changed to remove the non-adherent cells. The MSCs were passed once 90% confluence was reached. As described previously[26], anti-CD29 (102205; Biolegend), anti-CD90 (ab24904; Abcam, Cambridge, MA, United States), and anti-CD11b (101205; Biolegend, San Diego, CA, United States) antibodies were used to label MSCs, and the purity of the MSCs was analyzed using a BD FACSVerse (Becton, Dickinson and Company, Franklin Lakes, NJ, United States).

CA pretreatment of MSCs

CA (≥ 94% purity) was purchased from Cayman Chemical Company (Ann Arbor, MI, United States). The stoste used for MSC pretreatment included full medium and CA (200 g/mL) dissolved in DMEM as previously described[29]. After incubation for 72 h, the MSCs and $MSCs^{CA}$ were injected into mice, and the supernatants were used to treat mouse podocytes (MPC5) for 48 h.

Urine albumin-creatinine ratio

Random urine samples were collected, followed by determining the albumin concentration with a mouse albumin ELISA kit (Sangon Biotech, China) and creatinine with a creatinine assay kit (Nanjing Jiancheng, Jiangsu Province, China). The urine albumin-creatinine ratio was calculated by dividing the urine albumin concentration by the creatinine concentration.

Hematoxylin-eosin staining

Mouse kidneys were fixed in 4% neutral formaldehyde followed by paraffin embedding. The paraffin sections were rehydrated in a graded ethanol series and subjected to hematoxylin-eosin (HE) staining (Beyotime, Shanghai, China) as previously described[33].

Immunohistochemistry

The sections underwent antigen retrieval in 0.01 M citric acid solution (pH 6.0) in a microwave oven for 10 min after deparaffinization and rehydration. To inhibit endogenous peroxidase, the slices were incubated with 5% H_2O_2 for 15 min. The sections were then further blocked for 30 min at room temperature with 5% bovine serum albumin (BSA), and then incubated overnight at 4 °C with anti-p-Smad3 antibody (C25A9; Cell Signaling Technology, Danvers, MA, United States). The slices were treated with secondary antibodies for 1 h at room temperature following PBS washing. Images were recorded with a light microscope (Eclipse 80i; Nikon, Japan).

TUNEL assay

TUNEL assay was used to evaluate podocyte apoptosis in the kidneys after ADR induction, as previously described[34]. After the mouse kidneys were fixed in 4% neutral formaldehyde followed by paraffin embedding, the paraffin sections were used for staining. Podocyte apoptosis was measured through the utilization of a One-step TUNEL In Situ Apoptosis Assay Kit (AF488; Green) (E-CK-A321; Elabscience, China). The images were captured with an orthotopic fluorescence microscope (DM4B; Leica, Germany).

Cell culture and treatment

Prof. San-Tao Ou (Department of Nephrology, Southwest Medical University) kindly donated the conditionally immortalized MPC5 cell line. The cells were grown at 33 °C in RPMI-1640 medium supplemented with 10 IU/mL recombinant interferon and 10% FBS. After the MPC5 cells were cultured at 37 °C for 14 d to induce differentiation, the differentiated cells were treated with different concentrations of ADR for 24 h. A Smad3 overexpressing MPC5 cell line was established with the Smad3 overexpression plasmid pcDNA3.1-Smad3 which was described previously[35].

Immunofluorescence

After treatment, the MPC5 cells or frozen sections were fixed with 4% paraformaldehyde for 10 min, permeabilized with 0.25% Triton X-100 (in PBS), and blocked with 5% BSA for immunofluorescence. After that, the frozen sections or MPC5 cells were incubated with anti-podocin (BA0290; Boster, Wuhan, China), anti-Bax (AF0120; Affinity, United States), and anti-Bcl-2 (AF6139; Affinity) antibodies at 4 °C overnight. After washing with PBS, the frozen sections or MPC5 cells were incubated with Alexa Fluor 594 Donkey anti-mouse/rabbit secondary antibodies (Thermo Fisher Scientific, Waltham, MA, United States) for 1 h at room temperature. The nuclei were stained with 4¢,6-diamidino-2-phenylindole (Sangon Biotech). Images were captured with a fluorescence microscope (EVOS FL Auto, Thermo Fisher Scientific, United States).

Real-time quantitative polymerase chain reaction

TRIzol reagent (Invitrogen, Carlsbad, CA, United States) was used to separate total RNA from cells or kidneys, and a Reverse Transcription Kit (Promega, Madison, WI, United States) was used to obtain cDNA. Using Master Mixture (TaKaRa, Dalian, China) and LightCycler 480 equipment (Roche, Germany), the podocin mRNA expression levels were assessed. The internal control used was GAPDH. Using $2^{-\Delta\Delta Ct}$ analysis, the relative expression of the target gene was standardized to GAPDH expression. The primer sequences used are shown in Supplementary Table 1.

Western blot analysis

Using RIPA lysis buffer (Beyotime), total proteins were extracted from kidneys or cells. The protein concentrations were determined with a BCA protein assay kit (Beyotime). Proteins were transferred onto polyvinylidene difluoride membranes after being separated by 12% SDS-PAGE. Then the membranes were incubated with anti-podocin (BA0290; Boster), anti-p-Smad3 (C25A9; Cell Signaling Technology), anti-Smad3 (C67H9; Cell Signaling Technology), anti-Bax (AF0120; Affinity), anti-Bcl-2 (AF6139; Affinity), and anti-GAPDH (AB0037; Abways, China) antibodies at 4°C overnight. The membranes were treated with the relevant secondary antibody at room temperature for 1 h after being rinsed with Tris-buffered saline with Tween (TBST). The protein bands were depicted with an enhanced ECL kit (Boster) and a chemiluminescence imaging system (ChemiScope 6200; Clinx, China). ImageJ software (NIH, Bethesda, MD, United States) was used to calculate the band gray intensity.

Apoptosis detection by flow cytometry

The cells were digested with trypsin-EDTA solution (C0201; Beyotime), collected in a centrifuge tube, and centrifuged for 5 min at 1800 rpm, and the supernatant was discarded. The cells were resuspended with 1 mL precooled PBS. According to the Annexin V-FITC/PI Apoptosis Detection kit's instructions (Vazyme, Nanjing, China), the prepared propyl iodide staining solution was added to the cells and incubated at 37 °C for 10 min without light. Red fluorescence was detected at an excitation wavelength of 488 mm and light scattering was detected with a BD FACSVerse (Becton, Dickinson).

Statistical analysis

The mean and standard deviation of the data are displayed. Using SPSS 21.0 software (IBM Corp., Chicago, IL, United States), one-way analysis of variance was used to compare the data. $P < 0.05$ was considered statistically significant.

RESULTS

MSCs^{CA} enhance the protective effect of MSCs on podocyte injury in ADR-induced FSGS

To investigate whether CA pretreatment enhances the protective effect of MSCs on podocyte injury in ADR-induced FSGS mice, we treated mice with MSCs, CA, or MSCs^{CA}. Due to MSCs, CA, and MSCs^{CA} being dissolved in DMEM, a DMEM group was separately designed as the solvent control group to exclude the protective effect of DMEM-containing nutrients on podocytes (Figure 1A). The identification of MSCs, the chemical formula of CA, and its appropriate concentration can be found in our previous research[26]. Eight weeks after ADR injection, increased urinary albumin excretion was detected in ADR-treated mice, and MSCs^{CA} reversed this more significantly than MSCs or CA alone. However, there was no difference between the DMEM group and the model group (Figure 1B). HE staining showed that glomerular atrophy and FSGS were prominent in the ADR and DMEM groups, but MSCs^{CA} treatment reversed this change and was

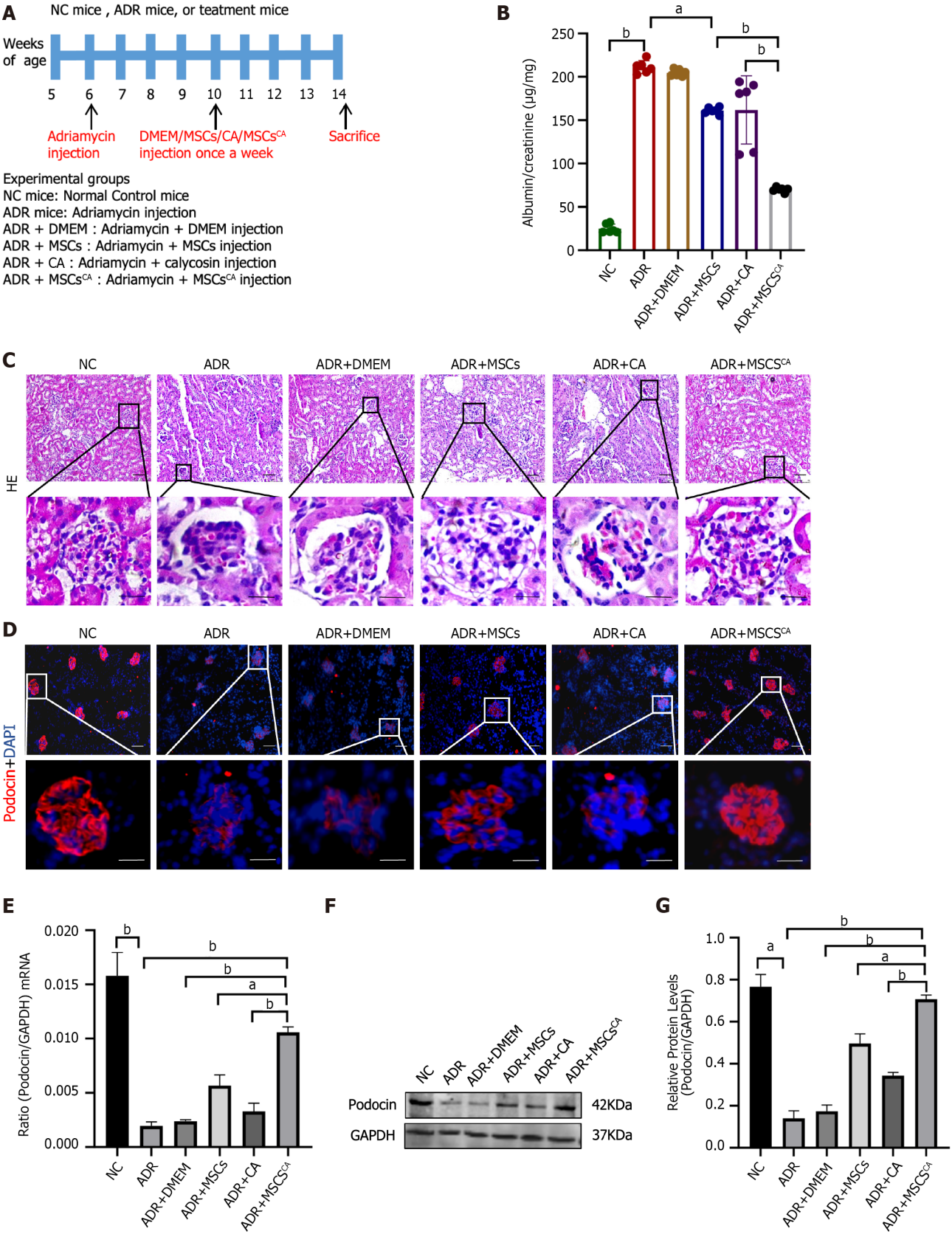

DOI: 10.4252/wjsc.v15.i6.617

Figure 1 Mesenchymal stem cells pretreated with calycosin enhance the protective effect of mesenchymal stem cells on podocyte injury in adriamycin-induced focal segmental glomerulosclerosis mice. A: Mice received adriamycin injections through the tail vein at week 6, were injected with Dulbecco's modified eagle medium, mesenchymal stem cells (MSCs), calycosin (CA), and MSCs pretreated with CA (MSCs^{CA}) at week 10, respectively, and were sacrificed at week 14; B: Levels of albumin/creatinine ratio in urine (n = 6), $^{a}P < 0.05$, $^{b}P < 0.001$; C: Pathological changes in the kidneys of mice examined by hematoxylin-eosin staining. Typical glomeruli are indicated by black boxes and enlarged to the next row. Bar = 50 μm; D: Changes in the kidneys of mice examined by

podocin immunofluorescence staining. Glomeruli are indicated by white boxes and enlarged to the next row. Bar = 50 μm; E: Relative (podocin/GAPDH) mRNA expression analyzed by real-time quantitative polymerase chain reaction. Data are expressed as the mean ± SD (n = 6). $^{a}P < 0.05$, $^{b}P < 0.001$; F and G: Relative protein levels (podocin/GAPDH) detected by Western blot. Data are expressed as the mean ± SD (n = 3). $^{a}P < 0.05$, $^{b}P < 0.001$. NC: Normal control; ADR: Adriamycin; DMEM: Dulbecco's modified eagle medium; MSCs: Mesenchymal stem cells; CA: Calycosin; MSCs^{CA}: Mesenchymal stem cells pretreated with calycosin.

superior to MSCs and CA treatment (Figure 1C). Immunostaining, real-time quantitative polymerase chain reaction (RT-PCR), and Western blot analysis showed that the expression of podocin, a podocyte-specific marker, was significantly reduced in the ADR and DMEM groups; however, MSCs^{CA} treatment best restored its expression (Figure 1D-G). The above evidence indicated that MSCs^{CA} treatment better protected podocytes from ADR injury in FSGS mice.

The capacity of MSCs to prevent apoptosis in ADR-induced FSGS is improved by CA pretreatment

To determine the effect of MSCs^{CA} on renal cell apoptosis, Western blot and TUNEL assay were performed. Expression of Bax protein as an apoptosis marker was significantly increased in the ADR and DMEM groups compared with the normal group, and their levels were reduced after MSC or CA treatment (Figure 2A and B). MSCs^{CA} reduced ADR-induced Bax protein expression more significantly than MSCs or CA. The changing trend in Bcl-2 protein expression was opposite to that of Bax in each group (Figure 2A and C). TUNEL assay showed an obvious increase in the brightness and range of green fluorescence in the ADR group, which was weakened by MSCs^{CA} treatment (Figure 2D). The above data indicated that MSCs^{CA} enhanced the antiapoptotic effect of MSCs on kidney cells of ADR-induced FSGS mice.

P-Smad3 is upregulated in podocytes of ADR-induced FSGS mice and reversed after MSCs^{CA} treatment

It has been reported that the Smad3 protein is involved in podocyte apoptosis[13], so we examined the effect of MSCs^{CA} on the expression of Smad3 and p-Smad3 proteins. As expected, we found by Western blot and immunohistochemistry that MSCs^{CA} treatment significantly reversed the upregulation of p-Smad3 in ADR-treated mouse renal podocytes, and the effect was superior to that of MSC and CA treatment (Figure 3). The above evidence suggested that p-Smad3 was involved in the ADR-induced injury of podocytes and the recovery after MSCs^{CA} treatment.

The capacity of MSCs to reduce the injury caused by ADR-stimulated MPC5 cells in vitro is improved by CA pretreatment

To further demonstrate the enhanced potential of MSCs^{CA} to protect podocytes from ADR injury, we cultured and treated MPC5 cells. Immunofluorescence staining, RT-PCR, and Western blot showed that 1.2 μM/mL ADR decreased the expression of podocin mRNA and protein, while the expression was significantly promoted by treatment with conditioned medium from MSCs, or CA. Importantly, conditioned medium from MSCs^{CA} further elevated the expression of podocin mRNA and protein compared with the ADR group (Figure 4). Therefore, MSCs^{CA} protected podocytes from ADR injury better than MSCs or CA alone.

CA pretreatment enhances the ability of MSCs to inhibit apoptosis in ADR-stimulated MPC5 cells

Immunofluorescence staining and Western blot demonstrated that the protein level of Bax was upregulated in MPC5 cells treated with ADR, but its expression was significantly inhibited by treatment with a conditioned medium from MSCs, or CA alone (Figure 5). The effects of the conditioned medium from MSCs^{CA} were more pronounced. The trend for Bcl-2 protein expression was the opposite. These findings revealed that Ca-pretreated MSCs enhanced the inhibitory effect of MSCs on podocyte apoptosis.

MSCs^{CA} improve ADR-induced podocyte apoptosis by targeting p-Smad3 expression

As described previously, p-Smad3 is involved in ADR-induced FSGS mice. Further experiments were conducted to explore whether MSCs^{CA} inhibit podocyte apoptosis by targeting p-Smad3. Expression of p-Smad3 in MPC5 cells was markedly elevated by ADR stimulation and subsequently significantly downregulated by MSCs^{CA} treatment. The upregulated expression of p-Smad3 was also reversed by MSCs or CA, but to a lesser extent (Figure 6A and B). When Smad3 accompanied by p-Smad3 in MPC5 cells was overexpressed, Bax protein expression was upregulated but Bcl-2 protein expression was downregulated. Meanwhile, MSCs^{CA} treatment no longer showed a protective effect against ADR-induced podocyte apoptosis compared with the group without Smad3 overexpression (Figure 6C-G). Flow cytometry was used to detect apoptosis, and it was found that the apoptosis rate of MPC5 cells was significantly increased after ADR induction compared with the normal group, and MSCs^{CA} reversed this increase. However, after overexpression of Smad3, the apoptosis rate was increased compared with the normal group and the model group regardless of whether MSCs^{CA} were administered. This means that treatment with MSCs^{CA} did not improve the apoptosis of podocytes with Smad3 overexpression (Figure 6H-L). The graphical abstract (created in BioRender.com) is shown in Figure 6M. The above evidence suggested that MSCs^{CA} improved podocyte apoptosis through targeted inhibition of p-Smad3.

DISCUSSION

Increasing evidence has shown that MSCs and derived extracellular vesicles can ameliorate renal deterioration in CKD [36,37]. However, because of a hostile environment with several stresses such as inflammation, high acidity, hypoxia, and

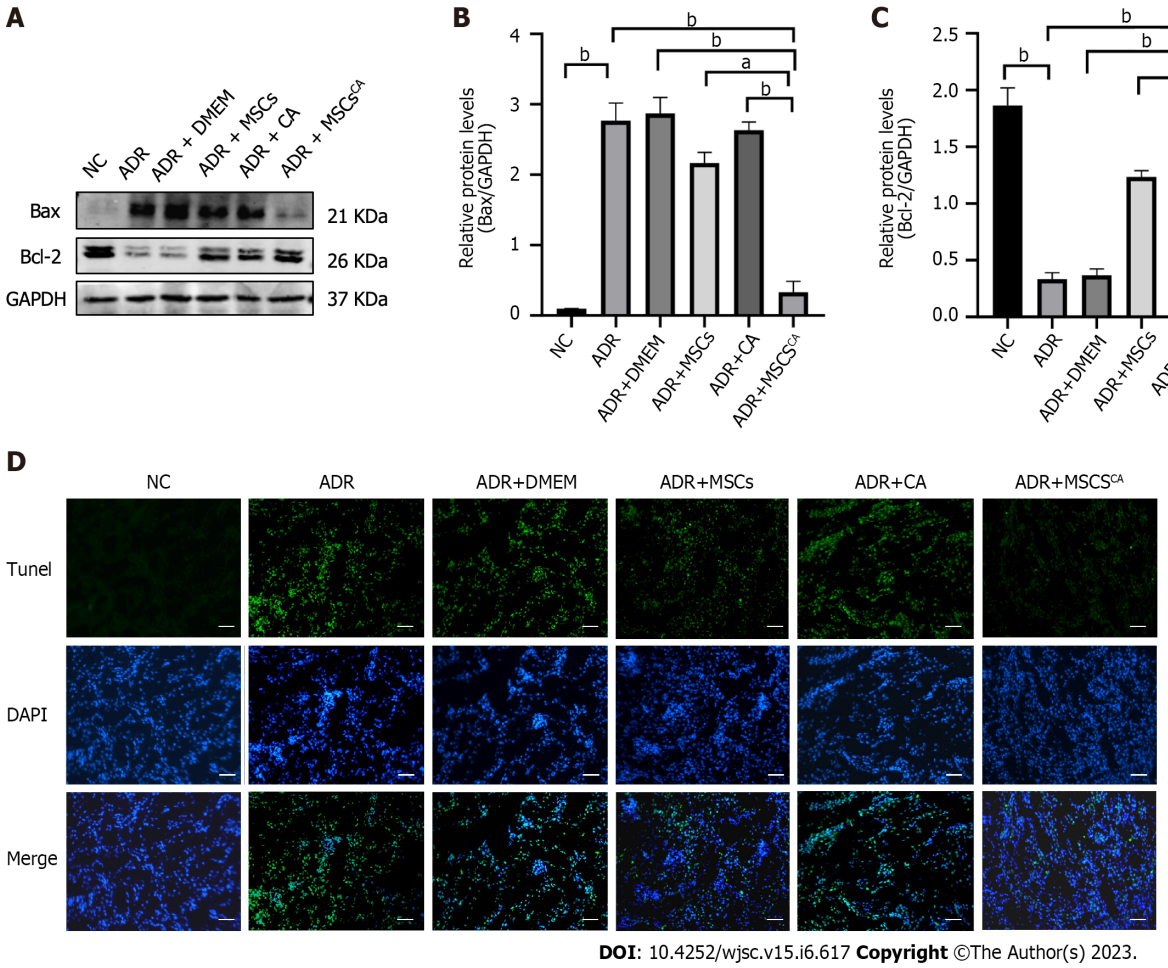

DOI: 10.4252/wjsc.v15.i6.617 **Copyright** ©The Author(s) 2023.

Figure 2 Calycosin pretreatment enhances the ability of mesenchymal stem cells to inhibit apoptosis in adriamycin-induced focal segmental glomerulosclerosis mice. A-C: Protein expression levels of Bax and Bcl-2 in the kidneys measured by Western blot and normalized to control. Data are expressed as the mean ± SD (n = 3). $^{a}P < 0.05$, $^{b}P < 0.001$; D: Apoptosis in each group as determined by TUNEL assay. Bar = 50 μm. NC: Normal control; ADR: Adriamycin; MSCs: Mesenchymal stem cells; CA: Calycosin; MSCs^{CA}: Mesenchymal stem cells pretreated with calycosin.

depleted energy reserve, few MSCs survive *in vivo* after intravenous or direct local injection[38-40]. The question of whether preconditioning BMSCs can shield them from the damaging environment at the injury site and enhance their functionality has drawn more attention in research. These pretreatments involve the application of supportive materials, cytokines, and natural or synthetic chemicals[41-44]. Researchers have been investigating the preconditioning of MSCs using Chinese herbal medicine or its primary monomer components. There is evidence that resveratrol-pretreated adipose-derived stem cells show increased regenerative capacity in a rat model of diabetes-induced cardiomyopathy[45]. Further research has shown that preconditioning MSCs obtained from umbilical cords with the active ingredient of a Chinese herb, triptolide, primed MSCs to be activated and inhibited the immune response before being delivered[46]. Previous results from our group have also shown that CA-pretreated BMSCs show enhanced antifibrotic activity in UUO mice and inhibit tubular epithelial cell necrosis[29]. Therefore, we investigated whether MSCs^{CA} enhance podocyte protection. Similar to previous studies, MSCs^{CA} protected podocytes from ADR-induced apoptosis, both *in vivo* and *in vitro*, which means that they may be a potential therapy for FSGS.

CA is the top ingredient in *Astragalus*, which is one of the most widely used herbs in Chinese medicine to treat kidney disease[47-49]. The effectiveness of CA in CKD has been confirmed in recent years[50-52]. However, whether its combination with MSCs can enhance their efficacy in treating CKD remains to be seen. It has been shown that human MSCs are stimulated to enhance osteogenesis and mineralization by CA-7-O-glucoside obtained from *Astragalus membranaceus*[53]. This result gave us confidence and we also identified the advantages and potential of MSCs^{CA} in the treatment of FSGS, which extends the application of CA and MSCs in FSGS.

The main pathological manifestations of FSGS are podocyte injury and the therapeutic options for FSGS are limited, requiring further research and exploration. Therefore, we explored the mechanism of podocyte injury. Podocyte apoptosis is the main type of podocyte injury, which includes podocyte dedifferentiation, autophagy, and epithelial-mesenchymal transformation[54]. Podocyte apoptosis is caused by many factors, including drugs, infection, and immune disorders[55-57]. ADR is one of the drugs that causes podocyte apoptosis due to its pharmacological action and distribution[58]. However, how to protect podocytes from ADR needs further research to find more effective targeted drugs.

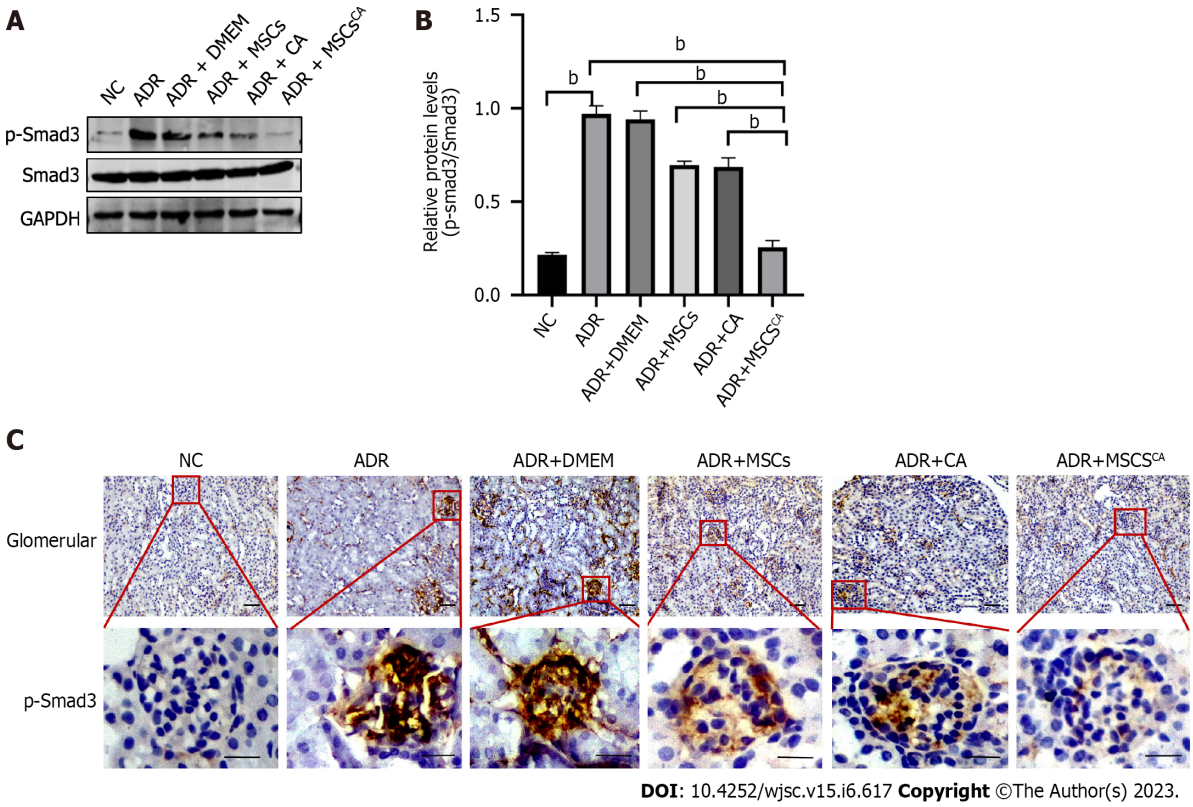

DOI: 10.4252/wjsc.v15.i6.617

Figure 3 P-Smad3 is upregulated in podocytes of adriamycin-induced focal segmental glomerulosclerosis mice and reversed after treatment with mesenchymal stem cells pretreated with calycosin. A and B: Protein expression levels of p-Smad3 and Smad3 detected using Western blot and normalized to control. Data are expressed as the mean ± SD (n = 3). $^{b}P < 0.001$; C: Immunohistochemistry staining for p-Smad3 in mouse glomeruli, which are indicated by red boxes and enlarged to the next row. Bar = 50 μm. NC: Normal control; ADR: Adriamycin; MSCs: Mesenchymal stem cells; CA: Calycosin; MSCs^{CA}: Mesenchymal stem cells pretreated with calycosin.

Smad3 is involved in apoptosis, and podocytes are no exception[59,60]. Activation of Smad3 and its related pathway proteins induces podocyte apoptosis[14,61]. The canonical Smad pathway is a crucial regulatory route in the etiology of renal inflammation and fibrosis, according to earlier research. Major receptor-associated Smads include Smad2 and Smad3. Mad-homology 2 domain is located at the C-terminus of Smad3, which has unique phosphorylation sites and sequences triggered by transforming growth factor (TGF)-β1. The binding of phosphorylated Smad3 to TGF-β1 signaling receptors promotes fibrosis[62]. Our study showed that MSCs^{CA} significantly downregulated the expression of p-Smad3 in the kidneys of ADR-induced FSGS mice and ADR-induced MPC5 cells. Subsequently, we overexpressed Smad3 in MPC5 cells and confirmed that MSCs^{CA} targeted inhibition of p-Smad3 to improve podocyte apoptosis using rescue experiments. This provides a new possible mechanism and target for preventing podocyte apoptosis by MSCs^{CA}.

There were some limitations to this study. Although we have revealed that MSCs^{CA} improve podocytes apoptosis by inhibiting Smad3 signaling, this study still has certain limitations and the underlying mechanism deserves further exploration. First, how does MSCs^{CA} intervene in the Smad3 signal, directly or indirectly? We speculate that CA may activate the anti-apoptotic activity of MSCs or affect the differentiation, mobilization, and homing of BMSCs as well as the abundance of beneficial exosomes, but the main mechanism and responsible factors are still unknown. Second, it is still unclear which molecules in podocytes respond to the activity of MSCs and what are their potential relationship with Smad3. Understanding these mechanisms is conducive in expanding the application of MSCs^{CA}, and we will answer each question one by one in future research.

CONCLUSION

This study showed that MSCs^{CA} improve ADR-induced podocyte apoptosis by targeting Smad3 inhibition, and are superior to MSCs or CA. Thus, our study provides a new perspective on the synergistic application of MSCs and a new theory for the mechanism of improvement of podocyte apoptosis.

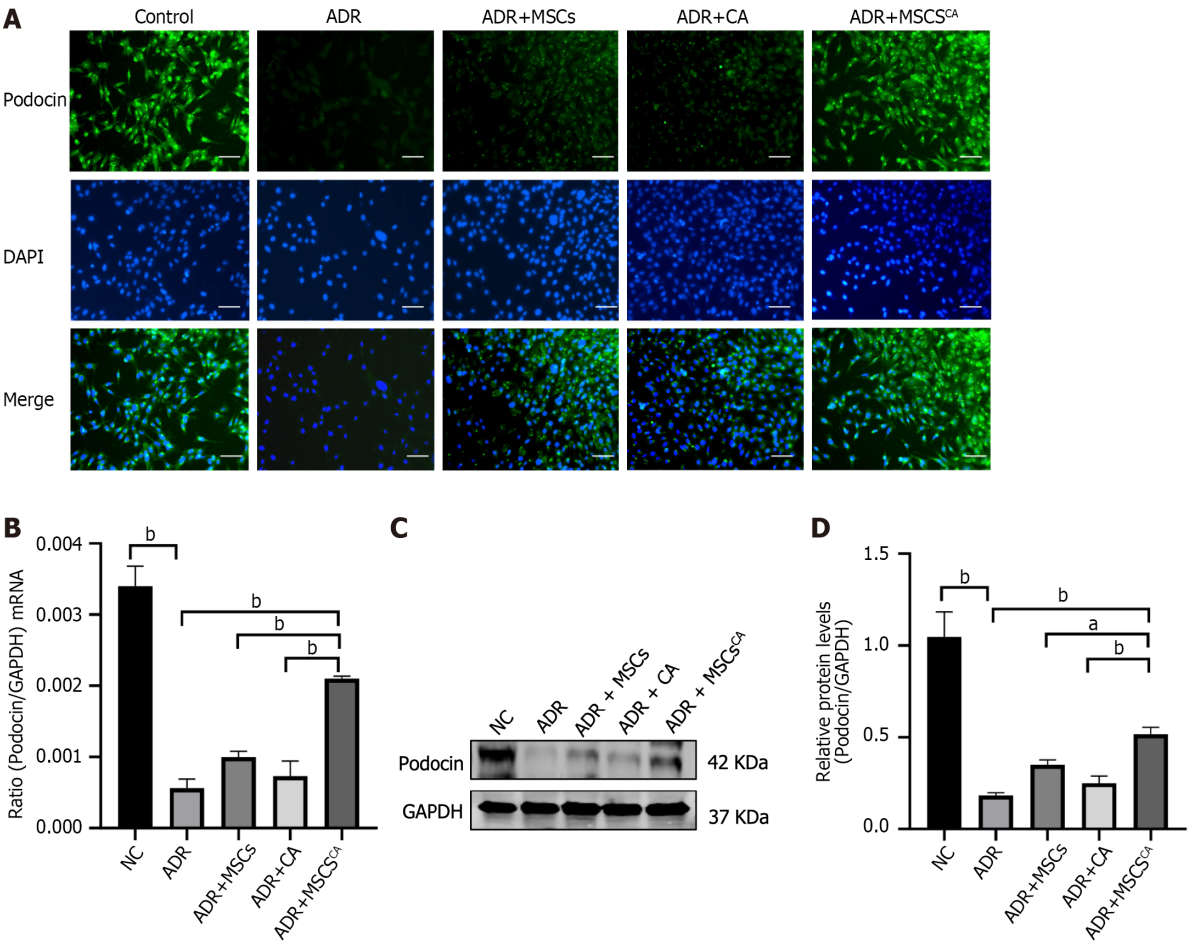

DOI: 10.4252/wjsc.v15.i6.617

Figure 4 Calycosin pretreatment enhances the ability of mesenchymal stem cells to ameliorate the injury of adriamycin-stimulated mouse podocyte cells *in vitro*. A: Podocin expression in each group as determined by immunofluorescence staining. Bar = 50 μm; B: Analysis of relative (podocin/GAPDH) mRNA expression by real-time quantitative polymerase chain reaction. Data are expressed as the mean ± SD (n = 3). $^{b}P < 0.001$; C and D: Protein expression levels of podocin detected by Western blot and normalized to control. Data are expressed as the mean ± SD (n = 3). $^{a}P < 0.05$, $^{b}P < 0.001$. NC: Normal control; ADR: Adriamycin; MSCs: Mesenchymal stem cells; CA: Calycosin; MSCs^{CA}: Mesenchymal stem cells pretreated with calycosin.

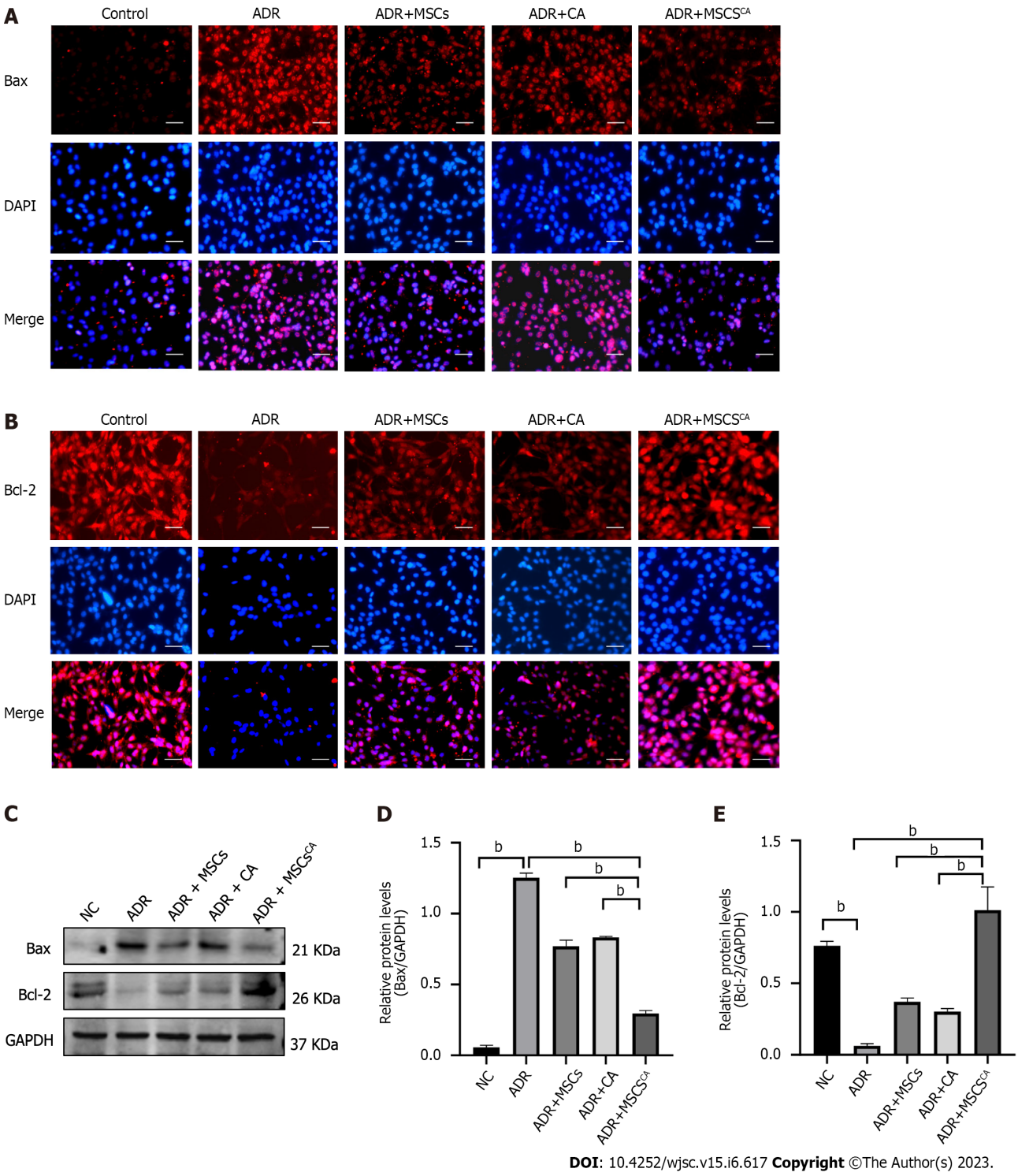

DOI: 10.4252/wjsc.v15.i6.617

Figure 5 Calycosin pretreatment enhances the ability of mesenchymal stem cells to inhibit apoptosis in adriamycin-stimulated mouse podocyte cells. A and B: Expression of Bax and Bcl-2 in each group as determined by immunofluorescence staining. Bar = 50 μm; C-E: Protein expression levels of Bax and Bcl-2 detected by Western blot and normalized to control. Data are expressed as the mean ± SD (n = 3). $^{b}P < 0.001$. NC: Normal control; ADR: Adriamycin; MSCs: Mesenchymal stem cells; CA: Calycosin; MSCs^{CA}: Mesenchymal stem cells pretreated with calycosin.

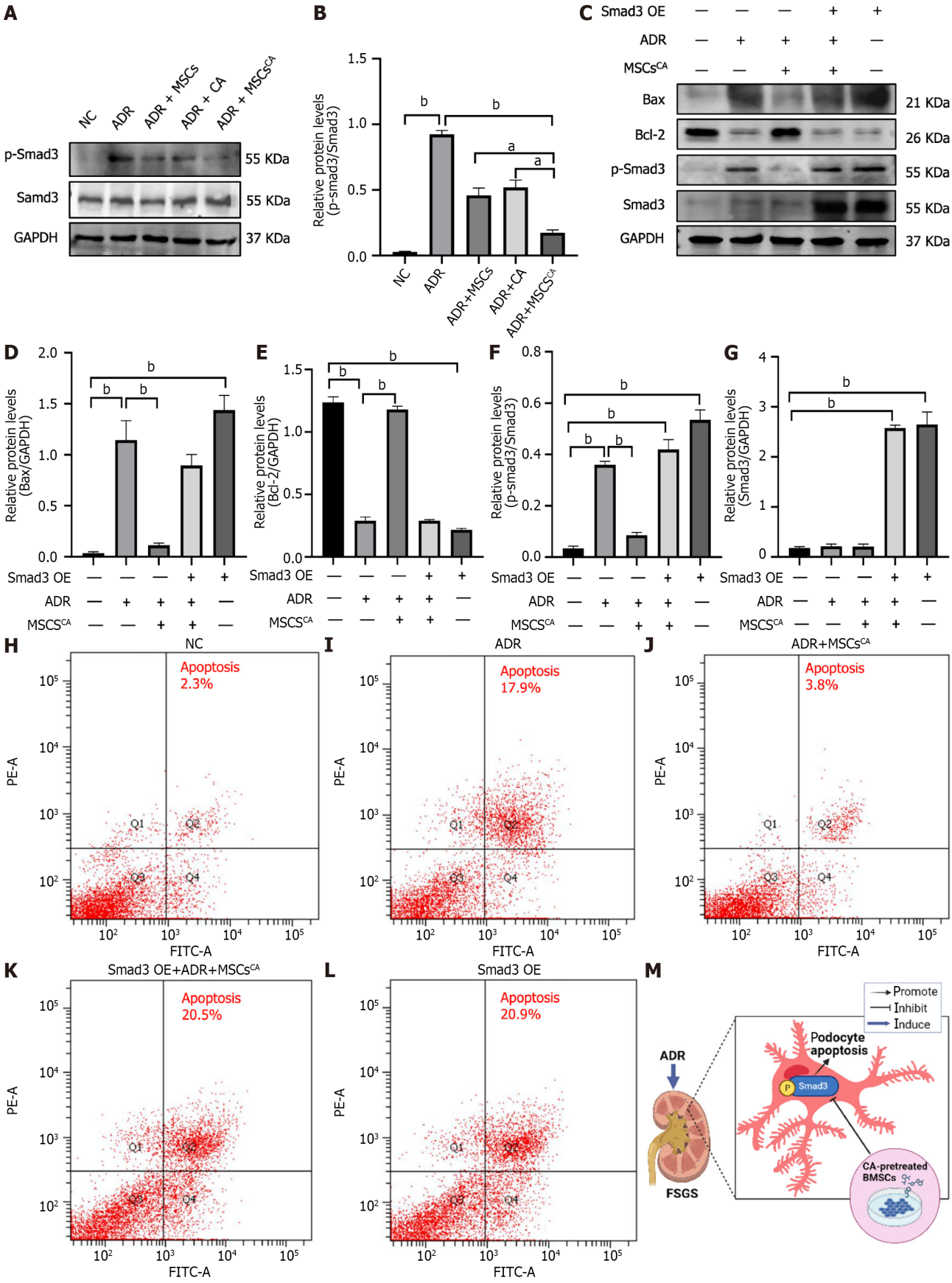

DOI: 10.4252/wjsc.v15.i6.617

Figure 6 Calycosin-pretreated mesenchymal stem cells improve adriamycin-induced podocyte apoptosis by targeting p-Smad3 expression. A and B: Protein expression levels of p-Smad3 and Smad3 in mouse podocyte cells (MPC5) detected by Western blot and normalized to control. Data are expressed as the mean ± SD (n = 3). $^{a}P < 0.05$, $^{b}P < 0.001$; C-G: Protein expression levels of Bax, Bcl-2, p-Smad3, and Smad3 in Smad3-overexpressing MPC5

cells detected by Western blot and normalized to control. Data are expressed as the mean ± SD (n = 3). $^{b}P < 0.001$; H-L: Cell apoptosis detected by flow cytometry; M: Graphical abstract (created in BioRender.com). NC: Normal control; ADR: Adriamycin; MSCs: Mesenchymal stem cells; CA: Calycosin; MSCs^{CA}: Mesenchymal stem cells pretreated with calycosin; FSGS: Focal segmental glomerulosclerosis.

ARTICLE HIGHLIGHTS

Research background

Focal segmental glomerulosclerosis (FSGS) has become a global public health problem due to its high incidence and lack of treatment. Prevention of podocyte apoptosis is essential in the treatment of FSGS. Bone marrow-derived mesenchymal stem cells (BMSCs) have been found to protect podocytes, but have some limitations, such as low survival rate *in vivo* and poor homing function. In our previous study, calycosin (CA)-pretreated BMSCs enhanced the antifibrotic activity in kidneys compared with BMSCs. Therefore, CA-pretreated MSCs are expected to be a new method to protect podocytes in the treatment of FSGS.

Research motivation

Although MSCs have been confirmed to improve podocyte apoptosis in mice, their availability and effectiveness *in vivo* are limited. Currently, there is still a lack of effective therapeutic methods for FSGS, and their mechanism of action is not clear.

Research objectives

To evaluate the therapeutic effect of CA-pretreated BMSCs in a mouse model of adriamycin (ADR)-induced FSGS *in vivo* and MPC5 cells *in vivo*.

Research methods

MSCs^{CA} were compared with MSCs or CA to observe their inhibitory effects on podocyte apoptosis in mice with ADR-induced FSGS *in vivo* and ADR-treated MPC5 cells *in vitro*, to explore the possible mechanism by which MSCs^{CA} improves podocyte apoptosis.

Research results

In vivo results showed that MSCs^{CA} reduced podocyte apoptosis, improved podocyte injury and depletion, alleviated glomerulosclerosis and albuminuria, and downregulated p-Smad3 expression in ADR-induced FSGS mice, which were superior to MSCs and CA. Similar to *in vivo* studies, MSCs^{CA} alleviated ADR-induced apoptosis of MPC5 cells more significantly than MSCs and CA. Through rescue experiments, we found that the potential of MSCs^{CA} to protect podocytes may be realized through targeted inhibition of p-Smad3 expression.

Research conclusions

MSCs^{CA} improve ADR-induced podocyte apoptosis by targeting Smad3 inhibition, which are superior to MSCs or CA.

Research perspectives

Our findings provide a new potential strategy for the treatment of FSGS.

FOOTNOTES

Author contributions: Wang L and Fahsai K contributed equally to this article as co-corresponding authors; Wang L and Fahsai K designed the study and supervised the laboratory experiments; Hu QD conducted the experiments and drafted the manuscript; Tan RZ assisted with the experiments; Zou YX and Li JC collected the samples; Fan JM and Wang L contributed new reagents and analytic tools; and all authors read and approved the final manuscript.

Supported by the National Natural Science Foundation of China (General Program), No. 82205002; Science and Technology Project of Sichuan Province, No. 2022YFS0621, No. 21ZDYF0348, and No. 2022NSFSC1459; Luzhou-Southwest Medical University Science and Technology Strategic Cooperation Project, No. 2021LZXNYD-P04; and Southwest Medical University of Affiliated Traditional Medicine Hospital Project, No. 2022-CXTD-03.

Institutional animal care and use committee statement: All animal experiments were reviewed and approved by the Animal Ethics Committee of Southwest Medical University (Approval No. 20221031-012).

Conflict-of-interest statement: The authors have no conflicts of interest to declare.

Data sharing statement: All data are available from the corresponding author upon reasonable request Wangli120@swmu.edu.cn.

ARRIVE guidelines statement: The authors have read the ARRIVE guidelines, and the manuscript was prepared and revised according to

the ARRIVE guidelines.

Country/Territory of origin: China

ORCID number: Qiong-Dan Hu 0000-0003-3712-056X; Fahsai Kantawong 0000-0003-0323-3021; Li Wang 0000-0003-3881-3149.

S-Editor: Chen YL
L-Editor: Wang TQ
P-Editor: Zhang XD

REFERENCES

1 **Wheeler DC**, Jongs N, Stefansson BV, Chertow GM, Greene T, Hou FF, Langkilde AM, McMurray JJV, Rossing P, Nowicki M, Wittmann I, Correa-Rotter R, Sjöström CD, Toto RD, Heerspink HJL; DAPA-CKD Trial Committees and Investigators. Safety and efficacy of dapagliflozin in patients with focal segmental glomerulosclerosis: a prespecified analysis of the dapagliflozin and prevention of adverse outcomes in chronic kidney disease (DAPA-CKD) trial. *Nephrol Dial Transplant* 2022; **37**: 1647-1656 [PMID: 34850160 DOI: 10.1093/ndt/gfab335]

2 **Rajasekeran H**, Reich HN, Hladunewich MA, Cattran D, Lovshin JA, Lytvyn Y, Bjornstad P, Lai V, Tse J, Cham L, Majumder S, Bowskill BB, Kabir MG, Advani SL, Gibson IW, Sood MM, Advani A, Cherney DZI. Dapagliflozin in focal segmental glomerulosclerosis: a combined human-rodent pilot study. *Am J Physiol Renal Physiol* 2018; **314**: F412-F422 [PMID: 29141939 DOI: 10.1152/ajprenal.00445.2017]

3 **Peev V**, Hahm E, Reiser J. Unwinding focal segmental glomerulosclerosis. *F1000Res* 2017; **6**: 466 [PMID: 28491286 DOI: 10.12688/f1000research.10510.1]

4 **Shabaka A**, Tato Ribera A, Fernández-Juárez G. Focal Segmental Glomerulosclerosis: State-of-the-Art and Clinical Perspective. *Nephron* 2020; **144**: 413-427 [PMID: 32721952 DOI: 10.1159/000508099]

5 **Margos G**, Fingerle V, Oskam C, Stevenson B, Gofton A. Comment on: Gupta, 2019, distinction between Borrelia and Borreliella is more robustly supported by molecular and phenotypic characteristics than all other neighbouring prokaryotic genera: Response to Margos' *et al*. "The genus Borrelia reloaded" (PLoS One 13(12): e0208432). PLoS One 14(8):e0221397. *Ticks Tick Borne Dis* 2020; **11**: 101320 [PMID: 31722850 DOI: 10.1016/j.ttbdis.2019.101320]

6 **Agrawal V**, Prasad N, Jain M, Pandey R. Reduced podocin expression in minimal change disease and focal segmental glomerulosclerosis is related to the level of proteinuria. *Clin Exp Nephrol* 2013; **17**: 811-818 [PMID: 23377573 DOI: 10.1007/s10157-013-0775-y]

7 **Campbell KN**, Tumlin JA. Protecting Podocytes: A Key Target for Therapy of Focal Segmental Glomerulosclerosis. *Am J Nephrol* 2018; **47** Suppl 1: 14-29 [PMID: 29852493 DOI: 10.1159/000481634]

8 **Liu XQ**, Jiang L, Li YY, Huang YB, Hu XR, Zhu W, Wang X, Wu YG, Meng XM, Qi XM. Wogonin protects glomerular podocytes by targeting Bcl-2-mediated autophagy and apoptosis in diabetic kidney disease. *Acta Pharmacol Sin* 2022; **43**: 96-110 [PMID: 34253875 DOI: 10.1038/s41401-021-00721-5]

9 **Fan Y**, Yang Q, Yang Y, Gao Z, Ma Y, Zhang L, Liang W, Ding G. Sirt6 Suppresses High Glucose-Induced Mitochondrial Dysfunction and Apoptosis in Podocytes through AMPK Activation. *Int J Biol Sci* 2019; **15**: 701-713 [PMID: 30745856 DOI: 10.7150/ijbs.29323]

10 **Xu J**, Deng Y, Wang Y, Sun X, Chen S, Fu G. SPAG5-AS1 inhibited autophagy and aggravated apoptosis of podocytes *via* SPAG5/AKT/mTOR pathway. *Cell Prolif* 2020; **53**: e12738 [PMID: 31957155 DOI: 10.1111/cpr.12738]

11 **Chen A**, Feng Y, Lai H, Ju W, Li Z, Li Y, Wang A, Hong Q, Zhong F, Wei C, Fu J, Guan T, Liu B, Kretzler M, Lee K, He JC. Soluble RARRES1 induces podocyte apoptosis to promote glomerular disease progression. *J Clin Invest* 2020; **130**: 5523-5535 [PMID: 32634130 DOI: 10.1172/JCI140155]

12 **Liu Y**, Li Y, Xu L, Shi J, Yu X, Wang X, Li X, Jiang H, Yang T, Yin X, Du L, Lu Q. Quercetin Attenuates Podocyte Apoptosis of Diabetic Nephropathy Through Targeting EGFR Signaling. *Front Pharmacol* 2021; **12**: 792777 [PMID: 35069207 DOI: 10.3389/fphar.2021.792777]

13 **Chen Y**, Zhang L, Liu S, Yao B, Zhang H, Liang S, Ma J, Liang X, Shi W. Sam68 mediates high glucose-induced podocyte apoptosis through modulation of Bax/Bcl-2. *Mol Med Rep* 2019; **20**: 3728-3734 [PMID: 31485651 DOI: 10.3892/mmr.2019.10601]

14 **Guo W**, Gao H, Pan W, Yu P, Che G. High glucose induces Nox4 expression and podocyte apoptosis through the Smad3/ezrin/PKA pathway. *Biol Open* 2021; **10** [PMID: 33046439 DOI: 10.1242/bio.055012]

15 **Thanaskody K**, Jusop AS, Tye GJ, Wan Kamarul Zaman WS, Dass SA, Nordin F. MSCs vs. iPSCs: Potential in therapeutic applications. *Front Cell Dev Biol* 2022; **10**: 1005926 [PMID: 36407112 DOI: 10.3389/fcell.2022.1005926]

16 **Zhang L**, Xiang J, Zhang F, Liu L, Hu C. MSCs can be a double-edged sword in tumorigenesis. *Front Oncol* 2022; **12**: 1047907 [PMID: 36439438 DOI: 10.3389/fonc.2022.1047907]

17 **Bian D**, Wu Y, Song G, Azizi R, Zamani A. The application of mesenchymal stromal cells (MSCs) and their derivative exosome in skin wound healing: a comprehensive review. *Stem Cell Res Ther* 2022; **13**: 24 [PMID: 35073970 DOI: 10.1186/s13287-021-02697-9]

18 **Kwon DG**, Kim MK, Jeon YS, Nam YC, Park JS, Ryu DJ. State of the Art: The Immunomodulatory Role of MSCs for Osteoarthritis. *Int J Mol Sci* 2022; **23** [PMID: 35163541 DOI: 10.3390/ijms23031618]

19 **Khalilpourfarshbafi M**, Hajiaghaalipour F, Selvarajan KK, Adam A. Mesenchymal Stem Cell-Based Therapies against Podocyte Damage in Diabetic Nephropathy. *Tissue Eng Regen Med* 2017; **14**: 201-210 [PMID: 30603477 DOI: 10.1007/s13770-017-0026-5]

20 **Wang Y**, Liu J, Zhang Q, Wang W, Liu Q, Liu S, Song Y, Wang X, Zhang Y, Li S, Yang X, Lv S, Liu G. Human umbilical cord mesenchymal stem cells attenuate podocyte injury under high glucose *via* TLR2 and TLR4 signaling. *Diabetes Res Clin Pract* 2021; **173**: 108702 [PMID: 33609619 DOI: 10.1016/j.diabres.2021.108702]

21 **Sun J**, Zhao F, Zhang W, Lv J, Yin A. BMSCs and miR-124a ameliorated diabetic nephropathy *via* inhibiting notch signalling pathway. *J Cell Mol Med* 2018; **22**: 4840-4855 [PMID: 30024097 DOI: 10.1111/jcmm.13747]

22 **Yang RC**, Zhu XL, Wang J, Wan F, Zhang HQ, Lin Y, Tang XL, Zhu B. Bone marrow mesenchymal stem cells attenuate the progression of focal segmental glomerulosclerosis in rat models. *BMC Nephrol* 2018; **19**: 335 [PMID: 30466397 DOI: 10.1186/s12882-018-1137-5]

23 **Li Y**, Liu Q, Ou ST, Wu WH, Gan LW. Research on mechanism of MAPK signal pathway induced by BMSCs for the proteinuria of rat's kidney, glomerulosclerosis and activity of RAS. *Eur Rev Med Pharmacol Sci* 2021; **25**: 795-803 [PMID: 33577034 DOI: 10.26355/eurrev_202101_24643]

24 **Zhao T**, Jin Q, Kong L, Zhang D, Teng Y, Lin L, Yao X, Jin Y, Li M. microRNA-15b-5p shuttled by mesenchymal stem cell-derived extracellular vesicles protects podocytes from diabetic nephropathy *via* downregulation of VEGF/PDK4 axis. *J Bioenerg Biomembr* 2022; **54**: 17-30 [PMID: 34806156 DOI: 10.1007/s10863-021-09919-y]

25 **Duan Y**, Luo Q, Wang Y, Ma Y, Chen F, Zhu X, Shi J. Adipose mesenchymal stem cell-derived extracellular vesicles containing microRNA-26a-5p target TLR4 and protect against diabetic nephropathy. *J Biol Chem* 2020; **295**: 12868-12884 [PMID: 32580945 DOI: 10.1074/jbc.RA120.012522]

26 **Hu C**, Li L. Preconditioning influences mesenchymal stem cell properties in vitro and in vivo. *J Cell Mol Med* 2018; **22**: 1428-1442 [PMID: 29392844 DOI: 10.1111/jcmm.13492]

27 **Feng D**, Li XR, Wang ZY, Gu NN, Zhang SX, Li CF, Chen Y, Ma ZQ, Lin RC, Zhang HG, Zhao C. Integrated UPLC-MS and Network Pharmacology Approach to Explore the Active Components and the Potential Mechanism of Yiqi Huoxue Decoction for Treating Nephrotic Syndrome. *Front Pharmacol* 2021; **12**: 775745 [PMID: 35295738 DOI: 10.3389/fphar.2021.775745]

28 **Li AP**, He SS, Zhang WN, Zhang LC, Liu YT, Li K, Qin XM. Exploration the active compounds of Astragali Radix in treatment of adriamycin nephropathy by network pharmacology combined with transcriptomic approach. *J Ethnopharmacol* 2020; **258**: 112537 [PMID: 31901455 DOI: 10.1016/j.jep.2019.112537]

29 **Hu Q**, Zhu B, Yang G, Jia J, Wang H, Tan R, Zhang Q, Wang L, Kantawong F. Calycosin pretreatment enhanced the therapeutic efficacy of mesenchymal stem cells to alleviate unilateral ureteral obstruction-induced renal fibrosis by inhibiting necroptosis. *J Pharmacol Sci* 2023; **151**: 72-83 [PMID: 36707181 DOI: 10.1016/j.jphs.2022.12.001]

30 **Dou Y**, Shang Y, Shen Y, Qu J, Liu C, Cao J. Baicalin alleviates adriamycin-induced focal segmental glomerulosclerosis and proteinuria by inhibiting the Notch1-Snail axis mediated podocyte EMT. *Life Sci* 2020; **257**: 118010 [PMID: 32598932 DOI: 10.1016/j.lfs.2020.118010]

31 **Liu G**, He L, Yang X, Tang L, Shi W, She J, Wei J. MicroRNA-155-5p Aggravates Adriamycin-Induced Focal Segmental Glomerulosclerosis through Targeting Nrf2. *Nephron* 2023; **147**: 108-119 [PMID: 35728579 DOI: 10.1159/000525233]

32 **Peister A**, Mellad JA, Larson BL, Hall BM, Gibson LF, Prockop DJ. Adult stem cells from bone marrow (MSCs) isolated from different strains of inbred mice vary in surface epitopes, rates of proliferation, and differentiation potential. *Blood* 2004; **103**: 1662-1668 [PMID: 14592819 DOI: 10.1182/blood-2003-09-3070]

33 **Dong L**, Li JC, Hu ZJ, Huang XR, Wang L, Wang HL, Ma RCW, Lan HY, Yang SJ. Deletion of Smad3 protects against diabetic myocardiopathy in db/db mice. *J Cell Mol Med* 2021; **25**: 4860-4869 [PMID: 33733577 DOI: 10.1111/jcmm.16464]

34 **Xing L**, Fang J, Zhu B, Wang L, Chen J, Wang Y, Huang J, Wang H, Yao X. Astragaloside IV protects against podocyte apoptosis by inhibiting oxidative stress *via* activating PPARγ-Klotho-FoxO1 axis in diabetic nephropathy. *Life Sci* 2021; **269**: 119068 [PMID: 33476631 DOI: 10.1016/j.lfs.2021.119068]

35 **Peng Z**, Guo HY, Li YQ, Li JC, Yang XH, Liu J, Hu QD, Wang HL, Wang L. The Smad3-dependent microRNA let-7i-5p promoted renal fibrosis in mice with unilateral ureteral obstruction. *Front Physiol* 2022; **13**: 937878 [PMID: 36091385 DOI: 10.3389/fphys.2022.937878]

36 **Grange C**, Skovronova R, Marabese F, Bussolati B. Stem Cell-Derived Extracellular Vesicles and Kidney Regeneration. *Cells* 2019; **8** [PMID: 31614642 DOI: 10.3390/cells8101240]

37 **Yun CW**, Lee SH. Potential and Therapeutic Efficacy of Cell-based Therapy Using Mesenchymal Stem Cells for Acute/chronic Kidney Disease. *Int J Mol Sci* 2019; **20** [PMID: 30939749 DOI: 10.3390/ijms20071619]

38 **Chen Y**, Shen H, Ding Y, Yu Y, Shao L, Shen Z. The application of umbilical cord-derived MSCs in cardiovascular diseases. *J Cell Mol Med* 2021; **25**: 8103-8114 [PMID: 34378345 DOI: 10.1111/jcmm.16830]

39 **Wang C**, Tian C, Cai D, Jiang H, Zhang W, Liu S, Peng L, Hu X. BDNF-overexpressing MSCs delivered by hydrogel in acute ischemic stroke treatment. *Ann Transl Med* 2022; **10**: 1393 [PMID: 36660688 DOI: 10.21037/atm-22-5921]

40 **Nie WB**, Zhang D, Wang LS. Growth Factor Gene-Modified Mesenchymal Stem Cells in Tissue Regeneration. *Drug Des Devel Ther* 2020; **14**: 1241-1256 [PMID: 32273686 DOI: 10.2147/DDDT.S243944]

41 **Philipp D**, Suhr L, Wahlers T, Choi YH, Paunel-Görgülü A. Preconditioning of bone marrow-derived mesenchymal stem cells highly strengthens their potential to promote IL-6-dependent M2b polarization. *Stem Cell Res Ther* 2018; **9**: 286 [PMID: 30359316 DOI: 10.1186/s13287-018-1039-2]

42 **Li C**, Lv H, Du Y, Zhu W, Yang W, Wang X, Wang J, Chen W. Corrigendum to "Biologically modified implantation as therapeutic bioabsorbable materials for bone defect repair" [Regen Ther 19 (2022) 9-23]. *Regen Ther* 2023; **22**: 191 [PMID: 36874475 DOI: 10.1016/j.reth.2023.01.010]

43 **Fatima A**, Malick TS, Khan I, Ishaque A, Salim A. Effect of glycyrrhizic acid and 18β-glycyrrhetinic acid on the differentiation of human umbilical cord-mesenchymal stem cells into hepatocytes. *World J Stem Cells* 2021; **13**: 1580-1594 [PMID: 34786159 DOI: 10.4252/wjsc.v13.i10.1580]

44 **Ulpiano C**, da Silva CL, Monteiro GA. Mesenchymal Stromal Cells (MSCs): A Promising Tool for Cell-Based Angiogenic Therapy. *Curr Gene Ther* 2021; **21**: 382-405 [PMID: 34533444 DOI: 10.2174/1566523221666210917114353]

45 **Chen TS**, Chuang SY, Shen CY, Ho TJ, Chang RL, Yeh YL, Kuo CH, Mahalakshmi B, Kuo WW, Huang CY. Antioxidant Sirt1/Akt axis expression in resveratrol pretreated adipose-derived stem cells increases regenerative capability in a rat model with cardiomyopathy induced by diabetes mellitus. *J Cell Physiol* 2021; **236**: 4290-4302 [PMID: 33421145 DOI: 10.1002/jcp.30057]

46 **He H**, Takahashi A, Mukai T, Hori A, Narita M, Tojo A, Yang T, Nagamura-Inoue T. The Immunomodulatory Effect of Triptolide on Mesenchymal Stromal Cells. *Front Immunol* 2021; **12**: 686356 [PMID: 34484183 DOI: 10.3389/fimmu.2021.686356]

47 **Zhang HW**, Lin ZX, Xu C, Leung C, Chan LS. Astragalus (a traditional Chinese medicine) for treating chronic kidney disease. *Cochrane Database Syst Rev* 2014; CD008369 [PMID: 25335553 DOI: 10.1002/14651858.CD008369.pub2]

48 **Han C**, Jiang YH, Li W, Liu Y. Astragalus membranaceus and Salvia miltiorrhiza ameliorates cyclosporin A-induced chronic nephrotoxicity through the "gut-kidney axis". *J Ethnopharmacol* 2021; **269**: 113768 [PMID: 33383113 DOI: 10.1016/j.jep.2020.113768]

49 **Yoshino T**, Horiba Y, Mimura M, Watanabe K. Oral Astragalus Root Supplementation for Mild to Moderate Chronic Kidney Disease: A Self-

Controlled Case-Series. *Front Pharmacol* 2022; **13**: 775798 [PMID: 35300298 DOI: 10.3389/fphar.2022.775798]

50 **Huang D**, Shen P, Wang C, Gao J, Ye C, Wu F. Calycosin plays a protective role in diabetic kidney disease through the regulation of ferroptosis. *Pharm Biol* 2022; **60**: 990-996 [PMID: 35587919 DOI: 10.1080/13880209.2022.2067572]

51 **Yosri H**, El-Kashef DH, El-Sherbiny M, Said E, Salem HA. Calycosin modulates NLRP3 and TXNIP-mediated pyroptotic signaling and attenuates diabetic nephropathy progression in diabetic rats; An insight. *Biomed Pharmacother* 2022; **155**: 113758 [PMID: 36271546 DOI: 10.1016/j.biopha.2022.113758]

52 **Zhang N**, Guan C, Liu Z, Li C, Yang C, Xu L, Niu M, Zhao L, Zhou B, Che L, Wang Y, Xu Y. Calycosin attenuates renal ischemia/reperfusion injury by suppressing NF-κB mediated inflammation *via* PPARγ/EGR1 pathway. *Front Pharmacol* 2022; **13**: 970616 [PMID: 36278223 DOI: 10.3389/fphar.2022.970616]

53 **Park KR**, Park JE, Kim B, Kwon IK, Hong JT, Yun HM. Calycosin-7-O-β-Glucoside Isolated from Astragalus membranaceus Promotes Osteogenesis and Mineralization in Human Mesenchymal Stem Cells. *Int J Mol Sci* 2021; **22** [PMID: 34768792 DOI: 10.3390/ijms222111362]

54 **Dai H**, Liu Q, Liu B. Research Progress on Mechanism of Podocyte Depletion in Diabetic Nephropathy. *J Diabetes Res* 2017; **2017**: 2615286 [PMID: 28791309 DOI: 10.1155/2017/2615286]

55 **Yu S**, Ren Q, Yu L, Tan J, Xia ZK. Role of autophagy in Puromycin Aminonucleoside-induced podocyte apoptosis. *J Recept Signal Transduct Res* 2020; **40**: 273-280 [PMID: 32102592 DOI: 10.1080/10799893.2020.1731536]

56 **Hall G**, Wyatt CM. Mechanisms of Proteinuria in HIV. *Front Med (Lausanne)* 2021; **8**: 749061 [PMID: 34722586 DOI: 10.3389/fmed.2021.749061]

57 **Bao W**, Xia H, Liang Y, Ye Y, Lu Y, Xu X, Duan A, He J, Chen Z, Wu Y, Wang X, Zheng C, Liu Z, Shi S. Toll-like Receptor 9 Can be Activated by Endogenous Mitochondrial DNA to Induce Podocyte Apoptosis. *Sci Rep* 2016; **6**: 22579 [PMID: 26934958 DOI: 10.1038/srep22579]

58 **Qu G**, He T, Dai A, Zhao Y, Guan D, Li S, Shi H, Gan W, Zhang A. miR-199b-5p mediates adriamycin-induced podocyte apoptosis by inhibiting the expression of RGS10. *Exp Ther Med* 2021; **22**: 1469 [PMID: 34737809 DOI: 10.3892/etm.2021.10904]

59 **Lee JH**, Mellado-Gil JM, Bahn YJ, Pathy SM, Zhang YE, Rane SG. Protection from β-cell apoptosis by inhibition of TGF-β/Smad3 signaling. *Cell Death Dis* 2020; **11**: 184 [PMID: 32170115 DOI: 10.1038/s41419-020-2365-8]

60 **Qiu M**, Li T, Wang B, Gong H, Huang T. miR-146a-5p Regulated Cell Proliferation and Apoptosis by Targeting SMAD3 and SMAD4. *Protein Pept Lett* 2020; **27**: 411-418 [PMID: 31544687 DOI: 10.2174/0929866526666190911142926]

61 **Song S**, Shi C, Bian Y, Yang Z, Mu L, Wu H, Duan H, Shi Y. Sestrin2 remedies podocyte injury *via* orchestrating TSP-1/TGF-β1/Smad3 axis in diabetic kidney disease. *Cell Death Dis* 2022; **13**: 663 [PMID: 35908070 DOI: 10.1038/s41419-022-05120-0]

62 **Wu W**, Wang X, Yu X, Lan HY. Smad3 Signatures in Renal Inflammation and Fibrosis. *Int J Biol Sci* 2022; **18**: 2795-2806 [PMID: 35541902 DOI: 10.7150/ijbs.71595]

World Journal of Stem Cells

Submit a Manuscript: https://www.f6publishing.com

World J Stem Cells 2023 June 26; 15(6): 632-653

DOI: 10.4252/wjsc.v15.i6.632

ISSN 1948-0210 (online)

SYSTEMATIC REVIEWS

Current overview of induced pluripotent stem cell-based blood-brain barrier-on-a-chip

Arielly da Hora Alves, Mariana Penteado Nucci, Nicole Mastandrea Ennes do Valle, Juliana Morais Missina, Javier Bustamante Mamani, Gabriel Nery Albuquerque Rego, Olivia Furiama Metropolo Dias, Murilo Montenegro Garrigós, Fernando Anselmo de Oliveira, Lionel Fernel Gamarra

Specialty type: Cell and tissue engineering

Provenance and peer review: Invited article; Externally peer reviewed.

Peer-review model: Single blind

Peer-review report's scientific quality classification

Grade A (Excellent): 0
Grade B (Very good): 0
Grade C (Good): C, C
Grade D (Fair): D
Grade E (Poor): 0

P-Reviewer: Chen YJ, China; Lu Q, China; Thummer RP, India

Received: February 15, 2023
Peer-review started: February 15, 2023
First decision: April 10, 2023
Revised: April 10, 2023
Accepted: May 8, 2023
Article in press: May 8, 2023
Published online: June 26, 2023

Arielly da Hora Alves, Mariana Penteado Nucci, Nicole Mastandrea Ennes do Valle, Juliana Morais Missina, Javier Bustamante Mamani, Gabriel Nery Albuquerque Rego, Olivia Furiama Metropolo Dias, Murilo Montenegro Garrigós, Fernando Anselmo de Oliveira, Lionel Fernel Gamarra, Hospital Israelita Albert Einstein, São Paulo 05529-060, São Paulo, Brazil

Mariana Penteado Nucci, Hospital das Clínicas HCFMUSP, Faculdade de Medicina, Universidade de São Paulo, São Paulo 05403-010, São Paulo, Brazil

Corresponding author: Lionel Fernel Gamarra, PhD, Academic Research, Professor, Research Associate, Teacher, Hospital Israelita Albert Einstein, Av. Albert Einstein, 627/701, Morumbi, São Paulo 05529-060, São Paulo, Brazil. lgamarra@einstein.br

Abstract

BACKGROUND

Induced pluripotent stem cells (iPSCs) show great ability to differentiate into any tissue, making them attractive candidates for pathophysiological investigations. The rise of organ-on-a-chip technology in the past century has introduced a novel way to make *in vitro* cell cultures that more closely resemble their *in vivo* environments, both structural and functionally. The literature still lacks consensus on the best conditions to mimic the blood-brain barrier (BBB) for drug screening and other personalized therapies. The development of models based on BBB-on-a-chip using iPSCs is promising and is a potential alternative to the use of animals in research.

AIM

To analyze the literature for BBB models on-a-chip involving iPSCs, describe the microdevices, the BBB *in vitro* construction, and applications.

METHODS

We searched for original articles indexed in PubMed and Scopus that used iPSCs to mimic the BBB and its microenvironment in microfluidic devices. Thirty articles were identified, wherein only 14 articles were finally selected according to the inclusion and exclusion criteria. Data compiled from the selected articles were organized into four topics: (1) Microfluidic devices design and fabrication; (2) characteristics of the iPSCs used in the BBB model and their differentiation conditions; (3) BBB-on-a-chip reconstruction process; and (4) applications of BBB

microfluidic three-dimensional models using iPSCs.

RESULTS

This study showed that BBB models with iPSCs in microdevices are quite novel in scientific research. Important technological advances in this area regarding the use of commercial BBB-on-a-chip were identified in the most recent articles by different research groups. Conventional polydimethylsiloxane was the most used material to fabricate in-house chips (57%), whereas few studies (14.3%) adopted polymethylmethacrylate. Half the models were constructed using a porous membrane made of diverse materials to separate the channels. iPSC sources were divergent among the studies, but the main line used was IMR90-C4 from human fetal lung fibroblast (41.2%). The cells were differentiated through diverse and complex processes either to endothelial or neural cells, wherein only one study promoted differentiation inside the chip. The construction process of the BBB-on-a-chip involved previous coating mostly with fibronectin/collagen IV (39.3%), followed by cell seeding in single cultures (36%) or co-cultures (64%) under controlled conditions, aimed at developing an *in vitro* BBB that mimics the human BBB for future applications.

CONCLUSION

This review evidenced technological advances in the construction of BBB models using iPSCs. Nonetheless, a definitive BBB-on-a-chip has not yet been achieved, hindering the applicability of the models.

Key Words: Induced pluripotent stem cells; Cell differentiation; Blood-brain barrier; Neurovascular unit; Organ-on-a-chip; Microfluidic device

Core Tip: This systematic review provided a current perspective on the applicability of induced pluripotent stem cells within blood-brain barrier (BBB)-on-a-chip with high technology advances in commercial chips and promotion of an efficient human neurovascular unit, able to screen for drugs, mimic brain dysfunctions, such as stroke and Huntington's disease, and suitable for future personalized therapeutic approaches. However, the composition and construction of the BBB models lack consensus in the literature.

Citation: Alves ADH, Nucci MP, Ennes do Valle NM, Missina JM, Mamani JB, Rego GNA, Dias OFM, Garrigós MM, de Oliveira FA, Gamarra LF. Current overview of induced pluripotent stem cell-based blood-brain barrier-on-a-chip. *World J Stem Cells* 2023; 15(6): 632-653

URL: https://www.wjgnet.com/1948-0210/full/v15/i6/632.htm

DOI: https://dx.doi.org/10.4252/wjsc.v15.i6.632

INTRODUCTION

Induced pluripotent stem cells (iPSCs) have been largely studied for their numerous applications in drug screening, toxicological studies, cell therapy, and disease modeling[1]. Their relevance may be justified by their resemblance to embryonic stem cells, given their ability to differentiate into any one of the three germ layers: ectoderm, mesoderm, and endoderm[1,2], making them attractive candidates for cell therapy-based regenerative medicine[3].

Different from primary cells, iPSCs are easily attainable and able to mature into almost any desired cell type. In general, they can be formed by reprogramming cells obtained from a tissue biopsy or from more accessible sources such as peripheral blood, renal epithelial cells, or dental pulp[4,5]. These characteristics, as opposed to primary cells, have promoted more reliable models for complex human structures such as the blood-brain barrier (BBB)[6].

The BBB secures the brain with a homeostatic environment, controlling the interaction, communication, and molecular and ion exchange between the central nervous system (CNS) and the peripheral blood[7]. The neurovascular unit (NVU) is generally composed of brain microvascular endothelial cells (BMECs), astrocytes (ACs), and pericytes (PCs), being directly involved in regulating CNS blood flow, and consequently, neuronal activity[8].

Recreating the BBB microenvironment *in vitro* allows for the investigation of barrier dysfunction in neurodegenerative diseases, and drug delivery to the CNS, in addition to the evaluation and screening of the permeability of substances across the BBB[9,10]. In this regard, classic BBB *in vitro* models have traditionally utilized Transwell® technology, which enables the construction of multicellular models with paracrine interactions between the co-cultures of ECs and ACs or PCs. Notwithstanding its usefulness, Transwell® technology lacks a key element for the *in vivo*-like functioning of ECs: Laminar flow[6,9]. Moreover, many of the existing BBB models employ primary BMECs, immortalized BMECs, or human umbilical vein ECs (HUVECs) as EC-layer cultures. Even though they can constitute fair BBB constructs, access to primary cell sources can be difficult for ethical purposes and immortalized lines often fail to mimic the actual BBB function found *in vivo*[6,9].

In the building of *in vitro* BBB mimics, iPSC-derived BMECs (iBMECs) present improved barrier properties compared to primary BMECs, allowing for the modeling of genetic diseases and personalized therapy approaches[2]. These properties become more apparent when iBMECs are cultured in a complex environment. The traditional *in vitro* culture model, despite being simple and reproducible, fails to mimic cell-cell and cell-extracellular matrix (ECM) interactions[11]. Animal models, which present ideal barrier permeability, transport mechanisms, and morphological characteristics, present low reliability given that 80% of clinical trials fail in drug-delivery tests[12]. These limitations may be overcome with the development of organs-on-a-chip that simulate complex morphology in a three-dimensional (3D) culture[13].

The construction and applications of BBB-on-a-chip using microfluidic devices provide a lower-cost alternative with an impact on ethical issues, allowing for the reduced use of animals, reagents, and sample volume, and also permitting real-time microscopic analysis, with shortened reaction and analysis times, high throughput, automation, and portability[14, 15]. Furthermore, from a morphological point of view, the microdevices assure a compatible reproduction of the BBB model due to the presence of laminar flow and shear stress, which convey better maintenance of barrier functions, homeostasis, and transport. This model has already been applied to several studies of neurological disorders such as Alzheimer's disease, stroke, infectious diseases, and brain cancer[15]. Despite being the best alternative for simulation and in-depth study of the BBB, studies involving microfluidic devices lack clear protocols for large-scale manufacturing and adequate liquid perfusion, making the process imprecise and hard to operate, in addition to the difficulty in collecting channel material for detailed assessments[16].

Regarding the construction of BBB *in vitro* models on-a-chip using iPSCs, the literature still lacks a consensus on the best conditions to mimic BBB dysfunction upon CNS disorders and to screen for drugs and other therapeutic approaches. In view of these gaps, this systematic review searched the current literature for examples that meet the abovementioned criteria, that is, iPSCs, BBB models, and microfluidic devices.

MATERIALS AND METHODS

Search strategy

The articles used in this review were identified through searches performed in the PubMed and Scopus databases following the PRISMA guidelines[17]. The following selected criteria of interest, keyword strings ((Induced Pluripotent Stem Cell) AND (Microfluidic Device) AND (Blood-Brain Barrier)) and Boolean operators (DecS/MeSH) were used:

PubMed: (((((((“organs-on-chips”[Title/Abstract]) OR (“organs-on-a-chip”[Title/Abstract])) OR (“microfluidic device”[Title/Abstract])) OR (“lab-on-chips”[Title/Abstract])) OR (microfluidics[Title/Abstract])) AND ((((“blood-brain barrier”[Title/Abstract]) OR (“Brain Blood Barrier”[Title/Abstract])) OR (“Blood Brain Barrier”[Title/Abstract]))) AND (((“Induced Pluripotent Stem Cell”[Title/Abstract]) OR (“Induced pluripotent stem cells”[Title/Abstract])) OR (iPSC[Title/Abstract]))) NOT (review[Publication Type]);

Scopus: ((TITLE-ABS-KEY (ipsc) OR TITLE-ABS-KEY (“induced pluripotent stem cell”) OR TITLE-ABS-KEY (“induced pluripotent stem cells”))) AND (((TITLE-ABS-KEY (“organs-on-chips”) OR TITLE-ABS-KEY (“organs-on-a-chip”) OR TITLE-ABS-KEY (“microfluidic device”) OR TITLE-ABS-KEY (“lab-on-chips”) OR TITLE-ABS-KEY (microfluidics) OR TITLE-ABS-KEY (“lab-on-chip”))) AND ((TITLE-ABS-KEY (“blood brain barrier”) OR TITLE-ABS-KEY (“brain blood barrier”) OR TITLE-ABS-KEY (“blood-brain barrier”)))) AND (LIMIT-TO (LANGUAGE, “English”)) AND (LIMIT-TO (DOCTYPE, “ar”)).

Inclusion and exclusion criteria

Only original full-text articles written in English have been included, without publication year limit, containing: (1) iPSCs; (2) microfluidic devices; and (3) simulation of the BBB by specialized cells. From the perspective of the Problem, Intervention, Comparison, and Outcome criterion, the addressed Problem was unclear literature on the best conditions to mimic the BBB using microfluidic device technology (BBB-on-a-chip) and IPSCs; the Intervention was to analyze the conditions for BBB-on-a-chip manufacture regarding the design and material for an adequate construction of the NVU with a functional environment for testing; the Comparison was related to conventional analyses; and the Outcome was a microdevice that mimics the BBB applied in neurological conditions or not. The exclusion of articles followed the following criteria: (1) Book chapters; (2) reviews; (3) duplicate articles in the databases; and (4) a study that did not report the use of iPSCs in the BBB-on-a-chip.

Data extraction

The selected articles under evaluation were analyzed under four topics, which were represented in three tables and one figure that addressed the following characteristics: (1) Microfluidic devices design and fabrication; (2) characteristics of the iPSCs used in the BBB models and their cultivation conditions; (3) iPSC differentiation process into iBMECs for reconstruction of the BBB-on-a-chip model; and (4) applications of BBB microfluidic 3D models using iPSCs.

Data compilation and review

In this systematic review, the preselection of titles was performed by authors Alves ADH and Gamarra LF from the defined search strategies. The ten authors (Alves ADH, Nucci MP, Ennes do Valle NM, Missina JM, Rego GNA, Mamani JB, Dias OFM, Garrigós MM, de Oliveira FA, Gamarra LF), in pairs, independently, and randomly reviewed and analyzed the eligibility of the articles according to the selection criteria mentioned above. In case of discrepancy in study selection between two authors, the criteria were discussed with a third reviewer and resolved.

Ennes do Valle NM and Mamani JB searched for the fabrication and characteristics of microfluidic devices; Alves ADH, Nucci MP, Ennes do Valle NM, Missina JM, and Rego GNA searched for differentiation and characterization protocols for iPSCs; Alves ADH, Nucci MP, Ennes do Valle NM, Missina JM, and Gamarra LF searched for the insertion and manipulation of cells in the microfluidic device; de Oliveira FA, Mamani JB, Dias OFM, and Garrigós MM searched for the objectives and applications of the selected studies. Analyses of data extracted from tables and flowcharts were performed by full peer consensus, respecting the above distribution. In this review, all authors wrote the entire text.

Risk of bias assessment

The selection of articles was performed in pairs and a third independent author decided if the articles should be included. The data selected in the tables were divided by the authors into the groups already described above, and data verification was carried out by the following group. The final inclusion of studies into the systematic review was by agreement of all reviewers.

Data analysis

The variables grouped in the tables and charts were distributed in percentages or range of distribution and used to characterize and illustrate the most frequently used results in this review.

RESULTS

Overview of the reviewed literature

A search was performed based on the abovementioned selection strategy and keywords, resulting in 30 original articles in English: 11 from PubMed and 19 from Scopus. Following the exclusion criteria, 5 of the 11 articles from PubMed were excluded: 4 under the "review article" criterion and 1 under the "book chapter" criterion. Regarding the studies found in Scopus, 10 were manuscripts duplicated by the other database. After the eligibility analysis, only two articles were withdrawn: One for not having reported a study using iPSCs, and the other for not involving BBB functionality. Finally, this systematic review included 14 articles[18-31] that met all selection and inclusion criteria established by the authors (Figure 1).

Microfluidic device design and fabrication

The main theme of this review has been studied in current years (2017-2022), as shown in Table 1. The latest studies were performed in commercial chips[18-21], whereas older studies were performed using chips manufactured in-house[22-31]. In general, the studies with commercial chips did not detail the type of polymer[18-20] or the technology or mold used [18-21]. Only one of them specified the use of polydimethylsiloxane (PDMS), a well-known polymer for manufacturing microfluidic chips[21]. The majority of studies that manufactured the chip in-house used PDMS (57%)[22,25-29,31], but two studies adopted the less than usual materials polymethylmethacrylate (PMMA)[23] and Objet VeroClear® photopolymer[30]. Most of the chips fabricated in-house were molded by soft lithography[24-29,31], except the study by Choi *et al*[23], which employed computer numerical control; and the study by Wang *et al*[30], which used a 3D object printer. Details about mold material and fabrication were seldom explored in soft lithography applications; however, the mainly reported material was SU-8 made by photolithography[25-27].

Half of the articles evaluated displayed membrane-free microfluidic chips[18-20,24,25,29,31], as shown in Table 1. The remaining studies reported the presence of a membrane dividing the channels within the chip: Three (21%) made of PDMS[21,26,27], one made of polyethylene terephthalate (PE)[28], two made of polyester (PETE)[22,23], and one of porous polycarbonate (PC)[30]. Almost all microfluidic chips with membranes were designed to comprise a top and a bottom channel[21-23,26-28]. An exception was found in the study by Wang *et al*[30], whose chip design was more complex, containing four parts that were stacked to compose the BBB model. Five studies (36%) presented three-channel microfluidic chips: Two side channels that were generally used to perfuse medium, and one middle channel where the cells were generally cultured[18-20,25,29]. The remaining studies employed simpler chip designs that comprised a single [24] or multiple channels[31] parallel to each other. Channel dimensions were largely variable (from 160 μm to 2200 μm) among the selected articles, defined according to the desired use of the chip.

Characteristics of the iPSCs used in the BBB models and their cultivation and differentiation conditions

To build the BBB, as shown in Table 2 and Figure 2A, IMR90-C4 from human fetal lung fibroblasts was the main iPSC line used (41.1%)[18,19,21,23,24,28,30], commonly cultivated in Matrigel-coated flasks. Few studies (17.6%) have reported the use of different iPSC lines[20,26,27], one of which used nine different types of iPSCs[27] that were extracted from skin fibroblasts or the peripheral blood of healthy (5) or unhealthy donors (2). Two of these skin fibroblast lines from unhealthy donors were modified by clustered regularly interspaced short palindromic repeat (CRISPR)[27]. These diverse cell lines were useful in modeling BBB dysfunctions and their corrections[27].

Concerning the coating applied for culturing the iPSC lines, fibronectin was selected for cultivation of human iPSC (hiPSC)-ECs (11.8%)[25,29]. Other particular iPSC lines, such as Ax0018 (neural stem cells)[20] and BC1-hiPSC (bone marrow)[31], were cultured on Matrigel, whereas GM25256 (skin fibroblast)[22], and ACS-1024 (bone marrow)[24] were cultured on laminin. The ECM on which EZ-Spheres (neural progenitors) were grown was not defined[26]. Interestingly, the study by Motallebnejad *et al*[24] compared cultivation of the ACS-1024 line on different laminin isoforms (LN511 and LN411), or on collagen IV associated with fibronectin[24]. Overall, Matrigel was the coating of choice in the majority of

Table 1 Microfluidic device design and fabrication

Ref.	Manufacturing					Characteristics of microdevices
	Fabrication	Main material of device	Technology used	Mold details	Membranes	Dimensions as width × height
Kurosawa *et al* [18], 2022	MIMETAS® (OrganoPlate® 3-lane plate)	Unspecified polymer	NR	NR	Membrane-free	Top and bottom channels: 320 μm × 220 μm. Gel channels: 360 μm × 220 μm. PhaseGuides®: 100 μm × 55 μm
Fengler *et al* [19], 2022	MIMETAS® (OrganoPlate® 3-lane plate)	Unspecified polymer	NR	NR	Membrane-free	Top and bottom channels: 320 μm × 220 μm. Gel channels: 360 μm × 220 μm. PhaseGuides®: 100 μm × 55 μm (width × height)
Wevers *et al* [20], 2021	MIMETAS® (OrganoPlate® 3-lane plate)	Unspecified polymer	NR	NR	Membrane-free	Top and bottom channels: 320 μm × 220 μm. Gel channels: 360 μm × 220 μm. PhaseGuides®: 100 μm × 55 μm
Noorani *et al* [21], 2021	Emulate® (brain on-a-chip)	PDMS	NR	NR	PDMS membrane	Brain channel: 1 mm × 1 mm. Blood channel: 1 mm × 0.2 mm
Middelkamp *et al*[22], 2021	In house	PDMS	Soft lithography	Material: PMMA. Fabrication: Microm-milling	PETE membrane (5 μm thick)	Straight bottom channel: 500 μm × 500 μm. Open-top compartment: 500 μm × 1500 μm
Choi *et al*[23], 2021	In house	PMMA	CNC	NA	PETE membrane	HUVEC microchannels: 800 μm × 200 μm. iBMECs microchannels: 800 μm × 500 μm
Motallebnejad *et al*[24], 2020	In house	NR	Soft lithography	NR	Membrane-free	800 μm × 100 μm
Lee *et al*[25], 2020	In house	PDMS	Soft lithography	Material: SU-8. Fabrication: Photolithography	Membrane-free	Fluidic channel: 1340 μm × 150 μm. Main channel: 2200 μm × 150 μm
Jagadeesan *et al* [26], 2020	In house	PDMS	Soft lithography	Material: SU-8. Fabrication: Photolithography	PDMS membrane (50 μm thick)	Top microchannel: 1 mm × 1 mm. Bottom microchannel: 1 mm × 0.2 mm
Vatine *et al*[27], 2019	In house	PDMS	Soft lithography	Material: SU-8. Fabrication: Photolithography	PDMS membrane (50 μm thick)	Top microchannel: 1 mm × 1 mm. Bottom microchannel: 1 mm × 0.2 mm
Park *et al*[28], 2019	In house	PDMS	Soft lithography	Material: Prototherm. Fabrication: 3D printed (Proto labs)	PE membrane (20 μm thick)	Hollow microchannels: 1 mm × 1 mm. Top channel: 1 mm × 1 mm. Bottom channel: 1 mm × 0.2 mm
Campisi *et al* [29], 2018	In house	PDMS	Soft lithography	Material: Silicon Wafer. Fabrication: NR	Membrane-free	Fluidic channel: 1000 μm × 150 μm. Main channel: 1300 μm × 150 μm. Distance between posts: 200 μm
Wang *et al*[30], 2017	In house	Objet VeroClear photopolymer	3D object printer (Objet 30Pro, Stratasys Ltd., Rehovot, Israel)	NA	PC membrane (0.4 μm pore size)	Main channel: 300 μm × 160 μm
DeStefano *et al* [31], 2017	In house	PDMS	Soft lithography	Material: Aluminum mold. Fabrication: NR	Membrane-free	390 μm, 450 μm, 550 μm, and 770 μm (different width)

3D: Three-dimensional; CNC: Computer numerical control; hBMECs: Human brain microvascular endothelial cells; HUVEC: Human umbilical vein endothelial cells; NA: Not applied; NR: Not reported; PDMS: Polydimethylsiloxane; PC: Porous polycarbonate; PE: Polyethylene terephthalate; PETE: Polyester track-etched; PMMA: Poly(methyl methacrylate); SU-8: Negative photoresist.

the selected studies (47.4%)[18-20,23,24,27,28,30,31]. The least common coatings, such as basement membrane matrix coating[26] and geltrex[20], appeared in 5.3% of the analyzed articles (Figure 2A and Table 2).

The iPSCs generally go through a complex differentiation process, involving multiple medium replacements with the addition of supplements and composition changes. Most iPSC cultivation protocols were undertaken in mTeSR1 medium (53.3%) associated[23] or not[18,19,24,26-28,30,31] with essential medium 8 (E8, 6.7%) for about 3 d, mainly for culturing the IMR90-C4 cell line. Part of these studies (35.7%)[18,19,21,24,31] added the Rho-associated, coiled-coil containing protein kinase inhibitor (Y27632) to the cultures overnight to inhibit cell proliferation before differentiation[32,33].

Table 2 Characteristics of the induced pluripotent stem cells used in the blood-brain barrier model, their cultivation and differentiation conditions

Ref.	Cell origin	Cell differentiation				BBB components model	
		iPSCs line	Flask coating	Medium	Supplement	Differentiated cell/medium	Co-culture/medium
Kurosawa *et al* [18]	Human fetal lung fibroblast	IMR90-C4	Matrigel	Day 3-2: mTeSR1-cGMP	Day 3: With Y27632 Day 2: Without Y27632	iBMECs (10^7) in ESFM	NA
				Day 0-5: UM	KOSR (20%) + glutamax (0.5%) + NEAA (1%) + β-mercaptoethanol (0.0007%)		
				Day 6-8: $EC^{+/+}$ (HESFM)	hPDS (1%) + RA (10 μM) + hFGF2 (20 ng/mL)		
Fengler *et al*[19]	Human fetal lung fibroblast	IMR90-C4	Matrigel	Day 3-1: mTeSR1	Y27632 (10 μM)	iBMECs purified[1] (10^6) in HBVP conditioned	NA
				Day 0-5: UM (DMEM/F12-HEPES)	Glutamax + KOSR + NEAA + β-Mercapto-ethanol		
				Day 6: $EC^{+/+}$ (HESFM)	bPPP (1%) + RA (10 μM) + bFGF (20 ng/mL)		
Wevers *et al*[20]	Human astrocytes	iPSCs	Geltrex	DMEM	FBS (10%) + N2 (1 ×) + P/S (1%)	iBMECs (10^4) in NR medium	Astrocyte-neuron cells (1:4) (1.5×10^4 cells/μL) in N2B27
	Human neural stem cells	Ax0018	Matrigel-GFR	Day 0-21: N2B27	BDNF (20 ng/mL) + GDNF (10 ng/mL) + AAc (100 μM) + db-cAMP1 (10 μM)		
Noorani *et al*[21]	Human fetal lung fibroblast	IMR90-C4	NR	Day 1: E8	Y27632 (10 μm)	iBMECs (1.5×10^7 cells/mL) in NR medium	Primary ACs (10^6 cells/mL) and PCs (3.5×10^5 cells/mL) (3:1) in NR medium
				Day 0-6: UM	KOSR (20%) + NEAA (1%) + Glutamax (0.5%) + β-Mercapto-ethanol (0.1 mM)		
				Day 7-8: $EC^{+/+}$ (HESFM)	bPPP (1%) + bFGF (20 ng/mL) + RA (10 μm)		
				Day 9: $EC^{-/-}$ (HESFM)	Without bFGF and RA		
Middelkamp *et al*[22]	Adult skin fibroblasts	GM25256	Laminin	Day 1: DMEM/F12	Primocin (0.1 mg/mL) + DX (4 μg/mL) + N2 (1 ×) + MEM-NEAA (1 ×) + NT3-RHP (10 ng/mL) + BDNF-RHP (10 ng/mL)	iNeurons (10^4) in E8	Rat ACs (1:1) and HUVECs (4×10^4) in ECGM-2
				Day 1 (after two hours): E8	RevitaCell (1 ×) + DX (4 μg/mL)		
				Day 3-38: Neurobasal	Day 3: Primocin (0.1 mg/mL) + B-27 (1 ×) serum free + glutamax (1 ×) + DX (4 μg/mL) + NT-3 (10 ng/mL) + BDNF (10 ng/mL) + arabinoside hydrochloride (2 μm) Day 5: Refresh medium without arabinoside hydrochloride (2 μm)		

					Day 9-38: Refresh medium with 2.5% fetal calf serum		
Choi *et al*[23]	Human fetal lung fibroblast	IMR90-C4	Matrigel	Day 3: mTeSR1™-E8™	NR	iBMECs purified[1] (1.2×10^7 cells/mL) in HESFM	AC (10^6 cells/mL) in $EC^{-/-}$
				Day 0-5: UM (DMEM/F12)	KOSR (20%) + NEAA (100x) + glutamax (0.5%) + β-Mercapto-ethanol (0.007%) (5% O_2)		
				Day 6-8: $EC^{+/+}$ (HESFM)	Human serum (1%) + bFGF (20 ng/mL) + RA (10 μm) (5% O_2)		
				Day 9: $EC^{-/-}$ (HESFM)	Without bFGF and RA		
Motallebnejad *et al*[24]	Human fetal lung fibroblast	IMR90-C4	Matrigel	Days 3-1: mTeSR1-cGMP	Day 3: Y27632 (10 μm)	iBMECs purified[1] in NR medium	NA
					Day 2: Without Y27632		
				Days 0-5: UM	NR		
				Days 6-8: $EC^{+/+}$ (HESFM)	Days 6-7: hPDS (1%) + RA (10 μM) + FGF2 (20 ng/mL)		
					Day 8: bPPP (1%) or FBS (2%) + FGF (20 ng/mL) + RA (10 μM)		
				Day 9: $EC^{-/-}$ (HESFM)	Without bFGF and RA		
	Healthy human African American male from the bone marrow CD34+ cells	ACS-1024	LN 511-E8 or LN 411-E8 or collagen IV + fibronectin	HESFM	Day 8: bPPP (1%) or FBS (2%) + FGF (20 ng/mL) + RA (10 μM)		
					Day 9: Without bFGF and RA		
Lee *et al*[25]	Endothelial cells	hiPSC-ECs	Human fibronectin	VascuLife VEGF	iCell media supplement	hiPSC-ECs (6×10^6 cells/mL) in VascuLife VEGF with thrombin	PCs and ACs (10^6 cells/mL) in VascuLife VEGF with thrombin
Jagadeesan *et al*[26]	Neural progenitors	EZ-Spheres	NA	Day 1: EZ-sphere medium (DMEM/F12)	bFGF (100 ng/mL) + EGF (100 ng/mL) + heparin (5 μg/mL) + B27 (2%)	iNPCs (10^6 cells/mL) in NDM	ACs (9×10^5 cells/mL) and PCs (3×10^5 cells/mL) in in DMEM
					B27 (2%) + vitamin A + N2 (1%) + hBDNF, (20 ng/mL)		
	NR	hiPSCs	Basement membrane matrix-coated	Day 1: mTeSR1	NR	iBMECs [(14-20) × 10^6 cells/mL] in $EC^{-/-}$ (HESFM)	
				Day 2-8: UM (DMEM/F12)	KOSR (10%) + NEAA (1%) + glutamine (0.5%) + β-Mercapto-ethanol (100 μm)		
				Day 9-10: $EC^{+/+}$ (HESFM)	bPPP (1%) + bFGF (20 ng/mL) + RA (10 μM)		
				Day 11: $EC^{-/-}$ (HESFM)	Without bFGF and RA		
Vatine *et al*[27]	Adult skin fibroblasts	CS03iCTR CS83iCTR CS03iCTR$^{mut, 2}$ CS01iMCT8	Matrigel	Day 3: mTeSR1	NR	iNPCs (10^6 cells/mL) in NDM and iBMECs (1.4×10^4 cells/mL)	ACs (9×10^5 cells/mL) and PCs (3×10^5 cells/mL) in DMEM

		CS01iMCT-8^{cor,2}					
	Peripheral blood	CS0172iCTR					
		CS0188iCTR		Day 0: UM	Without bFGF		
		CS0617iCTR					
	Huntington's disease	CS81iHD					
Park *et al*[28]	Human fetal lung fibroblast	IMR90-C4	Matrigel	Day 3: mTeSR1	NR (5% O_2)	iBMECs purified[1] (2.3×10^7 cells/mL) in EC	ACs (7×10^5 cells/mL) and PCs (3×10^5 cells/mL) in ACM
				Day 0-6: UM (DMEM/F12)	KOSR (100 mL) + NEAA (5 mL) + glutamax (2.5 mL) + β-Mercaptoethanol (3.5 µL) (5% O_2)		
				Day 7-9: $EC^{+/+}$	RA (5% O_2)		
Campisi *et al*[29]	Blood from 30-39-year-old healthy females	hiPSC-ECs	Human fibronectin	VascuLife VEGF	iCell media supplement + VEGF (50 ng/mL)	hiPSC-ECs (2×10^6 cells/mL) in EBM-2	Monoculture hiPSC-ECs (6×10^6 cells/mL) in EBM-2
							PCs (2×10^6 cells/mL) in EGM-2 MV
							PCs and ACs (2×10^6 cells/mL) in EGM-2 MV
Wang *et al*[30]	Human fetal lung fibroblast	IMR90-C4	Matrigel	Day 3: mTeSR1	NR	iBMECs in HESFM	Rat primary ACs in AGM
				Day 0-5: UM (DMEM/F12)	HEPES + KOSR (20%) + MEM-NEAA (1 ×) + L-glutamine (1 mM) + β-Mercaptoethanol (0.1 mM)		
				Day 6-8: $EC^{+/+}$ (HESFM)	hPDS (1%) + bFGF (20 ng/mL) + RA (10 µM)		
DeStefano *et al*[31]	CD34 positive bone marrow	BC1-hiPSCs	Matrigel	Day 4-3: mTeSR1-E8	NR Day 3: Y27632 (10 µm)	iBMECs (10^5) in EC	NA
				Day 0-5: UM (DMEM/F12)	KOSR (20%) + NEAA (1%) + L-Glutamine (0.5%) + β-Mercaptoethanol (0.84 µm)		
				Day 6-7: $EC^{+/+}$ (HESFM)	hPDS (1%) + bFGF (20 ng/mL) + RA (10 µm)		
				Day 8: EC (HESFM)	DB-cAMP (400 µm) or Y27632 (10 µm)		

[1]Induced pluripotent stem cell-derived brain microvascular endothelial cells were selectively expanded before to seed in the chip.

[2]Modified by clustered regularly interspaced short palindromic repeats. For human induced pluripotent stem cells-brain microvascular endothelial cells purification, day 8: ECM [1 µg/cm^2 LN 511-E8 or LN 411-E8 (iMatrix, iWAi), 1 µg/cm^2 full length laminin 511 (Biolamina), 100 µg/mL fibronectin (Millipore Sigma), or a mixture of 400 µg/mL collagen IV (Millipore Sigma) and 100 µg/mL of fibronectin] protein-coated ThinCert cell culture inserts (Greiner Bio-One), well plates or ibidi µ-slides. AT: Adipose tissue; BDNF-RHP: Brain-derived neurotrophic factor recombinant human protein; EGF: Epidermal growth factor; BM: Bone marrow; bPPP: Platelet-poor plasma derived bovine serum; CXCR4: C-X-C chemokine receptor type 4; db-cAMP1: 2′-O-Dibutyryladenosine-3′,5′-cyclic monophosphate; DMEM: Dulbecco's modified eagle medium; E8 medium: Essential 8 medium; EGF: Epidermic growth factor; FDF2: Fibroblast growth factor 2; FL: Fetal lung; GFP: Green fluorescent protein; HESFM: Human endothelial serum free medium; hFGF2: Human fibroblast growth factor 2; hiPSC: Human induced pluripotent stem cell; HOXB4: Homeobox B4; hPDS: Human serum from platelet-poor human plasma; IB: Intrabone; IP: Intraperitoneal; IV: Intravenous; KOSR: Knockout serum replacement; Matrigel-GFR: Growth factor reduced matrigel; MEC: Brain microvascular endothelial cell; MEM: Minimum essential medium; NA: Not applied; NEAA: Non-essential amino acids; Nos2$^{-/-}$: Deficient in type 2 nitric oxide; NR: Not reported; NT3-RHP: Neurotrophin-3 recombinant human protein; P/S: Penicillin/streptomycin; PDGFB: Platelet-derived growth factor subunit B; PPDS: Platelet poor derived serum; AAc: Ascorbic acid; SDF-1: Stromal cell-derived factor 1; solG-CSFR: Soluble granulocyte colony-stimulating factor decoy receptor; TPO: Thrombopoietin; UCB: Umbilical cord blood; MMP3: Matrix metallopeptidase 3.

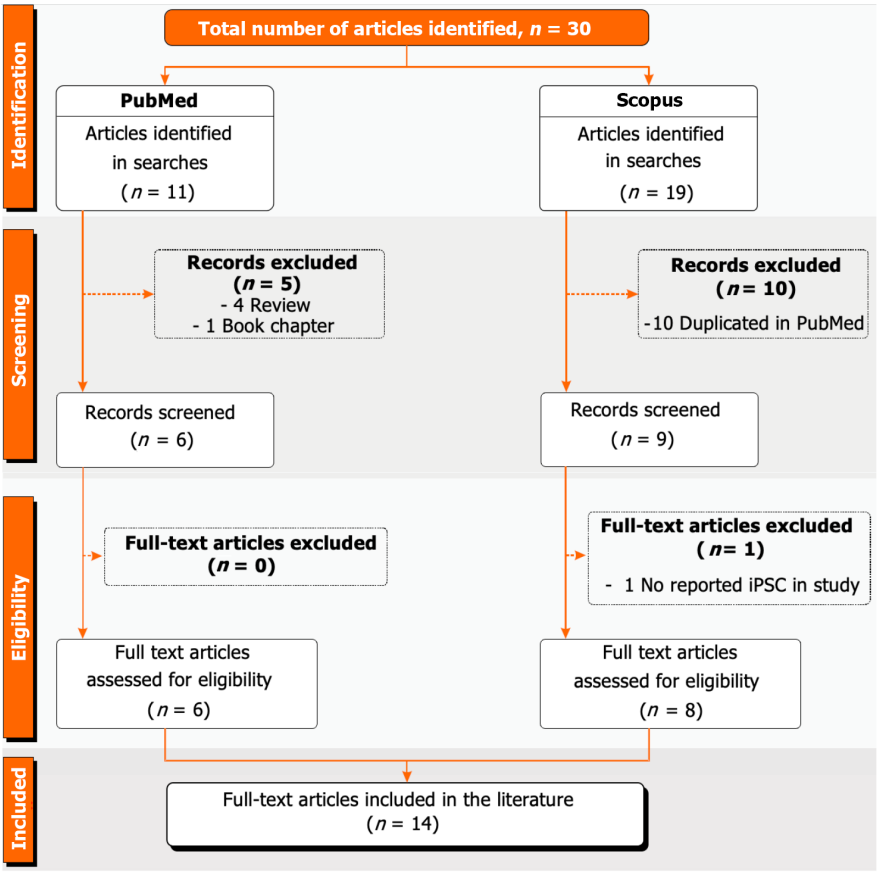

DOI: 10.4252/wjsc.v15.i6.632

Figure 1 PRISMA flow chart of the study selection process applied in this systematic review. iPSC: Induced pluripotent stem cell.

Unconditioned medium (UM), normally composed of Dulbecco's modified Eagle medium (DMEM)/F12 supplemented with knockout serum replacement + non-essential amino acids (NEAA) or minimum essential medium (MEM) with NEAA (MEM-NEAA) + glutamax or L-glutamine + β-mercaptoethanol, was used in 71.4% of the studies[18,19,21,23,24,26-28,30,31] to promote differentiation to ECs (for 6 d on average), followed by a change to human endothelial serum-free medium containing diverse substances, such as retinoic acid (RA), platelet-poor-derived bovine serum (bPPP) or human serum from platelet-poor human plasma (hPDS), and basic fibroblast growth factor, to induce BMEC formation (Figure 2A and Table 2).

Few studies have described different processes to generate iBMECs. Lee *et al*[25] used solely vasculife vascular endothelial growth factor medium with iCell media supplement[29]. The study by Wevers *et al*[20] used DMEM/F12 and N2B27 supplemented with brain-derived neurotrophic factor (BDNF) + glial cell line-derived neurotrophic factor + ascorbic acid + 2'-O-Dibutyryladenosine-3',5'-cyclic monophosphate. Finally, the study by Middelkamp *et al*[22] utilized DMEM/F12 supplemented with primocin + doxycycline (DX) + N2 + MEM-NEAA + neurotrophin-3 (NT3) recombinant human protein + BDNF recombinant human protein, followed by a change to E8 supplemented with revitacell + DX, and a later change to neurobasal medium supplemented first with primocin + B27SF + glutamax + DX + NT3 + BDNF, in addition to arabinoside hydrochloride for 24 h, followed by the addition of fetal calf serum. DX induced the overexpression of neurogenin 2 in GM25256 iPSCs, being one of the key factors for the differentiation of GM25256 into iNeurons (Table 2).

All of the abovementioned processes were described for iPSC differentiation on a plate, with the exception of the study by Campisi *et al*[29], whose cell differentiation step occurred inside the microfluidic chips. Furthermore, two studies used hypoxic conditions during the cell differentiation process[23,28].

BBB-on-a-chip reconstruction process

To build the BBB-on-a-chip model, the microdevices must first receive a coating layer to sustain 3D cell growth, as depicted in Figure 2B. From this perspective, diverse coating substances and different cell-seeding strategies have been described, depending on the chip design. As seen in Figure 2B, previously to cell culture on-a-chip, fibronectin was the principal ECM component coating the microfluidic channels (39.3%)[18,21,23-26,28-31], among which 28.6% corresponded to a mixture of fibronectin + collagen type IV. More recent studies have applied an ECM composed of collagen type I + 4-(2-hydroxyethyl)-1-piperazineethanesulfonic acid + sodium bicarbonate (10.7%)[18-20]. Laminin coating was used in 14.3% of the analyzed studies[22,26,27], wherein a mixture of different types of laminin + fibronectin was employed in the study by Motallebnejad *et al*[24]. Additionally, one study utilized only Matrigel[20], and another utilized collagen type I[23] as channel coating. The mentioned coatings were carefully selected for each channel, depending on the

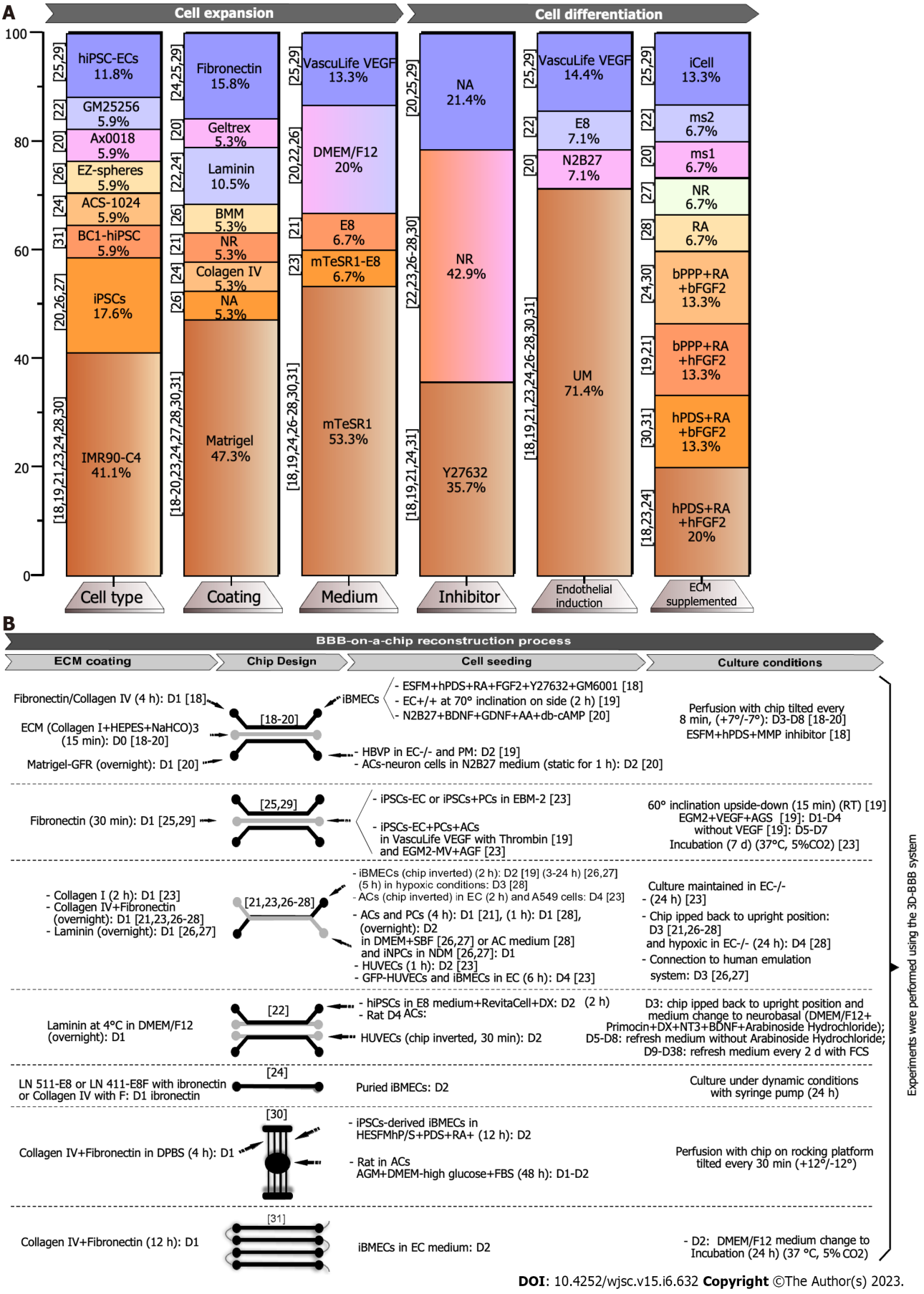

DOI: 10.4252/wjsc.v15.i6.632

Figure 2 Induced pluripotent stem cell differentiation process into induced pluripotent stem cell-derived brain microvascular endothelial-like cells for reconstruction of the blood-brain barrier-on-a-chip model. A: Percent analysis of cells and culture media used in induced pluripotent stem

cell expansion and differentiation before blood-brain barrier (BBB)-on-a-chip reconstruction; B: Schematic summary of the main findings in this systematic review on the cells and culture conditions applied in the BBB-on-a-chip reconstruction process. Studies were grouped by similar device designs. AAc: Ascorbic acid; AC: Astrocyte; ACS-1024: Bone-induced pluripotent stem cell line; AGF: Astrocyte growth factor; AGM: Astrocyte growth medium; BC1: Lymphoma cell line; BDNF: Brain-derived neurotrophic factor; bFGF: Bovine fibroblast growth factor; BMM: Basement membrane matrix; bPPP: Basic platelet-poor plasma; D1: Day 1; D2: Day 2; D3: Day 3; D38: Day 38; D4: Day 4; D5: Day 5; D6: Day 6; D8: Day 8; D9: Day 9; db-cAMP1: 2'-O-Dibutyryladenosine-3',5'-cyclic monophosphate; DMEM/F12: Dulbecco's modified Eagle medium with F12; DPBS: Dulbecco's phosphate-buffered saline; DX: Doxycycline; E8: Essential 8 medium; EC-/-: Human endothelial serum-free medium without retinoic acid + basic fibroblast growth factor; EC: Endothelial cell; EC+/+: Human endothelial serum-free medium with retinoic acid + basic fibroblast growth factor; ECM: Extracellular matrix; EGM-2MV: Microvascular endothelial cell growth medium-2; ESFM: Endothelial serum-free medium; FBS: Fetal bovine serum; FCS: Fetal calf serum; FGF2: Fibroblast growth factor 2; GDNF: Glial cell line-derived neurotrophic factor; GFP: Green fluorescent protein; GFR: Growth factor reduced; GM25256: Cell line of induced pluripotent stem cell derived from adult skin fibroblasts; GM6001: Broad spectrum MMP inhibitor; HBVP: Human brain vascular pericytes; HEPES: 4-(2-hydroxyethyl)-1-piperazineethanesulfonic acid; HESFM: Human endothelial serum-free medium; hFGF: Human fibroblast growth factor; hiPSC-EC: Human-induced pluripotent stem cell-derived endothelial cell; hPDS: Human serum from platelet-poor human plasma; hPDS: Platelet-poor plasma-derived human serum; HUVEC: Human umbilical vein endothelial cell; iBMECs: Induced pluripotent stem cell-derived brain microvascular endothelial cells; IMR90-C4: Induced pluripotent stem cell line; iPSCs: Induced pluripotent stem cells; LN: Laminin; ms1: Brain-derived neurotrophic factor + glial cell line-derived neurotrophic factor + ascorbic acid + 2'-O-Dibutyryladenosine-3',5'-cyclic monophosphate; ms2: Primocin + glutamax + doxycycline + neurotrophin-3 + brain-derived neurotrophic factor + fetal calf serum; mTeSR1: Basal medium type for induced pluripotent stem cells; N2B27: Culture medium; NA: Not applied; NR: Not reported; NT3: Neurotrophin-3; P/S: Penicillin/streptomycin; PCs: Pluripotent cells; PM: Pericyte medium; RA: Retinoic acid; RA: Retinoic acid; RT: Room temperature; SFB: Serum-free medium; UM: Unconditioned medium; VEGF: Vascular endothelial growth factor; Y27632: Dihydrochloride inhibitor.

desired environment and cultured cell type.

Regarding cell seeding, five studies have described an iBMEC single culture[18,19,24,29,31], in which two studies applied a selective cell expansion step before seeding[19,24]. A co-culture of iBMEC + ACs was reported in three studies [20,23,30], one of which used PCs in the co-culture[29]. Yet, most studies have built their BBB models based on an approach involving more than two cell types in co-culture, normally associating ACs and PCs with other ECs such as HUVECs[22], iBMECs[21,28], and iPSC-ECs[25], with the exception of Jagadeesan *et al*[26] and Vatine *et al*[27], who associated neural progenitor cells with ACs and PCs in the brain-side, and iBMECs in the blood-side of their BBB model (Figure 2B).

The particular aspects of cell culture inside the chips are displayed in Figure 2B. Among the observed aspects, we highlight the inversion or inclination of the chip to seed the cells[21-23,25-28], maintenance of the chip under hypoxic conditions[28], and tilting of the chips for gravity-dependent bidirectional medium flow[18-20,30].

Applications of BBB microfluidic 3D models using iPSCs

Regarding the general objective of the studies (Table 3), the great majority of the articles (roughly 80%)[18-21,23,24,26-30] were aimed at developing a microfluidic BBB model, as well as assessing the convenience of the manufactured model by quantifying common molecular markers that are normally expressed in cells that make up the BBB *in vivo*. Five of these studies (35.7%) analyzed drug transport for BBB characterization purposes[18,19,27,28,30]. Only two studies described actual applications for their models: Wevers *et al*[20] used their developed chip to model BBB disruption upon ischemic stroke, and Lee *et al*[25] tested the permeability of their model to commercial and synthesized polymer nanoparticles (NPs). Middelkamp *et al*[22] compared a 2D Transwell BBB model to one built on-a-chip, whereas DeStefano *et al*[31] evaluated the effect of shear stress on their BBB microfluidic chips.

The characterization of the BBB model was performed by means of structural and functional analyses. Concerning structural analyses, the expression of tight junction proteins was evaluated in 85.7% of the studies using immunocytochemistry (85.7%)[18-21,23-31]. Part of these studies also performed quantitative polymerase chain reaction (qPCR) (42.9%)[23-25,29,31]. Less frequently used techniques were fluorescence (F-actin staining)[24], transcriptional analysis [27], mass spectrometry (MS) (proteomics)[28], and western blot analysis[31]. Transport protein and receptor expression was evaluated in 57.1% of the cases[18,20,21,23,26-28,31] by immunocytochemistry (42.9%)[18,21,23,26-28], qPCR (21.4%) [18,20,31], fluorescence (permeability glycoprotein inhibition, 14.3%)[20,21], transcriptional analysis (7.1%)[27], and MS (7.1%)[28]. Two studies (14.3%) characterized neuronal differentiation by immunocytochemistry[22,26], one of which also applied RNA sequencing and transcriptomic analysis to further characterize the HUVECs[22]. Structural characterization of ACs and PCs was performed by immunocytochemistry by Campisi *et al*[29]. Lastly, DeStefano *et al*[31] used microscopic techniques to structurally and functionally characterize ECs seeded on-a-chip[31] (Table 3).

Functional characterization of the BBB model was more varied, with the use of diverse techniques. Tight junction functionality (71.4%) was mostly analyzed by fluorescence (50%)[18-20,22,24,26,30] using diverse fluorescent markers[18, 23,24,26,28-30] such as zonula occludens-1 (ZO-1), claudin-5[21,22,26,28], occludin (OCLN)[21,22], glucose transporter type 1[21,24,26], platelet/EC adhesion molecule-1 (PECAM-1)[22,24,26,27], and vascular endothelial (VE)-cadherin[22]. Other techniques used to evaluate tight junction functionality were transepithelial electrical resistance (TEER) measurements (42.9%)[19,20,24,27,28,30], enzyme-linked immunosorbent assay (21.4%)[19,27,28], (ultra or high performance) liquid chromatography with tandem MS (LC-MS/MS) (21.4%)[18,27,30], immunocytochemistry[23,27] (14.3%), transendothelial migration of cancer cells[23], electron transmission microscopy (7.1%)[28], and transmitted light microscopy (7.1%)[27]. Microvessel permeability (57.1%)[19-21,25,27-30] and microvessel integrity (7.1%)[19] were assessed by fluorescence (57.1%)[19-21,25,27-30]. Transport protein function was evaluated by 21.4% of the studies[18,27, 28] by fluorescence (14.3%)[27,28] and high-performance LC-MS (7.1%)[18]. Neuronal functionality was evaluated by calcium fluorescence imaging (14.3%)[20,27] and immunocytochemistry (7.1%)[27]. Mitochondrial membrane potential was analyzed by luminescence and ATP quantification (7.1%)[20]. In a diverse approach, the study by Vatine *et al*[27],

Table 3 Applications of blood-brain barrier microfluidic three-dimensional models using induced pluripotent stem cells

Ref.	Application	Characterization	Evaluation technique	Outcomes
Kurosawa *et al*[18]	Build and evaluate a BBB 3D *in vitro* model	Capillary structure formation and tight junction proteins expression	Immunocytochemistry	Formation of the capillary structure, functional tight proteins; lower expression of ABC transporters than levels found *in vivo*, except for BCRP; expression of functional SLC transporters
		Transport proteins and receptors expression	Immunocytochemistry	
			qPCR	
		Tight junction functionality	Fluorescence (lucifer yellow and antipyrine)	
			HPLC-MS/MS (test-drug transport)	
		Transport proteins function	HPLC-MS/MS (test-drug transport)	
Fengler *et al*[19]	Build and evaluate a BBB 3D *in vitro* model	Tight junction proteins expression	Immunocytochemistry	Capillary diameter CA. 40 times larger than *in vivo* brain vessels; physiologically relevant TEER values; physiologically similar localization of BCRP and GLUT-1 proteins. Promising BBB model for future drug screening tests
		Microvessel integrity	Fluorescence (DEX-A647 and sodium fluorescein)	
		Microvessel permeability	Diazepam, Emricasan, Ac-YVAD-CMK, Z-DEVD-FMK, ZVAD (OH)-FMK, Staurosporine, and IL-1β	
		Tight junction functionality	ELISA (Diazepam)	
			TEER measurements	
Wevers *et al*[20]	Build and evaluate a BBB 3D *in vitro* model	Tight junction proteins expression	Immunocytochemistry	Barrier functionality similar to that found *in vivo*; microfluidic model suitable for evaluating disruption of the BBB; successful ischemic stroke modeling. Potential use for modeling the BBB under sub-optimal conditions (disease) and for evaluating potential therapies
		Tight junction functionality	TEER measurements	
		Microvessel permeability	Fluorescence (sodium fluorescein)	
		Transport proteins expression	Fluorescence: P-gp inhibition	
			qPCR	
		Neuronal functionality	Calcium fluorescence imaging	
	Ischemic stroke modeling	Microvessel permeability	Fluorescence (FITC-dextran)	
		Mitochondrial membrane potential	Luminescence (CellTiter-GLO)	
			ATP quantification	
Noorani *et al*[21]	Build and evaluate a BBB 3D *in vitro* model	Tight junction proteins expression	Immunocytochemistry	BBB functionality remains intact for up to 7 d and is similar to that found *in vivo*; a more physiologically relevant BBB model; shear stress contributes positively to BBB tightness
		Microvessel permeability	UPLC-MS/MS: [$^{13}C_{12}$] sucrose and [$^{13}C_6$] mannitol	
		Transport proteins expression	Immunocytochemistry	
			Fluorescence: P-gp inhibition	
Middelkamp *et al*[22]	Compare 2D cultures to microfluidic chip cultures	Neuronal differentiation and characterization of HUVECs	Immunocytochemistry	Culture in microfluidic chips promotes gene expression that more closely resembles that found *in vivo*
			RNA sequencing	
			Transcriptomic analysis	
Choi *et al*[23]	Build and evaluate a BBB 3D *in vitro* model	Tight junction proteins expression	Immunocytochemistry	cECMTE membrane with 10 m pores in microfluidic device were successful in mimicking the *in vivo* BBB, also allowing for cancer cell tissue migration. Promising BBB model for studying cancer metastasis, cell communication, and migration
			qPCR	
		Tight junction functionality	Fluorescence (lucifer yellow)	
			Transendothelial migration of cancer cells (CellMask)	
			Immunocytochemistry	
		Transport proteins expression	Immunocytochemistry	

Motallebnejad *et al*[24]	Build and evaluate a BBB 3D *in vitro* model	Tight junction proteins expression	Immunocytochemistry	LM511-E8 ECM contributes to long-lasting endothelial cell and BBB function, in addition to promoting better shear stress responses. Authors recommend the use of LM511-E8 ECM for future studies involving BBB function
			Fluorescence (F-actin staining)	
			qPCR	
		Tight junction functionality	TEER measurements	
			Fluorescence (rhodamine B-labeled neutral dextran)	
Lee *et al*[25]	BBB permeability to polymer nanoparticles	Tight junction and transport proteins expression	qPCR	Fast analysis of polymer nanoparticles permeability; physiologically reliable BBB model
		Permeability to polymer nanoparticles	Fluorescence (polymer nanoparticles and FITC-dextran)	
			3D fluorescence intensity maps	
Jagadeesan *et al*[26]	Build and evaluate a BBB 3D *in vitro* model	Tight junction proteins expression	Immunocytochemistry	Successful fabrication of BBB model personalized for different human individuals; BBB models were able to mimic physiological differences between healthy and ill individuals
		Tight junction functionality and microvessel permeability	Fluorescence: FITC-dextran	
		Transport proteins expression	Immunocytochemistry	
		Neuronal differentiation		
Vatine *et al*[27]	Build and evaluate a BBB 3D *in vitro* model	Tight junction proteins expression	Immunocytochemistry	Successful fabrication of BBB model personalized for different human individuals; BBB models were able to mimic physiological differences between healthy and ill individuals
			Transcriptional analysis	
		Microvessel permeability and tight junction functionality	Fluorescence (FITC-dextran and 2NDBG)	
			ELISA (human albumin, IgG and transferrin)	
			LC-MS/MS (T_3, colchicine, levetiracetam and retigabine)	
			Transmission light microscopy	
			TEER measurements	
			Immunocytochemistry	
		Transport proteins expression	Immunocytochemistry	
			Transcriptional analysis	
		Transport protein function	Fluorescence (rhodamine-123)	
		Whole-blood neuronal toxicity	Colorimetric assay (quantification of lactic dehydrogenase)	
		Neuronal functionality	Immunocytochemistry	
			Calcium fluorescence imaging	
Park *et al*[28]	Build and evaluate a BBB 3D *in vitro* model	Tight junction proteins expression	Immunocytochemistry	BBB functionality remains intact for up to 7 d. Promising BBB model for future drug and antibody transport studies
			Multiplex qPCR	
			MS (proteomics)	
		Tight junction functionality and microvessel permeability	Electron transmission microscopy	
			TEER measurements	
			Fluorescence (dextrans, cetuximab, angiopep-2, MEM75, 13E4)	
			ELISA (dextrans, cetuximab)	
		Transport proteins expression	Immunocytochemistry	
			MS	
		Transport proteins function	Fluorescence (rhodamine-123 and doxorubicin)	

Campisi *et al*[29]	Build and evaluate a BBB 3D *in vitro* model	Tight junction proteins expression	Immunocytochemistry qPCR	Tri-culture of human iPSC-derived endothelial cells, astrocytes and pericytes spontaneously arranged into a BBB-like model. Promising BBB model for future preclinical experiments
		Tight junction functionality and microvessel permeability	Fluorescence (FITC-dextran)	
		Characterization of astrocytes and pericytes	Immunocytochemistry	
Wang *et al*[30]	Build and evaluate a BBB 3D *in vitro* model	Tight junction proteins expression	Immunocytochemistry	Pumpless media perfusion system that resembles the blood residence time within brain tissues; physiologically relevant TEER values maintained for up to 10 d. Promising BBB model for future drug permeability studies
		Tight junction functionality and microvessel permeability	TEER measurements Fluorescence: FITC-dextran and doxorubicin LC-MS/MS (caffeine and cimetidine)	
DeStefano *et al*[31]	Evaluate BBB upon shear stress	Characterization of iPSC-derived endothelial cells morphology and function	Microscopy (time-lapse imaging analysis using ImageJ)	BBB endothelial cells display unique features that differ from endothelial cells from other tissues; shear stress plays a key role in BBB-like function in microfluidic models
		Tight junction proteins expression	Immunocytochemistry Western blot qPCR	
		Transport proteins expression	qPCR	

2NDBG: 2-deoxy-2-[(7-nitro-2,1,3-benzoxadiazol-4-yl)-amino]-D-glucose; 3D: Three-dimensional; Ac-YVAD-CMK: Caspase-1 inhibitor; ATP: Adenosine triphosphate; UPLC-MS/MS: Ultra-performance liquid chromatography-mass spectrometry (tandem); BBB: Blood-brain barrier; BCRP: Breast cancer resistance protein; cECMTE: Condensed extracellular matrix track-etched; CellTiter-GLO: Luminescent cell viability assay; DEX-A647: Dextran conjugated to Alexa 647; ECM: Extracellular matrix; ELISA: Enzyme-linked immunoassay; FITC-dextran: Fluorescein isothiocyanate dextran; GLUT-1: Glucose transporter 1; hBMEC: Human brain microvascular endothelial cells; HPLC-MS/MS: High-performance liquid chromatography-mass spectrometry (tandem); HUVEC: Human umbilical vein endothelial cell; iBMEC: Induced pluripotent stem cell-derived brain microvascular endothelial-like cell; IgG: Immunoglobulin G; IL-1β: Interleukin 1 beta; iPSC: Induced pluripotent stem cell; LC-MS/MS: Liquid chromatography-mass spectrometry (tandem); LM511-E8: Fragment E8 of laminin 511; MS: Mass spectrometry; P-gp: Permeability glycoprotein; qPCR: Quantitative polymerase chain reaction; RNA: Ribonucleic acid; SLC: Solute carrier protein; TEER: Trans-epithelial electrical resistance; Z-DEVD-FMK: Caspase-3 inhibitor; ZVAD (OH)-FMK: Pan-caspase inhibitor.

among other evaluations, perfused whole human blood through the chip channels to perform a whole-blood neuronal toxicity assay using a colorimetric technique, focusing on the quantification of lactic dehydrogenase[27] (Table 3).

Overall, the analyzed studies were successful in building structural and functional BBB models on-a-chip using iPSCs. Most of them highlighted the future use of their models for drug screening tests, in addition to mimicking physiological conditions found in healthy and unhealthy individuals, wherein one of the studies reported the applicability of their device for modeling cancer cell invasion and migration through the BBB. The studies also focused on the potential for the development of personalized therapies, mainly in conditions of disease. Some interesting outcomes have reported long-lasting BBB function for the developed chips, with an average BBB function duration of 7 d[21,28] to 10 d[30] (Table 3).

DISCUSSION

This systematic review showed that this theme, BBB models with iPSCs in microdevices, is quite novel in the scientific literature; without setting a time limit, only articles from 2017 to 2022 were found. Furthermore, the articles published in the last 2 years have already shown great technological advances in BBB-on-a-chip in commercial devices[18-21]. Curiously, the same chip by MIMETAS® was used in three studies by different labs around the world (Japan[18], the Netherlands[19], and Germany[20]), and another commercial BBB-on-a-chip was also used by an American lab[21]. These advances in technological on-chip manufacturing allow the scientific community to direct further efforts to apply the developed BBB-on-a-chip to model pathological conditions, such as stroke[21], and design personalized therapeutic approaches.

Among the developed BBB models on a microdevice, some showed distinctive features, mainly for the chips fabricated in house. For example, the study by Choi *et al*[23] described a BBB microchip whose functionality was based on a track-etched 10 μm pore polyester membrane covered with a collagen type I ECM. This study reported that the ECM-covered membrane with a larger pore size allowed for better modeling of the communications between neural cells and ECs, in addition to enabling the evaluation of cancer cell metastasis through the BBB[23]. Other articles also based their 3D BBB models on microfluidic channels separated by porous membranes of various materials - PDMS[21,26,27], PC[30], PE[28], PETE[22,23] - and various pore sizes that ranged from 0.4 mm to 7 mm. Nevertheless, none of these studies focused on

the importance of the membrane material or pore size to the envisaged BBB function.

However, half of the selected articles, and curiously, the most recent ones, showed similar geometries with straight membrane-free channels. The advantage of the presence of a membrane is controversial in the literature regarding its role in the BBB model. Due to the relatively greater thickness of the artificial membrane compared to the basal lamina *in vivo*, cell-cell interactions are limited[34,35]. More recent articles use the diffusible factors produced by the cells in culture themselves for indirect communication between ACs and the BBB endothelium, without the physical restriction imposed by the artificial membrane[35].

Organs-on-chips are a currently sought alternative due to the possibility of physiologically relevant 3D *in vitro* single- or pluricellular culture and, more importantly, due to the possibility of laminar medium flow, mimicking the environment and shear stress found in capillary vessels. Also, the microchip culture of neural cells has shown more *in vivo*-like results, with more mature neurons and ACs[22]. However, the establishment of laminar flow might be cumbersome, given the need for apparatuses such as syringes, capillary tubes, and peristaltic pumps adapted for the sterile environment required for cell culture. Some studies have attempted to overcome this problem with creative alternatives, such as rocking platforms that allow the bidirectional flow of media within the microchips[18-20,30]. Regardless, the cerebral tissue is rather complex and involves a multitude of interacting cell types and ECM proteins. *In vitro* modeling at such a level is already challenging *per se*, whether or not the laminar flow is involved.

Regarding the material used for chip fabrication, conventional PDMS was used in most cases (57%)[22,25-29,31]. One of the studies adopted PMMA[23], which consists of the least hydrophobic material utilized in microfabrication. In addition, this material is ideal for mass production, and it is stiffer than PDMS. However, rapid prototyping is somewhat complicated by the fact that PMMA bonding is more difficult than the straightforward bonding of PDMS[36,37]. Conversely, PDMS may nonselectively adsorb proteins and hydrophobic molecules, which could possibly interfere with the characterization process of the BBB-on-a-chip and future drug screening applications[38]. Hence, some studies have presented alternatives to tackle this issue, such as covering the microchip surface with bovine serum albumin[39], grafting with anti-fouling molecules[40], or silanization[41].

For construction of the *in vitro* NVU, the cell cultures have been classically established in Transwell plates, mainly using primary brain ECs isolated from animal and human sources, which retain very tight barriers *in vitro* and may be useful tools for studying paracellular permeability[42,43]. Immortalized EC lines, such as HUVECs, have also been used in these BBB models, although they do not provide the permeability profile or the protein expression typically present in the human BBB[44]. Moreover, there is great difficulty in obtaining primary human brain ECs from healthy individuals [45].

The aforementioned drawbacks have been recently addressed with the use of iPSCs. After going through a complex differentiation protocol, these stem cells have shown *in vivo*-like barrier function[27]. Their BBB phenotype can be further enhanced by co-cultivation with other cells that exert barrier function *in vivo*, such as ACs and PCs[24,27]. In view of this aspect, we found in this systematic review a great diversity of iPSC commercially available cell lines from human sources, such as the IPS cell line IMR90-C4 from human fetal lung fibroblasts[18,19,21,23,24,28,30]. We further verified that one study used an iPSC line from unhealthy donors, with the advanced purpose of verifying BBB dysfunction in a pathological model and an attempt to correct this dysfunction through gene editing (CRISPR)[27]. In addition, building BBB models from human-derived iPSCs may be a valuable tool for personalized medicine, wherein a patient's CNS disease could be precisely modeled *in vitro*, enabling the evaluation of personalized treatment.

On the other hand, iPSC-based BBB models have shown short-lived BBB function, which is generally maintained for up to 2 d[21]. Current efforts have been aimed at extending the BBB profile of these cultures[21,28,30]. 3D BBB on-a-chip devices form more physical and physiologically accurate morphologies. The cell-cell and cell-matrix interactions produced in microfluidic models generally provide a robust BBB function, with permeability to different substances (drugs, antibodies, proteins) that resemble that observed *in vivo*[18,19,27,28].

Most of the studies featured in this review (86%) differentiated their iPSCs into BMECs. This is expected since BMECs are the specialized cells in the CNS vasculature that show barrier properties. On the other hand, four studies differentiated the iPSCs into neural cells (neurons and ACs)[20,22,26,27]. The NVU, which makes up the BBB, is mainly composed of strict interactions among BMECs, the ECM, basal lamina, PCs, ACs, and adjacent neurons[11,46]. Even though neurons are indeed considered to be part of the BBB, they are physiologically positioned farther from the microvessels that make up the NVU (10 μm to 20 μm) than ACs or PCs[47]. The studies that reported co-culture of ECs with neurons mentioned in the current review did not clearly state the reasons for using neurons in their BBB models, but some studies stated that co-culture of iBMECs with neurons induces the upregulation of membrane transporters typical of the BBB, promoting a more robust function[29,48], as reported in a study by Wevers *et al*[20]. Microfluidic chips co-cultured both with iBMECs and neural cells showed a more robust phenotype regarding BMECs and strong indicators of epithelial cell barrier integrity and permeability (TEER from 1000 to 4000 Ω × cm^2)[18,19,21,27,30].

Although studies have pointed out drawbacks using primary BMECs or iBMECs in the EC monolayer in BBB-on-a-chip, they still constitute a more reliable model. One of the biggest challenges in using iBMECs in BBB research is the difficulty in producing an *in vivo*-like BMEC phenotype *in vitro* following the currently available protocols, which generally result in more epithelial-like phenotypes with the suboptimal expression of membrane transporters[6,20,26,27,49]. A recent meta-analysis study showed that iPSCs could only be reliably differentiated into BMECs through exposition to endothelial ETS transcription factors ETS variant transcription factor 2, Friend leukemia integration 1 transcription factor, and Ets-related gene[49]. Nevertheless, the differentiation of iPSCs into iBMECs can further benefit from co-culture with neural cells, such as ACs and neurons[27,50]. While a more robust differentiation protocol is not established, some studies make use of alternative ways to make an EC layer, such as the use of HUVECs[22], primary BMECs[20], or even immortalized lines[10]. On the other hand, the isolation of human primary BMECs is a challenge, since they comprise less than 0.1% of the cells in the CNS and tend to de-differentiate in culture[27,51]. Studies with HUVECs generally point out

some limitations, such as the formation of an incomplete EC monolayer[22]. Immortalized cells, despite being easily commercialized, generally constitute BBB models with poor barrier properties[27,52].

Fully iPSC-based chips were useful in modeling BBB disruptions from diseased patients, such as the alterations found in Huntington's disease and in monocarboxylate transporter 8 deficiency[26,27]. Wevers *et al*[20] and Middelkamp *et al*[22] also differentiated the iPSCs into neurons, albeit not providing further justifications for doing so. With the exception of Vatine *et al*[27], who observed improved barrier functions with a fully iPSC-derived BBB chip, the other studies considered in this review have not versed on whether their obtained outcomes were positive or negatively dependent on the use of iPSCs.

Normally the microfluidic chips receive a coating made of collagen type IV/fibronectin before cell seeding[21,23,24,26-28,30,31]. These coating agents improve cell adhesion to the chip substrate through micropatterning, offering a fibrous base to guide cell differentiation and cell-to-cell contacts[16]. Motallebnejad *et al*[24] considered that the *in vivo* brain endothelial basement membrane is made up of laminins. Keeping this in mind, they compared the characteristics of the iPSC-derived ECs grown on an ECM based on E8 fragments of laminin 411 or laminin 511 (laminin511-E8) to ECs grown on the common collagen IV/fibronectin ECM. The authors found that the ECM made of laminin511-E8 presented more significant results, with the iPSC-ECs grown on this ECM exhibiting a longer-lasting EC phenotype and improved barrier stability compared to cells grown on the collagen IV/fibronectin ECM. iPSC-ECs grown on laminin511-E8 presented higher expression levels of junctional proteins such as claudin-5, VE-cadherin, and PECAM-1. Curiously, three other articles used a laminin ECM coating[22,26,27], but on the "brain side" channel of their microfluidic devices. One of the aforementioned studies also used the laminin coating on the "blood side" channel for culturing HUVECs, but without mentioning the importance of the laminin ECM[22].

Another important aspect of microfluidic device analyses in many studies is perfusion, whether by culture media or other biologically-relevant liquids, due to the shear stress and their important advantage in *in vitro* studies[10,16,53]. For BBB models, the role of shear stress on BBB function remains inconclusive. Among the studies selected for this review, eight (57%) considered shear stress[19-22,24,27,30,31], whereas two[22,30] designed their BBB mimics to minimize shear stress. Vatine *et al*[27] reported an increase in the expression of tight junction genes, such as tight junction protein 1/*ZO-1*, *OCLN*, *PECAM-1*, and cadherin 5/VE-cadherin, even under shear stress as low as 0.01 or 0.5 dyne/cm^2. A study by Noorani *et al*[21] found ambiguous results for cultures under shear stress; perfusion did not induce changes in tight junction gene expression but decreased the permeability levels of sucrose and mannitol. In turn, the work by DeStefano *et al*[31] focused solely on the effect of increasing shear stress (0, 4, or 12 dyne/cm^2) on the genotype and phenotype of iPSC-derived ECs. The authors found no correlation between the presence of shear stress and the expression of a more robust EC phenotype, since tight junctions are already formed under static conditions. Some authors considered that perfusion makes a bigger difference in BBB models made of non-iPSC-derived EC cultures such as HUVECs or primary ECs[31,54], whereas iPSC-derived ECs do not experience drastic changes in BBB markers upon shear stress[21,31]. Motallebnejad *et al*[24] gathered evidence that culturing iPSC-derived ECs on laminin511-E8 ECM improves the response of ECs to shear stress, wherein the cells exhibit changes in morphology, surface area, and the upregulation of tight junction proteins.

Regarding BBB applications, the specialized literature has not yet been able to establish a consistent microfluidic BBB model that can cover a broad range of applications, from modeling CNS disorders, including cancer metastasis, to screening for drugs able to permeate the BBB to treat such maladies. This is reflected in the goals of most studies selected to be part of this review. The great majority of the articles (roughly 80%) were aimed at developing a microfluidic BBB model, as well as assessing the convenience of the manufactured model by quantifying common molecular markers that are normally expressed in cells that make up the BBB *in vivo*[18-21,23,24,26-30]. Only one of the studies focused not on the BBB model itself but on the permeation potential of either commercial or synthesized polymer NPs through the *in vitro* 3D BBB mimic[25]. The BBB is a significant obstacle to the effective transport of large molecules for the treatment of brain disorders, and a study by Lee *et al*[25] showed that iPSC-ECs are appropriate for generating the 3D *in vitro* BBB model [25]. Surface modification of NPs with ligands for specific binding to BBB cells enhances NP accumulation in the brain through receptor-mediated endocytosis, providing good conditions to explore personalized therapies[25].

Another different application for the 3D BBB model was reported in a study by Wevers *et al*[20], which employed hypoxia together with hypoglycemia and lack of perfusion to successfully mimic ischemic stroke on-a-chip[20]. This hypoxic condition was also used to improve the iPSC differentiation to BMECs inside the microfluidic device by Park *et al*[28]. Based on the hypoxic environment found during the embryological development of the BBB *in vivo*, the whole differentiation step of iPSCs into ECs, both on a plate and in the microfluidic chip, was performed under low oxygen (5% O_2). For the cells cultured under hypoxia, the authors observed the upregulation of diverse tight junction proteins and membrane transporters, contributing to a more robust BBB function. Moreover, they found that the differentiated ECs produce hypoxia-inducible factor 1α, a molecular marker whose presence was found to improve the function and durability of the BBB model[28].

Concerning the characterization techniques, the structural evaluation of the BBB model was mainly targeted by immunocytochemistry, whereas functional aspects have been mainly assessed using fluorescence techniques. Immunocytochemistry assays are the golden standard for identifying proteins related to the BBB, as well as for identifying different stages of BBB maturation (early, intermediate, and late phases of BBB development)[55]. Fluorescence assays are easily accessible and generally offer a vast array of markers that can be used for various purposes, from evaluating BBB permeability and integrity to neuronal functionality. Many studies mentioned TEER measurements as an important method to characterize BBB function[20,21,24,27,28,30,56]. However, they pose a number of disadvantages. The TEER values across BBB culture models are frequently influenced by disregarded physical and technical factors such as temperature, viscosity, and current density, generated by various electrode types, surface size, circumference, and porosity of the insert membrane, leading to severalfold differences within the same biological model[57]. Additionally, these TEER values can vary according to cell type (primary, immortalized, iPSC-derived), cell source (animal or human),

and culture type (2D, 3D culture, co-culture)[58]. Therefore, the comparison of TEER values among different studies is highly discouraged in the relevant literature.

This systematic review highlights the main aspects of the current literature on BBB models on-a-chip, from iPSC differentiation to the NVU formation and characterization inside the microfluidic devices, also considering the functional duration of the proposed models by diverse approaches, focusing on future applications. However, the lack of uniform nomenclature and protocols made it a challenge to deeply analyze and comprehend all the steps in the processes involved.

The construction of BBB-on-a-chip still faces numerous challenges in producing feasible, reproducible, and reliable models. This becomes apparent in that, among the 14 articles studied in this review, 12 focused on the development of a robust *in vitro* model[18,19,21-24,26-31], and only 2 focused on the application of a model to study BBB disruption following ischemic stroke[20] and study the BBB permeability to polymer NPs[25]. Even though the use of iPSCs in microfluidic systems poses an advancement in these BBB constructs, there remain obstacles in the use of this type of cells, especially related to differentiation protocols, which need to be further developed in order to result in more dependable cell phenotypes. Moreover, on-chip technology remains a costly *in vitro* alternative, and the in-house manufacture of microfluidic devices is hampered by the need for a clean room and specialized equipment and personnel.

The integration of sensors to monitor barrier permeability and neuronal response to drug exposure is an important aspect scarcely addressed. The addition of such sensors could enable more precise and real-time measurements of drug transport across the BBB and its effects in brain cells. In terms of potential impacts, this technology can accelerate the development of new drugs by allowing for faster and more accurate screening of compounds that cross the BBB for therapeutic effects on the brain. One important step towards this scenario was already taken in the study by Vatine *et al* [27], who were successful in perfusing whole human blood through their microfluidic device, creating promising conditions to evaluate disease[27]. Moreover, more reliable BBB-on-a-chip constructs may help to better understand the *in vivo* functioning of the BBB across different individuals, representing a significant impact on personalized medicine.

CONCLUSION

Despite the well-known literature on iPSCs, microfluidic devices, and BBB *in vitro* models in isolation, the combination of the three subjects is a currently relevant theme, already presenting with advanced technology in the use of commercial microdevices for modeling the BBB. The BBB-on-a-chip models, in spite of their particularities in each study, have shown to be efficient for reconstructing the NVU *in vitro*, being able to reproduce the characteristics found *in vivo* in terms of structure and function. They have displayed promising qualities for investigating barrier disorders, drug delivery, mimicking disease, and personalized medicine.

ARTICLE HIGHLIGHTS

Research background

Induced pluripotent stem cells (iPSCs) offer a potential alternative to building blood-brain barrier (BBB)-on-a-chip models that more closely resemble the structure and functions found *in vivo*.

Research motivation

iPSC-derived BBB models on-a-chip are a promising field that still lacks improvements and uniformity within the specialized literature.

Research objectives

To search the literature and analyze the selected data on the cultivation of iPSCs within microfluidic environments to mimic the human BBB.

Research methods

A literature search using the PRISMA approach using the following terms: “iPSC,” “BBB,” and “microfluidic device,” wherein 14 studies were selected based on the inclusion and exclusion criteria, and data were organized into three tables and one flow chart.

Research results

Studies have been found from 2017 to 2022, wherein the microdevices were either commercially available or manufactured in-house using soft-lithography. iPSCs were differentiated into endothelial or neural cells and seeded in the chips individually or in co-culture onto an extracellular-matrix layer mainly made of collagen IV/fibronectin. The selected studies focused principally on the structural and functional design of the human BBB model on-a-chip, displaying future application potential for drug screening and disease modeling.

Research conclusions

Despite the lack of consensus in protocols, the studies analyzed herein were able to efficiently reproduce a human

microfluidic BBB *in vitro* making use of iPSCs.

Research perspectives

The developed BBB models on-a-chip have shown great potential to study physiopathological conditions related to the central nervous system, to apply advanced technology approaches for novel therapies (drug delivery through nanoparticles), and to develop genetic modification therapies for BBB dysfunctions through clustered regularly interspaced short palindromic repeats methodologies.

FOOTNOTES

Author contributions: Alves ADH, Nucci MP, Ennes do Valle NM, Missina JM, and Gamarra LF conceived and designed this study; Alves ADH, Nucci MP, Ennes do Valle NM, Rego GNA, and Gamarra LF performed the literature review; Alves ADH, Nucci MP, Ennes do Valle NM, Rego GNA, Mamani JB, and Missina JM performed the data extraction and critical review; Alves ADH, Nucci MP, Ennes do Valle NM, Missina JM, de Oliveira FA, and Mamani JB interpreted and analyzed the collected data; Alves ADH, Nucci MP, Ennes do Valle NM, Missina JM, Dias OFM, Garrigós MM, and Gamarra LF wrote this review; All authors reviewed and approved the final manuscript as submitted.

Supported by CNPq, Nos. 308901/2020-7 and 400856/2016-6; FAPESP, Nos. 2019/21070-3, 2017/17868-4, and 2016/21470-3; SisNANO 2.0/MCTIC, No. 442539/2019-3; and the National Institute of Science and Technology Complex Fluids, INCT-FCx.

Conflict-of-interest statement: The authors have no conflicts of interest to declare.

PRISMA 2009 Checklist statement: The authors have read the PRISMA guidelines, and the manuscript was prepared and revised according to the PRISMA 2009 Checklist.

Country/Territory of origin: Brazil

ORCID number: Arielly da Hora Alves 0000-0003-3570-0827; Mariana Penteado Nucci 0000-0002-1502-9215; Nicole Mastandrea Ennes do Valle 0000-0003-4523-1753; Juliana Morais Missina 0000-0002-6226-9932; Javier Bustamante Mamani 0000-0001-5038-0070; Gabriel Nery Albuquerque Rego 0000-0003-2011-0373; Olivia Furiama Metropolo Dias 0000-0003-0168-9367; Murilo Montenegro Garrigós 0000-0002-7082-8730; Fernando Anselmo de Oliveira 0000-0002-7226-1694; Lionel Fernel Gamarra 0000-0002-3910-0047.

S-Editor: Wang JJ
L-Editor: Filipodia
P-Editor: Zhang XD

REFERENCES

1 **Shi Y**, Inoue H, Wu JC, Yamanaka S. Induced pluripotent stem cell technology: a decade of progress. *Nat Rev Drug Discov* 2017; **16**: 115-130 [PMID: 27980341 DOI: 10.1038/nrd.2016.245]
2 **Lippmann ES**, Al-Ahmad A, Azarin SM, Palecek SP, Shusta EV. A retinoic acid-enhanced, multicellular human blood-brain barrier model derived from stem cell sources. *Sci Rep* 2014; **4**: 4160 [PMID: 24561821 DOI: 10.1038/srep04160]
3 **Wiegand C**, Banerjee I. Recent advances in the applications of iPSC technology. *Curr Opin Biotechnol* 2019; **60**: 250-258 [PMID: 31386977 DOI: 10.1016/j.copbio.2019.05.011]
4 **Ray A**, Joshi JM, Sundaravadivelu PK, Raina K, Lenka N, Kaveeshwar V, Thummer RP. An Overview on Promising Somatic Cell Sources Utilized for the Efficient Generation of Induced Pluripotent Stem Cells. *Stem Cell Rev Rep* 2021; **17**: 1954-1974 [PMID: 34100193 DOI: 10.1007/s12015-021-10200-3]
5 **Sundaravadivelu PK**, Raina K, Thool M, Ray A, Joshi JM, Kaveeshwar V, Sudhagar S, Lenka N, Thummer RP. Tissue-Restricted Stem Cells as Starting Cell Source for Efficient Generation of Pluripotent Stem Cells: An Overview. *Adv Exp Med Biol* 2022; **1376**: 151-180 [PMID: 34611861 DOI: 10.1007/5584_2021_660]
6 **Workman MJ**, Svendsen CN. Recent advances in human iPSC-derived models of the blood-brain barrier. *Fluids Barriers CNS* 2020; **17**: 30 [PMID: 32321511 DOI: 10.1186/s12987-020-00191-7]
7 **Sweeney MD**, Zhao Z, Montagne A, Nelson AR, Zlokovic BV. Blood-Brain Barrier: From Physiology to Disease and Back. *Physiol Rev* 2019; **99**: 21-78 [PMID: 30280653 DOI: 10.1152/physrev.00050.2017]
8 **Kugler EC**, Greenwood J, MacDonald RB. The "Neuro-Glial-Vascular" Unit: The Role of Glia in Neurovascular Unit Formation and Dysfunction. *Front Cell Dev Biol* 2021; **9**: 732820 [PMID: 34646826 DOI: 10.3389/fcell.2021.732820]
9 **Williams-Medina A**, Deblock M, Janigro D. In vitro Models of the Blood-Brain Barrier: Tools in Translational Medicine. *Front Med Technol* 2020; **2**: 623950 [PMID: 35047899 DOI: 10.3389/fmedt.2020.623950]
10 **Wevers NR**, Kasi DG, Gray T, Wilschut KJ, Smith B, van Vught R, Shimizu F, Sano Y, Kanda T, Marsh G, Trietsch SJ, Vulto P, Lanz HL,

Obermeier B. A perfused human blood-brain barrier on-a-chip for high-throughput assessment of barrier function and antibody transport. *Fluids Barriers CNS* 2018; **15**: 23 [PMID: 30165870 DOI: 10.1186/s12987-018-0108-3]

11 **Abbott NJ**, Patabendige AA, Dolman DE, Yusof SR, Begley DJ. Structure and function of the blood-brain barrier. *Neurobiol Dis* 2010; **37**: 13-25 [PMID: 19664713 DOI: 10.1016/j.nbd.2009.07.030]

12 **Van Norman GA**. Limitations of Animal Studies for Predicting Toxicity in Clinical Trials: Is it Time to Rethink Our Current Approach? *JACC Basic Transl Sci* 2019; **4**: 845-854 [PMID: 31998852 DOI: 10.1016/j.jacbts.2019.10.008]

13 **Clevers H**. Modeling Development and Disease with Organoids. *Cell* 2016; **165**: 1586-1597 [PMID: 27315476 DOI: 10.1016/j.cell.2016.05.082]

14 **Halldorsson S**, Lucumi E, Gómez-Sjöberg R, Fleming RMT. Advantages and challenges of microfluidic cell culture in polydimethylsiloxane devices. *Biosens Bioelectron* 2015; **63**: 218-231 [PMID: 25105943 DOI: 10.1016/j.bios.2014.07.029]

15 **Cui B**, Cho SW. Blood-brain barrier-on-a-chip for brain disease modeling and drug testing. *BMB Rep* 2022; **55**: 213-219 [PMID: 35410642 DOI: 10.5483/BMBRep.2022.55.5.043]

16 **Liang Y**, Yoon JY. *In situ* sensors for blood-brain barrier (BBB) on a chip. *Sens Actuators Rep* 2021; **3**: 100031 [DOI: 10.1016/j.snr.2021.100031]

17 **Liberati A**, Altman DG, Tetzlaff J, Mulrow C, Gøtzsche PC, Ioannidis JP, Clarke M, Devereaux PJ, Kleijnen J, Moher D. The PRISMA statement for reporting systematic reviews and meta-analyses of studies that evaluate health care interventions: explanation and elaboration. *PLoS Med* 2009; **6**: e1000100 [PMID: 19621070 DOI: 10.1371/journal.pmed.1000100]

18 **Kurosawa T**, Sako D, Tega Y, Debori Y, Tomihara Y, Aoyama K, Kubo Y, Amano N, Deguchi Y. Construction and Functional Evaluation of a Three-Dimensional Blood-Brain Barrier Model Equipped With Human Induced Pluripotent Stem Cell-Derived Brain Microvascular Endothelial Cells. *Pharm Res* 2022; **39**: 1535-1547 [PMID: 35411503 DOI: 10.1007/s11095-022-03249-3]

19 **Fengler S**, Kurkowsky B, Kaushalya SK, Roth W, Fava E, Denner P. Human iPSC-derived brain endothelial microvessels in a multi-well format enable permeability screens of anti-inflammatory drugs. *Biomaterials* 2022; **286**: 121525 [PMID: 35599022 DOI: 10.1016/j.biomaterials.2022.121525]

20 **Wevers NR**, Nair AL, Fowke TM, Pontier M, Kasi DG, Spijkers XM, Hallard C, Rabussier G, van Vught R, Vulto P, de Vries HE, Lanz HL. Modeling ischemic stroke in a triculture neurovascular unit on-a-chip. *Fluids Barriers CNS* 2021; **18**: 59 [PMID: 34906183 DOI: 10.1186/s12987-021-00294-9]

21 **Noorani B**, Bhalerao A, Raut S, Nozohouri E, Bickel U, Cucullo L. A Quasi-Physiological Microfluidic Blood-Brain Barrier Model for Brain Permeability Studies. *Pharmaceutics* 2021; **13** [PMID: 34575550 DOI: 10.3390/pharmaceutics13091474]

22 **Middelkamp HHT**, Verboven AHA, De Sá Vivas AG, Schoenmaker C, Klein Gunnewiek TM, Passier R, Albers CA, 't Hoen PAC, Nadif Kasri N, van der Meer AD. Cell type-specific changes in transcriptomic profiles of endothelial cells, iPSC-derived neurons and astrocytes cultured on microfluidic chips. *Sci Rep* 2021; **11**: 2281 [PMID: 33500551 DOI: 10.1038/s41598-021-81933-x]

23 **Choi B**, Choi JW, Jin H, Sim HR, Park JH, Park TE, Kang JH. Condensed ECM-based nanofilms on highly permeable PET membranes for robust cell-to-cell communications with improved optical clarity. *Biofabrication* 2021; **13** [PMID: 34479224 DOI: 10.1088/1758-5090/ac23ad]

24 **Motallebnejad P**, Azarin SM. Chemically defined human vascular laminins for biologically relevant culture of hiPSC-derived brain microvascular endothelial cells. *Fluids Barriers CNS* 2020; **17**: 54 [PMID: 32912242 DOI: 10.1186/s12987-020-00215-2]

25 **Lee SWL**, Campisi M, Osaki T, Possenti L, Mattu C, Adriani G, Kamm RD, Chiono V. Modeling Nanocarrier Transport across a 3D In Vitro Human Blood-Brain-Barrier Microvasculature. *Adv Healthc Mater* 2020; **9**: e1901486 [PMID: 32125776 DOI: 10.1002/adhm.201901486]

26 **Jagadeesan S**, Workman MJ, Herland A, Svendsen CN, Vatine GD. Generation of a Human iPSC-Based Blood-Brain Barrier Chip. *J Vis Exp* 2020 [PMID: 32176199 DOI: 10.3791/60925]

27 **Vatine GD**, Barrile R, Workman MJ, Sances S, Barriga BK, Rahnama M, Barthakur S, Kasendra M, Lucchesi C, Kerns J, Wen N, Spivia WR, Chen Z, Van Eyk J, Svendsen CN. Human iPSC-Derived Blood-Brain Barrier Chips Enable Disease Modeling and Personalized Medicine Applications. *Cell Stem Cell* 2019; **24**: 995-1005.e6 [PMID: 31173718 DOI: 10.1016/j.stem.2019.05.011]

28 **Park TE**, Mustafaoglu N, Herland A, Hasselkus R, Mannix R, FitzGerald EA, Prantil-Baun R, Watters A, Henry O, Benz M, Sanchez H, McCrea HJ, Goumnerova LC, Song HW, Palecek SP, Shusta E, Ingber DE. Hypoxia-enhanced Blood-Brain Barrier Chip recapitulates human barrier function and shuttling of drugs and antibodies. *Nat Commun* 2019; **10**: 2621 [PMID: 31197168 DOI: 10.1038/s41467-019-10588-0]

29 **Campisi M**, Shin Y, Osaki T, Hajal C, Chiono V, Kamm RD. 3D self-organized microvascular model of the human blood-brain barrier with endothelial cells, pericytes and astrocytes. *Biomaterials* 2018; **180**: 117-129 [PMID: 30032046 DOI: 10.1016/j.biomaterials.2018.07.014]

30 **Wang YI**, Abaci HE, Shuler ML. Microfluidic blood-brain barrier model provides in vivo-like barrier properties for drug permeability screening. *Biotechnol Bioeng* 2017; **114**: 184-194 [PMID: 27399645 DOI: 10.1002/bit.26045]

31 **DeStefano JG**, Xu ZS, Williams AJ, Yimam N, Searson PC. Effect of shear stress on iPSC-derived human brain microvascular endothelial cells (dhBMECs). *Fluids Barriers CNS* 2017; **14**: 20 [PMID: 28774343 DOI: 10.1186/s12987-017-0068-z]

32 **Watanabe K**, Ueno M, Kamiya D, Nishiyama A, Matsumura M, Wataya T, Takahashi JB, Nishikawa S, Muguruma K, Sasai Y. A ROCK inhibitor permits survival of dissociated human embryonic stem cells. *Nat Biotechnol* 2007; **25**: 681-686 [PMID: 17529971 DOI: 10.1038/nbt1310]

33 **Vernardis SI**, Terzoudis K, Panoskaltsis N, Mantalaris A. Human embryonic and induced pluripotent stem cells maintain phenotype but alter their metabolism after exposure to ROCK inhibitor. *Sci Rep* 2017; **7**: 42138 [PMID: 28165055 DOI: 10.1038/srep42138]

34 **Jiang L**, Li S, Zheng J, Li Y, Huang H. Recent Progress in Microfluidic Models of the Blood-Brain Barrier. *Micromachines (Basel)* 2019; **10** [PMID: 31195652 DOI: 10.3390/mi10060375]

35 **Kaisar MA**, Sajja RK, Prasad S, Abhyankar VV, Liles T, Cucullo L. New experimental models of the blood-brain barrier for CNS drug discovery. *Expert Opin Drug Discov* 2017; **12**: 89-103 [PMID: 27782770 DOI: 10.1080/17460441.2017.1253676]

36 **Young EW**, Berthier E, Guckenberger DJ, Sackmann E, Lamers C, Meyvantsson I, Huttenlocher A, Beebe DJ. Rapid prototyping of arrayed microfluidic systems in polystyrene for cell-based assays. *Anal Chem* 2011; **83**: 1408-1417 [PMID: 21261280 DOI: 10.1021/ac102897h]

37 **Chen Y**, Zhang L, Chen G. Fabrication, modification, and application of poly(methyl methacrylate) microfluidic chips. *Electrophoresis* 2008; **29**: 1801-1814 [PMID: 18384069 DOI: 10.1002/elps.200700552]

38 **Toepke MW**, Beebe DJ. PDMS absorption of small molecules and consequences in microfluidic applications. *Lab Chip* 2006; **6**: 1484-1486 [PMID: 17203151 DOI: 10.1039/b612140c]

39 **Ostuni E**, Chen CS, Ingber DE, Whitesides GM. Selective deposition of proteins and cells in arrays of microwells. *Langmuir* 2001; **17**: 2828-2834 [DOI: 10.1021/la001372o]

40 **Gokaltun A**, Yarmush ML, Asatekin A, Usta OB. Recent advances in nonbiofouling PDMS surface modification strategies applicable to microfluidic technology. *Technology (Singap World Sci)* 2017; **5**: 1-12 [PMID: 28695160 DOI: 10.1142/S2339547817300013]

41 **Jon S**, Seong J, Khademhosseini A, Tran TNT, Laibinis PE, Langer R. Construction of nonbiofouling surfaces by polymeric self-assembled monolayers. *Langmuir* 2003; **19**: 9989-9993 [DOI: 10.1021/la034839e]

42 **Lippmann ES**, Azarin SM, Kay JE, Nessler RA, Wilson HK, Al-Ahmad A, Palecek SP, Shusta EV. Derivation of blood-brain barrier endothelial cells from human pluripotent stem cells. *Nat Biotechnol* 2012; **30**: 783-791 [PMID: 22729031 DOI: 10.1038/nbt.2247]

43 **Helms HC**, Abbott NJ, Burek M, Cecchelli R, Couraud PO, Deli MA, Förster C, Galla HJ, Romero IA, Shusta EV, Stebbins MJ, Vandenhaute E, Weksler B, Brodin B. In vitro models of the blood-brain barrier: An overview of commonly used brain endothelial cell culture models and guidelines for their use. *J Cereb Blood Flow Metab* 2016; **36**: 862-890 [PMID: 26868179 DOI: 10.1177/0271678X16630991]

44 **Man S**, Ubogu EE, Williams KA, Tucky B, Callahan MK, Ransohoff RM. Human brain microvascular endothelial cells and umbilical vein endothelial cells differentially facilitate leukocyte recruitment and utilize chemokines for T cell migration. *Clin Dev Immunol* 2008; **2008**: 384982 [PMID: 18320011 DOI: 10.1155/2008/384982]

45 **Delsing L**, Herland A, Falk A, Hicks R, Synnergren J, Zetterberg H. Models of the blood-brain barrier using iPSC-derived cells. *Mol Cell Neurosci* 2020; **107**: 103533 [PMID: 32717317 DOI: 10.1016/j.mcn.2020.103533]

46 **Banerjee S**, Bhat MA. Neuron-glial interactions in blood-brain barrier formation. *Annu Rev Neurosci* 2007; **30**: 235-258 [PMID: 17506642 DOI: 10.1146/annurev.neuro.30.051606.094345]

47 **Wong AD**, Ye M, Levy AF, Rothstein JD, Bergles DE, Searson PC. The blood-brain barrier: an engineering perspective. *Front Neuroeng* 2013; **6**: 7 [PMID: 24009582 DOI: 10.3389/fneng.2013.00007]

48 **Appelt-Menzel A**, Cubukova A, Günther K, Edenhofer F, Piontek J, Krause G, Stüber T, Walles H, Neuhaus W, Metzger M. Establishment of a Human Blood-Brain Barrier Co-culture Model Mimicking the Neurovascular Unit Using Induced Pluri- and Multipotent Stem Cells. *Stem Cell Reports* 2017; **8**: 894-906 [PMID: 28344002 DOI: 10.1016/j.stemcr.2017.02.021]

49 **Lu TM**, Houghton S, Magdeldin T, Durán JGB, Minotti AP, Snead A, Sproul A, Nguyen DT, Xiang J, Fine HA, Rosenwaks Z, Studer L, Rafii S, Agalliu D, Redmond D, Lis R. Pluripotent stem cell-derived epithelium misidentified as brain microvascular endothelium requires ETS factors to acquire vascular fate. *Proc Natl Acad Sci U S A* 2021; **118** [PMID: 33542154 DOI: 10.1073/pnas.2016950118]

50 **Canfield SG**, Stebbins MJ, Morales BS, Asai SW, Vatine GD, Svendsen CN, Palecek SP, Shusta EV. An isogenic blood-brain barrier model comprising brain endothelial cells, astrocytes, and neurons derived from human induced pluripotent stem cells. *J Neurochem* 2017; **140**: 874-888 [PMID: 27935037 DOI: 10.1111/jnc.13923]

51 **Cecchelli R**, Berezowski V, Lundquist S, Culot M, Renftel M, Dehouck MP, Fenart L. Modelling of the blood-brain barrier in drug discovery and development. *Nat Rev Drug Discov* 2007; **6**: 650-661 [PMID: 17667956 DOI: 10.1038/nrd2368]

52 **Kamiichi A**, Furihata T, Kishida S, Ohta Y, Saito K, Kawamatsu S, Chiba K. Establishment of a new conditionally immortalized cell line from human brain microvascular endothelial cells: a promising tool for human blood-brain barrier studies. *Brain Res* 2012; **1488**: 113-122 [PMID: 23041702 DOI: 10.1016/j.brainres.2012.09.042]

53 **Seebach J**, Dieterich P, Luo F, Schillers H, Vestweber D, Oberleithner H, Galla HJ, Schnittler HJ. Endothelial barrier function under laminar fluid shear stress. *Lab Invest* 2000; **80**: 1819-1831 [PMID: 11140695 DOI: 10.1038/labinvest.3780193]

54 **DeStefano JG**, Williams A, Wnorowski A, Yimam N, Searson PC, Wong AD. Real-time quantification of endothelial response to shear stress and vascular modulators. *Integr Biol (Camb)* 2017; **9**: 362-374 [PMID: 28345713 DOI: 10.1039/c7ib00023e]

55 **Dermietzel R**, Krause D. Molecular anatomy of the blood-brain barrier as defined by immunocytochemistry. *Int Rev Cytol* 1991; **127**: 57-109 [PMID: 1880006 DOI: 10.1016/S0074-7696(08)60692-0]

56 **Srinivasan B**, Kolli AR, Esch MB, Abaci HE, Shuler ML, Hickman JJ. TEER measurement techniques for in vitro barrier model systems. *J Lab Autom* 2015; **20**: 107-126 [PMID: 25586998 DOI: 10.1177/2211068214561025]

57 **Vigh JP**, Kincses A, Ozgür B, Walter FR, Santa-Maria AR, Valkai S, Vastag M, Neuhaus W, Brodin B, Dér A, Deli MA. Transendothelial Electrical Resistance Measurement across the Blood-Brain Barrier: A Critical Review of Methods. *Micromachines (Basel)* 2021; **12** [PMID: 34208338 DOI: 10.3390/mi12060685]

58 **Shah B**, Dong X. Current Status of In vitro Models of the Blood-brain Barrier. *Curr Drug Deliv* 2022; **19**: 1034-1046 [PMID: 35240972 DOI: 10.2174/1567201819666220303102614]

Published by **Baishideng Publishing Group Inc**
7041 Koll Center Parkway, Suite 160, Pleasanton, CA 94566, USA
Telephone: +1-925-3991568
E-mail: bpgoffice@wjgnet.com
Help Desk: https://www.f6publishing.com/helpdesk
https://www.wjgnet.com